

REPORT SERIES IN AEROSOL SCIENCE

N:o 126 (2011)

**Proceedings of the Finnish Center of Excellence and Graduate School in
'Physics, Chemistry, Biology and Meteorology of Atmospheric
Composition and Climate Change'
Annual Workshop 18.–20.5.2011**

Editors: Markku Kulmala, Jaana Bäck, Hanna K. Lappalainen and Tuomo Nieminen

Helsinki 2011

ISBN 978-952-5822-49-6
<http://www.atm.helsinki.fi/FAAR/>

CONTENTS

Kulmala M. et al.: Finnish CoE in physics, chemistry, biology and meteorology of atmospheric composition and climate change, results in 2010-2011	19
Aalto J., Kolari P., Aaltonen H., Bäck J., Hari P. and Nikinmaa E.: Continuous measurements of Scots pine shoots show huge variation in VOC emissions during year 2010	31
Aaltonen H., Aalto J., Bäck J., Kolari P., Pihlatie M., Pumpanen J., Kulmala M., Nikinmaa E. and Vesala T.: Continuous chamber measurements of VOC fluxes from boreal pine forest floor	35
Acosta M., Haapanala S., Lohila A., Aurela M., Laurila T., Vesala T.: The effect of water table level on dissolved oxygen concentration and methane emissions in two Finnish wetland ecosystems	40
Ahmad I., Mielonen T., Portin H., Laaksonen A., Arola A., Romakkaniemi S.: Aerosol effect on Cumulus/Stratocumulus clouds: Comparison of ground based in-situ measurement and Satellite observations	43
Alekseychik P., Mammarella I. and Vesala T.: Nighttime thermal decoupling in a conifer forest canopy	48
Anttila T.: Numerical study on the importance of the particle mixing state to cloud droplet formation	52

Asmi A.:	
Weakness of weekly wavelets void indirect weekend effect	
.....	54
Asmi E., Kivekäs N., Komppula M., Hyvärinen A.-P., Hatakka J., Viisanen Y. and Lihavainen H.:	
Atmospheric secondary particle formation in Pallas 2000-2011	
.....	57
Babkovskaia N., Boy M., Smolander S., Romakkaniemi S. and Kulmala M.:	
A study of aerosol production at the cloud edge with DNS	
.....	60
Backman J., Rizzo L. V., Petäjä T., Manninen H.E., Nieminen T, Hakala J., Aalto P.P., Siivola E., Morais F., Hillamo R., Artaxo P. and Kulmala M.:	
Measuring optical properties and size distributions at São Paulo, Brazil: new particle formation events occur at the site	
.....	63
Bergman T., Kokkola H., Makkonen R., Kerminen V.-M., Kulmala M. and Lehtinen K.:	
Characteristics of global aerosol optical depth simulated with microphysical models SALSA and M7 within ECHAM5-HAM	
.....	67
Berninger F.:	
Long term temporal scaling of forest atmosphere relations using tree rings	
.....	71
Boy M., Babkovskaia N., Gierens R., Gopalkrishnan K.V., He Q., Makkonen R., Mogensen D., Rusanen A., Sihto S.-L., Smolander S., Vuollekoski H., Watcharapaskorn C. and Zhou L.:	
Overview about the activities in the atmosphere modelling group	
.....	72
Brus D., Neitola K., Hyvärinen A.-P. and Lihavainen H.:	
Nucleation and growth in sulfuric acid-water system: from nano scale to CCN	
.....	76

Bäck J., Kulmala M. and the CRAICC-team: Cryosphere-atmosphere interactions in a changing arctic climate (CRAICC)	79
Bäck J., Aalto J., Kolari P., Juurola E., Henriksson M. and Hakola H.: Temporal and between-tree variability of Scots pine monoterpene emissions in a boreal forest stand	81
Dal Maso M., Mentel T. F., Kiendler-Scharr A., Kleist E., Tillmann R., Sipilä M., Petäjä T., Hakala J., Liao L., Lehtipalo K., Junninen H., Ehn M., Vanhanen J., Mikkilä J., Kulmala M., Wildt J., Worsnop D.: Plant emissions and atmospheric nanoparticle formation	85
Franchin A., Schobesberger S., Lehtipalo K., Makhmutov V., Stozhkov Y., Gagné S., Nieminen T., Manninen H. E., Petäjä T., Kulmala M. and the CLOUD collaboration: Physical characterization of ions in the CLOUD chamber	87
Gagné S., Lehtipalo K., Manninen H.E., Nieminen T., Schobesberger S., Franchin A., Yli-Juuti T., Boulon J., Sonntag A., Mirme S., Mirme A., Hörrak U., Petäjä T., Asmi E. and Kulmala M.: Intercomparison of air ion spectrometers	89
Gagné S., Leppä J., Petäjä T., McGrath M.J., Vana M., Kerminen V.-M., Laakso L. and Kulmala M.: Ion-induced nucleation fraction and small ion concentration asymmetry in Helsinki	94
Gierens R., Laakso L., Lauros J., Makkonen R., Vakkari V., Mogensen D., Vuollekoski H. and Boy M.: Modelled new particle formation in Southern African savannah	98

Haapanala S., Hakola H., Hellén H., Vestenius M., Levula J. and Rinne J.: Is forest management a significant source of monoterpenes into the boreal atmosphere?	102
Hakala J., Sipilä M., Lehtipalo K., Järvinen E., Siivola E., Kulmala M. and Petäjä T.: A new nanoscale ion differential mobility particle sizer	108
Hamed A., Joutsensaari J. and Laaksonen A.: Does ammonia or trimethylamine participate in atmospheric nucleation? Examination based on gas-phase activities	111
Hao L.Q., Kortelainen A., Miettinen P., Jaatinen A., Portin H., Komppula M., Leskinen A., Romakkaniemi S., Smith J.N., Worsnop D.R. and Laaksonen A.: Chemical characterization of atmospheric sub-micron aerosols in a semi-urban aerosol- cloud interaction observation station using high-resolution aerosol mass spectrometer	116
He Q., Boy M., Bäck J., Rinne J., Hakola H., Guenther A., Smolander S. and Kulmala M.: A different model for estimating monoterpene emissions over boreal pine forest	121
Heinonsalo J., Juurola E., Lindén A. and Pumpanen J.: Different root-associated symbiotic ectomycorrhizal fungal species affect carbon allocation of Scots pine	124
Hellén H. and Hakola H.: Online-GC-MS measurements and receptor modelling studies of VOCs in urban air	126

Hirsikko A., Tiitta P., Vakkari V., Manninen H.E., Laakso H., Kulmala M., Mirme A., Mirme S., Mabaso D., Gagné S. and Laakso L.:	
Particle and ion formation and concentrations in the polluted area of Marikana, South- Africa	
.....	131
Hölttä T., Mencuccini M., Sevanto S., Vesala T. and Nikinmaa E.:	
Theory and testing of a new method for the continuous monitoring of phloem osmotic pressure of trees in the field	
.....	135
Hyvärinen A.-P., Neitola K., Asmi E., Brus D. and Lihavainen H.:	
Hygroscopic properties of sub-arctic aerosols: continuous HTDMA measurements from Pallastunturi, Finnish Lapland	
.....	139
Jaatinen A., Romakkaniemi S., Hao L.Q., Kortelainen A., Miettinen P., Brus D., Portin H., Komppula M., Leskinen A., Smith J. N. and Laaksonen A.:	
Cloud droplet activation during the 2010 Puijo cloud experiment	
.....	141
Järvi L., Grimmond C.S.B., Nordbo A., Setälä H., Taka M., Siivola E., Ruth O. and Vesala T.:	
Evaluation of the surface urban energy and water balance scheme (SUEWS) in Helsinki	
.....	144
Joensuu J., Altimir N., Raivonen M., Kolari P., Keronen P., Vesala T., Bäck J., Hari P. and Nikinmaa E.:	
Technical improvements in shoot-level monitoring of O ₃ and NO _x fluxes of Scots pine	
.....	148
Jokinen T., Sipilä M., Petäjä T., Junninen H., Mauldin L., Worsnop D.R. and Kulmala M.:	
Sulfuric acid and sulfuric acid cluster detection with CI-API-TOF	
.....	151

Kabiri K., Havimo M., Hölttä T., Sievänen R. and Hari P.: Can we apply the knowledge of Scots pine ecosystems to Norway spruce?	154
Kajos M. K., Nordin E., Eriksson A., Nilsson P., Hellén H., Roldin P., Carlsson J., Rissler J., Svenningsson B., Swietlicki E., Boghard M., Kulmala M., Ruuskanen T. M. and Pagels J.: SOA formation from gasoline exhaust	156
Keskinen H., Jaatinen A., Joutsensaari J., Romakkaniemi S., Miettinen P., Kortelainen A.-M., Hao L., Smith J. N. and Laaksonen A.: Cloud droplet activation of salt and dust with secondary organic matter: differences between light and dark chemistry	159
Kieloaho A.-J., Héllen H., Hakola H. and Pihlatie M.: Semi-quantitative ambient air measurements of amines in Hyytiälä	164
Kivekäs N., Asmi E., Komppula M., Hyvärinen A.-P., Viisanen Y., Aalto P., Nieminen T., Svenningsson B., Arneth A. and Lihavainen H.: Spatial extent of new particle formation events in Northern Scandinavia	167
Kolari P., Hölttä T., Hari P. and Nikinmaa E.: Productivity of Scots pine under changing climate in Southern Finland and at northern timberline	171
Korhonen J.F.J., Pumpanen J. and Pihlatie M.: Estimating wet nitrogen deposition from bulk deposition measurements	175

Korhonen J.F.J., Pihlatie M., Pumpanen J., Levula J., Hari P., Nikinmaa E., Ilvesniemi H. and Vesala T.:	
Full nitrogen balance of a boreal Scots pine forest	
.....	179
Kortelainen A., Hao L. Q., Jaatinen A., Miettinen P., Smith J. N., Worsnop D. R. and Laaksonen A.:	
Aerosol mass spectrometry based chemical composition measurements of aerosol particles in Finnish boreal forest area at spring-time	
.....	181
Kulmala L., Pumpanen J., Levula J., Rantanen S., Laakso H., Siivola E., Kolari P. and Vesala T.:	
CO ₂ efflux before and after a clear cut and prescribed burning of a boreal spruce forest	
.....	184
Kulmala L., Pumpanen J. and Hari P.:	
The above ground respiration of ground vegetation in boreal pine forests	
.....	188
Kulmala M. et al.:	
General overview: European integrated project on aerosol cloud climate and air quality interactions (EUCAARI) - integrating aerosol research from nano to global scales	
.....	192
Kupiainen O., Ortega I.K., Paasonen P., Loukonen V., Kurtén T., Vehkamäki H. and Kulmala M.:	
Ammonia and amines in atmospheric particle formation	
.....	199
Kurtén T., Ortega I. K., Kupiainen O. and Vehkamäki H.:	
The use of computational chemistry in modeling the chemistry and physics of atmospheric nucleation and nucleation precursor gases	
.....	201

Kyrö E.-M., Virkkula A., Dal Maso M., Parshintsev J., Ruiz-Jimenez J., Manninen H. E., Heinonen P., Forsström L., Riekkola M.-L., Hartonen K. and Kulmala M.: Evidence of Antarctic aerosol formation due to continental biogenic precursors	204
Laakso L., Vakkari V., Laakso H., Kulmala M., Beukes P., Van Zyl P., Pienaar J.J., Tiitta P., Josipovic M., Venter A., Jaars K., Booyens W., Aurela M., Laurila T., Laaksonen A. and Worsnop D.: New continental African supersite for atmospheric observations	208
Lappalainen H.K., Sevanto S., Dal Maso M., Taipale R., Kajos M.K., Kolari P. and Bäck J.: Modelling day-time concentrations of biogenic volatile organic compounds in a boreal forest canopy based a source oriented approach	210
Lauri A., Bäck J., Vesala T., Laaksonen A., Keskinen J., Riekkola M.-L., Hallikainen M., Häme T., Jokiniemi J., Pellikka P., Nikinmaa E., Viisanen Y. and Kulmala M.: Doctoral programme in atmospheric composition and climate change: from molecular processes to global observations and models (ACCC)	213
Lehtipalo K., Franchin A., Schobesberger S., Vanhanen J., Mikkilä J., Nieminen T., Worsnop D., Kulmala M. and the CLOUD collaboration: The use of particle size magnifier for detection of particles smaller than 2 nm at the CLOUD experiment	222
Leppä J., Gagné S., Laakso L., Kulmala M. and Kerminen V.-M.: Influence of asymmetric concentrations of small ions on the aerosol charging state	225
Liao L., Boy M., Mentel T. F., Kleist E., Mogensen D., Kulmala M. and Dal Maso M.: Simulation on the contribution of biogenic VOCs to the new particle formation from Jülich plant chamber measurements	230

Lindén A.S., Heinonsalo J., Oinonen M. and Pumpanen J.: Energy availability increases nitrogen mineralization	232
Lohila A., Minkkinen K., Aurela M., Tuovinen J.-P., Penttilä T. and Laurila T.: A forestry-drained peatland in Southern Finland is a large CO ₂ sink	234
Lönn G., McGrath M.J., Junninen H., Schobesberger S., Franchin A., Petäjä T., Worsnop D.R. and Kulmala M.: Chemical composition and correlation of ions in a marine atmosphere	237
Loukonen V., McGrath M. J., Väänänen R., Karinkanta R., Viisanen K., Dal Maso M. and Vehkamäki H.: sPARCK - simple program for atmospherically relevant cluster kinetics	241
Malila J., Lehtinen K.E.J., Napari I., McGraw R. and Laaksonen A.: The first nucleation theorem with coagulation scavenging of precritical clusters	243
Mammarella I., Peltola O., Nordbo A., Rannik Ü. and Vesala T.: EddyUH – an advanced software for eddy covariance flux calculations	247
Manninen H.E., Hirsikko A., Nieminen T., Yli-Juuti T., Asmi E., Kontkanen J., Franchin A., Gagné S., Lehtipalo K., Kerminen V.-M., Petäjä T. and Kulmala M.: Direct detection of atmospheric particle formation using ion spectrometers	253
Merikanto J., Carslaw K., Korhonen H. and Kulmala M.: Historical trends in global and regional CCN concentrations from 1850 to 2000	256

Miettinen P., Tiitta P., Jaatinen A., Kortelainen A., Hao L., Smith J. and Laaksonen A.: Aerosol size resolved vertical flux measurements	259
Mikkonen S., Romakkaniemi S., Smith J. N., Korhonen H., Petäjä T., Plass-Duelmer C., Boy M., McMurry P. H., Lehtinen K.E.J., Joutsensaari J., Hamed A., Mauldin R.L., Birmili W., Arnold F., Kulmala M. and Laaksonen A.: Statistical proxy for sulphuric acid concentration	261
Mogensen D., Smolander S., Nolscher A., Williams J., Sinha V., Zhou L., Guenther A., Nieminen T., Kajos M., Rinne J., Sogachev A., Kulmala M. and Boy M.: OH-reactivity and concentration in summertime boreal forest	265
Mølgaard B., Hussein T., Corander J. and Hämeri K.: Bayesian forecast model for size-fractionated urban particle number concentrations	270
Napari I., Julin J. and Vehkamäki H.: Performance of some nucleation theories with a non-sharp droplet-vapor interface	272
Neitola K., Brus D., Sipilä M., Jokinen T., Paasonen P. and Lihavainen H.: Amines inhibit the particle growth: H ₂ SO ₄ -H ₂ O-amine flow tube experiment	276
Nieminen T., Junninen H., Schobesberger S., Lönn G., Ehn M., Petäjä T., Worsnop D. R. and Kulmala M.: Physical and chemical characteristics of air ions during autumn 2010 in Hyytiälä, Finland	279
Nordbo A., Järvi L., Haapanala S. and Vesala T.: Multisite analysis of urban flux measurements in Helsinki	281

Nyman M., Laurila T., Kulmala L., Juurola E., Sorvari S., Haapanala S., Keronen P., Kolari P., Mammarella I., Komppula M., Lehtinen K., Juuti S., Aalto T., Aurela M., Laakso L., Viisanen Y. and Vesala T.:	
Ecosystem and atmospheric measurements in ICOS-Finland	
.....	287
Olascoaga B., Porcar-Castell A. and Nikinmaa E.:	
Influence of temperature in the recovery from photodamage in <i>Pinus sylvestris</i> L.	
.....	290
Ortega I.K., Kurtén T., Kupiainen O., Vehkamäki H. and Kulmala M.:	
Using quantum mechanics to improve our knowledge about climate change	
.....	294
Paasonen P., Kajos M. K., Rantala P., Junninen H., Petäjä T. and Kulmala M.:	
Particle growth rate from nucleation mode to cloud condensation nuclei in boreal forest	
.....	297
Paramonov M., Petäjä T., Aalto P.P., Kerminen V.-M. and Kulmala M.:	
The analysis of size-segregated cloud condensation nuclei counter (CCNC) data from SMEAR II and its implications for aerosol-cloud relations	
.....	300
Patokoski J., Kajos M. K., Ruuskanen T. M., Schallhart S., Rantala P. and Rinne J.:	
Total OH reactivity measurements in boreal forest	
.....	302
Peltola O., Mammarella I., Haapanala S. and Vesala T.:	
Intercomparison of four methane gas analysers for eddy covariance flux measurements	
.....	305
Petäjä T., Sipilä M., Lehtipalo K., Manninen H. E., Junninen H., Ruuskanen T., Ehn M., Vanhanen J., Vehkamäki H., Worsnop D. R. and Kulmala M.:	
An overview of recent instrument development at University of Helsinki	
.....	309

Pihlatie M., Riis Christiansen J., Aaltonen H., Korhonen J., Nordbo A., Rasilo T., Benanti G., Giebels M., Helmy M., Hirvensalo J., Jones S., Juszczyk R., Klefoth R., Lobo Do Vale R., Rosa A.P., Shreiber P., Serga D., Vicca S., Wolf B. and Pumpanen J.: Comparison of static chambers to measure CH ₄ fluxes from soils	315
Porcar-Castell A., Garcia-Plazaola I., Nichol C., Kolari P., Olascoaga B., Esteban R. and Nikinmaa E.: Physiological factors uncoupling the photochemical reflectance index (PRI) from the photosynthetic light use efficiency (LUE)	318
Prisle N. L., Topping D., Romakkaniemi S., Dal Maso M., McFiggans G. and Kokkola H.: Importance of surfactant representations for predicted cloud droplet numbers in global scale simulations	321
Pulliaainen J., Kyrö E. and Viisanen Y.: Satellite CAL-VAL activities and facilities of FMI at Sodankylä	327
Pumpanen J., Heinonsalo J., Rasilo T. and Ilvesniemi H.: Effect of increased soil temperature on CO ₂ exchange and net biomass accumulation in Norway spruce, Scots pine and silver birch; preliminary results of a microcosm experiment	329
Rantala P., Kajos M. K., Patokoski J., Ruuskanen T. M., Schallhart S., Taipale R. and Rinne J.: Ecosystem scale VOC emissions measured by surface layer gradient technique	331
Rasilo T., Ojala A., Starr M. and Pumpanen J.: DOC concentration and quality in the riparian zone of a forested boreal catchment	334

Reissell A., De Noblet–Ducoudré N., Kabat P. and Yakir D.: Land–use–induced land–cover changes and functioning of the earth system	339
Riekkola M.-L., Hartonen K., Parshintsev J., Laitinen T., Ruiz-Jimenez J., Petäjä T. and Kulmala M.: Recent advances in sampling and in chemical analysis of atmospheric aerosols	343
Rinne J., Haapanala S., Peltola O., Pihlatie M., Aurela M., Hatakka J., Schurig C., Mammarella I., Laurila T., Tuittila E.-S. and Vesala T.: Long term measurements of methane emission from a boreal fen by eddy covariance method	353
Rinne J., Ruuskanen T.M., Taipale R., Kajos M.K., Patokoski J., Ghirardo A., Schnitzler J.-P., Aalto J., Aaltonen H., Hakola H., Bäck J. and Boy M.: Ecosystem scale VOC emission from Scots pine forest	357
Romakkaniemi S., Keskinen H., Jaatinen A., Smith J.N., Joutsensaari J. and Laaksonen A.: Adsorption activation of insoluble aerosol particles	360
Ruuskanen T. M., Müller M., Schnitzhofer R., Karl T., Graus M., Bamberger I., Hörtnagl L., Wohlfahrt G. and Hansel A.: Emission and deposition of VOC above grassland, eddy covariance fluxes with PTR- TOF	363
Ruusuvuori K., Kurtén T., McGrath M. J., Ortega I.K., Vehkamäki H. and Kulmala M.: Stability of clusters containing water, pyridine and ammonia	366

Schallhart S., Ruuskanen T. M., Kajos M. K., Junninen H., Rinne J. and Kulmala M.: VOC flux and concentration measurements with PTR-TOF in Hyytiälä	368
Schobesberger S., Franchin A., Junninen H., Ehn M., Lehtipalo K., Gagné S., Nieminen T., Petäjä T., Kulmala M., Worsnop D.R. and the CLOUD collaboration: Measurements of ions and ion clusters by mass spectrometry during sulfuric acid-induced nucleation in the CLOUD chamber at CERN	370
Sundström A.-M., Kolmonen P., Sogacheva L., Rodriguez E., Hannukainen M., Atlaskina K. and De Leeuw G.: Aerosol optical properties over China observed with satellite remote sensing	373
Tomasic M., Hölttä T., Getzieh R., Brovkin V., Vesala T., Smolander S., Kleinen T., Reick C., Raivonen M., Susiluoto J. and Valdebenito A.: Methane emissions from boreal wetlands: a modelling study with the JSBACH model	376
Tu M. K., Hellsten A., Markkanen T. and Vesala T.: Large eddy simulation model for studying atmospheric turbulence	377
Tupek B., Minkkinen K., Kolari P., Starr M., Alm J., Vesala T., Pumpanen J., Pulkkinen M., Laine J. and Nikinmaa E.: CO ₂ anomalies along forest and mire hydrological ecotone	383
Vaattovaara P., Cravigan L., Talbot N., Olivares G., Law C., Harvey M., Ristovski Z. and Laaksonen A.: Surface southern pacific ocean SOA	388

Vakkari V., Laakso H., Kulmala M., Mabaso D. and Laakso L.: Sub-micron aerosol particle size distributions in clean and polluted Southern African savannah	391
Vesala T., Nordbo A., Haapanala S., Mammarella I., Pumpanen J., Eugster W., Huotari J. and Ojala A.: On eddy covariance flux measurements over lakes	395
Vestenius M., Anttila P., Hansson K., Hellèn H., Brorström-Lunden E. and Hakola H.: Sources of persistent organic pollutants in atmosphere at Pallas, Finland	399
Virkkula A., Levula J., Pohja T., De Leeuw G., Schultz D., Clements C., Kukkonen J., Nikmo J., Sofiev M., Pirjola L., Kulmala L., Pumpanen J., Vesala T., Kieloaho A.-J., Aaltonen H., Pihlatie M., Häkkinen S., Manninen H.E., Junninen H., Nieminen T. and Kulmala M.: Prescribed forest burning experiment in June 2009	402
Virkkula A., Makkonen U., Mäntykenttä J. and Hakola H.: Gas and aerosol measurements with MARGA in urban and rural environments in Finland	408
Vuollekoski H., Korhonen H., Zhou L., Lehtinen K. E. J., Kerminen V.-M., Boy M. and Kulmala M.: UHMAEMO – University of Helsinki multicomponent aerosol module: a revised and modularized version	414
Väänänen R., Paananen K., Petäjä T., Virkkula A., Aalto P.P., Pohja T., Kortetjärvi L. and Kulmala M.: Airborne aerosol measurements over Southern Finland at October 2010 and April 2011	417

Yli-Juuti T., Zardini A.A., Kulmala M., Bilde M., Pagels J., Eriksson A., Swietlicki E., Worsnop D. and Riipinen I.:

Organic acid – inorganic salt aqueous solution droplets: a study on equilibrium vapour pressure of succinic acid

..... 421

Zhou L., Boy M., Vuollekoski H., Watcharapaskorn C., Mogensen D., Smolander S., Sogachev A. and Kulmala M.:

The first long-term model study of particle formation and growth with detailed chemistry and aerosol dynamics in and above boreal forest

..... 426

Äijälä M., Junninen H., Ehn M., Petäjä T., Aalto P. P., Kulmala M. and Worsnop D. R.:

Aerosol chemical composition measurements at a boreal forest site in Southern Finland during different seasons

..... 429

FINNISH CoE IN PHYSICS, CHEMISTRY, BIOLOGY AND METEOROLOGY OF ATMOSPHERIC COMPOSITION AND CLIMATE CHANGE, RESULTS IN 2010-2011

MARKKU KULMALA¹, JAANA BÄCK^{1,2}, ARI LAAKSONEN^{3,4}, EERO NIKINMAA², MARJA-LIISA RIEKKOLA⁵, TIMO VESALA¹, YRJÖ VIISANEN³, MICHAEL BOY¹, MIIKKA DAL MASO¹, HANNELE HAKOLA³, PERTTI HARI², KARI HARTONEN⁵, VELI-MATTI KERMINEN³, ANTTI LAURI¹, TUOMAS LAURILA³, HEIKKI LIHAVAINEN³, TUUKKA PETÄJÄ¹, JANNE RINNE¹, SAMI ROMAkkANIEMI⁴, SANNA SORVARI^{1,3}, HANNA VEHKAMÄKI¹ + the FCoE TEAM

¹Department of Physics, University of Helsinki, Finland

²Department of Forest Sciences, University of Helsinki, Finland

³Finnish Meteorological Institute, Finland

⁴Department of Physics, University of Eastern Finland, Kuopio Unit, Finland

⁵Department of Chemistry, University of Helsinki, Finland

BACKGROUND

Our main objective is to contribute to the reduction of scientific uncertainties concerning global climate change issues, particularly those related to aerosols and clouds. We aim at creating a deep understanding on the dynamics of aerosol particles and ion and neutral clusters in the lower atmosphere, with the emphasis of biogenic formation mechanisms and their linkage to biosphere-atmosphere interaction processes, biogeochemical cycles and trace gases. The relevance and usage of the results in the context of global scale modelling, and the development and utilisation of the newest measurement techniques are addressed. The cores of activities are a) in continuous measurements and database of atmospheric and ecological mass fluxes and aerosol precursors and CO₂/aerosol/trace gas interactions in SMEAR field stations and GAW station and b) in focused experiments and modelling to understand the observed patterns.

In order to be able to meet our objectives, and to answer our research questions, we are committed to supra-disciplinary research with a high level of technological and scientific innovation. Understanding the complex, non-linear system requires a diverse range of scientific and technological expertise in the areas of chemistry, physics, biology, and meteorology, and involves laboratory studies, ground, ship, and airborne field studies, satellite remote-sensing and numerical modelling studies ranging from the molecular *ab initio* level to the global scale Earth system models. Our research approach covers all those observational, experimental and theoretical aspects. Actually the amount and representativeness of field data collected within the recent efforts like EUCAARI (European Integrated project on Aerosol Cloud Climate and Air Quality Interactions; Kulmala et al., 2009) will allow us to test the overall performance of different hypotheses and parameterize obtained process understanding for global models.

METHODS AND ACTIVITIES

The Centre of Excellence is a core in a large variety of activities (see Figure 1). We act as an active partner in the climate change research community in national, Baltic/Nordic, European and Global level. We participate in different projects, and are responsible for organization or leadership of several international projects. E.g. in 2010, two Nordic centers of excellence were nominated, namely CRAICC and DEFROST, where members of our FCoE are active partners. The unique performance of our FCoE can be seen e.g. with the fact that our FCoE is part of international aerosol, carbon, nitrogen, atmospheric chemistry etc. projects although the research communities typically are separate ones.

The backbone of our research activities is our efficient infrastructure, namely the network of field stations like SMEARs and GAW stations. The data obtained in our comprehensive continuous measurements over 15 years can be used to make significant conceptual development, and links the different disciplines in a unique manner.

In practice the research under the CoE is performed under five specific work packages:

- WP1) Formation and growth of atmospheric aerosol particles
- WP2) Ion and neutral clusters
- WP3) Aerosol-cloud interactions
- WP4) Biosphere-atmosphere interactions
- WP5) Earth system behavior

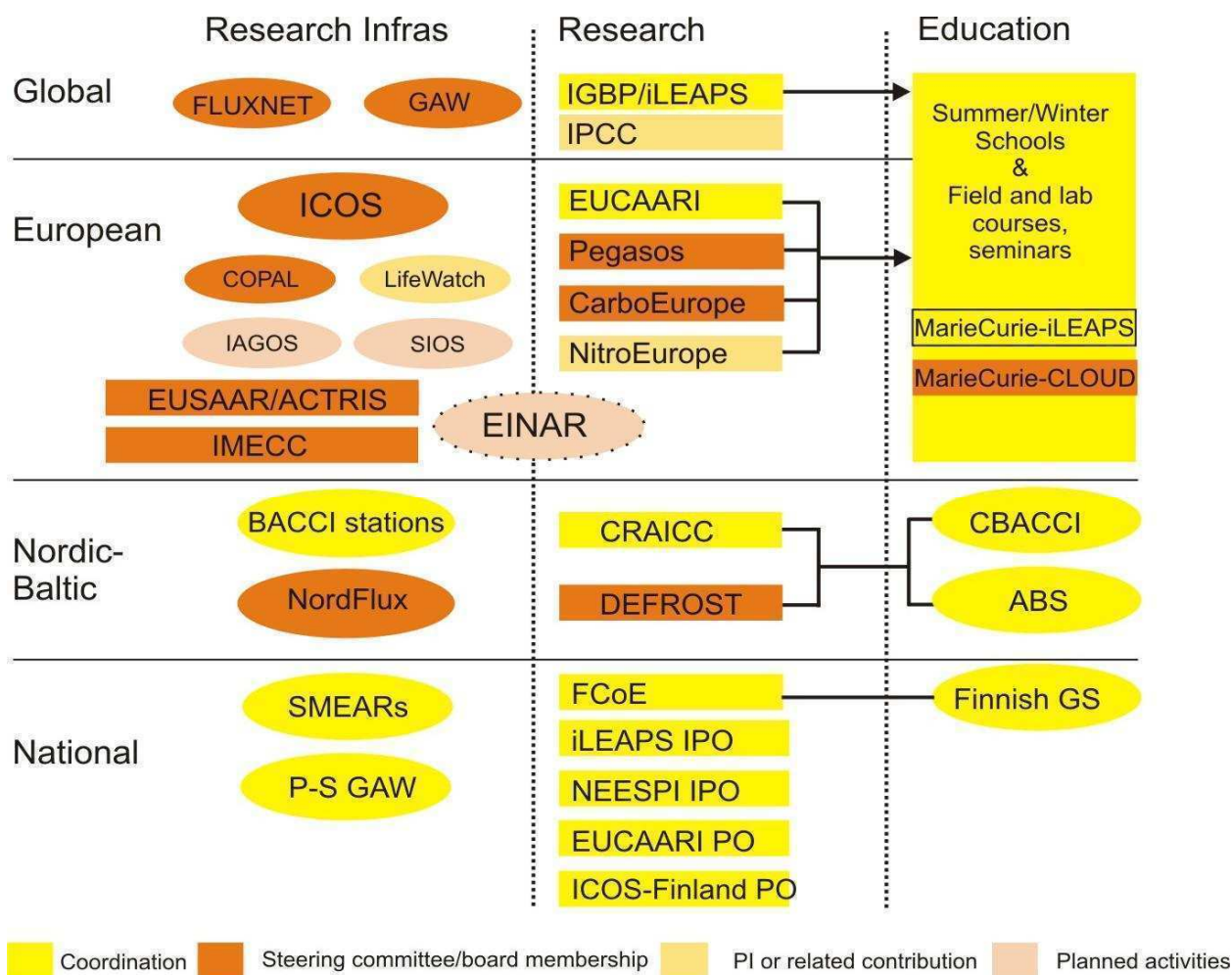


Figure 1. Scheme of the Network of FCoE activities in education, research and research infrastructures

Abbreviations:

ABS=Atmosphere-Biosphere Studies; ACTRIS = European aerosol and atmospheric chemistry infrastructure; BACCI= Biosphere-Aerosol-Cloud-Climate Interactions; CBACCI=Carbon- Biosphere-Atmosphere-Cloud-Climate- Interactions; CLOUD = Cosmics Leaving Outdoor Droplets; COPAL= COMMunity heavy-PAYload Long endurance Instrumented Aircraft for Tropospheric Research in Environmental and Geo-Sciences; CRAICC= Cryosphere-Atmosphere Interactions in a Changing Arctic Climate; DEFROST = A changing cryosphere – depicting ecosystem-climate feedbacks as affected by permafrost, snow and ice; EINAR= European Institute of Atmospheric Sciences and Earth System Research; EUCAARI= European Integrated Project on Aerosol-Cloud-Climate-Air Quality Interactions; EUSAAR= European Supersites for Atmospheric Aerosol Research;

EXPEER = Distributed Infrastructure for EXPERimentation in Ecosystem Research; FCoE=Finnish Centre of Excellence in Physics, Chemistry, Biology and Meteorology of Atmospheric Composition and Climate Change; FLUXNET = Integrated CO₂ flux measurement network; GHGEurope = Greenhouse gas management in European land use system (<http://www.ghg-europe.eu/>); GAW = Global Atmospheric Watch; GS= Finnish graduate school; IAGOS= In-service Aircraft for Global Observing System; ICOS =Integrated Carbon Observation System; IGBP= International Geosphere-Biosphere Program; iLEAPS=integrated Land Ecosystem Atmosphere Processes Study; IMECC= Infrastructure for Measurements of the European Carbon Cycle; IPCC = Intergovernmental Panel for Climate Change; LifeWatch = e-science and technology infrastructure for biodiversity data and observatories; NordFlux = A Nordic research network for greenhouse gas exchange from northern ecosystems; P-S GAW= Pallas- Sodankylä Global Atmosphere Watch Station; PEGASOS= Pan-European Gas-Aerosols-climate interaction Study; SIOS= Svalbard Integrated Arctic Earth Observing System; SMEAR=Station for Measuring Ecosystem-Atmosphere Relations

HIGHLIGHTS OF RECENT RESULTS

During the past year we have published one paper in both in Nature and in Science as well as one in Nature Geoscience. The total number of all peer reviewed publications by members of the FCoE in 2010-11 (until May 15th) is more than 160. Altogether over 20 MSc's and 19 PhD's finalized their theses within the FCoE during 2010-2011 (until May 15th).

Our most important recent results are specified in following highlights. The relations of the highlights to certain WPs are shown in brackets after the description of the highlight. The highlights of WPs 1, 2 and 4 are pronounced. WP3 has several highlights and some more are coming. The highlights for WP5 (global modeling) are anticipated during the last two years of the present FCoE period.

We have focused on instrument development (e.g. Junninen et al., 2010, Vanhanen et al., 2010). The instrument development presented in these two papers brings the aerosol particle measurements and atmospheric mass spectrometric methods together. In the future these tools will enable us to expand the research to other fields. **WP1 and WP2.**

We have used both field measurements and atmosphere-plant simulation results in order to elucidate the specific roles of plant emissions on the particle formation. Chamber simulations at atmospheric concentrations have clearly shown that particle formation rate is directly connected to emission strength of terpenoid species (Dal Maso et al., 2011); analysis of field data has also shown that atmospheric nucleation is a kinetic type process, in which organic vapours are involved (Paasonen et al., 2010). **WP1, WP2, WP4**

Field data from Antarctica has brought evidence of strong biogenic organics-induced new particle formation plumes acting as a major particle source. (Kyrö et al., 2011). **WP1**

Sawmill plumes of monoterpenes were found to act as a strong particle source, with similar particle population characteristics than naturally produced biogenic aerosol (Liao et al., 2010). **WP1, WP4**

Recently Massolini et al. (2010) showed the importance of atmospheric oxidation and ageing to aerosol hygroscopicity. In the laboratory we showed that the organic aerosol will be more prone to water vapor condensation after aging. This will have large effects in the aerosol-cloud interactions and in particular in determining the human influence on the climate change. **WP1 and WP3.**

A large collaborative effort (Kerminen et al., 2010) highlighted the phenomenological results obtained during the EUCAARI campaign. We were able to connect detailed studies into a global framework both in terms of observations and in modelling perspectives. This work continues, but the EUCAARI project will be used as a benchmark appraising the results obtained in the future collaborative research. **WP1, WP2 and WP5.**

A review of the atmospheric air ion concentrations enabled us to constrain the observed ion concentrations and reconcile them with observations of ion production rates; the atmospheric range of ion-induced aerosol formation was also mapped (Hirsikko et al., 2010), and the ambient ion-induced nucleation rates parameterized (Nieminen et al., 2011). **WP1 and WP2**

Laboratory made laser aerosol mass spectrometer was utilized in the measurements of atmospheric particles (Laitinen et al., 2011). The two main findings from the laser AMS samples were black carbon and the possible presence of amines. The black carbon was seen as a distinct ion plume in the spectrum produced already by the IR desorption laser at mass range about 150-400 amu. Two most abundant amines were found at 143 amu and 185 amu, and they are tentatively assigned to alkyl-substituted amines. Here, some amines were found in nearly all samples, but relatively highest concentrations were at particle sizes from 10 to 25 nm and on the samples when one or more new particle formation events occurred. **WP1**

Particle-into-liquid sampler was on-line coupled with solid-phase extraction-liquid chromatography-mass spectrometry for the first time (Parshintsev et al., 2010). This combination made possible to perform the whole analysis of ambient aerosols in a closed system, which minimized artefacts and shortened the analysis time. **WP1**

The differential mobility analyzer (DMA) was used for size separation of aerosols before filter sampling with Teflon or quartz. Zero sample collection system was built in order to detect positive artefacts due to adsorption of gas-phase compounds onto filter media. It was noticed that both filter media adsorb gas-phase compounds extremely well and thus simultaneous zero sample collection must be done prior filter sampling every time the DMA is used (Parshintsev et al., 2011). **WP1**

Comprehensive two-dimensional gas chromatography-mass spectrometry (GC×GC-TOF-MS) was utilized in the analysis of aerosol samples size separated with DMA. Due to superior separation efficiency and sensitivity, it was concluded to be essential for this kind of samples, where concentrations are small and the number of compounds is very high. In addition, data processing was built to handle the data produced with the GC×GC-TOF-MS. This system made the new approach for the aerosol composition research possible. In some applications the detailed information of each compound present in aerosols is not needed, whereas the distribution of compounds by the groups is of interest. Thus, comparison of samples can be done in a more comprehensive way, before the detailed examination, if needed (Ruiz-Jimenez et al., 2011). **WP1**

We have underlined the importance of sulfuric acid in atmospheric nucleation. However, the participation of e.g. amines and organics in the early growth is still not ruled out (Sipilä et al., 2010). **WP2.**

Homogeneous nucleation rates of sulfuric acid and water were measured by using a flow tube technique. The nucleated particle counts were measured with particle size magnifier (PSM) and an ultrafine condensation particle counter (UCPC) TSI model 3025A. The gas phase sulfuric acid concentration in this study was measured with the chemical ionization mass spectrometer (CIMS). The wall losses of sulfuric acid were estimated from measured concentration profiles along the flow tube. The initial concentrations of sulfuric acid estimated from loss measurements ranged from 10^8 to $3 \cdot 10^9$ molecules cm^{-3} . The nucleation rates obtained in this study cover about three orders of magnitude from 10^{-1} to 10^2 with the UCPC and from 10^1 to 10^4 with the PSM. The nucleation rates show good agreement with the latest atmospheric nucleation data. To the best of our knowledge, this is the first experimental work providing temperature dependent nucleation rate measurements using a high efficiency particle counter with a cut-off-size of 1.5 nm together with direct measurements of gas phase sulfuric acid concentration. **WP2**

The most detailed molecular-resolution experimental data in nucleation studies are cluster distributions, which are steady-state results of the inherently dynamic cluster birth-death processes. Computational studies typically yield evaporation rates, which need to be converted into cluster distributions using kinetic models. We have developed a fully time-dependent multicomponent cluster dynamics code; ACDC (Atmospheric Clusters Dynamics Code). A parallel version (Loukonen et al., 2011) capable of treating also larger cluster size is under development. Using ACDC, we have shown that the commonly used form of the first nucleation theorem fails in the presence of pre-critical stable clusters, manifested as free energy minima (Vehkamäki et al., 2011). Such minima likely exist in the atmospherically relevant sulfuric acid - amine system (Kupiainen et al., 2011; Kurtén et al., 2011a). In collaboration with experimental researchers, we have investigated the details of cluster charging and detection in instruments. We have shown that the experimentally observed (Petäjä et al., 2011) strongly bound neutral sulfuric acid dimers

very likely contain a base molecule in addition to the two acids, but that this base evaporates after the charging, and is thus not detected (Petäjä et al. 2011; Kurtén et al., 2011a; 2011b). **WP2**

We proposed a simple and computationally light representation of surface active organics to be used to parameterise CCN activation (Prisle et al., 2011). **WP3**

We present a model study (Romakkaniemi et al 2011) demonstrating that surface partitioning of volatile surfactants enhances their uptake by submicron liquid droplets. Our model simulations show an order of magnitude higher uptake of methylglyoxal in aqueous aerosols of cloud condensation nuclei sizes (less than 200 nm in radius) when surface partitioning is taken into account, compared to when surface partitioning is neglected. As a consequence, the production of SOA through the aqueous phase chemical processing of methylglyoxal is also enhanced, but to a lesser degree, because condensation of the hydroxyl radical from gas phase limits the production. **WP3**

The new developed model SOSA (Boy et al., 2011) was finalized, evaluated and used to estimate the vertical profiles of possible organic precursors in the atmospheric nucleation process. Lauros and co-workers (Lauros et al., 2010) confirmed this results by comparing measured and modelled vertical profiles of new formed particles inside and above the mixed layer with the model MALTE. The hydroxyl-radical - as the most important precursor for sulphuric acid in the atmosphere - was investigated with SOSA, and in comparison with the measured OH-reactivity, a missing unexplained sink term by more than 50 % was defined during two campaigns at the SMEAR II in Hyytiälä (Mogensen et al., 2011). **WP1 and WP4**

We investigated the biogenic SOA particles formed from oxidation products of VOCs in plant chamber experiments and in boreal forests within a few hours after atmospheric nucleation events (Virtanen et al 2010). On the basis of observed particle bouncing in an aerosol impactor and of electron microscopy we conclude that biogenic SOA particles can adopt an amorphous solid - most probably glassy - state. This amorphous solid state should provoke a rethinking of SOA processes because it may influence the partitioning of semi-volatile compounds, reduce the rate of heterogeneous chemical reactions, affect the particles' ability to accommodate water and act as cloud condensation or ice nuclei, and change the atmospheric lifetime of the particles. **WP1 and WP4**

Hao et al. (2011) presented smog chamber laboratory work, focusing on SOA formation via oxidation of the emissions of two dominant tree species from boreal forest area, Scots pine (*Pinus sylvestris* L.) and Norway spruce (*Picea abies*), by hydroxyl radical (OH) and ozone (O₃). Condensable products from OH-dominated chemistry showed a higher volatility than those from O₃-initiated systems during aerosol growth stage. Particulate phase products became less volatile via aging process which continued after input gas-phase oxidants had been completely consumed. **WP1 and WP4**

Leaf gas exchange and tree growth were linked to water and assimilate transport. The approach explained well the observed behavior and provides thus a direct connection between leaf control of water vapor and CO₂ fluxes, soil moisture conditions and tree structure (Nikinmaa et al 2011, Hölttä et al, 2010). Formulation that combined embolisation avoidance and maximal water transport per invested carbon in stem was able to explain observed structural features of tree stems (Hölttä et al. 2011). Diurnal variation in stem diameter was connected to carbohydrate transport in stems providing a new potential measurement (Hölttä et al 2011) of the observed rather rapid transport of photosynthates to roots and subsequent release back to atmosphere (Heinonsalo et al 2010, Vargas et al 2010). The sugar input to soil accelerates decomposition of old carbon and influences plant nitrogen uptake (Linden et al 2011). **WP4**

We have shown a clear seasonal pattern in the carbohydrate and VOC concentrations and monoterpene synthase enzymes in Scots pine needles, suggesting strong linkages to acclimation and winter-summer transitions. We also developed continuous fluorescence method for observation of these transitions (Porcar-Castell et al. 2011). We showed that growing shoots are proportionally a dominating source of pine stand monoterpene emissions (Aalto et al manuscript) and that a chemotype-specific emission spectrum within a homogeneous forest stand can be distinguished, highlighting the need for more detailed description of vegetation structure and dynamics for regional VOC emission estimates (Bäck et al 2011). Pine forest floor emits several VOCs both in summer and in wintertime, monoterpene fluxes being clearly the highest with clear diurnal and seasonal pattern, and early summer and late fall (litter fall period) are

the seasons of highest fluxes (Aaltonen et al 2011). Laboratory experiments showed distinct VOC emission patterns in various soil fungi (Bäck et al 2010). Variation in soil temperature influenced the composition of archeal populations in soil with possible consequences on methane emissions with warming climate (Bomberg et al 2011). **WP4**

We have taken into use an on-line ion-chromatograph MARGA and successfully measured inorganic gases and aerosols in urban and rural air. The most important new information that can be obtained from this instrument is the concentration of the trace gases NH_3 , HNO_3 , HNO_2 , and HCl at a 1-hour time resolution so that for instance diurnal cycles can be observed. A very clear diurnal cycle of NH_3 , HONO and HNO_3 was observed, especially in July. The clear diurnal cycles of ammonia and nitric acid suggest that they may at least partly be due to evaporation of ammonium nitrate particles in the hottest time of the warm July 2010 and condensation on particles at the cooler nighttimes. Recently we also have set up a system measuring VOC emission rates from a Norway spruce twig, and this will greatly improve our ability to upscale emissions from individual tree and branch scale to stand scale and beyond. **WP1 and WP4**

We have shown the monoterpene emission from boreal forest ecosystems to originate via two emission pathways: First, directly from monoterpene synthesis, and second, as evaporation from large plant internal storage pools (Ghirardo et al., 2010). Measurements during HUMPPA-COPEC-2010 campaign showed that a large fraction of total OH reactivity is not accounted for, indicating the existence of unmeasured reactive biogenic compounds (Sinha et al., 2010). **WP4**

Ecosystem scale methane emission measurements by eddy covariance method have been conducted continuously at Siikaneva since 2005 (e.g. Rinne et al., 2007). This is one of the longest continuous methane emission time series. The methane emission is an important part of the carbon balance of the fen ecosystem as around 20 % of carbon sequestered as carbon dioxide is re-released as methane. Even though the emission is mostly correlated with temperature, the measurements have shown that simple temperature and water table relations cannot describe the emission dynamics. **WP4**

The long-term surface-atmosphere exchange measurements by meteorological techniques have been continued in forest, wetland, lake and urban sites. The data can be utilized in understanding of feedback processes related to the biosphere. Globally, the various feedbacks tend to warm the atmosphere and substantially reduce and potentially even eliminate the cooling effect owing to carbon dioxide fertilization of the terrestrial biota (Arneeth et al., 2010). The first determination of the energy balance for a lake based on the eddy-covariance technique revealed the similarity with forest ecosystems although the dynamics of the energy balance components differ drastically (Nordbo et al., 2011). To understand the effect of the forest thinning to aerosol particle deposition requires multi-layer (canopy), size-resolved (particles) and second-order (turbulence models (Katul et al., 2011)). The first, preliminary results on global methane emission estimates by plant-mediated transport have been achieved by JSBACH model. The instalment of absolute greenhouse gas concentration measurements have started at SMEAR II station and the existing tower was extended to 127 m. **WP4 and WP5**

We estimated the magnitude of the radiative forcing (RF) due to changes in albedo following the forestation of peatlands, and calculated the net RF by taking into account changes in both albedo and greenhouse gas (GHG) fluxes during one forest rotation (Lohila et al 2010). The magnitude of the albedo-induced RF was similar to that caused by the carbon sequestration of the growing trees. At three site cases out of four the drainage induced a cooling or negative RF, the tendency for cooling being higher at sites with a higher nutrient level. Our results show that the decreasing albedo resulting from peatland forestation contributes significantly to the RF, balancing out or even exceeding the cooling effect due to the changing GHG fluxes. **WP4 and WP5**

Forestry-drainage of peatlands is one of the most important land-use practices affecting the greenhouse gas balance of the forestry sector in Finland (Lohila et al 2011). The carbon balances of these forests are very uncertain because of methodological difficulties. We measured, using the micrometeorological EC method, the net ecosystem exchange of CO_2 in a nutrient poor forestry-drained peatland in southern Finland. The measurements show that the studied drained peatland forest is a large sink of CO_2 mainly due

to (1) the low nutrient status of the site, which decreases the peat decomposition rate and increases the allocation of C into the roots and (2) actively photosynthesising and dense ground vegetation. **WP4 and WP5**

Nitrous oxide (N₂O) fluxes were measured by automated and manual chambers in a sedge fen in northern Finland. In addition, nitrogen deposition and lateral flows were measured. Measurements showed that northern mires are characterized by high organic nitrogen pools and lateral aquatic flows. Emission of N₂O was low but we estimated that N₂ production was significant based on measured N₂O emissions and soil concentrations (Lohila et al 2010, Drewer et al 2010). **WP4**

We analyzed the relationships between net ecosystem exchange of carbon (NEE) and climate factors using the eddy covariance method at 125 unique sites in various ecosystems over six continents with a total of 559 site-years (Yi et al 2010). We found that NEE observed at eddy covariance sites is (1) a strong function of mean annual temperature at mid- and high-latitudes, (2) a strong function of dryness at mid- and low-latitudes, and (3) a function of both temperature and dryness around the mid-latitudinal belt (45°N). **WP4 and WP5**

RECENT NATURE AND SCIENCE PAPERS

1. Sipilä, M., Berndt, T., Petäjä, T., Brus, D., Vanhanen, J., Stratmann, F., Patokoski, J., Mauldin III, R.L., Hyvärinen, A.-P., Lihavainen, H. and Kulmala, M. (2010) The role of sulfuric acid in atmospheric nucleation, *Science*, 327, 1243-1246.
2. Virtanen, A, Joutsensaari, J, Koop, T, Kannosto, J, Yli-Pirilä, P, Leskinen, J, Mäkelä, JM, Holopainen, JK, Pöschl, U, Kulmala, M, Worsnop, DR, Laaksonen, A (2010) An amorphous solid state of biogenic secondary organic aerosol particles, *Nature*, 467, 824-827.
3. Arneth, A, Harrison, SP, Zaehle, S, Tsigaridis, K, Menon, S, Bartlein, PJ, Feichter, J, Korhola, A, Kulmala, M, O'Donnell, D, Schurgers, G, Sorvari, S, Vesala, T (2010) Terrestrial biogeochemical feedbacks in the climate system', *Nature Geoscience*, 3, 525-532.

OTHER REFERENCES

Aaltonen H., Pumpanen J., Pihlatie M., Hakola H., Hellén H., Kulmala L., Vesala T. and Bäck J. (2011) Boreal pine forest floor biogenic volatile organic compound emissions peak in early summer and autumn. *Agricultural and Forest Meteorology* 151: 682-691

Arneth, A., S.P. Harrison, S. Zaehle, K. Tsigaridis, S. Menon, P.J. Bartlein, J. Feichter, A. Korhola, M. Kulmala, D. O'Donnell, G. Schurgers, S. Sorvari and T. Vesala (2010) Terrestrial biogeochemical feedbacks in the climate system. *Nature Geoscience* 3, 525-532.

Bomberg et al. (2011) Archaeal communities in boreal forest tree rhizospheres respond to changing soil temperatures. *Microbial Ecology*. DOI: 10.1007/s00248-011-9837-4.

Boy, M., Sogachev, A., Lauros, J., Zhou, L., Guenther, A. and Smolander, S. (2011) SOSA - a new model to simulate the concentrations of organic vapours and sulphuric acid inside the ABL - Part I: Model description and initial evaluation, *Atmos. Chem. Phys.* 11, 43-51.

Brus, D., Neitola, K., Petäjä, T., Vanhanen, J., Hyvärinen, A.-P., Sipilä, M., Paasonen, P., Lihavainen, H., and Kulmala, M. (2010) Homogenous nucleation of sulfuric acid and water at atmospherically relevant conditions, *Atmos. Chem. Phys. Discuss.*, 10, 25959-25989, doi:10.5194/acpd-10-25959-2010.

Bäck J., Aalto, J., Henriksson M., Hakola H., He Q. and Boy M. (2011) Chemodiversity in terpene emissions at a boreal Scots pine stand. MS, *submitted to Biogeosciences Discussions*.

- Bäck J., Aaltonen H., Hellén H., Kajos M., Patokoski J., Taipale R., Pumpanen J. and Heinonsalo J. (2010) Variable emissions of microbial volatile organic compounds (MVOCs) from root-associated fungi isolated from Scots pine. *Atmospheric Environment* 44: 3651-3659.
- Dal Maso, M., Mentel, T.F., Kiendler-Scharr, A., Kleist, E., Tillmann, R., Sipilä, M., Petäjä, T., Hakala, J., Liao L., Lehtipalo, K., Junninen, H., Ehn, M., Vanhanen, J., Mikkilä J., Kulmala, M., Wildt, J. and Worsnop, D. (2011) Direct observation of atmospheric nanoparticle formation from sulphuric acid and a biogenic organic precursor, in preparation. *Proceedings of the FCoE Annual Meeting 2011 (this issue)*
- Drewer J., Lohila A., Aurela M., Laurila T., Minkkinen K., Penttilä T., Dinsmore K.J., McKenzie R., Helfter C., Flechard C., Sutton M.A., Skiba U.M. (2010). Comparison of greenhouse gas fluxes and nitrogen budgets from an ombrotrophic bog in Scotland and a minerotrophic sedge fen in Finland. *European Journal of Soil Science* 61, 640-650.
- Ghirardo, A., K. Koch, R. Taipale, I. Zimmer, J.-P. Schnitzler and J. Rinne, (2010) Determination of de novo and pool emissions of terpenes from four common boreal/alpine trees by ¹³CO₂ labeling and PTR-MS analysis. *Plant, Cell & Environment*, 33, 781-792. doi: 10.1111/j.1365-3040.2009.02104.x
- Hao, L. Q., Romakkaniemi, S., Yli-Pirilä, P., Joutsensaari, J., Kortelainen, A., Kroll, J. H., Miettinen, P., Vaattovaara, P., Tiitta, P., Jaatinen, A., Kajos, M. K., Holopainen, J. K., Heijari, J., Rinne, J., Kulmala, M., Worsnop, D. R., Smith, J. N., and Laaksonen, A. (2011). Mass yields of secondary organic aerosols from the oxidation of α-pinene and real plant emissions. *Atmos. Chem. Phys.*, 11, 1367-1378:
- Heinonsalo, J, Pumpanen, J, Rasilo, T, Hurme, K and Ilvesniemi, H. (2010) Carbon partitioning in ectomycorrhizal Scots pine seedlings. *Soil Biology, Soil Biology & Biochemistry*. 42: 1614-1623.
- Hirsikko, A., Nieminen, T., Gagné, S., Lehtipalo, K., Manninen, H.E., Ehn, M., Hörrak, U., Kerminen, V.-M., Laakso, L., McMurry, P.H., Mirme, A., Mirme, S., Petäjä, T., Tammet, H., Vakkari, V., Vana, M. and Kulmala, M. (2011) Atmospheric ions and nucleation: a review of observations. *Atmos. Chem. Phys.*, 11, 767-798.
- Hölttä, T, Mäkinen, H, Nöjd, P, Mäkelä-Carter, A, and Nikinmaa, E. (2010) A physiological model of softwood cambial growth. *Tree Physiology*, 30, 1235-1252.
- Hölttä et al. (2011). An optimality model explains the structure of plant vascular systems. *Plant Cell Env.*, *accepted*
- Hölttä et al. (2011). Theory and testing of a new method for the continuous monitoring of phloem osmotic pressure of trees in the field. Manuscript in preparation
- Junninen, H., Ehn, M., Petäjä, T., Luosujärvi, L., Kotiaho, T., Kostianen, R., Rohner, U., Gonin, M., Fuhrer, K., Kulmala, M. and Worsnop, D.R. (2010) API-ToFMS: a tool to analyze composition of ambient small ions. *Atmos. Meas. Technol.*, 3, 1039-1053.
- Katul, G., S. Launiainen, T. Grönholm and T. Vesala (2011) The effects of the canopy medium on dry deposition velocities of aerosol particles in the canopy sub-layer above forested ecosystems. *Atmospheric Environment* 45, 1203-1212.
- Kerminen, V.-M., Petäjä, T., Manninen, H.E., Paasonen, P., Nieminen, T., Sipilä, M., Junninen, H., Ehn, M., Gagné, S., Laakso, L., Riipinen, I., Vehkamäki, H., Kurtén, T., Ortega, I.K., Dal Maso, M., Brus, D., Hyvärinen, A., Lihavainen, H., Leppä, J., Lehtinen, K.E.J., Mirme, A., Mirme, S., Hörrak, U., Berndt, T., Stratmann, F., Birmili, W., Wiedensohler, A., Metzger, A., Dommen, J., Baltensperger, U., Kiendler-Scharr, A., Mentel, T.F., Wildt, J., Winkler, P.M., Wagner, P.E., Petzold, A., Minikin, A., Plass-Dülmer, C., Pöschl, U., Laaksonen, A. and Kulmala, M. (2010) Atmospheric nucleation: highlights of the EUCAARI project and future directions. *Atmos. Chem. Phys.* 10, 10829-10848.
- Kupiainen, O., Ortega, I. K., Paasonen, P., Loukonen, V., Kurtén, T., Vehkamäki, H. and Kulmala, M. (2011) Ammonia and amines in atmospheric particle formation. *Proceedings of the FCoE Annual Meeting 2011 (this issue)*

- Kurtén, T., Ortega, I. K., Kupiainen, O. and Vehkamäki, H. (2011a) The use of computational chemistry in modelling the chemistry and physics of atmospheric nucleation and nucleation precursor gases. *Proceedings of the FCoE Annual Meeting 2011 (this issue)*
- Kurtén, T., Petäjä, T., Smith, J., Ortega, I. K., Sipilä, M., Junninen, H., Ehn, M., Vehkamäki, H., Mauldin, L., Worsnop, D. R. and Kulmala, M. (2011b) The effect of H₂SO₄- amine clustering on chemical ionization mass spectrometry (CIMS) measurements of gas-phase sulfuric acid. *Atmos. Chem. Phys.* 11, 3007-3019.
- Kyrö, E.-M., Virkkula, A., Dal Maso, M., Parshintsev, J., Ruíz-Jimenez, J., Manninen, H.E., Forsström, L., Heinonen, P., Riekkola, M.-L., Hartonen K. and Markku Kulmala (2011) Evidence of antarctic aerosol formation due to continental biogenic precursors; *Proceedings of the FCoE annual meeting 2011 (this issue)*
- Lauros, J., Sogachev, A., Smolander, S., Vuollekoski, H., Sihto, S.-L., Laakso, L., Mammarella, I., Rannik, U. and Boy, M. (2010) Particle concentration and flux dynamics in the atmospheric boundary layer as the indicator of formation mechanism, *Atmos. Chem. Phys. Discuss.* 10, 20005-20033.
- Liao, L., Dal Maso, M., Taipale, R., Rinne, J., Ehn, M., Junninen, H., Äijälä, M., Nieminen, T., Alekseychik, P., Hulkkonen, M., Kerminen V.-M. and Kulmala M. (2011) Monoterpene pollution episodes in a forest environment: indication of anthropogenic origin and association with aerosol particles *Boreal Env. Res.*, in press
- Lindén A. et al. (2011). Energy limitation restricts nutrient cycling in boreal forest soils; potential effects on the nitrogen availability. *Proceedings of the FCoE Annual Meeting 2011 (this issue)*
- Lohila A., Aurela M., Hatakka J., Pihlatie M., Minkkinen K., Penttilä T., Laurila T. (2010). Responses of N₂O fluxes to temperature, water table and N deposition in a northern boreal fen. *European Journal of Soil Science* 61, 651-661.
- Lohila A., Minkkinen K., Aurela, M., Tuovinen J.-P., Penttilä T., Laurila T. (2011) Forestry-drained peatland in southern Finland is a large CO₂ sink. *Proceedings of the FCoE Annual Meeting 2011 (this issue)*
- Lohila A., Minkkinen K., Laine J., Savolainen I., Tuovinen J.-P., Korhonen L., Laurila T., Tietäväinen H., Laaksonen A. (2010). Forestation of boreal peatlands - impact of changing albedo and greenhouse gas fluxes on radiative forcing. *Journal of Geophysical Research* 115, G04011, doi:10.1029/2010JG001327.
- Laitinen, T. et al. (2011) Characterization of organic compounds in 10 to 50 nm aerosol particles in a boreal forest with laser desorption ionization aerosol mass spectrometer and comparison with other techniques. *Atmos Environ*, doi:10.1016/j.atmosenv.2011.04.023.
- Loukonen, V., McGrath, M. J., Väänänen, R., Karinkanta, R., Viisanen, K., Dal Maso, M. and Vehkamäki, H. (2011) sPARCK - simple program for atmospherically relevant cluster kinetics. *Proceedings of the FCoE Annual Meeting 2011 (this issue)*
- Massoli, P., Lambe, A.T., Ahern, A.T., Williams, L.R., Ehn, M., Mikkilä, J., Canagaratna, M.R., Brune, W.H., Onasch, T.B., Jayne, J.T., Petäjä, T., Kulmala, M., Laaksonen, A., Kolb, C.E., and Davidovits, P. and Worsnop, D.R. (2010) Relationship between aerosol oxidation level and hygroscopic properties of laboratory generated secondary organic aerosol (SOA) particles. *Geophys. Res. Lett.*, L24801, doi: 10.1029/2010GL045258.
- Mogensen, D., Smolander, S., Sogachev, A., Zhou, L., Sinha, V., Guenther, A., Williams, J., Nieminen, T., Kajos, M., Rinne, J., Kulmala, M. and Boy, M. (2011) Modelling atmospheric OH-reactivity in a boreal forest ecosystem, *Atmos. Chem. Phys. Discuss.*, 11, 9133-9163.
- Nieminen, T., Paasonen, P., Manninen, H.E., Sellegri, K., Kerminen, V.-M. and Kulmala, M. (2011) Parameterization of ion-induced nucleation rates based on ambient observations. *Atmos. Chem. Phys.*, 11, 3393-3402.

- Nikinmaa E. et al. (2011). Assimilate transport in phloem sets conditions for leaf gas exchange. Manuscript in preparation
- Nordbo, N., S. Launiainen, I. Mammarella, M. Leppäranta, J. Huotari, A. Ojanen and T. Vesala (2011) Long-term energy flux measurements and energy balance over a small boreal lake using eddy covariance technique. *J. Geophys. Res.* 116, DOI: 10.1029/2010JD014542.
- Paasonen, P., Nieminen, T., Asmi, E., Manninen, H.E., Petäjä, T., Plass-Dülmer, C., Flentje, H., Birmili, W., Wiedensohler, A., Hörrak, U., Metzger, A., Hamed, A., Laaksonen, A., Facchini, M.C., Kerminen, V.-M. and Kulmala M. (2010) On the roles of sulphuric acid and low-volatility organic vapours in the initial steps of atmospheric new particle formation: *Atmos. Chem. Phys.*, 10, 11223-11242.
- Parshintsev, J, Kivilompolo, M, Ruiz Jimenez, J, Hartonen, K, Kulmala, M, Riekkola, M. (2010) Particle-into-liquid sampler on-line coupled with solid-phase extraction-liquid chromatography-mass spectrometry for the determination of organic acids in atmospheric aerosols. *J. Chromatogr. A* **1217**, 5427.
- Parshintsev, J. et al. (2011) Comparison of quartz and teflon filters for simultaneous collection of size-separated ultrafine aerosol particles and gas-phase zero samples, *Anal. Bioanal. Chem.* doi: 10.1007/s00216-011-5041-0.
- Petäjä, T., Sipilä, M., Paasonen, P., Nieminen, T., Kurtén, T., Berndt, T., Stratmann, F., Vehkamäki, H. and Kulmala, M. (2011) Experimental observation of strongly bonded sulphuric acid dimers. *Phys. Rev. Lett.*, in press.
- Porcar-Castell A. (2011) A high resolution portray of the annual dynamics of photochemical and non-photochemical quenching in needles of *Pinus sylvestris*. *Physiologia Plantarum*. in press
- Prisle, N. L., Dal Maso, M. and Kokkola, H. (2011) A simple representation of surface active organic aerosol in cloud droplet formation, *Atmos. Chem. Phys.*, 11, 4073-4083.
- Rinne, J., T. Riutta, M. Pihlatie, M. Aurela, S. Haapanala, J.-P. Tuovinen, E.-S. Tuittila & T. Vesala, (2007) Annual cycle of methane emission from a boreal fen measured by the eddy covariance technique. *Tellus*, 59B, 449-457.
- Ruiz-Jimenez, J. et al. (2011) Comprehensive GCxGC, a valuable technique for the screening of different chemical compounds in ultrafine aerosol particles, Submitted to *Environ. Monitoring*
- Romakkaniemi, S., H. Kokkola, J. N. Smith, N. L. Prisle, A. N. Schwier, V. F. McNeill, and A. Laaksonen (2011) Partitioning of semivolatile surface-active compounds between bulk, surface and gas phase. *Geophys. Res. Lett.*, 38, L03807, doi:10.1029/2010GL046147:
- Sinha, V., J. Williams, J. Lelieveld, T. Ruuskanen, M. Kajos, J. Patokoski, H. Hellén, H. Hakola, D. Mogensen, M. Boy, J. Rinne, M. Kulmala (2010) OH Reactivity Measurements within a Boreal Forest: Evidence for Unknown Reactive Emissions. *Environmental Science & Technology*, 44, 6614-6620.
- Sipilä, M., Berndt, T., Petäjä, T., Brus, D., Vanhanen, J., Stratmann, F., Patokoski, J., Mauldin III, R.L., Hyvärinen, A.-P., Lihavainen, H. and Kulmala, M. (2010) The role of sulfuric acid in atmospheric nucleation. *Science*, 327, 1243-1246.
- Vanhanen, J., Mikkilä, J., Lehtipalo, K., Sipilä, M., Manninen, H.E., Siivola, E., Petäjä, T. and Kulmala, M. (2011) Particle size magnifier for nano-CN Detection *Aerosol Sci. Technol.*, 45, pp. 533-542.
- Vargas, R, Baldocchi, D.D., Allen, M.F., Bahn, M, Black, A.T., Collins, S.L., Curiel Yuste, J, Hirano, T, Jassal, R.S., Pumpanen, J, and Tang, J. (2010) Looking deeper into the soil: biophysical controls and seasonal lags of soil CO₂ production and efflux. *Ecological Applications* 20, 1569-1582.
- Virtanen, A., Joutsensaari, J., Koop, T., Kannosto, J., Yli-Pirilä, P., Leskinen, J., Mäkelä, J.M., Holopainen, J.K., Pöschl, U, Kulmala, M, Worsnop D.R. and Laaksonen, A. (2010). An amorphous solid state of biogenic secondary organic aerosol particles. *Nature* 467, 824-827:
- Yi C., Ricciuto D., Li R., Wolbeck J. Xu X., Nilsson M., Aires L., Albertson J.D., Ammann C., Arain M.A., Araujo A.C., Aubinet M., Aurela M., Barcza Z., Barr A., Berbigier P., Beringer J., Bernhofer C.,

Black A.T., Bolstad P.V., Bosveld F.C., Broadmeadow M.S., Buchmann N., Burns S.P., Cellier P., Chen J.M., Chen J., Ciais P., Clement R., Cook B.D., Curtis P.S., Dail D.B., Dellwik E., Delpierre N., Desai A.R., Dore S., Dragoni D., Drake B.G., Dufrene E., Dunn A., Elbers J., Eugster W., Falk M., Feigenwinter C., Flanagan L.B., Foken T., Frank J., Fuhrer J., Gianelle D., Goldstein A., Goulden M., Granier A., Gruenwald T., Gu L., Guo H., Hammerle A., Han S., Hanan N.P., Haszpra L., Heinesch B., Helfter C., Hendriks D., Hutley L.B., Ibrom A., Jacobs C., Johansson T., Jongen M., Katul G., Kiely G., Klumpp K., Knohl A., Kolb T., Kutsch W.L., Lafleur P., Laurila T., Leuning R., Lindroth A., Liu H., Loubet B., Manca G., Marek M., Margolis H.A., Martin T.A., Massman W.J., Matamala R., Matteucci G., McCaughey H., Merbold L., Meyers T., Migliavacca M., Miglietta F., Misson L., Moelder M., Moncrieff J., Monson R.K., Montagnani L., Montes-Helu M., Moors E., Moureaux C., Mukelabai M.M., Munger J.W., Myklebust M., Nagy Z., Noormets A., Oechel W., Oren R., Pallardy S.G., Kyaw T.P., Pereira J.S., Pilegaard K., Pinter K., Pio C., Pita G., Powell T.L., Rambal S., Randerson J.T., Randow C.V., Rebmann C., Rinne J., Rossi F., Roulet N., Ryel R.J., Sagerfors J., Saigusa N., Sanz M.J., Mugnozza G., Schmid H.P., Seufert G., Siqueira M., Soussana J., Starr G., Sutton M.A., Tenhunen J., Tuba Z., Tuovinen J.-P., Valentini R., Vogel C.S., Wang J., Wang S., Wang W., Welp L.R., Wen X., Wharton S., Wilkinson M., Williams C.A., Wohlfahrt G., Yamamoto S., Yu G., Zampedri R., Zhao B., Zhao X., (2010). Climate control of terrestrial carbon exchange across biomes and continents. *Environmental Research Letters* 5, 034007, doi: 10.1088/1748-9326/5/3/034007.

CONTINUOUS MEASUREMENTS OF SCOTS PINE SHOOTS SHOW HUGE VARIATION IN VOC EMISSIONS DURING YEAR 2010

J. AALTO¹, P. KOLARI¹, H. AALTONEN², J. BÄCK¹, P. HARI¹ AND E. NIKINMAA¹

¹Department of Forest Sciences, University of Helsinki, Finland.

²Finnish Meteorological Institute, Helsinki, Finland

Keywords: SCOTS PINE, VOC EMISSION, CONTINUOUS MEASUREMENTS

INTRODUCTION

Various VOCs (volatile organic compounds) are essential in tropospheric chemistry influencing new particle formation and growth (Clayes et al. 2004, Kulmala et al. 2004, Tunved et al. 2006) and other reactions such as production and destruction of tropospheric ozone (Atkinson and Arey 2003) and competition for OH with methane thus affecting the lifetime of latter (Kaplan et al. 2006). Because of these multiple impacts on atmospheric composition BVOCs interact with climate in many ways (Kulmala et al. 2004). Biogenic sources play a key role in VOC budget over extensive areas, one example being boreal coniferous forests (Rinne et al. 2009), where trees are the main contributor to VOC emissions over year. Continuous, very long term measurements of VOC fluxes from boreal trees are rarely conducted. However, continuous measurements are essential when it comes to characterizing the phenomena causing VOC synthesis and emissions and when various models (emission model, air chemistry model etc.) are developed and tested. To provide extensive data sets about emissions of VOCs from boreal forests, we have conducted various VOC emission measurements. Here we introduce some results concerning two Scots pine (*Pinus sylvestris* L.) shoots, measured during year 2010.

MATERIAL AND METHODS

The measurements were conducted at the SMEAR II measurement station (Station for Measuring Forest Ecosystem – Atmosphere Relations) in Hyytiälä, Southern Finland (61°N, 24°E, 180 m a.s.l.). The forest around the station is dominated by 48-year-old Scots pine, and the canopy reaches a height of about 17 m. With a scaffolding tower there is an access to the crowns of three pines and an aspen. The automatic gas-exchange system consists of 3.5-dm³ cylindrical shoot chambers, sampling tubing, and analyzers. The chambers are made of acrylic plastic and their internal surfaces coated with Teflon FEP film. The chambers remain open most of the time and close intermittently for 3 minutes, four times per every third hour. While open, the chamber interior is in contact with ambient unfiltered air. During a closure, air is drawn from the chambers to the gas analyzers along the sample lines. Ambient air is allowed to enter the chamber through small holes in the chamber walls to compensate the sample air flow taken from the chamber. Two cylindrical chambers were installed in the beginning of March 2010: one with a mature shoot inside (hereafter ‘mature shoot’) and the other with only a terminal bud inside chamber (hereafter ‘growing shoot’). All buds of the mature shoot and all axillary buds of the growing shoot were removed before installation. The growth of the growing shoot was recorded with photographic measurements.

Teflon PTFE tubes of 50 m length and with internal diameter of 4 mm are leading the air towards the CO₂ and H₂O analyser at flow rate of 1 dm³ min⁻¹. VOC sample air is drawn from those tubes before CO₂ and H₂O analysers and led to VOC analyser through a PTFE tube with internal diameter of 1,57 mm and length of about 5 meters. VOC concentrations were recorded with a proton transfer reaction-mass spectrometer (PTR-MS, Ionicon Analytik, Innsbruck, Austria). The sample air intake of PTR-MS was a little less than 0.1 dm³ min⁻¹. The operation of PTR-MS, calibrations and the concentration calculations are explained in detail in Taipale et al. 2008. One set of PTFE tubings are led to provide sample air for O₃

and NO_x analysers. Ambient atmospheric concentrations of CO₂, H₂O, O₃, NO_x as well as air temperature and PPFD, are measured during and before chamber closure and the values recorded at 5-s intervals. VOC concentrations are recorded at about 12.5 s intervals. The flux calculations were conducted using mass balance equation, where the emission can be solved. The results from the VOC measurements are expressed with the measured protonated mass symbol (amu+1, e.g. M33 = methanol). Measured masses and the potential contributing compounds were: M33 methanol, M45 acetaldehyde, M59 acetone, M69 isoprene, M79 benzene, M81 monoterpenes, M99 hexenal, M101 hexanal, M137 monoterpenes, and M153 methyl salicylate.

In 2010, the emission measurements started in the end of March and continued until December. There are several short calibration, maintenance and other gaps in the data series.

RESULTS AND DISCUSSION

The monitored Scots pine shoots emitted all of the recorded masses except M153. During cold seasons there was weak or no diurnal pattern with all of the recorded masses, but from the beginning of May to the middle of September there was clear diurnal pattern with most of the recorded masses (Fig. 1). The monitored shoots were sources for most of the recorded masses nearly all of the time; in nighttime and during cold seasons the emissions were close to zero, but in daytime during active season both shoots showed significant emissions. The most clear diurnal and temporal variation was recorded for masses 33, 45, 59, 81 and 137, but also masses 69, 79, 99 and 101 showed some diurnal and temporal variation.

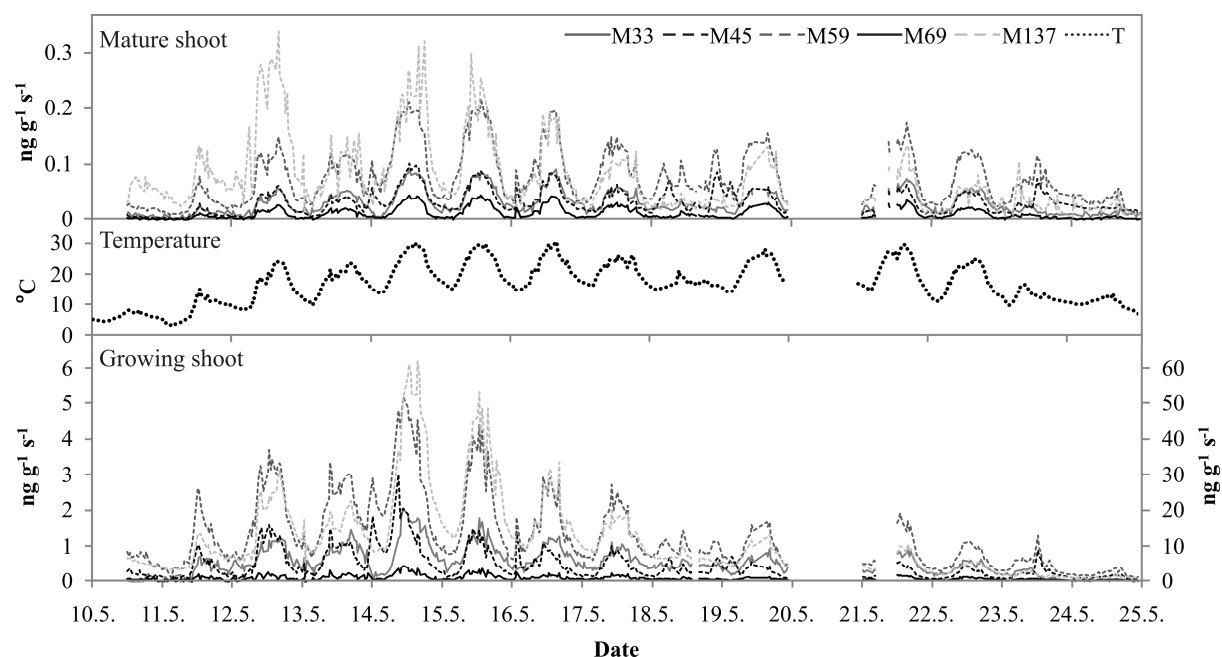


Figure 1. Scots pine shoot VOC emissions measured between 10th and 25th of May 2010. In the lowest panel, the Y-axis on the left side stands for masses 33, 45, 59 and 69, and the right one stands for mass 137.

During spring, when the growth was most intense, and also before that, the emissions of the growing shoot were ten-fold (masses 33, 45, 59 and 69) or even 200-fold (mass 137) when compared to mature shoot (Fig. 1). During April and May the growing shoot was stronger source of VOCs than the mature shoot even when the emissions were not scaled to the masses of the shoots. These differences nearly disappeared during summer when the growing shoot reached the full length and size. This shows that growing Scots pine shoots are significant sources of several VOCs during springtime, although their total mass is not very high.

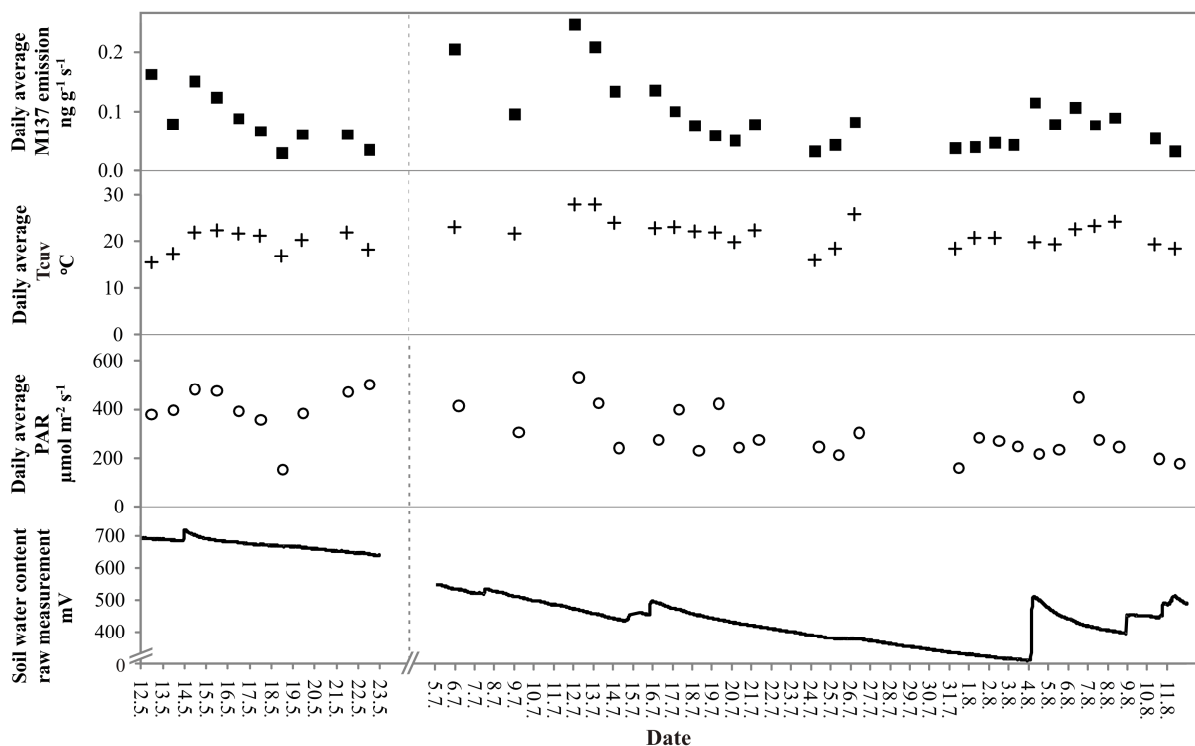


Figure 2. Daily average monoterpene emissions from one pine shoot during hot seasons of summer 2010. The lower panels show daily average temperature inside cuvette in the beginning of closure, daily average photosynthetically active radiation and soil water content.

Summer 2010 included two heatwaves. The first one in the middle of May was unseasonable hot. The second one was not unusually hot but it was very long, lasting over one month (Fig. 2). During heatwaves there were days between totally cloudless and full overcast (Fig. 2). During both heatwaves the monoterpene emissions from mature shoot were high in the beginning of period but decreased when heatwave dragged on. During the later heatwave there was some correlation between soil water content and monoterpene emissions, but during the first one the correlation was not that clear (Fig. 2). There was not clear decline in the emissions of other measured masses during heatwaves. It remains open and under ongoing research if the decrease in monoterpene emissions during heatwaves has something to do with drought effects or is it due to emptying storages of monoterpenes.

ACKNOWLEDGEMENTS

This work was supported by the Academy of Finland Centre of Excellence program (project no 1118615) and the graduate school in Physics, Chemistry and Meteorology of Atmospheric Composition and Climate Change.

REFERENCES

- Atkinson R. & Arey J. 2003. Gas-phase tropospheric chemistry of biogenic volatile organic compounds: a review. *Atmos. Environ.* **37**: 197–219.
- Claeys M., Grahan B., Vas G., Wang W., Vermeylen R., Pashynska V., Cafmeyer J., Guyon P., Andreae M.O., Artaxo P. & Maenhaut W. 2004. Formation of secondary organic aerosols through photooxidation of isoprene. *Science* **303**: 1173–1176.
- Kaplan J.O., Folberth G. & Hauglustaine D.A. 2006. Role of methane and biogenic volatile organic compound sources in late glacial and Holocene fluctuations of atmospheric methane concentrations. *Global Biogeochem. Cycles* **20**, GB2016
- Kulmala M., Suni T., Lehtinen K.E.J., Dal Maso M., Boy M., Reissell A., Rannik Ü., Aalto P., Keronen

- P., Hakola H., Bäck J., Hoffmann T., Vesala T. & Hari P. 2004. A new feedback mechanism linking forests, aerosols, and climate. *Atmos. Chem. Phys.* **4**: 557–562.
- Rinne J., Bäck J. & Hakola H. 2009. Biogenic volatile organic compound emissions from the Eurasian taiga: current knowledge and future directions. *Boreal Env. Res.* **14**: 807-826.
- Tunved P., Hansson H.-C., Kerminen V.-M., Ström J., Dal Maso M., Lihavainen H., Viisanen Y., Aalto P. P., Komppula M. & Kulmala M. 2006. High natural aerosol loading over Boreal forests. *Science* **312**: 261–263.

CONTINUOUS CHAMBER MEASUREMENTS OF VOC FLUXES FROM BOREAL PINE FOREST FLOOR

H. AALTONEN^{1, 2}, J. AALTO², J. BÄCK^{2, 3}, P. KOLARI², M. PIHLATIE³, J. PUMPANEN², M. KULMALA³, E. NIKINMAA² and T. VESALA³

¹Air Quality Laboratories, Finnish Meteorological Institute, P.O. Box 503, FI-00101 Helsinki, Finland

²Department of Forest Sciences, University of Helsinki, P.O. Box 27, FI-00014 University of Helsinki, Finland

³Department of Physics, University of Helsinki, P.O. Box 64, FI-00014 University of Helsinki, Finland

Keywords: VOC, MONOTERPENE, BOREAL FOREST, FOREST FLOOR, PTR-MS

INTRODUCTION

Biogenic sources are the main contributors to global volatile organic compound (VOC) emissions into the atmosphere, where VOCs take part in numerous chemical reactions, the new particle formation and particle growth as an example (Kulmala et al., 2000). From the air chemistry point of view, the VOC fluxes from boreal forest canopies have been the most intensively studied biogenic source, in contrast to forest floor VOC fluxes, which have mainly been measured on short campaign wise basis (Hellén et al., 2006; Aaltonen et al., 2011). As VOCs have a short lifetime due their reactivity, the air chemistry below the canopy plays more important role for the fluxes originating from the forest floor (Rinne et al., 2007).

Continuous, long term measurements of VOC fluxes from the forest floor have not been carried out so far. However, the forest floor has been shown to have an important role in boreal forest ecosystem VOC emissions especially in the spring and in the autumn (Hellén et al., 2006; Aaltonen et al., 2011). Forest floor VOC fluxes consist of fluxes from both vegetation and soil, however their proportions as well as the contributing processes in soil are not sufficiently known. The soil VOC emissions are assumed to originate from several sources: degradation of organic matter, microbes taking part in soil processes and living roots (e.g. Hayward et al., 2001; Asensio et al., 2008; Leff and Fierer, 2008; Bäck et al., 2010).

To increase the level of understanding of biogenic VOC fluxes we conducted continuous VOC measurements on the boreal pine forest floor during snow-free season. These automated measurements will show the overall level of forest floor VOC fluxes as well as to demonstrate the shorter and the longer scale temporal variations in fluxes. One aim of this study was also to provide data for air chemistry models, which lack the measured data on below-canopy VOC fluxes.

METHODS

We measured VOC fluxes from a pine forest floor at the SMEAR II (Station for Measuring Forest Ecosystem–Atmosphere Relations II), in southern Finland. The forest stand at the SMEAR II is 48 years old and dominated by Scots pine (*Pinus sylvestris*). The stand height is ~18 m and the canopy is open, with an average tree density of ~1370 ha⁻¹ (Ilvesniemi et al., 2009). The most common vascular plant species and mosses at ground level are lingonberry (*Vaccinium vitis-idaea*), bilberry (*Vaccinium myrtillus*), wavy hair-grass (*Deschampsia flexuosa*), heather (*Calluna vulgaris*), Schreber's big red stem moss (*Pleurozium schreberi*) and a dicranum moss (*Dicranum* sp.) (Ilvesniemi et al., 2009). The soil above the homogeneous bedrock is Haplic podzol formed in a glacial till, with an average depth of 0.5–0.7 m. The 30-year average annual precipitation at SMEAR II station is 713 mm and annual mean temperature 3.3 °C (Drebs et al. 2002). During the sampling period, from May to November 2010, weather at the station was warmer and dryer than the average, the cumulative precipitation being 463 mm

and mean temperature 9.9 °C. The 30-year average for the cumulative precipitation of May–November is 494 mm, while the average of mean temperature for the same period is 8.8 °C (Drebs et al., 2002).

The VOC fluxes were measured between 6 May and 15 November 2010 with three permanently installed dynamic non-steady-state chambers. The chambers (80 cm x 40 cm x 25 cm) were made of an aluminium frame while the sides and the top were covered with transparent fluorinated ethylene–propylene film (0.05 mm) from the inside. Two small fans were continuously mixing air in the chamber. The operation of the chambers was automated; each chamber was pneumatically closed for 15 min once every three hours, i.e. eight times per day. The chambers were connected to a proton transfer reaction-mass spectrometer (PTR-MS, Ionicon Analytik, Innsbruck, Austria) with a polytetrafluoroethylene tubing. The operation of PTR-MS, calibrations and the flux calculations are explained detail in Taipale et al. (2008). We were measuring ten masses and six of them were calibrated by the standard gas (Table 1). The results from the PTR-MS analyses are expressed with the measured protonated mass symbol (amu+1, e.g. M33 = methanol).

Measured mass	Potential contributing compounds
33	Methanol*
45	Acetaldehyde*
59	Acetone*, methyl vinyl ether
69	Isoprene*, 3-methyl-2-buten-1-ol, furan
79	Benzene*
81	Monoterpene fragment
99	Hexenal
101	Hexanal, <i>cis</i> -3-hexen-1-ol
137	α -Pinene*, monoterpenes
153	Methyl salicylate

Table 1. Masses measured with the PTR-MS and potential compounds contributing these masses. Asterisk (*) indicates compounds in the calibration gas.

RESULTS AND DISCUSSION

The boreal pine forest floor showed emissions for all the masses we selected to measure with the PTR-MS. The measurements were conducted with three randomly installed chambers and the spatial variation in the fluxes was evident. Chambers were placed on fairly different spots regarding to forest floor vegetation and dense vegetation seemed to affect VOC fluxes negatively. The maximum fluxes of the masses 81 and 137 (monoterpenes) were one magnitude higher than the others (Figure 1), the highest peaks reaching 1000 ng m⁻² s⁻¹ level. In contrast, the fluxes of M59, M69 and M79 were really low, being all the time below 10 ng m⁻² s⁻¹. The monoterpene emissions were approximately one magnitude higher than earlier measured with manual chambers in the same site (Aaltonen et al., 2011). However, manual measurements have been made with different technique (adsorbent tube sampling, GC-MS analysis) and targeted just certain monoterpenes, while PTR-MS measures all the compounds occurring in the masses 81 and 137.

All masses showed regular diurnal variations, the forest floor being clearly a source during day times, while the fluxes declined close to zero during nights. In the night-time, also negative flux values were frequently observed, probably because of the increased humidity inside the chambers. Especially oxygenated compounds stick easily on moist inner surfaces of chambers as well as plant and moss surfaces. During the periods of higher day time fluxes the night time values were always close to zero and the high fluxes consisted of a few mid-day values only. This suggests that higher temperatures, increasing volatility and biological activity and decreasing humidity, are essential for high VOC fluxes.

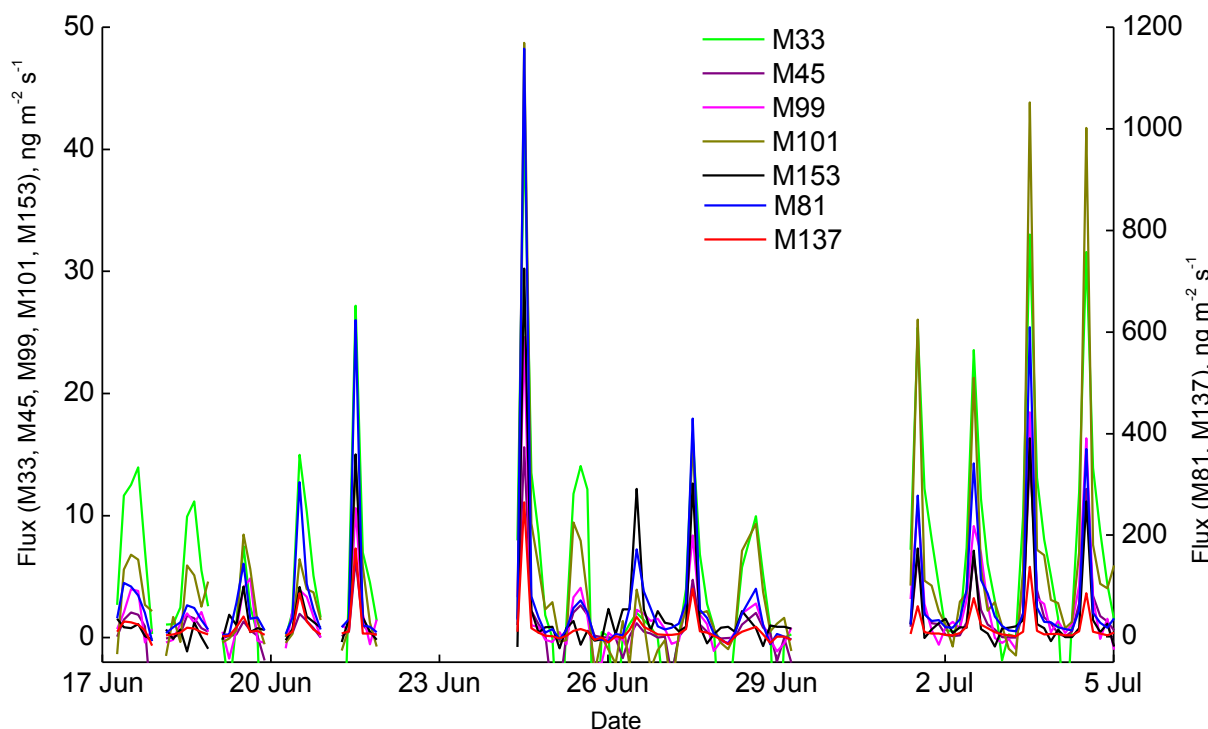


Figure 1. Boreal forest floor VOC fluxes measured between 17 June and 5 July 2010 with one automated chamber.

In addition to diurnal variation, the fluxes of almost all of the masses showed a larger temporal fluctuation during the measurement period (Figure 2). The biologically most active part of the growing season, from the end of May to mid July, was also the time of the highest VOC fluxes. Hellén et al. (2006) measured similar levels of terpenes with manual chambers at SMEAR II during springs 2004 and 2005, but in their study the fluxes decreased earlier, already in April. Another period poked out from the data was just before the chamber removal in November, after a long stable period of quite low fluxes. This increase of fluxes was observable only with heavier masses (M69→), except the monoterpene masses (M81 and M137). A similar behaviour of high late autumn VOC fluxes was measured in the year 2008 (Aaltonen et al., 2011) as well, with the exception that in 2008 the flux peaked already in October and that the peak was observable also with monoterpenes. Besides plant roots, also microbes (bacteria, fungi, algae) have been connected to soil VOC emissions (e.g. Leff and Fierer, 2008; Bäck et al., 2010). Large emissions of low molecular weight oxygenated compounds were measured from common soil fungi in a laboratory study (Bäck et al., 2010). Since in this field study the high emissions were only heavier compounds, it seems that the autumnal flux peak we measured might not be originating from fungal activity.

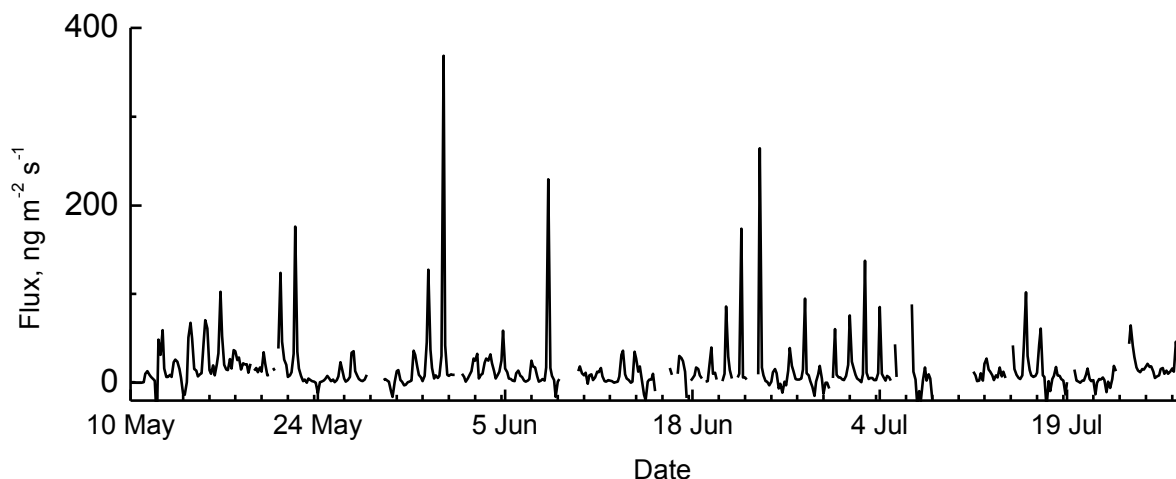


Figure 2. Temporal fluctuation of flux of the mass 137 (monoterpenes), measured between 10 May and 27 July 2010.

CONCLUSIONS

The pine forest floor emitted several VOC compounds, including oxygenated compounds and terpenoids. Monoterpene fluxes were clearly the highest; approximately one magnitude higher than with the other compounds. All the masses showed diurnal variation as well as larger scale fluctuation, early summer being the season of higher fluxes. The spatial variation of fluxes was remarkable, dense forest floor vegetation having a negative effect on fluxes. Further studies both in a field and a laboratory on surface reactions occurring on the chamber walls and inside the sample lines, as well as on the below ground processes are needed to assess the measurement errors and verify the VOC sources and their potential roles in emissions from below canopy space. However, this study provides new data of boreal forest floor VOC fluxes and their seasonality, which can be used for air chemistry and climate modelling.

ACKNOWLEDGEMENTS

The financial support by the Vilho, Yrjö and Kalle Väisälä Fund, Maj and Tor Nessling Foundation and the Academy of Finland Centre of Excellence program (project no 1118615) is gratefully acknowledged.

REFERENCES

- Aaltonen, H., J. Pumpanen, M. Pihlatie, H. Hakola, H. Hellén, L. Kulmala, T. Vesala and J. Bäck (2011). Boreal pine forest floor biogenic volatile organic compound emissions peak in early summer and autumn, *Agr. Forest Meteorol.* **151**, 682-691.
- Asensio, D., J. Peñuelas, P. Prieto, M. Estiarte, I. Filella and J. Llusà (2008). Interannual and seasonal changes in the soil exchange rates of monoterpenes and other VOCs in a Mediterranean shrubland, *Eur. J. Soil Sci.* **59**, 878-891.
- Bäck, J., H. Aaltonen, H. Hellén, M.K. Kajos, J. Patokoski, R. Taipale, J. Pumpanen and J. Heinonsalo (2010). Variable emissions of microbial volatile organic compounds (MVOCs) from root-associated fungi isolated from Scots pine, *Atmos. Environ.* **44**, 3651-3659.
- Drebs, A., A. Nordlund, P. Karlsson, J. Helminen and P. Rissanen (2002). Climatological statistics of Finland 1971–2000, (Finnish Meteorological Institute, Helsinki, Finland).
- Hellén, H., H. Hakola, K.-H. Pystynen, J. Rinne and S. Haapanala (2006). C₂–C₁₀ hydrocarbon emissions from a boreal wetland and forest floor, *Biogeosciences* **3**, 167-174.
- Hayward, S., R.J. Muncey, A.E. James, C.J. Halsall and C.N. Hewitt (2001). Monoterpene emissions from soil in a Sitka spruce forest, *Atmos. Environ.* **35**, 4081-4087.

Ilvesniemi, H., J. Levula, R. Ojansuu, P. Kolari, L. Kulmala, J. Pumpanen, S. Launiainen, T. Vesala and E. Nikinmaa (2009). Long-term measurements of the carbon balance of a boreal Scots pine dominated forest ecosystem, *Boreal Environ. Res.* **14**, 731-753.

Kulmala, M., K. Hämeri, J.M. Mäkelä, P.P. Aalto, L. Pirjola, M. Väkevä, E.D. Nilsson, I.K. Koponen, G. Buzorius, P. Keronen, Ü. Rannik, L. Laakso, T. Vesala, K. Bigg, W. Seidl, R. Forkel, T. Hoffmann, J. Spanke, R. Janson, M. Shimmo, H.-C. Hansson, C. O'Dowd, E. Becker, J. Paatero, K. Teinilä, R. Hillamo, Y. Viisanen, A. Laaksonen, E. Swietlicki, J. Salm, P. Hari, N. Altimir and R. Weber (2000). Biogenic aerosol formation in the boreal forest, *Boreal Environ. Res.* **5**, 281-297.

Leff, J.W. and N. Fierer (2008). Volatile organic compound (VOC) emissions from soil and litter samples, *Soil Biol. Biochem.* **40**, 1629-1636.

Rinne, J., R. Taipale, T. Markkanen, T.M. Ruuskanen, H. Hellén, M.K. Kajos, T. Vesala and M. Kulmala (2007). Hydrocarbon fluxes above a Scots pine forest canopy: measurements and modeling, *Atmos. Chem. Phys.* **7**, 3361-3372.

Taipale, R., T.M. Ruuskanen, J. Rinne, M.K. Kajos, H. Hakola, T. Pohja and M. Kulmala (2008). Technical Note: Quantitative long-term measurements of VOC concentrations by PTR-MS – measurement, calibration, and volume mixing ratio calculation methods, *Atmos. Chem. Phys.* **8**, 6681-6698.

THE EFFECT OF WATER TABLE LEVEL ON DISSOLVED OXYGEN CONCENTRATION AND METHANE EMISSIONS IN TWO FINNISH WETLAND ECOSYSTEMS

M. ACOSTA¹, S. HAAPANALA¹, A. LOHILA², M. AURELA², T. LAURILA², T. VESALA¹

¹ Department of Physical Science, University of Helsinki, Helsinki, Finland

² Climate Change Research, Finnish Meteorological Institute, Helsinki, Finland

Keywords: BOREAL WETLAND, DISSOLVED OXYGEN, WATER TABLE LEVEL, METHANE

INTRODUCTION

The stability of the wetland carbon pool is sensitive to the availability of molecular oxygen (O₂) and thereby changes in hydrological status (Jobbagy and Jackson, 2000). In general, free O₂ is present above the water table (oxic zone). When a soil is flooded (anoxic zone), soil oxygen is rapidly depleted through aerobic respiration using O₂ as the terminal electron acceptor. This is because the rate of gaseous O₂ diffusion through water is much slower than through air. In the absence of O₂, other alternative electron acceptor (nitrate, manganese, iron, sulphate and carbon dioxide) are progressively reduced with decreasing energy to the microbial community (Puckett and Cowdery, 2002). Under anoxic conditions, the decomposition of organic matter involves coupled anaerobic degradation pathways, where methane (CH₄) is the main end product (Le Mer and Roger, 2001). The effect of water level on soil Dissolved Oxygen (DO) distribution and CH₄ emissions as well as potential feedback mechanisms to global warming remains unclear. Therefore, the importances of better understand the relationship between DO dynamics, water table level (WTL) and CH₄ in wetland ecosystems. The aims of our study were: 1) to present reliable measurements of dissolved oxygen (DO) at two boreal wetlands ecosystems, 2) to obtain diurnal dynamics of WTL, DO and CH₄; and 3) to identify the relationship between WTL, DO distribution and CH₄ emissions in the studied wetland ecosystems.

METHODS

The study was carried out at two boreal wetland sites in Finland, The Siikaneva and the Lompolojänkää site. The Siikaneva site is an oligotrophic fen located in Ruovesi in Southern Finland (61° 50 N, 24° 12 E, 162 m a.s.l.). The peat depth at the measurement site is up to four meters and has accumulated since the end of the last ice age, in about 9000 yr. The site has a relatively flat topography with no pronounced string and hollow structures. The vegetation at the site is dominated by peat mosses (*Sphagnum balticum*, *S. majus* and *S. papillosum*), Sedges (*Carex rostrata* Stokes, *C. limosa* L., *Eriophorum vaginatum* L.) and Rannochrush (*Scheuchzeria palustris* L.). The long-term (1971-2000) annual mean temperature and annual precipitation of the site are 3.3° C and 713 mm, respectively, (Rinne *et al.*, 2007).

At Siikaneva site, automatic continuous measurements of DO were carried out on June 2010 (from 3rd to 30th) applying optical dissolved oxygen sensors (6150 ROX sensor, YSI incorporated, Ohio, USA). The sensors were installed at three different depths (15 cm, 25 cm and 35 cm). The CH₄ fluxes were measured using the micrometeorological eddy covariance technique. Moreover, meteorological parameters such as air temperature, relative humidity, precipitation, soil temperature profile and WTL were recorded continuously during the period of the experiment.

The Lompolojänkki site is an open, pristine and nutrient-rich sedge fen located in Northern Finland in the Aapa mire region (67°59 N, 24°12 E, 269 m above sea level). The peat depth at the site is up to 3 m at the center of the fen. The relatively dense vegetation layer is dominated by *Betula nana*, *Menyanthes trifoliata*, *Salix lapponum*, *Carex lasiocarpa* and *C. rostrata*. The moss cover on the ground is patchy, consisting mainly of peat mosses (*Sphagnum angustifolium*, *S. riparium*, *S. teres*, *S. warnstorfi*, *S. subsecundum* and *S. fallax*) and some brown mosses (*Warnstorfia exannulata*), (Aurela *et al.*, 2009). The long-term (1971-2000) annual temperature and precipitation at the site are -1.4° C and 484 mm, respectively.

At Lompolojänkki site, the concentration of dissolved oxygen (DO) was measured continuously using a Troll-9500 multiparameter water quality sensor. The sensor head, equipped with the RDO® Optical Dissolved Oxygen sensor (In-Situ Inc., USA), was buried at the depth of approximately 10 cm into the peat. Data was logged hourly during the measurement period May-June 2009. The CH₄ flux at the site has been measured during the snow-free period with two automatic chambers (Lohila *et al.*, 2010).

RESULTS

At both sites, a positive correlation between WTL and DO was found, indicating that the reducing conditions in the peat soil were controlled by the water table level. At Siikaneva site a significant difference in DO concentration between different peat depths was observed. In the surface layer (15cm) the diurnal dynamics in DO could be explained by the change in peat temperature. At lower depths, diurnal variation was not observed – conditions being anoxic with values close to 0.2 mg/L. Rain events were another factor influencing DO concentration in the surface layer, increase in DO was observed after rain events in the majority of the occasions. Emissions of CH₄ were very stable during the experiment period and did not correlate with DO. However, occasionally a slight increase in CH₄ flux was observed with increased WTL.

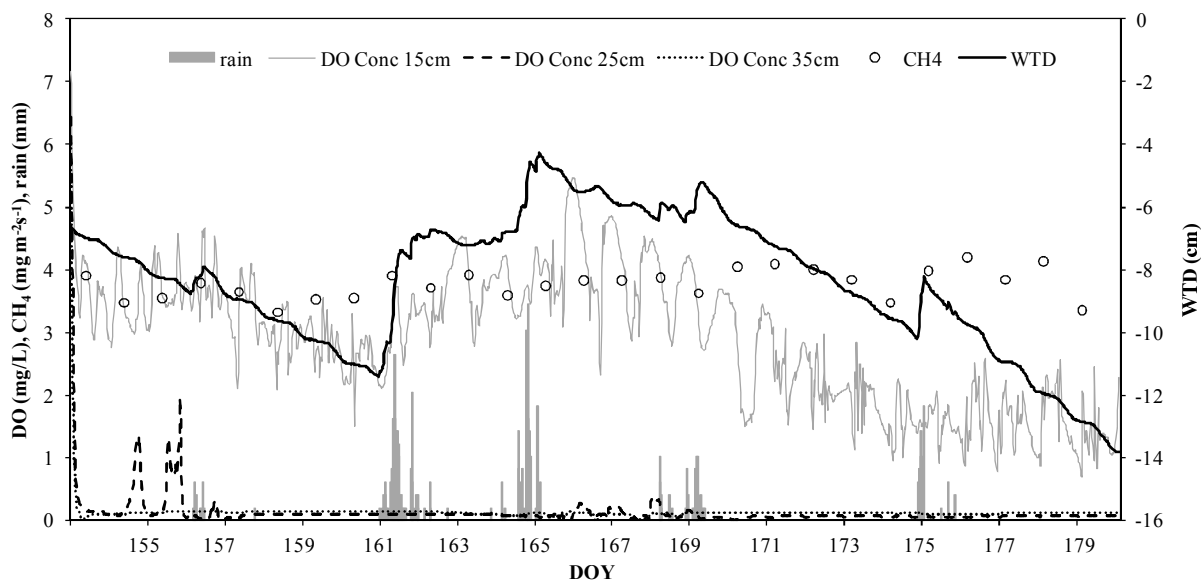


Figure 1. Diurnal courses of dissolved oxygen concentration (DO) at three different depths (15cm, 25cm and 35cm), methane emissions (CH₄, daily averaged), rain events and water table level (WTL) at Siikaneva wetland site during the measurement period (from 3rd to 30th of June 2010).

At Lompolojänkki, the peat at the measurement depth stayed anoxic for most of the summer. However, in May during the flooding and in June after some rainy days, the DO concentration peaked right after a rise in WTL. This was likely due to the input of oxygen-rich water from precipitation and from the surface runoff water originating from the surrounding forest. In June 15, lowered methane flux was observed for a short time at the same time with the rise in WTL and the first, smaller increase in DO

concentration. This increase in DO may be connected with the diffusion of dissolved oxygen from the better aerated horizons above.

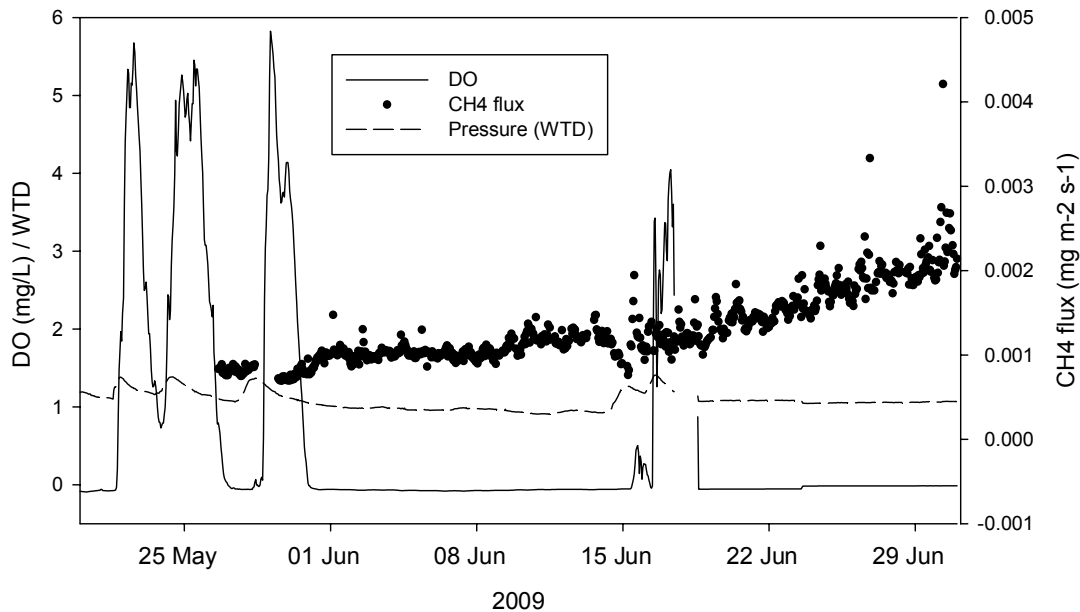


Figure 2. Concentration of dissolved oxygen (DO), CH₄ flux (measured by automatic chamber) and pressure in the peat soil, indicating fluctuations in water level (WTD) at Lompolojänkkä in May-June 2009.

CONCLUSIONS

Although previous investigations on the effects of water level change on CH₄ efflux from wetlands have shown that water levels stimulate anaerobic decomposition and CH₄ efflux, our short field studies suggest a complex relationship and poor correlation between water level status and CH₄. The both sites showed a different relationship between water level and dissolved oxygen. At Siikaneva a strong effect of water level on dissolved oxygen distribution in peat soil was observed compared to Lompolojänkkä site. Moreover in Siikaneva site water table level showed temporally dynamic in response to precipitations.

REFERENCES

- Aurela, M., Lohila, A., Tuovinen, J.-P., Hatakka, J., Riutta, T. & Laurila, T. (2009). Carbon dioxide exchange on a northern boreal fen. *Boreal Environment Research*, 14, 699–710.
- Jobbagy, E.G. and Jackson, R.B. (2000). The vertical distribution of soil organic carbon and its relation to climate and vegetation. *Ecological Applications* 10 (2), 423–436.
- Le Mer, J. and Roger, P. (2001). Production, oxidation, emission and consumption of methane by soils: a review. *European Journal of Soil Science* 37, 25–50.
- Lohila, A., Aurela, M., Hatakka, J., Pihlatie, M., Minkkinen, K., Penttilä, T., and Laurila, T. (2010). Responses of N₂O fluxes to temperature, water table and N deposition in a northern boreal fen. *European Journal of Soil Science* 61, 651–661.
- Puckett, L.J. and Cowdery, T.K. (2002). Transport and fate of nitrate in a glacial outwash aquifer in relation to ground water age, land use practices, and redox processes. *Journal of Environmental Quality* 31 (3), 782–796.
- Rinne, J., Riutta, T., Pihlatie, M., Aurela, M., Haapanala, S., Tuovinen, J.P., Tuittila, E.S. and Vesala, T. (2007). Annual cycle of methane emission from a boreal fen measured by the eddy covariance technique. *Tellus* 59B, 449–457.

Aerosol effect on Cumulus/Stratocumulus clouds: Comparison of ground based in-situ measurement and Satellite observations

I. AHMAD¹, T. MIELONEN², H. PORTIN², A. LAAKSONEN¹, A. AROLA², S. ROMAkkANIEMI¹

¹Department of Applied Physics, University of Eastern Finland (Kuopio).

²Finnish Meteorological Institute, Kuopio Unit (Finland).

Keywords: Cloud droplet effective radii, Cloud Optical Thickness, Liquid Water Path, Aerosol particle concentration, MODIS.

INTRODUCTION

Suspended particulate matter in the atmosphere (aerosol) plays an important role in the earth's radiation budget. They affect earth's atmosphere directly (extinction of solar radiation) and indirectly by acting as a cloud condensation nuclei (CCN). The interaction between aerosol and cloud is not a trivial process. This complex interaction is producing large uncertainty in the estimates of earth's radiation budget (IPCC report, 2007), as aerosol can affect cloud's life time and cloud optical thickness (COT), which is a function of liquid water content and cloud droplet effective radii (R_{eff}) in the cloud. Therefore it is important to analyze the effect of aerosol on cloud using different approaches, like; ground based in-situ measurement, satellite cloud retrieval and combination/validation of them. There is always a discrepancy between any of the two approaches, and that should be analyzed for more accurate aerosol cloud interaction.

In this work R_{eff} , LWP and COT were analyzed from the two MODIS instruments onboard Aqua and Terra satellite respectively, for quantitative assessment of the effect of particle number concentration on R_{eff} . The relation between number concentrations of accumulation mode particles (N_{acc}) from ground based measurements and R_{eff} , from MODIS was studied to see how aerosol affects cloud's optical properties. Hypothetically, the increase in aerosol number concentration should decrease the droplet effective radii. Additionally, R_{eff} measurement from Puijo was compared with MODIS R_{eff} measurement for comparison. Normally there is a difference in effective radii at bottom and top of cloud, but by knowing the depth of cloud some estimate of R_{eff} can be achieved if cloud vertical profile is assumed to be adiabatic.

GROUND BASED DATA

Puijo measurement station is located ($62^{\circ} 54'$, $27^{\circ} 40'$, 224 m above the surrounding lake) on the roof of Puijo tower, in Kuopio (Finland). The station has provided continuous aerosol particle and meteorological data since June, 2006. Detailed description of Puijo station can be found from Leskinen et al., (2009) and Portin et al., (2009). In this study accumulation mode (100nm–800nm) particle number concentration (N_{acc}) data from Puijo was used to see the effect of aerosol burden on R_{eff} . N_{acc} data was achieved from Differential Mobility Particle Sizer (DMPS).

For comparison of ground based measurements and MODIS data it is crucial that only single layer cloud exist. For detecting single layered cloud events were chosen using data from Vaisala CT25K Ceilometer from Savilahti measurement site. The site is located in the campus area of UEF, Kuopio and around 2 km southeast from Puijo, and 5m above the lake level. To make sure clouds are in the boundary layer it was limited that the cloud base must be less than 800m from the lake level. To select warm (liquid water) and non precipitating clouds we kept limits for some weather parameters like temperature and rain intensity

from Puijo weather station. A limit of satellite derived R_{eff} ($3\mu\text{m} \leq R_{eff} \leq 30\mu\text{m}$) is also applied for making the selection of water cloud more reliable (Nakajima and King 1990; Quaas et al., 2005). This was done so that our analysis of aerosol-cloud interaction is not affected by precipitation and ice phased clouds. We limit temperature, pressure, rain intensity and visibility to (>265)K , (>700) hpa, (< 0.2) mm/h and visibility (<200) meter respectively. Pressure was also considered in MODIS data for assuring low level cloud selection. Accumulation mode particle concentration was averaged to one hour in accordance to MODIS retrieval, as we have cloud retrieval from 5x5 pixels which gives us good estimation of aerosol cloud interaction.

We divided our data into two groups; (a) – water cloud with cloud base height less than 800 meter above the surrounding lake. (b) – water cloud with cloud base less than 224 meter above the surrounding lake.

In the later case Puijo tower itself is in the cloud, and cloud droplet number distribution could be measured with Cloud Droplet Probe (CDP) in the range 3–50 μm .

In both cases we were confined by multilayered clouds, mixed phased cloud, no satellite overpass and missing satellite data and the number of days with good observations were limited to 54 (for data group-a) and 17 (for data group-b).

For determining R_{eff} and LWC from puijo data we followed the equations given by (Liu and Hallett, 1997; Hansen and Travis, 1974; Rosenfeld and Lensky, 1998; Nakajima and King, 1990).

$$R_{eff} = \frac{\int_0^{\infty} r^3 n(r) dr}{\int_0^{\infty} r^2 n(r) dr} \quad \text{Equation. 1}$$

$$LWC = \int_0^{\infty} \rho \cdot n(r) \cdot \frac{4}{3} \pi r^3 \quad \text{Equation. 2}$$

Where; $n(r)$ is the cloud droplet size distribution, r is the cloud droplet radius and ρ is density of water. Since $n(r)$ depends on CCN present at the cloud base (Portin et al., 2009) therefore we expect a relation between CCN and $n(r)$ and their effect on R_{eff} as under;

$$R_{eff} \sim \left(\frac{3LWC}{4\pi n_d \rho} \right)^{1/3} \quad \text{Equation. 3}$$

We are more interested in R_{eff} , as this parameter is playing a vital role in calculation of the radiative properties of water clouds (Hansen and Travis, 1974).

We also used our air parcel model to investigate and compare cloud properties with ground based and satellite measurements. The model was used to estimate cloud top R_{eff} based on measured number of cloud droplets and estimate for the cloud depth from MODIS instrument.

SATELLITE DATA

MODIS instruments onboard Aqua and Terra polar synchronous orbiting satellites were used to retrieve cloud microphysical parameters like R_{eff} , COT, LWP from top of the cloud. MODIS scanning spectroradiometer consists of 36 channels. Six of these (visible and near infrared) bands are used in cloud retrieval algorithm (MODIS ATBT–cloud products). The swath width of the scanner is 2330 km with 55° on each side of nadir view (total of 110° width), which is covering more area as compared to CloudSat and CALIPSO satellites. Collection 5.1 from atmosphere level 2 was selected from LAADS WEB website (<http://ladsweb.nascom.nasa.gov/data/search.html>). The 5x5 km spatial resolution was used from both MODIS instruments for coincident cloud events (single layered water cloud). A 1x1 km pixel data was also used

for quality assurance flags purposes. Cloud parameters like R_{eff} , COT and LWP are averaged from 1 by 1 to 5 by 5 km, as cloud top properties are available for 5x5 km. Data with applying the same limits of temperature and pressure was taken for our task. Here in MODIS data we also checked the uncertainty (which comes from atmospheric correction and data measurement, and library generating algorithm) in cloud retrieval for excluding low quality data. Data field ‘Cloud Phase’ information was very useful to eliminate ice, uncertain and mixed phased cloud.

RESULTS AND CONCLUSION

Our case (a), where we choose clouds of base height less than 800 meter, gives an indication of the effect of aerosol on the microphysics of stratus/stratocumulus clouds Fig. 1. Cloud droplet effective radii are decreasing with increasing CCN (100–800) nm, which is theoretical given in equation 3. The data has been screened for any possible chance of contamination, e.g., ice cloud, mixed/uncertain phase cloud, multilayered clouds, quality assurance, etc as mentioned in ‘ground based data’ section. But still we have some higher values of R_{eff} from MODIS at higher concentration of CCN. This might be due to cloud dynamics or uncertainties caused by surface reflection contribution in the retrieval.

For second case (b) when Puijo tower is inside the clouds, i.e., cloud’s base height is less than 224 meter above surrounding lake, we did not get the congenial results. There is no clear correlation between ground base measurements and MODIS retrieval but somehow there are some data points which are considerably comparable with modelled cloud droplet effective radii, shown in Figure 2. We can divide the data into two groups according to COT values (optically thick and thin clouds), but then we will have very less data for comparison and analysis. Unfortunately the number of good days, i.e. when the tower is in the cloud, and Aqua or Terra is over-passing when only one cloud layer exists, is still quite low. Further analysis has to be done to get more cloud retrieval from MODIS by averaging the cloud parameters to larger region but this would make results less comparable as aerosol measurements can be affected by local aerosol emissions. We will continue our analysis using data from MODIS and from Puijo measurement station to get more cloud events.

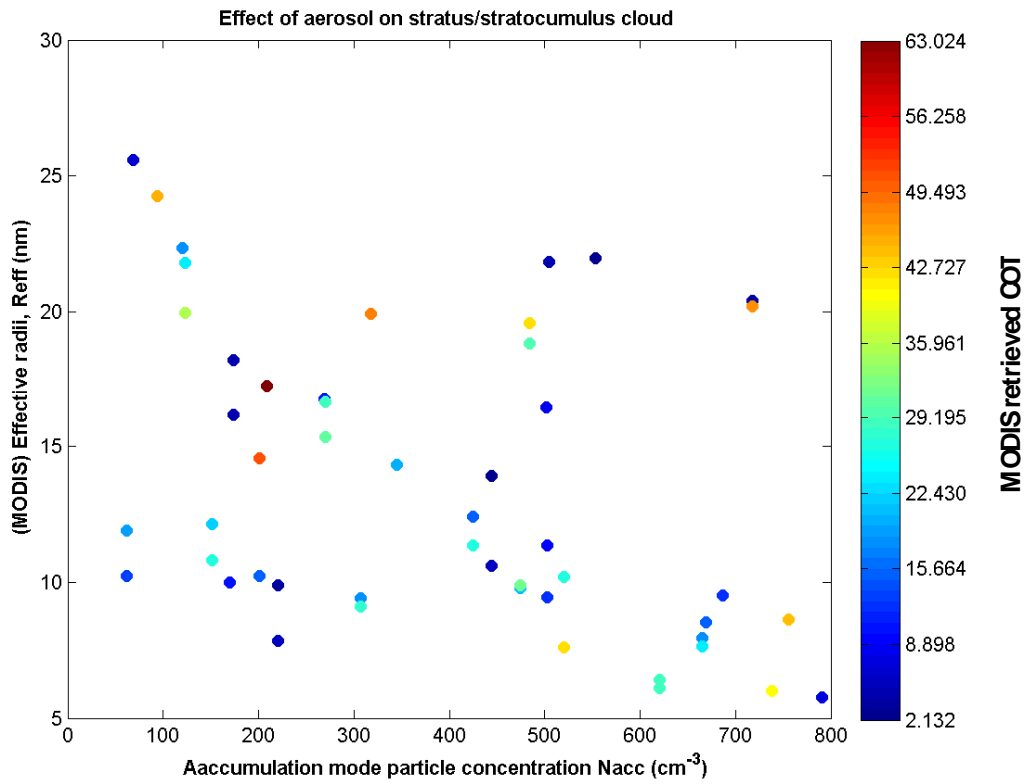


Fig 1: Cloud top effective radius as a function of number concentration of accumulation mode aerosol particles. Color is for cloud optical thickness.

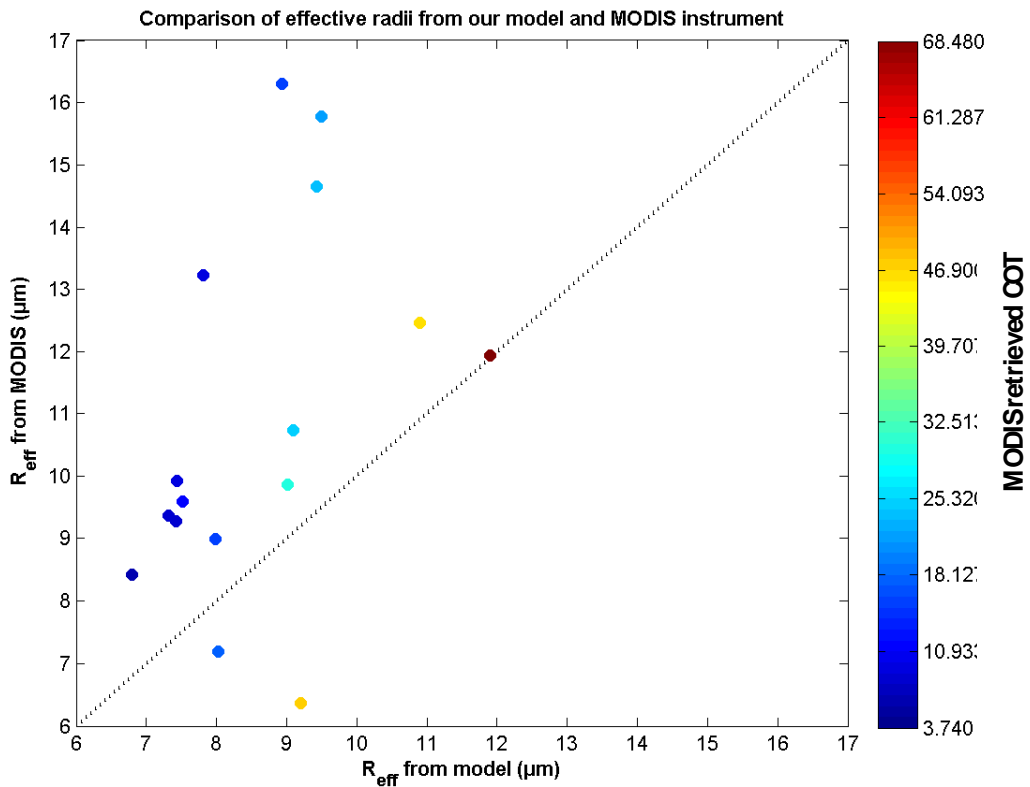


Fig 2: MODIS retrieved cloud top effective radius vs modelled effective radius, which is based on in situ measured cloud droplet number concentration and estimated cloud thickness.

ACKNOWLEDGEMENTS

This work was supported by Maj ja Tor Nessling Foundation and Academy of Finland (project number 123466)

REFERENCES

Leskinen, A., Portin, H., Komppula, M., Miettinen, P., Arola, A., Lihavainen, H., Hataka, J., Laaksonen, A., and Lehtinen, K. E. J., (2009). *Overview of the research activities and results at the Puijo semi-urban measurement station. Boreal Env. Res.*, 14, 576-590

Hansen, J. E., and L. D. Travis, (1974). *Light scattering in planetary atmospheres. Space Sci. Rev.*, 16, 527-610.

IPCC Report 2007, Climate Change 2007: Synthesis Report. Contribution of Working Groups I, II and III to the Fourth Assessment Report of the Intergovernmental Panel on Climate Change [Core Writing Team, Pachauri, R.K and Reisinger, A.(eds.)]. IPCC, Geneva, Switzerland, 104 pp.

King, M. D., Tsay, S., Platnick, S. E., Wang, M. And Liou, K., (1997). *MODIS Algorithm Theoretical Basis Document No. ATBD-MOD05, MOD06-Cloud product. Version 5.*

Liu, Y, and Hallett., J., (1997). The ‘ $1/3$ ’ power law between effective radius and liquid water-content’. *Quarterly journal of the royal meteorological society* 123, 1789-1795.

Nakajima, T. and King, M. D (1990). *Determination of the optical thickness and effective particle radius of clouds from reflected solar radiation measurements. Part I: Theory, J. Atmos. Sci.*, 47, 1878-1893.

Portin, J. H., Mika Komppula, Leskinen, A.P., Romakkaniemi, S., Laaksonen, A., and Lehtinen, K. E. J., (2009). *Overview of the aerosol-cloud interaction at the Puijo semi-urban measurement station. Boreal Env. Res.*, 14: 641-653.

Quaas, J., Boucher, O. and Lohmann, U. (2005). *Constraining the total aerosol indirect effect in the LMDZ and ECHAM4 GCMs using MODIS satellite data. Atmos. Chem. Phys. Discuss.*, 5, 9669-9690.

Rosenfeld, D., and Lensky, I. M., 1998. *Satellite-based insights into precipitation formation processes in continental and maritime convective clouds, Bulletin of the American Meteorological Society*, 79. 2457-2476.

NIGHTTIME THERMAL DECOUPLING IN A CONIFER FOREST CANOPY

P. ALEKSEYCHIK, I. MAMMARELLA and T. VESALA

University of Helsinki, Department of Physics,
Helsinki, Finland.

Keywords: eddy-covariance, stability, decoupling, drainage flow.

INTRODUCTION

Many environmental issues can be investigated with the help of eddy-covariance (EC) measurement technique, which employs the measurements of wind and scalars (e.g. $[\text{CO}_2]$) to infer the vertical turbulent flux (of carbon dioxide). However, the performance of EC technique is particularly sensitive to nighttime stable conditions, which usually lead to significant flux underestimation by the EC measurements [1].

The EC technique is unable to capture the real flux at stable conditions, which frequently occur at night time and lead to severe biases in flux measurements. At that time of day, there is no turbulence generation by ground heating. At weak winds and clear skies at night time (very stable BL), an open forest canopy allows for an intensive cooling of the ground. Consequently, an inversion forms in the whole layer from the ground to above-canopy level. Strong stratification sets in, so that the turbulence becomes effectively lifted and decoupled from the ground [2]. The CO_2 flux, emitted near the ground or by the lower part of the canopy, starts flowing away in a gravity force-induced drainage flow.

SITE DESCRIPTION

The study utilizes the measurement data from the Station for Measuring Forest Ecosystem-Atmosphere Relations (SMEAR II) located in southern Finland (61.51°N , 24.17°E). The station tower is at 180m asl within the relatively homogeneous pine (*Pinus sylvestris* L.) stand established in 1962, which stretches 1 kilometer to the North. The vegetation homogeneity is retained along the distance of about 150 meters in all directions from the mast; farther on the other species are also represented, most notably the spruce stand 150 meters to the South. The average height of the local pine stand is 15 m, all-sided LAI (leaf area index) is $6 \text{ m}^2/\text{m}^2$. The tower is situated atop a slanting ridge approximately 40 meters high and 1 km long (from North to East), bordered by a lake from South-West. The largest slope gradient is in the vicinity of the lake, whereas the smallest is on the eastern side of the ridge.

MATERIALS AND METHODS

In this study, we generally used the measurement data from the years 2004-2006. Data employed in this study included: at the main mast - profiles of air temperature, wind speed, wind direction and CO_2 concentration at 4.2, 8.4, 16.8, 33.6, 50.4 and 67.2 meter levels, and CO_2 flux measured by 2 EC setups at 23.3m height (main mast) and 3.2m height (small mast nearby).

In order to register the decoupling, we made use of the wind direction profile and defined the wind directional shear (WDdiff) for the trunk space (3.2-8.4m) and the canopy space (8.4m-16.8m). Decoupling within a layer was defined as the period of $\text{WDdiff} > 60^\circ$. When WDdiff was high in both layers, the situation was described as “complex decoupling”. In parallel with WDdiff, we used the quantities characterizing turbulence (friction velocity, u_* , vertical wind velocity standard deviation, σ_w), and dynamic stability (bulk Richardson number, Ri).

The turbulent friction velocity, u_* , was used as a measure of turbulent mixing. It is expressed via Reynolds turbulent stress as

$$u_* = \left(\frac{\tau}{\rho} \right)^{1/2}, \quad (1)$$

where u_* is the friction velocity, τ the Reynolds turbulent stress, ρ the air density. In turn, the bulk Richardson number is a measure of dynamic stability inside a layer:

$$Ri = \frac{g\Delta\bar{\theta}z}{\bar{\theta}(\bar{u})^2}, \quad (2)$$

where g is the gravity acceleration, $\Delta\bar{\theta}$ the potential temperature difference between the top and the bottom of a layer, $\bar{\theta}$ the potential temperature at the top, and \bar{u} the mean wind speed at the top, z the height at the top of a layer. Thus, we could obtain Ri for two layers, 4.2-8.4m (trunk space) and 8.4-16.8m (canopy space).

EC technique was used for the CO_2 flux calculation. It is based on the action of turbulence, which, according to Reynolds decomposition, is represented for some quantity s as

$$s = \bar{s} + s', \quad (3)$$

Here, the varying quantity s is decomposed into the mean (overbar) and fluctuating (prime) components. Assumptions that the terrain in the measurement area is horizontally homogeneous and the flux is stationary (no change with time) lead to a conclusion that at a certain height inside surface layer the vertical CO_2 flux can be expressed as a covariance of vertical wind speed and CO_2 concentration:

$$F_{CO_2} = \overline{w'c_{CO_2}'}, \quad (4)$$

The model of respiration was formulated using the nonlinear regression of the nighttime CO_2 flux at sufficient turbulence ($u_* > 0.25$) versus soil temperature:

$$R_{mod} = R_{ref} Q_{10}^{(T-T_{ref})/10}, \quad (5)$$

where R_{ref} is the reference respiration at the T_{ref} of 10 degrees Celsius, Q_{10} the temperature sensitivity, and T the humus temperature. The reference respiration was recalculated inside a 15-day moving window, while the temperature sensitivity was kept constant at 2.6.

We also calculated the Net Ecosystem Exchange (NEE) and normalized NEE (NEEnorm) so that to investigate the impact of the nighttime decoupling on EC CO_2 flux:

$$NEEnorm = NEE / R_{mod} = (R_{tot} - GPP) / R_{mod}, \quad (6)$$

where NEE is the Net Ecosystem Exchange, R_{tot} the total ecosystem respiration, GPP the gross primary productivity of the ecosystem, and R_{mod} the respiration model. In practice, NEE was calculated as the sum of the EC CO_2 flux and the storage flux below EC measurement height of 23.3m.

RESULTS

Inspection of WDdiff revealed that decoupling was frequent on summer nights at our site; about 10-20% of all nighttime periods could be characterized as decoupling conditions.

We have found that the onset of decoupling conditions and change of the drainage flow depth are related to the magnitude of stability and turbulence. At low stability, subcanopy wind followed the above-canopy

wind, but at high stability, subcanopy wind was downslope even when above-canopy wind was upslope (Figure 1).

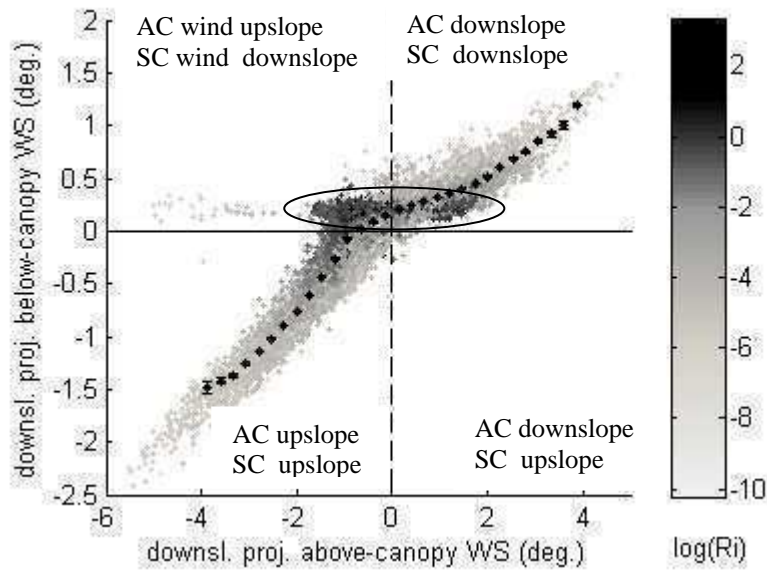


Figure 1. Downslope projected above-canopy (16.8m) wind speed versus downslope projected below-canopy (8.4m) wind speed. Color coding is done using the values of $\log(Ri)$. The black dots with the error bars are the bin-averages \pm std. The ellipsoid marks the data at high-stability, decoupling conditions (canopy-space decoupling here), where the subcanopy wind is downslope regardless of the above-canopy wind. AC – above-canopy; SC – subcanopy.

Moreover, it was found that the depth of the drainage flow increased with the increase of stability. At low and at high dynamic stability, trunk and canopy decoupling become more probable, correspondingly (Figure 2). This observation implies that stronger stability allows for the generation of a deeper decoupled layer, inside which a more powerful drainage flow can be initiated.

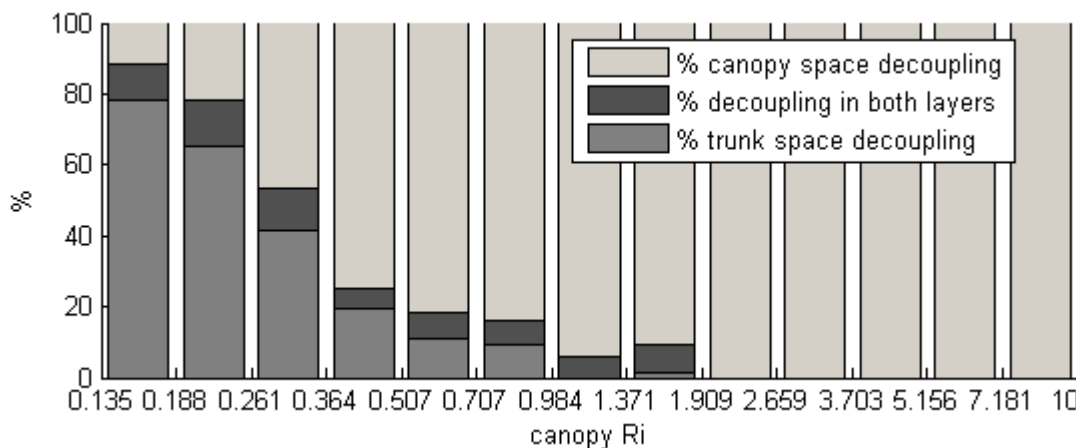


Figure 2. Occurrence of the 3 decoupling regimes (trunk, canopy and both layers) at varying canopy Ri , in percents of all periods with decoupling. While dynamic stability is low, trunk space decoupling prevails. As Ri increases, the fraction of trunk space decoupling cases drops rapidly. Cases of decoupling in both layers, when the wind direction profile is especially complex, are distributed evenly over Ri , but also vanish at $Ri > \sim 2$.

Besides that, some important quantities ($[CO_2]$ profile, temperature, long-wave radiation, EC CO_2 flux) have exhibited highly correlated behaviour during the nighttime decoupling periods. It is of special interest that the EC CO_2 flux was varying when high $WD_{diff_{3.2-8.4m}}$ and $WD_{diff_{8.4-16.8m}}$ indicated trunk and canopy space decoupling, correspondingly (Figure 3).

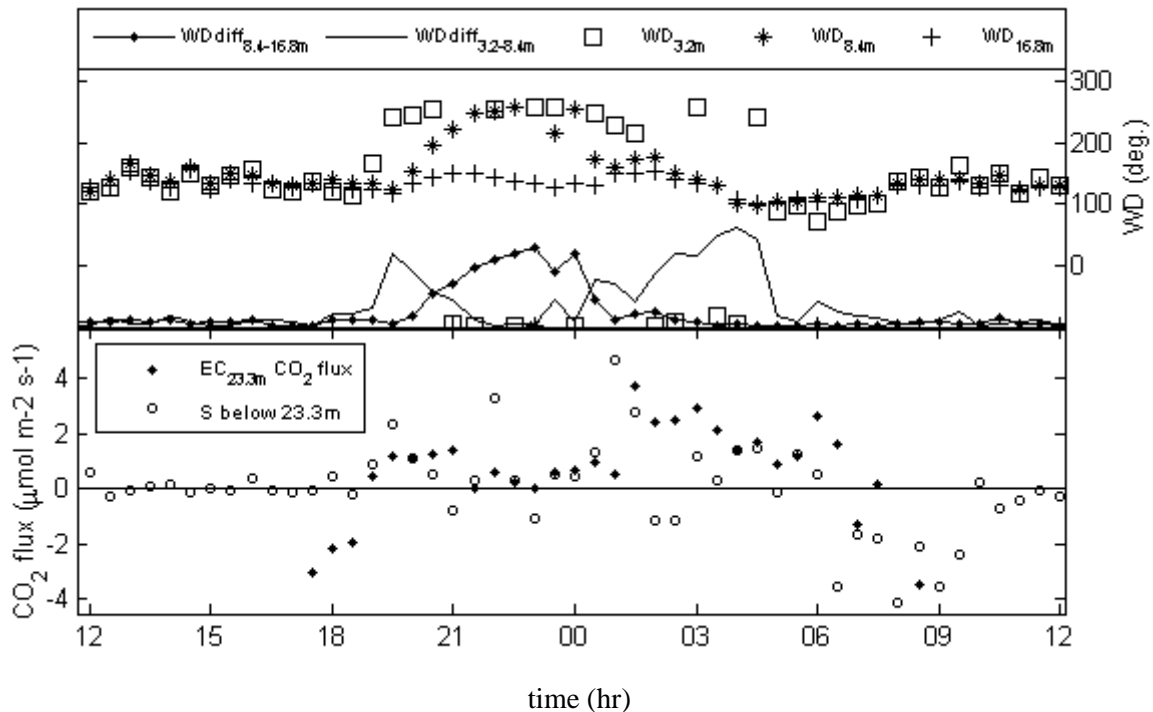


Figure 3. Casestudy of 06-07.08.04. Upper panel: wind directions at 3.2, 8.4 and 16.8m levels and WD_{diff} for the layers 3.2-8.4m and 8.4-16.8m; lower panel: EC flux and storage flux of CO_2 . WD_{diff} indicates 3 stages of decoupling: in the trunk space (19-21 PM and 01-05 AM) and in canopy space (21 PM-01 AM). Note the drop in the EC CO_2 flux during the canopy space decoupling.

CONCLUSIONS

The study has demonstrated high applicability of the wind direction profile for the nighttime decoupling detection. The decoupling regimes were clearly distinguished by the characteristic evolution of the EC CO_2 flux, stability and turbulence indicators. The changes in the depth of the decoupled layer were reflected in the variation of the turbulent CO_2 flux.

REFERENCES

- M.L. Goulden, J.W. Munger, S.-M. Fan, B.C. Daube, S.C. Wofsy (1996). Measurements of carbon sequestration by long-term eddy covariance: methods and a critical evaluation of accuracy, *Glob. Ch. Biol.* **2**, 169-182.
- L. Mahr, X. Lee, A. Black, H. Neumann, R. Staebler (2000). Nocturnal mixing in a forest subcanopy, *Agric. For. Meteorol.* **101**, 67-78.

NUMERICAL STUDY ON THE IMPORTANCE OF THE PARTICLE MIXING STATE TO CLOUD DROPLET FORMATION

T. ANTTILA¹

¹ Finnish Meteorological Institute, P.O.Box 503, FI-00101 Helsinki, Finland

Keywords: Aerosol-cloud interactions, Cloud modelling, Aerosol chemistry

INTRODUCTION

One of the open issues related to aerosol-cloud interactions is the connection between the aerosol mixing state and the cloud microphysical properties (McFiggans et al., 2006). The aerosol mixing state is related to the heterogeneity of the chemical composition of a particle distribution: internally mixed particles have similar composition whereas particles in an externally mixed population are chemically differentiated. The mixing state has relevance to the cloud formation because the ability of a particle to act as a cloud condensation nuclei (CCN) depends nonlinearly on the particle hygroscopicity and on the chemical composition in general (McFiggans et al., 2006). Consequently erroneous or simplified description of the mixing state might be reflected in the simulated or inferred properties of clouds. There are several experimental techniques that can be used to probe the aerosol mixing state, including approaches based on Hygroscopic Tandem Differential Mobility Analyzer (H-TDMA) instruments (Swietlicki et al., 2008). Here we have utilized the existing H-TDMA and size distribution data sets and employed an adiabatic air parcel model to simulate size-dependent aerosol activation. The main goal of the study is to find out how complex representation of the particle hygroscopicity and mixing state is needed to model the cloud droplet activation process accurately.

MODEL DESCRIPTION

The approach consists of the following steps: 1) specifying the particle size distribution, 2) specifying the treatment of the aerosol mixing state and hygroscopicity, 3) mapping the hygroscopicity data to the particle CCN activation properties, and 4) simulating the cloud formation process.

Size-dependent activation of particles into cloud droplets is modeled using a cloud parcel model that is described in detail by Anttila and Kerminen (2002). Briefly, the model solves equations governing the time development of a population of aerosol particles and cloud droplets in an air parcel that rises adiabatically with a constant updraft velocity. In the reference case, particles are distributed into the bins according to both their size and hygroscopicity. For each bin, the critical supersaturation needed is calculated using the approach of Rissler et al. (2004). The H-TDMA data sets were mainly taken from Swietlicki et al. (2008). Regarding the particle size distribution, four scenarios were considered: marine, continental background, rural and polluted (urban). The size distribution parameters were taken from the measurement data reported in the literature for each scenario. Finally, the results from simulations where the representation of particle mixing state and hygroscopicity were simplified were compared with the corresponding reference model runs.

RESULTS

The results show that describing the hygroscopicity and mixing state of an aerosol population by a single parameter, a size-independent water-soluble mass fraction, induced errors of up to 12% in the predicted cloud droplet number concentration (CDNC) in marine and continental background areas. Particles displayed a greater degree of external mixing in urban and rural environments compared to the marine and

continental background areas, and the error in the cloud droplet concentrations was up to 35% if the aerosol was assumed to be internally mixed. Under the internal mixture assumption, accounting for the size dependence of the particle hygroscopicity led to smaller errors in CDNC such that the errors, averaged over updraft velocity, decreased from 29 to 28% and from 15 to 11% in the urban and rural scenarios, respectively. It was also found that a computationally efficient and relatively accurate approach is to treat less and more hygroscopic particles separately using the size-averaged properties of each population. In this case, the average error in CDNC was around 12 and 13% in the urban and rural scenarios, respectively. If the size-dependence is further accounted for, the average error in CDNC decreased down to 2 and 4% in the urban and rural scenarios, respectively. Regarding other findings, the model calculations suggest that the mixing state of a particle distribution is reflected in size-resolved activation efficiency (fraction of particles activated into cloud droplets versus particle dry diameter). The results presented here thus indicate that size-resolved measurements of cloud droplet activation may provide information on the mixing state of the sampled particle population.

CONCLUSIONS

The results of this study support the notion that the particle chemical composition and mixing state play a role in CCN activation only in areas in the vicinity of urban emissions. Taken together, the results imply that numerical models focusing on the atmospheric impacts of urban pollution may benefit by using model configurations where the less and more hygroscopic particles are tracked separately, rather than assuming an internal mixture. Because of the aging processes, however, freshly-emitted particles with a high degree of external mixing make only a small contribution to the total number of climatically important particles. Therefore it is viable to hypothesize that describing the hygroscopicity of a particle population with a single parameter is sufficient for modeling cloud droplet formation in a global modeling context.

ACKNOWLEDGEMENTS

This research was supported by the Academy of Finland Center of Excellence program (project number 1118615).

REFERENCES

- Anttila, T., and V.-M. Kerminen (2002), Influence of organic compounds on cloud droplet activation - a model investigation considering the volatility, water-solubility and surface activity of organic matter, *J. Geophys. Res.* **107** (D22), 4662, doi: 10.1029/2001JD001482.
- McFiggans, G., P. Artaxo, U. Baltensperger, H. Coe, M.C. Facchini, G. Feingold, S. Fuzzi, M. Gysel, A. Laaksonen, U. Lohmann, T.F. Mentel, D.M. Murphy, C.D. O'Dowd, J.R. Snider, and E. Weingartner (2006), The effect of physical and chemical aerosol properties on warm cloud droplet activation, *Atmos. Chem. Phys.* **6**, 2593–2649.
- Rissler, J., E. Swietlicki, J. Zhou, G. Roberts M. O. Andreae, L.V. Gatti, and P. Artaxo (2004), Physical properties of the sub-micrometer aerosol over the Amazon rain forest during the wet-to-dry season transition – comparison of modeled and measured CCN concentrations, *Atmos. Chem. Phys.* **4**, 2119–2143.
- Swietlicki, E., H.-C. Hansson, K. Hameri, B. Svenningsson, A. Massling, G. McFiggans, P.H. McMurry, T. Petäjä, P. Tunved, M. Gysel, D. Topping, E. Weingartner, U. Baltensperger, J. Rissler, A. Wiedensohler, and Kulmala, M. (2008), Hygroscopic properties of submicrometer atmospheric aerosol particles measured with H-TDMA instruments in various environments - A review, *Tellus B* **60**, 432–469.

WEAKNESS OF WEEKLY WAVELETS VOID INDIRECT WEEKEND EFFECT

A. Asmi

Dept of Physics, University of Helsinki, Finland

Keywords: CCN, Wavelets, Weekend-effect

INTRODUCTION

We have studied the background of so called aerosol "weekend-effect", or aerosol emission influence on the regional meteorology, using multi-station European long-time measurements of number size distributions of CCN-sized aerosol particles and CCNs. With notably rare exceptions we could not find weekly cycle in in CCN or CCN proxy number concentrations, suggesting the CCN-sized aerosol number concentrations are too homogeneous to produce strong indirect-effect based weekend effect.

METHODS

As the datasets for actual CCN concentrations were not available, we constructed different CCN analogies from more widely measured aerosol number size distributions. The idea was to follow (Asmi et al., 2011) in general approach and calculated from the size distributions different cut-off diameters to represent potential cut-off diameters of CCN activation. These approaches do not take into account particle composition and are thus non-ideal proxies for the CCN numbers, but are consistent with many modelling approaches.

We used as the main dataset the dataset from three boundary layer low-land stations in Germany and Northern Europe, namely Pallas (Lihavainen et al., 2008) and SMEAR II (Hyytiälä) (Hari and Kulmala, 2005) stations in Northern and Southern Finland respectively and Melpitz station (Engler et al., 2007) in Eastern Germany. The stations were chosen for their long-period continuous measurements of size distribution. The data was collected from EBAS web-interface (ebas.nilu.no) and from the station operators. As additional data source, we used the field data from two years of measurements in low-land EUSAAR and GUAN stations as described in (Asmi et al., 2011).

From the size distributions, we calculated some representative "CCN-sized" concentrations of aerosols. Three overlapping size ranges were used: 50-500 nm (N_{50}), 100-500 nm (N_{100}) and 250-500 nm (N_{250}). The upper limit of 500 nm was due instrumental limitations. In addition to these, the air-parcel model calculated CDNC numbers were calculated from the size distribution ($CDNC_{ap}$) and for SMEAR II station, the measured CCN number at water supersaturation of $S=0.04$ was used ($NCCN_{0.04}$). See Appendix A for details of the measurements, initial data preparation and instrumentation used. We used years 2009–2010 data for the analysis on NCCN.

The data was then tested against a series of statistical significance tests. Concentration histogram tests were done to show if there is a statistically significant difference between mean weekday concentrations of three concentration ranges N_{50} , N_{100} and N_{250} . We separated the datasets by weekdays and calculated histograms of concentrations for each weekday. The test was done for all-year datasets and separately for seasonal (DJF, MAM, JJA, SON) subsets of the data. The test used was Kruskal-Wallis non-parametric test (Kruskal and Wallis, 1957) with null hypothesis that the mean concentrations of weekdays were all from the same distribution with similar median

and shape. The daily means were used to remove the high autocorrelation of measurements done in the same day.

The statistical tests of concentration histograms was not supportive of a strong weekend effect either CCN proxy or NCCN number concentrations. None of the tests for concentrations studied could reject the null hypothesis ($p=0.05$), and thus there is no reason to believe at least statistically significant differences between weekdays in the concentrations studied, even in seasonal datasets. The closest to rejecting null hypothesis was NCCN_{0.04} data with $p=0.13$ for all-season dataset, with Sunday concentrations being smaller than other weekdays. We further extended our analysis to 1-2 year data from additional 21 stations around Europe from (Asmi et al., 2011), but with similar results - only 6 of 315 statistical tests (21 stations, 4 seasons + all seasons, 3 size ranges). Based on these test results, we can conclude that there is no strong consistent difference between weekday concentrations of CCN-sized particles in regional background of European boundary layer.

Even though there is no strong variation between weekdays in seasonal or annual medians or histogram shapes, there is a possibility of an intermittent signal in weekly periodicity. To find such signals, spectral analytic methods can be used to extract signal from background noise. However, using a pure spectral analysis could be also misleading, as many signals could also be from natural sources, or just occurring from random fluctuations in the atmosphere, or instrumental noise. For this reason, we considered a "weekend" cycle to only occur if two consecutive tests could be passed: 1) The observed periodicity should be statistically significantly over the background noise level, determined from the sampling-time variance and autocorrelation; and (2) the observed signal should also be consistently connected to specific weekdays. The first test shows that the signal is unlikely from random fluctuations, and the second connects it to anthropogenic sources. We used the wavelet analysis for the datasets from the 3 main stations. The comparison spectrum for spectral analysis was modified red-noise spectrum. However, the tests done do not show any 7-day variability, detectable above the background noise, for any of the concentrations studied, effectively making any further tests for weekly variability unnecessary.

CONCLUSIONS

The lack of CCN number weekly cycle does not support indirect-effects based weekly cycle in European meteorology, at least in regional background environment. There are still potential for such cyclicities based on the methodological limitations of current measurements, mostly on particle composition (hygroscopicity), optical properties and changes in giant CCNs. Also differences between surface concentrations and cloud base aerosol concentrations could affect the actual aerosol-cloud interactions.

We also conclude that the overall lack of reliable long-term measurements of CCN number concentrations and overall aerosol number size spectra between 0.5 and 2 μm hamper the studies for potential aerosol-cloud interactions in European boundary layer.

ACKNOWLEDGEMENTS

This work has been partially funded by EUSAAR (Contract No. RII3-CT-2006-026140) and EU-CAARI, (Contract no 36833) projects of the 6th Framework programme of European Commission. The financial support by the Academy of Finland Centre of Excellence program (project no 1118615) is gratefully acknowledged. The help of EUSAAR and GUAN station managers is highly appreciated, especially from Prof. M. Kulmala, Dr. P. Aalto and Mr. M. Paramonov (SMEAR II station), Dr. A. Wiedensohler and Dr. W. Birmili (Melpitz station) and Dr. H. Lihavainen and Dr. E. Asmi (Pallas station). Wavelet software was provided by C. Torrence and G. Compo.

REFERENCES

- Asmi, A., Wiedensohler, A., Laj, P., Fjaeraa, A.-M., Sellegri, K., Birmili, W., Weingartner, E., Baltensperger, U., Zdimal, V., Zikova, N., Putaud, J.-P., Marinoni, A., Tunved, P., Hansson, H.-C., Fiebig, M., Kivekäs, N., Lihavainen, H., Asmi, E., Ulevicius, V., Aalto, P. P., Swietlicki, E., Kristensson, A., Mihalopoulos, N., Kalivitis, N., Kalapov, I., Kiss, G., de Leeuw, G., Henzing, B., Harrison, R. M., Beddows, D., O'Dowd, C., Jennings, S. G., Flentje, H., Weinhold, K., Meinhardt, F., Ries, L., and Kulmala, M. (2011). Number size distributions and seasonality of submicron particles in Europe 2008-2009. *Atmospheric Chemistry and Physics Discussions*, 11(3):8893–8976.
- Engler, C., Rose, D., Wehner, B., Wiedensohler, A., Brüggemann, E., Gnauk, T., Spindler, G., Tuch, T., and Birmili, W. (2007). Size distributions of non-volatile particle residuals ($d_p < 800$ nm) at a rural site in germany and relation to air mass origin. *Atmospheric Chemistry and Physics*, 7(22):5785–5802.
- Hari, P. and Kulmala, M. (2005). Station for measuring Ecosystem-Atmosphere relations (SMEAR II). *Boreal Env. Res.*, 10:315–322.
- Kruskal, W. H. and Wallis, W. A. (1957). Use of ranks in one-criterion variance analysis. *Journal of the American Statistical Association*, 47(260):583–621.
- Lihavainen, H., Kerminen, V.-M., Komppula, M., Hyvrinen, A.-P., Laakia, J., Saarikoski, S., Makkonen, U., Kivekäs, N., Hillamo, R., Kulmala, M., and Viisanen, Y. (2008). Measurements of the relation between aerosol properties and microphysics and chemistry of low level liquid water clouds in northern finland. *Atmospheric Chemistry and Physics*, 8(23):6925–6938.

ATMOSPHERIC SECONDARY PARTICLE FORMATION IN PALLAS 2000-2011

E. ASMI¹, N. KIVEKÄS¹, M. KOMPPULA¹, A.-P. HYVÄRINEN¹, J. HATAKKA¹, Y. VIISANEN¹ and H. LIHAVAINEN¹

¹Finnish Meteorological Institute, Erik Palménin aukio 1, 00560 Helsinki, Finland

Keywords: PARTICLE FORMATION AND GROWTH, ARCTIC AEROSOL, DMPS, LONG-TERM TRENDS.

INTRODUCTION

Secondary new particle formation (NPF) has been recognised as an important source of atmospheric aerosol particles worldwide (Kulmala *et al.* 2004). Yet, there are numerous open questions on how this process proceeds or what its climatic importance at different geographic regions is. These questions relate to e.g. particle formation mechanisms, compounds involved in the process, environmental boundaries required as well as the ability of freshly formed tiny particles to grow up to the sizes of climatic relevance. To contribute for answering these questions, we analysed nearly 11-years (April 2000 – December 2010) of continuous measurement data from Finnish sub-Arctic GAW (Global Atmospheric Watch) station Pallas with the focus on NPF events. We classified the days into NPF event, undefined and non-event days following Dal Maso *et al.* (2005), determined the particle formation and growth rates, examined which factors (air mass properties, local meteorology, condensation sink, sulphuric acid concentration, etc.) promote or hinder particle formation, analysed the long-term trends, and in addition, the probability of particles to grow up to the CCN (Cloud Condensation Nuclei) sizes.

METHODS

The analysis of NPF relied on Differential Mobility Particle Sizer (DMPS) measurements on particle number size distributions (Komppula *et al.* 2003). From the measured distributions, we determined the particle formation and growth rates following the procedure presented in Komppula *et al.* (2003). Auxiliary data on local meteorological variables, as well as on air mass backward trajectories, calculated with FLEXTRA (Stohl *et al.* 1995), were used. Sulphuric acid has been suggested to be a key parameter in atmospheric NPF, and while lacking the direct measurement of H₂SO₄, we used a proxy based on global radiation, condensation sink (CS) and SO₂ (Petäjä *et al.* 2009).

RESULTS

Seasonal variation of NPF events was congruent with previous studies, showing a spring maximum and a winter minimum (Komppula *et al.* 2003). Equally, NPF was found to be favoured by clean Arctic air masses and bright, sunny weather. The observed seasonal trend was by a large part explained by inter-annual changes in climatic and meteorological conditions. Monthly median growth rates varied within the limits of 1.9 and 4.6 nm h⁻¹, being highest in summer months, and as such providing evidence of the significance of organic vapours for the particle growth. It was calculated that in all seasons a major fraction of the particle growth could not be explained by the sulphuric acid alone. To get further evidence on the contribution of organics for the particle growth, biogenic emissions for marine and mixed air masses were estimated similarly as in Tunved *et al.* 2006. In general, the growth rate showed increase with biogenic emissions, as expected (Fig. 1.)

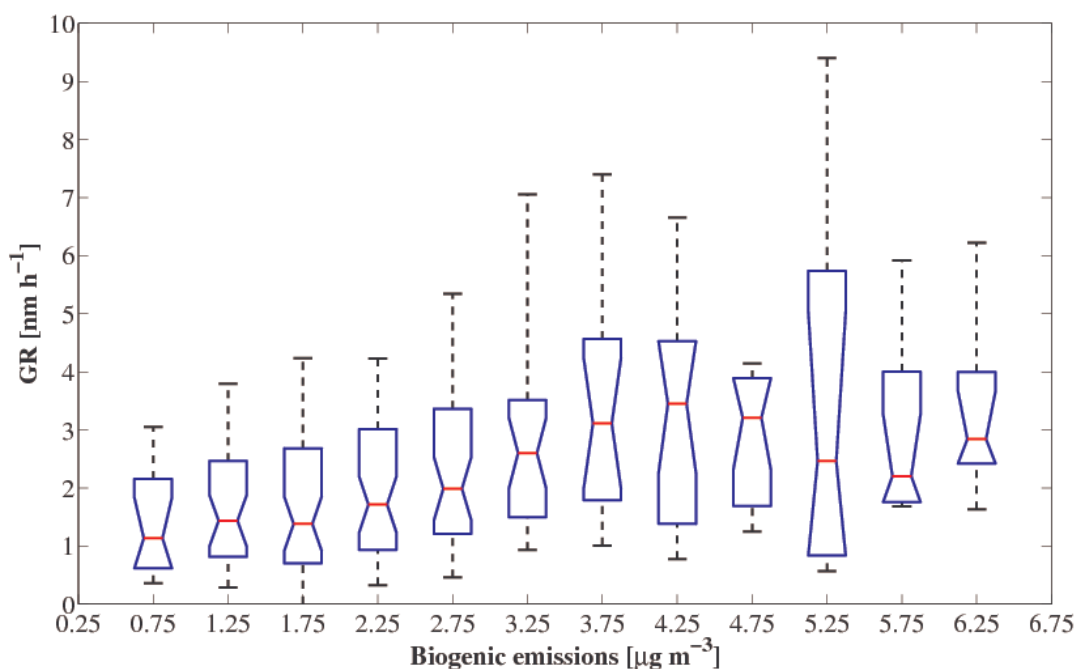


Figure 1. Particle growth rate as a function of biogenic emissions for marine and mixed air masses.

The inter-annual trend of NPF days versus non-event days suggests a decrease in the beginning of the decade and vice versa, increases in the end of the decade (Fig. 2). As the external climatic and meteorological quantities seemed to predict the NPF occurrence fairly well, we developed a proxy for NPF based on air mass origin, visibility and global radiation. It however turned out that this proxy was insufficient for predicting the inter-annual trend and thus other non-specified factors played a role in particle formation, our best guess of these being the quantity of nucleating or condensable vapours. This idea was supported by the similar inter-annual trend in particle growth rates (not shown).

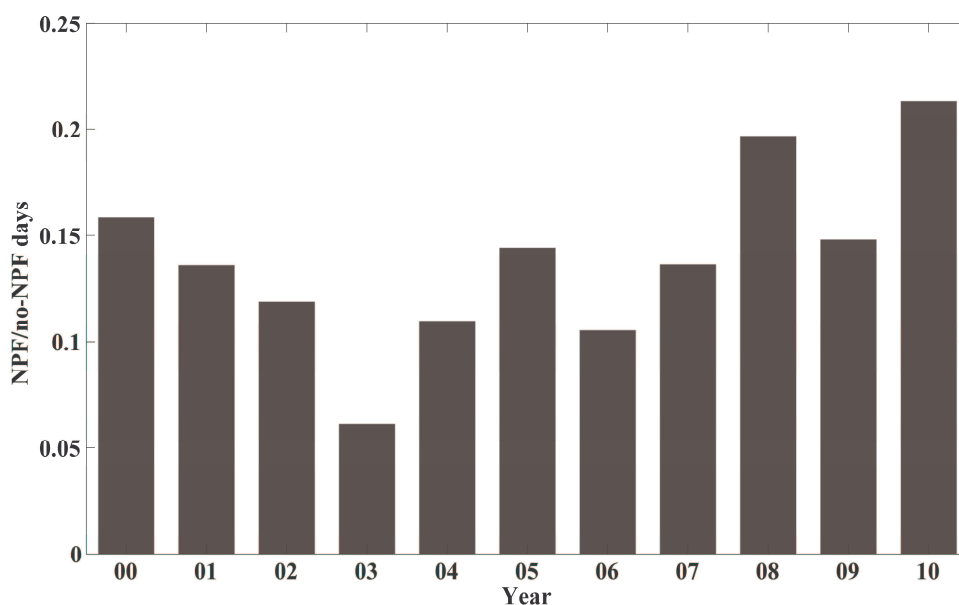


Figure 2. NPF days vs. non-event days – 11 year trend.

Finally, the climatic impact of NPF was examined by separating the events with the growing mode exceeding 80 nm size, previously found to be a good approximation of CCN size limit in Pallas (Komppula et al 2005). In 34% of the class I (for definition, see Dal Maso *et al.* 2005) events this limit was reached with the maximum probability of CCN₈₀ formation in summer season. This is in agreement with the higher growth rates observed in summer. We may conclude on the climatic importance of NPF that while the observable CCN₈₀ formation from NPF was infrequent, its impact on CCN number was large; the average increase in CCN₈₀ number by NPF was 211 %.

CONCLUSIONS

Based on over 10-years of continuous measurements in sub-Arctic Pallas station, following can be concluded on the observed new particle formation (NPF) events: 1) NPF has clear seasonal cycle, with maximum in spring and minimum in winter, 2) organic vapours from boreal forests seem to be mainly responsible for the particle growth and 3) if growth up to CCN sizes is observed, NPF increases CCN numbers significantly (over 3-fold).

ACKNOWLEDGEMENTS

This work was conducted as a part of the Finnish Centre of Excellence in Physics, Chemistry, Biology and Meteorology of Atmospheric Composition and Climate Change.

REFERENCES

- Dal Maso, M., Kulmala, M., Riipinen, I., Wagner, R., Hussein, T., Aalto, P.P. and Lehtinen K.E.J. (2005). Formation and growth of fresh atmospheric aerosols: eight years of aerosol size distribution data from SMEAR II, Hyytiälä, Finland, *Boreal Environ. Res.* **10**, 323-336.
- Komppula, M., Lihavainen, H., Kerminen, V.-M., Kulmala, M. and Viisanen, Y. (2005). Measurements of cloud droplet activation of aerosol particles at a clean subarctic background site. *J. Geophys. Res.* **110**(D06204), doi: 10.1029/2004JD005200.
- Komppula, M., Lihavainen, H., Hatakka, J., Paatero, J., Aalto, P., Kulmala, M. and Viisanen, Y. (2003). Observations of new particle formation and size distributions at two different heights and surroundings in subarctic area in northern Finland. *J. Geophys. Res.* **108**(D9), 4295.
- Kulmala, M., Vehkamäki, H., Petäjä, T., Dal Maso, M., Lauri, A., Kerminen, V.-M., Birmili, W. and McMurry, P.H. (2004). Formation and growth rates of ultrafine atmospheric particles: A review of observations, *J. Aerosol Sci.* **35**, 143-176.
- Petäjä, T., Mauldin III, R.L., Kosciuch, E., McGrath, J., Nieminen, T., Paasonen, P., Boy, M., Adamov, A., Kotiaho, T. and Kulmala M. (2009). Sulfuric acid and OH concentrations in a boreal forest site, *Atmos. Chem. Phys.* **9**, 7435-7448.
- Stohl, A., Wotawa, G., Seibert, P. and Kromp-Kolb, H. (1995). Interpolation errors in wind fields as a function of spatial and temporal resolution and their impact on different types of kinematic trajectories, *J. Appl. Meteor.* **34**, 2149-2165.
- Tunved, P., Hansson, H.-C., Kerminen, V.-M., Ström, J., Dal Maso, M., Lihavainen, H., Viisanen, Y., Aalto, P.P., Komppula, M. and Kulmala, M. (2006). High natural aerosol loading over boreal forests, *Science* **312**, 261-263.

A STUDY OF AEROSOL PRODUCTION AT THE CLOUD EDGE WITH DNS

N. BABKOVSKAIA¹, M. BOY¹, S. SMOLANDER¹, S. ROMAkkANI², M. KULMALA¹

¹ Department of Physical Sciences, University of Helsinki, Finland.

² Department of Physical Sciences, University of Kuopio, Finland.

Keywords: aerosol production, cloud physics, DNS.

Spatial distribution of aerosol particles, turbulent mixing of clouds with the environment, the influence of turbulence on aerosol dynamics (and vice versa) are the key issues in the study of aerosol clouds. One of the possible ways of understanding these issues is to use direct numerical simulations (DNS).

In this project we use a high-order public domain finite-difference code for compressible hydrodynamic flows (Pencil Code, 2001). The code advances the equations in non-conservative form. The degree of conservation of mass, momentum and energy can then be used to assess the accuracy of the solution. The code uses six-order centered finite differences. For turbulence calculation we normally use the RK3-2N scheme for the time advancement. This scheme is of Runge - Kutta type, third order. On a typical processor, the cache memory between the CPU and the RAM is not big enough to hold full three-dimensional data arrays. Therefore, the Pencil Code has been designed to evaluate first all the terms on the right-hand sides of the evolution equations along a one-dimensional subset (pencil) before going to the next pencil. This implies that all derived quantities exist only along pencils. Only in exceptional cases do we allocate full three-dimensional arrays to keep derived quantities in memory.

The code is highly modular and comes with a large selection of physics modules. Recently, a detailed chemistry module has been implemented, including an accurate description of all necessary quantities, such as diffusion coefficients, thermal conductivity, reaction rates etc (N. Babkovskaia et al., 1975). This module was well tested by using the commercial code for calculation of the turbulent combustion process (Chemkin). The other module with description of the aerosol dynamics is also completed now. The implemented material is prepared for calculating an evaporation and condensation processes of aerosol particles, which consists of a solid core covered by liquid water.

Since initially the Pencil Code was elaborated for studying turbulent motions, it is well suitable to modeling the fluid mechanical processes in the atmospheric clouds. Additionally, due to an accurate description of the chemistry, the Pencil Code is a powerful tool for studying the aerosol dynamics in a turbulent medium with complicated chemical composition.

In this project we study the activation process at the cloud edge. We consider the flux of aerosol particles of the size of 100 nm, which goes through the boundary between the dry and wet air. For test purposes we start from a 0-D problem and take into account the condensation and evaporation of the aerosol particles covered by liquid water. Initially we take a lognormal distribution of particles and supersaturation of 0.1 - 0.3 %. After several seconds we get a splitting of the initial distribution into two peaks. This results is in a good agreement with the theory of aerosol dynamics (Seinfeld and Pandis, 2006).

Next we consider a one dimensional problem and study the motion and evolution of the front between the dry and wet air. The dry air flux (supersaturation is 0 %) with 1000 aerosol particles is coming into the domain with an inlet velocity of 0.3 m/s and interacts with a wet cloud edge.

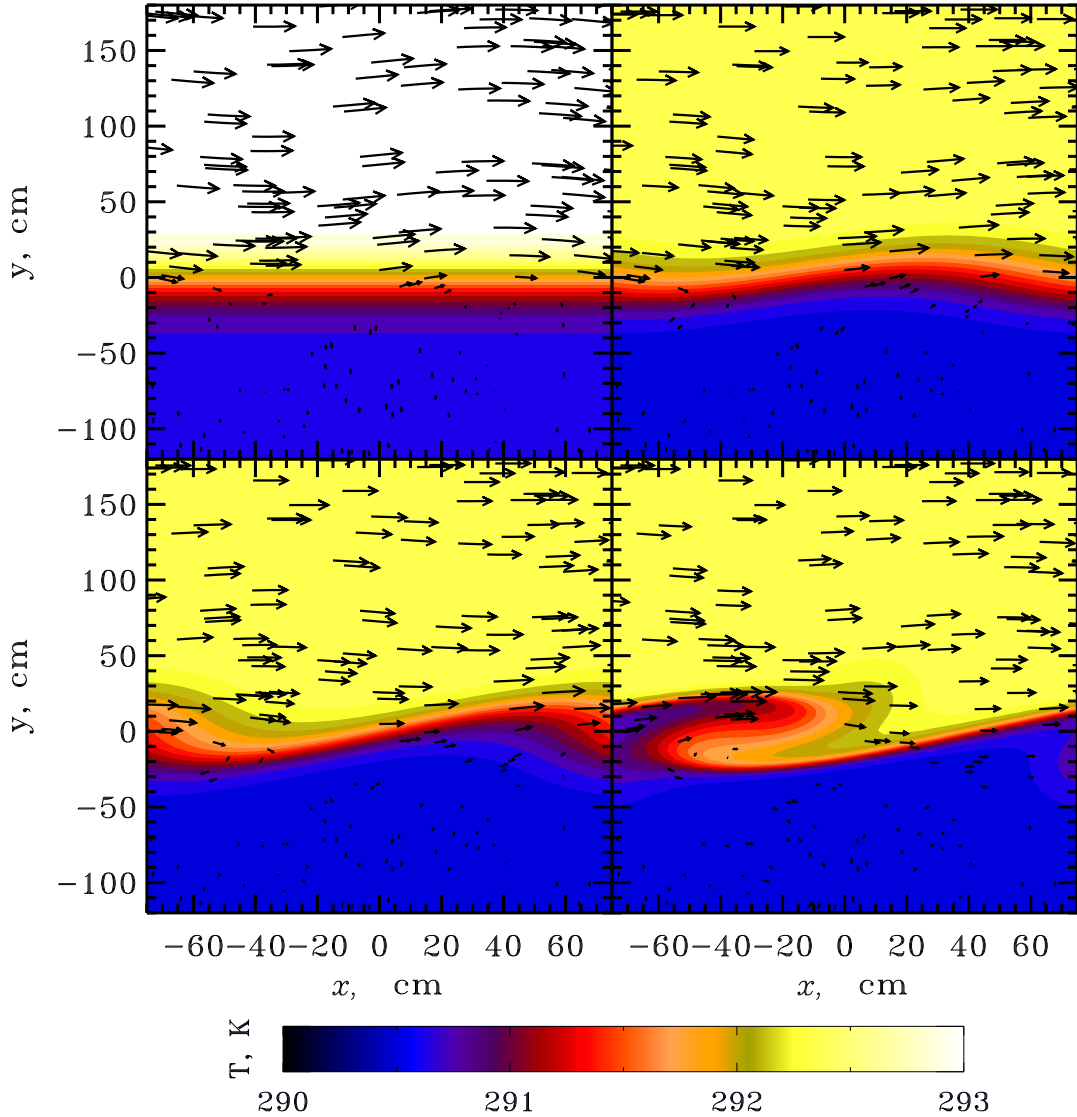


Figure 1: Velocity and temperature fields in the 2D calculated domain at $t = 0$ s (*upper left panel*), $t = 0.8$ s (*upper right panel*), $t = 0.16$ s (*lower left panel*) and $t = 3.2$ s (*lower right panel*).

This approach allows us to analyze the effect of the fluid mechanics on the aerosol dynamics (and vice versa) in a laminar regime.

Finally, we consider a two dimensional problem with a more complicated velocity field at the cloud edge. We assume that the dry air flux is coming in the middle of the computational domain and coming out at its boundaries (see Figure 1). After several seconds the cloud edge is transformed and we analyze the final distribution of the aerosol particles there. In Figure 2 we present the distribution of $0.2 \mu\text{m}$, $0.4 \mu\text{m}$, $1.1 \mu\text{m}$ and $1.6 \mu\text{m}$ particles at $t = 1.6$ s. One can see that the large particles are located at the cloud edge, that is in a good agreement with the observational data.

Comparing the result of one dimensional and two dimensional simulations we conclude that in both models particle distribution inside a boundary between wet and dry air are very close, if the cloud edge is not destroyed because of the complicated gas motion. In a case of destroyed cloud edge the further study is needed.

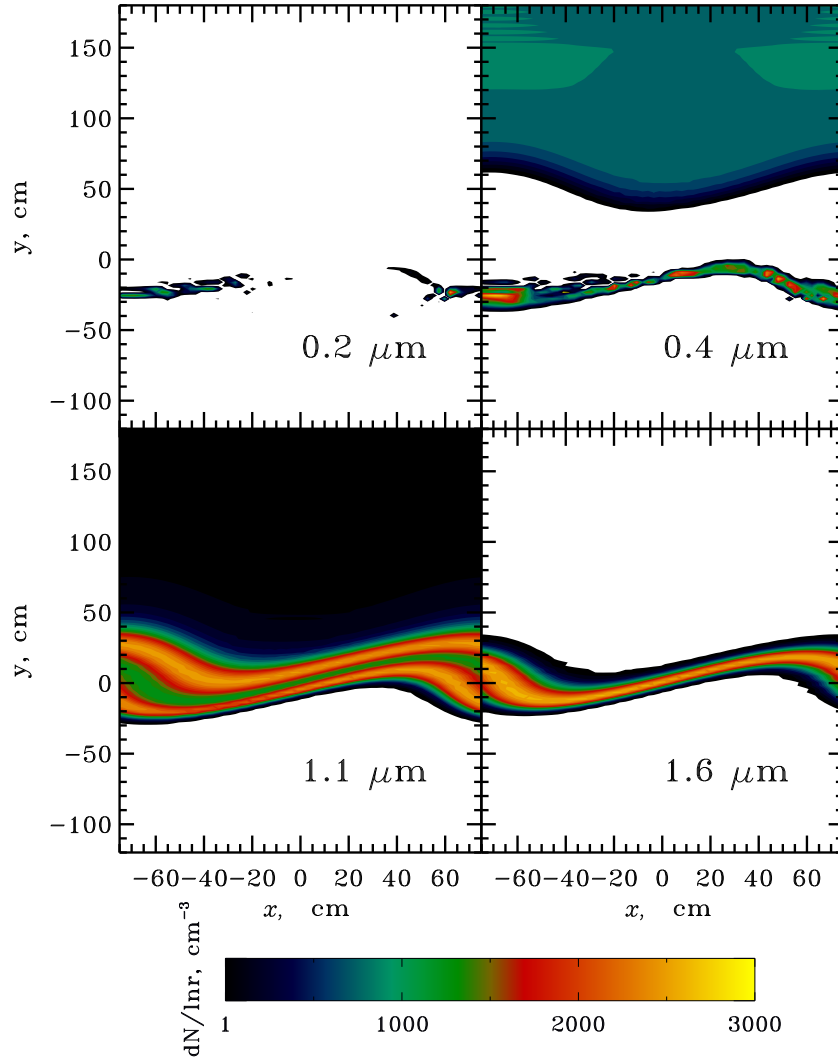


Figure 2: 2D distributions of $0.2 \mu\text{m}$ (upper left panel), $0.4 \mu\text{m}$ (upper right panel), $1.1 \mu\text{m}$ (lower left panel) and $1.6 \mu\text{m}$ (lower right panel) at $t = 1.6 \text{ s}$.

REFERENCES

The Pencil Code, <http://pencil-code.googlecode.com>, (2001).

Seinfeld, J. H. and Pandis S. N., (2006). *Atmospheric chemistry and physics: From Air pollution to Climate Change*. (John Wiley & Sons, Inc).

Babkovskaia, N., Haugen, N., Brandenburg, A. (2011). A high-order public domain code for direct numerical simulations of turbulent combustion. *J. of Computational Physics*, **230**, 1.

MEASURING OPTICAL PROPERTIES AND SIZE DISTRIBUTIONS AT SÃO PAULO, BRAZIL: NEW PARTICLE FORMATION EVENTS OCCUR AT THE SITE

J. BACKMAN¹, L.V. RIZZO², T. PETÄJÄ¹, H.E. MANNINEN¹, T. NIEMINEN¹, J. HAKALA¹, P.P. AALTO¹, E. SIIVOLA¹, F. MORAIS³, R. HILLAMO⁴, P. ARTAXO³, and M. KULMALA¹

¹Division of Atmospheric Sciences, Department of Physics, University of Helsinki, Finland

²Department of Earth and Exact Sciences, Federal University of São Paulo, Brazil

³Institute of Physics, University of São Paulo, Brazil

⁴Finnish Meteorological Institute, Helsinki, Finland

Keywords: AIR QUALITY, BIOFUELS, MEGACITIES, NUMBER SIZE DISTRIBUTIONS

INTRODUCTION

Atmospheric aerosols have been shown to affect human health and well-being (Nel, 2005). They also influence visibility and the radiation balance as they scatter (Cabada, Khlystov, Wittig, Pilinis, & Pandis, 2004) and absorb (M. Z. Jacobson, 2001) solar radiation. Atmospheric aerosols and trace gases are tightly connected via physical, chemical and meteorological processes. New ethanol based fuels for the world's vehicular fleet have been developed to reduce the dependence on fossil fuel, as well as to reduce carbon dioxide emissions. However, little is still known about their impacts on human health, air quality and climate (Farrell, 2006; M. Z. Jacobson, 2007). Megacities cover a relatively small area of land, but they are a significant source of anthropogenic emissions to the total pollution budget by mankind. At MASP, it has been estimated that out of the 7.2 million passenger and commercial vehicles 55 % of the burnt fuel is alcohol (CETESB, 2007). The addition of ethanol to vehicle fuels reduces carbon monoxide emissions but results in increased aldehyde emissions resulting in a photochemical smog problem (Graham, Belisle, & Baas, 2008; Haagensmit, 1952; Seinfeld & Pandis, 2006). The vehicular fleet accounts for roughly 80 % of the hydrocarbon (HC) emissions which are subsequently oxidised in the atmosphere resulting in products with low enough vapour pressures to be found in the condensed phase.

The aim of this study is to characterize number size distributions and total number concentrations of sub-micron particulate matter in MASP, as well as the optical properties. The aim is to continue the measurements for up to a year revealing diurnal patterns along with seasonal cycles and wintertime inversion induced pollution events. The observations reported here were taken as a part of the BIOFUSE project ("The effects of intensive BIO-Fuel production and USE on regional air quality and global climate", a cooperation between the University of Helsinki (UHEL), University of São Paulo (USP), and the Finnish Meteorological Institute (FMI).

MEASUREMENTS

The measurement site is located roughly 10 km from the city centre, at the western edge of the most densely populated area. São Paulo city is surrounded by vast suburban areas populated by 20 million people, resulting in the world 7th biggest metropolitan area. It is located in the Armando Salles de Oliveira campus area of USP. The campus area is vast, totalling an area of 7.4 km², making the site ideal for tracking the urban ambient particulate pollutants without the uncertainty and noise of local sources. The city of São Paulo is located on a plateau of 860 meters above sea level (a.s.l.) surrounded by hills rising up

to about 1200 meters a.s.l. The measurement equipment sits inside a temperature controlled room at the roof of a four story building.

The measurement equipment at the site are a dual-flow differential mobility particle sizer (DMPS) and a Neutral cluster and Air Ion Spectrometer (NAIS) measuring number size distributions from 6 to 800 nm and 0.8 to 42 nm respectively. In addition there are a three wavelength TSI Inc. 3563 three wavelength nephelometer and a Thermo Scientific Multi Angle Absorption Photometer (MAAP) measuring light scattering and absorption coefficients respectively.

RESULTS

New particle formation events have been observed all over the world, from pristine atmospheric conditions like Antarctica, to heavily polluted environments like Mexico City (Dunn et al., 2004) to oceanic new particle formation events in the South Pacific (Kulmala et al., 2004 and references there in). Here we present the first measured new particle formation events measured in São Paulo, Brazil (Figure 1).

The occurrence of new particle formation (NPF) depends on the competition between the initial growth of the nuclei and their scavenging by the pre-existing particulate pollution (Kulmala et al., 2005). When the condensation sink (CS) is low, also small condensable vapour source rates are able to produce enough material for the small particles to form and grow. However, when the CS is large, the source rate needed for the particles to grow and to survive to observable sizes need to be substantially larger (Kulmala et al., 2005). In this study we show that the new particle formation events also occur in heavily polluted areas such as São Paulo, Brazil. While the CS can be a limiting factor for new particle formation, the fact that these events are observed at heavily polluted areas demonstrates that a large abundance of condensable vapours can result in new particle formation events. New particle formation events has also been seen in New Delhi, India (Mönkkonen et al., 2005), Beijing, China (Wehner et al., 2004) and Mexico City, Mexico (Dunn et al., 2004).

During the first month a total of seven new particle formation events were observed with growth rates ranging from 9 to 25 nm h⁻¹. During these events the condensation sink, vapour abundance explaining the growth, and vapour production rates were calculated. Interestingly enough there were also events where condensed vapours were evaporating from the condensed phase thus shrinking the size of the particles in all sizes.

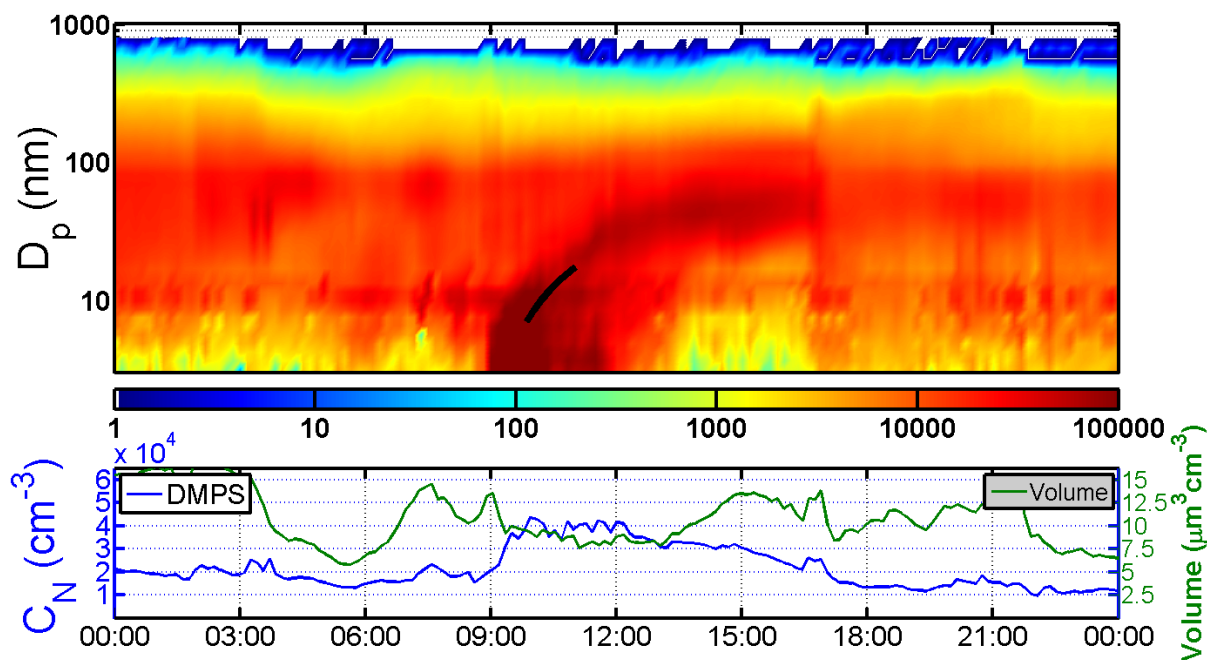


Figure 1. The first nucleation event measured on the 2nd of November 2010. The growth rate of 9.3 nm h⁻¹ was calculated using DMPS data from 6 to 20 nm indicated by the black line.

CONCLUSIONS

During the first three months we have observed seven new particle formation events in Sao Paolo, Brazil. From four of these growth rates could be calculated ranging from 9 – 25 nm h⁻¹. From these events we could calculate the vapour abundance explaining the growth of the particles and the production rate of the vapour to sustain the growth. We found that the condensation sink (CS) during the events were double that of pristine conditions but lower than in the heavily polluted New Delhi in India. Similarly the vapour abundance of the nucleating vapours and their production rate in São Paulo much was less than New Delhi in India but greater than the pristine conditions of the boreal forests of Nordic countries.

ACKNOWLEDGEMENTS

The effects of intensive BIO-Fuel production and USE on regional air quality and global climate (BIOFUSE) was supported by the Academy of Finland's Sustainable Energy Research Programme (SusEn) and by the Brazilian National Council for Scientific and Technological Development (CNPq). The financial support by the Academy of Finland Centre of Excellence program (project no 1118615) is also gratefully acknowledged.

REFERENCES

- Cabada, J. C., Khlystov, A., Wittig, A. E., Pilinis, C., & Pandis, S. N. (2004). Light scattering by fine particles during the pittsburgh air quality study: Measurements and modeling. *Journal of Geophysical Research-Atmospheres*, 109(D16), D16S03. doi:10.1029/2003JD004155
- CETESB. (2007). Relatório de qualidade das águas interiores do estado de são paulo No. 2007). São Paulo: CETESB.

- Dunn, M. J., Jimenez, J. L., Baumgardner, D., Castro, T., McMurry, P. H., & Smith, J. N. (2004). Measurements of Mexico City nanoparticle size distributions: Observations of new particle formation and growth. *Geophysical Research Letters*, 31(10), L10102. doi:10.1029/2004GL019483
- Farrell, A. E. (2006). Ethanol can contribute to energy and environmental goals (vol 311, pg 506, 2006). *Science*, 312(5781), 1748-1748.
- Graham, L. A., Belisle, S. L., & Baas, C. (2008). Emissions from light duty gasoline vehicles operating on low blend ethanol gasoline and E85. *Atmospheric Environment*, 42(19), 4498-4516. doi:10.1016/j.atmosenv.2008.01.061
- Haagensmit, A. J. (1952). Chemistry and physiology of Los Angeles smog. *Industrial and Engineering Chemistry*, 44(6), 1342-1346.
- Jacobson, M. Z. (2001). Strong radiative heating due to the mixing state of black carbon in atmospheric aerosols. *Nature*, 409(6821), 695-697.
- Jacobson, M. Z. (2007). Effects of ethanol (E85) versus gasoline vehicles on cancer and mortality in the United States. *Environmental Science & Technology*, 41(11), 4150-4157. doi:10.1021/es062085v
- Kulmala, M., Petaja, T., Monkkonen, P., Koponen, I. K., Dal Maso, M., Aalto, P. P., et al. (2005). On the growth of nucleation mode particles: Source rates of condensable vapor in polluted and clean environments. *Atmospheric Chemistry and Physics*, 5, 409-416.
- Kulmala, M., Vehkamäki, H., Petaja, T., Dal Maso, M., Lauri, A., Kerminen, V. M., et al. (2004). Formation and growth rates of ultrafine atmospheric particles: A review of observations. *Journal of Aerosol Science*, 35(2), 143-176. doi:10.1016/j.jaerosci.2003.10.003
- Mönkkönen, P., Koponen, I. K., Lehtinen, K. E. J., Hameri, K., Uma, R., & Kulmala, M. (2005). Measurements in a highly polluted Asian mega city: Observations of aerosol number size distribution, modal parameters and nucleation events. *Atmospheric Chemistry and Physics*, 5, 57-66.
- Nel, A. (2005). Air pollution-related illness: Effects of particles. *Science*, 308(5723), 804-806. doi:10.1126/science.1108752
- Seinfeld, J. H., & Pandis, S. N. (2006). *Atmospheric chemistry and physics - from air pollution to climate change* (2nd edition) John Wiley & Sons.
- Wehner, B., Wiedensohler, A., Tuch, T. M., Wu, Z. J., Hu, M., Slanina, J., et al. (2004). Variability of the aerosol number size distribution in Beijing, China: New particle formation, dust storms, and high continental background. *Geophysical Research Letters*, 31(22), L22108. doi:10.1029/2004GL021596

Characteristics of global aerosol optical depth simulated with microphysical models SALSA and M7 within ECHAM5-HAM

T. BERGMAN¹, H. KOKKOLA¹, R. MAKKONEN², V-M. KERMINEN³, M. KULMALA² and K. LEHTINEN^{1,4}

¹ Finnish Meteorological Institute, FI-70211, Kuopio, Finland

²University of Helsinki, Department of Physics, FI-00014, Helsinki, Finland

³Finnish Meteorological Institute, FI-00101, Helsinki, Finland

⁴University of Eastern Finland, Dept. Physics and Mathematics, FI-70211, Kuopio, Finland

Keywords: aerosol, optical depth, aerosol-climate model, global modeling

INTRODUCTION

Aerosols affect the radiative balance of atmosphere through multiple mechanisms. Aerosols absorb and scatter radiation and by acting as cloud condensation nuclei they can alter the radiative characteristics of clouds. The impact of aerosols in the atmosphere persists to have large uncertainties. Global climate models generally describe aerosols with modal or moment approaches. However, sectional models enable more flexibility in terms of describing the aerosol size distribution and the particle size dependent chemical composition, which have implications in e.g. aerosols' ability to form cloud droplets. By selection of significant microphysical processes and with increasing computational power sectional models are a viable choice for representation of aerosols within global atmospheric models.

METHODS

We have implemented a sectional aerosol model SALSA (Sectional Aerosol module for Large Scale Applications) by Kokkola et al. (2008) within the ECHAM5-HAM (Stier et al. 2005) aerosol-climate model. We compare the optical depths simulated with SALSA and with the original ECHAM5-HAM aerosol model M7 (Vignati et al. 2004) to satellite and in-situ observations.

The SALSA module describes the aerosol population with 20 sections. There are 10 size dependent sections with parallel sections depending on the external mixing of particles. M7 describes the aerosol population with 7 lognormal modes. There are 4 soluble modes with 3 insoluble modes in parallel for external mixing of particles. Both models consider five compounds: sulphate, organic carbon, black carbon, sea salt and dust. In addition to these water uptake is also considered. Aerosol optical depths (AOD) are calculated using Mie theory following Toon and Ackerman (1981). Due to computational requirements the AOD is determined from lookup tables using Mie parameter, and real and imaginary parts of refractive index as input parameters. The particle refractive indices are the volume weighted average of all compounds.

To evaluate the AOD characteristics of the aerosol populations produced by the microphysical models we have made nudged simulation runs with both M7 and SALSA for year 2008. We have used half a year spin-up before the actual simulation year for the aerosol and trace gas concentrations to develop. T63 resolution is used which corresponds to approximately $1.9^\circ \times 1.9^\circ$ in the gaussian grid. For the vertical resolution of the atmosphere we have used 31 levels which go up to 10 hPa.

RESULTS

Simulated global AOD is compared to satellite retrieval MODIS (Tanré et al. 1997) and ground-based sun-photometry robotic network AERONET (Holben et al. 2001). The MODIS satellite retrieval provides the observed AOD in global scale. MODIS retrieval has low uncertainty for areas over oceans while its ability to capture AOD over land has significant uncertainties. AERONET robotic network operates in-situ measurements of the AOD.

	Observation	SALSA	M7
MODIS	0.15	0.10	0.14
AERONET	0.17	0.12	0.17

Table 1: Averages of observed and simulated AOD for year 2008.

In Table 1 we have the global means of AOD for SALSA and M7 calculated for gridpoints with MODIS data and means of gridpoints corresponding to AERONET sites. In both cases SALSA has much lower AOD while M7 captures the AOD almost perfectly.

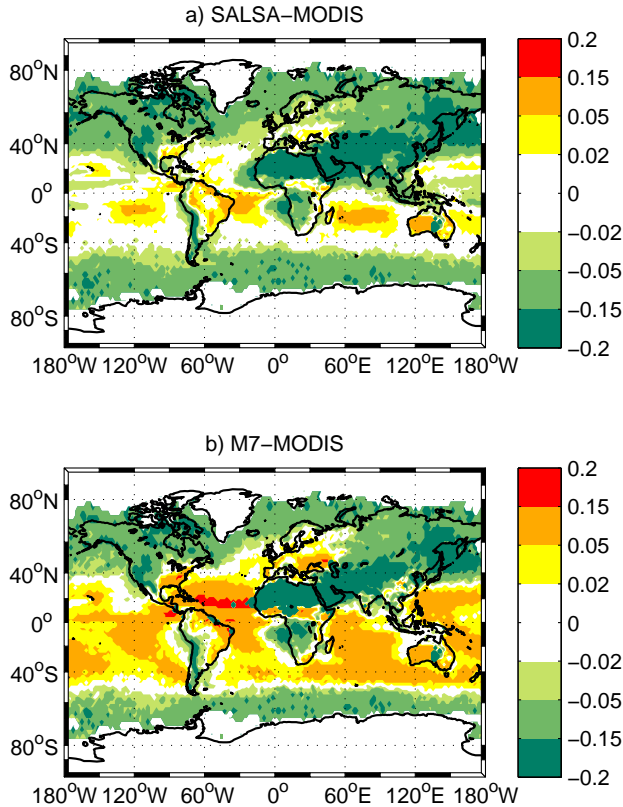


Figure 1: Difference in aerosol optical depth between a) SALSA and b) M7 and MODIS satellite retrieval. Green color indicates underestimation with a model and yellow indicates overestimation with a model.

We have in Fig. 1 the difference in annual mean for year 2008 between simulated AOD and MODIS retrieval. Both SALSA (Fig. 1a) and M7 (Fig. 1b) underestimate the AOD at high latitudes. One of the reasons for underestimation is too strong wet deposition of aerosols. In the mid-latitude ocean regions the difference in simulated AOD with SALSA to satellite retrieval is lower than with

M7. M7 shows clear overestimation in large part of ocean regions. Over the Atlantic Ocean to the west of Saharan desert the AOD with M7 is at least 0.15 higher than MODIS retrieval. In Europe and the East coast of USA the difference to MODIS with SALSA is less than 0.05 while with M7 the difference to MODIS is small in China and India. Furthermore both models show poor performance over Sahara and Arabian peninsula. However, the MODIS retrieval is unreliable over land areas with high reflection. Therefore the differences over land, especially over desert areas, should be viewed with caution.

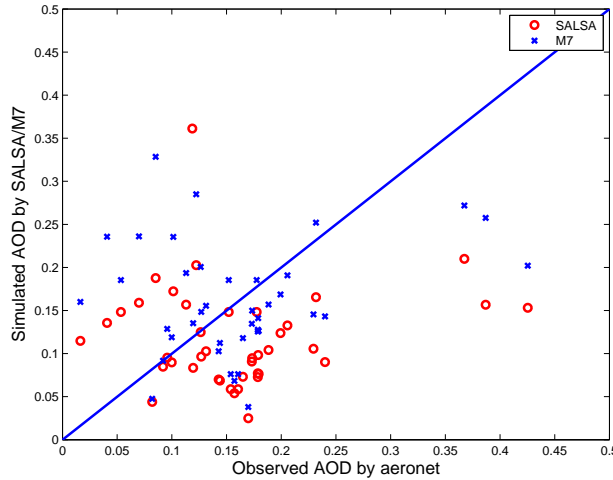


Figure 2: Scatterplot of simulated aerosol optical depth with SALSA (red \circ) and M7 (blue \times) compared to AERONET robotic network stations.

The AERONET provides a ground-based sun-photometry AOD statistics. We have in Fig. 2 scatterplot of the AOD for SALSA and M7 compared to AERONET robotic network. The overall annual mean AOD for gridpoints corresponding to AERONET sites for SALSA is 0.12 and for M7 the mean is 0.17 while the annual average over the AERONET sites is 0.17. From Fig. 2 we can see that the simulated AOD at these sites is overestimated for low values and underestimated for high values. In all cases except one the AOD with SALSA is smaller than AOD with M7. Due to lower overestimation SALSA shows better agreement with AERONET for observed AODs under 0.15 while M7 shows better agreement for observed AODs larger than 0.15.

CONCLUSIONS

The global aerosol optical depth simulated with the two microphysical models SALSA and M7 within aerosol-climate model ECHAM5-HAM was compared to MODIS and AERONET observations. Annual global mean AOD is produced quite well with M7 but underestimated using SALSA. Regionally both models underestimate the AOD at high-latitudes. Possible reasons for this are poor description of the transport and too high removal rate of aerosols. With M7 the global average AOD of 0.14 is in good agreement with the MODIS retrieval of 0.15 but regionally the differences to observed AOD are significant with differences as high as 0.15. With SALSA we have good agreement in mid-latitude oceans, while the global annual mean AOD is underestimated with 0.10. We found also that SALSA is unable to reproduce the high AODs related to highly polluted areas such as India and China.

ACKNOWLEDGEMENTS

This work was supported by the Academy of Finland.

REFERENCES

- Kokkola, H., Korhonen, H., Lehtinen, K. E. J., Makkonen, R., Asmi, A., Järvenoja, S., Anttila, T., Partanen, A.-I., Kulmala, M., Järvinen, H., Laaksonen, A., and Kerminen, V.-M. (2008). SALSA - a Sectional Aerosol module for Large Scale Applications *Atmos. Chem. Phys.*, 8, 2469-2483.
- Stier, P., Feichter, J., Kinne, S., Kloster, S., Vignati, E., Wilson, J., Ganzeveld, L., Tegen, I., Werner, M., Balkanski, Y., Schulz, M., Boucher, O., Minikin, A., and Petzold, A. (2005). The aerosol-climate model ECHAM5-HAM *Atmos. Chem. Phys.*, 5, 1125-1156.
- Vignati, E., Wilson, J., and Stier, P. M7: An efficient size-resolved aerosol microphysics module for large-scale aerosol transport models *J. Geophys. Res.*, 109, (2004) D22202, doi: 10.1029/2003JD004485.1.
- Holben, B.N., Tanré, D., Smirnov, A., Eck, T.F., Slutsker, I., Abuhassan, N., Newcomb, W. W., Schafer, J. S., Chatenet, B., Lavenu, F., Kaufman, Y. J., Castle, J. V., Setzer, A., Markham, B., Frouin, D. C. R., Halthore, R., Karneli, A., O'Neill, N. T., Pietras, C., Pinker, R. T., Voss, K., and Zibordi, G.: An emerging ground-based aerosol climatology: Aerosol optical depth from AERONET *J. Geophys. Res.* 106, 12067 - 12098, 2001
- Tanré, D., Kaufman, Y.J., Herman, M., and Mattoo, S.: Remote sensing of aerosol properties over oceans using MODIS/EOS spectral radiances *J. Geophys. Res.*, 102, 16971 - 16988, 1997
- Toon, O. B. and Ackerman, T. P.: Algorithms for the calculation of scattering by stratified spheres, *Appl. Opt.*, 20, 3657-3660, 1981

Long term temporal scaling of forest atmosphere relations using tree rings

Frank Berninger
Department of Forest Sciences
University of Helsinki
Finland

Introduction

Forests have been exposed to increased CO₂ and to atmospheric pollutants over a long time period and the functioning and the growth of forests have been changed by the atmosphere. Since the effects of both CO₂ and many atmospheric pollutants may be cumulative, we require tools to detect and scale effects over a long time periods. Effects may be cumulative and trees may respond to slowly over the long term.

In this presentation I try to trace how long term changes in the atmospheric composition can be traced back using tree rings using a few published examples and ongoing work. The talk is more a summary of ongoing and preexisting work that tries to discuss both potential and problems to infer forest atmosphere relations from tree rings.

According to Cook and Kariutskis (1987, modified here) tree ring growth is the result of the interactions of several and internal processes of trees.

$$I_t = f(\text{age}) \oplus f(\text{disturbance}) \oplus f(\text{climate}) \oplus f(\text{competition}) \oplus f(\text{pollution}) \oplus f(\text{previous growth})$$

Which indicates that tree growth is the overlaid signal of several processes. Usually scientists try to separate these different signals by replicating their samples over many trees sampled from different stands using different conditions. The extraction standard techniques are, in addition focusing pretty much on the extraction of the climate signal from tree rings. In addition the dependence of tree growth on the growth of the previous years (or the so called autocorrelation) is pretty strong and impedes to some extend inference from tree rings.

I subsequently present three case studies on tree growth that show, how in spite of these methodological difficulties useful conclusions can be drawn from tree ring data.

In the case study one we try to establish links between tree rings and photosynthetic production of jack pine and black spruce in Canada. The study reveals that inter site differences in ring width are related to differences in photosynthetic production while intra site variation in growth is much less limited by photosynthetic production.

Case study two investigates the relationships between atmospheric turbidity and tree rings, revealing changes in the sensitivity of tree ring growth within solar cycles.

Case study three reveals a large scale growth decline of Scots pine forests due to Sulphur deposition.

OVERVIEW ABOUT THE ACTIVITIES IN THE ATMOSPHERE MODELLING GROUP

M. BOY, N. BABKOVSKAIA, R. GIERENS, K.V. GOPALKRISHNAN, Q. HE, R. MAKKONEN, D. MOGENSEN, A. RUSANEN, S.-L. SIHTO, S. SMOLANDER, H. VUOLLEKOSKI, C. WATCHARAPASKORN, L. ZHOU

Department of Physics, University of Helsinki, P.O.Box 64,FI-00014 University of Helsinki, Finland

Keywords: ATMOSPHERE MODELLING, VOC'S, AEROSOLS, CLOUDS

INTRODUCTION

Today it is crucial to point out in any statement given from the scientific community to politicians that many of our future climate predictions are based on simplified and more or less empirically achieved parameterizations without knowing the detailed processes. Facing the huge impacts by the increased CFC-concentrations in the stratosphere some decades ago, coupled with our insufficient knowledge about the reason for the ongoing ozone-depletion we should have learned our lesson: the atmosphere is a very complex system (always with surprises) and we can only reach a complete picture if we invest strong efforts in understanding the detailed mechanisms. The overall aim of the Atmosphere Modelling Group is to achieve a better process-based knowledge in many atmosphere relevant fields, starting by the emissions of volatile organic compounds, the still for many molecules unclear atmospheric chemistry up to the direct and indirect aerosol effect and its implications on the local and global climate.

OBJECTIVES

The Atmosphere Modelling Group in the Division of Atmospheric Sciences at the University of Helsinki, was established in the beginning of 2009. The group currently includes beside Dr. Boy who is leading the group two post-doctoral scientists, four PhD-, three Master and two Bachelor students. The model activities are on different time-scales reaching from milliseconds in the cloud-process-studies to years in the global climate model and cover a wide spatial range from centimetres up to the globe. The strength of the group arises from a strong collaboration between the group members and in this manner also between the different models. This cross line through time and space with different models in one group offers a very unique and powerful setup and enables the investigation in many important atmospheric fields like chemistry and aerosols from the process level up to their implications on the global climate. Regarding the complexity of atmospheric processes valuable results are only achieved if people from different fields are collaborating very close together like it is in the Atmosphere Modelling Group. The main objectives of the group activities are:

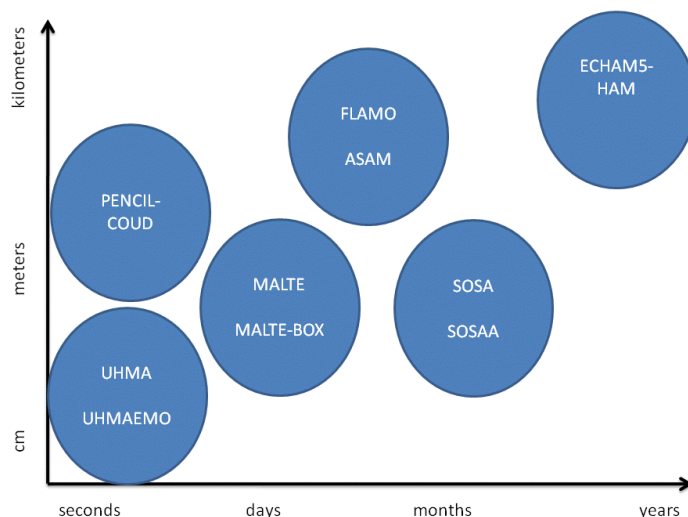
- to quantify the emissions of volatile organic compounds (VOCs) from different ecosystems and to pinpoint the fraction of organic compounds which are not identified by novel instrumentation up today
- to improve our capability in modelling the formation of SOA in the atmosphere and their ability to act as cloud condensation nuclei (CCN)
- to gain a better understanding in the cloud formation processes and the influence of turbulence on the aerosol dynamic and vice versa the influence of aerosol dynamics on the turbulence
- to discover and investigate possible feedback mechanisms in the biosphere-atmosphere system which could have a crucial role in future climate predictions
- to parameterize the new achieved results on a more process-based understanding and implement them in large-scale models

METHODS

In order to achieve the objectives, the following research questions are addressed and build the main scientific goals for the group activities:

- Do the emissions of VOCs measured and simulated for different ecosystems with empirical and process-based models present a satisfying representation of all emitted species and how large is the fraction we are still not able to quantify? Is the seasonal trend captured and how important is the emission of VOCs from soil and litter?
- What are the key processes related to the formation of SOA and are the main mechanism understood and parameterized in an acceptable way? Is the sulphuric acid molecule really the key component in the atmospheric nucleation mechanism and what are the roles of amines?
- How important is vertical mixing in terms of photochemistry and SOA formation processes, taking the strong gradients of certain parameters such as reactive gases (e.g. sesquiterpenes) into account?
- Under what chemical, physical and meteorological conditions biogenic SOA act as CCN and will this change under future climate scenarios? How strong is the influence of turbulence on the aerosol dynamics (and vice versa) inside and at the edge of a cloud?
- Do the emissions of VOCs and the subsequent production of SOA cause a cooling or warming effect for the boreal forest regions in the future compared to the biomass increase by rising temperature and CO₂ concentrations?
- Will the formation of new particles in the future increase or decrease and what impact could this have on the climate through the direct and indirect aerosol effect?
- Do undiscovered feedback mechanisms in the complex atmosphere-biosphere system still exist and if yes how important is their role for our future climate?

To answer this questions the group uses different models. A schematic time-space plot and a short description of the different models used are presented in below.



Schematic time-space plot of the models developed and/or applied in the group of atmosphere modelling.

The UHMA model (University of Helsinki Multi component Aerosol model) and the new improved version UHMAEMO (EMO stands for aErosol MOdule) includes comprehensive aerosol dynamics (nucleation, condensation, coagulation and deposition) and has already been successfully tested in different atmospheric models. This code was developed at the University of Helsinki during the last ten years and is one of the most detailed aerosol dynamic codes available (Korhonen et al., 2004). A new version with an improved condensation scheme and a more up to date numerical solution has been constructed by the group recently.

The PENCIL-CLOUD code is a high-order finite-difference code for compressible hydrodynamic flows. It is highly modular and can easily be adapted to different types of problems. An aerosol dynamic module was implemented to study the effects of turbulence on the cloud formation processes (and vice versa) and to investigate the effects of different CCN-concentrations with variable chemical properties on the number of cloud droplets formed. This project started last autumn and a manuscript explaining the model structure and presenting the first results is under preparation.

MALTE / MALTE-BOX (Model to predict new Aerosol formation in the Lower Troposphere) is a zero- and/or one-dimensional model which includes several modules for the simulation of boundary layer dynamics and both chemical and aerosol dynamical processes. The aerosol dynamics are solved by the size-segregated aerosol model UHMA, the emissions are predicted by MEGAN (Model for Emissions of Gases and Aerosols in Nature, Guenther et al., 2006) and gas phase chemistry is solved with the kinetic preprocessor (KPP, <http://people.cs.vt.edu/~asandu/Software/Kpp/>) in combination with the Master Chemical Mechanism (MCM, <http://mcm.leeds.ac.uk/MCM/>). The model was developed during the last six years at the University of Helsinki and the National Centre for Atmospheric Research in Boulder, Colorado, USA (Boy et al., 2006, 2008, Lauros et al., 2010).

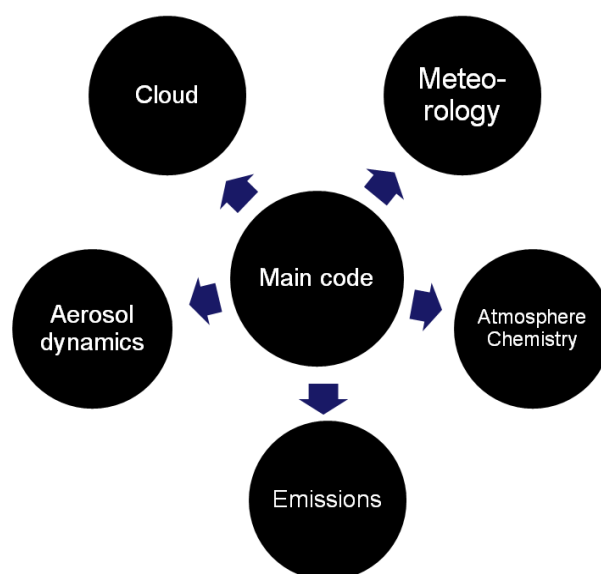
SOSA / SOSAA (model to Simulate the concentrations of Organic vapours, Sulphuric Acid and Aerosols) in its current version includes similar modules for emissions of organic vapours and gas phase chemistry as MALTE. It is a one-dimensional parallelized model operating at the high-performance supercluster Murska at the IT Center for Science in Helsinki, which gives the possibility to run long-term simulations with detailed processes in chemistry and meteorology within reasonable time (Boy et al., 2010). Recently the already in MALTE tested UHMAEMO code was parallelized and implemented in SOSA. This is the first model using a comprehensive aerosol dynamic code coupled with detailed chemistry to investigate the formation of secondary organic aerosols for long periods with a high vertical resolution.

FLAMO (Flexible Atmosphere Model) is a regional model with high temporal and spatial resolution. It is currently developed by Dr. Henri Vuollekoski and PhD-student KV Gopalkrishnan. The model provides a parallelized interface and simplifies the implementation of different modules constructed and tested in other models like for meteorology, emissions, chemistry and aerosol dynamics. This task will be finalized until next summer.

ASAM (All Scale Atmosphere Model) developed at the Institute for Tropospheric Research (Leipzig, Germany) is a large eddy simulation model with simplified aerosol and chemistry modules. This model will be intensively used in combination with the PENCIL-CLOUD model to provide the input parameters at the edge of clouds or other interested spaces. The model was transferred to our group in the beginning of this year and a strong collaboration including student exchange was agreed with the responsible scientists at IfT for further model development and applications.

The ECHAM-HAM (currently version ECHAM5_HAM) is an aerosol-climate modelling system. It is based on a flexible microphysical approach and, as the number of externally imposed parameters is minimised, allows the application in a wide range of climate regimes. ECHAM-HAM predicts the evolution of an ensemble of micro-physically interacting internally- and externally-mixed aerosol populations as well as their size-distribution and composition. This model is operated in the group and enables the testing of new developed parameterizations and the effect of selected feedback mechanism in one global climate models involved in the next IPCC predictions (Makkonen et al., 2009).

The development and application of various models over many magnitudes in space and time is a great challenge. Inside the group each module (see figure below) is organized by one responsible person on an extra place organised by version control (BAZAAR). This enables every model beside the ECHAM-HAM to get the updated information achieved by new results. This structure is an important part to ensure that different people do not waste their time by implementing the results from others inside their code but automatically by pushing the button receive all updates achieved inside the group.



Schematic picture of the structure inside the group for individual modules used

ACKNOWLEDGEMENTS

This work was supported by the Helsinki University Centre for Environment (HENVI). The financial support by the Academy of Finland Centre of Excellence program (project no 1118615) is gratefully acknowledged. This work was also supported by the European Integrated Project on Aerosol Cloud Climate and Air Quality Interactions (EUCAARI).

REFERENCES

- Boy, M., Hellmuth, O., Korhonen, H., Nillson, D., ReVelle, D., Turnipseed, A., Arnold, F. and Kulmala, M.: MALTE – Model to predict new aerosol formation in the lower troposphere, *Atmos. Chem. Phys.*, 6, 4499–4517, 2006.
- Boy, M., Sogachev, A., Lauros, J., Zhou, L., Guenther, A. and Smolander, S.: SOSA - a new model to simulate the concentrations of organic vapours and sulphuric acid inside the ABL - Part I: Model description and initial evaluation, *Atmos. Chem. Phys.* 11, 43-51, 2011.
- Guenther, A., Karl, T., Harley, P., Wiedinmyer, C., Palmer, P.I., and Geron, C.: Estimates of global terrestrial isoprene emissions using MEGAN (Model of Emissions of Gases and Aerosols from Nature), *Atmos. Chem. Phys.*, 6, 3181-3210, 2006.
- Korhonen, H., Lehtinen, K. E. J., and Kulmala, M.: Multicomponent aerosol dynamics model UHMA: model development and validation, *Atmos. Chem. Phys.*, 4, 471–506, 2004.
- Lauros, J., Sogachev, A., Smolander, S., Vuollekoski, H., Sihto, S.-L., Laakso, L., Mammarella, I., Rannik, U. and Boy, M.: Particle concentration and flux dynamics in the atmospheric boundary layer as the indicator of formation mechanism, *Atmos. Chem. Phys. Discuss.* 10, 20005-20033, 2010.
- Makkonen, R., Asmi, A., Korhonen, H., Kokkola, H., Jarvenoja, S., Raisanen, P., Lehtinen, K. E. J., Laaksonen, A., Kerminen, V.-M., Jarvinen, H., Lohmann, U., Bennartz, R., Feichter, J. and Kulmala, M.: Sensitivity of aerosol concentrations and cloud properties to nucleation and secondary organic distribution in ECHAM5-HAM global circulation model, *Atmos. Chem. Phys.*, 9, 1747-1766, 2009.

NUCLEATION AND GROWTH IN SULFURIC ACID – WATER SYSTEM: FROM NANO SCALE TO CCN

D. BRUS^{1,2}, K. NEITOLA¹, A.-P. HYVÄRINEN¹ and H. LIHAVAINEN¹

¹Finnish Meteorological Institute, Erik Palménin aukio 1, P.O. Box 503, FIN-00100 Helsinki, Finland

²Laboratory of Aerosol Chemistry and Physics, Institute of Chemical Process Fundamentals Academy of Sciences of the Czech Republic, Rozvojová 135, CZ-165 02 Prague 6, Czech Republic

Keywords: sulfuric acid, nucleation, CCN, flow tube.

INTRODUCTION

Atmospheric new particle formation consists of rather complicated sets of processes, the first of them is gas-to-particle nucleation which occurs naturally but might be also easily influenced by anthropogenic emissions of gases such as SO₂. It is generally accepted that sulfuric acid is a robust source of new particles and plays a central role in atmospheric new particle formation. Aerosol particles serving as cloud condensation nuclei (CCN) play an important role in the formation of clouds, precipitation, and they have influence on atmospheric chemistry and physics, the water cycle in nature and Earth's climate (Seinfeld and Pandis, 1998). One of the largest uncertainties in present understanding of climate change is the response of cloud characteristics and precipitation processes to currently increasing anthropogenic aerosol concentrations. The CCN activation is determined by particle composition, size and water vapor supersaturation. The CCN measurements are continually performed both in laboratories and field experiments around the globe to provide reliable data of atmospheric CCN concentration and size distribution as function of water vapor supersaturation. Since increasing demand is put on quantitative description, assessment of the effects of natural background aerosol on CCN and description of the impact on the atmosphere and climate (Andreae *et al.* 2005). In this laboratory study we focused on CCN activation of sulfuric acid particles produced with flow tube technique.

METHODS AND RESULTS

Flow tube technique was used to produce particles in the size range from about 10 to 130 nm by homogeneous nucleation of sulphuric acid and water (Brus *et al.* 2010). Sulfuric acid vapour was produced by using a thermally controlled one meter long saturator with I.D. of 6 cm which was partially filled with pure (97%) sulfuric acid. Dry, purified, and particle free air is flown through the saturator with constant flow rate (0.1 slpm) to saturate the flow with sulphuric acid vapour. The concentration of sulfuric acid is controlled by the temperature of the saturator. The sulphuric acid concentration was measured at the end of two meter long temperature controlled flow tube with Chemical Ionization Mass Spectrometer (CIMS) (Petäjä *et al.*, 2009) or Atmospheric Pressure Interface Time-of-Flight mass spectrometer API-TOF (Junninen *et al.*, 2010). The concentration of nucleated particles was monitored with Particle Size Magnifier (PSM, Vanhanen *et al.*, 2010) and CPC TSI model 3010. The size of the particles was measured with DMPS system (HAUKE DMA, UCPC, TSI model 3025A) in the size range from 3 to 200 nm. The continuous flow Cloud Condensation Nuclei Counter (CCNC, Droplet Measurement Technologies) was used to measure CCN. The key parameters recorded during the typical experiment are shown in figure 1 as a time series: particle size distribution (DMPS), temperature of saturator, mean particle diameter, sulfuric acid concentration in a gas-phase (CIMS) and activated fraction of sulphuric acid particles (CCNC).

At water supersaturation 1% we are able to activate about 50% of sulfuric acid particles with the mean diameter of 28 nm (taken from DMPS particle size distribution).

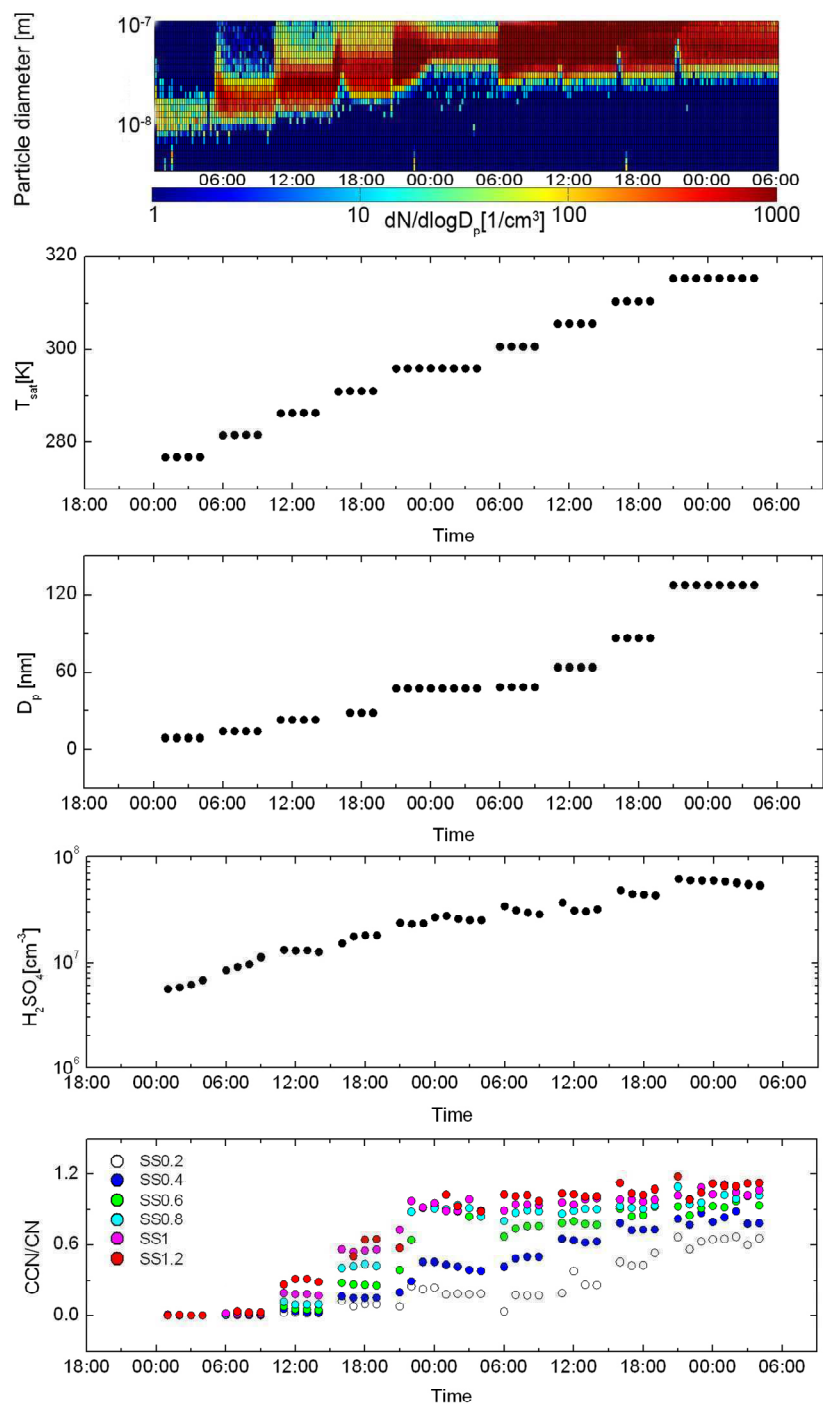


Figure 1. Key parameters of the experiment as a time series: particle size distribution (DMPS), temperature of saturator, mean particle diameter, sulphuric acid concentration in a gas-phase (CIMS) and activated fraction of sulphuric acid particles (CCNC).

ACKNOWLEDGEMENTS

This work was supported by the Academy of Finland Centre of Excellence program (project no. 1118615), KONE foundation, and Maj and Tor Nessling foundations.

REFERENCES

- Andreae, M. O., C. D. Jones and P. M. Cox (2005). Strong present-day aerosol cooling implies a hot future, *Nature*, 435, 1187-1190.
- Brus, D., K. Neitola, T. Petäjä, J. Vanhanen, A.-P. Hyvärinen, M. Sipilä, P. Paasonen, H. Lihavainen, and M. Kulmala (2010). Homogenous nucleation of sulfuric acid and water at atmospherically relevant conditions, *Atmos. Chem. Phys. Discuss.*, 10, 25959-25989.
- Junninen, H., M. Ehn, T. Petäjä, L. Luosujärvi, T. Kotiaho, R. Kostianen, U. Rohner, M. Gonin, K. Fuhrer, M. Kulmala and D. R. Worsnop (2010). A high-resolution mass spectrometer to measure atmospheric ion composition, *Atmos. Meas. Tech.*, 3, 1039–1053, doi:10.5194/amt-3-1039-2010.
- Petäjä T., R. L. Mauldin, III, E. Kosciuch, J. McGrath, T. Nieminen, P. Paasonen, M. Boy, A. Adamov, T. Kotiaho and M. Kulmala (2009). Sulfuric acid and OH concentrations in a boreal forest site, *Atmos. Chem. Phys.*, 9, 7435–7448.
- Seinfeld, J. H. and S.N. Pandis (1998). *Atmospheric Chemistry and Physics: From Air Pollution to Climate Change*, New York: John Wiley & Sons, Inc.

CRYOSPHERE-ATMOSPHERE INTERACTIONS IN A CHANGING ARCTIC CLIMATE (CRAICC)

JAANA BÄCK^{1,2)}, MARKKU KULMALA¹⁾ and THE CRAICC -TEAM

¹⁾ Department of Physics, University of Helsinki, P.O. Box 64, FI-00014 University of Helsinki, Finland

²⁾ Department of Forest Sciences, University of Helsinki, P.O. Box 27, FI-00014 University of Helsinki, Finland

Keywords: ARCTIC AND BOREAL AREAS, CRYOSPHERE, ATMOSPHERE, ICE, SHORT-LIVED CLIMATE FORCERS, PALEOCLIMATOLOGY, REMOTE SENSING, ARCTIC WARMING

The surface radiation balance regulates the melting and freezing of the pack ice, which in turn is a key climate regulator in the Arctic. Important, yet poorly-quantified factors in this context are short-lived climate forcers (SLCF), including e.g. natural and anthropogenic aerosols. The climate impacts of SLCFs are tightly connected with cryospheric changes and associated human activities (Fig 1). For example, transport of black carbon aerosols to high latitudes and their deposition on snow are known to decrease the surface albedo which, together with decreased sulfate aerosol emissions, has probably contributed to the observed Arctic warming. Melting of the pack ice and sea ice are likely to result in increased numbers of aerosol particles and CCN from sources in the high Arctic, thereby increasing the reflectivity of clouds. Properties of high-latitude clouds may also be affected by the changing biogenic aerosol formation associated with warming and snow-cover changes over boreal forest regions. Albedo changes due to altering vegetation dynamics will further influence the feedbacks between biosphere, cryosphere and atmosphere.

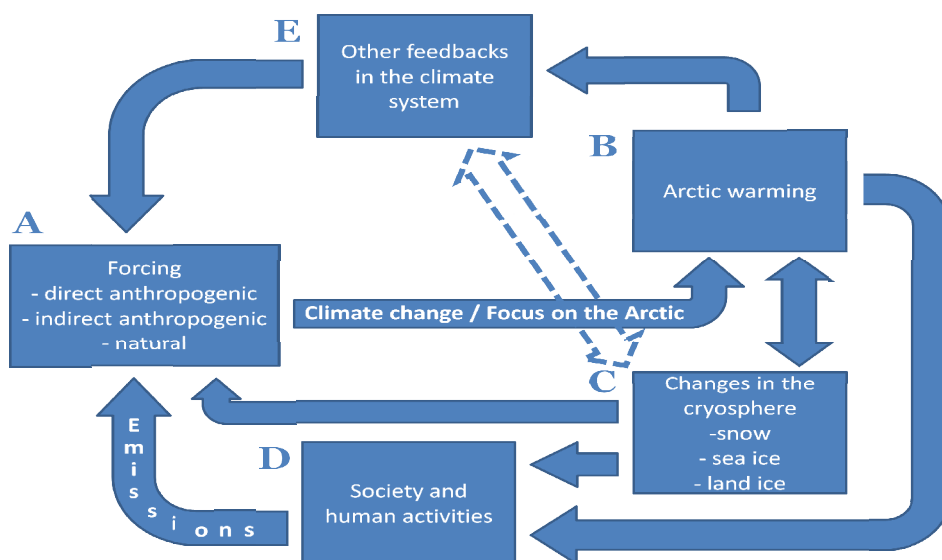


Figure 1. Links and feedbacks between different components in climate change and cryosphere in Arctic areas.

The Nordic Center of Excellence CRAICC (CRYOSPHERE-ATMOSPHERE INTERACTIONS IN A CHANGING ARCTIC CLIMATE) aims at analyzing and quantifying the natural and anthropogenic feedback processes and their impacts on Arctic warming in different time scales, from nanoseconds to decades and millennia. The obtained knowledge will be implemented into Earth System climate models, thus improving their accuracy related to Arctic areas. The project includes over 130 participants from all Nordic countries in 17 research groups, and is coordinated by the University of Helsinki. Funding is provided by Nordforsk.

CRAICC Work packages include: Coordination, Cryospheric changes, Natural emissions associated with warming and cryospheric changes, SLCF and cryosphere, Cryosphere-aerosol-cloud-climate interactions, Atmosphere-cryosphere-societal interactions Past long-term changes in the Arctic, and Synthesis, Integration and Earth System modeling. The funding allows short- and long-term fellowships and researcher mobility between Nordic countries. An important part of the NCoE is researcher training, where expertise from all involved disciplines and research areas will be utilized. CRAICC also facilitates joint use of research infrastructures such as intensive field stations (Fig 2) and field campaigns.

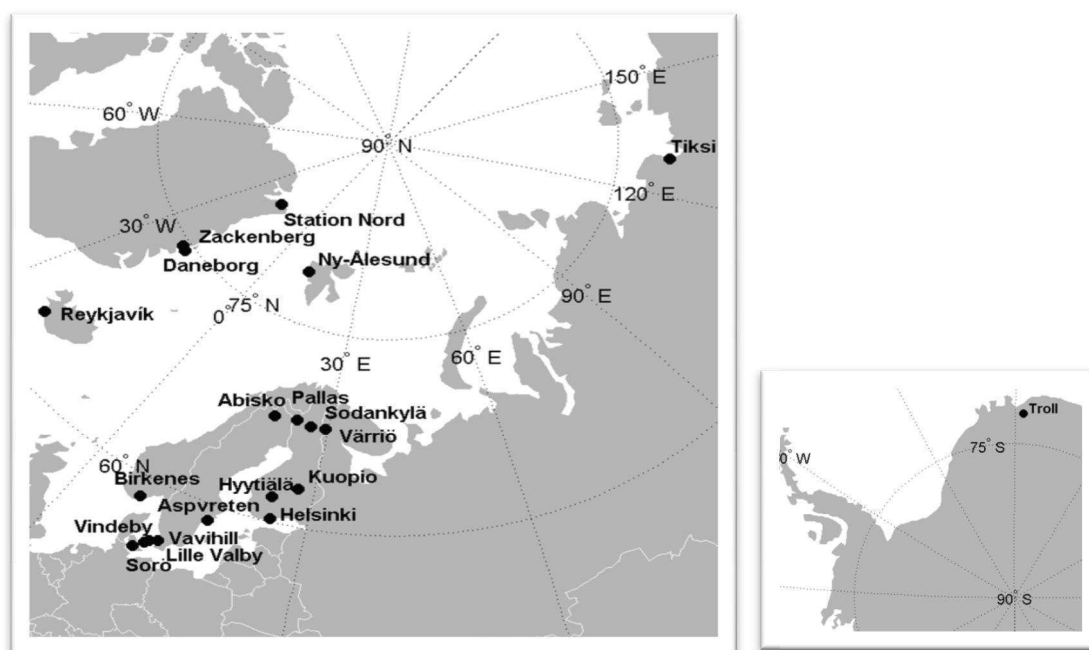


Figure 2. CRAICC field stations in Arctic and Antarctic areas.

TEMPORAL AND BETWEEN-TREE VARIABILITY OF SCOTS PINE MONOTERPENE EMISSIONS IN A BOREAL FOREST STAND

J. BÄCK^{1,2}, J. AALTO^{2,3}, P. KOLARI², E. JUUROLA², M. HENRIKSSON⁴ and H. HAKOLA⁴

¹Dept. of Physics, P.O. Box 64, FI-00014 University of Helsinki, Finland.

²Dept. of Forest Sciences, P. O. Box 27, 00014 University of Helsinki, Finland

³Hyytiälä Forestry Field Station, Hyytiäläntie 124, FI-35500 Korkeakoski, Finland.

⁴Finnish Meteorological Institute, P.O. Box 503, FI-00101 Helsinki, Finland

Keywords: MONOTERPENE EMISSIONS, SCOTS PINE, SEASONALITY, CHEMOTYPE, ATMOSPHERIC CHEMISTRY.

INTRODUCTION

Atmospheric chemistry in background areas is strongly influenced by natural vegetation. Boreal coniferous forests are known to produce large quantities of volatile vapours, especially isoprenoids to the surrounding air (e.g. Guenther *et al.*, 2006, Rinne *et al.*, 2009). These compounds react with OH and O₃, and contribute to the formation and growth of atmospheric new particles (Kulmala *et al.*, 2004, Tunved *et al.*, 2006). Normally emission rates are modelled using semi-empirical models where emission parameters are derived from a few measurements done at standardized conditions (Guenther *et al.*, 2006). However, emission rates vary significantly with species, with individual and over time. Especially in boreal forests the seasonality of emissions can be clearly distinguished (Hakola *et al.*, 2006). Moreover, different parts of the tree canopy and also the below-canopy processes influence the stand-level emission patterns. This strongly suggests that better knowledge of this variability is needed, in order to upscale emissions from branch scale to regional scale and for modeling the atmospheric chemistry.

Our aim was to analyse the variability of monoterpene emissions of Scots pine trees during a prolonged period under field conditions. We also tested variation in emission quality and quantity between individual trees. The results can be used to clarify the potential errors in atmospheric chemistry models caused by applying parameterizations from emission data obtained from only a few trees and only at a single point in time.

METHODS

The measurements were conducted at the SMEAR II measurement station (Station for Measuring Forest Ecosystem – Atmosphere Relations) in Hyytiälä, Southern Finland (61°N, 24°E, 180 m a.s.l.). We measured the monoterpene emission rates from Scots pine (*Pinus sylvestris* L.) branches in the field using a dynamic shoot enclosure and a proton-transfer reaction –mass spectrometer (PTR-MS) on-line during 2009-2010. We also measured the detailed emission spectrum of one pine tree with a gas chromatograph-mass spectrometer (GC-MS) over one full year. To clarify the population-level variability in emissions, we sampled 40 trees and measured their emissions in laboratory conditions with GC-MS.

RESULTS AND DISCUSSION

Monoterpene emissions from Scots pine varied greatly with the season (Fig 1). The highest emissions, totalling up to 4 ug g⁻¹ h⁻¹, were measured in spring and summer period. Emissions were poorly correlated

with incident PAR or temperature (Fig 2), indicating that large storage pools can influence the emissions from Scots pine foliage.

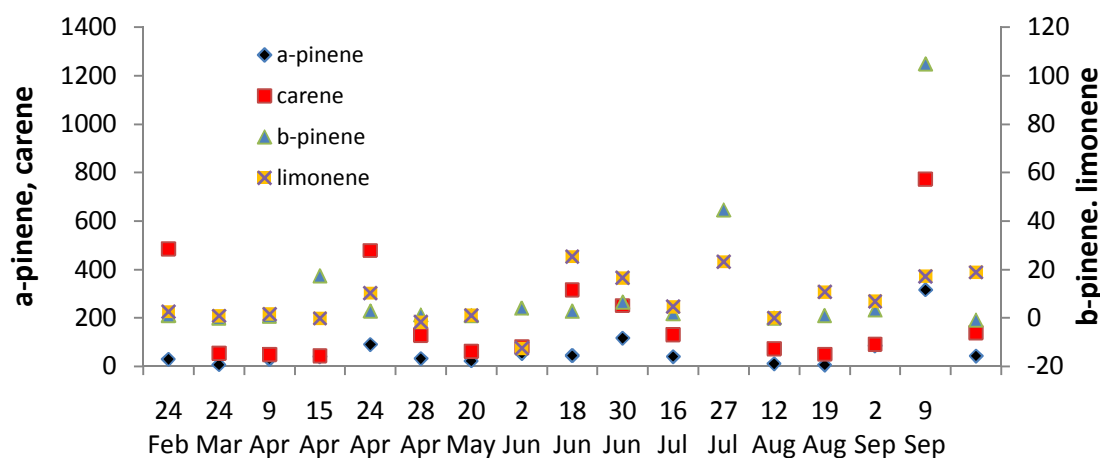


Figure 1. Emission rates of four main monoterpenes from a Scots pine branch (includes both current and previous year needles) between February 24 and September 15, 2009. Measurements from tree no 3 in Figure 4.

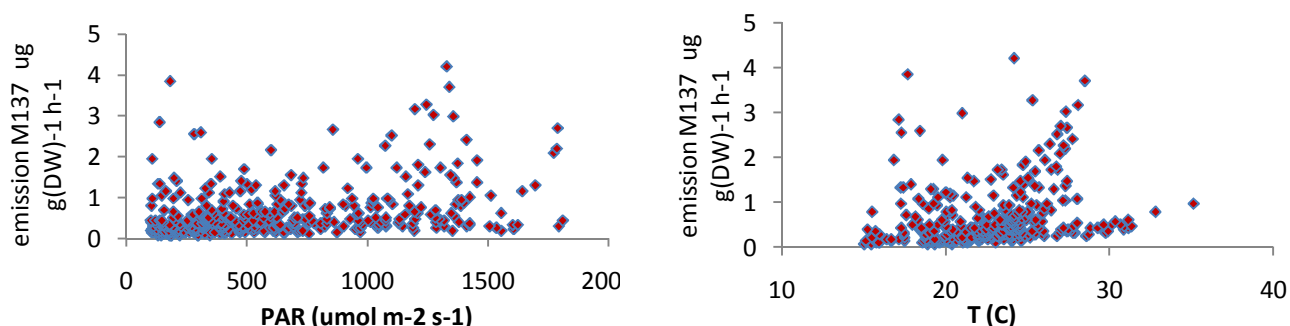


Figure 2. Correlations between monoterpene emissions (M137) and incident photosynthetically active radiation (a) and temperature (b). Measurements from one-yr-old pine branch with PTR-MS in summer 2010.

When the variation in monoterpene emission quality was analyzed, two main compounds, α -pinene and Δ^3 -carene, were seen to form on average 40-97 % of the monoterpenes in the emissions (Fig. 1). The population-level data showed a bimodal distribution in emission composition, in particular in Δ^3 -carene emission within the studied population. 10% of the trees emitted mainly α -pinene and almost no Δ^3 -carene at all, whereas 20% of the trees were characterized as high Δ^3 -carene emitters, with some α - and β -pinene emissions (Fig. 3). In addition to variations in emitted monoterpene spectrum, emission rates vary with a factor of about 10 between trees growing close together (Fig 4).

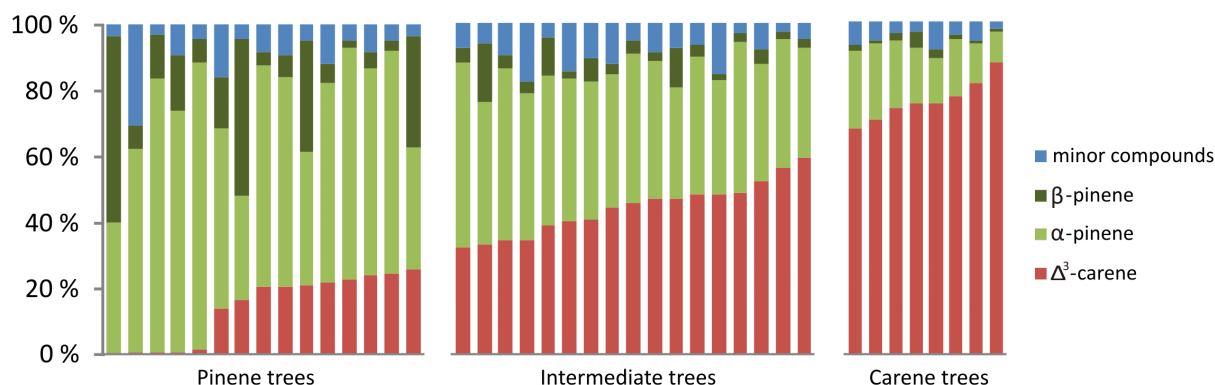


Figure 3. The relative emission patterns of 40 Scots pine trees at SMEAR II, classified in three chemotype groups with cluster analysis.

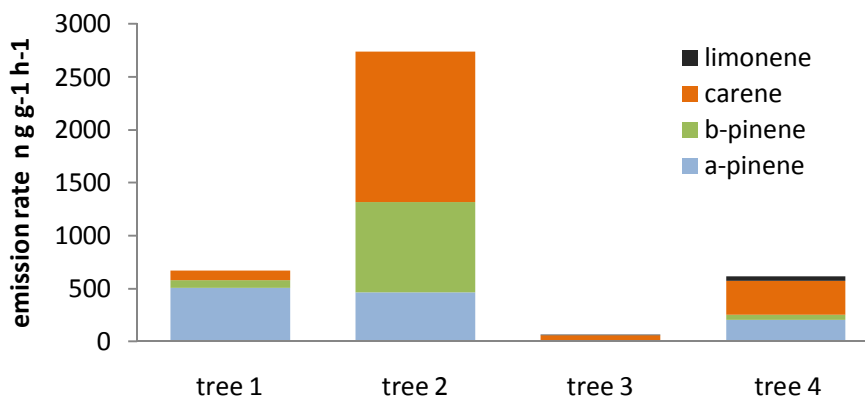


Figure 4. Emission rates and emitted monoterpene spectrum of four Scots pine trees at the SMEAR II stand in August 2009. Tree 1 is pinene type, tree 2 is carene type and other two trees show an intermediate emission pattern.

CONCLUSIONS

The monoterpene emission rates and spectrum vary greatly temporally and a chemotype-specific emission spectrum within a homogeneous forest stand can be distinguished. The data clearly points out that for understanding the total atmospheric monoterpene concentrations, knowledge of the chemotype composition and temporal variations in emission rates are essential.

ACKNOWLEDGEMENTS

This work was supported by the Academy of Finland Center of Excellence (project no1118615) and the Doctoral programme in Atmospheric Composition and Climate Change: From molecular processes to global observations and models (ACCC).

REFERENCES

- Boy, M., Sogachev, A., Lauros, J., Zhou, L., Guenther, A., and Smolander, S. (2011) SOSA a new model to simulate the concentrations of organic vapours and sulphuric acid inside the ABL - Part 1: Model description and initial evaluation. *Atmos. Chem. Phys.* **11**, 43–51, 30 doi:10.5194/acp-11-43-2011
- Guenther, A., Karl, T., Harley, P., Wiedinmyer, C., Palmer, P. I., and Geron, C. (2006) Estimates of global terrestrial isoprene emissions using MEGAN (Model of Emissions of Gases and Aerosols from Nature). *Atmos. Chem. Phys.* **6**, 3181–3210, doi:10.5194/acp-6-3181-2006
- Hakola, H., Tarvainen, V., Bäck, J., Ranta, H., Bonn, B., Rinne, J., and Kulmala, M. (2006) Seasonal variation of mono- and sesquiterpene emission rates of Scots pine. *Biogeosciences* **3**, 93-101.
- Kulmala, M., Suni, T., Lehtinen, K. E. J., Dal Maso, M., Boy, M., Reissell, A., Rannik, Ü., Aalto, P., Keronen, P., Hakola, H., Bäck, J., Hoffmann, T., Vesala, T., and Hari P. (2004) A new feedback mechanism linking forests, aerosols, and climate. *Atmos. Chem. Phys.* **4**, 557-562.
- Rinne, J., Bäck, J., and Hakola, H. (2009) Biogenic volatile organic compound emissions from the Eurasian taiga: current knowledge and future directions. *Boreal Environ. Res.*, **14**, 807-826.
- Tunved, P., Hansson, H.-C., Kerminen, V.-M., Ström, J., Dal Maso, M., Lihavainen, H., Viisanen, Y., Aalto, P. P., Komppula, M., and Kulmala, M. (2006) High Natural Aerosol Loading over Boreal Forests. *Science* **312**, 261-263.

PLANT EMISSIONS AND ATMOSPHERIC NANOPARTICLE FORMATION

DAL MASO, MIIKKA^{1,2}, MENDEL, THOMAS F.², KIENDLER-SCHARR, ASTRID², KLEIST, EINHARD², TILLMANN, RALF², SIPILÄ, MIKKO¹, PETÄJÄ, TUUKKA¹, HAKALA, JANI¹, LIAO, LI¹, LEHTIPALO, KATRIANNE¹, JUNNINEN, HEIKKI¹, EHN, MIKAEL¹, VANHANEN, JOONAS¹, MIKKILÄ JYRI¹, KULMALA, MARKKU¹, WILDT, JÜRGEN², WORSNOP, DOUGLAS¹

¹Department of Physics, University of Helsinki, P.O.Box 48, 00014, Helsinki, Finland

²Institut für Chemie und Dynamik der Geosphäre (ICG), Forschungszentrum Jülich, 52425 Jülich, Germany

Keywords: nanoparticle formation, BVOCs, sulphuric acid, laboratory experiments.

INTRODUCTION

The atmosphere is an oxidising medium and oxidation reactions play a major role in the chemical and physical cycles of various compounds in the terrestrial atmosphere. Oxidation reactions of volatile organic compounds, most of which are emitted by terrestrial vegetation, lead to the formation of non- or semivolatile products, which may subsequently undergo a phase transition and enter the atmospheric aerosol phase. The most likely candidates of precursors of aerosol-producing vapors are sulphur dioxide and plant-originated volatile organic compounds.

The controlling mechanism of tropospheric nanoparticle formation is currently still an open question. Field and laboratory measurements have clearly indicated a strong correlation between observed sulphuric acid – a product of SO₂ oxidation – and nanoparticle concentrations and formation rates (see eg. Riipinen et al., 2007). The observed seasonality and comparisons with plant VOC emission strengths, however, show that aerosol formation is also correlated with biogenic organic oxidation. Laboratory studies with real plant emissions have shown a clear dependence of aerosol formation on the VOC emission strength and also the chemical mixture (Mentel et al., 2009, Kiendler-Scharr et al., 2009), thereby ruling out the possibility that nanoparticle formation by nucleation would be completely independent of organic compounds.

Because of the possibility that atmospheric particle formation is caused by several different processes, each of which dominates in different precursor concentration ranges, reconciling the sulphuric acid and VOC-dependent explanations for aerosol formation requires detailed studies of the particle formation process at concentrations resembling the natural atmosphere.

MATERIALS AND METHODS

We investigated the formation of nanosized condensation nuclei (nano-CN) from sulphuric acid and plant emissions in the Jülich Plant Chamber setup. The extensive measurement setup consisted of several condensation nuclei counters (CPCs) including a pulse-height CPC and a CPC with a prototype Particle Size Magnifier for detection of sub-3 nm CN. Particle size distributions were monitored using an SMPS. Sulphuric acid levels were measured using chemical ionization mass spectrometry, while VOC concentrations were monitored with proton transfer mass spectrometers and a gas chromatograph – mass spectrometer. We also deployed an Atmospheric Pressure Interface TOF spectrometer (API-TOF) to monitor the concentrations and distribution of charged clusters and molecules in the chamber.

In the series of experiments performed we used boreal forest tree emissions at levels typically found in the boreal evergreen forest boundary layer. The sulphuric acid concentration in the chamber was varied by changing the intensity of hydroxyl radical production and addition of SO₂ to the chamber; sulphuric acid levels were on par with atmospheric observations. The reaction chamber was flushed with ozone to achieve a steady-state concentration of 60 ppb when no OH was produced.

RESULTS AND DISCUSSION

We found that while the variation of the VOC concentration had a strong impact on the gas phase chemistry and also the hydroxyl radical and sulphuric acid levels, the changes in particle formation rates were not explainable by sulphuric acid concentration variations alone, but the particle formation process is directly influenced by the organic compounds.

We will present a detailed description of the evolution of the early nano-CN distribution and the influence of both sulphuric acid and biogenic organic oxidation products on it. The connections to the dynamics of the charged cluster and large molecule distribution as a function of ongoing oxidation by both ozone and the hydroxyl radical will also be discussed. We will present a comparison of our results to findings from atmospheric field observations of natural nano-CN formation, and give an overview of the implications of our findings.

ACKNOWLEDGEMENTS

We acknowledge the EUCAARI project for financial support. M. Dal Maso wishes to thank the Academy of Finland for financial support of this project (No. 128731). We also wish to thank the Maj and Tor Nessling foundation for financial support (grant No 2010363). The financial support by the Academy of Finland Centre of Excellence program (project No 1118615) is gratefully acknowledged.

REFERENCES

- Mentel, Th. et al., *Atmos. Chem. Phys.*, 9, 4387–4406 (2009)
Kiendler-Scharr, A., et al., *Nature*, 461, (7262): 381-384, 2009. DOI: 10.1038/nature08292
Riipinen et al., *Atmos. Chem Phys* 7, 1899-1914, 2007

PHYSICAL CHARACTERIZATION OF IONS IN THE CLOUD CHAMBER

A. FRANCHIN,¹ S. SCHOBESBERGER¹, K. LEHTIPALO¹, V. MAKHMUTOV², Y. STOZHKOVA², S. GAGNÉ¹, T. NIEMINEN¹, H. E. MANNINEN¹, T. PETÄJÄ¹, M. KULMALA¹ and THE CLOUD COLLABORATION.

¹Department of Physics, University of Helsinki, P.O. Box 64, FI-00014, Helsinki, Finland

²Lebedev Physical Institute RAS, 119991, Moscow, Russia.

Keywords: ATMOSPHERIC IONS, ION-INDUCED NUCLEATION, SULFURIC ACID, CLOUD EXPERIMENT.

INTRODUCTION

Aerosol particles have a significant influence on the Earth climate. Several studies have shown a correlation between past variations in climate, and solar and cosmic ray variability (Kirkby 2007). Nanoparticle formation in the boundary layer is a frequent phenomenon (Kulmala *et al.*, 2004). Sulfuric acid has been identified as playing an essential role in atmospheric nucleation (Weber *et al.* 1996). Ion-induced nucleation is one of the possible pathways for new particle formation in the atmosphere, but it is still unclear how important the contribution of ions is with respect to neutral pathways. Ion concentration and their size distribution are key quantities to understand ion-induced nucleation processes and dynamics.

METHODS

During the CLOUD (Cosmics Leaving OUtdoor Droplets) 2010 fall campaign, several experiments of sulfuric acid-water neutral and ion induced nucleation were performed in an aerosol chamber. In this experiment, Galactic Cosmic Rays (GCR) and the Proton Synchrotron (PS) accelerator at CERN were used as sources to generate ions in the 26.1 m³ CLOUD aerosol chamber under precisely controlled conditions. Both GCR and the PS pion beam were constantly monitored by a GCR counter and by an hodoscope, respectively.

The ion concentration in the CLOUD chamber was measured with a Neutral cluster and Air Ion Spectrometer, (NAIS, Kulmala *et al.*, 2007). The NAIS is able to measure air ion number size distributions in the mobility equivalent diameter range of 0.8 to 40 nm and correspondingly neutral particle number size distributions from ~2 to 40 nm mobility diameter.

It was also possible to use an Airmodus A09 Particle Size Magnifier (PSM; Vanhanen *et al.*, 2011), a scanning CPC with a cut off varying from 1 to 2 nm, to retrieve the size distribution of the atmospheric ions created in the chamber and compare it to the NAIS in absence of neutral particles in the chamber.

CONCLUSIONS

Based on the measured GCR and beam intensities we were able to calculate the expected ion concentrations in the chamber as a function of beam intensity. The calculated ion concentrations were then compared with the measured values in the NAIS, therefore we retrieved the ion-ion recombination coefficient, performing a dedicated set of experiments at different conditions: varying the internal temperature of the chamber, its relative humidity and the trace gas concentration such as sulfur dioxide, ozone and sulfuric acid.

The ratio of formation rates of charged and total particles give information about the contribution of ion-induced nucleation. Charged nucleation rates were retrieved from the NAIS ion mode and from two CPCs one of which was equipped with a switchable ion trap both results will be compared. The size

distribution of the atmospheric ions created in the chamber in absence of neutral particles in the chamber was measured using two different instruments based on different working principles: PSM, based on vapour condensation and optical detection and NAIS, based on mobility discrimination and electrical detection (Figure 1).

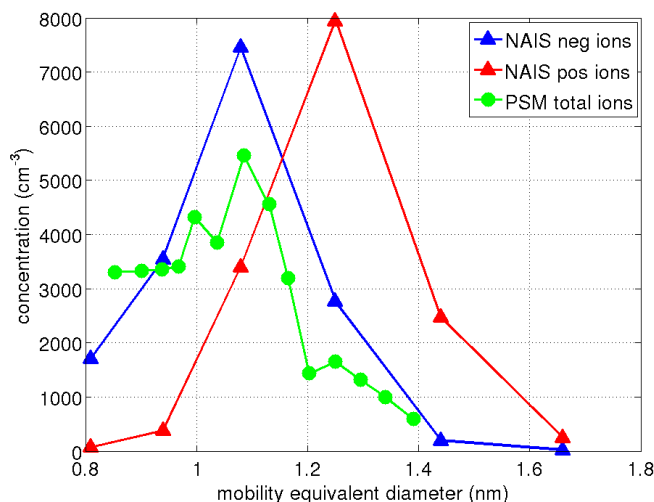


Figure 1. Comparison of number size distribution of ions from NAIS (blue for negative ions red for positive) and from PSM (green).

ACKNOWLEDGEMENTS

We would like to thank CERN for supporting CLOUD with important technical resources, and for providing a particle beam from the CERN Proton Synchrotron. This research has received funding from the EC's Seventh Framework Programme under grant agreement number 215072 (Marie Curie Initial Training Network "CLOUD-ITN"), from the German Federal Ministry of Education and Research (project number 01LK0902A), from the Swiss National Science Foundation and from the Academy of Finland Centre of Excellence program (project number 1118615).

REFERENCES

- Kulmala, M., Vehkamäki H., Petäjä, T., Dal Maso, M., Lauri, A., Kerminen, V.-M., Birmili, W., McMurry, P.H. (2004). Formation and growth rates of ultrafine atmospheric particles: a review of observations. *J. Aerosol Sci.*, 35, 143 – 176.
- Kulmala, M., Riipinen, I., Sipilä, M., Manninen H. E., Petäjä, T., Junninen, H., Dal Maso, M., Mordas, G., Mirme, A., Vana, M., Hirsikko, H., Laakso, L., Harrison, R. M., Hanson, I., Leung, C., Lehtinen, K. E. J. and Kerminen, V.-M. (2007). Toward Direct Measurement of Atmospheric Nucleation. *Science*, 318: 89-92.
- Kirkby, J. (2007). Cosmic Rays and Climate. *Surv. Geophys.*, 28, 333-375.
- Vanhanen, J., Mikkilä, J., Lehtipalo, K., Sipilä, M., Manninen, H. E., Siivola, E., Petäjä, T., Kulmala, M. (2011). Particle Size Magnifier for Nano-CN Detection. *Aerosol Sci. Tech.*, 45, 4, 533-42.
- Weber, R. J., Marti, J., McMurry, P. H., Eisele, F., Tanner, D. J., and Jefferson, A. (1996). Measured atmospheric new particle formation rates: implications for nucleation mechanisms. *Chem. Eng. Commun.*, 151, 53–64.

INTERCOMPARISON OF AIR ION SPECTROMETERS

S. GAGNÉ¹, K. LEHTIPALO¹, H.E. MANNINEN¹, T. NIEMINEN¹, S. SCHOBESBERGER¹,
A. FRANCHIN¹, T. YLI-JUUTI¹, J. BOULON², A. SONNTAG³, S. MIRME⁴, A. MIRME⁴, U.
HÖRRAK⁴, T. PETÄJÄ¹, E. ASMI⁵ and M. KULMALA¹

¹Department of Physics, University of Helsinki, P.O. Box 64, 00014 Helsinki, Finland.

²Laboratoire de Météorologie Physique, Blaise Pascal Univ., 63000 Clermont-Ferrand, France.

³Leibniz Institute for Tropospheric Research, Permoserstrasse 15, 04303 Leipzig, Germany.

⁴Institute of Physics, University of Tartu, Ülikooli 18, 50090 Tartu, Estonia.

⁵Finnish Meteorological Institute, P.O. Box 503, 00101 Helsinki, Finland.

Keywords: Air Ion Spectrometers, Instrumentation, Intercomparison, EUCAARI.

INTRODUCTION

The Air Ion Spectrometer was developed by Airel ltd. (AIS, Mirme et al., 2007) to measure the size distribution of charged particles in the atmosphere in the size range 0.8-42 nm. The later developed Neutral cluster and Air Ion Spectrometer (NAIS, Manninen et al., 2009) can also measure the size distribution of total particles (charged+neutral) in addition to charged particles. These instruments allow measurement of the particle size distribution with a very good size and time resolution: 28 channels between 0.8 and 42 nm, size distribution every 1 to 5 minutes (integration time is user defined).

This instrument is widely in use around the world in field or chamber measurements (see e.g. Manninen et al., 2010; Duplissy et al., 2010). In order to insure that the measurements made with different individual instruments are comparable, we performed two calibration and intercomparison workshops. The first one took place in winter 2008 (Asmi et al., 2009) and focused on the mobility and concentration detection performance of the instruments. The second workshop, on which this abstract is based, took place in summer 2009 (Gagné et al., 2011) and focused on providing insights for ion spectrometer users and for data interpretation.

METHODS

Eleven ion spectrometers were investigated during the second workshop: 5 AISs, 5 NAISs and 1 Airborne NAIS (ANAIS, a modified NAIS suitable for aircraft measurements). The ion spectrometers consist of two Differential Mobility Analyzers (DMA), one for each polarity, with 21 vertically stacked electrometers (see Fig. 1). The design of the AIS is similar to the NAIS, except for the particle mode modules.

Upon arrival in Helsinki, each instrument was cleaned and the flows were adjusted so that the instrument's performance is not hindered in any way. After insuring that the instruments were in good condition, they were calibrated with mobility standards or silver particles using a high resolution DMA or Hermann DMA (HDMA) to select the mobility of the particles and a commercial TSI electrometer to measure the concentration. This setup, that we call the HDMA setup, was used to assess the instrument's performance for particles of 5 nm in diameter and smaller. The Hauke setup, calibrating solely with silver particles, was used to assess the performance of the

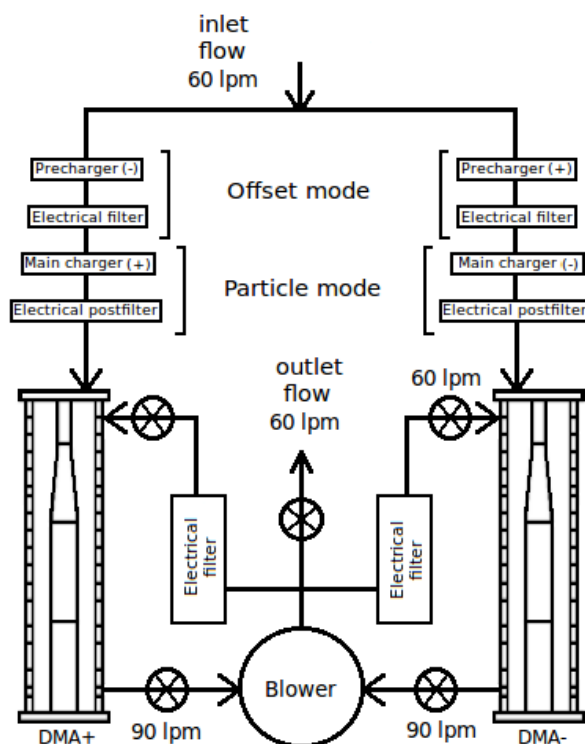


Figure 1: Schematic figure of the NAIS. The air sample is divided between the positive and negative columns. The sheath flow of the DMA is arranged in a closed loop of 60 lpm so that the total flow in the DMA is 90 lpm. The offset mode module charges and filters the particles to allow measurements of zero air. The particle mode module charges particles so that the total particle concentration can be estimated. The AIS does not have a particle mode module and the ANAIS has several blowers to control the flows more accurately.

instrument for particles between 4 and 40 nm in diameter. The mobility of the silver particles was selected using the Hauke DMA and the concentration was measured by an electrometer and a Condensation Particle Counter (CPC, TSI 3025). The ion spectrometers were tested for their mobility and concentration detection in ion mode (both setups) and in particle (total) mode (Hauke setup only).

When the instruments were not being calibrated in the setups described above, they were measuring in the intercomparison room, along with reference instruments: a Differential Mobility Particle Sizer (DMPS, 10-300 nm), a Balance Scanning Mobility Analyzer (BSMA, 0.8-7 nm), and an Ion-DMPS (2.2-11.5 nm). In the intercomparison room, the instruments were measuring ambient indoor air as well as outdoor-indoor mixed air when the door of the room, giving on a balcony, was opened. New Particle Formation (NPF) events were provoked in the intercomparison room and measured by all the ion spectrometers and the reference instruments.

RESULTS

The calibration results (Fig. 2) show that the instruments detected the mobility accurately for all instruments, in all modes. The concentration measurements were accurate in the ion mode but the ion spectrometers overestimated the particle concentration by a factor two to three. The NAISs almost always saw bigger concentrations than the AISs in the ion operation mode and the BSMA. Moreover, the NAIS overestimated the particle concentration compared to the DMPS. In general,

the negative column of the ion spectrometers performed better than the positive column.

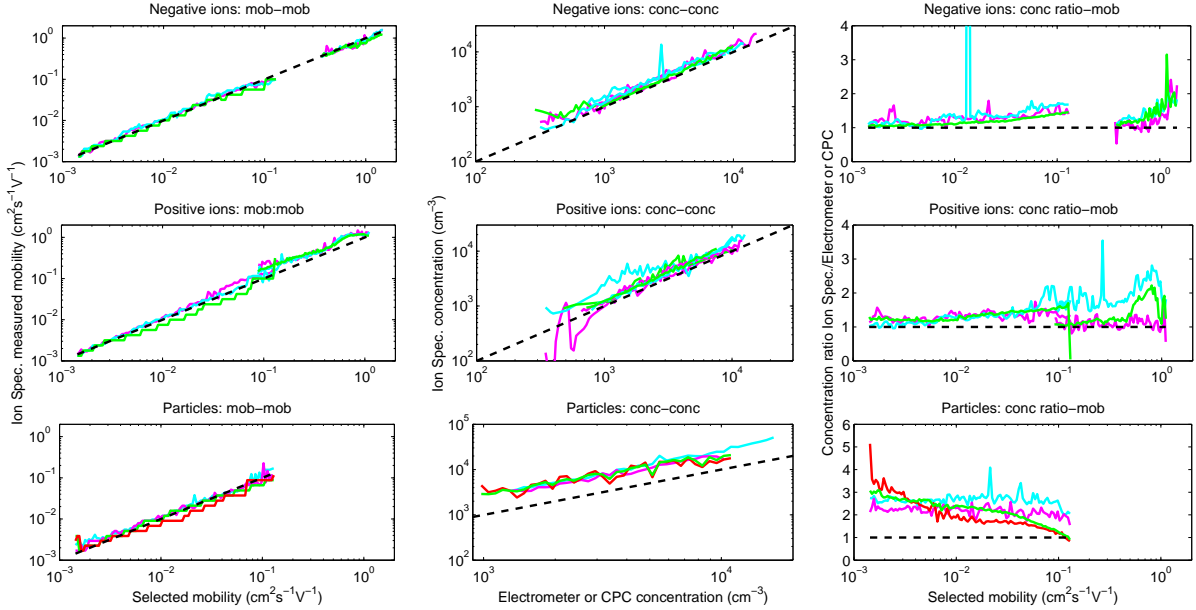


Figure 2: Results from the calibrations. Lines: 1-negative ions, 2-positive ions, 3-particles (NAISs only). Columns: 1-mobility-mobility, 2-concentration-concentration, 3-concentration ratio-mobility. In the first two lines, magenta: mean of AISs, cyan: mean of NAISs, green: ANAIS. In the particle line (3rd), magenta: mean of the positive column of the NAISs, cyan: mean of the negative column of the NAISs, red: positive column of the ANAIS, green: negative column of the ANAIS.

We calculated and compared the formation and growth rates of a NPF event for all ion spectrometers and relevant reference instruments (Table 1). The formation rates detected with the AISs was smaller than those detected with the NAISs. Also, the growth rates were about the same for AISs and NAISs. These results are consistent with our calibration results. The ANAIS behaved similarly to other NAISs, but is not included in the NAIS averages. The charged fraction calculated with the NAISs was compared to the charged fraction based on the Ion-DMPS and agreed well. This is unexpected given that the particle concentration was overestimated during calibration and indoor/outdoor air measurements. This particular feature of the NAISs is currently under investigation.

CONCLUSIONS

The ion spectrometer intercomparison workshop lead to nine main conclusions that one must bear in mind when interpreting data from an AIS or an NAIS:

- 1 The mobility detection of AISs and NAISs is accurate, provided that the instrument is kept clean and its flows are unobstructed.
- 2 The growth rates obtained from the ion spectrometers are reliable.
- 3 The concentration can vary by up to 10% from one individual ion spectrometer to the other.
- 4 In ion mode, the NAISs give slightly higher concentrations than the AISs. The AISs agree better with the BSMA.

Instrument	J_2 ($\text{cm}^{-3} \text{s}^{-1}$)			GR (nm h^{-1})					
	neg.	pos.	part.	2–3 nm (–/+)		3–7 nm (–/+)		7–20 nm (–/+)	
AIS 1	–	–	–	–	–	–	–	–	–
AIS 2	0.13	–	–	12.3	–	24.5	–	34.9	–
AIS 3	0.18	–	–	12.8	–	22.6	–	33.8	–
AIS 6	–	–	–	–	–	–	–	–	–
AIS 7	0.15	–	–	16.3	–	33.8	–	37.7	–
NAIS 1	0.21	0.08	2.2	15.2	13.3	21.4	23.4	39.6	39.3
NAIS 2	0.23	–	–	9.6	–	27.5	–	37.1	–
NAIS 3	0.20	–	3.9	11.2	–	27.1	–	34.6	–
NAIS 4	0.21	0.07	1.6	13.7	10.8	22.7	19.1	37.3	36.2
NAIS 5	0.24	0.09	1.3	15.8	12.2	22.9	25.1	34.9	38.9
A-NAIS	0.20	0.08	4.7	16.2	13.2	25.3	22.0	38.1	–
DMPS	–	–	1.1	–	–	–	–	–	37
BSMA	0.27	–	–	11.4	–	23.0	–	–	–
AIS (mean and st. dev.)	0.15 ± 0.03	–	–	13.8 ± 2.2	–	27.0 ± 7.0	–	35.5 ± 2.0	–
NAIS (mean and st. dev.)	0.22 ± 0.02	0.08 ± 0.01	2.7 ± 1.5	13.6 ± 2.7	12.4 ± 1.2	24.5 ± 2.5	22.4 ± 2.5	38.1 ± 1.7	–

Table 1: Analysis of the a NPF event on 12 June 2009 by reference instruments and 11 ions spectrometers. The mean and standard deviation for the AISs and NAISs are shown in the last two rows.

- 5 The NAISs can overestimate the particle concentration (particle mode) by a factor 2-3.
- 6 The formation rates vary from one individual instrument to the other, it also changes widely depending on the analysis method.
- 7 The ion formation rates calculated from NAIS data are higher than those calculated from the BSMA or AISs.
- 8 The particle formation rates of the NAISs is overestimated compared to the DMPS.
- 9 The charged fraction calculated from NAISs is considered unreliable because of conclusions 4, 5, 6 and 7. However, the analysis of an NPF yielded similar charged fractions for the NAISs and the Ion-DMPS.

ACKNOWLEDGEMENTS

Jani Hakala and Jyri Mikkilä are acknowledged for their help in various tasks throughout the workshop. Ella-Maria Kyrö and Anna Frey are acknowledged for their help in preparing the instruments for calibration. This research was supported by the Academy of Finland Center of Excellence program (project number 1118615), the European Commission 6th Framework program project EUCAARI, contract no 036833-2 (EUCAARI) and the Estonian Science Foundation, grant number 8342. The work of A. Franchin and S. Schobesberger was supported by the European Commission under the 7th Framework Programme (grant agreement number 215072: Marie Curie Initial Training Network, CLOUD-ITN).

REFERENCES

- Asmi, E., Sipilä, M., Manninen, H. E., Vanhanen, J., Lehtipalo, K., Gagné, S., Neitola, K., Mirme, A., S. M., Tamm, E., Uin, J., Komsaare, K., Attoui, M., and Kulmala, M. (2009). Results of the first air ion spectrometer calibration and intercomparison workshop. *Atmos. Chem. Phys.*, **9**, 141–154.
- Duplissy, J., Enghoff, M. B., Aplin, K. L., Arnold, F., Aufmhoff, H., Avngaard, M., Baltensperger, U., Bondo, T., Bingham, R., Carslaw, K., Curtius, J. David, A., Fastrup, B., Gagné, S., Hahn, F., Harrison, R. G., Kellett, B., Kirkby, J., Kulmala, M., Laakso, L., Laaksonen, A., Lillestol, E., Lockwood, M., Mäkelä, J., Makhmutov, V., Marsh, N. D., Nieminen, T., Onnela, A., Pedersen, E., Pedersen, J. O. P., Polny, J., Reichl, U., Seinfeld, J. H., Sipilä, M., Stozhkov, Y., Stratmann, F., Svensmark, H., Svensmark, J., Veenhof, R., Verheggen, B., Viisanen, Y., Wagner, P. E., Wehrle, G., Weingartner, E., Wex, H., Wilhelmsson, M., and Winkler, P. M. (2010). Results from the CERN pilot CLOUD experiment. *Atmos. Chem. Phys.*, **10**, 1635–1647.
- Gagné, S., Lehtipalo, K., Manninen, H. E., Nieminen, T., Schobesberger, S., Franchin, A., Yli-Juuti, T., Mirme, A., Mirme, S., Hörrak, U., Petäjä, T., Asmi, E., and Kulmala, M. (2011). Intercomparison of air ion spectrometers: a basis for data interpretation. *Atmos. Meas. Tech. Discuss.*, **4**, 1139–1180.
- Manninen, H. E., Nieminen, T., Asmi, E., Gagné, S., Häkkinen, S., Lehtipalo, K., Aalto, P. P., Vana, M., Mirme, A., Mirme, S., Hörrak, U., Plass-Dülmer, C., Stange, G., Kiss, G., Hoffer, A., Törö, N., Moerman, M., Henzing, B., de Leeuw, G., Brinkenberg, M., Kouvarakis, G. N., Bougiatioti, A., Mihalopoulos, N., O’Dowd, C., Ceburnis, D., Arneth, A., Svenningsson, B., Swietlicki, E., Tarozzi, L., Decesari, S., Facchini, M., Birmili, W., Sonntag, A., Wiedensohler, A., Boulon, J., Sellegri, K., Laj, P., Gysel, M., Bukowiecki, N., Weingartner, E., Wehrle, G., Laaksonen, A., Hamed, A., Joutsensaari, J., Petäjä, T., Kerminen, V.-M., and Kulmala, M. (2010). EUCAARI ion spectrometer measurements at 12 european sites – analysis of new particle formation events. *Atmos. Chem. Phys.*, **10**, 7907–7927.
- Manninen, H. E., Petäjä, T., Asmi, E., Riipinen, I., Nieminen, T., Mikkilä, J., Hörrak, U., Mirme, A., Mirme, S., Laakso, L., , Kerminen, V.-M., and Kulmala, M. (2009). Long-term field measurements of charged and neutral clusters using Neutral cluster and Air Ion Spectrometer (NAIS). *Boreal Env. Res.*, **14**, 591–605.
- Mirme, A., Tamm, A., Mordas, G., Vana, M., Uin, J., Mirme, S., Bernotas, T., Laakso, L., Hirsikko, A., and Kulmala, M. (2007). A wide-range multi-channel air ion spectrometer. *Boreal Env. Res.*, **12**, 247–264.

ION-INDUCED NUCLEATION FRACTION AND SMALL ION CONCENTRATION ASYMMETRY IN HELSINKI

S. GAGNÉ¹, J. LEPPÄ², T. PETÄJÄ¹, M.J. MCGRATH¹, M. VANA^{1,3}, V.-M. KERMINEN²,
L. LAAKSO^{1,2,4} and M. KULMALA¹

¹Department of Physics, University of Helsinki, P.O. Box 64, 00014 Helsinki, Finland.

²Finnish Meteorological Institute, P.O. Box 503, 00101 Helsinki, Finland.

³Institute of Physics, University of Tartu, Ülikooli 18, 50090 Tartu, Estonia.

⁴School of Physical and Chemical Sciences, North-West University, Private Bag x6001, Potchefstroom 2520, South Africa.

Keywords: Ion-induced nucleation, urban, Ion-DMPS, small ion asymmetry.

INTRODUCTION

New particle formation (NPF), nucleation and growth of particles to climatically relevant sizes takes place frequently in the atmosphere (Kulmala et al., 2004). Several nucleation mechanisms have been proposed, and despite frequent observation of the phenomena, the exact contribution of these mechanism is still unclear. Nucleation mechanisms can be separated into two categories: ion-induced nucleation (IIN) and neutral nucleation. On the one hand, IIN is all nucleation involving an electric charge; neutral nucleation on the other hand happens without the presence of an electric charge.

The contribution of IIN to new particle formation is under discussion as a possibly important source of particles for Cloud Condensation Nuclei (CCN). If IIN would indeed be important, it would have an effect on the Earth's climate through its control of the cloud cover (Carslaw et al., 2002). Although its importance in the upper troposphere, where it is predicted to thrive, is still badly known, its contribution in the boundary layer is becoming increasingly clear (Iida et al., 2006; Laakso et al., 2007; Iida et al., 2008; Gagné et al., 2008; Manninen et al., 2009; Gagné et al., 2011).

This paper contributes to the knowledge on the participation of IIN to new particle formation using the longest measurement dataset in an urban area: Helsinki. Moreover, a method used to calculate the charging state in Air Ion Spectrometers (Vana et al., 2006) data is adapted to the Ion-DMPS and its performance evaluated. Also, we analyze the data using a new theoretical framework (Leppä et al., 2011) allowing the concentration of small ions to be different for different polarities.

METHODS

We used an Ion-DMPS (Ion-Differential Mobility Particle Sizer, Laakso et al., 2007) to measure the charging ratio as a function of size and time between December 2008 and February 2010 at the SMEAR III station in Helsinki, Finland. The charging ratio is obtained by dividing the air ion concentration in ambient mode to the concentration in neutralized mode (bipolar charge equilibrium). When a particle population is at charge equilibrium, the charging ratio is one. When there are more charges than at equilibrium, the charging ratio is above one. Similarly, when there are less charges than at equilibrium, the charging ratio is below one. The Ion-DMPS yielded

charging ratios for sizes between about 2 and 12 nm for both the positive and negative polarity, with a time resolution of about 27 minutes.

For a NPF event day, the charging ratio is typically presented as one average value during the event time as a function of particle size. The charge distribution of a particle population generally tends to the charge equilibrium as the new particles grow. This is reflected in that the charging ratio tends to one as the particle size increases. This is the case when the equilibrium is the bipolar equilibrium. There are cases, as we will discuss later, where the equilibrium is not the bipolar equilibrium. The value towards which the charging ratio tends as the particle size increases is called the asymptotic charging ratio.

A new method for analyzing the Ion-DMPS data was developed and tested. The old method consists in finding the median value of the charging ratio during the time of the NPF event, for each size channel. The new method consists in plotting the concentration of ions in the ambient mode as a function of the concentration of ions in the neutralized mode. The slope (forced through the origin) is then the average charging ratio for the size channel. The uncertainty can be estimated through the scattering of the points around the slope.

A new theoretical description of the behavior of the charging state as a function of particle size developed by Leppä et al. (2011) and reproduced in Eq. 1 that allows the concentration of small ions to be different for negative and positive ions was used for the first time. This equation gives the charging state (the charging ratio at the size where nucleation takes place) as a function of the diameter d_p .

$$S_{asy}^{\pm}(d_p) = 1 - \frac{1}{k^{\pm}d_p} + \frac{(S_{asy,0}^{\pm} - 1)k^{\pm}d_0 + 1}{k^{\pm}d_p} e^{-k^{\pm}(d_p - d_0)} \quad (1)$$

where

$$k^{\pm} = \frac{\alpha N_c^{\mp}}{GR} \quad (2)$$

and d_p is the particle diameter, $S_{asy,0}$ and d_0 are the asymmetric charging state and diameter of newly formed particles, respectively, N_c^{\pm} is the number concentration of ion clusters (the polarity is indicated by the superscripts), GR is the particle growth rate and α ($\sim 1.6 \times 10^{-6} \text{ cm}^3\text{s}^{-1}$) is the ion-ion recombination coefficient. The asymptotic charging ratio in such asymmetric cases is the ratio of the small ion concentrations so that $S_{asymptotic}^{\pm} = N_c^{\pm}/N_c^{\mp}$.

For each NPF event day, the charging ratio as a function of particle size is plotted with an uncertainty box around each point. Points are normally generated in these uncertainty boxes 2000 times and Eq. 1 is fitted through these data points each time. For each day, the median value for S_{asy} is kept along with its corresponding k value and the Median Average Deviation, or MAD, of the 2000 fits is representative of the uncertainty of the fits.

RESULTS AND CONCLUSIONS

NPF event days took place on 15% of the days when the Ion-DMPS was measuring, 15% were undefined days and 70% were non-event days (Figure 1).

The IIN fraction in a NPF event is calculated using the charging state, multiplied by the equilibrium charged fraction at the size at which nucleation takes place. This means that the IIN fraction is the fraction of particles that are formed charged. An average IIN contribution of 0.7% has been found using both methods for calculating the charging state. The MAD using the new method was about half of the MAD using the old method, meaning that the new method significantly reduces the uncertainty of the charging state.

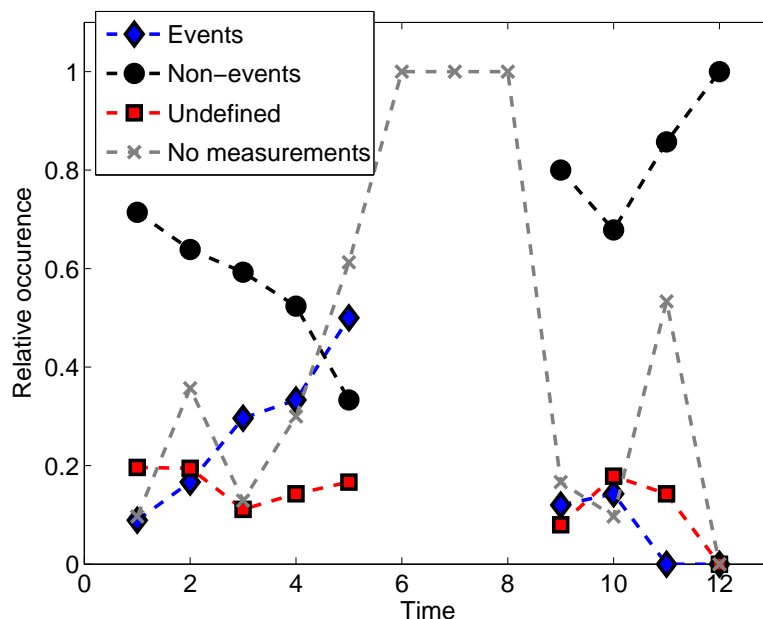


Figure 1: Classification of days on which Ion-DMPS measurements took place. The NPF event days seem to peak in spring in agreement with Hussein et al. (2008)

The new theoretical framework, allowing polarity asymmetry for small ions, also yielded a similar IIN contribution to NPF as the previously used method (Kerminen et al., 2007). The advantage of the new theoretical framework is that it explains why the asymptotic charging ratio is not one but rather slightly above one for one polarity and below one for the other. It also allows to capture the polarity asymmetry in the fitting and thus yields better charging state values.

In this study, we find that the fraction of ion-induced nucleation in the Helsinki urban area is very small (0.7%). This is in agreement with the results of Iida et al. (2006) and 2008 where the fraction of ion-induced nucleation has been found to be below 1% both in Boulder, Colorado and Mexico City. Based on these two results, this study and those of Gagné et al. (2008, 2010) and Manninen et al. (2009), the fraction of IIN seems to be bigger in Hyytiälä and cleaner areas, and smaller in polluted areas. According to Gagné et al. (2010), the contribution of neutral nucleation increases as the condensable vapor availability increases. In polluted areas, the saturation ratio of sulphuric acid is expected to be bigger than in a clean area. This could explain the tendency for IIN to be less important in urban areas.

ACKNOWLEDGEMENTS

This research was supported by the Academy of Finland Center of Excellence program (project number 1118615), and the European Commission 6th Framework program project EUCAARI, contract no 036833-2 (EUCAARI). Bjarke Molgaard is acknowledged for providing the DMPS event classification. Petri Keronen and Pasi P. Aalto are acknowledged for maintaining the SMEAR III station and providing the DMPS data.

REFERENCES

Carslaw, K. S., Harrison, R. G., and Kirkby, J. (2002). Cosmic rays, clouds and climate. *Science*, **298**, 1732–1737.

- Gagné, S., Laakso, L., Petäjä, T., Kerminen, V.-M., and Kulmala, M. (2008). Analysis of one year of Ion-DMPS data from the SMEAR II station, Finland. *Tellus*, **60B**, 318–329.
- Gagné, S., Leppä, J., Petäjä, T., McGrath, M., Vana, M., Laakso, L., and Kulmala, M. (2011). Measurements of charged ratios during new particle formation in Helsinki, Finland. Manuscript submitted to ACP.
- Gagné, S., Nieminen, T., Kurtén, T., Manninen, H. E., Petäjä, T., Laakso, L., Kerminen, V.-M., Boy, M., and Kulmala, M. (2010). Factors influencing the contribution of ion-induced nucleation in a boreal forest, Finland. *Atmos. Chem. Phys.*, **10**, 3743–3757.
- Hussein, T., Martikainen, J., Junninen, H., Sogacheva, L., Wagner, R., Dal Maso, M., Riipinen, I., Aalto, P. P., and Kulmala, M. (2008). Observation of regional new particle formation in the urban atmosphere. *Tellus*, **60B**, 509–521.
- Iida, K., Stolzenburg, M., McMurry, P. H., Dunn, M. J., Smith, J. N., Eisele, F., and Keady, P. (2006). Contribution of ion-induced nucleation to new particle formation: Methodology and its application to atmospheric observations in Boulder, Colorado. *J. Geophys. Res.*, **111**. D23201, doi:10.1029/2006JD007167.
- Iida, K., Stolzenburg, M. R., McMurry, P. H., and Smith, J. N. (2008). Estimating nanoparticle growth rates from size-dependent charged fractions: Analysis of new particle formation events in Mexico City. *J. Geophys. Res.*, **113**. D05207, doi:10.1029/2007JD009260.
- Kerminen, V.-M., Anttila, T., Petäjä, T., Laakso, L., Gagné, S., Lehtinen, K. E. J., and Kulmala, M. (2007). Charging state of the atmospheric nucleation mode: Implications for separating neutral and ion-induced nucleation. *J. Geophys. Res.*, **112**. D21205, doi:10.1029/2007JD008649.
- Kulmala, M., Vehkamäki, H., Petäjä, T., Dal Maso, M., Lauri, A., Kerminen, V.-M., Birmili, W., and McMurry, P. H. (2004). Formation and growth rates of ultrafine atmospheric particles: a review of observations. *J. Aerosol Sci.*, **35**, 143–176.
- Laakso, L., Gagné, S., Petäjä, T., Hirsikko, A., Aalto, P. P., Kulmala, M., and Kerminen, V. M. (2007). Detecting charging state of ultra-fine particles: instrumental development and ambient measurements. *Atmos. Chem. Phys.*, **7**, 1333–1345.
- Leppä, J., Gagné, S., Laakso, L., Kulmala, M., and Kerminen, V.-M. (2011). Behaviour of the aerosol charging state under asymmetric concentrations of small ions. Manuscript in preparation.
- Manninen, H. E., Nieminen, T., Riipinen, I., Yli-Juuti, T., Gagné, S., Asmi, E., Aalto, P. P., Petäjä, T., Kerminen, V.-M., and Kulmala, M. (2009). Charged and total particle formation and growth rates during EUCAARI 2007 campaign in Hyytiälä. *Atmos. Chem. Phys.*, **9**, 4077–4089.
- Vana, M., Tamm, E., Hörrak, U., Mirme, A., Tammet, H., Laakso, L., Aalto, P. P., and Kulmala, M. (2006). Charging state of atmospheric nanoparticles during the nucleation burst events. *Atmos. Res.*, **82**, 536–546.

MODELLED NEW PARTICLE FORMATION IN SOUTHERN AFRICAN SAVANNAH

R. GIERENS¹, L. LAAKSO^{1,2,3}, J. LAUROS¹, R. MAKKONEN¹, V. VAKKARI¹, D. MOGENSEN¹,
H. VUOLLEKOSKI¹ and M. BOY¹

¹Department of Physics, Division of Atmospheric Sciences, University of Helsinki,
Helsinki, 00014, Finland.

²Finnish Meteorological Institute, Research and Development, P.O. BOX 503, FI-00101, Finland.

³School of Physical and Chemical Sciences, North-West University, Potchefstroom, South Africa.

Keywords: AEROSOL MODELLING, PARTICLE FORMATION AND GROWTH, BOUNDARY LAYER,
SOUTH AFRICAN SAVANNAH.

INTRODUCTION

Africa is one of the least studied continents in respect to atmospheric aerosols. In this study we used measurements from a relatively clean savannah environment in South Africa to model new particle formation and growth. We were able to simulate the aerosol concentrations with a reasonable good agreement with the measurements.

METHODS

MALTE (Model to predict new Aerosol formation in the Lower TropospherE) is a one-dimensional model, which includes modules for boundary layer meteorology as well as aerosol dynamical and chemical processes (Boy *et al.*, 2006). The model used in this study is a further developed version, where the original turbulence scheme is replaced with that of SCADIS to get more reliable results considering vertical turbulent fluxes (Lauros *et al.*, 2010). The aerosol dynamic processes are simulated with UHMA (University of Helsinki Multicomponent Aerosol model). UHMA focuses on new particle formation and growth (Korhonen *et al.*, 2004), and thereby MALTE is well suited to study these phenomena. The emissions of monoterpenes and other organic vapours from the canopy are calculated with MEGAN (Model of Emissions of Gases and Aerosols from Nature) (Günther *et al.*, 2006). The chemistry is calculated using the Kinetic PreProcessor (KPP) (Damian *et al.*, 2002), and chemical reaction equations are from the Master Chemical Mechanism (<http://mcm.leeds.ac.uk/MCM/>). Previous studies indicate that this model is able to predict new particle formation events at the surface (Boy *et al.*, 2006 and Lauros *et al.*, 2010) and in the boundary layer (Siebert *et al.*, 2007) with good agreement compared with measurements.

The measurements utilized in this study were done at a relatively clean background savannah site in central southern Africa (Laakso *et al.*, 2008). The location is characterized with relatively low pollutant concentrations with occasional polluted air masses from the industrial areas 100-300 km to the east. New particle formation at the site has been found to take place during most of the sunny days, 69% of the days showing clear nucleation with additional 14 % of the days with non-growing nucleation mode (Vakkari *et al.*, 2011). The measurements utilized include meteorological variables (temperature, relative humidity, wind speed and direction, precipitation, and radiation), trace gas concentrations (SO₂, NO_x, CO, and O₃) and aerosols (number size distribution, particulate mass, and ion number size distribution) and concentration of volatile organic compounds (VOC's).

RESULTS

The observational data was used for input and comparisons with the simulations. Figure 1 shows the measured and modeled particle size distributions for one day, the 14th of October 2007, during which a relatively polluted airmass was present on the site. The model is able to reproduce the nucleation event and the growth of the particles, but the particles grow to the detected size, which is shown in the figure, later than observed. At noon the wind direction starts to change, leading to a change of airmass to less polluted and

thus no high particle concentrations are observed in the late afternoon hours. Since the model is one dimensional it's not able to simulate the change of air mass and thus the particle concentrations differ clearly from that observed.

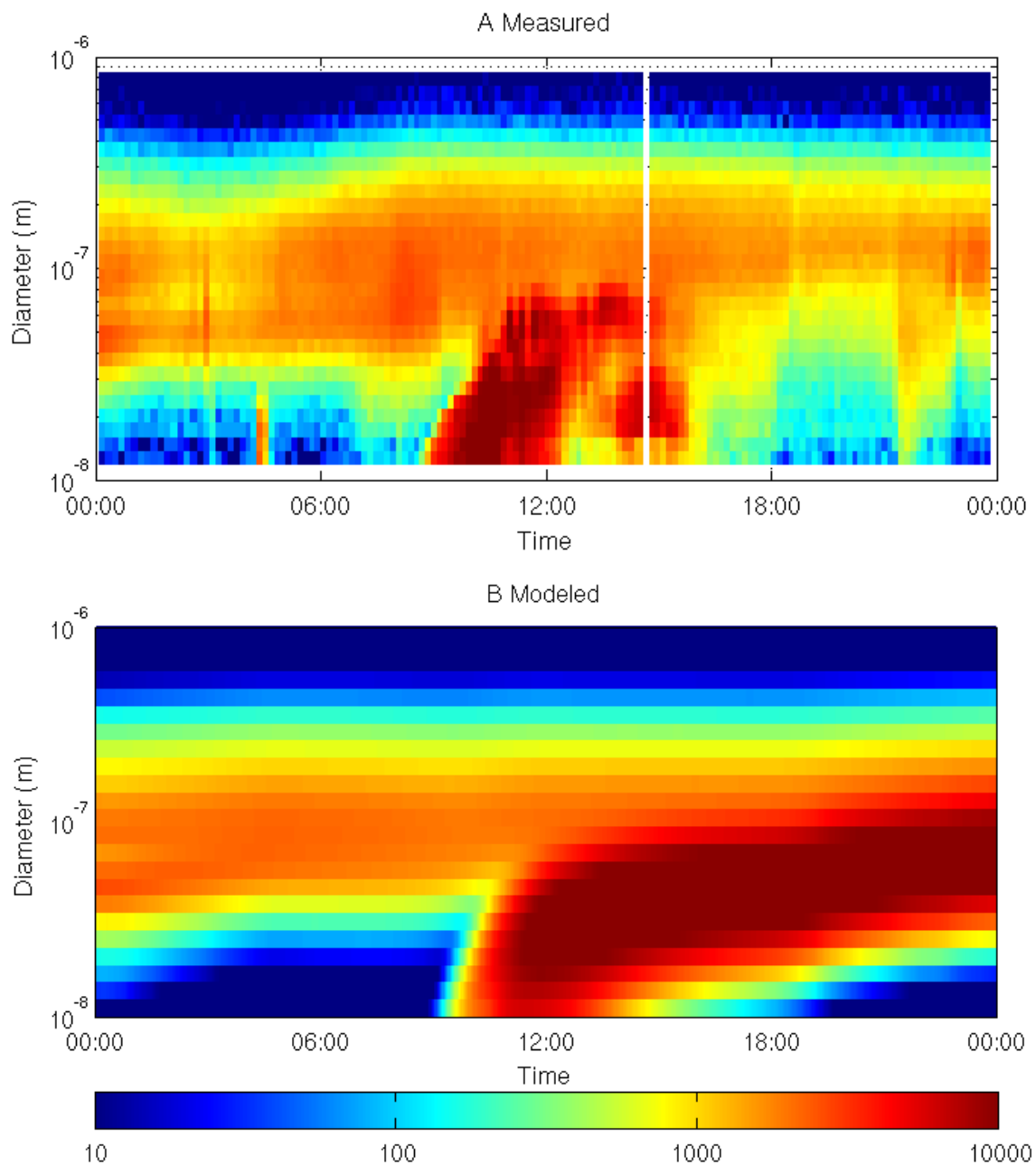


Fig 1. Measured (a) and modeled (b) particle size distribution on the 14th of October 2007. At noon the wind direction starts to change leading to a change of air mass and difference in measured and modeled particle concentrations.

Figure 2 shows the measured and modeled isoprene and monoterpene concentrations for the same day (14th of October 2007). The measured values are clearly lower as the model predicts, but due to the limited number of measurements we can't make any solid conclusions on the reliability of the model based on this comparison. These gases also contribute to the growth of the particles, and the particle size distribution shown in figure 1 does not give a reason to believe the VOC-concentrations in the model would be highly overestimated.

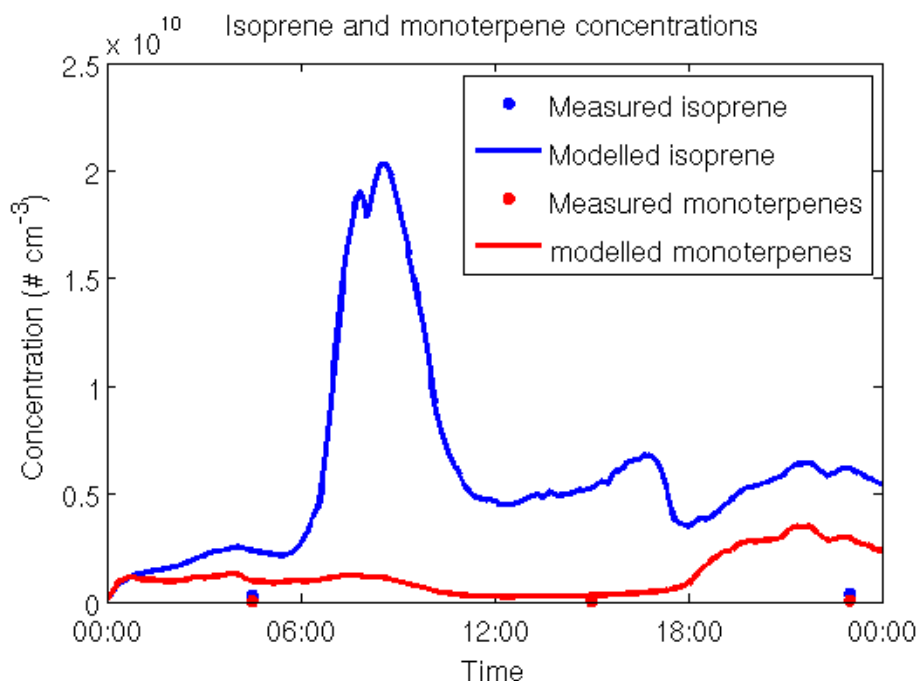


Figure 2. Measured (dots) and modelled (solid line) monoterpene (red) and isoprene (blue) concentrations on the 14th of October 2007. The model seems to give higher values compared to the measurements, but no proper conclusions can be drawn from this comparison due to the limited amount of measurements.

CONCLUSIONS

We selected a couple of days of continuous data and varying conditions of clean and polluted background air. The frequent new particle formation events and particle growth during this period was evaluated in detail. This work will present new model results to explain the high observed nucleation event frequency and discuss the reasons for high frequency of nucleation episodes observed.

ACKNOWLEDGEMENTS

This work was supported by the Finnish Academy, Finnish Center of Excellence and Helsinki University Centre for Environment.

REFERENCES

- Boy, M., Hellmuth, O., Korhonen, H., Nilsson, E. D., ReVelle, D., Turnipseed, A., Arnold, F., and Kulmala M. (2006). MALTE – model to predict new aerosol formation in the lower troposphere, *Atmos. Chem. Phys. Discuss.*, **6**, 3465-3512.
- Damian, V., Sandu, A., Damian, M., Potra, F., and Carmichael, G. R. (2002). The Kinetic PreProcessor KPP -- A software environment for solving chemical kinetics, *Comput. Chem. Eng.*, **26**, 1567-1579.
- Günther, A., Karl, T., Harley, P., Wiedinmyer, C., Palmer, P. I., and Geron, C. (2006). Estimates of global terrestrial isoprene emissions using MEGAN (Model of Emissions of Gases and Aerosols from Nature), *Atmos. Chem. Phys.*, **6**, 3181–321.
- Korhonen, H., Lehtinen, K. E. J., and Kulmala, M. (2004). Multicomponent aerosol dynamics model UHMA: model development and validation, *Atmos. Chem. Phys.*, **4**, 471.
- Laakso, L., Laakso, H., Aalto, P. P., Keronen, P., Petäjä, T., Nieminen, T., Pohja, T., Siivola, E., Kulmala, M., Kgabi, N., Molefe, M., Mabaso, D., Phalatse, D., Pienaar, K., and Kerminen, V.-M. (2008). Basic characteristics of atmospheric particles, trace gases and meteorology in a relatively clean Southern African Savannah environment, *Atmos. Chem. Phys.*, **8**, 4823–4839.
- Lauros, J., Sogachev, A., Smolander, S., Vuollekoski, H., Sihto, S.-L., Laakso, L., Mammarella, I., Rannik,

- Ü., and Boy, M. (2010). Particle concentration and flux dynamics in the atmospheric boundary layer as the indicator of formation mechanism, *Atmos. Chem. Phys. Discuss.* **10**: (8), 20005-20033.
- Siebert, H., Wehner, B., Hellmuth, O., Stratmann, F., Boy, M. and Klumala, M. (2007). New-particle formation in connection with a nocturnal low-level jet: Observations and modeling results, *Geophys. Res. Lett.*, **34**, L16822.
- Vakkari, V., Laakso, H., Kulmala, M., Laaksonen, A., Mabaso, D., Molefe, M., Kgabi, N. and Laakso, L. (2011). New particle formation events in semi-clean South African savannah, *Atmos. Chem. Phys.*, **11**, 3333-3346.

IS FOREST MANAGEMENT A SIGNIFICANT SOURCE OF MONOTERPENES INTO THE BOREAL ATMOSPHERE?

S. HAAPANALA¹, H. HAKOLA², H. HELLÉN², M. VESTENIUS², J. LEVULA³ and J. RINNE¹

¹Department of Physics, University of Helsinki, P.O. box 64, Helsinki, Finland.

²Air Quality Research, Finnish Meteorological Institute, P.O. box 503, Helsinki, Finland.

³Hyttiälä forestry field station, University of Helsinki, Hyttiäläntie 124, 35500 Korkeakoski, Finland.

Keywords: forest management, monoterpene, VOC emission, stump, logging residue.

INTRODUCTION

Biogenic volatile organic compounds (VOCs) have many important effects on the atmosphere and climate. Although the emissions of biogenic VOCs in boreal areas have been studied quite intensively, there are still large gaps remaining in our knowledge. In particular, the seasonality of the emission rates is poorly known (Rinne et al., 2009). The emission rates from Scots pine (*Pinus sylvestris*) have been measured throughout the growing season (Tarvainen et al., 2005) and there are few measurements from Norway spruce (*Picea abies*) also during dormant periods (Hakola et al., 2003). These studies show that few biogenic VOCs are emitted during the winter, and the emission rates are quite low due to low temperatures (Tarvainen et al., 2005).

Mechanical damage on trees is known to enhance the VOC emissions from coniferous trees (e.g. Juuti et al., 1990; Loreto et al., 2000) and birch species (Hakola et al., 2001). For coniferous trees this is expected to be particularly important as they store significant amounts of monoterpenes within their resin ducts. Lots of forestry work is conducted during winter and spring in boreal forests. Cut stumps and logging residue can provide a source of VOCs into the atmosphere, possibly also in biologically inactive periods. In winter, the lifetimes of VOCs are also longer and are thus transported to larger area. The spring period is of great interest because the maximum of aerosol particle formation events are observed at that time (Dal Maso et al., 2005), and it is expected to be strongly affected by VOCs in the atmosphere (Kulmala et al., 2004).

In boreal coniferous forests some measurements of monoterpene concentrations in air close to forestry work areas have been reported (Strömvall and Petersson, 1991; Räisänen et al., 2008). In these studies a clear increase in the monoterpene concentrations were observed. Strömvall & Petersson (1991) measured up to 500 fold monoterpene concentration in air above fresh branch wood of Scots pine and Norway spruce as compared to the background level. Räisänen et al. (2008) reported 2-3 fold concentration in air on a Scots pine clear cut area for 7 weeks after the felling. During thinning of a ponderosa pine (*Pinus ponderosa*) plantation, tenfold monoterpene fluxes have been measured in California, USA (Schade and Goldstein, 2003). However, no long-term measurements of emissions from cut forests have been reported to our knowledge.

The aim of the present study was to measure the VOC emission rates and composition from tree stumps and forest felling areas, and to study their temporal evolution and dependence on environmental parameters. From the results we can evaluate the possible importance of the VOC emissions from forestry work in comparison to intact ecosystems.

METHODS

The measurements took place in the southern Finland, close to the Hyytiälä Forestry Field Station (61°51' N, 24°17' E, 180 m a.s.l.). The area belongs to the southern boreal vegetation zone, with mean annual temperature of about 3°C and mean annual precipitation of about 700 mm. The emission rates and composition were measured from fresh felling areas during summers 2007 and 2008.

In 2007 the measurements were conducted on a clear cut area of about 4.3 ha, felled in November 2006. The forest biomass was dominated by Norway spruce. The emissions from single stumps of Norway spruce, Scots pine and birch (*Betula* spp.) were measured using enclosures. The same spruce stump was measured in May, June and August of 2007. The emissions from a birch and a pine stump were measured only on one day in June.

In 2008 we conducted the measurements on a seed tree felling area of about 4.0 ha, felled in the end of April. Beginning in May, the emissions of two Scots pine stumps were measured using enclosures. In addition to the enclosure measurements, the ecosystem scale emission was measured using disjunct eddy accumulation.

The enclosure measurements were carried out by placing a Teflon bag around a tree stump. Air was pumped through the bag with a flow rate of about 4 l min⁻¹. The inlet air was passed through a MnO₂ ozone scrubber. The samples were taken from the inlet and the outlet port to Tenax-TA/Carbopack-B adsorbent tubes with a constant flow rate of about 0.1 l min⁻¹. The emission rates were normalized to the cross sectional area of the stump. Temperature inside the enclosure and photosynthetic photon flux density (PPFD) outside the enclosure were recorded at the same time.

The ecosystem scale emission flux was measured using disjunct eddy accumulation (DEA) method (Rinne et al., 2000; Turnipseed et al., 2009). During the operation, a large primary sampling valve was opened once a minute for 200 ms. This allowed the pre-evacuated intermediate storage reservoir (V=1 l) made of electro-polished stainless steel to fill with sample air. The vertical wind speed, measured by a sonic anemometer (Metek USA-1) placed above the accumulator, about 2 m above ground level, was recorded simultaneously. After the sampling, air was drawn through one of the adsorbent tubes reserved for updraft and downdraft samples. The decision on which tube should be used was based on the direction of the vertical flow at the time of sampling. The duration of the adsorbent flow was proportional to the vertical wind velocity resulting in linearly proportional sample volume, and hence true eddy accumulation. Two similar samplers were operated simultaneously in turns resulting in 30 s sample interval and altogether 110 samples during 55 minutes sampling period.

All adsorbent samples were later analyzed for isoprene, monoterpenes and sesquiterpenes using an automatic thermodesorption device (Perkin-Elmer ATD-400) connected to a gas chromatograph (HP-5890), with a mass-selective detector (HP-5972).

RESULTS AND DISCUSSION

The birch stump emitted some monoterpenes, mainly α -pinene, β -pinene, limonene and camphene. The average monoterpene emission was 40 $\mu\text{g m}^{-2} \text{h}^{-1}$. Sesquiterpene emission of the birch stump was negligible. It was not possible to identify whether the stump was silver or downy birch. Both of these birch species are known to have variable mono- and sesquiterpene emissions from their leaves (Hakola et al., 2001; Vuorinen et al., 2005). However, the emission from the wooden parts (stem, bark), or their terpenoid content are not well known. As birches don't have resin ducts or other large storage structures for terpenoids, it is easy to understand that the emission was not very strong after the trees were cut down.

Both spruce and pine stump emitted large amounts of monoterpenes and some sesquiterpenes. The average monoterpene emission from spruce and pine stumps, measured in 2007, were 5100 $\mu\text{g m}^{-2} \text{h}^{-1}$

and $52000 \mu\text{g m}^{-2} \text{h}^{-1}$, respectively. The average mono- and sesquiterpene emissions from the pine stumps measured in 2008 were $25000 \mu\text{g m}^{-2} \text{h}^{-1}$ and $600 \mu\text{g m}^{-2} \text{h}^{-1}$, respectively. These emission rates were significantly higher than those of birch, which is easily understood due to existence of resin ducts in coniferous trees.

For the spruce stump, the monoterpene emission rate remained almost constant for the whole summer and it was not dependent on temperature or on the PPFD. The sesquiterpene emission rates increased in August compared to the measurements earlier in summer. In August the sesquiterpene contribution was about 4 % of the monoterpene emission. Earlier, in May and in June it was only less than 1 %. Hakola et al., (2003) measured the emission rates from living Norwegian spruce and they found out that the contribution of the sesquiterpenes was quite small in comparison with monoterpene emission rates early summer, but in July the emission rates of sesquiterpenes increased contributing more than monoterpenes to the total VOC emission. These high emissions of sesquiterpenes are probably not stored in a tree but released for defensive or other purposes.

Ecosystem scale emissions were measured on six different days, resulting altogether 30 flux values. The monoterpene emissions ranged between 0 and $20000 \mu\text{g m}^{-2} \text{h}^{-1}$. The emissions were dominated by α -pinene and Δ^3 -carene. The measurements conducted on the first day, June 13, were later discarded from the further analysis since the vertical wind measurement was contaminated by horizontal wind due to tilted mast. We normalised the measured emission rates to 15°C using the exponential temperature dependency of monoterpene evaporation. Figure 1 show the temporal change of the total monoterpene emission of the whole ecosystem. There is a clear trend of decaying emission. During the first months there was some fresh resin on the pine stump surface, probably causing the high emission.

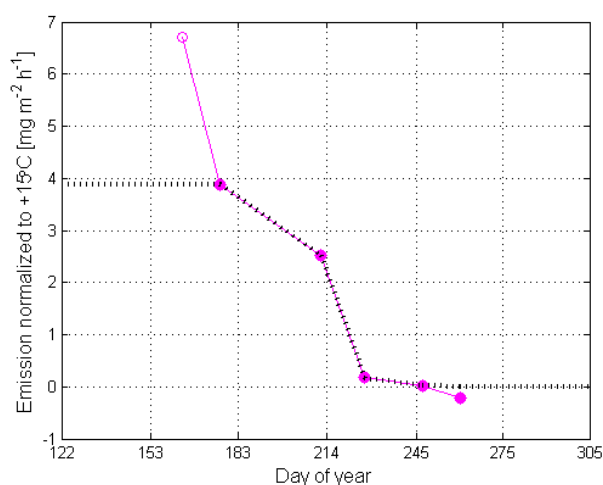


Figure 1. Temporal evolution of normalized monoterpene emission rate of the whole ecosystem. The first measurement point (indicated by open circle) was not used in the analysis because it was unreliable due to contaminated wind measurement. The dotted line is the interpolation used in the upscaling.

In order to estimate the significance of forest management to the total VOC emission in Finland we conducted simple upscaling. First we estimated the total monoterpene emission from intact and cut forest areas during one growing season using temperature data from Hyytiälä station during summer 2008. Pine forest emission potential is from Rinne et al., (2007). As the cut forest emission we used the decaying curve shown in Figure 1. Figure 2a show the daily minima and maxima temperatures used in the calculation. The resulting daily fluxes are shown in Figure 2b. Cumulative sum emission

during the 6 month period is shown in Figure 2c. The total monoterpene emissions from intact and cut forests are about 1000 mg m^{-2} and 8000 mg m^{-2} , respectively.

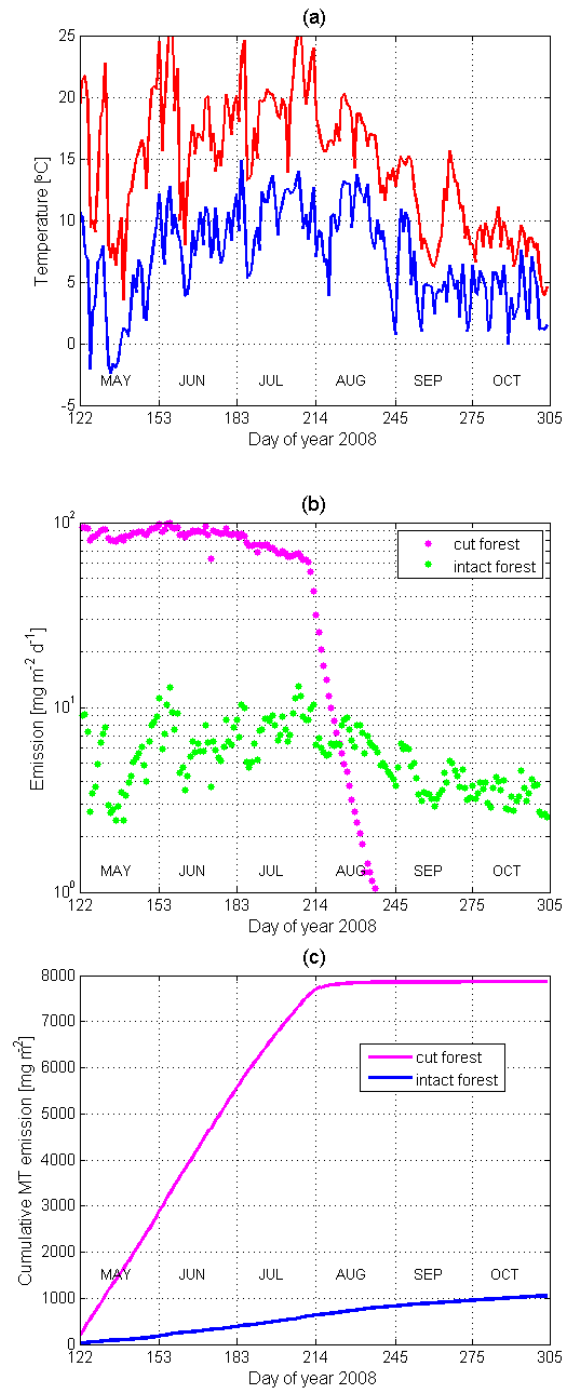


Figure 2. a) The temperature time series from Hyttiälä station was used to estimate the total monoterpene emissions during one summer. b) Daily fluxes of monoterpenes from clear cut area and intact forest. c) Accumulated monoterpene emission from clear cut area and intact forest during summer 2008.

To estimate the total amount of monoterpenes emitted annually due to forestry operations in Finland we upscaled this to cover all cutting methods. Instead of area, we used harvested volume as a scaling factor because the emissions are expected to be dependent on the amount of felling waste rather than on the treated area. Besides, the statistics on the harvested volume are very precise and easily available. In the seed tree felling area, where our measurements were conducted, the drain was 135 m³ ha⁻¹. Since the monoterpene emission for the six month period was 8 g m⁻², this yields to total monoterpene release of about 590 g m⁻³. According to the cutting statistics from 1998-2007 (Finnish Forest Research Institute, 2008), the total annual drain of coniferous trees from the Finnish forests is about 53 000 000 m³ which leads to monoterpene release of about 30 kilotonnes per year. The total annual emissions of monoterpenes from intact forests in Finland are estimated to be about 114 kilotonnes (Tarvainen et al., 2007). Surprisingly, the monoterpene emission caused by forestry operations seems to be as high as about 1/4 of the natural emission. This number is very rough estimate, but demonstrates that forest management might affect heavily to the local air chemistry soon after logging.

CONCLUSIONS

Large monoterpene emissions were measured from both single stumps and from the whole felling area. The emissions of sesquiterpenes were small and the emissions of isoprene were negligible. In the present study, only a very limited dataset was collected. Small dataset leads to large uncertainty in the results. Especially the upscaling results are uncertain. The exact result depends heavily on the extrapolation and interpolation of the emission. However, we believe that the order of magnitude of the upscaling result presented is correct and our conclusion on the importance of the forest management to the aerial concentration of monoterpenes is justified. In any case, the amount of the monoterpenes emitted by the forestry operations is significant. In addition to the amount of monoterpenes emitted into the atmosphere, forestry work may alter the timing of the emissions over the year. Forestry work conducted in the wintertime could provide a source of VOCs into the atmosphere also during biologically inactive winter period. However, the emissions from logging waste should be smaller in the wintertime due to low temperatures.

ACKNOWLEDGEMENTS

The financial support by the Academy of Finland Centre of Excellence program (project no 1118615) is gratefully acknowledged. S. Haapanala acknowledges Maj and Tor Nessling Foundation for financial support.

REFERENCES

- Dal Maso M.; Kulmala, M.; Riipinen, I.; Wagner, R.; Hussein, T.; Aalto, P. P.; Lehtinen, K. E. J. (2005). Formation and growth of fresh atmospheric aerosols: eight years of aerosol size distribution data from SMEAR II, Hyytiälä, Finland. *Boreal Env. Res.*, **5**, 323–336.
- Finnish Statistical Yearbook of Forestry 2008. (2008). Finnish Forest Research Institute, Vantaa, Finland, ISBN 978-951-40-2131-2.
- Hakola, H.; Laurila, T.; Lindfors, V.; Hellén, H.; Gaman, A.; Rinne, J. (2001). Variation of the VOC emission rates of birch species during the growing season. *Boreal. Env. Res.*, **6**, 237-249.
- Hakola, H.; Tarvainen, V.; Laurila, T.; Hiltunen, V.; Hellén, H.; Keronen, P. (2003). Seasonal variation of VOC concentrations above a boreal coniferous forest. *Atmos. Environ.*, **37**, 1623-1634.
- Juuti, S., Arey, J., Atkinson, R. (1990). Monoterpene emission rate measurements from a monterey pine. *J. Geophys. Res.*, **95**, 7515-7519.
- Kulmala, M.; Vehkamäki, H.; Petäjä, T.; Dal Maso, M.; Lauri, A.; Kerminen, V.-M.; Birmili, W.; McMurry, P. H. (2004). Formation and growth rates of ultrafine atmospheric particles: a review of observations, *J. Aerosol Sci.*, **35**, 143-176.

- Loreto, F., Nascetti, P., Graverini, A. and Mannozi, M. (2000). Emission and content of monoterpenes in intact and wounded needles of the Mediterranean pine, *Pinus pinea*. *Funct. Ecol.*, **14**, 589–595.
- Rinne, J.; Delany, A.; Greenberg, J.; Guenther, A. (2000). A true eddy accumulation system for trace gas fluxes using disjunct eddy sampling method. *J. Geophys. Res.*, **105**, 24791-24798.
- Rinne, J., Taipale, R., Markkanen, T., Ruuskanen, T.M., Hellén, H., Kajos, M.K., Vesala, T., Kulmala, M. (2007). Hydrocarbon fluxes above a Scots pine forest canopy: measurements and modeling. *Atmos. Chem. Phys.*, **7**, 3361-3372.
- Rinne, J., J. Bäck & H. Hakola, (2009): Biogenic volatile organic compound emissions from Eurasian taiga: Current knowledge and future directions. *Boreal Env. Res.*, **14**, 807-826.
- Räisänen, T., Ryppö, A., Kellomäki, S. (2008). Impact of timber felling on the ambient monoterpene concentration of a Scots pine (*Pinus sylvestris* L.) forest. *Atmos. Environ.*, **42**, 6759-6766.
- Schade, G. W. and Goldstein, A.H. (2003). Increase of monoterpene emissions from a pine plantation as a result of mechanical disturbances. *Geophys. Res. Lett.*, **30**, 1380.
- Strömvall, A.-M. and Petersson, G. (1991) .Conifer monoterpenes emitted to air by logging operations. *Scand. J. Forest Res.*, **6**, 253-258.
- Tarvainen, V., Hakola, H., Hellén, H., Bäck, J., Hari, P., Kulmala, M. (2005). Temperature and light dependence of the VOC emissions of Scots pine. *Atmos. Chem. Phys.*, **5**, 989-998.
- Turnipseed, A.; Pressley, S.; Karl, T.; Lamb, B.; Nemitz, E.; Allwine, E.; Cooper, W.; Shertz, S.; Guenther, A. (2009). The use of disjunct eddy sampling methods for the determination of ecosystem level fluxes of trace gases. *Atmos. Chem. Phys.*, **9**, 981-994.

A NEW NANOSCALE ION DIFFERENTIAL MOBILITY PARTICLE SIZER

J. HAKALA, M. SIPILÄ, K. LEHTIPALO, E. JÄRVINEN, E. SIIVOLA, M. KULMALA and
T. PETÄJÄ

Department of Physics, Division of Atmospheric Sciences, PL 64, 00014 University of Helsinki

Keywords: ATMOSPHERIC AEROSOLS, ATMOSPHERIC IONS.

INTRODUCTION

The first steps of the new particle formation (NPF) in the atmosphere are still unclear. There are several candidates responsible for the NPF including e.g. sulphuric acid (Weber *et al.* 1996, Petäjä *et al.* 2009) and organic vapors (Metzger *et al.* 2009). Also the role of ions in the process is under a heated debate as some results point towards negligible (Eisele *et al.* 2006), or at most minor (Gagné *et al.* 2008) or almost 100% (Yu and Turco, 2011) contribution of ions to the overall observed formation rate. Thus, without a doubt, more work needs to be done to clarify the role of ions in the NPF.

Laakso *et al.* 2007 introduced ion-Differential Mobility Analyzer (ion-DMPS), which is an instrument that is able to determine concentration of naturally charged ions and particle concentration after bipolar charging for both negative and positive polarity. This data can be used to extract charging state of the ambient particle population in the size range 3-15 nm (Laakso *et al.* 2007, Gagne *et al.* 2009). Furthermore, theoretical considerations by Kerminen *et al.* (2007) showed that the ion-DMPS data can actually be extrapolated down to smaller sizes as the growth aerosol mode carries information on the initial charging state. Thus, the relative contribution of ion induced and neutral nucleation pathways can be determined. The memory effect, however, depend on the ambient cluster ion concentration as well as on the growth rate of the particles. If the growth is small and the concentration of cluster ions is high, the growing mode rapidly loses its information on the initial charging state. One way to improve this is to develop an ion-dmps which is able to measure the charging state well below 3 nm in size. The new Nanoscale Ion Differential Mobility Particle Sizer (nano-IDMPS) constructed at the Division of Atmospheric Sciences of the University of Helsinki was optimized for measuring the size distribution of particles and naturally charged ions below the diameter of 7 nm. The instrument is currently deployed in a measuring campaign in SMEAR II station in Hyytiälä forest station.

METHODS

The basic setup of the nano-IDMPS is similar to conventional DMPS systems. It contains an aerosol neutralizer for ensuring the charge equilibrium of the particles, a Differential Mobility Analyzer (DMA) for classifying the particles according to their electrical mobility, and a Condensation Particle Counter (CPC) for counting the particles. The difference is, that in nano-IDMPS the radioactive source of the neutralizer can be blocked, so the sample aerosol goes through the same geometry if the sample line, but without being exposed to the radiation. With this kind of setup, the user can measure the size distribution of the naturally charged particles, or the size distribution of the particles in charge equilibrium (Laakso *et al.* 2007, Gagné *et al.* 2008). The nano-IDMPS is equipped with a TSI Model 3085 Nano DMA, which is designed for measuring nanoscale particles with minimal losses (Chen *et al.* 1998). The CPC is Pulse Height-CPC (PH-CPC), a modified TSI CPC 3025, where the optics is changed to measure the forward scattered pulse height of the white light from a particle. Also the saturator and condenser temperatures were optimized for better response for small particles (Marti *et al.*, 1996, Sipilä *et al.* 2009). The DMA is operated with bipolar voltage source to measure particles with both negative and positive charge. The length of the tubing between different parts of the instrument is kept as short as possible, to minimize the diffusion losses.

The full measuring cycle contains the measuring of naturally charged particles (ions) of both polarities, and both polarities of particles gone through the aerosol neutralizer. After measuring the size distribution of a particle type, the DMA voltage is set to zero to get the background of the PH-CPC. The background resulting from homogenous nucleation of butanol inside the PH-CPC can be separated by pulse-height analysis, and was excluded from the data.

CONCLUSIONS

The nano-IDMPS is a brand new instrument and currently performing its first measurements at field. The preliminary results seem promising, but a more detailed data analysis is still needed. As an example, in figure 1 are represented the size distributions of particles and ions of different polarities in Hyytiälä April the 19th 2011. In every panel of the figure, the onset of the nucleation is clearly visible starting roughly at 9:00 am. These size distribution plots are raw data, without inversion or loss corrections. Clearly, the nano-IDMPS can detect the start of the nucleation event more accurately and from smaller sizes than the conventional DMPS. From the data, the charging state of nano-particles as well as growth rates between 2-7 nm can be calculated, and thus get more information on the new particle formation process.

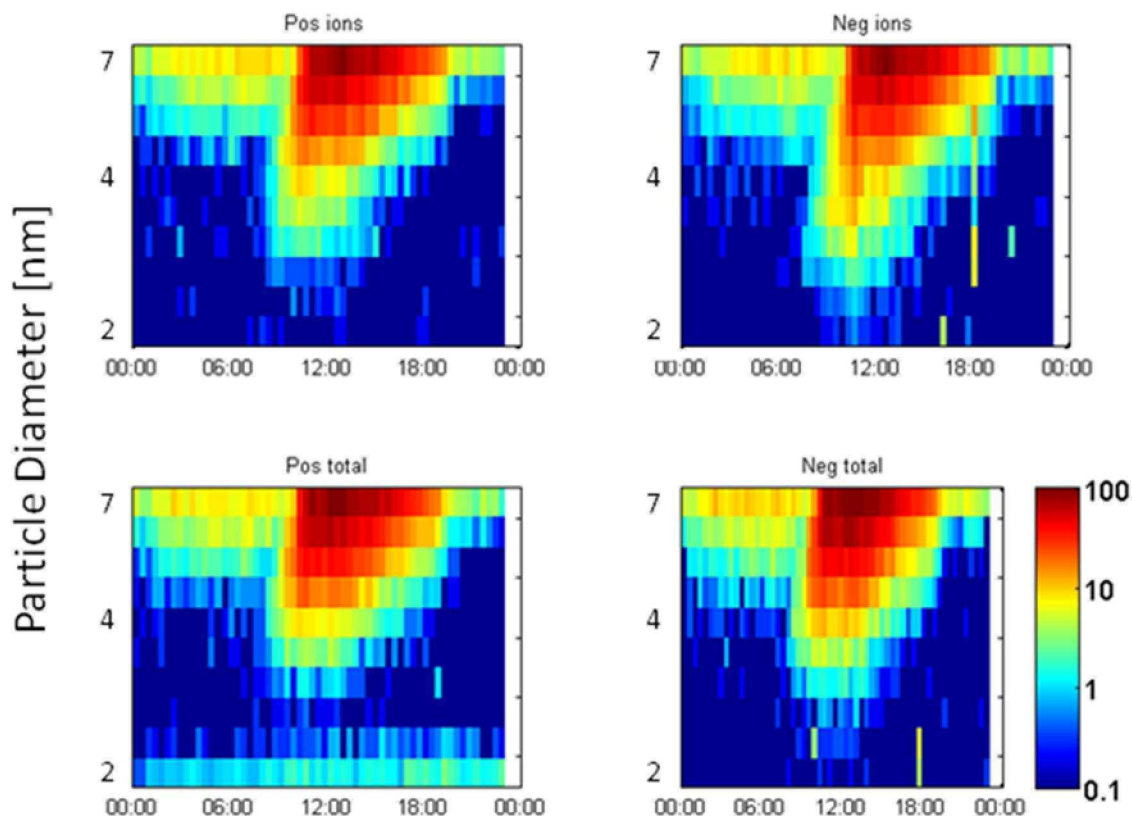


Figure 1. The size distributions of ions and particles in Hyytiälä on a nucleation event day April the 19th 2011 measured with a new nano-IDMPS. Pos/Neg ions refer to positive/negative naturally charged ions, whereas total is the neutralized charge distribution. The band in the lowest channels in pos total –mode comes from ions formed inside the neutralizer.

ACKNOWLEDGEMENTS

This work was supported by the Finnish Center of Excellency.

REFERENCES

- Chen, D.-R., D. Y. H. Pui, D. Hummes, H. Fissan, F. R. Quant and G. J. Sem (1998). Design and evaluation of a nanometer aerosol differential mobility analyzer (Nano-DMA). *J. Aerosol Sci.* **29**:497-509.
- Eisele, F. L., E. R. Lovejoy, E. Kosciuch, K. F. Moore, R. L. Mauldin III, J. N. Smith, P. H. McMurry and K. Iida (2006). Negative atmospheric ions and their potential role in ion-induced nucleation, *J. Geophys. Res.*, **111**:D04305, doi:10.1029/2005JD006568.
- Gagné, S., L. Laakso, T. Petäjä, V.-M. Kerminen and M. Kulmala (2008). Analysis of One Year of Ion-DMPS Data from the SMEAR II Station, Finland. *Tellus*, **60B**: 318-329.
- Gagné, S., T. Nieminen, T. Kurtén, H. E. Manninen, T. Petäjä, L. Laakso, V.-M. Kerminen, M. Boy, and M. Kulmala (2010). Factors Influencing the Contribution of Ion-Induced Nucleation in a Boreal Forest, Finland. *Atmos. Chem. Phys.*, **10**:3743-3757.
- Kerminen, V.-M., T. Anttila, T. Petäjä, L. Laakso, S. Gagné, K. E. J. Lehtinen, and M. Kulmala (2007). Charging state of the atmospheric nucleation mode: Implications for separating neutral and ion-induced nucleation, *J. Geophys. Res.*, **112**:D21205, doi:10.1029/2007JD008649.
- Laakso, L., S. Gagné, T. Petäjä, A. Hirsikko, P. P. Aalto, M. Kulmala and V.-M. Kerminen (2007). Detecting charging state of ultra-fine particles: instrumental development and ambient measurements. *Atmos. Chem. Phys.*, **7**:1333-1345.
- Marti, J. J., R. J. Weber, M. T. Saros, J. G. Vasilou and P. H. McMurry (1996). Modification of the TSI 3025 Condensation Particle Counter for Pulse Height Analysis, *Aerosol Sci. Tech.*, **25**: 2, 214-218.
- Metzger, A., B. Verheggen, J. Dommen, J. Duplissy, A. S. H. Prevot, E. Weingartner, I. Riipinen, M. Kulmala, D. V. Spracklen, K. S. Carslaw and U. Baltensperger (2009). Evidence for the role of organics in aerosol particle formation under atmospheric conditions. *PNAS*, **117**:6646-6651.
- Petäjä, T., R. L. Mauldin III, E. Kosciuch, J. McGarth, T. Nieminen, P. Paasonen, M. Boy, A. Adamov, T. Kotiaho and M. Kulmala (2009). Sulfuric acid and OH concentrations in a boreal forest site. *Atmos. Chem. Phys.*, **9**:7435-7448.
- Sipilä, M., K. Lehtipalo, M. Attoui, K. Neitola, T. Petäjä, P. P. Aalto, C. D. O'Dowd and M. Kulmala (2009). Laboratory Verification of PH-CPC's Ability to Monitor Atmospheric Sub-3 nm Clusters, *Aerosol Sci. Tech.*, **43**: 2, 126-135.
- Weber, R. J., J. J. Marti, P. H. McMurry, F. L. Eisele, D. J. Tanner and A. Jefferson (1996). Measured atmospheric new particle formation rates: Implications for nucleation mechanisms, *Chemical Engineering Communications*, **151**:53-64.
- Yu, F. and R. Turco (2011). The size-dependent charge fraction of sub-3-nm particles as a key diagnostic of competitive nucleation mechanisms under atmospheric conditions. *Atmos. Chem. Phys. Discuss.*, **11**:11281-11309.

DOES AMMONIA OR TRIMETHYLAMINE PARTICIPATE IN ATMOSPHERIC NUCLEATION? EXAMINATION BASED ON GAS-PHASE ACTIVITIES

A. Hamed¹, J. Joutsensaari¹, and A. Laaksonen^{1,2}

¹Department of Applied Physics, University of Eastern Finland, P. O. Box 70211 Kuopio, Finland

²Finnish Meteorological Institute, P.O. Box 503, 00101 Helsinki, Finland

Keywords: new particle formation, nucleation, sulfuric acid, organics

INTRODUCTION

Several laboratory and field studies suggest that sulfuric acid monomers and/or sulfate clusters are likely participants in atmospheric nucleation and growth (e.g. Weber et al., 1997; Sipilä et al., 2010). However, there are also observations that imply that the ambient sulfuric acid concentrations seem not to be enough to explain the observed nucleation and growth completely (e.g. Laaksonen et al., 2008a, Kuang et al., 2010). Organic compounds represent a large fraction of secondary aerosol mass (Jimenez et al., 2009), are thus likely to play an important role in growing freshly-formed. Recently, Metzger et al., (2010) reported that in the laboratory conditions, nucleation between H₂SO₄ and low-volatility organic vapours has been observed. In addition to the laboratory study, direct measurements during the field study in Tecamac, Mexico, showed that the molecular composition of 8–30 nm diameter particles formed from nucleation was dominated by amines. (Smith et al, 2010).

This study has been designed to investigate the roles that sulfuric acid, ammonia and trimethyl amine (TMA) may have in atmospheric nucleation. Particularly, we studied how ammonia (NH₃), TMA and sulphuric acid concentration and activities were connected to the observed nucleation rate. The rationale behind this approach is that if the nucleation is kinetically limited, then it should only depend on vapor concentrations, whereas if it is thermodynamically limited (due to the energy barrier of critical cluster formation), it should depend mainly on gas-phase activities of the nucleating vapors.

METHODS

For our analysis, we use the QUEST (Quantification of Aerosol Nucleation in the European Boundary Layer) campaign measurement data from the Finnish Boreal forest atmosphere during spring 2003. During this QUEST campaign a large number of different quantities were measured; here we mention only the measurements relevant to this study. Data includes 1) particle size distribution data measured by Differential Mobility Particle Sizer (DMPS) (Sihto et al., 2006); 2) the gas-phase concentrations of sulphuric acid (H₂SO₄), measured by a Chemical Ionization Mass Spectrometer (CIMS) (Sihto et al., 2006); 3) Ammonia (NH₃) concentrations (Laaksonen et al., 2008b) and trimethyl amine (TMA) (Sellegrì et al., 2005) concentrations. TMA (C₃H₉N) are derivative of ammonia in which two or three of the hydrogen have been replaced by methyl groups. TMA was measured by CIMS with a time resolution of less than 1 s, but the data was averaged over 60 s in order to reduce statistical error and the sampling noise. Particle size distribution and several meteorological and gas data are continuously obtained in Hyttiälä station since 1996, unlike the measurements of sulfuric acid and organics that are only available during the campaign periods. In that sense, the QUEST 2003 data set is quite unique that during the campaign a large number of nucleation events were observed: from a total of 23 measurement days, 20 were new particle formation (NPF) days. The measured sulfuric acid, ammonia and TMA were simultaneously available from altogether 10 days.

The gas-phase sulfuric acid activity (AH₂SO₄), NH₃ activity (ANH₃), TMA activity (ATMA) and the nucleation rate of critical clusters of 1.5 nm in diameter (J_{1.5}) are central quantities in this analysis.

Generally, gas-phase activity is defined as the ratio between the partial vapour pressures to the saturation vapour pressures. In other words, activity is essentially the same quantity as saturation ratio. We used Antoine Equation Parameters to calculate the saturation vapour pressure for TMA (Aston, et al., 1944) in the temperature range 192.84 - 276.60 K; and for NH₃ (Stull, 1947) in the temperature range 190-333K. For H₂SO₄ we used Ayers et al (1980) in the temperature range 338-445 K. Although the upper limit of the TMA saturation vapour pressure range is 276.60 K, we used the expression in the whole experimental T-range, up to 282 K. $J_{1.5}$ was extrapolated from the time-shifted values of the formation rate of 3 nm particles (J_3) – where J_3 was calculated directly from the particle size distribution data – by incorporating the probability that a particle would grow from 1 to 3 nm by vapor condensation before being scavenged by the pre-existing aerosol. Particularly, the time delay was estimated between the peak in sulphuric acid and particle number concentration of 3-6 nm particles (N_{3-6}) (Sihto et al., 2006). Consequently, $J_{1.5}$ values were estimated by using the method described by Kerminen and Kulmala (2002).

In order to examine the data, we produced so called activity plots, and corresponding concentration plots for sulfuric acid – ammonia, and for sulfuric acid – TMA, respectively. In studies of binary nucleation, activity plots are used to indicate how the activities of the two nucleating vapors can be varied so that the nucleation rate stays constant. An example of an activity plot is shown in Fig. 1. Unlike in the laboratory, the atmospheric nucleation rate is uncontrollable, and we do not have enough data to produce activity (or concentration) plots with constant nucleation rates. Instead, we use colour coding to indicate the nucleation rate of each data point. If the system studied is in fact the one responsible for nucleation in the atmosphere, one would then expect to see two things from the activity (or concentration) plot: 1) An anticorrelation type of behavior of the cloud of data points, and 2) A distribution of the colours indicating the nucleation rate such that colours corresponding to high rates are in further from the origin than colours corresponding to low rates.

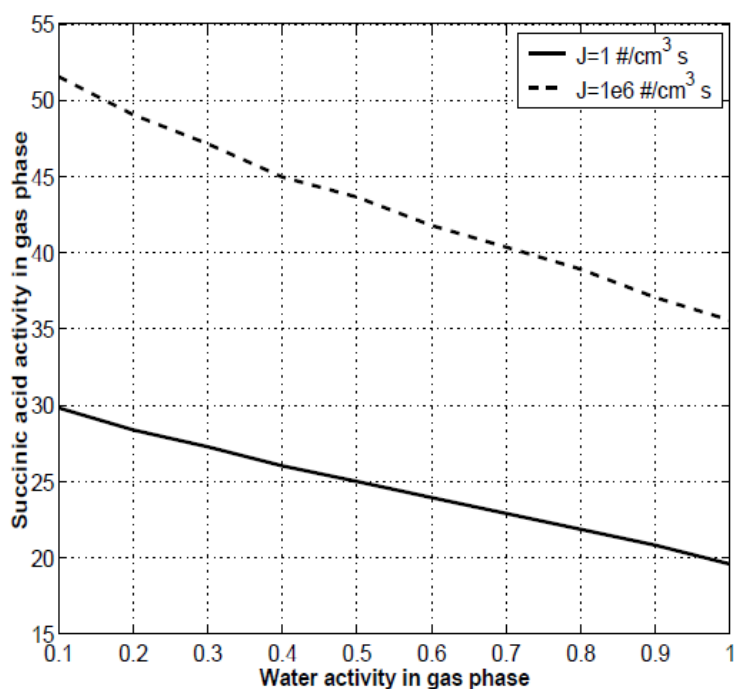


Figure 1. A theoretical activity plot of succinic acid/water nucleation (Gaman et al., 2004)

RESULTS

The measured ammonia concentrations were roughly on the same order as the TMA concentrations, whereas the ammonia activities were in general about one order of magnitude lower than TMA activities. Figure 2 a) and b) show logarithmic scatter plots of sulfuric acid and TMA concentrations and sulfuric acid and NH_3 concentrations, respectively, where the data points are color-coded according to $J_{1.5}$.

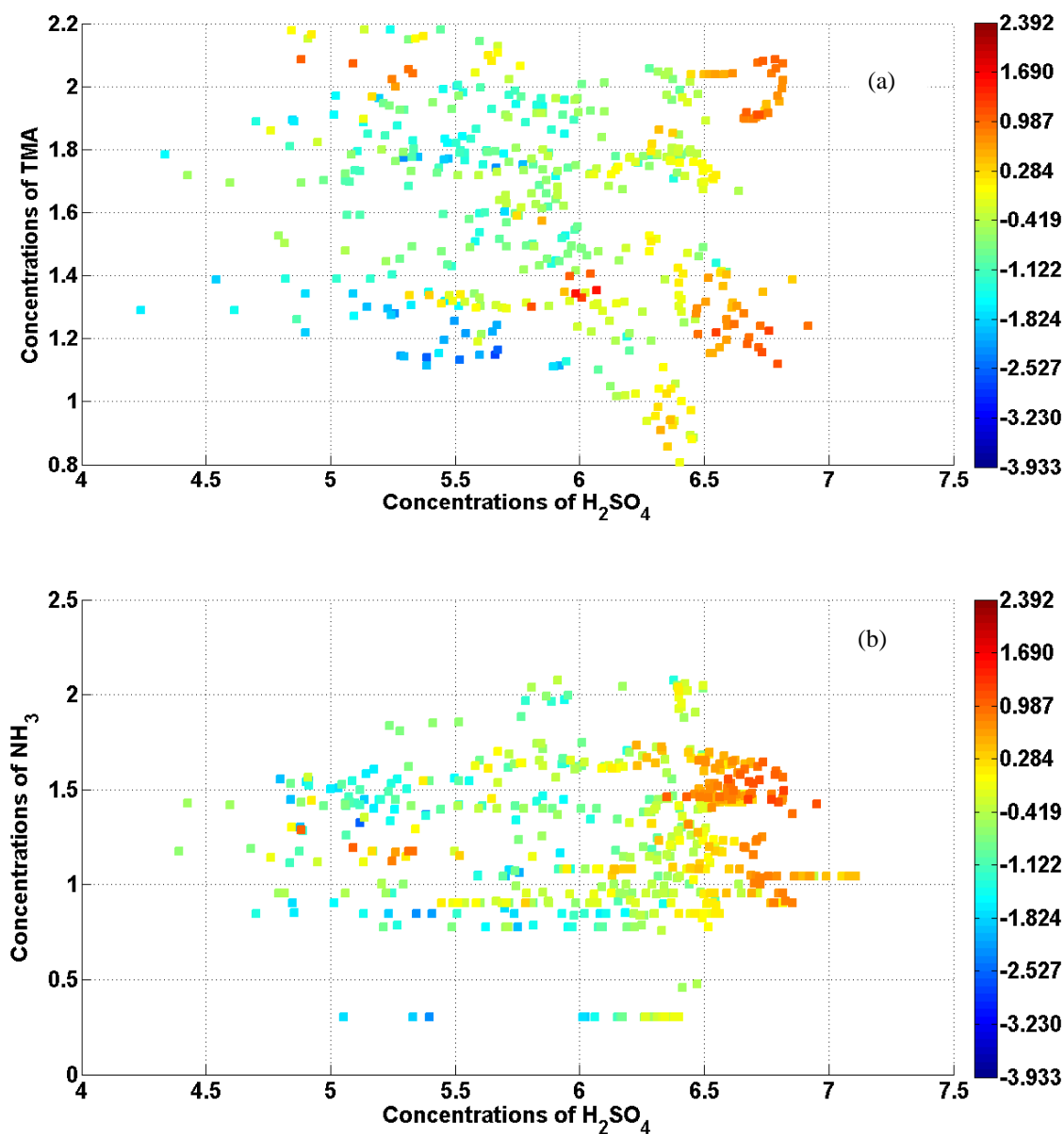


Figure 2. (a) Concentration of sulfuric acid [H_2SO_4] vs. concentration of TMA [TMA]; (b) [H_2SO_4] vs. concentration of NH_3 [NH_3] measured during the 2003 QUEST field campaign in Hyytiälä, Finland. Color coding indicates nucleation rate at 1.5 nm ($J_{1.5}$).

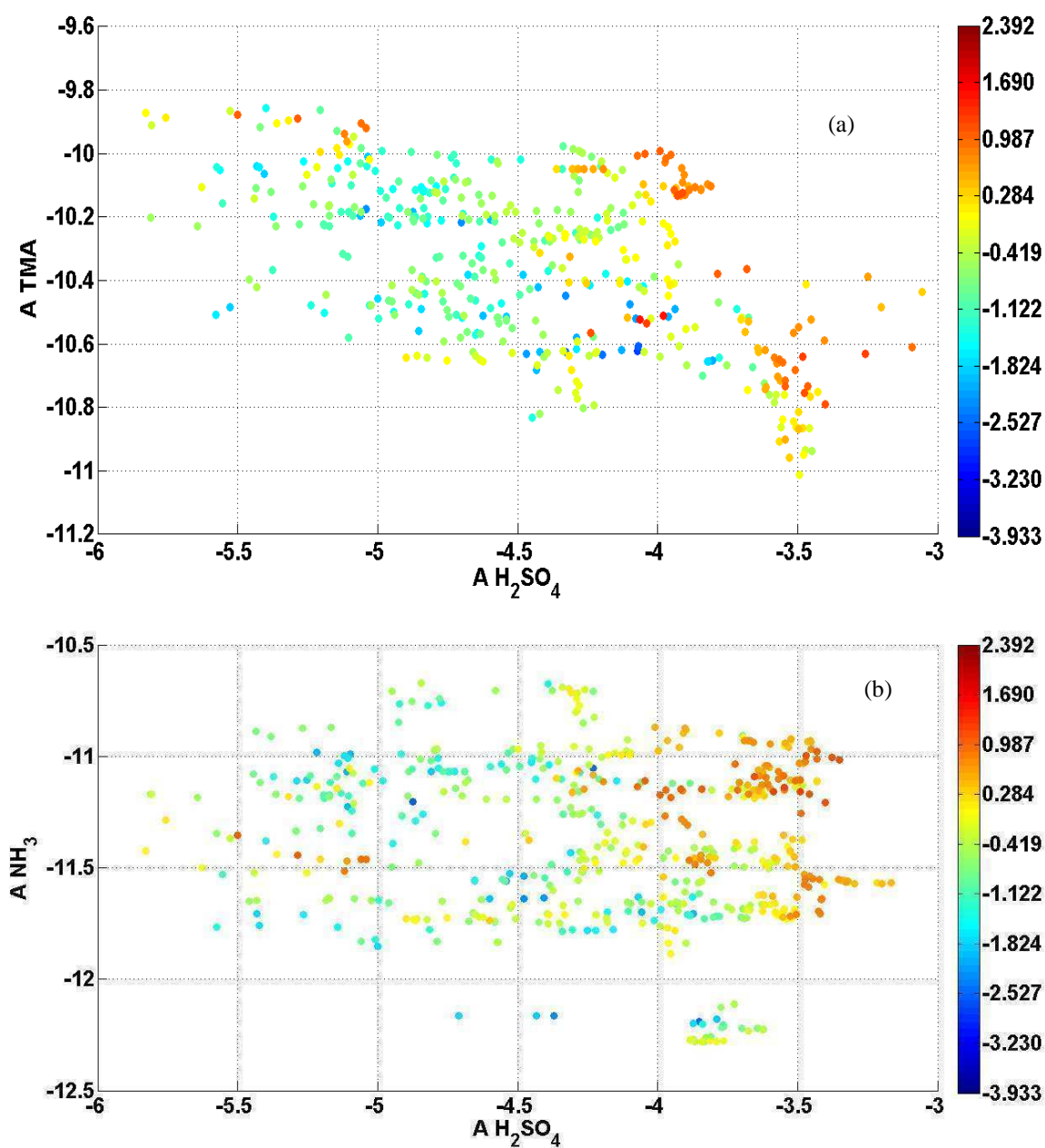


Figure 3. (a) A logarithmic scatter plot of activity of sulfuric acid ($A_{H_2SO_4}$) vs. TMA activity (A_{TMA}); (b) ($A_{H_2SO_4}$) vs. NH_3 activity (A_{NH_3}). The data points are color-coded according to $J_{1.5}$.

Figure 3 shows the logarithmic scatter plot of activity of sulfuric acid ($A_{H_2SO_4}$) and TMA activity (A_{TMA}). Figure 3b shows a similar plot for $A_{H_2SO_4}$ and A_{NH_3} . The data points are color-coded according to $J_{1.5}$. It is clearly seen from figures 2 b and 3 b that no significant correlation with ammonia can be detected. On the other hand there is a clear correlation between H_2SO_4 and TMA activities with value of $R^2 = 0.3$ (Fig 2a whereas the corresponding concentration plot shows only a very weak correlation if any (R^2 is 0.08)). The colours in Fig 2b are also distributed so that, in general, high nucleation rates are further from the origin than low nucleation rates. Taken together, there is indication from Figs. 2 and 3 that, 1) TMA was involved in the nucleation observed during the 2003 QUEST campaign but ammonia was not, and 2) the nucleation was thermodynamically rather than kinetically limited. However, the data is considerably noisy, so further examination is clearly needed.

ACKNOWLEDGEMENTS

Academy of Finland Centre of Excellence program (1118615) is gratefully acknowledged.

REFERENCES

- Aston, S., et al (1944). The heat capacity and entropy, heats of fusion and vaporization and the vapor pressure of trimethylamine. The entropy from spectroscopic and molecular data, *J. Am. Chem. Soc.*, 1944, 66, 1171-11.
- Gaman, A., et al (2004). Binary homogeneous nucleation in water-succinic acid and water-glutaric acid systems, *J. Chem. Phys.*, 120, 282–291.
- Jimenez, J. L. et al (2009). Evolution of organic aerosols in the atmosphere. *Science*, 326, 1525-1529.
- Kerminen, V.-M. and Kulmala, M.(2002). Analytical formulae connecting the “real” and the “apparent” nucleation rate and the nuclei number concentration for atmospheric nucleation events, *J. Aerosol Sci.*, 33, 609–622.
- Kuang, C. et al (2010). An improved criterion for new particle formation in diverse atmospheric environments. *Atmos. Chem. Phys. Discuss.*, 10, 491-521.
- Laaksonen, A., et al (2008a), The role of VOC oxidation products in continental new particle formation, *Atmos. Chem. Phys.*, 8, 2657-2665.
- Laaksonen A. et al (2008b). SO₂ oxidation products other than H₂SO₄ as a trigger of new particle formation. Part 2: Comparison of ambient and laboratory measurements, and atmospheric implications *Atmos. Chem. Phys.*, 8, 7255-7264.
- Metzger, A., et al (2010). Evidence for the role of organics in aerosol particle formation under atmospheric conditions, *PNAS*, 107 (15) , 6646-6651.
- Sellegri K. et al (2005). Measurements of organic gases during aerosol formation events in the boreal forest atmosphere during QUEST. *Atmos. Chem. Phys.*, 5, 373-384.
- Sihto, S.-L et al (2006), Atmospheric sulphuric acid and aerosol formation: implications from atmospheric measurements for nucleation and early growth mechanisms, *Atmos. Chem. Phys.*, 6, 4079.
- Sipilä, M., et al (2010), The Role of Sulphuric Acid in Atmospheric Nucleation, *Science.*, 327, 1234.
- Smith, J. N., et al (2010). Observations of aminium salts in atmospheric nanoparticles and possible climatic implications, *PNAS* (107), 6634-6639.
- Stull, D.R. (1947). Vapor Pressure of Pure Substances Organic Compounds, *Ind. Eng. Chem.*, 39, 517-540.
- Weber, et al. (1997). Measurements of new particle formation and ultrafine particle growth rates at a clean continental site, *J. Geophys. Res.* 102, 4375.

CHEMICAL CHARACTERIZATION OF ATMOSPHERIC SUB-MICRON AEROSOLS IN A SEMI-URBAN AEROSOL-CLOUD INTERACTION OBSERVATION STATION USING HIGH-RESOLUTION AEROSOL MASS SPECTROMETER

L.Q. HAO¹, A. KORTELAINEN¹, P. MIETTINEN¹, A. JAATINEN¹, H. PORTIN^{1,2}, M. KOMPPULA², A. LESKINEN², S. ROMAkkANIEMI¹, J.N. SMITH^{1,2,4}, D.R. WORSNOP^{1,3,5} AND A. LAAKSONEN^{1,3}

¹Department of Applied Physics, University of Eastern Finland, Kuopio, P.O. Box 1627, Finland

²Finnish Meteorological Institute, Kuopio Unit, Kuopio, P.O. Box 1627, Finland

³Finnish Meteorological Institute, Research and Development, Helsinki, P.O. Box 503, Finland

⁴National Centre for Atmospheric Research, Boulder, CO, P.O. Box 3000, USA

⁵Department of Physics, University of Helsinki, Helsinki, P.O. Box 64, Finland

Keywords: Puijo, Chemical composition, Aerosol Mass Spectrometer, Positive Matrix Factorization

INTRODUCTION

The largest uncertainties in our understanding of human-caused climate change are associated with the aerosol-cloud interactions. Atmospheric aerosol can act as cloud condensation nuclei (CCN) to affect the amount of cloud on the earth and thus the global climate. The aerosol CCN activity depends on both the size and chemical composition of the particles. Whereas the relation of CCN with particle size is relatively well understood, less is known about the link between aerosol chemical composition and CCN behaviour. For the real atmospheric aerosol populations where the chemical composition is size-dependent, the ability of aerosols to serve as CCN is getting more complicated.

Aircraft measurements can be carried out for the aerosol chemical composition-cloud interaction observations. Usually these measurements are short-term and intensive and requirements to the instrumentations are much higher than the ground-based measurements, such as faster data acquisition resolutions. An alternative way to conduct these kinds of studies can be made on the ground-based observations. Ideally this kind of station is convenient for the observation of cloud events. In 2005, such an observation station was established in Kuopio, Finland, for making long-term measurements of aerosol-cloud interactions (Leskinen et al., 2009; Portin et al., 2009). One measurement campaign was carried out in 2009. As an efficient and effective tool to measurement airborne aerosol, an Aerodyne high resolution time-of-flight aerosol mass spectrometer (HR-TOF-AMS, DeCarlo et al., 2006) was used to measure the chemical composition of ambient particles. Here in this abstract we present some preliminary results from the sub-micro aerosol measurements by AMS in this campaign. Another separate abstract will connect the aerosol chemical composition with the CCN activity.

MATERIALS AND METHODS

The measurement campaign was carried out in autumn during Sep. 21-Oct. 27, 2010 at Station for Measuring Forest Ecosystem -Atmosphere Relations IV, which is located at the top of Puijo tower, 306 m.a.s.l. and 224 m above the surrounding lake level, in Kuopio, Finland. Aerosol sources that impact the site include long-range transported aerosol from surrounding continents and oceans, as well as local pollution from traffic, a pulp mill, heating plant and other urban sources. A direct measurement of aerosol chemical composition was from AMS. AMS can provide the information from non-refractory sub-micron concentrations and size distributions. In this campaign, it was operated in a cycle of three modes every ten minutes, including: 2.5 min V-mode to obtain the mass concentrations of non-refractory species; 2.5 min PTOF (particle time-of-flight) mode to determine size distributions of species under the V-mode and 5 min W-mode to obtain the high resolution mass spectral data. Standard Tof-AMS data analysis software package were used to generate unit and high resolution mass spectra from V- and W-mode data respectively. For mass concentration calculations, a particle collection efficiency (CE) factor of 0.5 was applied to account for

the loss of particles in the transmission lens and heat vaporizer. The relative ionization efficiency values in this study were 1.4 for org, 1.1 for nitrate, 1.2 for sulfate and 4.5 for ammonium.

In the data analysis, we also applied positive matrix factorization (PMF) analysis to separate organic components (Paatero and Tapper, 1994, Ulbrich et al., 2009). In this analysis the observed data is represented as a bilinear factor model $x_{ij} = \sum g_{ip} f_{pj} + e_{ij}$ where x_{ij} are the measured values of j species in i samples. This model is solved with a least squares fitting process to obtain P factors comprised of constant source profiles (f_i , mass spectra for AMS data) and varying contributions over the time period of the dataset (g_i , time series). The fitting process minimizes Q , which is the summed squares of the ratios between the fit residuals and the error estimates of each data point. The residual at each point is e_{ij} .

Other supporting characterization methods in this campaign include the Hygroscopicity-, Volatility- and Organic- Tandem Differential Mobility Analyzer, CCN counter and Differential Mobility Particle Sizer for the measurements of particle properties. Meteorological condition data from wind speed, wind direction, ambient atmospheric pressure, temperature, relative humidity and precipitation as well as gas-phase measurements for NO_x , O_3 and SO_2 are also used for supporting the AMS data interpretations.

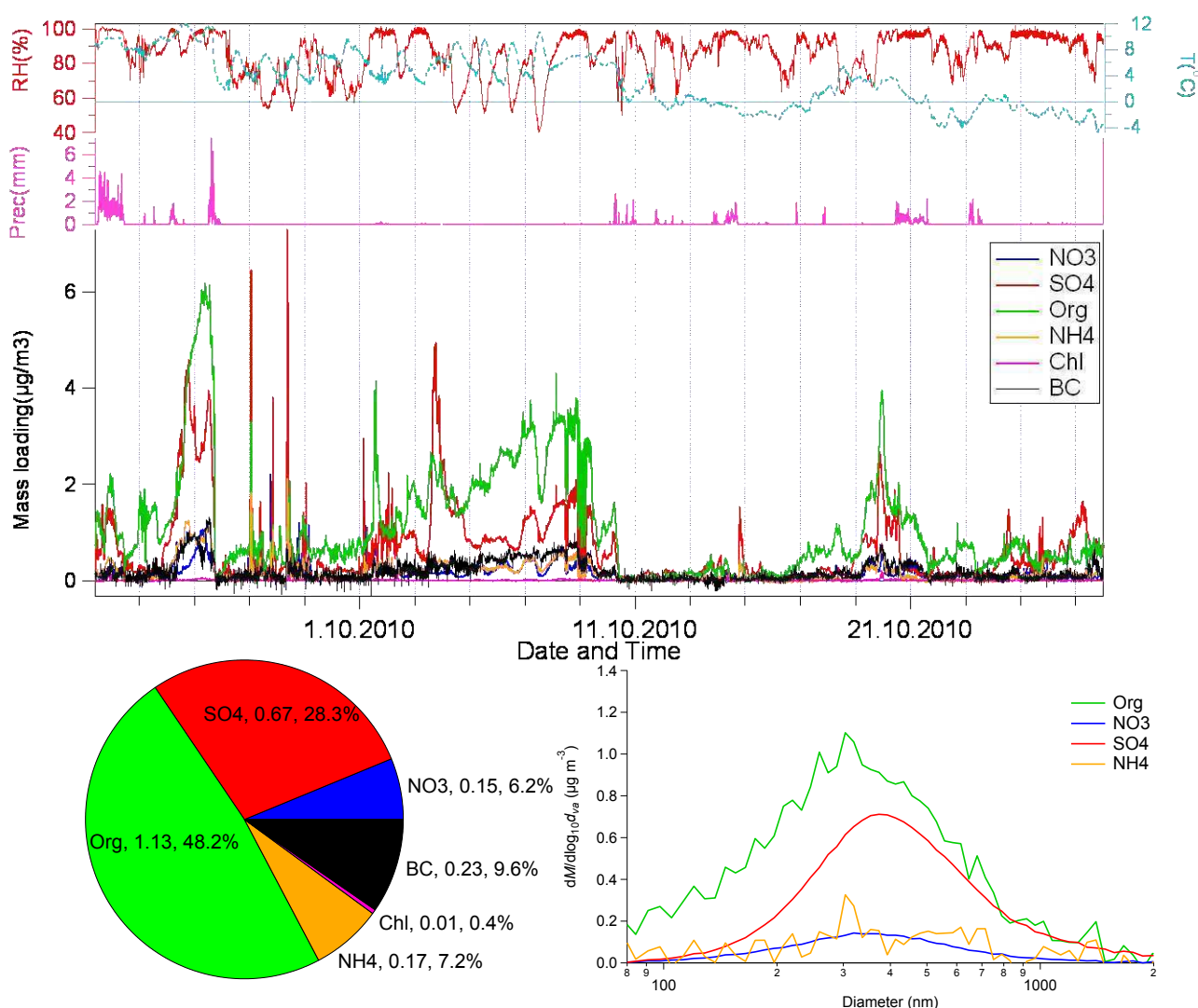


Figure 1 Upper panel: Time series of wind speed (WS, black), wind direction (WD, blue), relative humidity (RH, red), temperature (brown), precipitation (pink) and mass concentration from AMS plus black carbon. Bottom panels: chemical composition and size distribution of particles in this campaign.

RESULTS AND DISCUSSION

Figure 1 shows time-resolved variation of sulfate, nitrate, chloride, ammonium and organic concentrations measured with AMS and black carbon mass concentration as well as the corresponding time

series of the meteorological parameters in this campaign. On average, the mass loading of non-refractory species quantified with the AMS and black carbon is $2.36 \mu\text{g m}^{-3}$. Of this, organic, sulfate, nitrate, ammonia, chloride and black carbon mass contributed to 48.2%, 28.3%, 6.2%, 7.2%, 0.4% and 9.6%, respectively.

Aerosol number and mass concentrations show a strong dependence on the wind direction and precipitation as shown in Fig. 2 and 3. Wind from northeast where one pulp mill locates brings higher numbers of ultrafine particles in size range of 3-100nm than other directions (Fig. 2A). While the aerosol mass concentration is mainly subject to the wind from southwest and west, this is because that the particles from this direction are dominated in accumulation mode or coarse mode (Fig. 2B). Similarly, the masses of individual species such as sulfate, nitrate and ammonium shows strong influence by the wind from southwest (Fig. 2 C-E). There are occasional bursts of sulfate and nitrate from northeast direction, which can interpret the spikes observed in the time series in Fig. 1. Ammonia shows a close correlation with the sum of sulfate and nitrate concentrations. Measured ammonia concentration was less than 76% of predicted ammonia, indicating the observed aerosol in this campaign was acidic in nature. Organic aerosol mass is strong subject to the wind from north, west and southwest, which is slightly different from SO_4 , NO_3 and NH_4 cases. Precipitation has also been observed to have strong effect on aerosol mass concentrations shown in Fig. 1 and 3. Most probably they removed particles in a way of wet deposition.

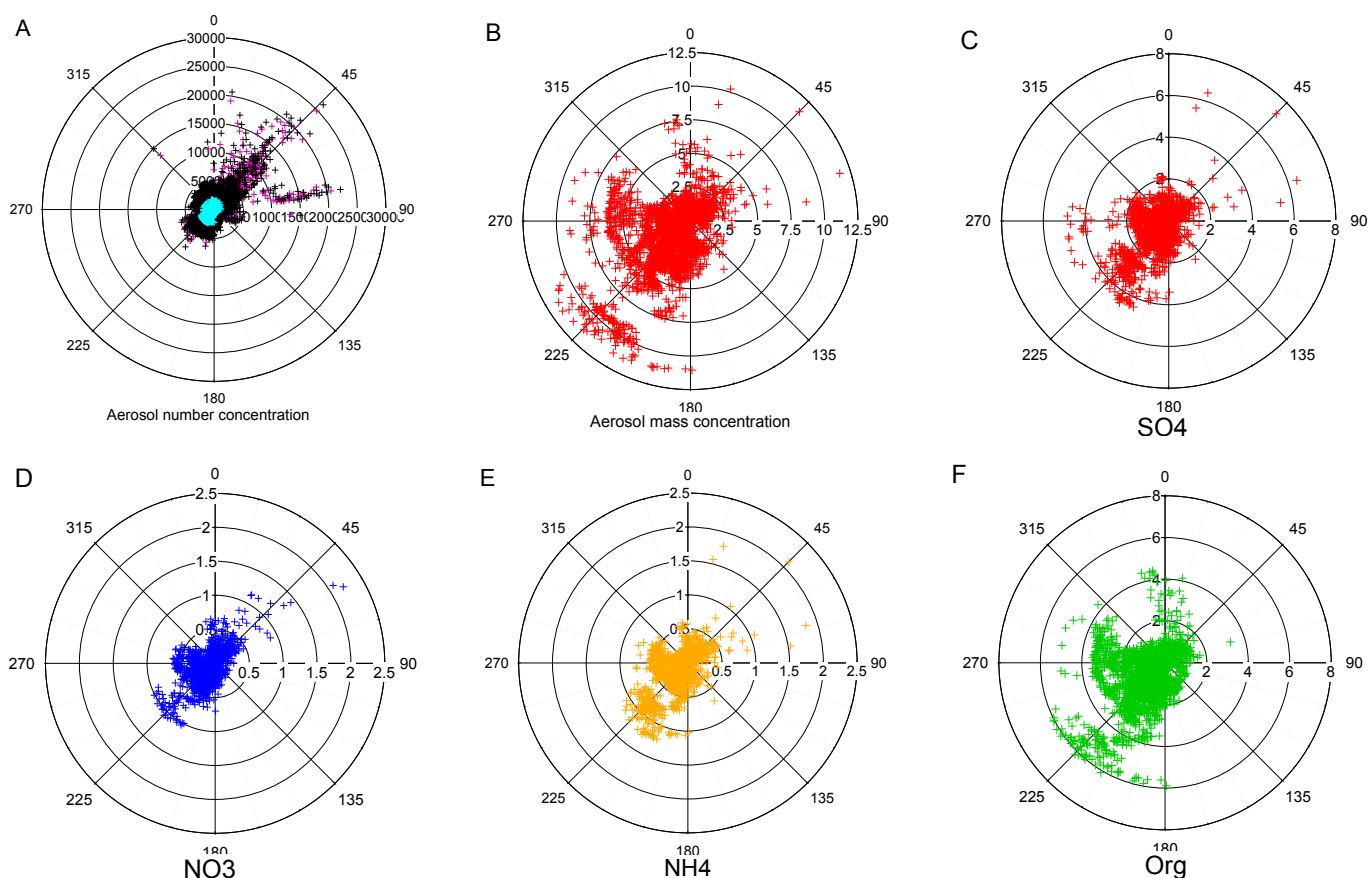


Figure 2 Wind roses for: (A) Aerosol number concentration, black for total number concentration, dark pink for total number concentration in Aiken mode (3-100nm) and green for accumulation mode (100-800nm). This plot shows the aerosol number concentration is dominated by the ultrafine mode; (B) Aerosol mass concentration; (C) sulfate; (D) Nitrate; (E) Ammonium; (F) Organic.

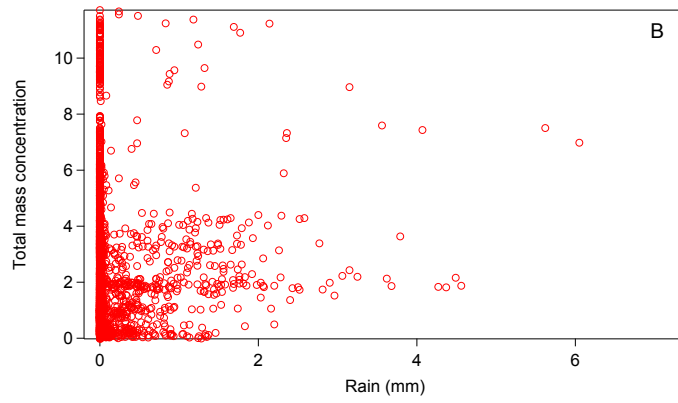


Figure 3 Relations of aerosol mass concentration to precipitation.

Five organic aerosol (OA) components were identified from AMS spectra using PMF (Figure 3): chemically-reduced urban primary emissions (hydrocarbon-like OA, HOA), low volatile OA (LV_OOA), semivolatile OA (SV_OOA) and biomass burning OA (BBOA_1 and BBOA_2), which contributed to 5.9%, 54.7%, 22.2%, and 16.7% of OA, respectively in mass loadings. LV_OOA and SV_OOA correlated with SO_4 and NO_3 , respectively. There are a few sulfate and nitrate spikes from northeast as freshly emissions, which mess up their correlations with LV_OOA and SV_OOA. BBOA_2 is from freshly emitted biomass burning aerosol, which shows correlation with black carbon. BBOA_1 is contributed from oxidized aerosol, showing a good correlation to levoglucosan, which is estimated from organic $m/z60$ after subtraction of 0.25% of total OA (Aiken et al, 2009). Contributions of HOA might be from the local traffic, which correlated to NO_2 .

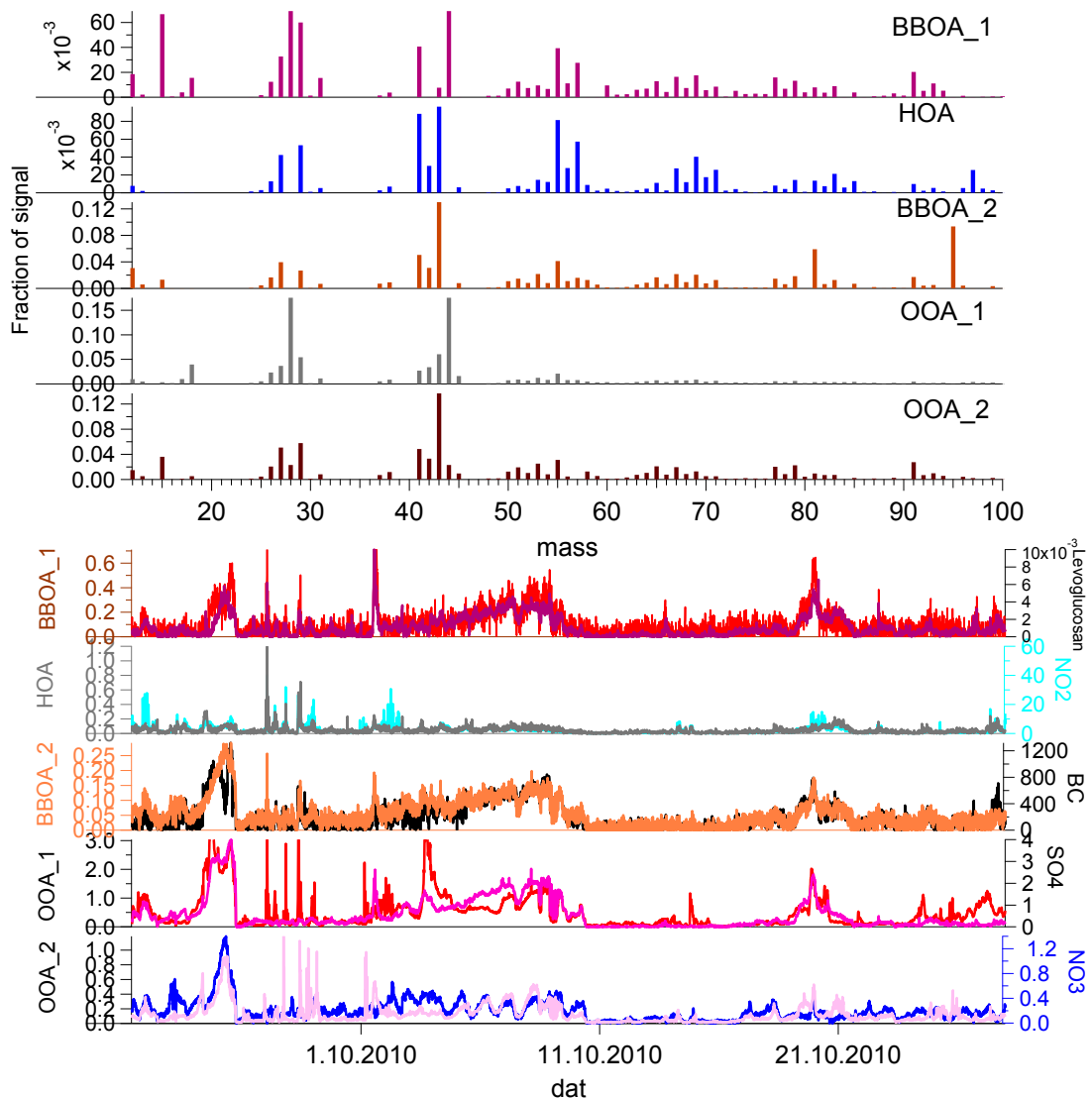


Figure 4 Time series of PMF-AMS sources and corresponding tracers. The bottom panel is in unit of $\mu\text{g}/\text{m}^3$.

ACKNOWLEDGEMENTS

This work was supported by the the Academy of Finland Centre of Excellence program (project no 1118615).

REFERENCES

- Aiken, A.C., et al. (2009). Mexico city aerosol analysis during MILAGRO using high resolution aerosol mass spectrometry at the urban supersite (T0)- Part 1: Fine particle composition and organic source apportionment, *Atmos. Chem. Phys.*, 9, 6633.
- DeCarlo, P.F., et al. (2006). Field-Deployable, High-Resolution, Time-of-Flight Aerosol Mass Spectrometer *Anal. Chem.*, 78, 8281.
- Leskinen, A., et al. (2009). Overview of the research activities and results at Puijo semi-urban measurement station. *Boreal Environ. Res.*, 14, 576.
- Paatero, P. and Tapper, U. (1994). Positive Matrix Factorization: a non-negative factor model with optimal utilization of error estimates of data values, *Environmetrics*, 5, 111.
- Portin, H., et al. (2009). Observations of aerosol-cloud interactions at the Puijo semi-urban measurement station. *Boreal Environ. Res.*, 14, 641.
- Ulbrich, I.M., et al. (2009). Interpretation of Organic Components from Positive Matrix Factorization of Aerosol Mass Spectrometric Data. *Atmos. Chem. Phys.*, 9, 2891.

A DIFFERENT MODEL FOR ESTIMATING MONOTERPENE EMISSIONS OVER BOREAL PINE FOREST

Q. HE¹, M. BOY¹, J. BÄCK², J. RINNE¹, H. HAKOLA³, A. GUENTHER⁴, S. SMOLANDER¹,
M. KULMALA¹

¹Department of Physics, PO Box 64, FI-00014 University of Helsinki, Finland

²Department of Forest Sciences, PO Box 27, FI-00014 University of Helsinki, Finland

³Finnish Meteorological Institute, Sahaajankatu 20 E, FI-00880 Helsinki, Finland

⁴National Center for Atmospheric Research, Boulder, CO 80303, USA

Correspondence to: Qingyang He (qingyang.he@helsinki.fi)

KEYWORDS: SOSA, MONOTERPENES

ABSTRACT

As one of the important biogenic volatile organic compounds (BVOCs) groups, monoterpene has been drawing more and more scientific attention in atmospheric research because of their chemical reactions to produce and destroy tropospheric ozone, their effects on aerosol growth and formation and their potential influence on global warming. Regional measurements and estimates are urgently needed to study carbon budgets and global climate. However, since various factors such as vegetation type, temperature light and humidity have complicated impacts on monoterpene emissions, comprehensive inventories are not so often reliably defined. To further track monoterpene concentrations and their chemical transformations, the model SOSA (model to Simulate the concentrations of Organic vapours and Sulphuric Acid) is applied to investigate Scots pine (*Pinus sylvestris*) tree emissions in a boreal coniferous forest at SMEAR II (Station for Measuring forest Ecosystem-Atmosphere Relations) in Hyytiälä, Finland.

INTRODUCTION

Finland, as a densely-forested country, the emission pattern of VOCs is always dominated by biogenic emissions. Therefore, BVOC study in Finland is particularly critical. Since previous research shows that many of the tree species in the European boreal zone are known to be monoterpene emitters (Janson, 1993; Hakola *et al.*, 1998; Hauff *et al.*, 1999), this study will focus on monoterpene emissions at Hyytiälä. Monoterpenes are emitted by plants because of their allelopathic function. They are of great importance in defence against insects and attraction of pollinators and enemies of other herbivores (Kesselmeier and Staudt, 1999). Temperature is the most significant factor of monoterpene emissions. Many other interlinked environmental and physiological parameters, such as light, humidity, CO₂ concentration, vegetation

type and metabolic activity also affect monoterpene emissions (Guenther *et al.*, 1995).

METHODS

SOSA is a model which combines meteorological transport, BVOC emissions and chemistry (Boy *et al.* 2011). To test the reliability of SOSA, simulation outputs are compared with measurement data collected from on-line chambers analysed by Proton-transfer-reaction mass spectrometry (PTR-MS) and Gas chromatography-mass spectrometry (GC-MS) analyzer.

RESULTS AND CONCLUSION

Result (Figure.1) indicates that modelling and observations of monoterpene concentrations reasonably agreed both day and night. However, the correlation coefficients still reveal some additional parameters like environmental stress, plant development and leaf maturation, nutrient and injury status also influencing monoterpene emissions, but were not taken into account in the model. In this case, the mechanisms of monoterpene emissions need to be understood better in order to improve the parameters used in model. May till September of the year was selected to make correlation test because emissions are productive and the simulation are representative during that period.

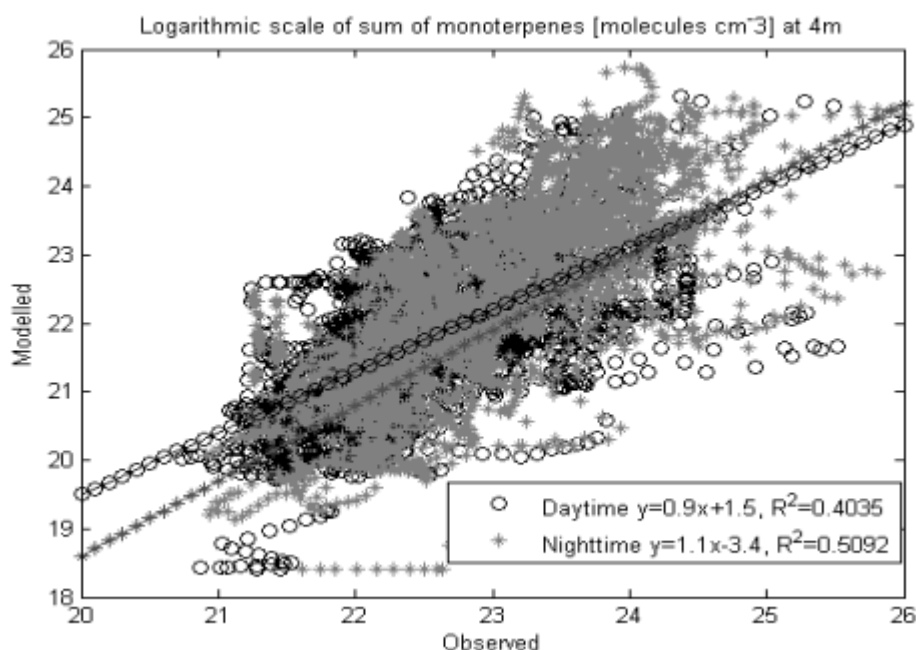


Fig 1. Correlation analysis between measured monoterpene concentration data with modelled from May to September 2007

The dominant monoterpenes species emitted from these coniferous trees are α -pinene and Δ^3 -carene with the proportion of 48% and 23% respectively. Monoterpene emissions did continue with low rates during the night. Diurnal and seasonal

variations are demonstrated both quantity and quality. Summer is the most active season and emission rate increases to the peak around 3pm during daytime. According to vertical profile, monoterpene concentrations are highest at lower height levels during night and well mixed during day. All the results are generally supported by measurement.

Another significant phenomenon for monoterpene emitters is the discrepancy between branch scale emissions and above-canopy concentrations. In order to reduce uncertainty in measuring and modeling, a more detailed chemotypic characterization blends needs to be constructed. SOSA is also used to estimate the contribution of different monoterpene distributions to the total OH reactivity. Results show that by selecting α -pinene and sabinene as the chemotype-species, the OH reactivity differs by a factor of almost 3.

ACKNOWLEDGMENTS

Financial support was from Finnish Center of Excellence in Physics, Chemistry, Biology and Meteorology of Atmospheric Composition and Climate Change. All the staff of the SMEAR II station is gratefully acknowledged.

REFERENCES

- Boy, M., Sogachev, A., Lauros, J., Zhou, L., Guenther, A., and Smolander, S.: SOSA – a new model to simulate the concentrations of organic vapours and sulphuric acid inside the ABL – Part I: Model description and initial evaluation; *J. Atmos. Chem. Phys.*, 2011,11, 43-51.
- Guenther, A., Hewitt, C. N., Erickson, D., Fall, R., Geron, C., Graedel, T., Harley, P., Klinger, L., Lerdau, M., McKay, W. A., Pierce, T., Scholes, B., Steinbrecher, R., Tallamraju, R., Taylor, J., and Zimmerman, P. A.: Global-Model of Natural Volatile Organic-Compound Emissions; *J. Geophys. Res.*, 1995, 100(D5), 8873-8892.
- Hakola, H., Rinne, J., and Laurila, T.: The hydrocarbon emission rates of tea-leaved willow (*Salix phylicifolia*), silver birch (*Betula pendula*) and European aspen (*Populus tremula*); *J. Atmos. Env.*, 1998,32, 1825-1833.
- Hauff, K., Rössler, J., Hakola, H., and Steinbrecher, R.: Isoprenoid emission in the European boreal forests, in Proceedings of EUROTRAC symposium 98; WIT press, 1999.
- Janson, R.: Monoterpene emission of scots pine and morwegian spruce; *J. Geophys. Res.*, 1993,98, 2839-2850.
- Kesselmeier, J., Staudt, M.: Biogenic volatile organic compounds (VOC): an overview on emission, physiology and ecology. *J. Atmos. Chem.*, 1999,33, 23-88.

FAAR abstract instructions and template

Please read carefully - the text contains instructions for abstract preparation

DIFFERENT ROOT-ASSOCIATED SYMBIOTIC ECTOMYCORRHIZAL FUNGAL SPECIES AFFECT CARBON ALLOCATION OF SCOTS PINE

J. Heinonsalo^{1,2}, E. Juurola¹, A. Lindén¹ and J. Pumpanen¹

¹Department of Forest Sciences, Faculty of Agriculture and Forestry, P.O. Box 27, FIN-00014, University of Helsinki, Finland.

²Viikki Biocenter, Department of Food and Environmental Sciences, Faculty of Agriculture and Forestry, PO.Box 56, FI-00014 University of Helsinki, Finland.

Keywords:

Photosynthesis, carbon, allocation, ectomycorrhiza, symbiosis, Scots pine

INTRODUCTION

In boreal forest ecosystems, major part of the fine roots of trees are in symbiotic association with a wide range of ectomycorrhizal fungal (ECM) species. Hundreds of fungal species or strains can be found even in one forest stand, indicating high biological diversity in root-associated fungal micro flora. We have studied the effects of different ectomycorrhizal fungal species on the complete carbon budget and the turnover rate of assimilated carbon in the Scots pine (*Pinus sylvestris* L.) tree seedlings growing on natural humus in microcosm conditions.

When ectomycorrhizal species *Suillus variegatus* was associated with the pine roots, the below-ground respiration increased and this carbon loss was compensated by higher photosynthetic activity. Other fungal species did not differ between each other in their effects on carbon balance (Heinonsalo *et al.*, 2010). Our findings indicate that some root-associated mycorrhizal fungal symbionts can significantly alter plant CO₂ exchange, biomass distribution, and the allocation of recently photosynthesized plant-derived carbon. These findings were made in natural humus conditions where the plant roots were associated with several different ectomycorrhizal species at the same time. Also in natural forests, the trees always host a wide variety of fungal symbionts. However, to confirm our result on the ectomycorrhizal fungal effect on photosynthetic capacity of the tree, we performed a new experiment using sterile pine seedling inoculated with single ECM species at a time.

METHODS

The surface sterilized pine seeds were germinated on glucose agar and transferred to glass tubes (diameter 22 mm) with Brown&Wilkins growth media. Until the first lateral short roots emerged, the seedlings were inoculated with eight (8) different ECM fungal species (N=16). The ECM species studied were *Piloderma croceum*, *Suillus variegatus*, *Amanita porphyria*, *Lactarius rufus*, *Suillus bovinus*, *Cenococcum geophilum*, *Tomentellopsis echinospora*, *Thelephora terrestris*. This selection of species are commonly found in boreal forests and represent a variety of different phylogenetic origins. Non-inoculated seedlings served as controls (N=16). After three months growth period in standardized and controlled growth chamber conditions, the photosynthetic capacity (P_{max}) was analysed using Walz GFS-3000 (Heinz Walz GmbH, Germany) in light levels 0-1400 $\mu\text{mol m}^{-2} \text{s}^{-1}$. The total and shoot and root biomass were measured to record the relative C allocation in biomass. The mycorrhizal and non-mycorrhizal root tips were counted to confirm the presence and intensity of fungal symbiotic association with the trees.

FAAR abstract instructions and template

Please read carefully - the text contains instructions for abstract preparation

PRELIMINARY RESULTS

The preliminary results show a clear trend that if seedlings are associated with different ECM species, more C is allocated into root biomass but the total seedling biomass is not significantly affected by the symbiosis, compared to non-inoculated seedlings. For several species this observation is statistically significant. The results concerning mycorrhization percentage (mycorrhizal roots vs. all short root tips), N uptake and photosynthesis (P_{max}) are under analysis and will be presented in the poster.

ACKNOWLEDGEMENTS

This research was supported by the Academy of Finland grants number 212915, 213093, 206085 and 130984. Mai Kugumäki MSc., Maria Domínguez Carrasco MSc. and Ulla Mikkola are acknowledged for their skillful technical assistance.

REFERENCES

Heinonsalo J., Pumpanen J., Rasilo T., Hurme K.-R. and Ilvesniemi H. 2010. Carbon partitioning in ectomycorrhizal Scots pine seedlings. *Soil Biol. & Biochem.* 42 (9): 1614-1623.

ONLINE-GC-MS MEASUREMENTS AND RECEPTOR MODELLING STUDIES OF VOCs IN URBAN AIR

H. HELLEN AND H. HAKOLA

Finnish Meteorological Institute, PL 503, 00101 Helsinki, Finland

Keywords: VOCs, NMHCs, receptor modeling, urban air, UNMIX

INTRODUCTION

Volatile organic compounds (VOCs) have great influence on tropospheric chemistry; they affect ozone formation and they or their reaction products may take part into new particle formation (Finlayson-Pitts and Pitts, 2000). Some of the VOCs are toxic or harmful themselves. In addition to this, halocarbons can cause ozone reduction in the stratosphere. Different VOCs may have totally different reaction paths, lifetimes and aerosol formation potentials in the atmosphere and therefore knowing the concentrations and the sources of individual VOCs is essential for different kind of atmospheric studies.

Concentrations and sources of VOCs have been studied in Helsinki by Hellén et al. (2003 and 2006). Traffic was found to be main local source, but also other sources e.g. wood combustion, had high contribution for some of the compounds. Some VOCs have also natural sources e.g. emissions from vegetation (Aaltonen et al. 2011, Tarvainen et al. 2007 and Hakola et al. 2006). Now with the improved measurement methods it is possible to measure concentrations continuously with higher time resolution. This gives more knowledge of the short term variations of concentrations and enables the use of multivariate receptor models for source apportionment studies. In this study VOC concentrations were measured first time in the city of Helsinki with an online gas chromatograph mass spectrometer (online-GC-MS) and source apportionments for different VOCs were estimated using UNMIX multivariate receptor model.

METHODS

Measurements were conducted at the 5th floor on the roof of Finnish Meteorological Institute in Helsinki, Finland, using a thermal desorpter (Markes Unity) with a gas chromatograph (Agilent 7890A) and a mass spectrometer (Agilent 5379N). Samples were taken every other hour in 20.1.-22.2.2011. Sampling time was 60 minutes and flow 30 ml min⁻¹. In the 5 m long stainless steel inlet line (1/4 O.D., heated to 70°C) extra flow of 1 L min⁻¹ was used to avoid losses of the compounds on the walls of the inlet tubes. Samples were collected directly to the cold trap of the thermal desorpter. Water was removed by keeping the hydrophobic cold trap at 10°C. Totally 27 different compounds were studied. For studying source compositions and contributions multivariate receptor model EPA Unmix 6.0 (Norri et. al. , 2007) was used.

RESULTS AND DISCUSSION

Table 1 shows average concentrations of measured compounds and Figure 1 concentration variations for one compound from each compound group. There is benzene for aromatics, ETBE for gasoline additives, heptane for alkanes, a-pinene for biogenic VOCs and tetrachloromethane for halogenated compounds. Highest concentrations were measured for aromatic hydrocarbons and lowest for biogenic hydrocarbons. For most halogenated compounds concentrations were at the same level during the whole campaign.

Table 1. Average concentrations (Conc) of different VOCs in Helsinki in winter 2011.

	Conc (ng m ⁻³)		Conc (ng m ⁻³)
<u>Aromatics HCs</u>		<u>Halogenated HCs</u>	
Benzene	1300	Chloroform	110
Toluene	1140	1,1,1-trichloroethane	50
Ethylbenzene	260	trichloroethene	50
p/m-xylene	690	1,2-dichloroethane	80
Styrene	50	Tetrachloromethane	630
o-xylene	270	Tetrachloroethene	50
Propylbenzene	50	<u>Biogenic HCs</u>	
3-ethyltoluene	110	Isoprene	30
4-Ethyltoluene	60	a-pinene	80
1,3,5-trimethylbenzene	50	Camphene	10
2-Ethyltoluene	50	b-pinene	30
1,2,4-trimethylbenzene	180	3-Carene	20
1,2,3-trimethylbenzene	40	p-cymene	20
<u>Alkanes</u>		Limonene	40
2,2,4-trimethylpentane	240	1,8-cineol	10
2-Methylpentane	410	<u>Gasoline additive</u>	
Hexane	320	ETBE	90
Heptane	230		
Octane	130		

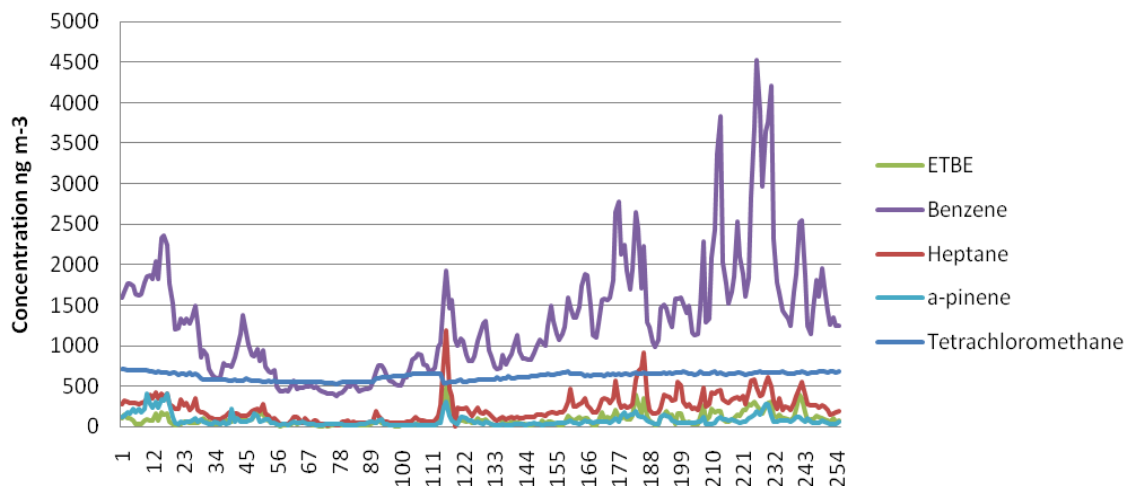


Figure 1. Concentration variations of selected VOCs 20.1.-22.2.2011 in Helsinki (N=255).

Halogenated hydrocarbons are not expected to have any local sources. Only exception is tetrachloroethene, which has some concentration peaks during the daytime. In the earlier study (Hellén et al., 2006) dry cleaning was found to be a source of it.

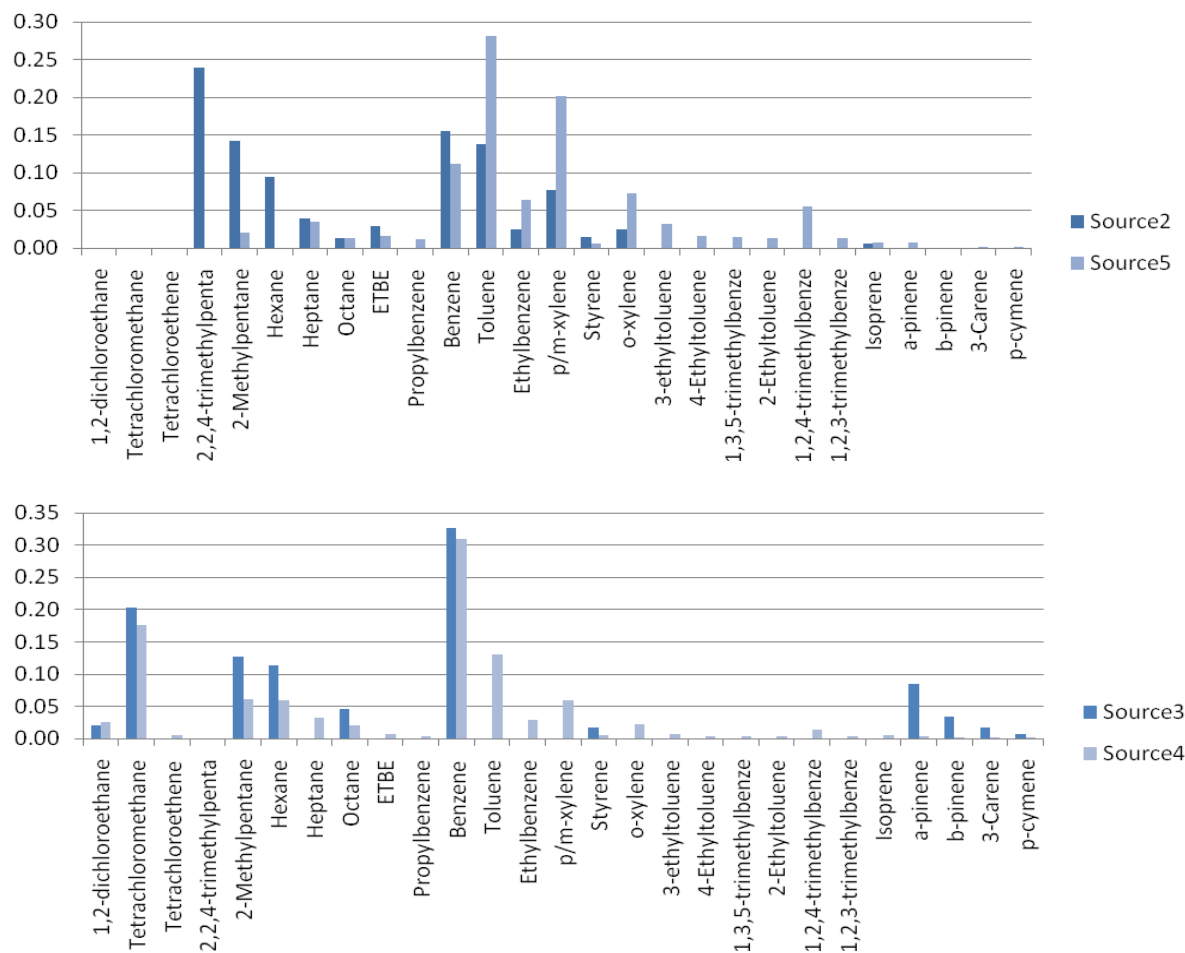


Figure 2. Source profiles of different sources found by UNMIX receptor model.

Different sources given by UNMIX were identified by source profiles and variations of source loading. Source 1 containing only tetrachloroethene and peaking during the daytime was identified as a dry cleaning based on earlier studies by Hellén et al. (2006). Sources 3 and 4 were identified as distant sources. They have high contribution of halogenated hydrocarbons (Figure 2), which are not expected to have any local sources. In addition to this, they do not show any diurnal variation (Figure 3). Also most of the monoterpenes were found from the source 3 and therefore this source is called as BVOCs/distant. Even though monoterpenes are fast reacting and not expected to be transported far from the emissions, in wintertime in Finland their lifetime is estimated to be from 6 h to 1.5 d and therefore transport from the background areas to Helsinki is possible. Sources 2 and 5 containing lots of aromatics and alkanes were identified as traffic related and local traffic sources. As shown in figure 3 these local traffic or traffic related sources have diurnal cycles with maxima during the rush hours. High contribution of most volatile alkanes and lack of less volatile aromatic

hydrocarbons in traffic related source profile indicates that this may be some gasoline evaporation e.g. from gasoline stations or during the cold starts of the cars.

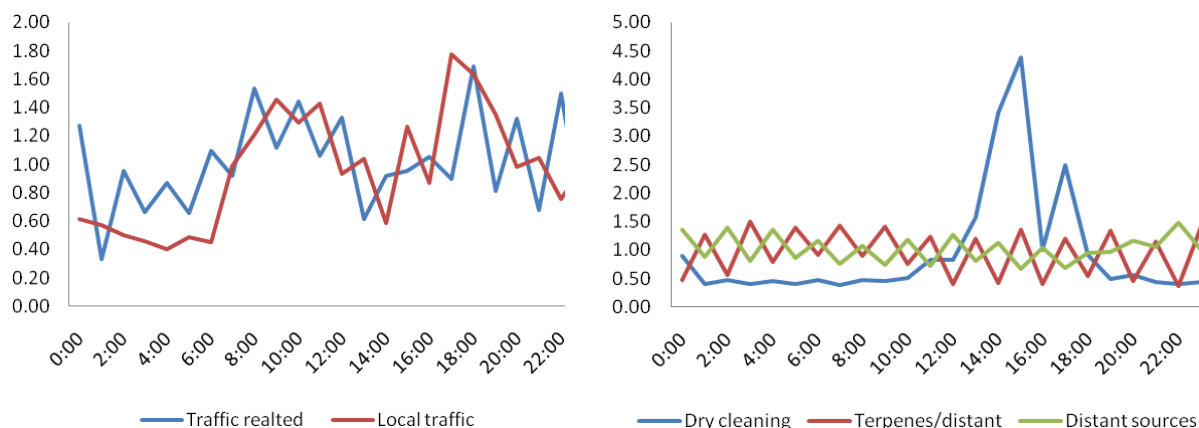


Figure 3. Diurnal variation of loadings of different sources (local winter time).

These UNMIX analysis show that for most of the aromatic hydrocarbons traffic is clearly the highest source (Figure 4). However, over 50% of benzene was found to be from distant sources. Also in the earlier study with chemical mass balance distant sources had high contribution especially for benzene (56%) (Hellén et al, 2006). Lifetime of benzene in the atmosphere is longer than lifetime of any other aromatic hydrocarbons.

Isoprene is a biogenic compound, but it exists also in gasoline exhaust. In this study 65% of isoprene was found in traffic or traffic related sources and 36% in distant sources. For other BVOCs source called as BVOCs/distant had the highest contribution (50-77 %), but for α -pinene and 3-carene also traffic had a small contribution. It is possible that some BVOCs were emitted from the construction site close by and mixed with traffic profile.

Traffic and traffic related sources had the highest contribution in some alkane concentrations (2,2,4-trimethylpentane, heptanes and 2-methylpentane), but for hexane and octane distant sources or BVOC/distant were higher. For 2,2,4-trimethylpentane (also known as iso-octane) only source was traffic related (gasoline exhaust/cold starts) and local traffic source did not have any contribution. 2,2,4-trimethylpentane is an important component of gasoline added as an anti-knocking agent.

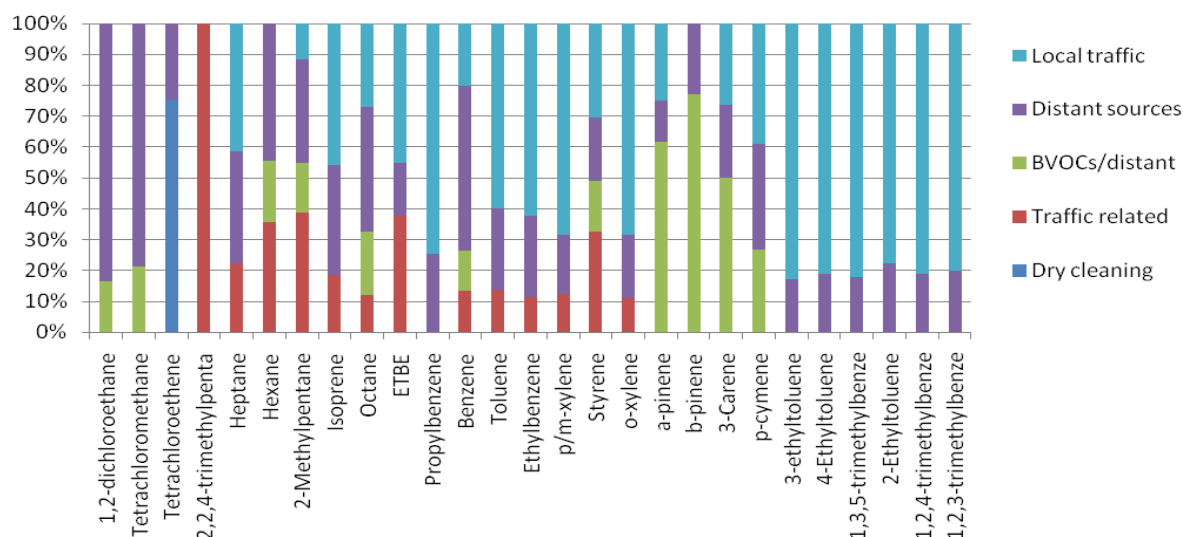


Figure 4. Source apportionment of different compounds.

REFERENCES

- Aaltonen H., Pumpanen J., Pihlatie M., Hakola H., Hellén H. and Bäck J., 2011. Emissions of biogenic volatile organic compounds from boreal Scots pine forest floor. *Agricultural and Forest Meteorology*, 151, 682-691.
- Finlayson-Pitts B. J. and Pitts J.N.(2000). *Chemistry of the upper and lower atmosphere*. (Academic Press, San Diego, CA).
- Hakola H., Tarvainen V., Bäck J., Rinne J., Ranta H., Bonn B., and Kulmala M., 2006. Seasonal variation of mono- and sesquiterpene emission rates of Scots pine. *Biogeosciences*, SRef-ID: 1726-4189/bg/2006-3-93, 93-101.
- Hellén H., Hakola H. and Laurila T. (2003). Source contributions of NMHCs in Helsinki using chemical mass balance (CMB) and multivariate (Unmix) receptor models. *Atmospheric Environment*, **37**, 1413-1424.
- Hellén H., Hakola H., Pirjola L., Laurila T. and Pystynen K.-H. (2006a) Ambient air concentrations, source profiles and source apportionment of 71 different C2-C10 volatile organic compounds in urban and residential areas of Finland. *Environmental Science and Technology*, **40**, 103-108.
- Norris G., Vedentham R. and Duvall R. (2007). EPA Unmix 6.0 Fundamentals & User Guide. U.S. Environmental Protection Agency, Office of Research and Development, Washington, DC 20460.
- Tarvainen V. Hakola H., Rinne J., Hellén H. and Haapanala S. (2007). Towards a comprehensive emission inventory of the Boreal forest. *Tellus*, **59 B**, 526-534

PARTICLE AND ION FORMATION AND CONCENTRATIONS IN THE POLLUTED AREA OF MARIKANA, SOUTH-AFRICA

A. HIRSIKKO¹, P. TIITTA^{2,3}, V. VAKKARI¹, H.E. MANNINEN¹, H. LAAKSO¹, M. KULMALA¹, A. MIRME⁴, S. MIRME⁴, D. MABASO⁵, S. GAGNÉ¹ and L. LAAKSO^{1,3,6}

¹Department of Physics, University of Helsinki, P.O. BOX 64, 00014 University of Helsinki, Finland

²University of Eastern Finland, Department of Physics, FI-70211 Kuopio, Finland

³School of Physical and Chemical Sciences, North-West University, Potchefstroom, South Africa

⁴Institute of Physics, University of Tartu, 18 Ülikooli Str., 50090 Tartu, Estonia

⁵Rustenburg Local Municipality, Rustenburg, Republic of South Africa

⁶Finnish Meteorological Institute, Research and Development, P.O. BOX 503, FI-00101, Finland

Keywords: AIR IONS, PARTICLE FORMATION, AIR QUALITY.

INTRODUCTION

Aerosol particle formation have been studied and characterised in various environments, including marine and continental, as well as urban and rural locations (e.g. Kulmala *et al.*, 2004; Hirsikko *et al.*, 2011). However, Africa is one of the least studied continents with respect to particle formation and air quality (Swap *et al.*, 2003; Laakso *et al.*, 2008; Vakkari *et al.*, 2011). Therefore, an atmospheric monitoring project was started in South-Africa in 2006. The project included monitoring of different meteorological parameters, trace gases, as well as air ion and particle size distributions. Recently, the measurements were updated with aerosol optical and ecosystem measurements. The measurements have been performed in background savannah, urban industrial and agricultural background areas (www.welgegund.org). The current study presents preliminary results of observations of air ion and particle formation and their concentrations, as well as connections to particle sources in Marikana, which is close to an informal settlement and mining areas.

METHODS

Measurements were carried out during February 2008-January 2010. The measurement set-up was described by Laakso *et al.* (2008) and Vakkari *et al.* (2011). Therefore, here we present only a short description of devices relevant for this study. Aerosol particle size distributions were measured with a Differential Mobility Particle Sizer (DMPS) in diameter range of 10-840 nm. The DMPS consisted of a Vienna-type Differential Mobility Analyser and a TSI-3010 Condensation Particle Counter. Ion size distributions were measured with an Air Ion Spectrometer (AIS, Airl Ltd., Mirme *et al.*, 2007). The AIS consisted of two (one for negative and one for positive ions) identical cylindrically symmetric multichannel differential mobility analysers, which measured natural air ion mobility distributions in the range $3.2\text{-}0.0013\text{ cm}^2\text{ V}^{-1}\text{ s}^{-1}$ (ca. $d = 0.8\text{-}42\text{ nm}$). Trace gases (SO₂, O₃, CO and NO_x) were monitored with a pulsed fluorescent Thermo-Electron 43S SO₂ analyser, Environnement s.a. 41M ozone analyser, Horiba APMA-360 CO analyser and Teledyne 200AU NO/NO_x analyser, respectively.

Due to the demanding environmental conditions in Marikana, our study had a special focus on data correction procedures. Combustion and mining produced soot and coarse particles, which blocked efficiently air flow pathways of the AIS. The flow pathways of the AIS were equipped with several dense nets to produce laminar flow (Mirme *et al.*, 2007). These nets and flower pump collected dirt and, consequently, the flow rate decreased. The smallest air ions are very mobile. Therefore, even a

small change in flow rate shifted the observed mobility distributions. Due to constant production of coarse particles the flow rate began to decrease from the desired level (ca. 1000 ccm) quickly after the instrument maintenance.

In aim to estimate the effect of the changing flow rate on mobility distributions we performed different theoretical simulations and field experiments. The results showed that the diameters of the smallest ions ($d < 3$ nm) were shifted immediately after any decrease in flow rate. If the flow rate decreased less than 20 %, the rest of the distribution ($d > 3$ nm) remained nearly unchanged. However, decreasing flow rate enhanced ion losses in all sizes. Additionally, laboratory calibrations by Gagné *et al.* (2011) have shown that the AISEs are slightly inaccurate when measuring ion concentrations.

We made the following decisions and corrections to the AIS data: 1) we were able to use the small ion data only when the flow rate was > 95 % of normal, 2) only the data for ions larger than 3 nm in diameter were used for detailed data analysis (e.g. formation and growth rates), 3) only the data with flow rate > 80 % of desired level were utilised, 4) we multiplied the concentration spectrums of positive and negative ions with factors 1.31 and 1.26, respectively, as derived from laboratory calibrations by Gagné *et al.* (2011), and 5) due to the decrease in flow rate, we multiplied the concentrations with size and flow rate dependent correction coefficients.

RESULTS AND CONCLUSIONS

In Marikana, aerosol particle concentrations were higher during the dry season (May-August) compared to the wet season (November-February), as was expected. However, the annual cycle of nucleation mode particle concentration was less pronounced compared to other size classes. Due to limited number of observation days with the AIS working with the desired flow rate, we were not able to study the annual cycle of small ion (smaller than ca. 1.6 nm) concentrations.

Diurnal cycle of particle concentrations was evident: 1) compared to other observations (e.g. Hirsikko *et al.*, 2011) small ion concentrations displayed a strong diurnal variation being the highest during night and the lowest during day-time, 2) nucleation mode particle concentrations were maximum around noon (Fig. 1), 3) Aitken mode particle concentrations showed three modes (the first early in the morning, the second in the afternoon and the third late in the evening), and 4) accumulation mode particle concentrations showed two peaks (one early in the morning and the other late in the evening). The diurnal cycle of small ion concentrations was determined mainly by the evolution of the boundary layer height, which had a strong night-time inversion. Further analysis and comparison with trace gas concentrations showed that Aitken and accumulation mode particles resulted from domestic burning in a nearby informal settlement. However, nucleation mode particle concentrations did not correlate with trace compounds (e.g. BC and CO) of combustion origin. Therefore, we concluded that these particles originated mainly from nucleation.

The investigation of secondary particle formation was initiated by means of visual event classification based on ion size distributions. Fortunately, the decreasing flow rate affected mainly the smallest ions and absolute concentration values, so we were able to use the whole available ion data for this qualitative analysis. The results showed that day-time particle formation was observed frequently (on 85 % and 79 % of the analysed days in negative and positive polarities, respectively) in Marikana (Fig. 2). The observations showed that the particle formation frequency was slightly suppressed during the wet season. Additionally, the in-situ particle formation took place in polluted atmosphere of Marikana. Despite the differences in measurement environments, our results of particle formation frequency were in accordance with the observations by Laakso *et al.* (2008) and Vakkari *et al.* (2011) in the South-African Savannah.

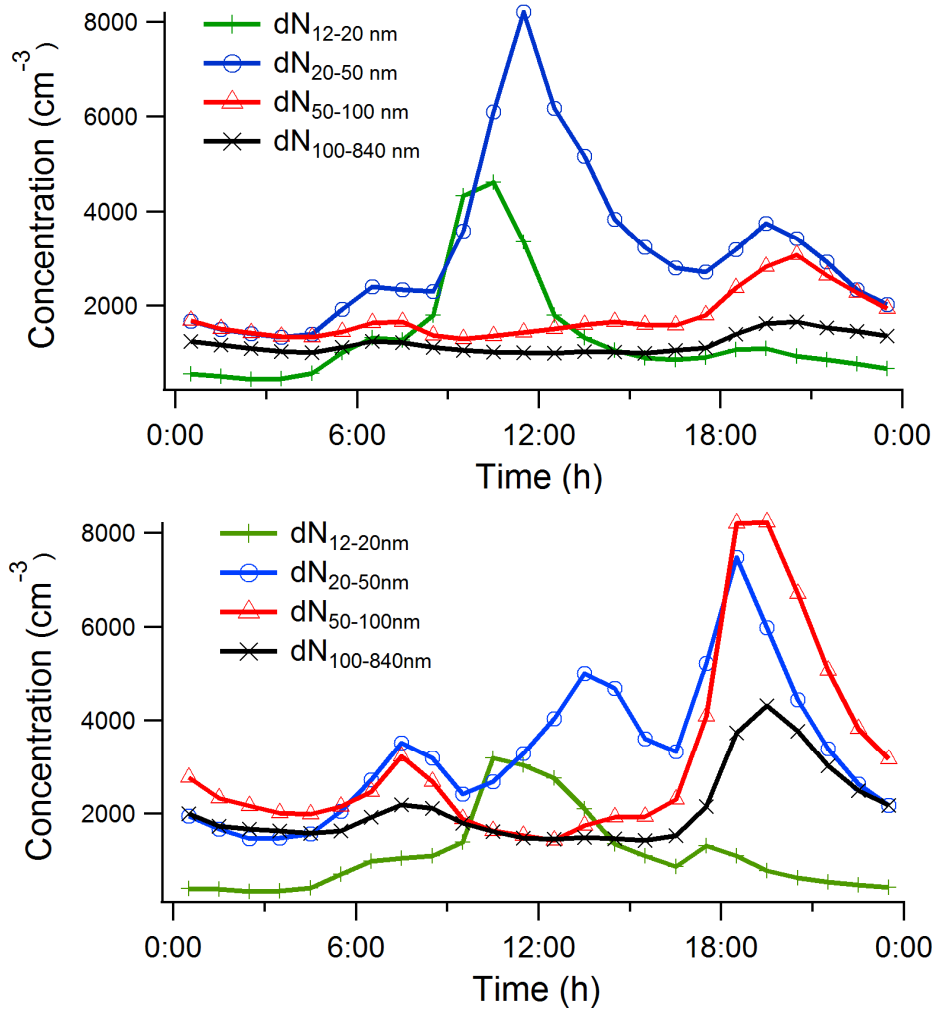


Figure 1. Average diurnal concentrations of nucleation (12-20 nm), Aitken (20-50 nm) and accumulation (50-840 nm) mode particles during the wet (upper panel) and dry (lower panel) seasons.

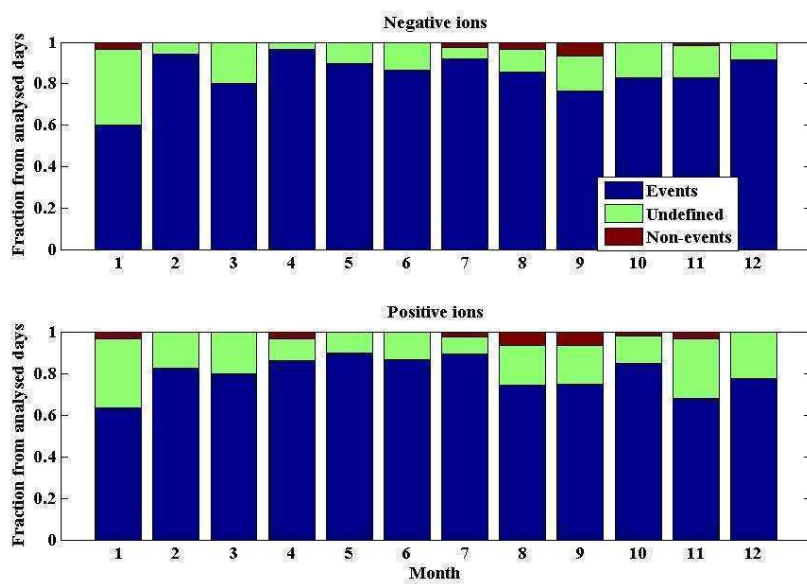


Figure 2. Particle formation frequency based on ion size distribution data.

ACKNOWLEDGEMENTS

This work was supported by the Academy of Finland and the Rustenburg local municipality.

REFERENCES

- Gagné, S., Lehtipalo, K., Manninen, H.E., Nieminen, T., Schobesberger, S., Franchin, A., Yli-Juuti, T., Boulon, J., Sonntag, A., Mirme, S., Mirme, A., Hörrak, U., Petäjä, T., Asmi, E., and Kulmala, M.: Intercomparison of air ions spectrometers: a basis for data interpretation (2011). *Atmos. Meas. Tech. Discuss.*, **4**, 1139-1180.
- Hirsikko, A., Nieminen, T., Gagné, S., Lehtipalo, K., Manninen, H. E., Ehn, M., Hörrak, U., Kerminen, V.-M., Laakso, L., McMurry, P. H., Mirme, A., Mirme, S., Petäjä, T., Tammet, T., Vakkari, V., Vana, M., and Kulmala, M. (2011). Atmospheric ions and nucleation: a review of observations. *Atmos. Phys. Chem.*, **11**, 767–798.
- Kulmala, M., Vehkamäki, H., Petäjä, T., Dal Maso, M., Lauri, A., Kerminen, V.-M., Birmili, W., and McMurry, P. H. (2004). Formation and growth rates of ultrafine atmospheric particles: a review of observations. *J. Aerosol Sci.*, **35**, 143–176.
- Laakso, L., Laakso, H., Aalto, P. P., Keronen, P., Petäjä, T., Nieminen, T., Pohja, T., Siivola, E., Kulmala, M., Kgabi, N., Molefe, M., Mabaso, D., Phalatse, D., Pienaar, K., and Kerminen, V.-M. (2008). Basic characteristics of atmospheric particles, trace gases and meteorology in a relatively clean Southern African Savannah environment. *Atmos. Chem. Phys.*, **8**, 4823–4839.
- Mirme, A., Tamm, E., Mordas, G., Vana, M., Uin, J., Mirme, S., Bernotas, T., Laakso, L., Hirsikko, A., and Kulmala, M. (2007). A wide-range multi-channel Air Ion Spectrometer. *Boreal Environ. Res.*, **12**, 247–264.
- Swap, R. J., Annegarn, H. J., Suttles, J. T., King, M. D., Platnick, S., Privette, J. L., and Scholes, R. J. (2003). Africa burning: a thematic analysis of the Southern African Regional Science Initiative (SAFARI 2000). *J. Geophys. Res.*, **108**, 8465, doi:10.1029/2003JD003747.
- Vakkari, V., Laakso, H., Kulmala, M., Laaksonen, A., Mabaso, D., Molefe, M., Kgabi, N., and Laakso, L. (2011). New particle formation events in semi-clean South African savannah. *Atmos. Chem. Phys.*, **11**, 3333-3346.
- www.welgegend.org (cited 27.4.2011)

THEORY AND TESTING OF A NEW METHOD FOR THE CONTINUOUS MONITORING OF PHLOEM OSMOTIC PRESSURE OF TREES IN THE FIELD

T. HÖLTTÄ¹, M. MENCUCINI², S. SEVANTO³, T. VESALA⁴ and E.. NIKINMAA¹

¹ Department of Forest Sciences, University of Helsinki, Helsinki, Finland

² School of GeoSciences, University of Edinburgh, Edinburgh, UK.

³ Los Alamos National Laboratory, Earth and Environment Science Division, Los Alamos, USA

⁴ Department of Physics, University of Helsinki, Helsinki, Finland.

Keywords: Phloem transport, Speed of link, Stem diameter change

INTRODUCTION

The measurement of the rate of transport of sugars from the leaves to the roots belowground via the phloem is currently possible only under laboratory conditions, using techniques such magnetic resonance imaging, or in the field using isotope pulse labelling or time series analysis of natural isotope discrimination at different positions along the translocation pathway. While these techniques are very powerful, they are also complex to employ and difficult to maintain over long periods of time, which also limits the possibilities for their spatial replication. This places considerable limitations on our possibility to further our understanding of the links between canopy photosynthesis and respiration of heterotrophic organisms, one of the most important unknowns in the interpretation of ecosystem level fluxes of carbon between atmosphere and terrestrial biosphere. While the in-situ measurement of phloem osmotic pressure is possible in free-bleeding species, there is a pressing need to develop new techniques that allow continuous unattended monitoring of phloem flow-related properties in the field.

High-resolution time-resolved measurements of stem and xylem diameter change with LVDT (linear variable displacement transducers) have been used for many years to monitor stem growth and/or estimate xylem water potential, although previous work has suggested that coupled bark and xylem measurements could also yield information over phloem properties and function.

We present here the basic theory for the interpretation of these measurements and show that coupled time-resolved measurements of bark and xylem diameter change can also be employed to estimate changes in phloem osmotic pressure. We apply this new theory to a dataset collected in Finland and show that the estimated phloem osmotic pressure at two positions along the stem of Scots pine trees correlates strictly with measured forest gross primary production estimated by eddy covariance. This correlation could be detected at time scales varying from hourly to diurnal and seasonal, suggesting that temporal variability in canopy photosynthesis can be rapidly transferred belowground by the phloem in the form of both fast waves of pressure-concentration waves and of slower moving mass flow.

METHODS

Simultaneous whole stem and xylem diameter change measurements have been conducted on 40-year old Scots Pine trees in Helsinki University research station in Hyytiälä, Southern Finland. Here we analyze this data from years 2006 and 2007 and compare it to CO₂ exchange measurements made by the eddy-covariance method.

Changes in xylem diameter Δd_x reflect changes in xylem pressure ΔP_x according to Hooke's law (Irvine & Grace 1997, Perämäki et al. 2001):

$$\Delta d_x \propto \Delta P_x \quad (1)$$

Similarly, changes in inner bark diameter Δd_b can be approximated to be proportional to change in inner bark pressure ΔP_b

$$\Delta d_b \propto \Delta P_b \quad (2)$$

Phloem tends towards equilibrium with the xylem by water exchange. The radial water flux (J) between the xylem and phloem is

$$J \propto (P_x - (P_b - \pi)) \quad (3)$$

where π is the osmotic pressure of the phloem.

MODEL DESCRIPTION

Step 1⁰: Assuming first no changes in the osmotic pressure of the inner bark, (constant π in Eq. 3), the expected diameter variation of the inner bark can be calculated from changes in xylem diameter alone using Eqs. (1) to (3), and assuming constant inner bark elasticity and radial permeability. Two constants of proportionality (having to do with the radial permeability and elasticities of the two tissues) are fitted from data to achieve this.

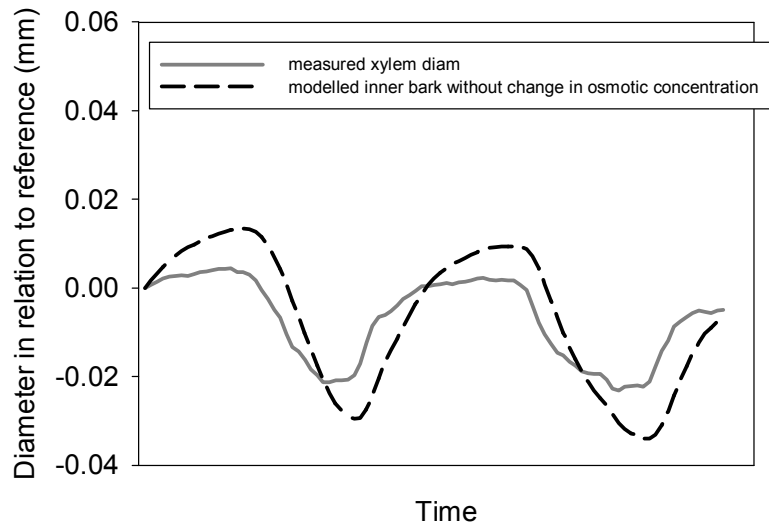


Fig. 1. Measured xylem diameter and the modelled inner bark diameter in the case its osmotic concentration remained constant.

Step 2⁰: The difference between the measured inner bark diameter and the inner bark diameter calculated according to step 1⁰ is due to changes in the osmotic concentration of the inner bark. An explicit equation (not shown here) can be written, which gives the dynamics of the osmotic pressure of the phloem.

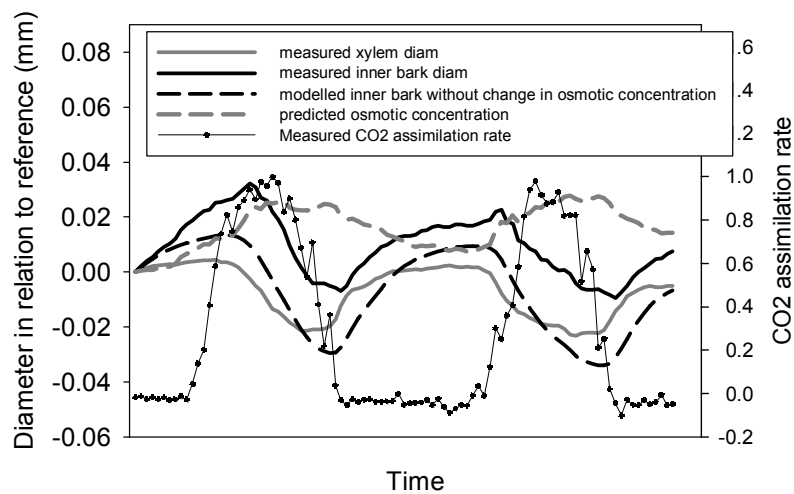


Fig. 2. In addition to Fig. 1, the measured inner bark diameter, the predicted change in osmotic concentration (units of the equivalent diameter change it induces), and the CO₂ assimilation rate measured by a cuvette.

CONCLUSIONS

The osmotic concentration predicted by the model (2 meters below the canopy) lags behind the measured photosynthetic production by approximately one to two hours. This short time lag is in correspondence with fast propagation of osmotic concentration in the phloem in the form of pressure-concentration waves (Mencuccini & Hölttä 2010). We also found a significant correlation between the daily cumulative GPP and the increase in osmotic concentration predicted by the model.

This new technique holds significant promise to allow high-resolution time-resolved monitoring of phloem osmotic and turgor pressure and provides a new tool that can be employed alongside other techniques to increase our understanding of phloem transport. We conclude by suggesting further avenues for testing of this new technique.

ACKNOWLEDGEMENTS

The financial support by the Academy of Finland Centre of Excellence program (project #1118615) is gratefully acknowledged. T. Hölttä received funding from Academy of Finland project #1132561.

REFERENCES

- Irvine J. and Grace J. (1997) Continuous measurements of water tensions in the xylem of trees based on the elastic properties of wood. *Planta* 202, 455–461.
- Mencuccini M. and Hölttä T. (2010) The significance of phloem transport for the speed of link between canopy photosynthesis and belowground respiration. *New Phytologist* 185, 189–203.

Perämäki M, Nikinmaa E, Sevanto S, Ilvesniemi H, Siivola E, Hari P, Vesala T. 2001. Tree stem diameter variations and transpiration in Scots pine: an analysis using a dynamic sap flow model. *Tree Physiology* 21, 889-897.

Sevanto S., Hölttä T., and Holbrook M. (2011) Effects of the hydraulic coupling between xylem and phloem on diurnal phloem diameter variation. *Plant Cell & Environment* 34, 690-703.

HYGROSCOPIC PROPERTIES OF SUB-ARCTIC AEROSOLS: CONTINUOUS HTDMA MEASUREMENTS FROM PALLASTUNTURI, FINNISH LAPLAND

A.-P. HYVÄRINEN¹, K. NEITOLA¹, E. ASMI¹, D. BRUS^{1,2} and H. LIHAVAINEN¹

¹Finnish Meteorological Institute, Erik Palménin aukio 1, P.O. Box 503, FIN-00100 Helsinki, Finland

²Laboratory of Aerosol Chemistry and Physics, Institute of Chemical Process Fundamentals Academy of Sciences of the Czech Republic, Rozvojová 135, CZ-165 02 Prague 6, Czech Republic

Keywords: H-TDMA, hygroscopic growth, Pallastunturi.

INTRODUCTION

Arctic climate has warmed twice as quickly as climate on average during the last century. Despite growing knowledge, climate models give still uncertain predictions for Arctic areas. The uncertainty arises for example from understanding the direct and indirect climate effects of aerosols. To address the knowledge gap in the properties of Arctic and sub-Arctic aerosols, FMI begun continuous measurements of aerosol hygroscopic growth at the Pallastunturi GAW station in the Finnish Lapland (Hatakka *et al.* 2003). The measurements were started on December 2008.

METHODS AND RESULTS

The measurements are conducted with a hygroscopicity tandem differential mobility analyser (HTDMA) built in-house FMI. The HTDMA was built according to the EUSAAR recommendations, and fulfils the EUSAAR criteria for continuous measurements. The main HTDMA features include:

- Measurement of hygroscopic growth factor (HGF) at a fixed RH of ~90 %
- Quality assurance with automated dry- and ammonium sulphate checks
- 8 dry diameters from 15 nm to 265 nm (1 cycle takes 1 hour)
- Aerosol humidification from the sample flow using a Gore-Tex humidifier
- DMA's in closed loop arrangement with a dew point analyser as the main humidity sensor

The 2009 annual average growth factors varied from 1.15 ± 0.08 measured for 15 nm dry particles to 1.44 ± 0.11 measured for the 265 nm dry particles. Figure 1 illustrates the corresponding HGF distributions. The growth factors had some seasonal variation, having highest values in the spring and lowest in the autumn (Table 1). However, the seasonal variation was weak and nearly within the standard deviation of the annual data.

Month	50 nm (Aitken mode)	165 nm (Accumulation mode)
Spring	1.23 ± 0.09	1.43 ± 0.09
Summer	1.18 ± 0.08	1.32 ± 0.10
Autumn	1.13 ± 0.07	1.32 ± 0.11
Winter	1.19 ± 0.08	1.42 ± 0.09

Table 1. Average growth factors with standard deviations for representative Aitken and Accumulation mode dry particles.

The mean growth factors were used to deduct the hygroscopicity parameter κ -values. These can be derived from the measured HTDMA growth factors (HGF) as follows (Good *et al.*, 2010):

$$\kappa_{HTDMA} = \frac{HGF^3 - 1}{RH} \exp\left(\frac{4\sigma_w M_w}{RT\rho_w D_d HGF}\right) + 1 - HGF^3. \quad (1)$$

The annual average κ -values for 2009 varied from 0.1 for 25 nm dry particles to 0.23 for 265 nm dry particles. Therefore, the Kelvin effect alone does not explain the increasing HGF towards larger dry particles.

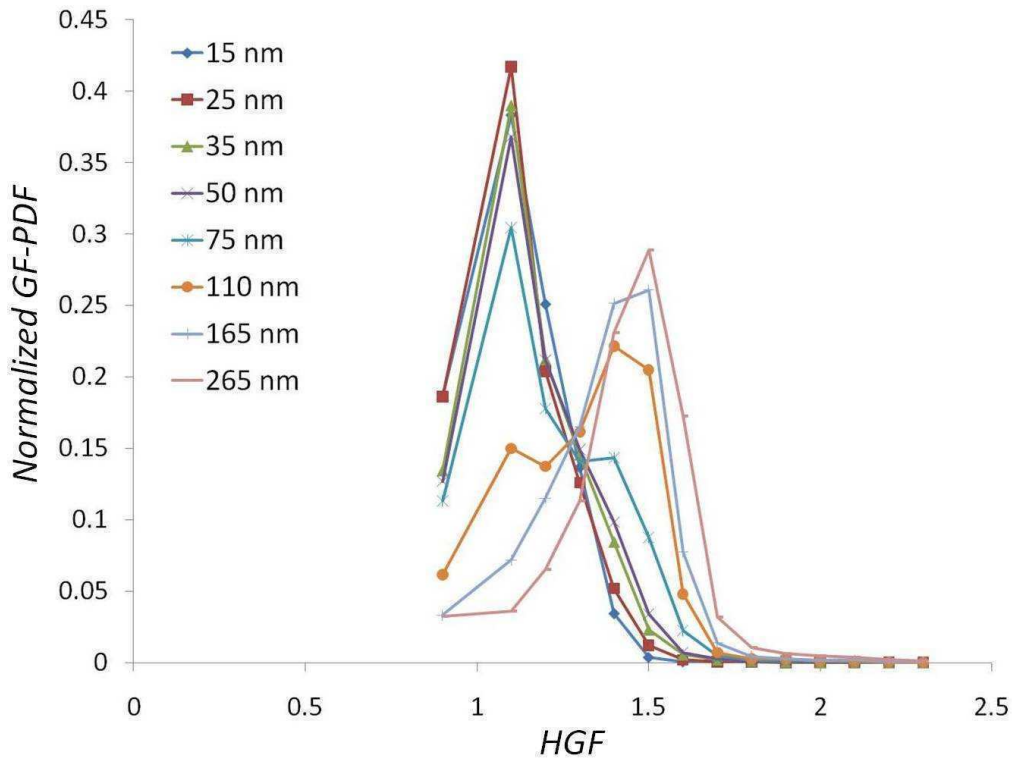


Figure 1. Average growth distributions for Pallastunturi aerosols.

The long term measurements of aerosol hygroscopic growth factors in Pallastunturi fill some of the knowledge gaps in aerosol properties in the sub-Arctic. This will be helpful when determining the climate effects of aerosols in the Arctic.

ACKNOWLEDGEMENTS

This work was supported by the Academy of Finland Centre of Excellence program (project no. 1118615), EUSAAR and the Maj & Tor Nessling foundation. Marting Gysel from PSI is acknowledged for providing the IGOR inversion algorithm for the HTDMA data.

REFERENCES

- Good, N., D. O. Topping, J. D. Allan, M. Flynn, E. Fuentes, M. Irwin, P. I. Williams, H. Coe, and G. McFiggans. (2010). Consistency between parameterisations of aerosol hygroscopicity and CCN activity during the RHaMBLe discovery cruise. *Atmos. Chem. Phys.*, 10, 3189-3203.
- Hatakka, J., T. Aalto, V. Aaltonen, M. Aurela, H. Hokola, M. Komppula, T. Laurila, H. Lihavainen, J. Paatero, K. Salminen and Y. Viisanen (2003). Overview of the atmospheric research activities and results at Pallas GAW station. *Boreal Env. Res.*, 8, 365–383.

CLOUD DROPLET ACTIVATION DURING THE 2010 PUIJO CLOUD EXPERIMENT

A. JAATINEN¹, S. ROMAkkANIEMI¹, L.Q. HAO¹, A. KORTELAINEN¹, P. MIETTINEN¹, D. BRUS³, H. PORTIN^{1,2}, M. KOMPPULA², A. LESKINEN², J.N. SMITH^{1,2,4} and A. LAAKSONEN^{1,3}

¹Department of Applied Physics, University of Eastern Finland, Kuopio, P.O. Box 1627, Finland

²Finnish Meteorological Institute, Kuopio Unit, Kuopio, P.O. Box 1627, Finland

³Finnish Meteorological Institute, Climate Change, Helsinki, P.O. Box 503, Finland

⁴National Center for Atmospheric Research, Boulder, CO, P.O. Box 3000, USA

Keywords: CLOUD EVENTS, CCN

INTRODUCTION

Aerosol particles act as condensation nuclei in the humid atmosphere with the potential to take on water and form cloud droplets. Newly formed aerosol particles become climatically important if they are able to grow to sizes of 50 nm and larger. Particles in this size range can act as cloud condensation nuclei (CCN) and therefore may contribute to the indirect aerosol effect, a series of proposed impacts that include increased cloud albedo due to increase in CCN concentration (Twomey, 1991) to increased lifetime of clouds (Albrecht, 1989). Once particles grow to a size where they can become CCN, their ability to activate into cloud droplets depends on their chemical composition, and the maximum water supersaturation in the air parcel forming cloud.

METHODS

The fourth Puijo Cloud Experiment (4th PuCE), an intensive campaign measuring aerosol and cloud properties, was conducted by the Finnish Meteorological Institute and University of Eastern Finland at the Puijo semi-urban measurement station. The measurement campaign was carried out during 30.9 – 28.10.2010. The station is located at the top of the Puijo sight-seeing tower, 306 m a. s. l. and 224 m above the surrounding lake level, thus being a very suitable site for aerosol-cloud interaction measurements (Leskinen et al., 2009; Portin et al., 2009). Aerosol sources for the observation are subject to the long-range transported particles from continent and ocean, but also the local pollution, likely from traffic, pulp mill, heating plant and the city.

In this work, the properties of cloud activation were studied using DMPS (Differential Mobility Particle Sizer), DMT CCNc (Cloud Condensation Nuclei counter), Aerodyne HR-TOF-AMS (High Resolution Time-Of-Flight Aerosol Mass Spectrometer) and the other aerosol properties such as volatility by V-TDMA (Volatility Tandem Differential Mobility Analyzer), organic growth by O-TDMA (Organic Tandem Differential Analyzer) and hygroscopic growth by H-TDMA (Hygroscopicity Tandem Differential Analyzer). During the measurements DMPS inlet was switched between PM1 (interstitial particles) and total line (all particles), and during the cloud events the particles activated to cloud droplets were resolved as a difference between the lines. In addition, we measured size-resolved CCN to get information about size dependency, and on the other hand data about the true supersaturation inside the cloud during a cloud event.

RESULTS

During the campaign, a total of seven cloud events were observed. The duration of the events ranged from a couple of hours up to about twenty hours. Figure 1 shows the time series of the CCNc derived critical diameter (D_{50}), i.e. the diameter where half of all particles are activated into cloud droplets. In addition, the DMPS derived critical diameters during cloud events are shown in Figure 1. The results show, that

during some cloud events (e.g the event on 20.10.2011) the mean supersaturation has been closer to 0.2%, but on most cases the real supersaturation inside the cloud has been 0.1% or less.

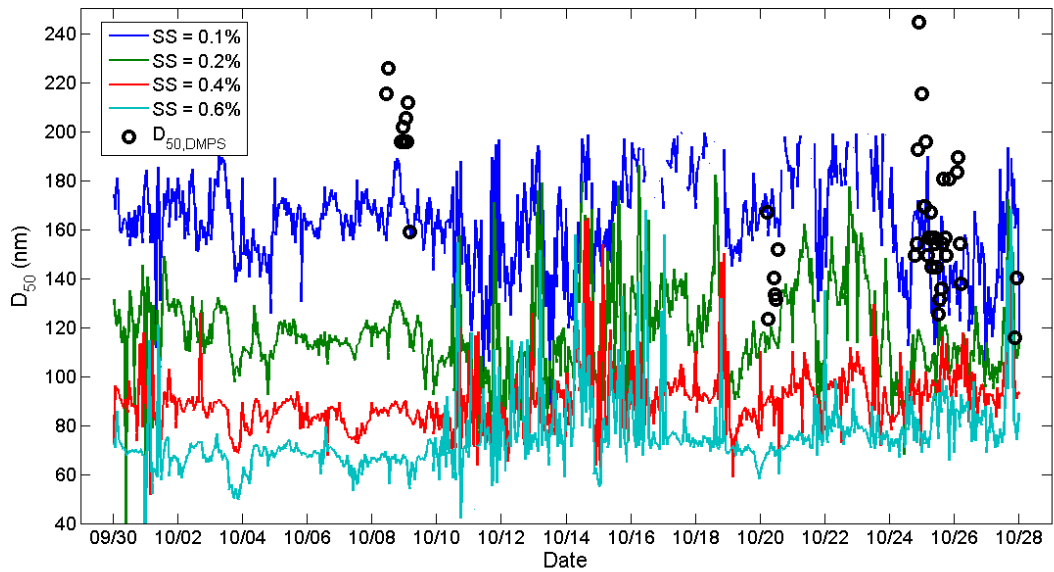


Figure 1. Time series of CCNc derived critical diameters (D_{50}) for four different supersaturations (lines) over the whole campaign time and DMPS derived critical diameters (black circles) during cloud events.

As an example, we have chosen one cloud event day for closer scrutiny, 9.10.2010, 00:00 – 05:45. From Figure 2 we can see that the minimum size of particles forming cloud events was around 100 nm and D_{50} -size, i.e. the size where blue and black line cross, is 195 nm. From CCN measurements the mean $D_{50}(SS=0.1\%)$ is 160 nm and $D_{50}(SS=0.2\%)$ is 120 nm. Thus the mean supersaturation during cloud formation has been less than 0.1%.

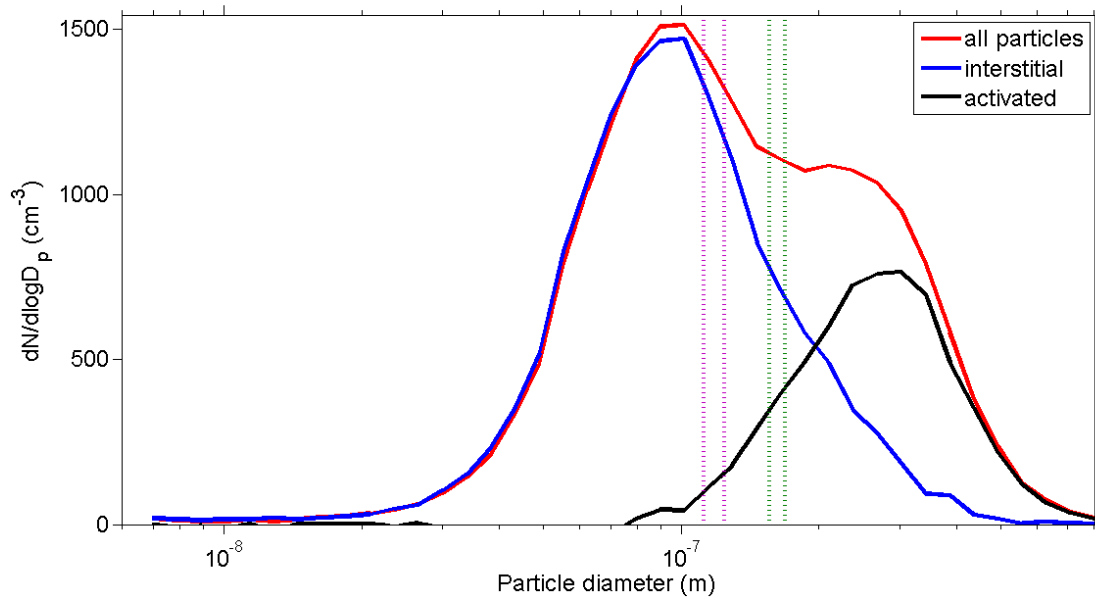


Figure 2. Size distributions of interstitial particles (blue) and all particles (red), and those forming cloud droplets (black). Green and purple dotted lines represent the range of the critical diameter (D_{50}) derived from the CCNc data during the cloud event, for $SS=0.1\%$ and $SS=0.2\%$ respectively.

During the cloud event the mass fraction of ammonium-sulphate was around 30% the rest being mainly organics. This is in good agreement with CCNc measurements.

In future analyses, we shall analyze other measured data (such as meteorological and chemical) to investigate how the size dependent composition of particles vary during cloud events, and how the diameter of smallest activated particles depend on the composition of particles.

ACKNOWLEDGEMENTS

This work was supported by the Academy of Finland (project 111865 and 123466) and by KONE foundation.

REFERENCES

- Albrecht, B. A.: Aerosols, cloud microphysics, and fractional cloudiness. *Science*, **245**(1229):1227–1230, 1989.
- Leskinen, A., et al. (2009) *Boreal Environ. Res.*, 14, 576-590.
- Portin, H., et al. (2009) *Boreal Environ. Res.*, 14, 641-653.
- Roberts, G. C. & Nenes, A. (2005). A continuous-flow streamwise thermal gradient CCN chamber for atmospheric measurements, *Aerosol Sci. Tech.*, 39, 206–221.
- Twomey, S. (1991). Aerosols, clouds and radiation, *Atmos. Environ.*, 25A, 2435–2442.

EVALUATION OF THE SURFACE URBAN ENERGY AND WATER BALANCE SCHEME (SUEWS) IN HELSINKI

L. JARVI¹, C.S.B. GRIMMOND², A. NORDBO¹, H. SETÄLÄ³, M. TAKA⁴, E. SIIVOLA¹, O. RUTH⁴ and T. VESALA¹

¹Division of Atmospheric Sciences, Department of Physics, University of Helsinki, P.O. Box 48, University of Helsinki, Finland.

²King's College London, Department of Geography, UK.

³Department of Environmental Sciences, University of Helsinki, Finland

⁴Department of Geography, University of Helsinki, Finland

Keywords: EVAPOTRANSPIRATION, HEAT, URBAN, WATER.

INTRODUCTION

In urban areas the typically high fraction of impervious surfaces affects the surface energy and water balances by increasing turbulent heat emissions to the atmosphere and surface runoff and by decreasing evapotranspiration. These processes affect human comfort, pollutant dispersion and increase the risk of flooding. The energy and water exchanges are not commonly measured so modeling approaches are needed particularly for urban planning and mitigation purposes. However, to date only a few urban water balance models have been developed (e.g. Grimmond *et al.*, 1986, Grimmond and Oke, 1991; Mitchell *et al.*, 2001; Berthier *et al.*, 2006; Xiao *et al.*, 2007). A model that can simulate both energy and water fluxes for extended periods of time (e.g. multiple years) with limited amount of input variables from standard meteorological stations is needed.

The Surface Urban Energy and Water Balance Scheme (SUEWS, Järvi *et al.*, 2011) is a new model which provides a simple tool to simulate both balances through the use of commonly measured meteorological variables and surface cover information. Previously, the model has been tested with three datasets from Vancouver, Canada, and two from Los Angeles, California (Järvi *et al.*, 2011), where it was found to simulate the net all-wave radiation (Q^*), sensible heat (Q_H) and latent heat (Q_E) fluxes well with rmse between 25-47, 30-59 and 20-55 W m⁻², respectively. In addition, the model was able to simulate surface wetness and soil moisture changes. In this study, the model is run and tested in an urban environment with strong seasonal variations.

METHODS

With SUEWS, the rates of evaporation-interception for a single layer with multiple surface types (paved, buildings, coniferous trees/shrubs, deciduous trees/shrubs, irrigated grass, non-irrigated grass and water) are calculated. Below each surface type, except water, there is a single soil layer. At each time step (5 min to 1 h) the moisture state of each surface and soil are calculated. Horizontal water movements at the surface and in the soil are incorporated. Q_E is calculated with a modified Penman-Monteith equation and Q_H as a residual from the available energy minus Q_E . The model contains several sub-models for e.g. Q^* , storage heat (ΔQ_s) and anthropogenic heat flux (Q_F) and external irrigation.

The forcing and evaluation data were observed at the SMEAR III station in Helsinki, Finland (Järvi *et al.*, 2009). The modeled Q^* , Q_H and Q_E are compared with the radiation and eddy covariance measurements carried out at 31 m on a lattice tower in 2010. The measurement setup consisted of a Metek ultrasonic anemometer (USA-1, Metek GmbH, Germany) to measure vertical wind speed and

sonic temperature and an closed-path infrared gas analyzers (LI-7000, LI-COR, Lincoln, Nebraska, USA) to measure CO₂ and H₂O mixing ratios. Temporal resolution for EC measurements was 10 Hz and in flux calculations the commonly accepted procedures were used (Aubinet *et al.*, 2000).

The complex surroundings of the tower can be divided into three types of surface cover by wind direction (Table 1). The results were divided according to the surface cover types and thermal seasons. In 2010, winter was from 1 January to 25 March and from 17 November to end of the year. Spring was from 26 March to 11 May, summer from 12 May to 25 September and fall from 26 September to 16 November.

	Surface cover fractions		
	Buildings	Paved	Vegetation
Urban (320-40°)	0.36	0.16	0.48
Road (40-180°)	0.26	0.31	0.43
Vegetation (180-320°)	0.19	0.17	0.64

Table 1. Surface cover fractions within a 600 m radius circle around the measurement tower. Fractions are given for the urban, road and vegetation sectors.

CONCLUSIONS

The model simulates Q^* well with rmse between 10.2 and 32.6 W m⁻². The largest uncertainty is related to the modeling of downward longwave radiation ($L\downarrow$), which is calculated from air temperature and relative humidity according to Loridan *et al.* (2011). When measured $L\downarrow$ is used to calculate Q^* , the rmse improves to 3.9-16.8 W m⁻². In spring and fall, when neither permanent snow cover nor external irrigation occur, the model simulates both Q_H and Q_E well (Figure 1, Q_H not shown). The underestimation of both fluxes in winter indicates underestimation of ΔQ_s and/or Q_F . Currently snow accumulation, which affects the availability of water in winter, is not accounted for but this is under development. Poor performance in summer is likely caused by underestimation of external irrigation. To date the irrigation sub-model has only been evaluated in a residential area in Vancouver where water consumption is likely lower than around the tower where allotment gardens and the University Botanical garden are located. Low Q_E (daytime difference on average 150 W m⁻²) were modeled in August, a period that was exceptionally warm and dry and irrigation was likely intense. In summer 2011, we plan to monitor water use in the Botanical garden, situated next to the station, in order to get more realistic irrigation values for the site.

Runoff has been monitored for October –November 2010 in two Helsinki catchments with different population densities. For both catchments SUEWS simulated the behavior of measured runoff well but overestimates runoff values when applied uncalibrated with the default model parameters ($r_{Mod} = 1.5r_{Meas}$, rmse = 0.17, $R^2 = 0.79$ and $r_{Mod} = 1.8r_{Meas} - 0.1$, rmse = 0.13, $R^2 = 0.57$). Future work will include analysis of the site specific parameters values for soil depth, drainage coefficients and surface store.

The new model SUEWS seems to simulate the energy and water balances well in Helsinki, but in order to draw any final conclusions, snow accumulation and irrigation model needs to be improved in the model.

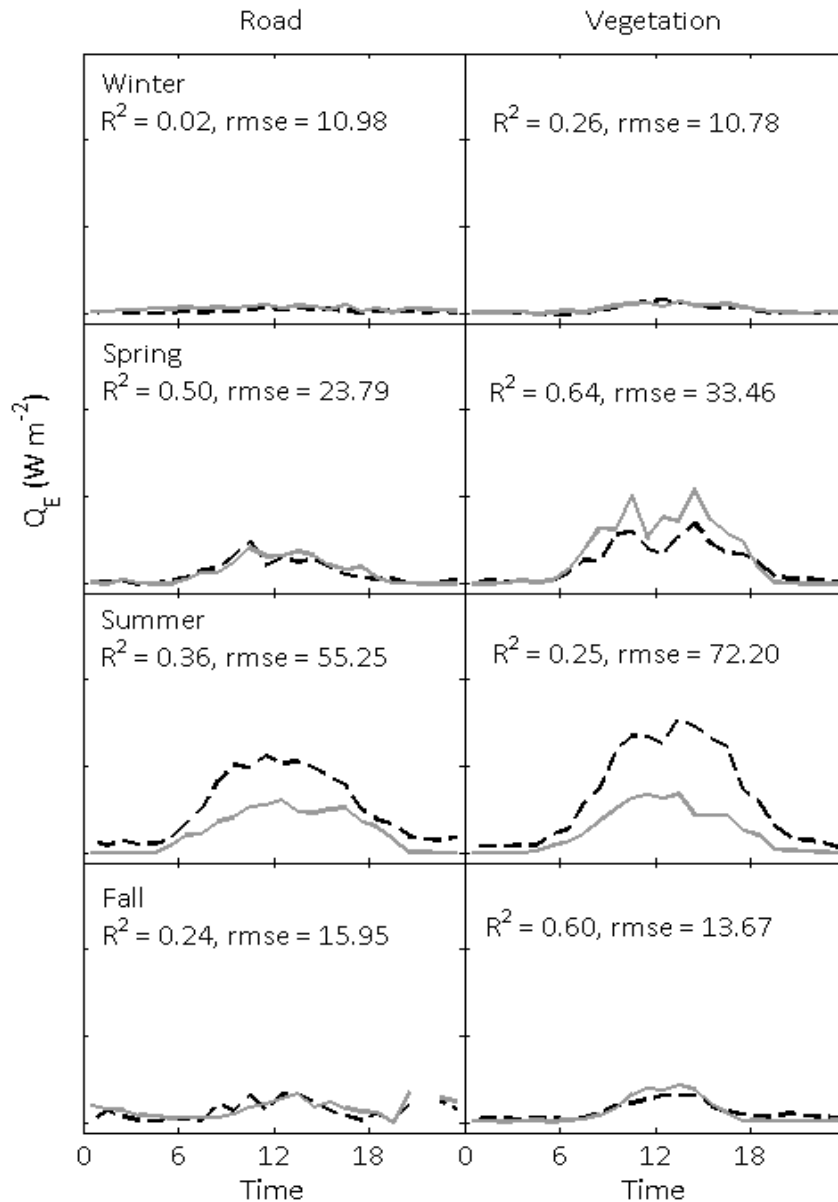


Figure 1. Diurnal behavior of measured and modeled latent heat fluxes (Q_E) in Helsinki in 2010.

ACKNOWLEDGEMENTS

This work was supported by the Finnish Academy (project no 138328) and EU project BRIDGE. We also thank the Academy of Finland Centre of Excellence program (project no1118615).

REFERENCES

- Aubinet M., A. Grelle, A. Ibrom, *et al.* (2000). Estimates of the annual net carbon and water exchange of European forests: the EUROFLUX methodology. *Adv. Ecol. Res.* 30, 114-175.
- Berthier E., S. Dupont, P.G. Mestayer and H. Andrieu (2006). Comparison of two evaporation schemes on a sub-urban site. *J. Hydrology* 328, 635-646.
- Grimmond C.S.B., Oke, T.R, 1986. Urban water balance 1. A model for daily totals. *Water Resour. Res.* 22, 1397-1403.
- Grimmond C.S.B. and T.R. Oke (1991). An Evaporation-Interception Model for Urban Areas. *Water Resour. Res.* 27, 1739-1755.

- Järvi L., C.S.B. Grimmond and A. Christen (2011). The Surface Urban Energy and Water Balance Scheme (SUEWS): Evaluation in Los Angeles and Vancouver. Submitted to *J. Hydrol.*
- Järvi L., H. Hannuniemi, T. Hussein, H. Junninen, P.P. Aalto, R. Hillamo, T. Mäkelä, P. Keronen, E. Siivola, T. Vesala and M. Kulmala (2009). The urban measurement station SMEAR III: Continuous monitoring of air pollution and surface-atmosphere interactions in Helsinki, Finland. *Boreal Env. Res* 14, 86-109.
- Loridan T., C.S.B Grimmond, B. Offerle, D. Young, T. Smith, L. Järvi and F. Lindberg (2010). Local-Scale Urban Meteorological Parameterization Scheme (LUMPS): longwave radiation parameterization and seasonality related developments. *J. Appl. Meteorol. Clim.*, <http://dx.doi.org/10.1175/2010JAMC2474.1>
- Mitchell V.G., R.G. Mein and T.A. McMahon (2001). Modelling the urban water cycle. *Environ. Modell. Softw.* 16, 615-629.
- Xiao Q., E.G. McPherson, J.R. Simpson and S.L. Ustin (2007). Hydrological processes at the urban residential scale. *Hydrol. Process.* 21, 2174-2188.

TECHNICAL IMPROVEMENTS IN SHOOT-LEVEL MONITORING OF O₃ AND NO_x FLUXES OF SCOTS PINE

J. JOENSUU¹, N. ALTIMIR¹, M. RAIVONEN^{1,2}, P. KOLARI¹, P. KERONEN², T. VESALA², J. BÄCK¹, P. HARI¹, E. NIKINMAA¹

¹University of Helsinki, Dept. Forest Sciences. PO box 27, FIN-00014 University of Helsinki, Finland.

²University of Helsinki, Dept. Physics. PO box 64, FIN-00014 University of Helsinki, Finland.

Keywords: ozone, nitrogen oxides, chamber measurements, flux.

INTRODUCTION

The SMEAR II station (Station of Measuring Forest Ecosystem-Atmosphere Relations) in Hyytiälä, Finland (61° N, 24° E) is well-known for its extensive series of measurements concerning the relationships of atmosphere and forest ecosystems in the boreal zone (Hari and Kulmala, 2005). As part of these measurements, shoot-level O₃ and NO_x fluxes of Scots pine (*Pinus sylvestris* L.) have been measured continuously since 1995. These measurements have provided valuable insights into O₃ and NO_x exchange and factors affecting them (Raivonen *et al.*, 2009, Altimir *et al.*, 2002).

TECHNICAL IMPROVEMENTS

Recently, the measurement system at SMEAR II has been improved with two technical changes concerning O₃ and NO_x measurements.

1) A new chamber type was designed to remove the enclosure effect caused by the shoot being somewhat shielded from ambient conditions at all times. The new chamber is built as a sliding box that encloses the shoot only for the short time needed to make a measurement and otherwise allows the shoot to experience all occurring ambient conditions, including wind and rain.

2) To measure NO_x concentrations in the chamber with the chemi-luminescence analyser used in the system, NO₂ is converted to NO. The molybdenum converter in use until 2006 is not specific to NO₂ but also converts other nitrogen-containing compounds. In order to allow targeted flux measurement of NO_x (instead of NO_y), the molybdenum converter of the NO_x analyser was replaced with a photolytic, NO₂-specific one.



Figure 1. Left: box chamber, right: sliding chamber. Photos: Pasi Kolari

AIMS OF THE PROJECT

In the first phase of the project, we are calculating O_3 and NO_y/NO_x fluxes for 2005–2011 and evaluating whether the measured fluxes or the observed effects of environmental factors have changed after the technical improvements. We are also studying the role and characteristics of the chamber blank (deposition or emission of the measured gases) caused by chamber walls in the new measurement system.

INITIAL RESULTS

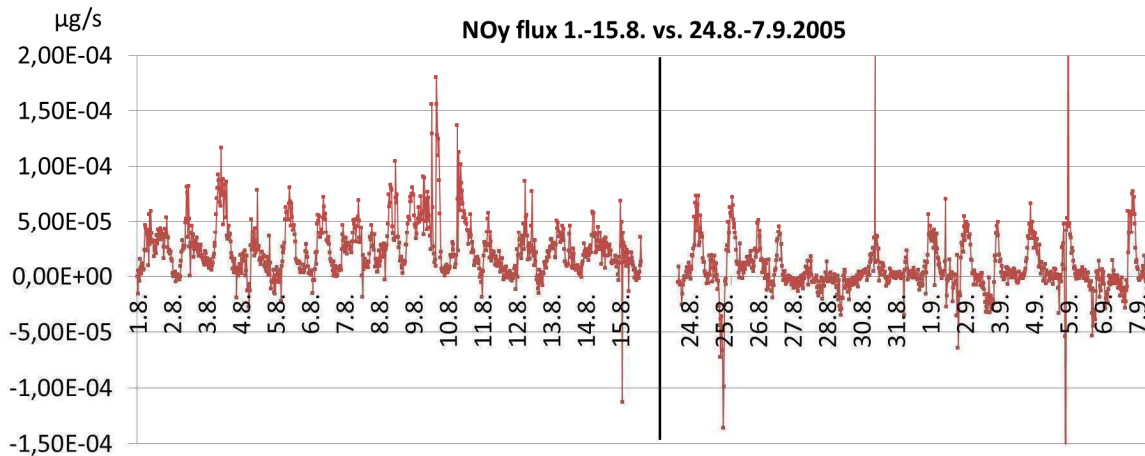


Figure 2. NO_y fluxes from a single chamber (chamber + shoot, chamber blank not calculated) with a box-type chamber (left) and a sliding chamber (right). Positive sign indicates emission from the shoot + chamber.

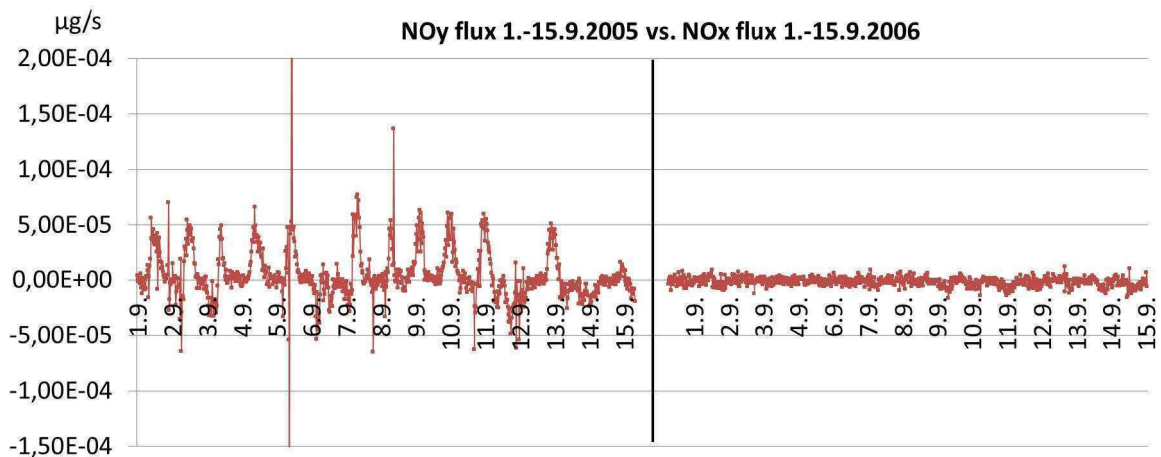


Figure 3. NO_y/NO_x fluxes from a single shoot chamber using a molybdenum converter (left) and a photolytic converter (right). Results with the Mo converter show UV-dependent NO_y emission. The effect of UV on NO_x fluxes will be evaluated.

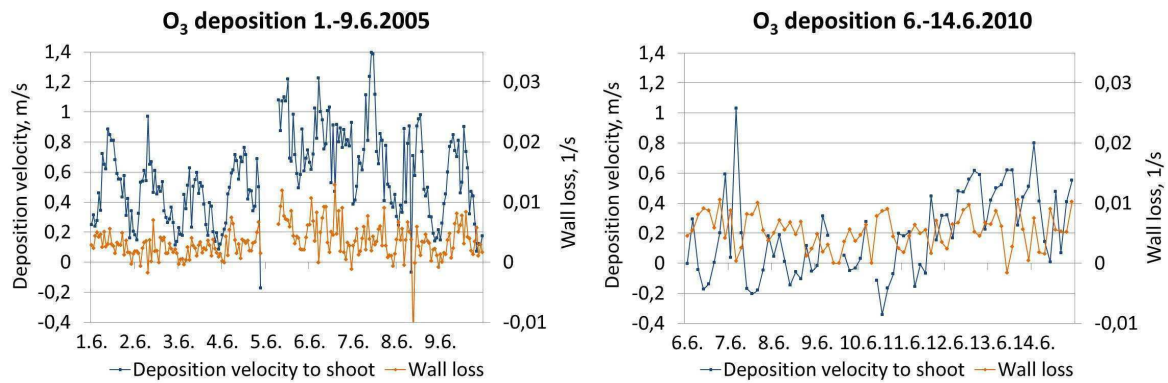


Figure 4. Ozone deposition in a box-type chamber (left) and a sliding chamber (right).

ACKNOWLEDGEMENTS

This work is supported by Maj and Tor Nessling Foundation.

REFERENCES

- Altimir, N., T. Vesala, P. Keronen, M. Kulmala and P. Hari (2002). Methodology for direct field measurements of ozone flux to foliage with shoot chambers. *Atmospheric Environment* **36**, 19.
- Hari, P. and M. Kulmala (2005). Station for Measuring Ecosystem-Atmosphere Relations (SMEARII). *Boreal Environment Research* **10**, 315.
- Raivonen, M., T. Vesala, L. Pirjola, N. Altimir, P. Keronen, M. Kulmala and P. Hari (2009). Compensation point of NO_x exchange: net result of NO_x consumption and production. *Agricultural and Forest Meteorology* **149**, 1073.

SULFURIC ACID AND SULFURIC ACID CLUSTER DETECTION WITH CI-API-TOF

T.B.A. JOKINEN, M. SIPILÄ, T. PETÄJÄ, H. JUNNINEN, L. MAULDIN, D.R. WORSNOP and M. KULMALA

Department of Physics, University of Helsinki, P.O.Box 64, Helsinki, Finland

Keywords: Sulphuric acid, nucleation, clusters, chemical ionization, APi-TOF.

INTRODUCTION

Sulfuric acid is a key compound in atmospheric nucleation (Sipilä et al., 2010, Zhao et al., 2010). In atmosphere, sulfuric acid is produced mainly photochemically via reaction of OH with SO₂. Concentration of sulfuric acid is typically very low, rarely exceeding 10⁸ molecules cm⁻³ (e.g. Paasonen et al., 2010). The low concentrations set certain requirements for the detector to be used for quantitative measurements. Method for measuring gas phase sulphuric acid by means of chemical ionization mass spectrometer were developed by Eisele and Tanner (1993). They used nitrate ion, NO₃⁻, and its clusters with nitric acid, HNO₃, for selective chemical ionization of H₂SO₄ via NO₃⁻·(HNO₃)_n + H₂SO₄ → n(HNO₃) + (HNO₃)·HSO₄⁻. Resulting (HNO₃)·HSO₄⁻ clusters together with remaining NO₃⁻·(HNO₃)_n were dissociated and HSO₄⁻ and NO₃⁻ were detected with a quadrupole mass spectrometer.

Here we present a measurement system in which the atmospheric pressure chemical ionization inlet, with geometry similar to Eisele and Tanner (1993), is combined with a high resolution atmospheric pressure interface time-of-flight mass spectrometer (Tofwerk Ag., Junninen et al., 2010). In the present setup, clusters are not broken on purpose, instead the high resolution and mass range of the TOF allows separation and summing of different clusters. Advantage of the method is that it allows one to seek for neutral sulphuric acid containing clusters formed by nucleation in the atmosphere (Zhao et al., 2010) or in laboratory systems (Sipilä et al., 2010).

LABORATORY EXPERIMENT

In the laboratory experiment we generated reagent ions by mixing a small amount of nitric acid to nitrogen flow and exposed it to a radioactive source (241Am). Sulfuric acid vapour was produced by leading synthetic air through a saturator containing pure 95-97% H₂SO₄. Sulfuric acid vapour was then introduced to the CI inlet with multiple different flow rates and diluted with laboratory air to create a constant sample flow of 10 lpm. The mixing with the reagent ions is done by applying voltage between a set of ion lenses.

The sample is guided to the TOF for mass per charge (m/Q) determination. Pressure is reduced to 10⁻⁶ mbar in three separately pumped chambers. Ions are guided to TOF using two quadrupoles and an ion lens assembly. We operated TOF in negative ion mode to monitor sulfuric acid and its dimer, trimer and tetramer at m/Q 97, 195, 293, 391 and nitric acid monomer, dimer and trimer at m/Q 62, 125 and 188.

Figure 1 shows increase in deprotonated sulfuric acid concentration when flow rate through the saturator is elevated from 0.1 lpm to 9.5 lpm. With flow rates under 1 lpm we only detect sulfuric acid monomer and dimer but at elevated flow rates, < 2 lpm, we can detect bigger clusters forming also. Nitric acid is been neutralized during ionization process which can be seen in descending signals of NO₃⁻, its dimer and trimer.

FIELD MEASUREMENTS

CI-TOF-MS was used to measure sulphuric acid and acidic aerosol clusters in ambient air during a spring campaign 2011 in Hyytiälä SMEAR II station. Naturally charged ion clusters were measured

simultaneously with an APi-TOF operating without charger. This data is needed to understand the contribution of naturally charged sulphuric acid clusters on the signals in CI-TOF-MS. For comparison, sulfuric acid was measured also with a CI-MS (Eisele and Tanner, 1993). Few different clusters have so far been identified in the CI-TOF-MS spectra. All of the detected clusters were associated with another peak in the mass spectrum with the same integer mass (Fig. 2). Besides observed acidic clusters, these contaminants tend to correlate with UV-radiation and thus sulfuric acid and particle formation. Therefore, the high resolution of APi-TOF helps in indentifying the nucleating clusters from molecular gas phase species. Question, which is not yet fully answered is that how much naturally charged sulfuric acid clusters, observed e.g. by Ehn et al. (2010), affect our measurement. Thus, these results should be taken as preliminary.

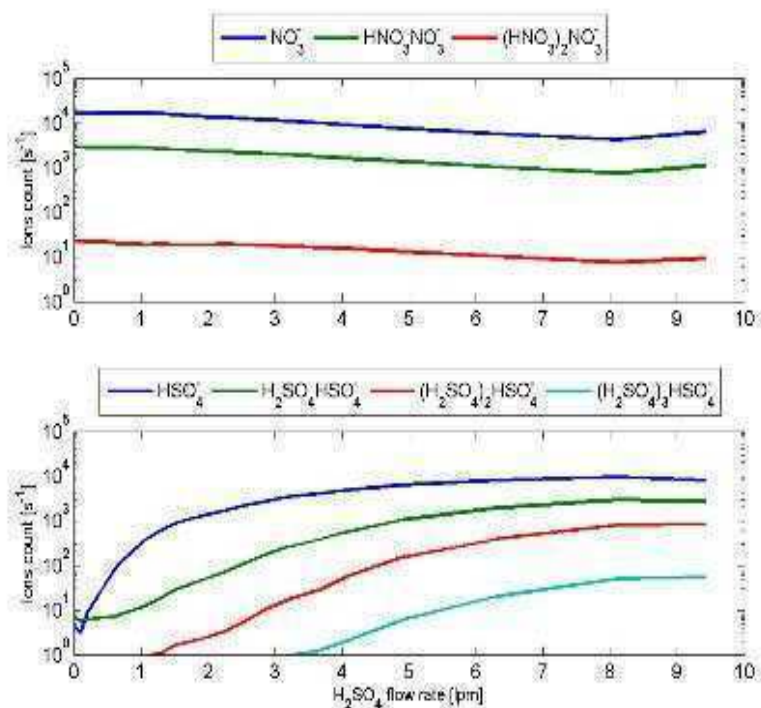


Figure 1. Sulfuric acid and reagent ion concentrations in CI-TOF-MS spectrum as a function of flow rate through H₂SO₄ saturator.

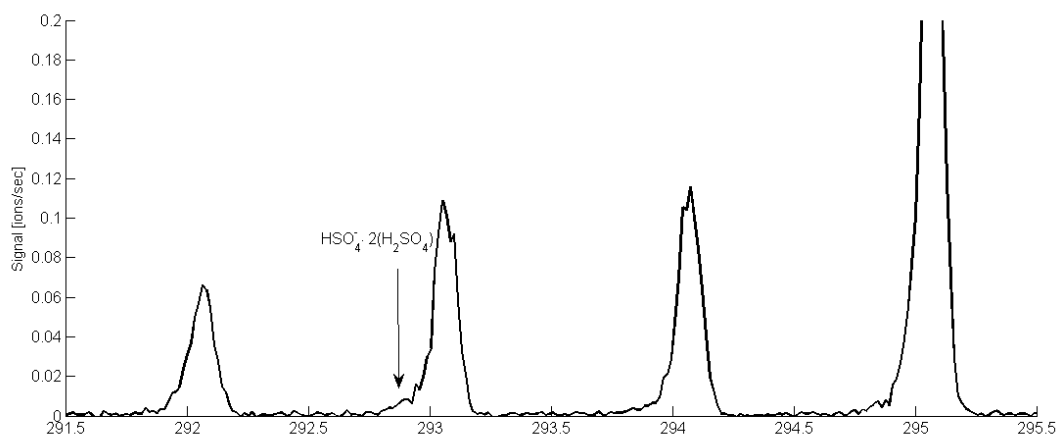


Figure 2. Example of the spectra around sulphuric acid trimer measured with CI-APi-TOF. Major fraction of the signal around an integer mass of 293 Da consists of unknown gas phase species. Distinguishing the tiny signal resulting from sulphuric acid cluster with an exact mass of 292.8949 Da is often difficult.

CONCLUSIONS

API-TOF equipped with nitric acid chemical ionization inlet is a promising tool for detection of very low concentration atmospheric acids and their clusters. At present the lowest detection limit for H₂SO₄ with 5 minute integration is around or slightly below 10⁻⁵ molecules cm⁻³ being comparable to that of CI-MS. However, the concentrations of clusters in the atmosphere are such low (per species) that even the naturally charged ion clusters can cover the weak signals from originally neutral, artificially charged, clusters. Future systems should therefore incorporate ion filter. In laboratory experiments, with higher concentrations of clusters, CI-API-TOF will, in the future, yield much new information on mechanistic steps of particle nucleation.

ACKNOWLEDGEMENTS

This work was supported by the Academy of Finland Finnish Center of Excellence Program.

REFERENCES

- Sipilä, M., Berndt, T., Petäjä, T., Brus, D., Vanhanen, J., Stratmann, F., Patokoski, J., Mauldin III, R. L., Hyvärinen, A.-P., Lihavainen, H., and Kulmala, M., *Science*, 327, 1243–1246, 2010.
- Paasonen, P., Nieminen, T., Asmi, E., Manninen, H.E., Petäjä, T., Plass-Dülmer, C., Flentje, H., Birmili, W., Wiedensohler, A., Hörrak, U., Metzger, A., Hamed, A., Laaksonen, A., Facchini, M.C., Kerminen, V.-M. and Kulmala, M., *Atmos. Chem. Phys. Discuss.* 10, pp. 1795–11850, 2010.
- Eisele, F. and Tanner, D., *J. Geophys. Res.*, 98, 9001–9010, 1993
- Junninen, H., Ehn, M., Petäjä, T., Luosujärvi, L., Kotiaho, T., Kostianen, R., Rohner, U., Gonin, M., Fuhrer, K., Kulmala, M. and Worsnop, D.R., *Atmos. Meas. Technol. Discuss.*, 3, pp. 599-636, 2010.
- Zhao et al., *J. Geophys. Res.*, 2010.
- Ehn et al., *Atmos. Chem. Phys.*, 2010.

CAN WE APPLY THE KNOWLEDGE OF SCOTS PINE ECOSYSTEMS TO NORWAY SPRUCE?

K. KABIRI¹, M. HAVIMO¹, T. HÖLTTÄ¹, R. SIEVÄNEN² and P. HARI¹

¹ Department of Forest Sciences, University of Helsinki, Finland.

² Finnish Forest Research Institute, Vantaa, Finland.

Keywords: SMEAR, MicroForest, climate change, structural regularities, photosynthesis, nitrogen deposition

INTRODUCTION

Metabolic processes generate carbon and nitrogen fluxes in forest ecosystems. The sugars formed in photosynthesis are the dominating source of energy and raw material for the life in forest ecosystems and nitrogen uptake provides raw material for synthesis of proteins, needed for enzymes, membrane pumps and pigments. The regularities in tree structure determine the allocation of sugars and nitrogen to needles, woody components and fine roots.

The dynamic ecosystem model MicroForest is based on carbon and nitrogen fluxes in trees, ground vegetation, soil organic matter and microbes in the soil. The regularities in tree structure determine the allocation of sugars and nitrogen. The core of the model describing trees is carbon and nitrogen balance equations; they include two unknowns, needle mass and fine root mass growth. They can be solved from the two mass balance equations.

The model is tuned to the Scots pine stands around SMEAR II station. The parameter values for the model have been determined utilising measurements at SMEAR II (Hari *et al.*, 2008). The aim of this study is to expand the model for spruce with measurements of trees in two stands in southern Finland.

METHODS

We measured stand density together with annual tree height and diameter at stump height for 30 trees in two spruce stands in Siuntio and Hyvinkää. There after we run the model constructed for Scots pine. We changed only the needle age from 3 to 5 years and we tuned the height growth sub model to correspond the height growth of the measured stands. We obtained the initial state of the seedlings in each size class in the model when the stand was 5 years old from the measurements.

RESULTS

The first run with Siuntio data indicated that the height growth model is Scots pine specific and we had to re-estimate the two parameter values in the height sub model. There after the runs with MicroForest were able to simulate the height and diameter growth in the size classes rather satisfactorily. Figure 1 shows the diameters and heights in the biggest (1st) and in the middle (3rd) size classes.

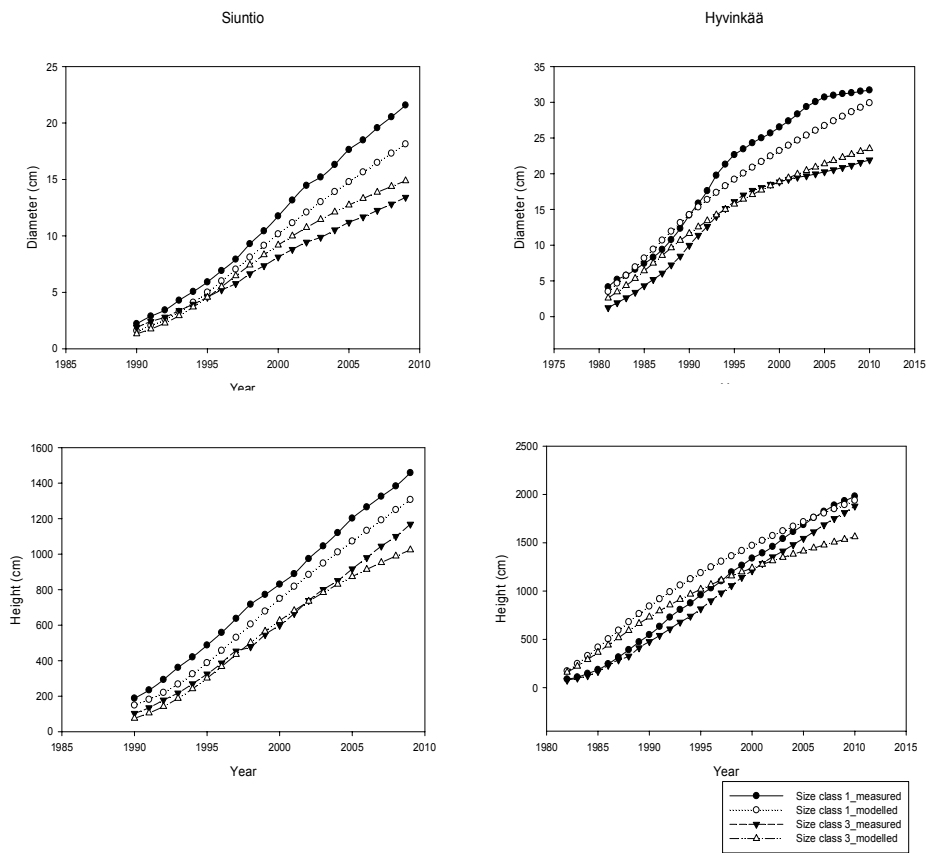


Fig.1. Diameter and height growth for Norway spruce and for biggest (1st) and middle (3rd) size classes measured and modelled with MicroForest.

This is the first attempt to apply the knowledge obtained in the research of Scots pine to Norway spruce. The obtained results are really promising, the same principles seem to govern the stand development in Scots pine and Norway spruce and the knowledge can be transferred between species.

ACKNOWLEDGEMENTS

This work was supported by the Center of Excellence (FCoE).

REFERENCES

Hari, P., Salkinoja-Salonen, M., Liski, J., Simojoki, A., Kolari, P., Pumpanen, J., Kähkönen, M., Aakala, T., Havimo, M., Kivekäs, R., and Nikinmaa, E. 2008. Growth and development of forest ecosystem; the MicroForest model. In: Hari, P., Kulmala, L. (Eds.) Boreal Forest and climate change. Springer, 582 pp.

SOA FORMATION FROM GASOLINE EXHAUST

M. K. KAJOS¹, E. Z NORDIN², A. ERIKSSON^{2,3}, P. NILSSON², H. HELLÉN⁴, P. ROLDIN³, J. CARLSSON², J. RISSLER², B. SVENNINGSSON³, E. SWIETLICKI³, M. BOGHARD², M. KULMALA¹, T. M. RUUSKANEN AND J. PAGELS²

¹Department of Physics, University of Helsinki, Finland

²Division of Ergonomics and Aerosol Technology, Lund University, Sweden

³Division of Nuclear Physics, Lund University

⁴Finnish Meteorological Institute, Finland

Keywords: AEROSOL, AROMATIC ORGANIC COMPOUNDS

INTRODUCTION

Atmospheric aerosol particles effect on the climate and human health. These particles can be emitted from primary sources such as windborne dust or sea spray. Secondary organic aerosol (SOA) particles are formed by gas-to-particle processes. Due to its importance in the atmospheric processes the formation of SOA is a widely studied phenomenon. However these studies often focus on SOA formation from biogenic organic gases such as mono- or sesquiterpenes. In addition photo oxidation of aromatic volatile organic compounds (VOCs) such as toluene and xylenes contribute to the atmospheric SOA formation (Ng et al., 2007, Hildebrandt et al., 2009). In densely populated areas traffic is a significant source of aromatic VOCs to the atmosphere. Especially cold starts or idling of vehicles lead to high VOC emissions since in these circumstances the catalysts do not remove the VOCs. Due to the lack of understanding of all of the complex chemical and physical processes related to the SOA formation of vehicle exhaust, the role of the aromatic VOCs on the SOA formation is not well understood (Hallquist et al., 2009). So far chamber studies on SOA formation from vehicle exhaust gases have been done by introducing only one aromatic compound at time. However, in order to understand the SOA formation of the complex mixture of VOCs present, that is not sufficient and studies on the gasoline exhaust are needed. The aim of this study was to improve the knowledge on the contribution of gasoline engine exhaust on the SOA formation.

METHODS

The chamber studies were done at the Lund University Ergonomics and Aerosol Technology laboratory in February-April 2010 and November-December 2010. (Nordin et al., 2010) The chamber used in the measurements was a 6 m³ Teflon (FEP) chamber that was housed inside an insulated 22 m² stainless steel chamber. During an experiment either gasoline exhaust or a mixture of pure toluene and m-xylene was added to the chamber and exposed to UV-radiation. In the gasoline exhaust experiments the exhaust of an idling Volvo V40 (1998) was diluted (1:10) and injected to the chamber with a flow rate of 50 lmin⁻¹ using a heated (140°C) stainless steel inlet. In experiments where pure toluene and m-xylene were used, liquid standards were added to a glass bulb and evaporated to the chamber. Ammonium sulphate was used as seed particles in all experiments. In some gasoline experiments also additional NO was used. The time evolution composition of the gas and particle phase was measured with several instruments (figure 1).

The aerosol mass yield, that is the ratio between formed SOA and reacted aromatic hydrocarbons, and the chemical composition of the formed aerosol are important parameters for understanding the mechanisms of SOA formation. The aerosol mass yield can be estimated using equation

$$Y = \frac{C_{SOA}}{C_{VOC}}$$

where C_{SOA} is the concentration of the formed SOA and C_{VOC} the concentration of the reacted VOCs. In the gasoline exhaust experiments the aerosol C_{VOC} was calculated for five different aromatic VOC compound: benzene, toluene, xylenes and C9- and C10-aromatics.

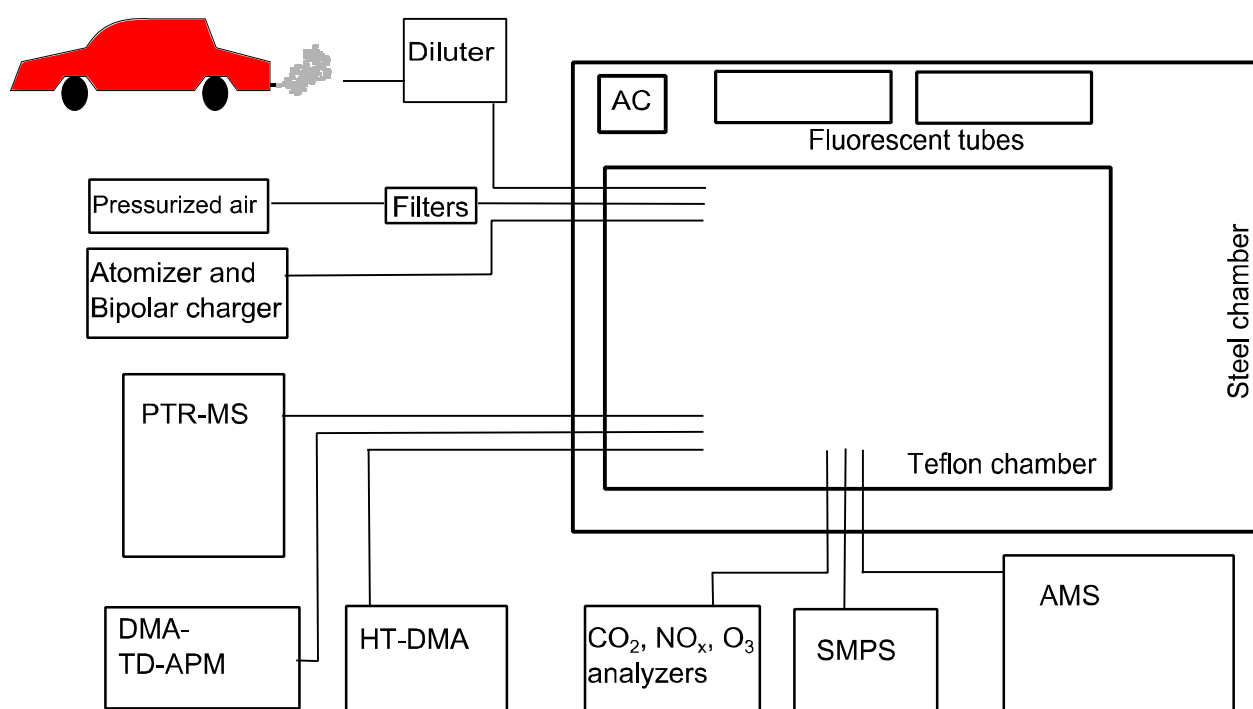


Figure1. A schematic picture of the measurement setup.

RESULTS

Preliminary results indicated that the measured aerosol mass yield of the gasoline exhaust was in the same range as the yields of the pure toluene + m-xylene experiments. Also previously reported (Odum et al. 1997) mass yields for pure light aromatic precursors were in the same range. This suggests that the C₆-C₁₀-aromatics are the major contributors of the SOA formation of the gasoline exhaust. Preliminary results will be presented in the FCoE meeting.

ACKNOWLEDGEMENTS

The financial support by the Academy of Finland Centre of Excellence program (project no 1118615) is gratefully acknowledged.

REFERENCES

- Hallquist, M., Wenger, J. C., Baltensperger, U., Rudich, Y., Simpson, D., Claeys, M., Dommen, J., Donahue, N. M., George, C., Goldstein, A. H., Hamilton, J. F., Herrmann, H., Hoffmann, T., Iinuma, Y., Jang, M., Jenkin, M. E., Jimenez, J. L., Kiendler-Scharr, A., Maenhaut, W., McFiggans, G., Mentel, Th. F., Monod, A., Prevot, A. S. H., Seinfeld, J. H., Surratt, J. D., Szmigielski, R., (Wildt, J. (2009). *The formation, properties and impact of secondary organic aerosol: current and emerging issues*. Atmos. Chem. Phys. Discuss., 9, 3555-3762.
- Hildebrandt, L., Donahue, N. M., Pandis, S. N. (2009) *High formation of secondary organic aerosol from the photo-oxidation of toluene*. Atmos. Chem. Phys., 9, 2973-2986.
- Ng N. L., Kroll J. H., Chan A.W. H., Chhabra P. S., Flagan R. C. and Seinfeld J.H (2007) *Secondary organic aerosol formation from m-xylene, toluene, and benzene*, Atmos. Chem. Phys., 7, 3909–3922.
- Nordin E. Z., Nilsson P., Eriksson A., Kajos M. K., Rissler J., Svenningsson B., Swietlicki E., Bohgard M., Kulmala M. and Pagels J. (2010) *Chamber studies of secondary aerosol formation from light duty vehicle exhaust*, conference proceedings, IAC 2010.
- Odum J. R., Jungkamp T. P. W., Griffin R. J., Forstner H. J. L, Flagan R. C, and Seinfeld J. H (1997) *Aromatics, Reformulated Gasoline, and Atmospheric Organic Aerosol Formation*, Environ. Sci. Technol., 31, 1890-1897.

Cloud Droplet Activation of Salt and Dust with Secondary Organic Matter: Differences between Light and Dark Chemistry

Keskinen Helmi¹, Jaatinen Antti¹, Joutsensaari Jorma¹, Romakkaniemi Sami¹, Miettinen Pasi¹, Aki-Matti Kortelainen¹, Liging Hao¹, Smith James N.^{1,2} and Laaksonen Ari^{1,3}

¹Dept. of Applied Physics, University of Eastern Finland, P.O. Box 1627, 70211 Kuopio, Finland.

²National Centre for Atmospheric Research, 80307, Boulder, CO USA.

³Finnish Meteorological Institute, 00101, Helsinki, Finland.

Keywords: Cloud droplet activation, ammonium sulphate, desert dust, α -pinene

INTRODUCTION

Atmospheric particulate matter contains salt, dust and organic matter from natural sources such as oceans, dust-storms and forests. Understanding the influence of these components on aerosol-cloud interactions is vital for predicting their impacts on present and future climate (IPCC, 2007). This has recently activated several predictive laboratory measurements of particulate matter (Roberts and Nenes, 2005), e.g., cloud droplet activation by desert dust (Kumar et al., 2010) and salts with secondary organic matter (Smith et al., 2009).

Atmospheric salts such as ammonium sulphate (AS) is known to be very hygroscopic and act efficiently as cloud condensation nuclei (CCN). Inorganic mineral and dust particles are not as hygroscopic but they still have ability act as CCN (Herich et al., 2009, Kumar et al., 2009). A recent study by Kumar et al. 2010 focused on the CCN activity of fresh dust particles from multiple sources (e.g. Arizona and Sahara). Their major implication was that freshly-emitted dust and mineral aerosols could act as CCN through the effects of water adsorption alone. Actually, they showed that 100 nm dust particles can exhibit comparable hygroscopicity to that of organic species or a particle with AS volume fraction of 10%. Salt and dust atmospheric particles contain very often organics (Halquist et al., 2009). The secondary organic matter (SOM) itself, e.g., formed by α -pinene oxidation as is typical in pine tree forests, is also known to be quite hygroscopic (Saathof et al., 2003). Actually, this organic matter can heterogeneously coat atmospheric salt and dust particles and thus affect on their hygroscopic properties and cloud droplet activation. Recently, Smith et al 2011 studied the SOM coating affect on deliquescence and efflorescence of AS nanoparticles and found that it was only minuscule. On the other hand, the hygroscopicity of nanoscale soot agglomerates clearly increases with SOM coating up to the level of pure SOM (Saathof et al., 2003).

The aim of this study is to measure the affect of partitioning of secondary organic matter on the cloud droplet activity of salt and dust particles, with and without UV-radiation. The measurements were done in the Kuopio aerosol chamber. The AS and Arizona test dust (ATD) particles were coated by secondary organic matter produced by α -pinene ozonolysis. The cloud droplet activation measurements were made with a CCN counter.

METHODS

We used the Kuopio aerosol research chamber (Hao et al., 2011) to process the AS and ATD nanoparticles with secondary organic matter formed from α -pinene ozonolysis (Figure 1). The nanoparticles were generated from a salt solution or suspension using an atomizer (Model 3076, TSI Inc., USA). The AS (Sigma Aldrich, 99.999%) /water (de-ionized) solution concentration was set to 1 wt %. Solid content in the water suspension of ATD (0 - 3 μ m, PTI, USA) was set to 0.1 wt %. The produced aerosol was fed to a diffusion drier (porous tube surrounded by silica gel) resulting relative humidity (RH) below 5 % (RH sensor, Rotronic).

The morphology of the ATD particles in the aqueous solution was studied by Transmission Electron Microscopy (TEM) (JEOL/ JEM 1200-EX). The TEM samples were collected on perforated carbon-copper grids (300 Mesh Cu, Agar, England) by depositing drops of a diluted suspension (0.005 wt%) directly on the grid for primary particle size image analysis and chemical composition analysis by energy dispersive spectroscopy (EDS).

Before each experiment the 6 m³ chamber was flushed and filled with pure filtered dry air. Secondly, the AS or ATD particles were introduced to the chamber and diluted achieving the desired concentration ($\sim 10^4$ /cm³). Following this, during some of the experiments fluorescent UV-lights were turned on. In next step the 2 μ l of α -pinene was injected to the chamber and, after 15 minutes of mixing, ozone was introduced to initiate oxidation. Ozone was generated by a UV lamp O₃ generator. Ozone enriched air (1.5 ppm) was introduced into the chamber (at 30 L/min) to achieve ozone concentration of 5 ppb. After that there was no flow into the chamber and chamber volume was slowly decreased by only the flow required by instruments (10.4 lpm). In all experiments, temperature was in the range of 25 \pm 2°C and RH in 5 \pm 2%, respectively.

During the experiment the particle size and concentration was monitored by scanning mobility particle sizer (SMPS) and condensation particle counter (CPC). Size-resolved CCN activity is carried out by using a differential mobility analyzer (DMA) parallel to the CCN counter. DMA was operated by stepping the voltage so that the dry particle diameters varied from 30 to 200 nm.

RESULTS AND DISSCUSSION

Figure 1 presents the morphology of the ATD nanoparticles. The ATD-nanoparticles shape varied from spheres to the clearly geometrical edged crystal shapes. This diverse morphology leads to the question of what shape factor we should use for these dust particles. The particle size measured by Image J from TEM-photos (Figure 1) was varying from 50 nm to 1 μ m. Si, Al, Fe, Mg, Ca, Cr, Mn and Au were detected from the particles by elemental mapping. This corresponded quite well with the composition provided by the manufacturer: SiO₂, Al₂O₃, Fe₂O₃, Na₂O, CaO, MgO, TiO₂ and K₂O. However, in addition Cr, Mn and Au were clearly detected from several samples.

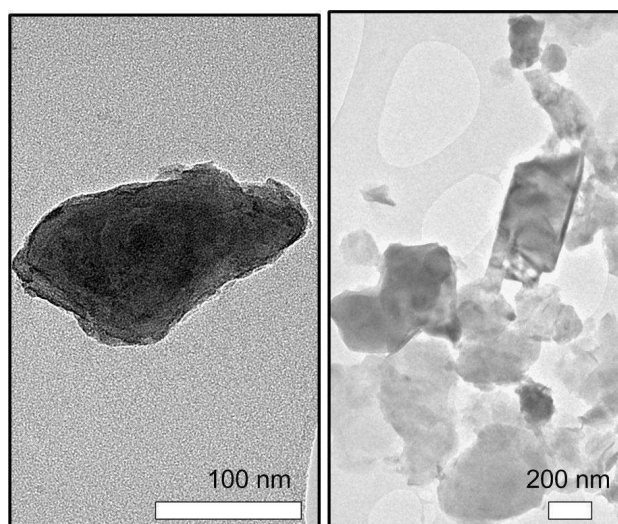


Figure 1. TEM micrographs from the ATD-nanoparticles, size, shape and composition of the dust particles is manifold. By Elemental mapping Si, Al, Fe, Ti, Mg, Ca, K, Cr, Mn and Au were detected.

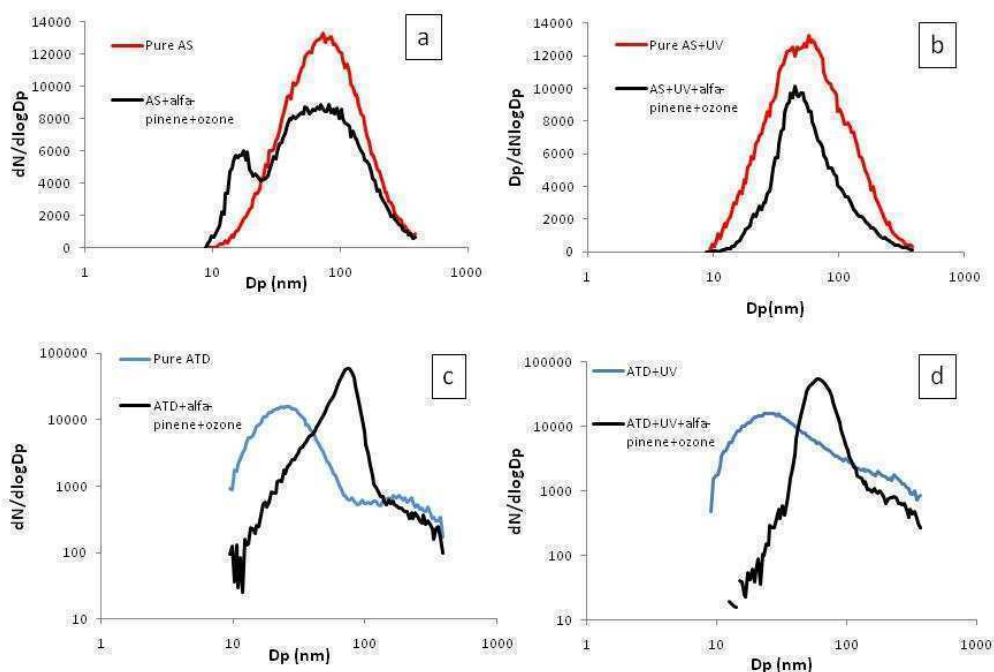


Figure 2. Size distributions from pure AS and SOM-coated AS without (a) and with UV (b) radiation, and pure ATD and SOM coated ATD without (c) and with UV (d).

The measured size distributions before and after SOM coating with and without UV-irradiation are presented in Figure 2. After SOM coating of AS (Figure 2a) the small mode was observed. Thus, most probably new particles were also formed in addition to condensation onto existing AS seed particles. The concentration drop from uncoated to coated can be explained by the dilution and wall losses over time. With the UV-light no new particle formation was observed (Figure 2b). However for the AS the SOM coating procedure was quite successful with and without UV-light. For the ATD clearly bimodal distributions were observed (Figure 2 c and d). The first mode with the mode diameter of 30 nm is most probably formed from water soluble fraction of the dust (including organics and salts) as we did not detect these particles with TEM (Figure 1). A similar bimodal distribution was observed by Gustavson et al. (2005). With SOM coating the particle number clearly increased and thus new SOM particles were formed. At the larger sizes, however, it appears that these primary particles have been coated by secondary organic matter.

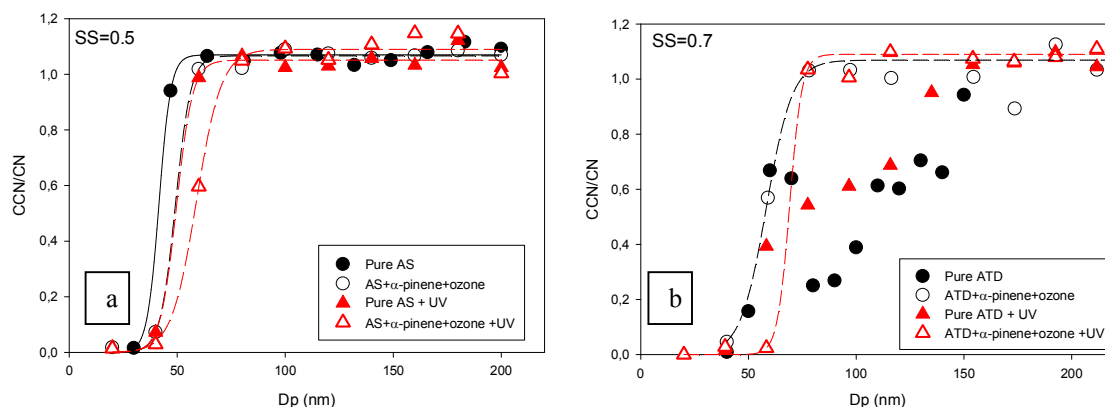


Figure 3 Measured activation curves for AS (filled symbols) and SOM coated AS (open symbols) without (spheres) and without UV (triangles) at 0.5% supersaturation (SS) (a) and for ATD (filled) and SOM

coated ATD (open) without (spheres) and without UV (triangles) at 0.7% SS. Lines are presenting the sigmoidal fit for each activation curve.

Figure 3 a shows the activation curves for pure and organic-coated AS with and without UV-light at 0.5% supersaturation (SS). The curves have a typical sigmoidal shape. The organic coating changed the AS dry activation diameter from 42 to 50 nm in dark and from 50 to 59 nm with UV-light, respectively. In fact, this small shift in activation diameter is expected and agreed well with other studies (e.g., King et al., 2007). The ~10 nm increase in activation diameter for organic-coated particles with UV-light is most probably caused by accelerated production of semivolatile compounds by UV radiation. For uncoated ATD we did not observed sigmoidal activation curves (Figure 3b, filled symbols). This is expected as they have strong variability in size dependent composition including soluble salts and organics and insoluble minerals from the natural ATD. However, the organic-coated particles had clear sigmoidal shaped activation curves. Again the UV-light shifted the dry activation diameter for coated particles from 57 to 69 nm at 0.7% SS.

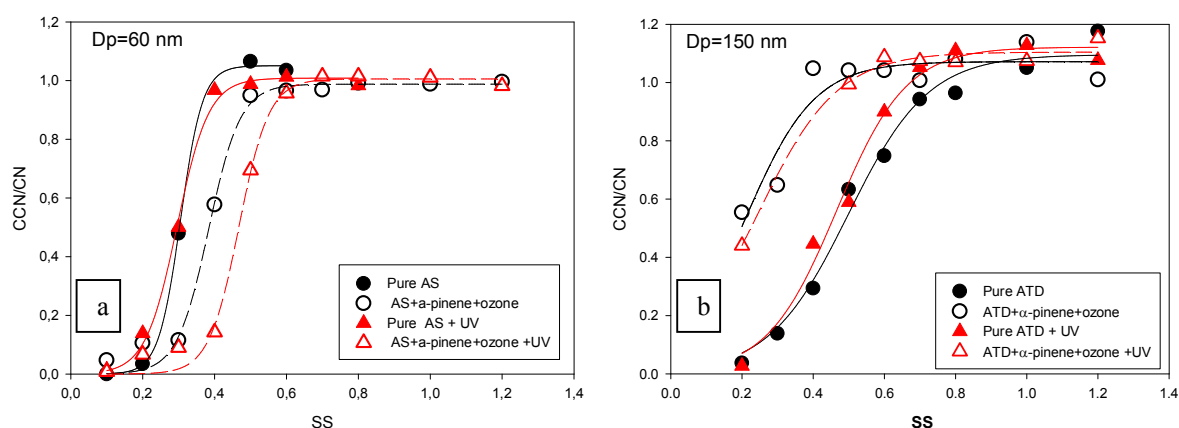


Figure 4 Measured activation curves for AS at $D_p = 60$ nm (a) and ATD at $D_p = 150$ nm (b) with and without organic coating and UV light. Lines are presenting the sigmoidal fit for each activation curve.

In Figure 4 a is presented the measured activation curves for the selected size $D_p = 60$ nm for AS with and without organic coating and UV light. The diameter is selected close to the particle maximum concentration (Figure 2a and b). The critical supersaturation (S_c) for pure AS in dark and with UV-light is now 0.3%. SOM coating increased the S_c to 0.39% in the dark and to 0.47% in UV light. For the dust particles the diameter of 150 nm was selected for the activation curve (Figure 4 b) to represent the real pure and coated dust particles and not the soluble fraction or newly-formed new SOM particles (Figure 1 and 2 c and d). The SOM coating clearly decreased the S_c both in dark and in UV-light at least by factor 2. In fact, the $S_c \sim 0.2$ at 150 nm for SOM coated dust is quite small and getting closer to the value observed for the pure SOM from α -pinene ozonolysis ($S_c = 0.15$, King et al., 2007). UV-light did not have clear effect to the activation for pure or coated dust.

CONCLUSIONS

These preliminary experiments showed that for AS the organic coating from the ozonolysis products of α -pinene depressed cloud condensation activation. On the other hand, for the ATD particles the activity was enhanced by organic coating. UV-light inhibited the activation with increased organic coating for AS nanoparticles. These experiments will be further developed by supporting size-selective measurements of hygroscopicity, volatility and chemical composition from the experimental conditions presented here.

ACKNOWLEDGEMENTS

This work was supported by the academy of Finland (Centre of Excellence, No 1118615 and decision numbers 123466, 118230, 138951), Kone foundation and Saastamoinen foundation. We gratefully thank Dr. Tiina Torvela for microscopic analysis. The National Center for Atmospheric Research is sponsored by the U. S. National Science Foundation

REFERENCES

- Hallquist, M., Wenger, J. C., Baltensperger, U., Rudich, Y., Simpson, D., Claeys, M., Dommen, J., Donahue, N. M., George, C., Goldstein, A. H., Hamilton, J. F., Herrmann, H., Hoffmann, T., Iinuma, Y., Jang, M., Jenkin, M., Jimenez, J. L., Kiendler-Scharr, A., Maenhaut, W., McFiggans, G., Mentel, Th. F., Monod, A., Prévôt, A. S. H., Seinfeld, J. H., Surratt, J. D., Szmigielski, R., and Wildt, J. (2009) The formation, properties and impact of secondary organic aerosol: current and emerging issues *Atmos. Chem. Phys.*, 9, 5155-5236.
- Hao, L. Q., Romakkaniemi, S., Yli-Pirilä, P., Joutsensaari, J., Kortelainen, A., Kroll, J. H., Miettinen, P., Vaattovaara, P., Tiitta, P., Jaatinen, A., Kajos, M. K., Holopainen, J. K., Heijari, J., Rinne, J., Kulmala, M., Worsnop, D. R., Smith, J. N., and Laaksonen, A. (2011) Mass yields of secondary organic aerosols from the oxidation of α -pinene and real plant emissions *Atmos. Chem. Phys.*, 11, 1367-1378.
- Herich, H., Tritscher, T., Wiacek, A., Gysel, M., Weingartner, E., Lohmann, U., Baltensperger, U., and Cziczo, D. J. (2009). Water uptake of clay and desert dust aerosol particles at sub- and supersaturated water vapor conditions, *Phys. Chem. Chem. Phys.*, 11, 7804–7809, doi:10.1039/b901585j.
- International Panel on Climate Change (IPCC) (2007). *Climate change 2007: the physical science basis. Contribution of working group I to the fourth assessment report of the Intergovernmental Panel on Climate Change*, Cambridge University Press, United Kingdom.
- King, S. M., Rosenoern, T., Shilling, J. E., Chen, Q., and Martin, S. T. (2007). Cloud Condensation Nucleus Activity of Secondary Organic Aerosol Particles Mixed with Sulfate. *Geophys. Res. Lett.* 34:L24806.
- Kumar, P., Nenes, A., and Sokolik, I. N. (2009). Importance of adsorption for CCN activity and hygroscopic properties of mineral dust aerosol *Geophys. Res. Lett.*, 36, L24804, (2009).
- Kumar P., I. N. Sokolik, and A. Nenes. (2010) Measurements of cloud condensation nuclei activity and droplet activation kinetics of fresh unprocessed regional dust samples and minerals, *Atmos. Chem. Phys. Discuss.*, 10, 31039–31081.
- Smith, M. L., Kuwata, M. and Martin, S. T. (2011) 'Secondary Organic Material Produced by the Dark Ozonolysis of α -Pinene Minimally Affects the Deliquescence and Efflorescence of Ammonium Sulfate', *Aerosol Science and Technology*, 45: 2, 244 - 261 (2010).
- Roberts, G. and Nenes, A. (2005). A continuous-flow streamwise thermal gradient CCN chamber for atmospheric measurements, *Aerosol Sci. Tech.*, 39, 206–221, (2005).
- Saathoff, H., Naumann, K. H., Schnaiter, M., Schock, W., Mohler, O., Schurath, U., Weingartner, E., Gysel, M., and Baltensperger, U. (2003). Coating of Sooth and (NH₄)₂SO₄ Particles by Ozonolysis Products of Alpha-Pinene. *J. Aerosol Sci.* 34:1297–1321.

SEMI-QUANTITATIVE AMBIENT AIR MEASUREMENTS OF AMINES IN HYYTIÄLÄ

A.-J. KIELOAHO^{1,2}, H. HÉLLEN², H. HAKOLA² and M. PIHLATIE¹

¹Division of Atmospheric Science, Department of Physics, University of Helsinki,
P.O. Box 48, FI-00014 Helsinki, Finland.

²Finnish Meteorological Institute, P.O. Box 503, FI-00101 Helsinki.

Keywords: ALIPHATIC AMINES, BOREAL FOREST, GAS PHASE.

INTRODUCTION

Although N cycling between the biosphere and the atmosphere has been intensively studied during the last decades, the missing key links in the research have been measuring flows of species that are difficult to quantify and identify. These N species include gaseous and particulate forms of nitrogen, like amines (Ge et al., 2011). The reactive N species like NH₃, HNO₃ and amines have been suggested to affect formation and growth of atmospheric aerosols (Kurtén et al., 2008; Ortega et al., 2008; Silva et al., 2008). Sample collection and analytical methods are based on methods introduced by Rampfl et al. (2008).

METHODS

Samples were collected from a Scots pine forest at SMEAR II station at Hyytiälä (61°15'N, 24°17'E) in southern Finland. Duration of a sample collection was 42 hours in weekdays and 72 hours during weekends throughout the measurement period from 2010 June to end of August. Measurement height was 1.5 m above the ground and a filter holder was shielded from rain and direct sunlight. Samples were collected with a flow of 16 L min⁻¹ through a PTFE membrane filter to a stack of phosphoric acid impregnated filters. The amines were trapped in the filters as salts, aminium ions. PTFE membrane filter was used to remove particles before the impregnated filters.

The aminium ions were extracted from the filters and the extract was analysed by high performance liquid chromatography electro spray ionisation ion trap mass spectrometer (HPLC-ESI/MS). In the LC system two columns were used at 40 °C, as analytical column Discovery® HS F5 HPLC and as pre-column HPLC SecurityGuard™ Cartridge. During the 30 minutes analysis constant flow (400 µL min⁻¹) of solvents, water (95%) and acetonitrile (5%) with 0.02% formic acid as a buffer, were used. Detection limit for the analytical method ranged from 0.6 ng m⁻³ to 6.8 ng m⁻³. Detection limits were lowest for DEA and TMA, 0.6 and 0.9 ng m⁻³, respectively. The highest detection limits were estimated for PA and EA, 6.8 and 3.9 ng m⁻³, respectively.

RESULTS AND DISCUSSION

Because of leakage in the sample collection holder the results are not quantitative and they are underestimations. From the seven measured aliphatic amines four compounds were over detection limit, TMA, EA, DMA, and DEA. Compound abundance during the measurement period is shown in figure 1. and amine species' air concentrations are shown in figure 2. Average air concentration for TMA, EA, DMA, and DEA are 9.7, 4.6, 3.2 and 2.6 ng m⁻³, respectively. The most abundant species were EA, TMA, and DEA which were constantly measured throughout the measurement period. DMA was abundant in the first half of the measurement period but was not detected after June.

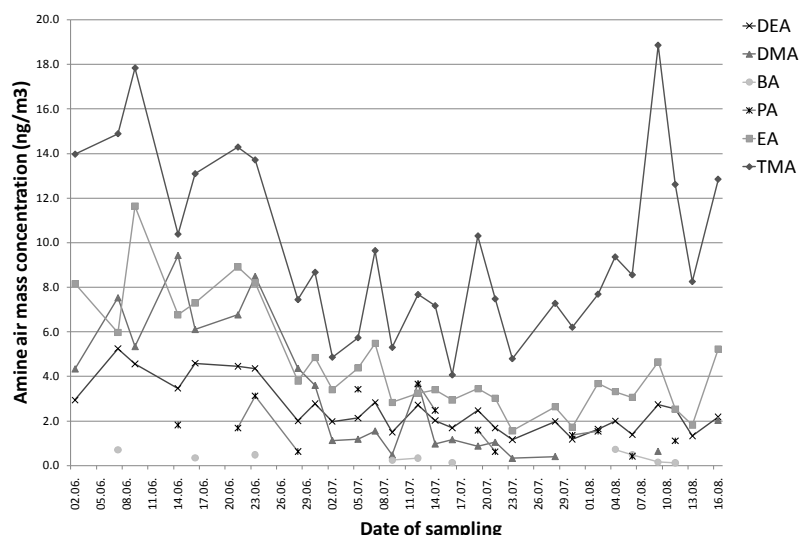


Figure 1. Air concentrations of measured amine compounds in ng m^{-3} . Results are underestimation due to leakage in a sample holder. Abbreviations refer to measured amine species. TMA : trimethylamine; TEA: triethylamine; EA: ethylamine; PA: propylamine; BA: butylamine; DMA: dimethylamine; DEA: diethylamine.

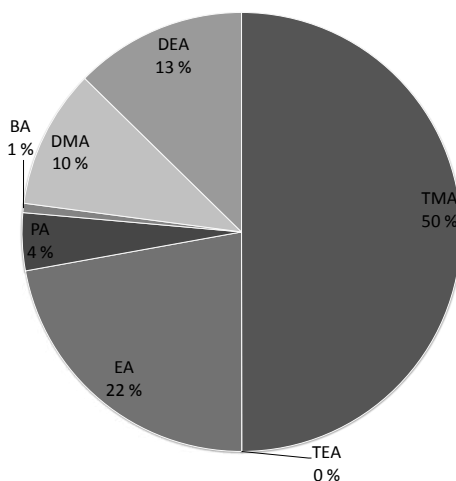


Figure 2. Amine species composition during the measurement period (2.6.-16.8. 2010). Abbreviations refer to measured amine species. TMA : trimethylamine; TEA: triethylamine; EA: ethylamine; PA: propylamine; BA: butylamine; DMA: dimethylamine; DEA: diethylamine.

REFERENCES

- Ge, X., A. S. Wexler and S. L. Clegg (2011). Atmospheric Amines - Part I. A Review. *Atmos. Env.* 45, 524-546.
- Kurtén, T., V. Loukonen, H. Vehkamäki and M. Kulmala (2008). Amines are likely to enhance neutral and ion-induced sulfuric acid-water nucleation in the atmosphere more effectively than ammonia. *Atmos. Chem. Phys.*, 8(14), 4095-4103.
- Ortega I. K., T. Kurtén, H. Vehkamäki, M. Kulmala (2008). The role of ammonia in sulfuric acid ion induced nucleation. *Atmos. Chem. Phys.*, 8(11), 2859-2867.
- Rampfl, M., S. Mair, F. Mayer, K. Sedlbauer, K. Breuer and R. Niessner (2008). Determination of primary, secondary, and tertiary amines in air by direct or diffusion sampling followed by

determination with liquid chromatography and tandem mass spectrometry. *Environ. Sci. Technol.*, 42, 5217-5222.

Silva. P. J., M. E. Erupe, D. Price, J. Elias, Q. G. J. Malloy, Q. Li, B. Warren and D. R. Cocker (2008). *Environ. Sci. Technol.*, 42, 4689-4696.

SPATIAL EXTENT OF NEW PARTICLE FORMATION EVENTS IN NORTHERN SCANDINAVIA

N. KIVEKÄS¹, E. ASMI¹, M. KOMPPULA¹, A-P. HYVÄRINEN¹, Y. VIISANEN¹, P. AALTO², T. NIEMINEN², B. SVENNINGSSON³, A. ARNETH⁴ And H. LIHAVAINEN¹

¹Research and Development, Finnish Meteorological Institute, Helsinki, PO. Box 503, Finland

²Department of Physics, University of Helsinki, Helsinki, 00101, Finland

³Department of Nuclear Physics, Lund University, Lund, 223 62, Sweden

⁴Department of Physical Geography and Ecosystems Analysis, Lund University, Lund, 223 62, Sweden

Keywords: PARTICLE FORMATION, PARTICLE GROWTH, AMBIENT AEROSOL, DMPS

INTRODUCTION

Atmospheric new particle formation (NPF) has been observed all around the world. Often the measurements have been carried out at a fixed location with instruments continuously measuring the air passing by. The growth of the newly formed particles can often be followed for several hours, even for several days after the particle production has ceased. This has led to an assumption that new particles are formed simultaneously over a large area, and as time passes by the particles observed later are those formed further and further from the station (Mäkelä *et al.*, 1997; Kulmala *et al.*, 1998). This allows us to study the spatial extent of NPF events by combining the observed event length with trajectory data.

METHODS

Continuous submicron aerosol size distribution data from three measurement stations in Northern Scandinavia were analysed. The stations Abisko (68° 21' N, 19° 03' E, 358m above sea level), Pallas (67° 58' N, 24° 07' E, 550 m asl.) and Värriö (67° 45' N, 29° 37' E, 370 m asl.) are located with approximately 200 km from each other on a west-east line. The analysed data period was years 2000-2010 from Pallas and Värriö, and 2005-2007 from Abisko with lower data coverage. The data was measured with DMPS (Pallas and Värriö) or SMPS (Abisko). All class 1a new particle formation events (dal Maso *et al.*, 2005) were taken into this study. At Abisko also 1b events were included to get better counting statistics. The number of analysed NPF events was 75, of which 11 were observed at Abisko, 34 at Pallas and 30 at Värriö. There were very few cases when a class 1a NPF event was observed at more than one measurement station, but often they were observed at two or three station during consecutive days.

The start and end times and the corresponding diameters of the observed growing nucleation modes were estimated from the data. The start time was the time when first particles of the later growing mode appeared in the measurements. The end time of the growing mode (later termed end time) was more difficult to define. Four criteria for the end time were used: 1) Particle number concentration in the mode decreases more than 50% within 3 hours while other modes remain stable, 2) The mean diameter of the mode starts to decrease, 3) The mode becomes unstable and 4) The mode gets mixed with other modes and can no longer be followed. The end time is reached at the first time point when any one of these criteria is met. In the beginning of the event most of the particles in the new mode have diameter below the smallest measurable size, and the observed start time is the time when the largest particles become measurable. To maintain coherency we defined the end diameter as the diameter of the largest particles in the mode at the end time (Figure 1). The start and end times of the growing mode allowed us to derive two important parameters: the average growth rate in each NPF event, and the duration of the mode, being the

time the particles have spent in atmosphere. The latter was corrected by extrapolating the mode from the measurement limit size (11 nm at Abisko, 7 nm at Pallas, 8 or 3 nm at Värriö) to 2 nm size to and adding the time needed for that growth to the observed mode duration.

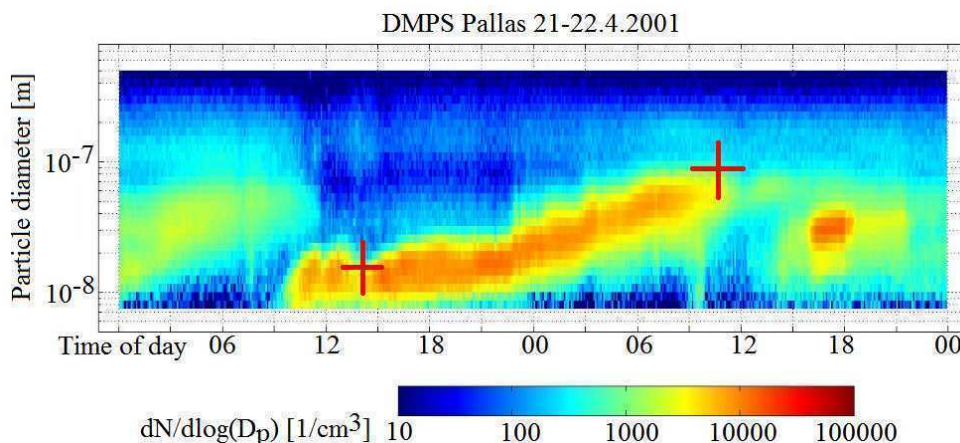


Figure 1. An example of a class 1a NPF event observed at Pallas. The red crosses show the start and end times and diameters of the growing mode.

For each station eight FLEXTRA trajectories (Stohl *et al.*, 1995) for each day with 3-hour intervals were calculated for the whole measurement period, the end point being the station at 925 hPa pressure level. The time the air mass had spent over land after last coming sea or ocean was also calculated for each trajectory. For each NPF event the last trajectory reaching the station before the end time was used to estimate where the particles had come from. That trajectory was followed back for the time of the corrected mode duration, giving us the approximate location where the first particles were formed (NPF start location).

The method used here for estimating the NPF start location contains several sources of uncertainty. The FLEXTRA trajectories can differ 100km in 24 hours from the true air mass path even in good conditions (Stohl and Siebert, 1998). The estimate for the growing mode end time is can easily vary a couple of hours for most events. Also the NPF event is assumed to start over a large area at the same time, and the growth rate is also assumed to be constant over the whole area.

RESULTS

The growing mode durations varied from 11 h to 39 h (5 and 95 percentiles) with mean and median of 21 and 20 h, respectively. The class 1b NPF events not included in this analysis had typically a shorter time during which the growing mode could be followed. In most analysed class 1a NPF events the growing mode duration was less than the time the air mass had spent over land (Figure 2), even though there were cases where the particles seemed to be formed prior the air mass entering areas over land. In some of these cases the air mass had entered over land from the Baltic Sea, and had recently been over land also before that. Such air masses are typically not clean marine air.

The Abisko-, Pallas- and Värriö stations are located approximately 5° apart from each other in east-west direction, but the mean NPF start locations were separated by only 2° and the median NPF start locations did not differ in systematic way. The 75 NPF start locations were also plotted on map (Figure 3).

The starting time of the NPF event was found to be connected to the time of day and season. This was expected, since the NPF events have been observed to typically start when there is enough solar radiation available (Kulmala *et al.*, 2004). The end time of the growing mode varied through the day without any clear correlation to time of day or solar radiation.

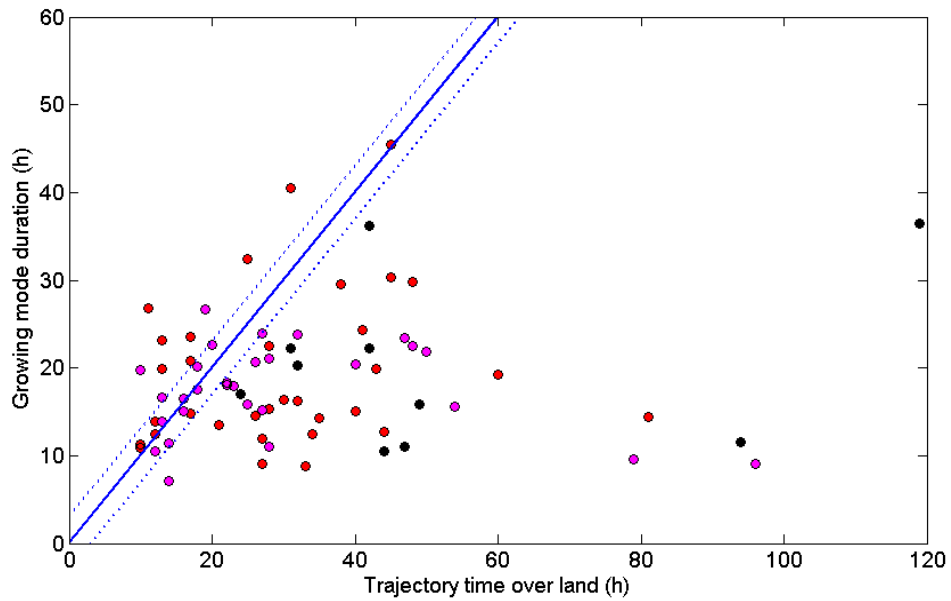


Figure 2. The corrected durations of the growing modes as a function of the time the air mass had spent over land. The black dots represent data from Abisko, red dots from Pallas and magenta dots from Värriö. The blue line is the time the trajectory passed coastal line and the dotted lines are ± 3 hours to that time.

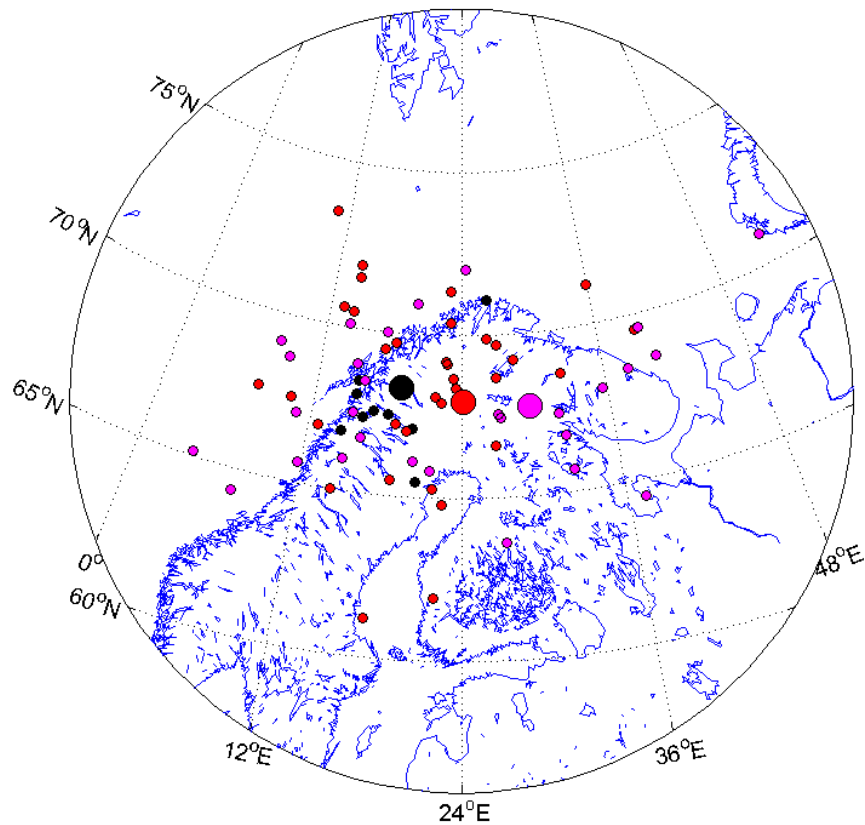


Figure 3. The NPF start locations. The small black dots represent data from Abisko, red dots from Pallas and magenta dots from Värriö. The large dots are the locations of the corresponding measurement stations.

CONCLUSIONS

The NPF start locations were typically not above ocean, which was seen in the comparison of growing mode duration and the time the trajectory had spent over land, as well as in the locations of the NPF start points. Also low correlation between the growing mode end times and time of day suggest that the growing mode end time is not determined by changes in solar radiation or boundary layer structure.

The ocean-continent boundary seems to be an important factor limiting the spatial extent of the new particle formation event. This is quite logical assuming that the air arriving from North Atlantic or Arctic Ocean contains only a few particles as well as very little condensable vapors. When the clean air arrives over land the vapor concentrations in the air start to increase. There is not enough pre-existing particle surface for the vapors to condense on, so new particles are formed.

A large fraction of the new particle formation events started clearly inland, also on the supposedly clean west-to-north-east sector. Including 1b events in the analysis would probably increase that fraction. This suggests that the ocean-continent boundary is not the only factor limiting the spatial extent of NPF events in the area. These events will be investigated more in the future. Also the NPF start times at the start location will be analysed in more depth. In addition to these the evolution of the NPF events will be analysed for those events passing over more than one measurement station.

ACKNOWLEDGEMENTS

This work was conducted as a part of the Finnish Centre of Excellence in Physics, Chemistry, Biology and Meteorology of Atmospheric Composition and Climate Change.

REFERENCES

- Dal Maso, M., Kulmala, I. Riipinen, R. Wagner, T. Hussein, P. Aalto, and K. Lehtinen (2005). Formation and growth of fresh atmospheric aerosols: eight years of aerosol size distribution data from SMEAR II, Hyytiälä, Finland, *Bor. Environ. Res.* 10, 323-336.
- M. Kulmala, H. Vehkamäki, T. Petäjä, M. Dal Maso, A. Lauri, V. -M. Kerminen, W. Birmili, P. H. McMurry (2004). Formation and growth rates of ultrafine atmospheric particles: a review of observations, *J. Aerosol. Sci.*, 35, 143-176.
- M. Kulmala, A. Toivonen, J.M. Mäkelä and A. laaksonen (1998). Analysis of the growth of nucleation mode particles in boreal forest, *Tellus* 50B, 449-462.
- J.M. Mäkelä, P. Aalto, V. Jokinen, T. Pohja, A. Nissinen, S. Palmroth, T. Markkanen, K. Seitsonen, H. Lihavainen and M. Kulmala (1997). Observations of ultrafine aerosol particle formation and growth in boreal forest. *Geophys. Res. Let.* 24: 1219-1222.
- A. Stohl and P. Seibert (1998): Accuracy of trajectories as determined from the conservation of meteorological tracers. *Q. J. Roy. Met. Soc.* 124, 1465-1484.
- A. Stohl, G. Wotawa, P. Seibert, and H. Kromp-Kolb (1995): Interpolation errors in wind fields as a function of spatial and temporal resolution and their impact on different types of kinematic trajectories. *J. Appl. Meteor.* 34, 2149-2165.

PRODUCTIVITY OF SCOTS PINE UNDER CHANGING CLIMATE IN SOUTHERN FINLAND AND AT NORTHERN TIMBERLINE

P. KOLARI, T. HÖLTTÄ, P. HARI and E. NIKINMAA

Department of Forest Sciences, P.O. Box 27, FI-00014 University of Helsinki, Finland

Keywords: climate change, photosynthesis, growth, Scots pine

INTRODUCTION

We estimated the potential increase in photosynthetic productivity in Scots pine (*Pinus sylvestris*) due to direct effects of increasing temperature and CO₂. Secondly, we studied how the direct changes in primary productivity and acceleration of soil nutrient cycling are reflected in the biomass production of pine. Thirdly, we estimated how drought will affect the fate of photosynthates in the accumulation of persistent biomass.

METHODS

Photosynthetic production of the trees was determined by integrating the instantaneous photosynthetic rate at leaf or shoot level over the whole stand. The integration was done with SPP (Stand Photosynthesis Program, Mäkelä et al. 2006) that combines a model of shoot photosynthetic production with the model of light interception in the canopy and soil water limitation to gas exchange. Shoot-scale photosynthetic production was calculated half-hourly using biochemical model of photosynthesis (Farquhar *et al.*, 1980) along with stomatal model of Leuning (1990). The seasonality of photosynthetic capacity and quantum yield were described as delayed temperature response (Mäkelä *et al.*, 2004). The model parameters were estimated from multiannual time series of pine shoot gas exchange in pine shoots in Hyytiälä, Southern Finland, and in Värriö, eastern Lapland. In the SPP simulations tree dimensions, leaf area index and tree density were typical for an established tree stand in a self-thinning phase well after canopy closure. The model was run with different climate change scenarios with increasing atmospheric CO₂ concentration and annual mean temperature. Modified weather data from Hyytiälä and Värriö was used as the model input. All half-hourly records of air temperature and atmospheric CO₂ were increased by the mean annual temperature rise and CO₂ increase, respectively. Water vapour concentration in the air was altered so as to keep relative humidity unchanged. Furthermore, the link between photosynthesis and growth during drought was studied with a growth model under development.

Stand development and biomass production was studied with MicroForest (Hari *et al.*, 2008) that incorporates soil nitrogen (N) cycling and changing allocation into foliage, wood and roots. The key parameters of the model are annual photosynthetic production in unshaded conditions, decomposition rate of proteins in the soil, and nitrogen deposition. The annual photosynthesis was obtained from simulations with increased CO₂ and temperature. In the climate change scenarios, annual maintenance respiration was assumed to change proportionally to photosynthesis. The rate of decomposition was increased by 6% per °C rise in temperature. Nitrogen deposition was assumed to remain at the present level in the future. No thinnings were performed in the simulations, only natural mortality was considered. The model was run with different climate change scenarios (Jylhä et al. 2009) that correspond to different future development in the emissions of CO₂ from fossil fuel combustion.

RESULTS

Simulations of photosynthesis and transpiration with SPP predict an increase in photosynthetic production and decline in instantaneous transpiration rates in Scots pine (Figure 1). Most of the temperature-induced increase in annual photosynthesis can be attributed to longer growing season. Increasing CO₂ enhances water-use efficiency as the stomata tend to open less at elevated CO₂ than in present CO₂. Due to the longer growing season in the future, however, the annual cumulative transpiration will remain approximately at the present level. Increasing stand foliage area, however, may offset the enhanced water-use efficiency. The free-air CO₂ enrichment studies have shown no significant change in the stomatal responses to CO₂. This means that drought will probably remain minor risk in Finnish conditions in the future.

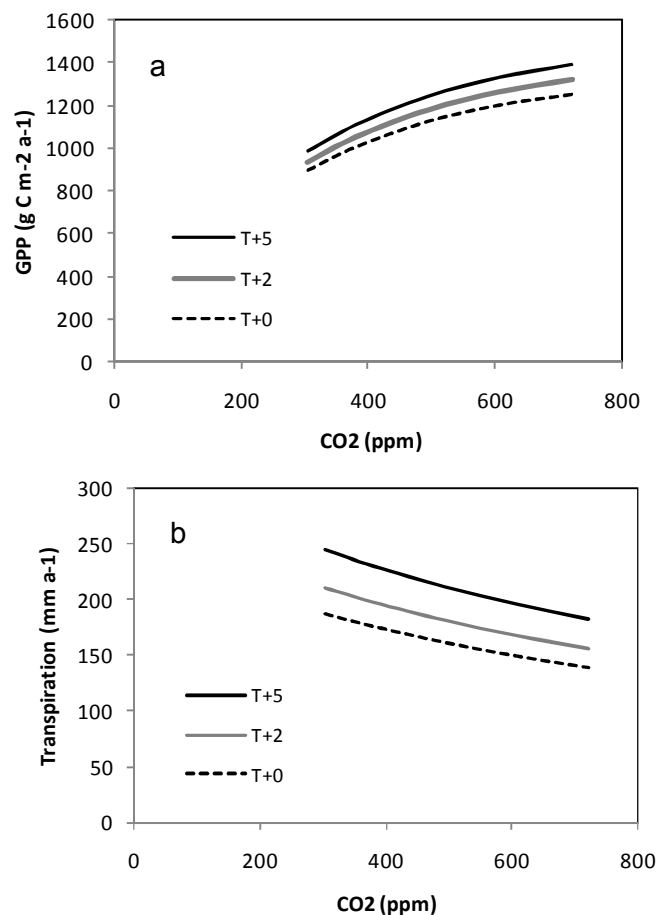


Figure 1. Variation in a) photosynthetic productivity and b) transpiration at different atmospheric CO₂ concentrations and average temperature rises in a typical middle-aged southern Finnish Scots pine stand. Stand foliage area remained constant in all simulations and there was no feedback from enhanced nutrient cycling in the soil.

MicroForest simulations with just increased photosynthetic productivity resulted in relatively smaller growth enhancement than increase in annual photosynthesis because soil nutrients were eventually depleted during stand development. However, enhanced nitrogen cycling and change in within-tree biomass allocation along with productivity changes allowed for increment of approximately 8% per °C

temperature rise in stemwood production in southern Finnish mature stand (Figure 2a). This largely resulted from lower allocation below ground. Average growth increment in closed-canopy stands with CO₂ scenario B1 and mean annual temperature rise of 2°C by the end of 21st century was 16% and 31% in southern Finland (Figure 2a) and in Lapland (Figure 2b), respectively. The extreme CO₂ scenario A2 and temperature rise of 5°C resulted in growth enhancement of 40% in southern Finland and 80% in the north.

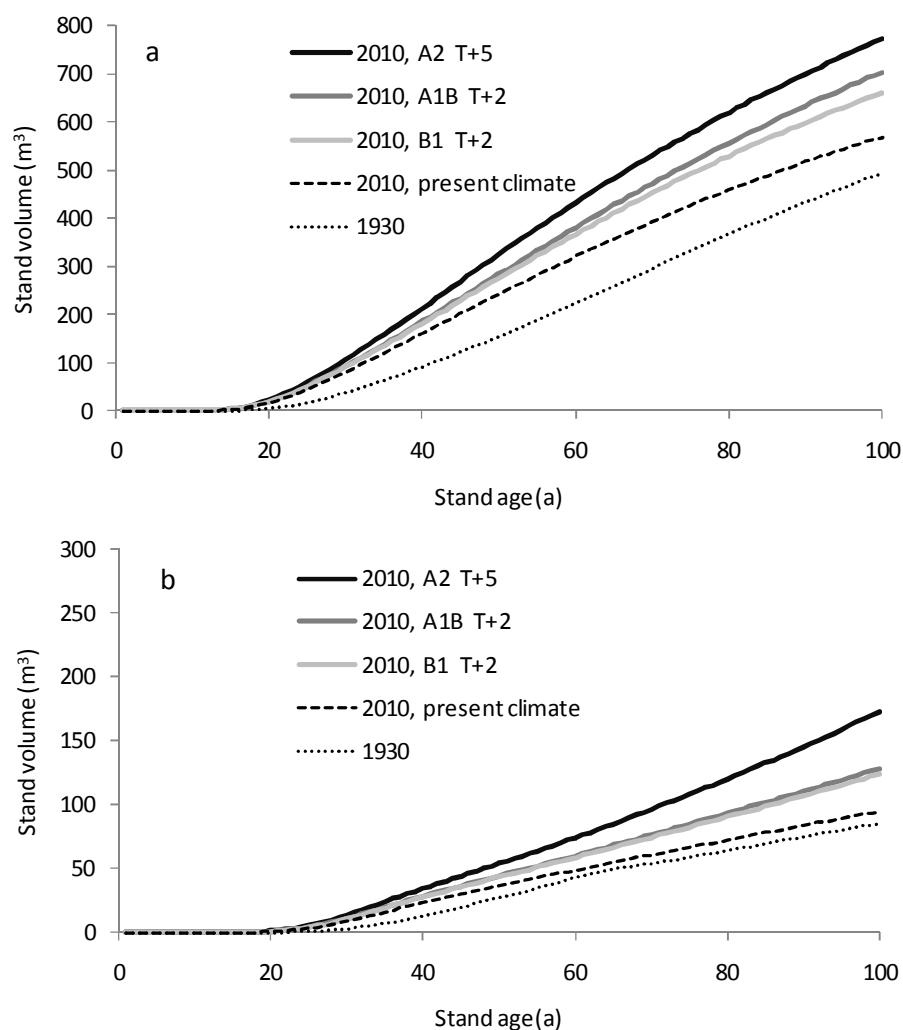


Figure 2. Projected development of stand volume in Scots pine stands in southern Finland (a) and in eastern Lapland (b). The simulated stands were established in 1930 (actual climate and nitrogen deposition history) and in 2010 with different CO₂ and temperature rise scenarios and assumption of nitrogen deposition remaining at present level of 0.5 g N m⁻² a⁻¹ in the south and 0.2 g N m⁻² a⁻¹ in the north.

Figure 3 shows how much earlier the growth starts to react to decrease in soil moisture compared to photosynthetic productivity. The growth influence of drought results from the growth process itself. Trees use water pressure to expand the newly differentiated cells to the size of mature cells that are then lignified in the cell wall formation process. The water pressure is created osmotically and trees use sugars for that. If they are under water stress more sugars are needed to just maintain the cell turgor not to mention the cell expansion. If drought is persistent, the achievable final cell size remains smaller. However, if the drought is reversed also growth may resume and rather rapid expansion may follow.

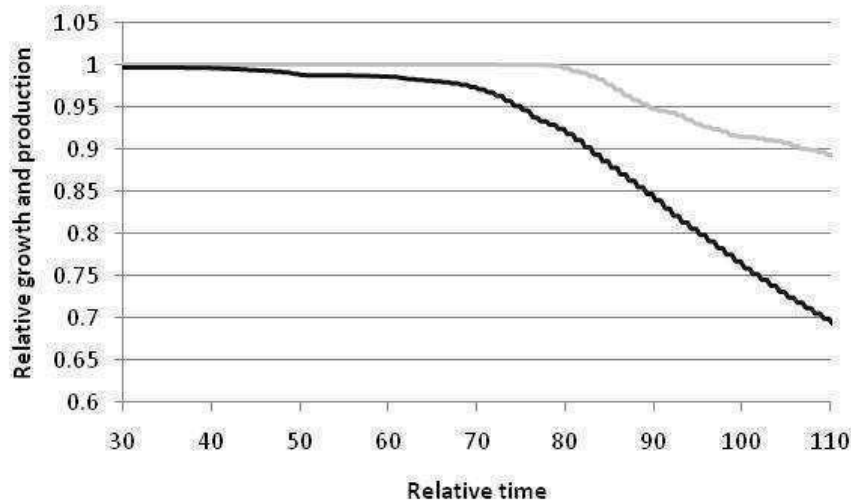


Figure 3. Relative decrease in modeled cumulative photosynthetic production (grey line) and modeled cumulative growth (black line) during 2006 drought year vs. no drought conditions. The time axis indicates days since 1 May.

ACKNOWLEDGEMENTS

This work was supported by the EU-funded project VACCIA (Vulnerability assessment of ecosystem services for climate change impacts and adaptation).

REFERENCES

- Farquhar, G.D., S. von Caemmerer and J.A. Berry (1980). A biochemical model of photosynthetic CO₂ assimilation in leaves of C₃ species. *Planta* **149**, 78.
- Hari, P., M. Salkinoja-Salonen, J. Liski, A. Simojoki, P. Kolari, J. Pumpanen, M. Kähkönen, T. Aakala, M. Havimo, R. Kivekäs and E. Nikinmaa (2008). Growth and development of forest ecosystems; The MicroForest Model. In: Hari, P. and L. Kulmala (eds.) *Boreal forest and climate change. Advances in Global Change Research, Vol. 34* (Springer Verlag), 433.
- Jylhä, K., K. Ruosteenoja, J. Räisänen, A. Venäläinen, H. Tuomenvirta, L. Ruokolainen, S. Saku and T. Seitola (2009). *Changing climate in Finland: estimates for adaptation studies*. Finnish Meteorological Institute, Reports 2009: 4.
- Leuning, R. (1990). Modelling stomatal behaviour and photosynthesis in *Eucalyptus grandis*. *Australian Journal of Plant Physiology* **17**, 159.
- Mäkelä, A., P. Hari, F. Berninger, H. Hänninen and E. Nikinmaa (2004). Acclimation of photosynthetic capacity in Scots pine to the annual cycle temperature. *Tree Physiology* **24**, 369.
- Mäkelä, A., P. Kolari, J. Karimäki, E. Nikinmaa, M. Perämäki and P. Hari (2006). Modelling five years of weather-driven variation of GPP in a boreal forest. *Agricultural and Forest Meteorology* **139**, 382.

ESTIMATING WET NITROGEN DEPOSITION FROM BULK DEPOSITION MEASUREMENTS

J.F.J. KORHONEN^{1,2}, JUKKA PUMPANEN² and MARI PIHLATIE^{3,1}

¹Division of Atmospheric Sciences, Department of Physics, University of Helsinki
P.O.Box 48, FI-00014, University of Helsinki, Finland

²Department of Forest Sciences, P.O. Box 27, FI-00014, University of Helsinki

³IMK-IFU, KIT, Kreuzteckbahnstr. 19, D-82467, Garmisch-Partenkirchen, Germany

Keywords: NITROGEN, DRY DEPOSITION, METHODOLOGY.

INTRODUCTION

Atmospheric deposition of nitrogen (N) has been studied intensively during the last decades. The deposition of reactive nitrogen (N_r) is linked with many environmental problems, such as eutrophication, loss of biodiversity, acidification of terrestrial and aquatic ecosystems, and health through air quality (NO_x) and quality of drinking water (NO_3^- ; Sutton et al., 2011).

Atmospheric deposition consists of two independent processes: wet and dry deposition. In case of N deposition, the wet and dry deposition are within the same order of magnitude. The implication of this is that to assess the total N deposition, reliable estimates of both are needed. However, measurement of wet, dry or total deposition is challenging. Wet deposition is usually measured from rain water collectors by multiplying the concentration of the substance in the water by the total amount of precipitation. Unfortunately these collectors also collect dry deposition, and thus the measured quantity is often called "bulk deposition". A use of constant factors for estimating the wet-only deposition from the bulk deposition have been suggested. Unfortunately, these methods can only give rough estimates. Some instrumental development has been made to measure wet-only deposition (e.g. Benitez et al. 2010), however, neither these methods are problem-free. Furthermore, these new methods do not give tools to estimate wet-only deposition from the existing measurements of deposition, such as data from the EMEP-network.

METHODS

We measured bulk deposition above the canopy of a young Scots pine (*Pinus sylvestris*) forest at SMEAR II station in Hyytiälä, Finland (61° 51' N, 24° 17' E). For estimating the wet-only and dry deposition, we used a time series of three years (2006-2008). Water collectors were emptied monthly in winter and fortnightly in summer. In case of heavy rain events, the collectors were emptied more often. Ammonium (NH_4^+), nitrate (NO_3^-) and total nitrogen concentrations (N_{tot}) were measured from the water samples at the Finnish Forest Research Institute, Vantaa Unit. Organic N (N_{org}) was determined using total nitrogen concentrations concentration in samples as follows

$$[N_{org}] = [N_{tot}] - [NH_4^+] - [NO_3^-], \quad (1)$$

where the N_{org} consist of dissolved organic nitrogen (DON) and particulate nitrogen.

Bulk N deposition rates were calculated as follows

$$F = c \, m \, A^{-1} \, t^{-1}, \quad (2)$$

where F is the nutrient flux to the precipitation collector ($\text{g m}^{-2} \text{d}^{-1}$), c is concentration of a compound in water sample (g m^{-3}), m is the mass of the water sample (g), A is the area of the collector (m^2) and t is the length of the collection period (days).

A simple model to fraction the bulk deposition into wet and dry deposition was developed as follows,

$$m = c_w P + D\Delta t, \quad (3)$$

where m is the mass of the compound in the collector (g), c_w is concentration of the nutrient (NH_4^+ , NO_3^- , N_{org}) in precipitation (g m^{-3}), P is total water mass in the collector, D is deposition constant and Δt is the length of the collection period. The model assumes that c_w and D are constant, and Δt is the length of the collection period. Total water mass in collector (P), m and Δt are measured, and c_w and D are unknown parameters. We fitted the model to the three year data set for concentrations of N_{org} , NH_4^+ and NO_3^- .

RESULTS AND DISCUSSION

The model predicts the pattern of the deposition to the sampler moderately well (Fig 1). As a result of the fit, the magnitude of the prediction was close to the measured one, as expected. However, there were clear events, when the model showed much smaller deposition than the measurements. These underestimations may be related to situations when dry deposition was accumulating for a longer period than that Δt was. The collector funnels were not cleaned during the sampling, and therefore dry deposition can accumulate for a longer time than what is modelled.

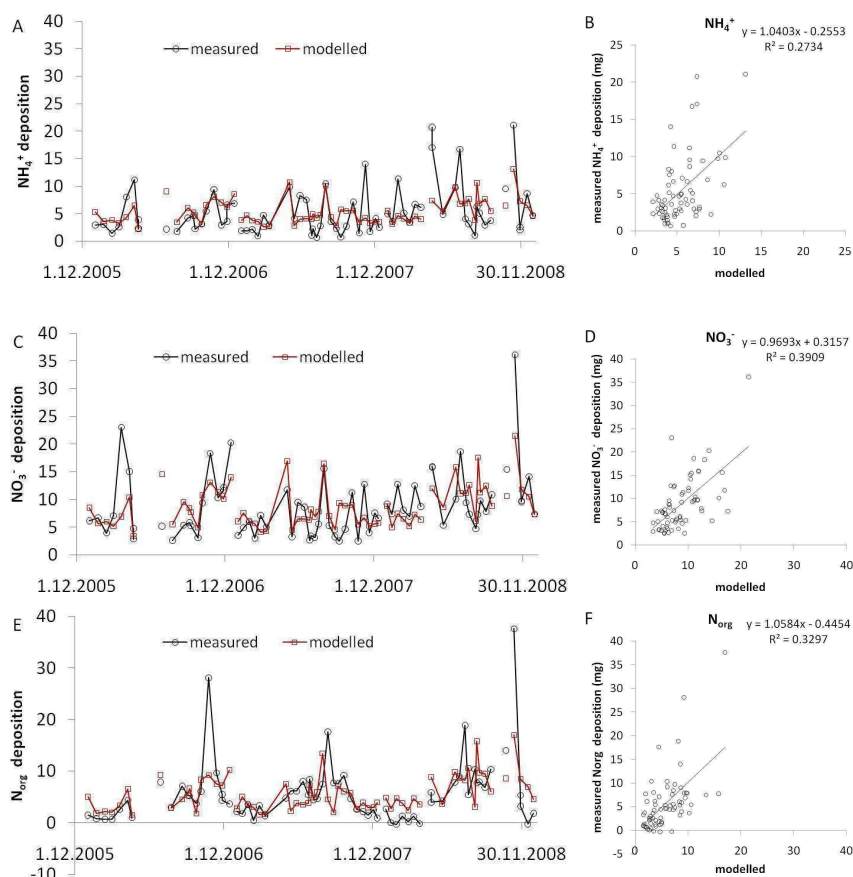


Figure 1. The predicted and measured bulk deposition of NH_4^+ , NO_3^- and N_{org} . The explaining variables are time and precipitation amount. Dry deposition constant and N content in precipitation are fitted to the model.

The model predicts that when precipitation intensity is very high, the concentration of nutrients in the water collector is dominated by the concentration in the precipitation. On the other hand, when precipitation intensity is very low, the model predicts that the water nutrient concentration is very high. The relationship between precipitation intensity and sampled water N concentrations are presented in Figure 2. For NO_3^- and NH_4^+ , precipitation intensity explains well the concentration in the sampler, suggesting that N is originating from both dry and wet deposition.

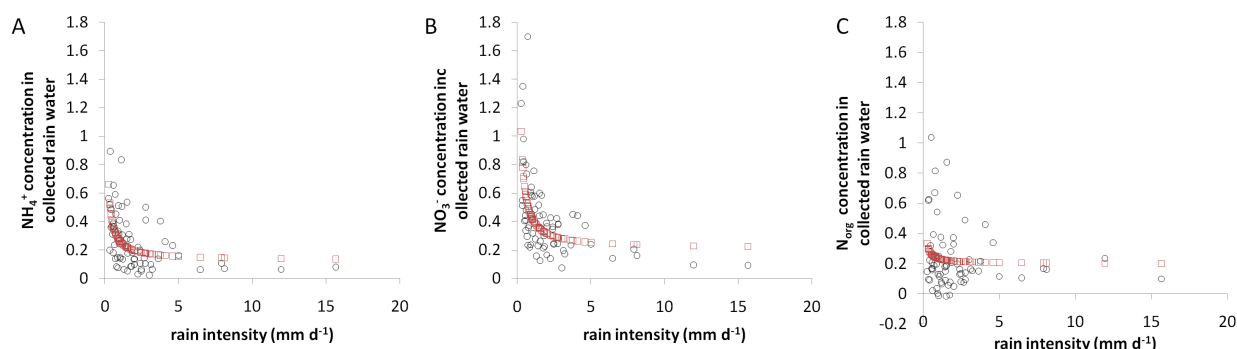


Figure 2. The relation with rain intensity to collected rainwater NH_4^+ , NO_3^- and N_{org} concentration. Red squares are modelled and black circles are measured concentrations.

Based on the model separation of wet only and dry deposition, the bulk deposition is 24.1% higher than wet deposition (Table 1). Therefore, using bulk deposition as a measure of wet deposition can cause severe bias to the N budget. The overestimation is largest for NH_4^+ and NO_3^- , but very small for N_{org} . Nitrate and organic nitrogen comprise 76% of the wet deposition, while nitrate and ammonia dominate the dry deposition with 96% fraction.

Table 1. The estimated effect of dry deposition to the “bulk deposition” and estimated composition of dry N deposition. Units are in $\text{kg N ha}^{-1} \text{a}^{-1}$.

	NH_4^+	NO_3^-	N_{org}	Total
Measured bulk deposition	1.42	2.33	1.66	5.41
Modelled contribution of wet deposition to the bulk deposition	1.03	1.71	1.62	4.36
Modelled contribution of dry deposition to the bulk deposition	0.39	0.62	0.04	1.05
Contribution of dry deposition to the measured bulk deposition	27.6 %	26.6 %	2.4 %	19.4 %
Modelled composition of dry deposition	37.2 %	59.0 %	3.8 %	100 %

Our approach is simple and we have to assume constant dry deposition rate and constant nutrient concentrations in the precipitation. When the method is applied over relatively long period (year or longer) of time and the variation of dry deposition and nutrient concentrations in precipitation are normally distributed, making these assumptions should not lead to systematic errors in determined wet deposition rates. It is also possible to determine the composition of dry deposition. This requires additional assumptions about the properties of the collector and forest surface. In the future, Δt could be replaced by the actual accumulation time for dry deposition.

CONCLUSIONS

In boreal region bulk deposition measurement overestimate wet nitrogen deposition markedly. Using the approach presented in this paper, it is possible to quantify this overestimation. In addition, the approach gives information on the composition of dry deposition. In our case the dry N deposition was dominated by mineral N (NH_4^+ and NO_3^-), whereas organic nitrogen was an important component in wet deposition.

ACKNOWLEDGEMENTS

This work was supported by Maj and Tor Nessling Foundation (project number 2011250), the Academy of Finland Centre of Excellence program (project number 1118615), the post-doctoral project 1127756, the Academy Fellow project 130984 and NitroEurope IP.

REFERENCES

- Benitez J. M. G., Cape J. N., Heal M. R., van Dijk N., Diez A. V. (2009). Atmospheric nitrogen deposition in south-east Scotland: Quantification of the organic nitrogen fraction in wet, dry and bulk deposition. *Atmospheric Environment*. 43, 4087 - 4094.
- Sutton M.A., Howard C.M., Erisman J.W., Billen G., Bleeker A., Grennfelt, P., van Grinsven, H., Grizzetti, B. (Eds; 2011). *The European Nitrogen Assessment – Sources, Effects and Policy Perspectives*. (Cambridge University Press, Cambridge, U.K).

FULL NITROGEN BALANCE OF A BOREAL SCOTS PINE FOREST

J.F.J. KORHONEN^{1,2}, M. PIHLATIE^{3,1}, J. PUMPANEN², J. LEVULA,⁴ P. HARI,² E. NIKINMAA,² H. ILVESNIEMI⁵ and T. VESALA¹

¹Division of Atmospheric Sciences, Department of Physics, University of Helsinki
P.O.Box 48, FI-00014, University of Helsinki, Finland

²Department of Forest Sciences, P.O. Box 27, FI-00014, University of Helsinki

³IMK-IFU, KIT, Kreuzteckbahnstr. 19, D-82467, Garmisch-Partenkirchen, Germany

⁴Hyytiälä Forestry Field Station, Hyytiäläntie 124, FI-35500, Korkeakoski, Finland

⁵Finnish Forest Research Institute, Vantaa Research Unit, PO. Box 18, FI-01301, Vantaa, Finland

Keywords: DEPOSITION, STORAGE, FLUX, BUDGET.

INTRODUCTION

We present a measurement-based N balance of boreal Scots pine (*Pinus sylvestris*) forest in Hyytiälä, Finland. All-year round measurements have been conducted continuously since 1996. The nitrogen budget consists of inputs, outputs, pools and internal cycling of nitrogen. The inputs consist of atmospheric N deposition and N fixation, both considered to be relatively small in the measurement area. In semi-natural ecosystems, the major outputs are considered to be leaching of NO_3^- and emission of N_2O from the soil to the atmosphere. In Hyytiälä, NO_3^- leaching is negligible and N_2O flux is relatively small.

There are large pools of N in the soil. The N in living biomass is in the order of around one tenth of the total N in the ecosystem. Still, based on fertilization experiments the productivity of boreal forests is typically considered as limited by low N availability. We explain this by low gross mineralization rate, which we assumed to be mainly dependent on the quality and quantity of litter fall and temperature. Furthermore, we emphasize the importance of N deposition and canopy N uptake for productivity of the forest.

METHODS

Except for dry deposition, all of the presented values are measured or calculated based on the measurements. Dry deposition estimates are from Flechard et al. (2011).

Measurements were conducted at SMEAR II-station in Hyytiälä, Southern Finland (61° 51'N, 24 ° 17'E). The stand is a young even-aged Scots pine forest regenerated by sowing after clear-cut, prescribed burning and soil preparation in 1962. Intensive all-year-round measurements of mass and energy fluxes and physiological and meteorological variables have been measured since 1996. The measurement station is established to a small hill containing two micro catchment areas (889 m² and 301 m²). These areas receive water only in precipitation and the water flow in soil is directed to two weirs, where the N concentration of water flowing out of the system is measured.

Precipitation, throughfall, stemflow, and runoff/percolation were measured and sampled bi-weekly to monthly intervals. In addition, soil water N content was analyzed in samples from suction cups at different soil horizons. Ammonium (NH_4^+), nitrate (NO_3^-) and total N concentrations were measured from the water

samples. Biomass pools and changes were calculated using data from annual biomass inventories. NO_x fluxes were measured using automatic chambers and N₂O flux was measured using automatic and manual chambers. Litterfall was measured monthly using 20 litter traps and 20 frames lying on the ground. Litter was separated into six groups, analyzed for C and N, and a time series of N concentration in each group was constructed.

RESULTS AND DISCUSSION

Soil is the greatest pool of N (150 - 200 g N m⁻²) in this forest stand. Other important storages of N are wood, bark, needles and fine roots (in total 15 - 25 g N m⁻²). More than 99.9% of the soil N is in organic form, directly unavailable to plants. Nitrogen in the woody tissue and bark is immobilized from decades to hundreds of years, whereas the N in the needles and fine roots is in constant cycling.

Nitrogen bulk deposition is approximately 4 kg N m⁻². Dry deposition is estimated to be around 3.5 kg N m⁻² (Flechar et al. 2011). Around 5% of the N deposition is lost in the runoff, mostly in the form of organic nitrogen. N loss in N₂O emissions from the soil is approximately 0.02 g N m⁻² a⁻¹, which is approximately 3% of the N deposition. NO_x emissions from the ecosystem are hardly within the measurement range. We estimate that more than 50% of the N deposition is retained in the canopy and ground vegetation.

During years from 1998 to 2009 annual aboveground litterfall from trees was on average 2.0 g N m⁻² and varied from 1.2 to 3.0 g N m⁻². Approximately half of the N in aboveground litterfall was in needles (1.1 g N m⁻² a⁻¹). Branches contributed about one fourth (0.47 g N m⁻² a⁻¹) of the N in aboveground litterfall. Retranslocation of needle litter was estimated to be 0.68 g N m⁻² a⁻¹. This resembles 34% of the N in aboveground litterfall.

Productivity of boreal forests is considered to be limited by low N availability. However, there are large pools of N not directly available for the plants. We deduce that N limitation is caused by low mineralization rate of litter and soil organic matter. We further suggest that main reasons for relatively low gross mineralization rate are low temperature and the quantity and chemical composition of the litter and SOM. Internal cycling of N and canopy N retention comprise a relatively large fraction in plant N uptake, thus boosting the productivity of the forest.

Challenges remain in the direct measurement of N₂ fixation, N₂ emission, dry deposition and canopy N uptake.

ACKNOWLEDGEMENTS

This work was supported by Maj and Tor Nessling Foundation (project number 2011250), the Academy of Finland Centre of Excellence program (project number 1118615), the post-doctoral project 1127756, the Academy Fellow project 130984 and the NitroEurope IP.

REFERENCES

- Flechar C. R., Nemitz, E., Smith, R. I., Fowler, D., Vermeulen, A. T., Bleeker A., Erisman, J. W., Simpson, D., Zhang, L., Tang, Y. S., and Sutton M. A. (2011). *Dry deposition of reactive nitrogen to European ecosystems: a comparison of inferential models across the NitroEurope network*. Atmos. Chem. Phys., 11, 2703–2728, doi:10.5194/acp-11-2703-2011
- Ivesniemi, H., Levula, J., Ojansuu, R., Kolari, P., Kulmala, L., Pumpanen, J., Launiainen, S., Vesala, T. & Nikinmaa, E. (2009). *Long-term measurements of the carbon balance of a boreal Scots pine dominated forest ecosystem*. Boreal Env. Res. 14(4): 731–753.

AEROSOL MASS SPECTROMETRY BASED CHEMICAL COMPOSITION MEASUREMENTS OF AEROSOL PARTICLES IN FINNISH BOREAL FOREST AREA AT SPRING-TIME.

A. KORTELAINEN¹, L. Q. HAO¹, A. JAATINEN¹, P. MIETTINEN¹, J. N. SMITH^{1,4}, D. R. WORSNOP^{1,2,3,5} and A. LAAKSONEN^{1,2}

¹Department of applied physics, University of Eastern Finland, Kuopio, 70211, Finland

²Finnish meteorological institute, Climate Change, Helsinki, 00101, Finland

³Department of physics, Division of Atmospheric Sciences, University of Helsinki, Helsinki, 00014, Finland

⁴National Center for Atmospheric Research, Boulder, Colorado, 80305, USA

⁵Aerodyne Research Inc., Billerica, MA, 01821, USA

Keywords: chemical composition, organics, AMS, PMF

INTRODUCTION

Atmospheric aerosol formation and aging are widely researched areas as the complexity of chemical compounds and ambient conditions are changing rapidly in nature. Secondary organic aerosols (SOA) form through the oxidation of gaseous emissions; as SOA age their oxidation ratio increases. In a remote forest setting, local organic compounds are not that oxidized as the long-range transported urban aerosol, which often correlates with particulate sulphate. Markers of combustion come out in long-range transported air mass plumes and correlate usually with substances like black carbon, levoglucosan and CO₂. The way to understand better the complex ambient organic aerosol compounds is to separate them into groups according to their properties such like oxidation, volatility, association with surrounding trace gases, other aerosol compounds and meteorology. Aerosol mass spectrometer based real-time measurements allow a change to understand better changes of organic aerosol in a ambient forest setting.

This work was first-time trial with PMF (Positive Matrix Factorization) analysis of W- mass spectrometer mode data in the clean northern boreal forest area at Hyytiälä. PMF method (Paatero, 1994; Ulbrich, 2009) was used for W-HR (High Resolution) organics data for tracking their sources and the results were compared to the recent analysis with V- mode, that has roughly two times lower mass resolution and with robust UMR (Unit Mass Resolution). It was found three different types of organics; LV-OOA (Low-Volatile Oxidized Organics Aerosol), SV-OOA (Semi-Volatile Oxidized Organics Aerosol) and BBOA (Biomass Burning Organics Aerosol), that had typical features of the recently published organics groups. After choosing more than five factors, on the other way called organic groups or types of organics, there was no new information in the upcoming factors. W-mode shared same information of the factors as in UMR and V-HR and if the lower sensitivity of W-mode doesn't have effect on PMF analysis the resulting number of factors in the Hyytiälä measurement site is 4 or 5.

METHODS

The ambient measurements were performed at the remote SMEARII (Station for Measuring Forest Ecosystem- Aerosol Relations) station, in the southern Finland at Hyytiälä (61° 51'N, 24° 17'E, 180m ASL) between 10.5-13.6.2009. Aerosol chemical composition was measured by Aerodyne HR-TOF-AMS (High Resolution Time-Of-Flight Aerosol Mass Spectrometer) and the other aerosol properties such as volatility by VTDMA (Volatility Tandem Differential Mobility Analyzer) and organic growth by UFO-TDMA (Ultra Fine Organic Tandem Differential Analyzer) (Vaattovaara, 2005). Other particle information (e.g. particle size distributions) and gas compounds (e.g. trace gases) were continuously collected at the site or by other research groups during the campaign.

Aerosol mass spectrometer measures real-time non-refractory aerosol particles of 50-1000 nm aerodynamic diameters. HR-TOF-AMS has two different mass spectrometric modes to quantify aerosol size and chemical composition. Basically V-mode was used to measure aerosol size and mass spectra as it is more sensitive than W-mode, which was used only to measure mass spectra with roughly two times better mass resolution. PMF method is powerful tool to classify complex organic compounds into groups by finding the solution for mass-balanced spectra and time-trends on minimizing the input matrix residual. Closer approach to the PMF method for the use of organics matrix is established in (Ulbrich, 2009). PMF was used for UMR, V- and W-HR organics data sets to quantify the organics sources at the site.

CONCLUSIONS

Recently it was found that in Hyytiälä there can be separated four different types of organic factors by HR-TOF-AMS. The factors were LV-OOA, SV-OOA, BBOA and HOA however the number of factors was changing between the PMF analysis of UMR and V-HR. In UMR there were two types BBOA, two types of LV-OOA and SV-OOA. In V-HR the number of factors rely on sorting the different factor types i.e in six-factor-solution it was found new factor HOA that alike-one was more BBOA-type in five-factor-solution. Therefore the number of factors wasn't concluded before the study of W-based PMF analysis. Usually taking more than four factors into PMF solution there was one factor that didn't correlate with any trace gases or aerosol components and it had low mass loading almost whole time. That factor was thought to be combined with the most alike factor in the last solution.

LV-OOA was more oxidized, long-range transported, low volatile and correlated with sulphate, nitrate and ammonium and diurnally increased during the daytime. SV-OOA was less oxidized, whose fraction increases during the daytime from new particle formation. It correlated with more organophilic aerosol fraction and nitrate and diurnally increased during the night. Biomass burning (BBOA) came out in air mass plumes originated from urban areas and correlated with black carbon, CO, CO₂, NO_x and nitrate. HOA seem to be related to local traffic at the measurement site with correlation to black carbon, CO, NO_x and nitrate in V-HR PMF analysis. The separation of BBOA and HOA was only slightly different and the difference was thought to be in the existence of levoglucosan mass peaks and partly different time trends. Normally levoglucosan seem to be really low in Hyytiälä and even hard to separate. In UMR levoglucosan seem to be higher than it really was because of low mass resolution. In V- and W-HR PMF, mass resolution gives better opportunity to separate mass peaks and it was thought that the group BBOA could not be decided only according to the existence of levoglucosan. In a nutshell there are two groups of BBOA/HOA-like groups where the one is more and the other less is oxidized.

Exploring the W HR PMF solutions, it seems that there's no new information after taking more than 5 factors into analysis. As in figure 1, there were two types of BBOA (more and less oxidized) and two LV-OOA and SV-OOA and the other LV-OOA in the bottom of figure 1 was the one with comparatively low mass loading. That group could perhaps be combined with the other LV-OOA group ensue the total number of groups to four, which allows two new factors at the site compared to Raatikainen et al. 2010, where he found two factors (OOA1 and OOA2) similar to types of SV- and LV-OOA with Q-AMS (Quadrupole Aerosol Mass Spectrometer). This work was the first time check with W HR PMF analysis at the site and it still has some uncertainties and they need to be taken more close check. There are few mass peaks that seem to have high residuals and their existence need to be taken care of and lower sensitivity of W- compared to V-mode need to be discussed does it have any effect on PMF.

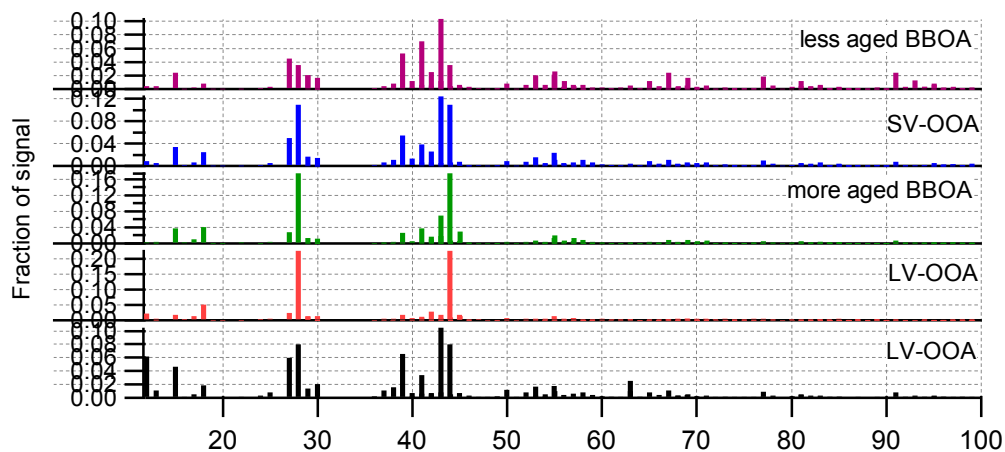


Figure 1. Organic groups for W-based HR PMF analysis.

ACKNOWLEDGEMENTS

The financial support by the Academy of Finland Centre of Excellence program (project no 1118615) is gratefully acknowledged.

REFERENCES

- Paatero, P. and Tapper, U.: Positive Matrix Factorization: a non-negative factor model with optimal utilization of error estimates of data values, *Environmetrics*, 5, 111-126, 1994.
- Ulbrich, I.M. , Canagaratna, M.R., Zhang, Q., Worsnop, D.R., and Jimenez J.L. Interpretation of Organic Components from Positive Matrix Factorization of Aerosol Mass Spectrometric Data. *Atmospheric Chemistry and Physics* , 9(9), 2891-2918, 2009.
- Vaattovaara, P., Räsänen, M., Kuhn, T., Joutsensaari, J. and Laaksonen, A., A method for detecting the presence of organic fraction in nucleation mode sized particles, *Atmospheric Chemistry and Physics*, 5, 3277-3287, 2005.
- Raatikainen, T., P. Vaattovaara, P. Tiitta, P. Miettinen, J. Rautiainen, M. Ehn, M. Kulmala, A. Laaksonen, and D.R. Worsnop. Physicochemical Properties and Origin of Organic Groups Detected in Boreal Forest Using an Aerosol Mass Spectrometer. *Atmospheric Chemistry and Physics*, 10(4), 2063-2077, 2010.

CO₂ EFFLUX BEFORE AND AFTER A CLEAR CUT AND PRESCRIBED BURNING OF A BOREAL SPRUCE FOREST

L. KULMALA^{1,2}, J. PUMPANEN¹, J. LEVULA³, S. RANTANEN³, H. LAAKSO³, E. SIIVOLA², P. KOLARI^{1,2}, and T. VESALA²

¹Department of Forest Sciences, P.O. Box 27, FIN-00014, University of Helsinki, Finland.

² Department of Physics, University of Helsinki, Finland.

³ Hyttiälä forestry field station, University of Helsinki, Korkeakoski, Finland.

Keywords: soil respiration, chamber method

INTRODUCTION

Soil respiration is the sum of CO₂ released 1) by root and rhizosphere respiration, which consists of autotrophic root respiration and respiration by root associated symbiotic fungi, mycorrhiza, and 2) by microbes and soil animals that decompose organic matter or other animals or microbes in the soil food web. Photosynthesis of plants has been shown to play a major role in the soil respiration by providing easily available carbon for the soil biota through root exudates (Högberg et al. 2001) whereas vegetation produces above- and belowground organic litter that microbes and soil animals decompose in a process that releases CO₂ back into the atmosphere. The third major component in soil respiration is the autotrophic respiration from tree roots. All together, the net primary production controls the amount of carbon input into the soil. In addition to biotic factors, soil respiration is, naturally, affected by abiotic factors controlling the enzymatic reactions such as the temperature and soil moisture (Davidson et al. 2006).

Fire is a natural part of forest ecology disturbing forest succession. During the fire, large amount of carbon dioxide is emitted into the atmosphere when the organic matter is burnt. Prescribed burning, meaning the anthropogenic burning of slash and other left over from logging, is a practise in forest management that has positive effects on biodiversity and tree regeneration. Logging removes trees and thereby most of the above- and belowground carbon input whereas wildfire and prescribed burning eliminate the ground vegetation and decrease the amount of organic matter in the soil i.e. litter and humus. Pietikäinen and Fritze (1993) found a decrease also in microbial biomass after prescribed burning treatments. After the removal of the above canopy by logging, soil is exposed to higher solar irradiation that increases soil temperature. The effect is even greater on the burnt surface due to lack of buffering ground vegetation and due to smaller albedo compared with a clear cut site.

In Fennoscandia, wildfires are effectively eliminated during the life span of a forest stand, which possibly increases the amount of soil organic matter in the humus layer in the long run (Wardle *et al.*, 1997). The thick humus layer could result in inefficient seeding and seedling establishment upon forest regeneration. Therefore prescribed burning is sometimes used to ease the seedling establishment by reducing the competition of ground vegetation and releasing important nutrients in the soil. Nowadays, also biodiversity issue (creating habitat for endangered species) has become more important, because efficient fire protection has decreased the area of forest fires in Fennoscandia. Successional patterns and the carbon balance after prescribed burning are well studied, but the consequences of prescribed burning (and natural forest fires) on the greenhouse gas fluxes and the changes in the contribution of different components of soil respiration following forest fire are still relatively poorly known.

The aim of this study was to quantify the changes taking place in soil respiration following clear-cutting and prescribed burning. We studied both the seasonal and diurnal pattern of the efflux and the

environmental variables affecting it. In addition, we studied the amount of carbon lost in the atmosphere instantaneously during the fire and its contribution to the forest carbon balance. We hypothesize that soil respiration and its diurnal amplitude are the smallest in the burnt area due to the lowest carbon input into the soil and the lowest amount of soil organic matter even if the soil surface temperatures were the highest in the dark soil surface exposed to solar radiation compared with an uncut control forest. We assume that the temperature response of soil respiration is the steepest in the forest and the effect of different weather events, such as drought or heavy rains, was larger compared to the burnt clear-cut site because trees contribute to the soil CO₂ efflux by autotrophic respiration and root exudates which are lost upon clear-cutting. In order to study these effects of prescribed burning on the CO₂ efflux of forest soil, we measured soil CO₂ efflux in 1) a mature spruce forest, 2) at a clear cut spruce forest, and 3) a clear cut and burnt spruce forest.

METHODS

The experimental site was a spruce (*Picea abies*) forest near the station for measuring ecosystem-atmosphere relations (SMEARII, Hari and Kulmala, 2005), southern Finland (61.52 N, 24.17 E). During the period from 1960 to 1990, the annual mean temperature was +2.9°C and precipitation, 709 mm. January was the coldest month (mean -8.9°C) and July the warmest (mean +15.9°C). The experimental site belongs to Myrtillus site type (MT) in the Finnish Classification system (Cajander 1926) with sparse occurrence of peat. The stem volume was app. 400 m³ ha⁻¹. Most common species on the forest floor are *Pleurozium schreberi*, *Maianthemum bifolium*, *Dicranum polysetum*, *Vaccinium myrtillus*, *Deschampsia flexuosa* and *Hylocomium splendens*.

The site was partly clear cut in February 2009 and the merchantable stem wood was collected but all slash was left on the site. The biomass of the above ground slash was 47000 kg ha⁻¹. Part of the clear cut area was burned in June 2009 resulting in three different treatments: a mature control forest, a clear cut site, and a clear cut and burnt site. 38 000 kg ha⁻¹ (78%) of slash, 2 300 kg ha⁻¹ (~100%) of ground vegetation, and 18 000 kg ha⁻¹ (22%) of organic soil in litter- and humus layer were burnt during the prescribed burning on the clear cut and burnt site.

Soil respiration was measured with automatic chambers made of transparent PMMA (acryl). Thickness of the sides and the UV-permeable cover is 6 mm and 3 mm, respectively. The chamber is 250 mm in height of which 70 mm is aluminium collar. The chamber opens towards the ground and the sides are 250 mm and 200 mm. CO₂ concentration (GMP343 Vaisala, Vantaa, Finland), temperature (Ptr-100) and relative humidity (HIH-4000-001, Honeywell International, Inc.) were measured inside the chamber. The air was mixed by a fan covered by a netted fabric to reduce the air flow rate. The performance of the chamber was tested on an artificial soil by a method described in detail by Pumpanen et al. (2004). The chamber was programmed to be open for 30 min and closed thereafter for 3 min. The rate of CO₂ exchange was estimated from linear regression that was fitted to the CO₂ readings. The automatic measurements started in 2008 in the area of mature forest that was later clear cut and burnt. The control forest as well as the unburnt clear cut area was measured with a similar chamber between June 2009 and October 2010.

Manual chamber measurements were performed on 11 collars at each treatment in circa two-week interval in 2008–2010. The manual chamber was 0.24 m in high and 0.22 m in diameter. The CO₂ concentration (GMP343), air humidity and temperature (HM70, Vaisala) were recorded for a 4-minute closure of the chamber. The rate of CO₂ exchange was estimated from linear regression that was fitted to the CO₂ readings.

PRELIMINARY RESULTS

The year 2008 was the rainiest and coolest of the studied years except for the relatively warm October. However, the soil moisture in the mature forest decreased several times during the summer, especially in late July and early August. The decrease in soil moisture decreased also the soil respiration (Figure 1A).

Before the clear-cutting, the level of soil respiration was similar at all experimental sites (Figure 1A). The differences between the sites started to arise after the burning in June 2009. The soil respiration was the lowest in the burnt area and the highest in the control forest whereas the soil temperatures (Figure 1B) were the lowest in the control forest (max. 15 °C) and highest in the burnt area (max. 21 °C). The same rank in soil temperatures remained in the warm summer of 2010 with maximum values of 19 °C and 24 °C at the control and burnt sites, respectively. Soil temperatures at the clear cut site were intermediate with maximum values of 17 °C and 21 °C in 2009 and 2010.

The temperature dependence of soil respiration was the weakest at the burnt site and the highest in the uncut control forest. In 2010, however, the soil respiration did not increase with soil temperatures from June to August in the forest, probably because of extremely low soil moisture. Simultaneously at the clear cut sites, soil respiration was similarly dependent of soil temperature as earlier indicating that the soil water content at the clear-cut site was not a limiting factor for soil respiration as in the uncut forest where the transpiration of trees and ground vegetation effectively dried out the soil.

The automatic measurements revealed the diurnal pattern of soil respiration. After the clear cut, the diurnal pattern was the highest at the clear cut site and smallest at the burnt site (Figure 2).

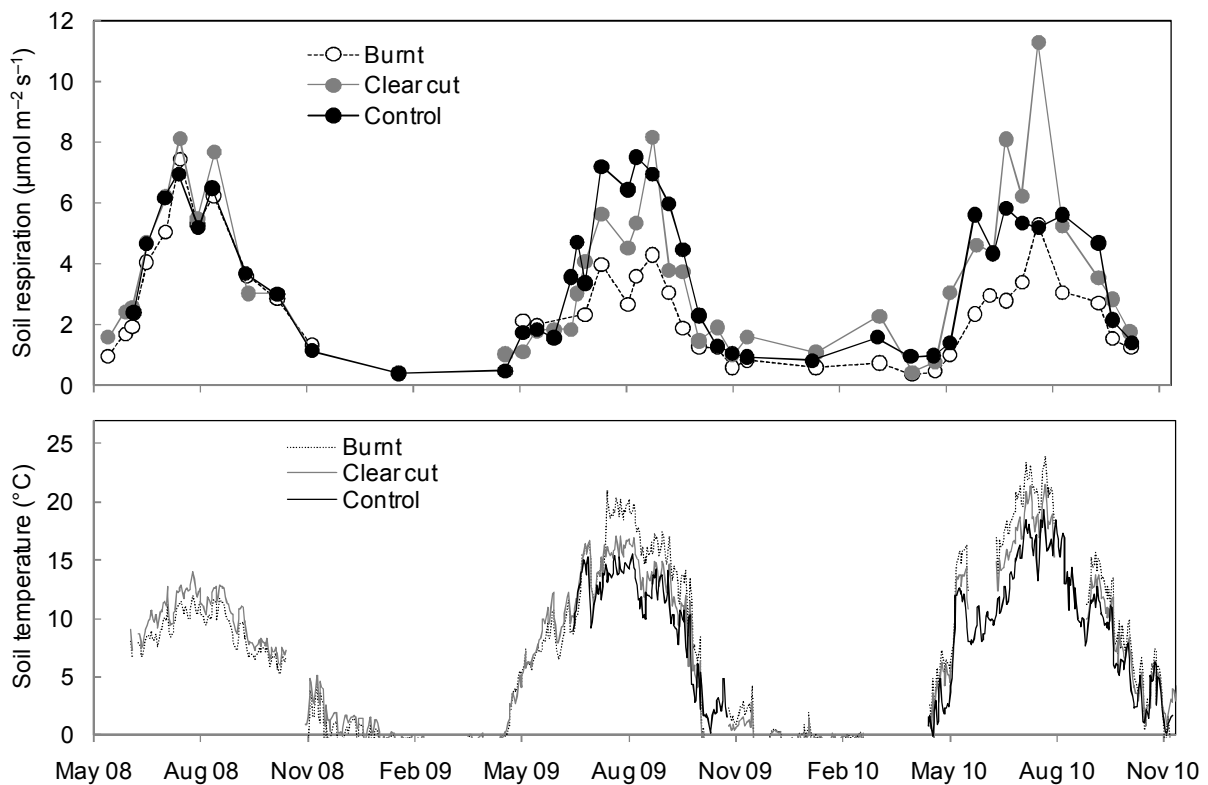


Figure 1: Soil respiration (A) measured by the manual chamber method and soil temperature (B) in the different treatments: clear cut and burnt site, clear cut site and uncut forest.

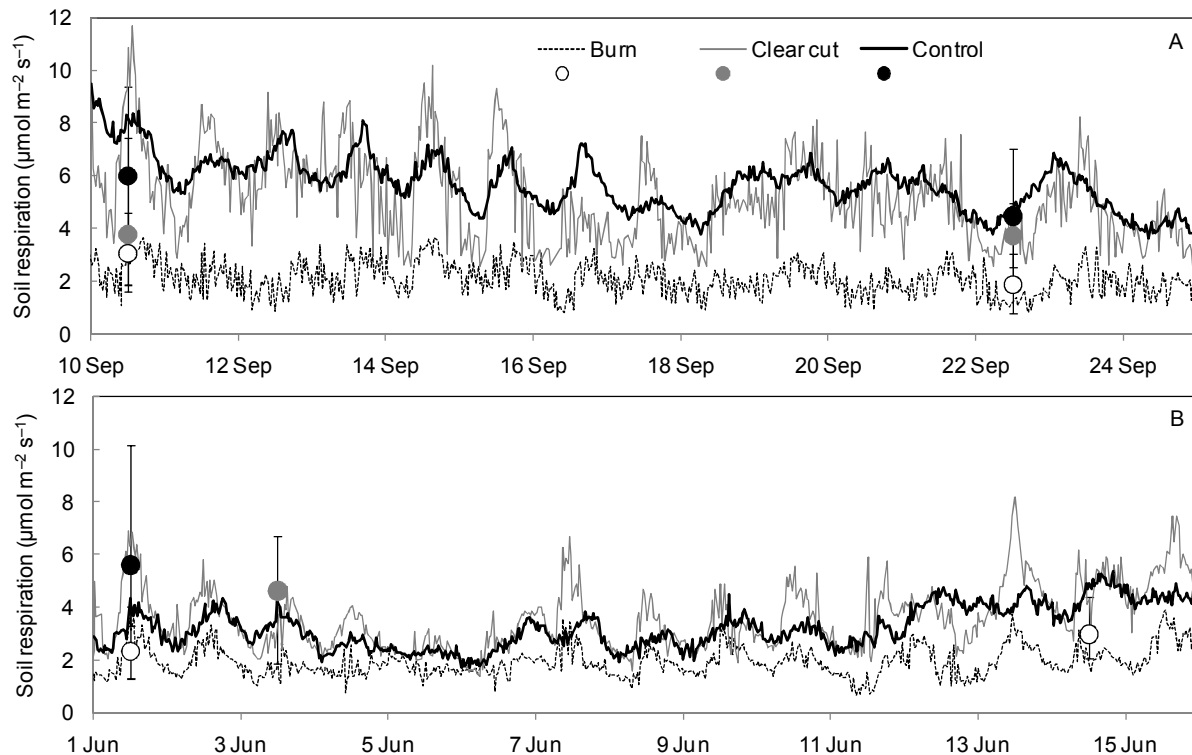


Figure 2: Soil respiration in September 2009 (A) and June 2010 (B) at the three different treatments (clear cut and burnt site, clear cut site and uncut forest) measured by the automatic (lines) and the manual chambers (spheres). The error bars in the manual measurements represent the range of soil respiration in the 11 measuring plots.

ACKNOWLEDGEMENTS

This research was supported by the Academy of Finland Centre of Excellence programme (project number 1118615), Academy of Finland (projects 130984, 137352, 206085 and 213093) and EU projects ICOS, GHG-Europe, and IMECC.

REFERENCES

- Hari, P. and M. Kulmala (2005). Station for measuring ecosystem-atmosphere relations (SMEAR II). *Boreal Environ.Res.* **10**, 315-322.
- Högberg P, A. Nordgren, N. Buchmann, A.F.S. Taylor, A. Ekblad, M.N Högberg, G. Nyberg, M. Ottosson-Lofvenius, D.J. Read (2001). Large-scale forest girdling shows that current photosynthesis drives soil respiration. *Nature* **411**, 789–792
- Davidson E.A. and I.A. Janssens (2006). Temperature sensitivity of soil carbon decomposition and feedbacks to climate change. *Nature* **440**,165-175
- Pietikäinen J. and H. Fritze (1993) Pietikainen, J., and Fritze, H. 1993. Microbial biomass and activity in the humus layer following burning: short-term effects of two different fires. *Can. J. For. Res.* **23**, 1275–1285.
- Pumpanen, J., P.Kolari, H. Ilvesniemi, K. Minkkinen, T. Vesala, S. Niinisto, A. Lohila, T. Larmola, M. Morero, M. Pihlatie, I. Janssens, C. Yuste, J.M. Grunzweig, S. Reth, J.A. Subke, K. Savage, W. Kutsch, G. Ostreng, W. Ziegler, P. Anthoni, A. Lindroth and P. Hari (2004). Comparison of different chamber techniques for measuring soil CO₂ efflux, *Agricultural and Forest Meteorology* **123**, 159–176
- Wardle, DA, O. Zackrisson, G. Hörnberg, and C. Gallet (1997). Influence of island area on ecosystem properties. *Science* **277**,1296–99.

THE ABOVE GROUND RESPIRATION OF GROUND VEGETATION IN BOREAL PINE FORESTS

L. KULMALA^{1,2}, J. PUMPANEN¹ and P. HARI¹

¹Department of Forest Sciences, P.O. Box 27, FIN-00014, University of Helsinki, Finland.

² Department of Physics, University of Helsinki, Finland.

Keywords: Chamber method, *Calluna vulgaris*, *Vaccinium vitis-idaea* and *V. myrtillus*

INTRODUCTION

Boreal forests have a vegetation structure of a tree layer and of a layer of ground vegetation comprising: ericaceous shrubs, herbs, grasses, mosses, and lichens. Research on carbon exchange in boreal forests has mainly focused on matured trees even ground vegetation plays a major role especially in the early phases of succession when the tree seedlings are small and do not shade the ground layer. Therefore, a study over the CO₂ exchange from ground vegetation is needed for understanding the forest carbon cycling and the responses of boreal forests to future climate.

Respiration is the chemical opposite of photosynthesis. It releases the captured energy for growth and maintenance by a series of chemical reactions that consume oxygen and release CO₂. Van't Hoff noted already in 1884 that the chemical reactions in a plant are dependent on temperature. Respiration as well is mostly dependent on temperature, often described as an exponential function, but respiration is influenced furthermore by species and growth form, age, oxygen concentration and nutrient and water supply, for example (Taiz and Zeiger, 2002). The aim of this study is to quantify the species-specific temperature responses of respiration of the most common ground vegetation species in boreal pine forest and clear cut sites.

METHODS

Most of the measurements were located at SMEARII (Hari and Kulmala, 2005) in Hyytiälä, southern Finland (61.52 N, 24.17 E). During the period from 1960 to 1990, the annual mean temperature was +2.9 °C and precipitation 709mm. January was the coldest month (mean -8.9 °C) and July, the warmest (mean +15.9 °C, Drebs *et al.*, 2002). The stand is comprised of a 45-year-old *Pinus sylvestris*. The soil at the site was exposed to prescribed burning and ploughing before sowing in 1962. In the summer of 2005, the dominant height of the stand was 16 m and the tree density 1100–1200 ha⁻¹. *Vaccinium vitis-idaea* L., *V. myrtillus* L. and mosses, mainly *Pleurozium schreberi* (Brid.) Mitt. and *Dicranum polysetum* Sw. dominated the forest floor. According to the Finnish forest site type classification (Cajander, 1926), the forest belongs to the *Vaccinium* site type (VT), that is of medium fertility.

We studied the respiration also at two clear-cut sites located nearly 1 km from each other and 7 km from the SMEAR II. Both sites were app. 1 hectare in size but differed substantially in soil fertility. According to the Finnish forest site type classification, the fertile site belonged mainly to the *Myrtillus* type (MT) and partly to *Oxalis Myrtillus* type (OMT). The infertile type belonged to *Calluna* type (CT). The fertile site was planted with Norway spruce and the infertile site was sown with Scots pine seeds. Fast-growing and opportunistic dominant species such as *Deschampsia flexuosa* (L.) Trin., *Epilobium angustifolium* (L.) Holub and *Rubus idaeus* L. dominated at the fertile site. The dominant species at the infertile site were evergreen and slow-growing such as *Calluna vulgaris* (L.) Hull and *Empetrum nigrum* L.

The majority of the respiration rates (*r*) of the most common plant species of ground vegetation were obtained at circa two-week intervals with a manual, cylindrical chamber based on the non-steady-state non-through-flow chamber technique (Kulmala *et al.*, 2008) during the growing seasons 2005 and 2006.

The darkened chamber was 0.30 m in diameter, 0.30 m in height and open downwards. CO₂ concentration (GMP343, Vaisala, Finland) inside the chamber was monitored during the measurement. The humidity and temperature values were obtained from a temperature and humidity probe (HMP75, Vaisala, Finland) also attached inside the chamber and connected to a data recorder (MI70, Vaisala, Finland). Pressure was measured at SMEAR II. The rate of respiration (r) was estimated from linear regression fitted to CO₂ readings over a 5-min time. During the measurements, the chamber was placed on a polyvinylchloride (PVC) collar that was perforated to allow air to circulate freely under the chamber. There was a 1-cm-thick sheet of cellular plastic between the collar and the chamber. The shoots entered the chamber through a cut in the plastic. Hence, we could measure the same shoots several times in their natural growing environment without causing any change or disturbance to the shoots. After the growing seasons, the shoots were dried and weighted.

The data set includes also respiration rates (r) with a different measurement setup in 2004. At that time, the above ground shoots were cut off and placed in a chamber on a plastic base. The chamber was 0.2 m in diameter and 0.255 m in height. Sample air was circulated between EGM-3 (PP-systems, UK) and the chamber for CO₂ concentration measurements over four minutes. Thereafter the shoots were dried and weighted. The measurement was repeated 60–80 times with *Calluna vulgaris*, *Vaccinium vitis-idaea* and *V. myrtillus* and few times with other vascular and non-vascular species. The chamber is introduced in detail by Pumpanen *et al.* (2004).

We fitted an exponential model of temperature dependence, $r(T)$, into the single species-specific respiration rates (r) and instantaneous air temperature (T , °C):

$$r(T) = r_0 Q_{10}^{\frac{T}{10}} \quad (1)$$

In the equation, Q_{10} and r_0 are species-specific constants. Q_{10} is the proportional change in $r(T)$ per 10 °C rise in temperature whereas the r_0 is respiration in 0 °C. The Q_{10} values were first calculated as follows:

$$Q_{10} = e^{10*\beta} \quad (2)$$

In the equation, β is the regression coefficient between the natural logarithm of r and air temperature (T). Then, r_0 (Eq. 1) was found using the obtained Q_{10} .

RESULTS AND DISCUSSION

Calluna vulgaris and *Vaccinium vitis-idaea*, the small shrubs with abundant wooden biomass and evergreen leaves, have quite similar temperature dependence (Q_{10}) of respiration and the respiration rate at 0 °C (r_0 , Table 1). The base level of respiration (r_0) of *Vaccinium myrtillus* is notably higher but the temperature dependence is even slightly smaller than in *Calluna vulgaris* and *Vaccinium vitis-idaea*, species with evergreen leaves. However, the coefficient of determination (r^2 , Table 1) of *V. myrtillus* is the lowest and the temperature dependence scattered (Figure 1B) probably due to the annual growth habit: the whole plant measurements included varying combination of leaves and wooden parts during the growing season. The small biomass of the experimental shoots most likely caused the scatter in the temperature dependence of *V. vitis-idaea*. The CO₂ release by respiration was weak and small biomass led to even a smaller signal which easily disappeared in the measuring noise.

Epilobium angustifolium and *Rubus idaeus* showed large variation in respiration rates and their temperature dependence was scattered at the clear cut sites (Figure 1F). In the middle-aged forest, the temperature response of grasses and herbs was even more spread (Figure 1E). Frantz *et al.* (2004) found that whole-plant respiration of rapidly growing plants had low sensitivity to temperature. In addition, the narrow temperature range during the measurement of deciduous species is also responsible for the blurred temperature dependence.

Table 1: Temperature response parameters r_0 and Q_{10} (Eq. 1) of *Calluna Vulgaris*, *Vaccinium vitis-idaea* and *Vaccinium myrtillus* in the middle-aged Scots pine stand (SMEAR II) in 2004–2006 based on above ground

respiration. The other columns represent the coefficient of determination (r^2), and a coefficient (a) and intercept (b) of the linear regression between observation and the model.

	r_0 ($\mu\text{g g}^{-1} \text{s}^{-1}$)	Q_{10}	r^2	a	b ($\mu\text{g g}^{-1} \text{s}^{-1}$)
<i>Calluna vulgaris</i>	0.016	2.81	0.55	0.66	0.030
<i>Vaccinium vitis-idaea</i>	0.020	2.76	0.39	0.43	0.069
<i>Vaccinium myrtillus</i>	0.030	2.66	0.35	0.41	0.094

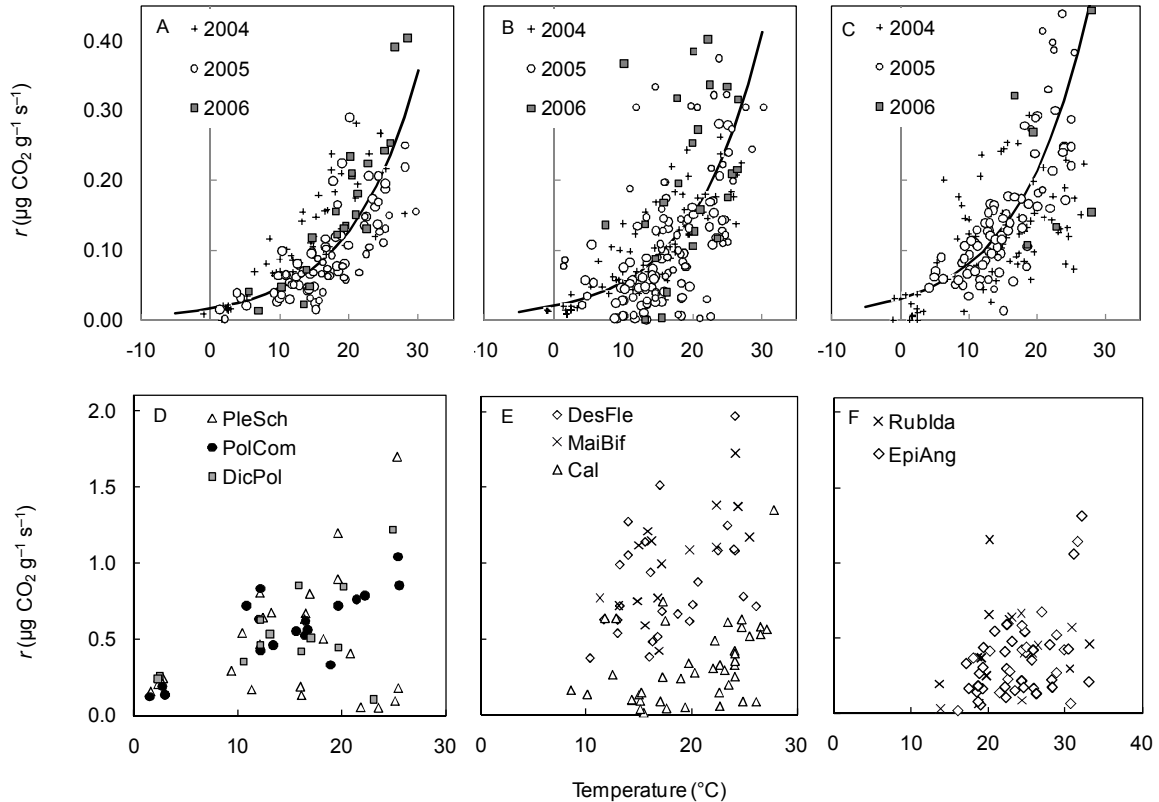


Figure 1: Respiration of the above ground biomass ($\mu\text{g CO}_2 \text{g}^{-1} \text{s}^{-1}$) of *Calluna Vulgaris* (A), *Vaccinium vitis-idaea* (B), *V. myrtillus* (C), mosses *Pleurozium schreberi*, *Polytrichum commune*, *Dicranum polysetum* (D), *Deschampsia flexuosa*, *Maianthemum bifolium*, *Calamagrostis sp.* (E) *Rubus Idaeus* and *Epilobium angustifolium* (F). Respiration was measured at SMEARII station in the middle-aged Scots pine stand in the figures A-E and at the clear cut sites in the figure F.

Leaves with high nitrogen content have high maintenance requirements and consequently they typically have higher dark respiration and therefore lose more carbon in respiration than low-nitrogen leaves (Chapin et al. 1987). *Epilobium angustifolium* grew both in the very poor and in the fertile site but the mass-based respiration rates do not differ from each other. Nevertheless, the mass-based respiration rates of deciduous species are in general notably higher than species with perennial leaves but the difference is explained also by the overwintering woody stem of low shrubs that has low maintenance requirements and therefore also slow respiration rates.

Besides the woody stem, low shrubs also have the longest life span that has been reported to decrease the respiration rates (Reich et al., 1998). At the clear cut sites, the measured respiration rates of above ground parts closely followed to the photosynthetic rate (Kulmala et al., 2009). Reich et al. (1998) observed a similar phenomenon. The temperature dependence of *Calluna vulgaris* at the clear cut site was equal to that in the middle-aged stand, but the base level value was slightly higher ($0.021 \mu\text{g g}^{-1} \text{s}^{-1}$).

It is noteworthy that sometimes the respiration rate of mosses in high temperatures is very low (Figure 1D). This might be a sign of dormancy that takes place after drying out (Peterson and Mayo, 1975).

Whole-plant maintenance respiration generally declines during water stress as a result of an overall slowing of metabolic activity.

It is well known that the temperature dependence of respiration differs in early and late season. However, partitioning respiration data to growth and maintenance respiration would require taking into account also the state of photosynthetic activity and water supply, for example, and the ages of leaf and wooden mass and the varying ratio between them. Including more affecting factors would, however, require more frequent and high-quality data.

The simple Q_{10} function is generally accepted in modelling leaf and ecosystem scale respiration but on the other hand, the use of it has been also widely criticised for not being capable for explaining the temperature sensitivity of respiration. There is also evidence that Q_{10} is not constant but dependent on the temperature range. Tjoelker (2000), for example, reported decreasing Q_{10} with increasing temperatures. Paembonan *et al.* (1991) studied *Chamaecyparis obtusa* and observed that Q_{10} decreases during the growing season with increasing night temperatures whereas r_0 was the smallest in the winter and increased in June-July. Skre (1975) reported that Q_{10} for *Vaccinium myrtillus* was 1.6–2.1 in July, 1.9 in August and 1.8 in September but in contrast, Tjoelker *et al.* (1999) did not notice such a decrease in Q_{10} with the night temperatures.

ACKNOWLEDGEMENTS

This study is performed within the framework of the Finnish Graduate School "Physics, Chemistry, Biology and Meteorology of Atmospheric Composition and Climate Change" and supported by the Academy of Finland Centre of Excellence programme (project number 1118615).

REFERENCES

- Cajander, A.K. (1926). The theory of forest types. *Acta Forestalia Fennica* **29**, 1–108.
- Chapin, F.S., A.J. Bloom, C.B. Field and R.H. Waring (1987). Plant-Responses to Multiple Environmental-Factors. *Bioscience* **37**, 49-57.
- Frantz, J.M., N.N. Cometti, and B. Bugbee (2004). Night temperature has a minimal effect on respiration and growth in rapidly growing plants. *Ann.Bot.* **94**, 155-166.
- Hari, P. and M. Kulmala (2005). Station for measuring ecosystem-atmosphere relations (SMEAR II). *Boreal Environ.Res.* **10**, 315-322.
- Kulmala, L., J. Pumpanen, T. Vesala and P. Hari (2009). Photosynthesis of boreal ground vegetation after a forest clear-cut. *Biogeosciences* **6**, 2495-2507.
- Paembonan, S.A., A. Hagihara and K. Hozumi (1991). Long-Term Measurement of CO₂ Release from the Aboveground Parts of a Hinoki Forest Tree in Relation to Air-Temperature. *Tree Physiol.* **8**, 399-405.
- Peterson, W.L. and J.M. Mayo (1975). Moisture Stress and its Effect on Photosynthesis in *Dicranum-Polysetum*. *Canadian Journal of Botany-Revue Canadienne De Botanique* **53**, 2897-2900.
- Reich, P.B., M.B. Walters, D.S. Ellsworth, J.M. Vose, J.C. Volin, C. Gresham and W.D. Bowman (1998). Relationships of leaf dark respiration to leaf nitrogen, specific leaf area and leaf life-span: a test across biomes and functional groups. *Oecologia* **114**, 471-482.
- Skre, O. (1975). CO₂ exchange in Norwegian tundra plants studied by infrared gas analyzer technique. In: *Wielgolaski, F.E. (ed.) Fennoscandian tundra ecosystems Vol. I. Plants and microorganisms. pp. 168–183. Springer, Berlin, DE.*
- Taiz, L. and E. Zeiger, (2002). *Plant Physiology*. Sinauer Associates, Sunderland, MA, pp 690.
- Tjoelker, M.G., P.B., Reich and J. Oleksyn, (1999) Changes in leaf nitrogen and carbohydrates underlie temperature and CO₂ acclimation of dark respiration in five boreal tree species. *Plant, Cell & Environment* **22**, 767-778
- Tjoelker, M.G. (2000) Modelling respiration of vegetation: evidence for a general temperature-depnt Q_{10} *Global Change biology* **7**, 223-230

GENERAL OVERVIEW: EUROPEAN INTEGRATED PROJECT ON AEROSOL CLOUD CLIMATE AND AIR QUALITY INTERACTIONS (EUCAARI) - INTEGRATING AEROSOL RESEARCH FROM NANO TO GLOBAL SCALES

M. KULMALA¹, A. ASMI¹, H.K. LAPPALAINEN^{1,2}, U. BALTENSPERGER³, J.-L. BRENGUIER⁴, M. C. FACCHINI⁵, H.-C. HANSSON⁶, Ø. HOV⁷, C.D. O'DOWD⁸, U. POESCHL⁹, A. WIEDENSOHLER¹⁰, R. BOERS¹¹, O. BOUCHER¹², G. DE LEEUW^{1,2,13}, H. DENIER VAN DEN GON¹³, J. FEICHTER¹⁴, R. KREJCI⁶, P. LAJ¹⁵, H. LIHAVAINEN², U. LOHMANN¹⁶, G. MCFIGGANS¹⁷, T. MENTEL¹⁸, C. PILINIS¹⁹, I. RIIPINEN^{1,20}, M. SCHULZ²¹, A. STOHL²², E. SWIETLICKI²³, E. VIGNATI²⁴, M. AMANN²⁵, M. AMMANN³, C. ALVES²⁶, S. ARABAS²⁷, P. ARTAXO²⁸, D.C.S. BEDDOWS²⁹, R. BERGSTRÖM³⁰, J.P. BEUKES³¹, M. BILDE³², J. F. BURKHART²², F. CANONACO³, S. CLEGG³³, H. COE¹⁷, S. CRUMEYROLLE³⁴, B. D'ANNA³⁵, S. DECESARI⁵, S. GILARDONI²⁴, M. FISCHER³⁶, A.M. FJÆRAA²², C. FOUNTOUKIS³⁷, C. GEORGE³⁶, L. GOMES⁴, P. HALLORAN¹², T. HAMBURGER³⁸, R.M. HARRISON³⁹, H. HERRMANN¹⁰, T. HOFFMANN⁴⁰, C. HOOSE⁴¹, M. HU⁴², U. HÖRRAK⁴³, Y. IINUMA¹⁰, T. IVERSEN⁷, M. JOSIPOVIC³¹, M. KANAKIDOU⁴⁴, A.KIENDLER-SCHARR¹⁸, A. KIRKEVÅG⁷, G. KISS⁴⁵, Z. KLIMONT²⁵, P. KOLMONEN², M. KOMPPULA⁴⁶, J.-E. KRISTJANSSON⁴⁷, L. LAAKSO^{1,2,31}, A. LAAKSONEN^{2,48}, L. LABONNOTE⁴⁹, V. LANZ³, K.E.J. LEHTINEN^{46,48}, R. MAKKONEN¹, G. MCMEEKING¹⁷, J. MERIKANTO¹, A. MINIKIN³⁸, S. MIRME³⁶, W.T. MORGAN¹⁷, E. NEMITZ⁵⁰, D. O'DONNELL¹⁴, TS. PANWAR⁵¹, H. PAWLOWSKA²⁷, A. PETZOLD³⁸, J.J. PIENAAR³¹, C. PIO²⁶, C. PLASS-DUELMER⁵², A.S.H. PRÉVÔT³, S. PRYOR⁵³, C.L. REDDINGTON⁵⁴, G. ROBERTS¹¹, D. ROSENFELD⁵⁵, J. SCHWARZ⁵⁶, Ø. SELAND⁷, K. SELLEGRI⁵⁷, X.J. SHEN⁵⁸, H. SIEBERT¹⁰, B. SIERAU¹⁶, D. SIMPSON⁷, J.Y. SUN⁵⁸, D. TOPPING¹⁷, P. TUNVED⁶, P. VAATTOVAARA^{46,48}, V. VAKKARI¹, J.P. VEEFKIND¹¹, A. VISSCHEDIJK¹³, H. VUOLLEKOSKI¹, R. VUOLO²¹, B. WEHNER¹⁰, J. WILDT¹⁸, S. WOODWARD¹⁴, D. R. WORSNOP^{1,2,59}, G.-J. VAN ZADELHOFF¹¹, A. A. ZARDINI^{32,60}, K. ZHANG¹⁴, P.G. VAN ZYL³¹, V.-M. KERMINEN², K.S. CARSLAW⁵⁴ AND S. N. PANDIS³⁷

¹University of Helsinki, Department of Physics, 00014 Helsinki, Finland

²Finnish Meteorological Institute, Research and Development, 00101 Helsinki, Finland

³Paul Scherrer Institut, Laboratory of Atmospheric Chemistry, Villigen PSI, Switzerland

⁴French Meteorological Service, 31057 Toulouse, France

⁵Institute of Atmospheric Sciences and Climate (ISAC), National Research Council (CNR), Bologna, Italy

⁶Stockholm University, Department of Applied Environmental Science (ITM), 10691 Stockholm, Sweden

⁷Norwegian Meteorological Institute, 0313 Oslo, Norway

⁸School of Physics & Centre for Climate and Air Pollution Studies, Environmental Change Institute, National University of Ireland, Galway, Ireland

⁹Max Planck Institute for Chemistry, Mainz, Germany

¹⁰Leibniz Institute for Tropospheric Research, 04318 Leipzig, Germany

¹¹Earth Observation and Climate Department, KNMI, The Netherlands

- /Climate and Seismology Sector, KNMI, The Netherlands
- ¹² Met Office Hadley Centre, Fitzroy Road, Exeter, Devon, EX1 3PB, UK
- ¹³ TNO Built Environment and Geosciences, Utrecht, The Netherlands
- ¹⁴ Max Planck Institute for Meteorology, Hamburg, Germany
- ¹⁵ Laboratoire de Glaciologie et Géophysique de l'Environnement (LGGE), CNRS/University of Grenoble, Grenoble, France
- ¹⁶ Institute of Atmospheric and Climate Science, ETH Zurich, Switzerland
- ¹⁷ School of Earth, Atmospheric and Environmental Sciences, University of Manchester, Manchester, UK
- ¹⁸ Institut fuer Energie- und Klimaforschung –Troposphaere, Forschungszentrum GmbH Juelich, 52425 Juelich, Germany
- ¹⁹ Department of Environment, University of the Aegean, Mytilene, Greece
- ²⁰ Carnegie Mellon University, Department of Chemical Engineering, Pittsburgh PA, USA
- ²¹ Laboratoire des Sciences du Climat et de l'Environnement, Gif-sur-Yvette, France
- ²² NILU, Norwegian Institute for Air Research, Kjeller, Norway
- ²³ Division of Nuclear Physics, Lund University, PO Box 118, S-22100 Lund,
- ²⁴ European Commission, Institute for Environment and Sustainability, Climate Change and Air Quality Unit, Ispra, Italy
- ²⁵ IIASA, International Institute for Applied Systems Analysis, Laxenburg, Austria
- ²⁶ CESAM & Department of Environment, University of Aveiro, Portugal
- ²⁷ Institute of Geophysics, Faculty of Physics, University of Warsaw, Warsaw, Poland
- ²⁸ Institute of Physics University of São Paulo Rua do Matão, Travessa R, 187 CEP05508-090, Sao Paulo, Brazil
- ²⁹ University of Birmingham, Division of Environmental Health and Risk Management, Birmingham, UK
- ³⁰ Department of Chemistry, University of Gothenburg, 412 96 Gothenburg, Sweden
- ³¹ School of Physical and Chemical Sciences, North-West University, Potchefstroom, South Africa
- ³² Department of Chemistry, University of Copenhagen, Copenhagen, Denmark
- ³³ School of Environmental Sciences, University of East Anglia, Norwich NR4 7TJ, UK
- ³⁴ Laboratoire de Météorologie Physique, Université Blaise Pascal, Clermont-Ferrand, France
- ³⁵ Institut de recherches sur la catalyse et l'environnement de Lyon, Villeurbanne, F-69626, France
- 36 Airel Ltd Tähe 4, 51010 Tartu, Estonia

- ³⁷Institute of Chemical Engineering and High Temperature Chemical Processes (ICE-HT) Foundation for Research and Technology Hellas (FORTH), Patras, 26504, Greece
- ³⁸Deutsches Zentrum fuer Luft- und Raumfahrt (DLR), Institute of Physics of Atmosphere, Oberpfaffenhofen, 82234 Wessling Germany
- ³⁹University of Birmingham, Division of Environmental Health and Risk Management, Birmingham, UK
- ⁴⁰Johannes Gutenberg-University Mainz, Germany
- ⁴¹Karlsruhe Institute of Technology, Germany
- ⁴²Peking University, China
- ⁴³Institute of Physics, University of Tartu, 18 Ülikooli St., Tartu, 50090, Estonia
- ⁴⁴Environmental Chemical Processes Laboratory, Department of Chemistry, University of Crete, 71003, P.O. Box 2208, Heraklion, Greece
- ⁴⁵Air Chemistry Group of Hungarian Academy of Sciences, University of Pannonia, P.O. Box 158, 8201 Veszprém, Hungary
- ⁴⁶Finnish Meteorological Institute, Kuopio Unit, 70211 Kuopio, Finland
- ⁴⁷Department of Geosciences, University of Oslo, Norway
- ⁴⁸University of Eastern Finland, Dept. Applied Physics, POB 1627, 70211 Kuopio, Finland
- ⁴⁹Laboratoire d'Optique Atmosphérique – Université des Sciences et Technologies de Lille/CNRS, Villeneuve d'Ascq Cedex, France
- ⁵⁰Centre for Ecology & Hydrology Bush Estate Penicuik Midlothian EH26 0QB
- ⁵¹TERI Darbari Seth Block IHC complex Lodhi Road, New Delhi -110003 India
- ⁵²Hohenpeissenberg Meteorological Observatory, Deutscher Wetterdienst, Germany
- ⁵³Risø National Laboratory Fredriksborgvej 399, P.O. Box 49 DK-4000 Roskilde, Denmark
- ⁵⁴University of Leeds, School of Earth and Environment, Leeds LS2 9JT, UK
- ⁵⁵Institute of Earth Sciences, The Hebrew University of Jerusalem, Israel
- ⁵⁶Institute of Chemical Process Fundamentals AS CR, Rozvojova 135, Prague, Czech Republic
- ⁵⁷Laboratoire de Météorologie Physique, UMR 6016, CNRS/University of Clermont-Ferrand, Clermont-Ferrand, France
- ⁵⁸Key Laboratory for Atmospheric Chemistry, CMA Centre for Atmosphere Watch and Services, Chinese Academy of Meteorological Sciences, Beijing 100081, China
- ⁵⁹Aerodyne Research, Inc. 45 Manning Rd, Billerica, MA 0182, USA
- ⁶⁰Institute for Energy, Sustainable Transport Unit, JRC-European Commission, 21027 Ispra (Va), Italy

Keywords: aerosols, clouds, climate, air quality

INTRODUCTION

The EU-FP6 EUCAARI project (2007-2010) is an Integrated Project (IP) of the 6th Framework Programme of the European Commission. The goals of EUCAARI are to quantify the effect of aerosols on cloud, climate and air quality interactions, to understand future climate change, and to develop strategies and implementation plans for global air quality monitoring. EUCAARI is a consortium of 48 partners coordinated by the University of Helsinki. The project has been motivated by the urgent need to quantify the effect of aerosols on our planet's radiative balance to understand future climate change. The uncertainty in aerosol radiative forcing has been typically greater than 100% and for some aerosol components it is more than 200%.

METHODS

The project was organized into elements studying the emission and formation of aerosols, their evolution and transformation during their atmospheric lifetime and their impact on clouds. This approach maximized the integration of methodologies and scales and ultimately our understanding of the effects of aerosols on air quality and climate. Ground-based, aircraft and satellite measurements were integrated with existing data to produce a global consistent dataset with the highest possible accuracy. The EUCAARI intensive measurement campaign in May, 2008, was designed around simultaneous airborne measurements together with measurements from several "super-site" stations around Europe. Furthermore, during EUCAARI, a hierarchy of new-generation models was developed based on the results of the laboratory and theoretical investigations. This new research concept of "all scales research chain" was the basis of the EUCAARI mission (Fig. 1). The EUCAARI work followed several research chains, in which small-scale models were used to interpret measurements and then integrated in to regional air quality and global climate models. In the end of the project this new knowledge was incorporated in policy-orientated models to analyze climate change and air quality for a range of global emission scenarios using updated economic and technological information.

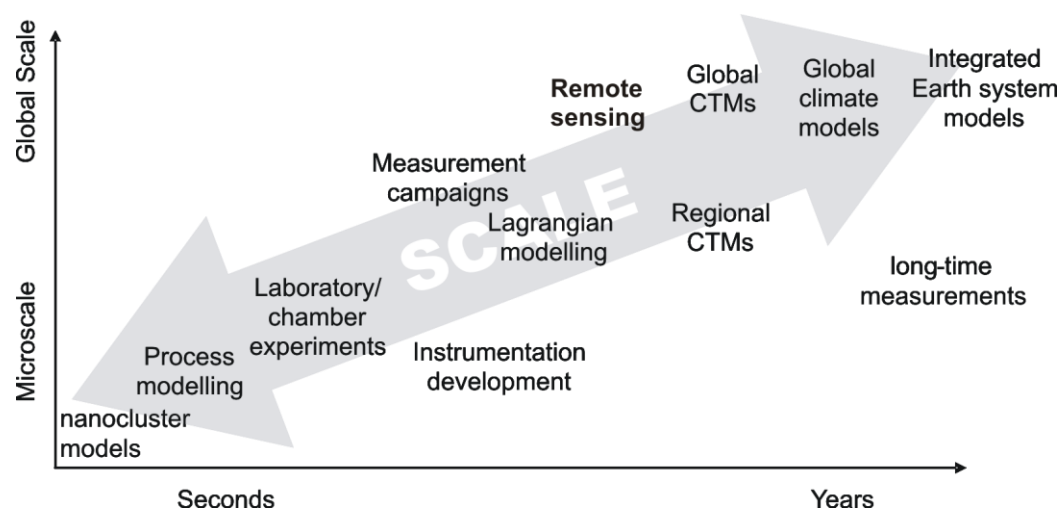


Figure 1. The "EUCAARI arrow" or research chain connecting molecular scale processes with the global scale through integrated measurements, modeling and theory (Kulmala et al., 2009).

RESULTS

One crucial task of EUCAARI was the quantification of the impact of aerosols and trace gases on clouds. The influence of aerosols on clouds depends on particle properties and cloud microphysics as well as on meteorological conditions. Before EUCAARI, the uncertainties related to aerosol properties were similarly high as those related to cloud microphysics and meteorology. Synthesizing the EUCAARI and related studies results, the uncertainty of key parameters in aerosol properties (aerosol particle hygroscopicity, size distribution, number concentration, etc.) and cloud microphysics (dilution ratio, effective radius, etc.) was reduced by about 50%. New formulations of turbulence in global models derived from EUCAARI observations give much better agreement with observations, yielding an overall 36% increase in predicted cloud droplet number concentrations and significantly reducing the model negative bias. With regard to climate modeling and air quality, aerosol properties and cloud microphysics appear now, after EUCAARI, well constrained relative to the uncertainties of meteorological conditions.

EUCAARI focused on the scientific questions related to aerosols with the greatest uncertainty at all relevant scales; from nanometers to global scale, from milliseconds to tens of years. The resulting improved understanding of the aerosol life cycle enabled us to also improve significantly the corresponding climate and air quality models. An example of such an improvement is the partitioning of complex organic compounds between the gas and the particulate phase. The work was based on laboratory experiments focusing on the micro scale. New models were then developed which greatly reduced the complexity of the organic aerosol (OA) partitioning problem to the point where they can be included in global OA models.

EUCAARI developed a set of new emission inventories and scenarios for Europe. For example the particle number emission inventory developed for Europe within EUCAARI is the first of its kind in the world. These inventories together with new knowledge on long-range transport of aerosol pollution provide valuable tools for air pollution policy making. The EUCAARI conclusions are also valuable inputs for future European air quality directives. Based on EUCAARI results the reduction in ammonia emissions is one of the most effective ways to reduce aerosol mass concentrations in Europe. Reduction in NO_x is also effective, but might lead to higher ozone levels in several areas. Reduction in SO₂ emissions will reduce particulate air pollution especially in the Eastern Mediterranean area. Reduction of organic aerosol concentrations is a lot more challenging and will require reductions of gas and aerosol emissions from transportation and biomass burning.

EUCAARI has also performed measurements, which provide new insights of the role of different types of aerosols on air quality and climate. EUCAARI has made significant progress in understanding the formation of biogenic secondary organic aerosol (BSOA). It has now shown that a large fraction of the OA in Europe is of modern origin, for which the main sources are BSOA (boreal forests), biomass burning and primary biogenic aerosol particles. These compounds have also been shown to contribute to the growth of newly formed particles into cloud condensation nuclei and are therefore important for the indirect radiative forcing. All these sources are expected to respond to climate change, although we are presently unable to gauge accurately the strength of the multitude of feedback mechanisms involved.

The large-scale interactions between air quality and climate have been largely unknown, although some links have been identified or even quantified. EUCAARI results highlight the potential impact of future climate change on air pollution and vice versa.

Good quality long-term data sets of physical, chemical, and optical characteristics of aerosols are rare. Long-term data sets are needed to estimate the effect of emission reductions and underpin European strategy on air pollution. EUCAARI leaves a legacy of data and advanced aerosol and cloud computer

codes, which are available via the EUCAARI Platform (<http://transport.nilu.no/projects/eucaari/>). The EUCAARI database, hosted by the Norwegian Institute for Air Research (NILU), builds on the efforts of the EMEP program and utilizes the developments of EU-FP6 infrastructure project EUSAAR (European Supersites for Atmospheric Aerosol Research). The construction of the European Research Area for the atmospheric science will require in the future that the strong connections between science and infrastructure programs be maintained. The database contains observation data of atmospheric chemical composition and physical properties in a common format. It also makes available transport modeling products (Lagrangian particle dispersion model FLEXPART) suitable for the identification of source regions of measured aerosols for the case studies. In order to expand the European activities of aerosol monitoring EUCAARI has built new field stations outside Europe: in polluted regions in China and South-Africa, in Amazon area in Brazil and rural areas in India. This selection of sites provides useful reference for evaluating European conditions and providing information for international negotiations.

EUCAARI contributed to expand the European activities of aerosol monitoring outside Europe: in polluted regions in China and South-Africa, in Amazon area in Brazil and rural areas in India. This selection of sites not only provides useful reference for evaluating European conditions and information for international negotiations but it also strengthened the positioning of Europe as an attractive place for advanced education in the atmospheric science. Support of the European Commission for extending long-term observing network in emerging and developing countries outside of Europe is an essential and unique contribution to GCOS.

The most important technical achievement of EUCAARI was the development of a new prototype of cluster spectrometer for measuring sub-3 nm size particle and cluster ion concentrations and thus allowing us to follow the initial steps of growth of new aerosol particles. This breakthrough will enable Europe to take a leading role in developing and applying environmental technologies and mobilize all stakeholders in the area of air pollution management.

In order to efficiently disseminate and ensure the continuity of EUCAARI measurement techniques, use of the instrumentation and running of the new stations the project has organized several workshops and training events for young scientist as an integral part of the research activity. EUCAARI has clearly strengthened the European research community working in different disciplines of aerosol research: physics, chemistry, meteorology and biology. The project has also set up the stage for further studies such as the continued development of global and regional models using EUCAARI findings and also the incorporation of its results in future air quality directives.

ACKNOWLEDGEMENTS

Main part of the work in this paper has been funded with FP6 project EUCAARI (Contract 34684). This work was performed in the framework of the Research Infrastructure Action under the FP6 "Structuring the European Research Area" Programme, EUSAAR Contract No. RII3-CT-2006-026140. The financial support by the Academy of Finland Centre of Excellence program (project No. 1118615) is gratefully acknowledged.

REFERENCES

Kulmala, M., Asmi, A., Lappalainen, H. K., Carslaw, K. S., Pöschl, U., Baltensperger, U., Hov, Ø., Brenquier, J.-L., Pandis, S. N., Facchini, M. C., Hansson, H.-C., Wiedensohler, A., and O'Dowd, C. D.: Introduction: European Integrated project on Aerosol Cloud Climate and Air Quality interactions (EUCAARI) – integrating aerosol research from nano to global scales, *Atmos. Chem. Phys.*, 9, 2825–2841, 2009.

Kulmala, M., Asmi, A., Lappalainen, H.K., Baltensperger, U., Brenguier, J.-L., Facchini, M. C., Hansson, H.-C., Hov, Ø., O'Dowd, C.D., Poeschl, U., Wiedensohler, A., Boers, R., Boucher, O., de Leeuw, G., Denier van den Gon, H., Feichter, J., Krejci, R., Laj, P., Lihavainen, H., Lohmann, U., McFiggans, G., Mentel, T., Pilinis, C., Riipinen, I., Schulz, M., Stohl, A., Swietlicki, E., Vignati, E., Amann, M., Ammann, M., Alves, C., Arabas, S., Artaxo, P., Beddows, D.C.S., Bergström, R., Beukes, J.P., Bilde, M., Burkhardt, J. F., Canonaco, F., Clegg, S., Coe, H., Crumeyrolle, S., D'Anna, B., Decesari, S., Gilardoni, S., Fischer, M., Fjærraa, A.M., Fountoukis, C., George, C., Gomes, L., Halloran, P., Hamburger, T., Harrison, R.M., Herrmann, H., Hoffmann, T., Hoose, C., Hu, M., Hörrak, U., Iinuma, Y., Iversen, T., Josipovic, M., Kanakidou, M., Kiendler-Scharr, A., Kirkevåg, A., Kiss, G., Klimont, Z., Kolmonen, P., Komppula, M., Kristjansson, J.-E., Laakso, L., Laaksonen, A., Labonnote, L., Lanz, V., Lehtinen, K.E.J., Makkonen, R., McMeeking, G., Merikanto, J., Minikin, A., Mirme, S., Morgan, W.T., Nemitz, E., O'Donnell, D., Panwar, T.S., Pawlowska, H., Petzold, A., Pienaar, J.J., Pio, C., Plass-Duelmer, C., Prévôt, A.S.H., Pryor, S., Reddington, C.L., Roberts, G., Rosenfeld, D., Schwarz, J., Seland, Ø., Sellegri, K., Shen, X.J., Siebert, H., Sierau, B., Simpson, D. Sun, J.Y., Topping, D., Tunved, P., Vaattovaara, P., Vakkari, V., Veefkind, J.P., Visschedijk, A., Vuollekoski, H., Vuolo, R., Wehner, B., Wildt, J., Woodward, S., Worsnop, D. R., van Zadelhoff, G.- J., Zardini, A.A., Zhang, K., van Zyl, P.G., Kerminen, V.-M., Carslaw, K.S., and Pandis, S. N.: General Overview: European Integrated project on Aerosol Cloud Climate and Air Quality interactions (EUCAARI) - integrating aerosol research from nano to global scales, submitted to ACPD .

AMMONIA AND AMINES IN ATMOSPHERIC PARTICLE FORMATION

O. KUPIAINEN, I.K. ORTEGA, P. PAASONEN, V. LOUKONEN, T. KURTÉN,
H. VEHKAMÄKI, M. KULMALA

University of Helsinki, Department of Physics, Division of Atmospheric Sciences,
Gustaf Hällströmin katu 2 A, P.O. Box 64, FI-00014 Finland.

Keywords: New particle formation, molecular clusters, amines, quantum chemistry.

INTRODUCTION

Atmospheric aerosols are known to affect the climate by absorbing and scattering radiation and acting as cloud condensation nuclei. According to recent estimates, 20–80 % of the aerosol particles are formed in the atmosphere by gas-to-particle nucleation. There remains, however, much uncertainty related to their actual birth-mechanism and composition. Consequently, aerosol forcing forms the largest uncertainty in global climate modeling.

New-particle formation rates have been observed to correlate strongly with sulfuric acid concentrations in a wide range of conditions, suggesting that sulfuric acid would be involved in the first steps of nucleation. However, particle formation can not be explained by homogeneous nucleation of sulfuric acid and water alone. Instead, some third compound is needed to stabilize the small sulfuric acid clusters and enable them to grow into particles. Ammonia and amines are good candidates, since their concentrations in the atmosphere are relatively high and, as base molecules, they bind strongly with sulfuric acid.

METHODS

We have studied positively charged and neutral sulfuric acid – ammonia – dimethylamine clusters using a multi-step quantum chemistry method for calculating their formation free energies. Cluster concentrations were studied using a collision and evaporation dynamics model.

For positively charged clusters, our computational results agree very well with measurements. Small neutral clusters, on the other hand, can not be measured directly, and the most accurate way to study them is by quantum chemistry.

CONCLUSIONS

We have found that the dynamics of neutral clusters is somewhat different than for the positive clusters, but in both cases DMA stabilizes the clusters strongly. According to our simulations, a large fraction of atmospheric sulphuric acid might be bound into dimethylamine clusters. (See Figure.) These clusters are long lived, and will probably be able to grow to larger sizes.

Ammonia is several orders of magnitude more abundant in the atmosphere than DMA, but it does not stabilize sulfuric acid clusters as effectively. Ammonia containing clusters are also present, but their concentrations are lower and they evaporate faster. These results suggest that dimethylamine or some other amines might be the key to understanding atmospheric new particle formation.

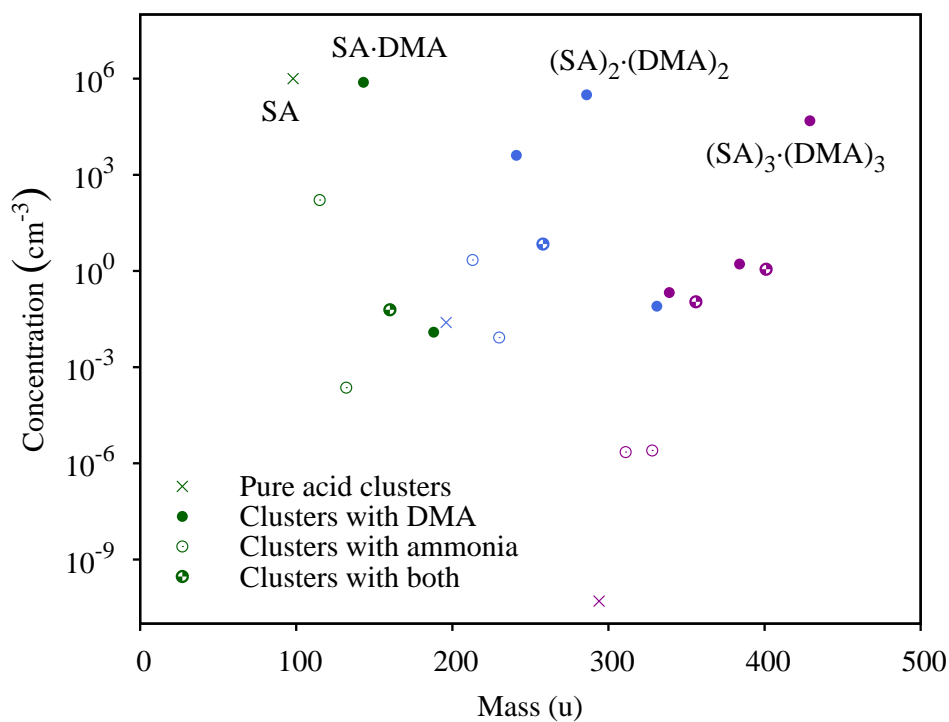


Figure: Simulated distribution of sulphuric acid – ammonia – dimethylamine clusters.
Green: one acid, blue: two acids, purple: three acids.

ACKNOWLEDGEMENTS

This work was supported by FP7-ATMNUCLE project No 227463 (ERC Advanced Grant), Academy of Finland LASTU program project number 135054 and FP7-MOCAPAF project No 257360 (ERC Starting grant). The authors thank the Scientific Computing Center (CSC), Espoo, Finland, for the computing time.

THE USE OF COMPUTATIONAL CHEMISTRY IN MODELING THE CHEMISTRY AND PHYSICS OF ATMOSPHERIC NUCLEATION AND NUCLEATION PRECURSOR GASES

T. KURTÉN, I. K. ORTEGA, O. KUPIAINEN AND H. VEHKAMÄKI

Division of Atmospheric Science, Department of Physics, University of Helsinki, Finland

Keywords: Nucleation, Atmospheric Chemistry, Sulfuric Acid, Computational Chemistry

INTRODUCTION

Nucleation - the agglomeration of gas-phase molecules into small clusters, and the growth of these clusters into larger particles - is one of the most challenging objects of study in the field of atmospheric science. This process very likely involves both reduced nitrogen compounds and oxidized sulfur compounds such as sulfuric acid. Thus, nucleation couples together the global biogeochemical sulfur and nitrogen cycles, and is ultimately one of the key factors in determining how compounds of low volatility flow through our atmosphere.

Due to the very small (nanometer or even sub-nanometer scale) size and low ambient concentration (normally only some hundreds or a few thousands per cm^3) of the nucleating clusters, experimental studies on their chemical identity are extremely difficult to carry out. Recent developments in cutting-edge high-resolution mass spectroscopy are starting to permit the unambiguous chemical characterization of charged atmospheric clusters starting from the molecular scale. However, mass spectrometric methods require the clusters to be charged, and therefore do not yield direct information on the atmospherically much more important neutral clusters. Depending on the charging mechanism used in the instruments, some cluster types may not be charged, others may be broken up or chemically completely altered by the process, and entirely new and artificial cluster types may be formed.

Computational chemistry, including both molecular dynamics and several flavours of quantum chemistry (semiempirical approaches, density functional theory and wavefunction-based methods), is becoming an increasingly common tool for modelling atmospheric chemical and physical processes such as nucleation. Especially quantum chemical methods are an attractive choice for treating new systems, as they do not need any system-specific parameters. Also, computational results can, at least in principle, be systematically improved upon by using higher levels of theory, allowing some estimate of the error margins.

RECENT RESULTS

Quantum chemistry methods have recently been used both to investigate the chemical reactions leading to the formation of aerosol precursor vapors, as well as the initial steps of the clustering of these precursors. For example, the night-time oxidation of the biogenic sulfur compounds DMS (dimethyl sulfide) and especially DMSO (dimethyl sulfide oxide) by the nitrate radical (NO_3) has been computationally shown (Kurtén et al., 2010a) to be an important component of their total atmospheric sink. Interestingly, the $\text{DMSO} + \text{NO}_3$ reaction proceeds mainly via an oxygen-transfer channel rather than a hydrogen-abstraction channel (see Figure 1). This illustrates that the atmospheric chemistry of sulfur compounds often displays features that are qualitatively different from that of carbon-hydrogen-oxygen-nitrogen (“CHON”) compounds, which normally do not undergo oxygen-transfer reactions as they have no hypervalent atoms able to accept two new bonds.

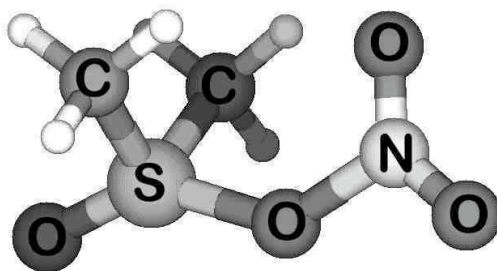


Figure 1. Transition state for the $\text{DMSO} + \text{NO}_3 \Rightarrow \text{DMSO}_2 + \text{NO}_2$ reaction.

Another increasingly common application of computational chemistry to aerosol science is the calculation of evaporation rates. Since the collision reactions forming the nucleation-relevant clusters are kinetically quite simple (and likely involve no significant activation energies or energy non-accommodation; see Kurtén et al., 2010b), the cluster evaporation rates can be straightforwardly calculated from the formation free energies using the law of mass balance. We have recently computed formation free energies and evaporation rates for a large set of clusters consisting of sulfuric acid together with several different nitrogen-containing base molecules; mainly ammonia and a variety of small amines. These results help estimate the relative importance of different base molecules in enhancing sulfuric acid nucleation, and also provide input for larger-scale modeling such as cluster dynamics or aerosol dynamics simulations.

Computed evaporation rates (Ortega et al., 2011) for clusters with 1-4 sulfuric acid molecules and 1 or 2 base molecules are shown in Figures 2 and 3, respectively. Ammonia and dimethylamine (DMA) are used as representative examples of atmospheric bases.

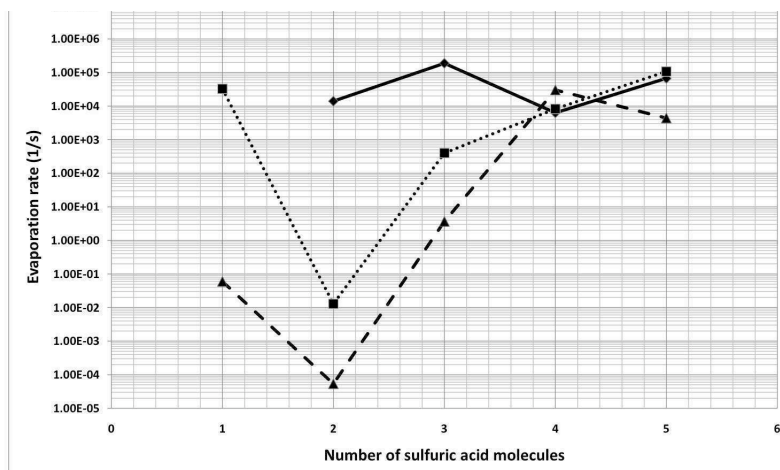


Figure 2. Evaporation rates of sulfuric acid clusters containing 0 or 1 base molecule. Solid line: clusters of pure sulfuric acid. Dotted line: clusters with one ammonia molecule. Dashed line: clusters with one dimethylamine molecule.

Figures 2 and 3 demonstrate how the presence of base molecules significantly stabilize sulfuric acid clusters with respect to acid evaporation, as shown also by laboratory and field experiments. Furthermore, the stabilizing effects of amines may in some conditions and for some cluster types be significantly larger than that of ammonia, though the precise comparison depends on the type of amine, the relative concentration of the different bases, and the cluster size. The figures also indicate that at some base concentrations, atmospheric nucleation may involve local minima on the free energy surface, in addition

to the free energy maximum known as the critical cluster. This is significant, as the existence of free energy minima renders the most common applications of the nucleation theorem invalid. Specifically, in the presence of local minima, the slope of the logarithm of the nucleation rate when plotted against the logarithm of the concentration of the nucleating vapor no longer yields any information on the size or composition of the critical cluster (Vehkamäki et al., 2011).

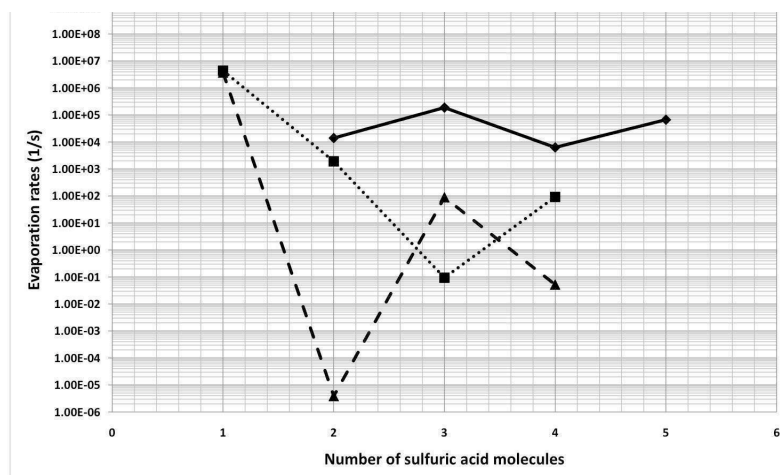


Figure 3. Evaporation rates of sulfuric acid of clusters containing 0 or 2 base molecule. Solid line: clusters of pure sulfuric acid. Dotted line: clusters with two ammonia molecules. Dashed line: clusters with two dimethylamine molecules.

CONCLUSIONS

Computational chemistry is a useful tool for studying the chemical and physical reactions of atmospheric nucleation precursors and nucleating clusters. Calculated evaporation rates demonstrate the importance of base molecules in stabilizing atmospheric sulfuric acid clusters, and also imply that stable pre-critical clusters (“local minima”) may exist in the atmosphere. The latter result may have significant implications for the analysis of field data on nucleation rates.

ACKNOWLEDGEMENTS

We thank the CSC IT centre in Espoo, Finland for computing time.

REFERENCES

- Kurtén, T., Lane, J. R., Jørgensen, S. and Kjaergaard, H. G. (2010a). Nitrate radical addition-elimination reactions of atmospherically relevant sulfur-containing molecules. *Phys. Chem. Chem. Phys.* **12**,12833.
- Kurtén, T., Kuang, C., Gómez, P., McMurry, P. H., Vehkamäki, H., Ortega, I. K., Noppel, M. and Kulmala, M. (2010b). The role of cluster energy nonaccommodation in atmospheric sulfuric acid nucleation. *J. Chem. Phys.* **132**, 024304.
- Ortega, I. K., Kurtén, T., Kupiainen, O., Olenius, T., Wilkman, O., McGrath, M., Kulmala, M., and Vehkamäki, H (2011). From quantum chemical formation free energies to evaporation rates. *Manuscript in preparation*.
- Vehkamäki, H., McGrath, M. J., Kurtén, T., and Kulmala, M. (2011). Rethinking the application of the first nucleation theorem to atmospheric nucleation. *Submitted to Phys. Rev. Lett.*

EVIDENCE OF ANTARCTIC AEROSOL FORMATION DUE TO CONTINENTAL BIOGENIC PRECURSORS

E.-M. KYRÖ¹, A. VIRKKULA², M. DAL MASO¹, J. PARSHINTSEV³, J. RUIZ-JIMENEZ³, H.M. MANNINEN¹, P. HEINONEN⁴, L. FORSTRÖM⁵, M.-L. RIEKKOLA³, K. HARTONEN³ and M. KULMALA¹

¹ University of Helsinki, Department of Physics, P.O.Box 48, 00014 University of Helsinki, Finland

² Finnish Meteorological Institute, Air Quality Research, Erik Palménin aukio 1, P.O.Box 503, 00101 Helsinki, Finland

³ University of Helsinki, Department of Chemistry, P.O.Box 55, 00014 University of Helsinki, Finland

⁴ Finnish Meteorological Institute, Finnish Antarctic Logistics, P.O.Box 503, 00101 Helsinki, Finland

⁵ University of Helsinki, Department of Biological and Environmental Sciences, P.O.Box 65, 00014 University of Helsinki, Finland

Keywords: Antarctic aerosols, new particle formation, secondary organic aerosols.

INTRODUCTION

Atmospheric aerosols present the largest uncertainties in future climate estimations. In Antarctica, their climatic feedbacks are poorly known due to the scarcity of experiments. The largest source of secondary aerosols in Antarctica is the surrounding ocean and its DMS emissions (Davis, 1998; Asmi, 2010), but also long-range transport (Ito, 1993) and intrusion of air from upper atmosphere (Virkkula, 2009) have been linked with the observed new particle formation.

Aerosol and atmospheric chemistry measurements were conducted at the Finnish Antarctic Research Station, Aboa ($73^{\circ}03'S$, $13^{\circ}25'W$), at Queen Maud Land, from December 2009 to January 2010. The purpose of the expedition was to study the sources of new particle formation (NPF) and subsequent growth of aerosols in Antarctica and the results can hopefully give new insight into this. It has already earlier been observed that at Aboa, the particle formation takes place in airmasses coming along the coast (Koponen, 2003) and even the contribution of the secondary organic aerosols (SOA) to the growth of aerosol particles has been discussed (Virkkula, 2006; Virkkula, 2009). In addition, the observed growth of the smallest cluster ions suggests that the nucleation in Antarctica can occur even in the boundary layer (Asmi, 2010).

Aboa is built on a nunatak Basen, approximately 500m ASL, 130km away from the open ocean. A small aerosol research laboratory (Fig.1), where the measurement devices were kept, is built some 200m away, North-East from the main station.

METHODS

The concentrations of neutral and charged particles as well as their size distribution, ozone concentration and filter samples were taken from the atmosphere, about 3m above the ground level. The prevailing wind direction at the station is North-East and thus the contamination by the main station can be greatly minimized.

The neutral particle size distribution from 10 – 500nm was measured using a Differential Mobility Particle Sizer (DMPS) (Aalto, 2001) and Air Ion Spectrometer (AIS) was used to measure the charged particle size distribution from 0.80 – 42nm (Hirsikko, 2005). A UV-photometric monitor was used to measure the ozone concentration and the filters were changed three times a week. Different chemical compounds from the filter samples were analyzed later in Finland with a comprehensive two dimensional gas chromatography-time-of-flight mass spectrometry (GCxGC–TOF–MS). With this methodology, a great amount of different organic compounds can be detected. Additionally, biological samples from top of Basen were taken in the beginning of January and they were kept frozen until they were analyzed.



Figure 1: Location of the aerosol research laboratory (ARL), Aboa main station and Wasa.

RESULTS AND DISCUSSION

The meteorological conditions were usual summertime conditions at Aboa. The median temperature, wind speed and relative humidity were -5°C , 4.6ms^{-1} and 76.0%, respectively. The median particle concentrations during the campaign can be seen from Table 1 and the timeseries of the total and nucleation mode neutral particle concentration from Fig. 2.

Device	Size range	Concentration (cm^{-3})
DMPS	Total	221.4
	Nucleation mode	14.9
	Aitken mode	101.1
	Accumulation mode	97.5
AIS, negative	Total	518.9
	Cluster ions	395.9
	Intermediate ions	1.7
AIS, positive	Total	356.0
	Cluster ions	283.7
	Intermediate ions	3.6

Table 1: Median particle concentrations during the measurement campaign.

During the campaign, three periods of NPF were observed — in the beginning of the campaign, in the beginning of January and in the end of the campaign (Fig. 2). On contrary to the observations by Virkkula *et al.* (2009), most of the events were not associated with intrusion of air from higher altitudes. The obtained formation and growth rates were comparatively high for Antarctica (Kulmala, 2004), order of 1 – 10nm/h.

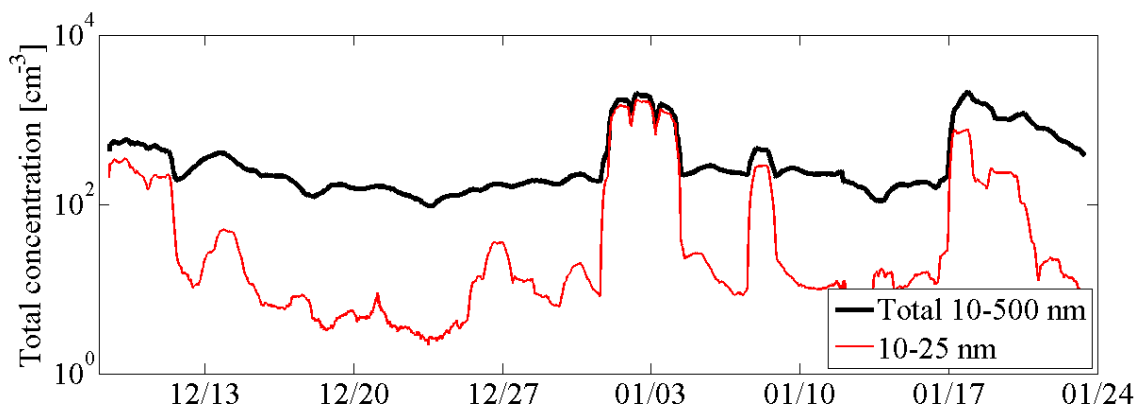


Figure 2: Time series of measured meteorological parameters as well as ozone and total particle concentration. Event-periods are separated by red vertical lines.

The most interesting nucleation period happened 1.1. – 3.1.2010, during which the NPF was unusually frequent and intense for Antarctica. Also, to our knowledge, this was the first time that apple-type events were observed with a DMPS system in Antarctica. During this time, the wind direction was North–East and the airmasses were arriving to the station along the coastline, but above the Gjelsvikfjella and Sør–Rondane -mountain ranges.

The possible connection between the biological activity on the nunatak and new particle formation and subsequent growth has been studied. The concentration of sulphuric acid that is needed to explain the observed growth and the one that is given by the kinetic nucleation $J = K[H_2SO_4]^2$ have been calculated.

If some of the observed particle formation proves to be originated in the nunatak, it would be the first evidence of Antarctic new particle formation due to continental biogenic precursors and would help in estimating the climatic feedbacks of aerosols in Antarctica.

ACKNOWLEDGEMENTS

This work was financed by the Academy of Finland (project no. 127534) and the Academy of Finland Centre of Excellence program (project no 1118615).

REFERENCES

- Aalto, P. *et al.* (2001). Physical characterization of aerosol particles during nucleation events. *Tellus*, **53B**, 344–358.
- Asmi, E. *et al.* (2010). Hygroscopicity and chemical composition of Antarctic sub-micrometre aerosol particles and observations of new particle formation. *Atmos. Chem. Phys.*, **10**, 4253–4271.
- Davis, D. *et al.* (1998). DMS oxidation in the Antarctic marine boundary layer: Comparison of model simulations and field observations of DMS, DMSO, DMSOz, H₂SO₄(g), MSA(g), and MSA(p). *JGR*, **103 (D1)**, 1657–1678.
- Hirsikko, A. *et al.* (2005). Annual and size dependent variation of growth rates and ion concentrations in boreal forest. *Boreal Environ. Res.*, **10**, 357–369.

- Ito, T. (1993). Size distribution of Antarctic submicron aerosols. *Tellus*, **45B**, 145–159.
- Koponen, I. K. *et al.* (2003). Number size distributions and concentrations of the continental summer aerosols in Queen Maud Land, Antarctica. *JGR*, **108 (D19)**, 4587.
- Kulmala, M. *et al.* (2004). Formation and growth rates of ultrafine atmospheric particles: a review of observations. *J. Aerosol Sci.*, **35**, 143–176.
- Virkkula, A. *et al.* (2006). Chemical size distributions of boundary layer aerosol over the Atlantic Ocean and at an Antarctic site. *JGR*, **111**, D05306.
- Virkkula, A. *et al.* (2009). Review of Aerosol Research at the Finnish Antarctic Research Station Aboa and its Surroundings in Queen Maud Land, Antarctica. *Geophysica*, **45**, 163–181.

NEW CONTINENTAL AFRICAN SUPERSITE FOR ATMOSPHERIC OBSERVATIONS

L. LAAKSO^{1,2,3}, V. VAKKARI¹, H. LAAKSO¹, M. KULMALA¹, P. BEUKES², P. VAN ZYL², J.J. PIENAAR², P. TIITTA², M. JOSIPOVIC², A. VENTER², K. JAARS², W. BOOYENS², M. AURELA³, T. LAURILA³, A. LAAKSONEN³, D. WORSNOP^{1,3,4}

¹Department of Physics, University of Helsinki, P.O. BOX 64, 00014 University of Helsinki, Finland

²School of Physical and Chemical Sciences, North-West University, Potchefstroom, South Africa

³Finnish Meteorological Institute, Research and Development, P.O. BOX 503, FI-00101, Finland

⁴Aerodyne Inc, USA

Keywords: SOUTH AFRICA, AEROSOLS, ECOSYSTEM, TRACE GASES, MEGACITIES

Megacities pose an increasing source of pollution due to migration to urban areas. This development is pronounced in developing countries, where economical possibilities for regional area planning are limited. Due to uncontrolled migration, new population often settle in informal settlements around the actual city areas. This is also the case in South Africa, where the Gauteng Metropolitan conurbation (Johannesburg, and Pretoria greater metropolitan areas) continuously grows and has become the most important economical area in Africa.

OBSERVATIONS

A new comprehensive measurement station (www.welgedund.org) was established 100 km West of Johannesburg on grazed savannah-grassland area with a few local pollution sources, but strongly impacted by the plumes from Gauteng and Mpumalanga industrial Highveld area with more than 10 million people. In addition to pollution plumes, the site experiences frequent injections of clean air from cleaner sparsely populated sector to the West-South-West.

The station is build in and around a mobile measurement trailer utilized in South Africa since 2006 (Laakso et al., 2008; Vakkari et al., 2010), which was placed on its permanent location in May 2010.

The continuous observations at the site are the following:

- Trace gases: SO₂, CO, NO_x, O₃ and anthropogenic and biogenic VOC's (2010-2011).
- Aerosol particles: air ion size distributions 0.4-40 nm, aerosol particle size distribution 10-840 nm, PM₁₀, black carbon, 3-λ aerosol scattering, aerosol chemical composition by online Aerosol mass spectrometer (2010-2011), and specific aerosol composition (2010-2011)
- Solar radiation: direct and reflected PPF (Photosynthetic Photon Flux Density) and global radiation, and net radiation
- Meteorology: precipitation, wind speed and direction, temperature at different heights and relative humidity.
- Ecosystem: sensible and latent heat fluxes, CO₂ flux, and soil temperature and moisture at different depths.

RESULTS AND CONCLUSIONS

The first year of measurements has revealed the advantages of the measurement location for the studies of the environmental impacts from Gauteng 'mega-city' area. During the easterly winds, concentration of accumulation mode aerosol particles and trace gases reach very high values (Figure

1), capable of affecting radiative balance and causing damages on the regional ecosystem, whereas during the westerly winds, all concentrations are low. During the dry season (May-September), the site was frequently hit by plumes of regional and local wild fires. The ecosystem measurements clearly showed the onset of photosynthesis and pulsed nature of the respiration following the precipitation events. The current focus of the studies is on ageing of the plume during the day time with high oxidising capacity and night-time with low O₃ and OH concentrations. Another research focus is on the validation of regional water balance models, which almost completely lack continuous boundary layer measurements of water exchange.

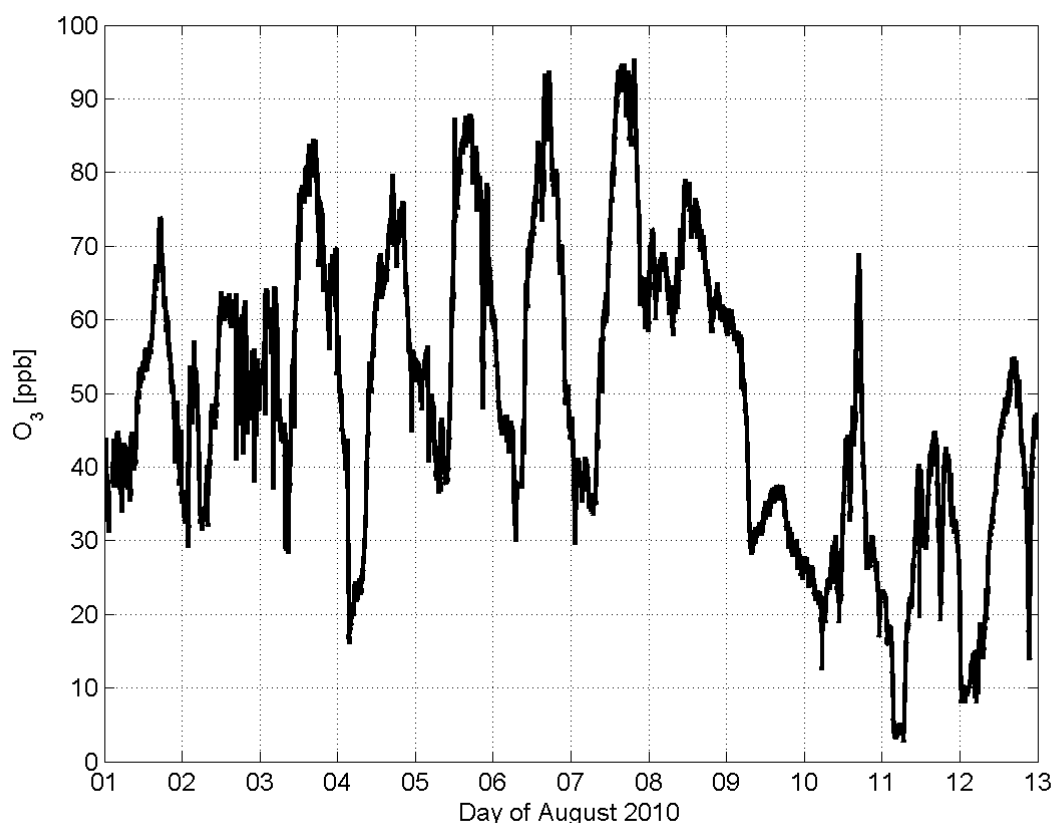


Figure 1. Ozone concentration at the Welgegund measurement site in the beginning of August 2010.

ACKNOWLEDGEMENTS

This work was supported by the Academy of Finland and the Rustenburg local municipality.

REFERENCES

- Laakso, L., Laakso, H., Aalto, P. P., Keronen, P., Petäjä, T., Nieminen, T., Pohja, T., Siivola, E., Kulmala, M., Kgabi, N., Molefe, M., Mabaso, D., Phalatse, D., Pienaar, K., and Kerminen, V.-M. (2008). Basic characteristics of atmospheric particles, trace gases and meteorology in a relatively clean Southern African Savannah environment. *Atmos. Chem. Phys.*, **8**, 4823–4839.
- Vakkari, V., Laakso, H., Kulmala, M., Laaksonen, A., Mabaso, D., Molefe, M., Kgabi, N., and Laakso, L. (2011). New particle formation events in semi-clean South African savannah. *Atmos. Chem. Phys.*, **11**, 3333-3346.
- www.welgegund.org (cited 27.4.2011)

MODELLING DAY-TIME CONCENTRATIONS OF BIOGENIC VOLATILE ORGANIC COMPOUNDS IN A BOREAL FOREST CANOPY BASED A SOURCE ORIENTED APPROACH

H.K. LAPPALAINEN^{1,2}, S. SEVANTO^{2,4}, M. DAL MASO², R. TAIPALE², M.K. KAJOS², P. KOLARI³ and J. BÄCK³

¹Finnish Meteorological Institute, P.O. Box 503, FI-00101 Helsinki, Finland

²Department of Physics, P.O. Box 64, FI-00014 University of Helsinki, Finland

³Department of Forest Ecology, P.O. Box 27, FI-00014 University of Helsinki, Finland

⁴Current address: Earth and Environmental Sciences Division, Los Alamos National Laboratory, Los Alamos, NM 87545 USA

Keywords: biogenic volatile organic compounds, temperature, photosynthesis, concentrations

INTRODUCTION

Integrated studies of measurements and modeling of atmospheric BVOC concentrations and emissions in different temporal scales are an important part of our attempts to understand biosphere-atmosphere interactions and atmospheric chemistry in the lower atmosphere. The production of BVOCs in plants, as well as the activity of the pathway for their release to the atmosphere is partly controlled by the same factors that control atmospheric chemistry and thus the concentration forming from the emissions. This makes it challenging both to measure and model BVOC concentration in the atmosphere (Penuelas and Llusia 2001).

The photosynthetic reactions are main biological processes synthesizing most of the precursors of biogenic VOCs and are strongly temperature driven. Temperature also affects physical properties of VOCs such as gas vapour pressure and the resistance in the emission pathway in the plant tissues (Niinemets et al. 2004). Furthermore, the same environmental factors, temperature and irradiation, controlling the instant photosynthetic activity and BVOC synthesis drive also the long term seasonal emissions via changes in seasonal photosynthetic capacity and this can be reflected in the atmospheric concentrations (Lappalainen et al 2009). In a boreal forest, the seasonal variation of photosynthetic capacity is strongly correlated with a temperature history (Mäkelä et al. 2004). Therefore, also seasonal variation in BVOC emissions could follow the temperature history with this same time constant. This could apply also to the canopy-layer concentrations if the main source of BVOCs is the forest and that the atmospheric life time of the substances is long enough compared to measurement frequency.

Due to the various and interlinked factors regulating emissions and atmospheric chemistry, estimating the atmospheric VOC budget is a very difficult task. The atmospheric chemistry-emission models include information both on BVOC emissions and their atmospheric chemistry reactions and are able to calculate BVOC fluxes (Forkel et al. 2006, Stroud et al 2005). This study was motivated by the fact that current models are heavily parameterized, and therefore their applicability is not as good as would be desired. In this study we analyzed the canopy level VOC concentrations with a simple, source-based approach, assuming they have mainly biogenic sources, and also assuming that potential chemical reactions would be too slow for the compounds in question to influence significantly the measured values.

METHODS

We used two physically separated measurements air concentration measurements of methanol, acetaldehyde, acetone, isoprene, and monoterpene from the SMEAR-II station (Station for Measuring Forest Ecosystem - Atmosphere Relations), in a boreal forest in Hyytiälä (61°51'N, 24°17'E, 181 m asl), southern Finland. The PTR-MS concentrations [ppbv] measured the upper canopy level, at 14 meter height, were conducted during June 2006- August 2007 and June-August 2008 (Taipale et al. 2008). We used this data to study three different, biologically justified statistical models for BVOC day-time atmospheric concentrations. The basis of all the models was on the exponential relationship between air temperature and the atmospheric concentration of volatile organic compounds (VOCs), which was earlier shown to describe well the concentrations above boreal forest (Lappalainen et al 2009).

The chamber measurements near the top of the tree crowns on Scots pine shoots were carried out between 23 March and 25 September 2007 (see Ruuskanen et al. 2005). This dataset was used to analyze the link between shoot emissions and canopy scale concentrations. Meteorological data was obtained from standard half-hourly micrometeorological measurements at the SMEAR-II station.

RESULTS

Preliminary results show that day-time concentrations in a shoot and upper canopy scale are significantly correlated. The high correlation coefficients indicate that the temporal variation in concentrations was remarkably similar, and suggest that the upper canopy measurements follow closely the emissions although these measurements represent different footprint areas.

Temperature model showed that the canopy level air concentrations of methanol and acetone can rather reliably be reproduced using a simple exponential relationship between temperature and concentrations, whereas the acetaldehyde, isoprene and monoterpene concentrations proved to be more difficult to predict with a simple temperature function (Lappalainen et al. 2010). The T-model could explain 66% of the day-time concentration variation of methanol, 0.27% of acetaldehyde, 0.66%, of acetone, 0.65 % of isoprene and 0.27 % monoterpene, respectively. The explanation level of the model improved slightly by adding a biological factor S, based on the temperature dependent recovery of photosynthesis, which was considered to represent the seasonal capacity of a tree to produce and emit volatiles. This T-S- model predicted the general level of daily and seasonal variation of the day-time concentrations somewhat better than the T model for all compounds. However, the model including the seasonal variation in photosynthetic capacity (S) was not able to capture the large variations in concentrations. In order to better capture the large variation, a trigger effect was incorporated to T-S model. Two triggers were tested: relatively high PAR and ozone. Although we attained better fit with the Trigger-model for the 2006-2007 data we were not able to improve the model predictability with the test dataset 2008.

CONCLUSIONS

According to our results a temperature based model could serve as a core approach for further development of a scarce parameterized BVOC concentration model for boreal forests and indicated the role of seasonal variations in photosynthetic efficiency on VOC concentrations. The study also presented the idea of a trigger model for explaining high peak concentrations of VOCs.

This analysis was based on the dataset covering the whole growing season. Although temperature and photosynthetic capacity seem to be the main driving factors on a daily scale, some other processes seem to replace them occasionally and can temporarily be main contributors to BVOC concentrations

above a forest stand. Next step is to analyze on specific time windows such as spring recovery of photosynthesis and drought.

ACKNOWLEDGEMENTS

This work was supported by the Academy of Finland Center of Excellence (project no1118615).

REFERENCES

- Lappalainen H., Sevanto S., Back J., Ruuskanen T., Kolari P., Taipale R., Rinne J., Kulmala M., and Hari P.: Day-time concentrations of biogenic volatile organic compounds in a boreal forest canopy and their relation to environmental and biological factors, *Atmos. Chem. Phys.* 9, 5447-5459, 2009.
- Lappalainen, H.K., Sevanto, S., Dal Maso, M., Taipale, R., Kajos, M.K., and Bäck, J.: Modelling day-time concentrations of biogenic volatile organic compounds in a boreal forest canopy. *Atmos. Chem. Phys. Discuss.*, 10, 20035-20068, 2010.
- Mäkelä, A., Hari, P., Berninger, F., Hänninen, H., and Nikinmaa, E.: Acclimation of photosynthetic capacity in Scots pine to the annual cycle temperature, *Tree Physiology*, 24, 369-378, 2004.
- Niinemets, U., Loreto, F., and Reichstein, M.: Physiological and physicochemical controls on foliar volatile organic compound emissions, *TRENDS in Plant Science*, 9, 180-186, 2004.
- Penuelas, J. and Llusia, J.: The complexity of factors driving volatile organic compound emissions by plants, *Biologia Plantarum*, 44, 481-487, 2001.
- Ruuskanen, T., Kolari, P., Bäck, J., Kulmala, M., Rinne, J., Hakola, H., Taipale, R., Raivonen, M., Altimir, N., and Hari, P.: On-line field measurements of monoterpene emissions from Scots pine by proton mass spectrometry, *Boreal Environment Research*, 10, 553-567, 2005.
- Schade, G.W. and Goldstein A.H.: Seasonal measurements of acetone and methanol: Abundances and implications for atmospheric budgets, *Global Biogeochemical Cycles*, 20, GB1011, doi:10.1029/2005GB002566, 2006.
- Taipale, R., Ruuskanen, T.M., Rinne, J., Kajos, M.K., Hakola, H., Pohja, T., and Kulmala, M.: Quantitative long-term measurements of VOC concentrations by PTR-MS – Part I: Measurement, calibration, and volume mixing ratio calculation methods, *Atmos. Chem. Phys.*, 8, 6681-6698, 2008.

DOCTORAL PROGRAMME IN ATMOSPHERIC COMPOSITION AND CLIMATE CHANGE: FROM MOLECULAR PROCESSES TO GLOBAL OBSERVATIONS AND MODELS (ACCC)

A. LAURI¹, J. BÄCK^{1,2}, T. VESALA¹, A. LAAKSONEN^{3,4}, J. KESKINEN⁵, M.-L. RIEKKOLA⁶, M. HALLIKAINEN⁷, T. HÄME⁸, J. JOKINIEMI⁹, P. PELLIKKA¹⁰, E. NIKINMAA², Y. VIISANEN⁴ and M. KULMALA¹

¹Department of Physics, P.O. Box 48, FI-00014, University of Helsinki

²Department of Forest Sciences, P.O. Box 27, FI-00014, University of Helsinki

³Department of Applied Physics, University of Eastern Finland, P.O. Box 1627, FI-70211 Kuopio

⁴Finnish Meteorological Institute, P.O. Box 503, FI-00101 Helsinki

⁵Department of Physics, Tampere University of Technology, P.O. Box 692, FI-33101 Tampere

⁶Department of Chemistry, P.O. Box 55, FI-00014 University of Helsinki

⁷Aalto University, School of Electrical Engineering, P.O. Box 13000 FI-00076 Aalto

⁸VTT Technical Research Centre of Finland, P.O. Box 1000, FI-02044 VTT

⁹Department of Environmental Science, University of Eastern Finland, P.O. Box 1627, FI-70211 Kuopio

¹⁰Department of Geosciences and Geography, P.O. Box 64, FI-00014 University of Helsinki

TRAINING AND KNOWLEDGE TRANSFER GOAL

The Doctoral Programme in Atmospheric Composition and Climate Change: From Molecular Processes to Global Observations and Models (ACCC) started in its present form in the beginning of 2010. The chief goal of the Programme is to educate a next generation of top-level scientists and experts with all the necessary multidisciplinary skills to tackle the future challenges of climate change, air quality matters and environmental technologies. The supra disciplinary education will enable those experts to serve at different challenging positions in society and industry. Beside classical curriculum skills and knowledge the education on the state-of-art measurement technologies (laboratory, ground-based and remote sensing) are emphasized. The ACCC Doctoral Programme is the only effort at a national level in advanced and comprehensive climate change research education with main focus on training of students in the field of atmospheric and biogeochemical sciences covering phenomena from the nanoscale to the global level and from nanoseconds to centuries.

ACCC PROGRAMME: FACTS AND FIGURES

The predecessor of the ACCC Doctoral Programme, the Graduate School in Physics, Chemistry, Biology and Meteorology of Atmospheric Composition and Climate Change, which involved three universities, two research institutes and one private enterprise, was very successful in combining and developing the doctoral training given in several physical, chemical, meteorological, and ecological research groups. The Graduate School had three strong backbones: an advanced research infrastructure (SMEAR stations and laboratories), a powerful researcher community (Finnish Centre of Excellence), and an existing training structure based on best practices collected from several universities in Nordic and Baltic countries (CBACCI, 2003). The investments made in the doctoral training have been extremely profitable. The participating research groups have gained a lot of international interest especially from students from different countries willing to carry out their PhD studies in the groups in Finland.

The ACCC Doctoral Programme is an extension of the former Graduate School. All the scientific fields of the previous Graduate School, namely Aerosol Physics and Technology, Meteorology, Atmospheric and Analytical Chemistry, Ecosystem Ecology and Ecophysiology are represented. Since the beginning of 2010, a new component in the Doctoral Programme has been the inclusion of global observations both from ground and space platforms – remote sensing technologies and applications, and radio science and engineering. The total number of students in the Doctoral Programme is currently 120. The ACCC Programme currently holds 12 doctoral student positions financed directly by the Ministry of Education and Culture.

From the beginning of 2010, the core of the Doctoral Programme has included four universities, four research institutes, and five private enterprises:

- University of Helsinki (Department of Physics, Department of Forest Sciences, Department of Chemistry, Department of Geography)
- University of Eastern Finland (Department of Physics and Mathematics, Department of Environmental Sciences)
- Tampere University of Technology (Department of Physics)
- Aalto University School of Science and Technology (Department of Radio Science and Engineering, Department of Surveying)
- Finnish Meteorological Institute (units in Helsinki and Kuopio)
- Finnish Geodetic Institute
- VTT Technical Research Centre of Finland
- Finland's Environmental Administration (SYKE)
- Vaisala Ltd.
- Beneq Ltd.
- Space Systems Finland Ltd.
- Helsinki Aerosol Consulting Ltd.
- Airmodus Ltd.

From the beginning of 2012, two new private enterprises will be involved:

- Arbonaut Ltd.
- MosaicMill Ltd.

The Doctoral Programme is operating within the Strategic Centre for Science, Technology and Innovation in Energy and Environment, coordinated by CLEEN Ltd.

The partners in the program are shown by a shell-shaped structure shown in Figure 1.

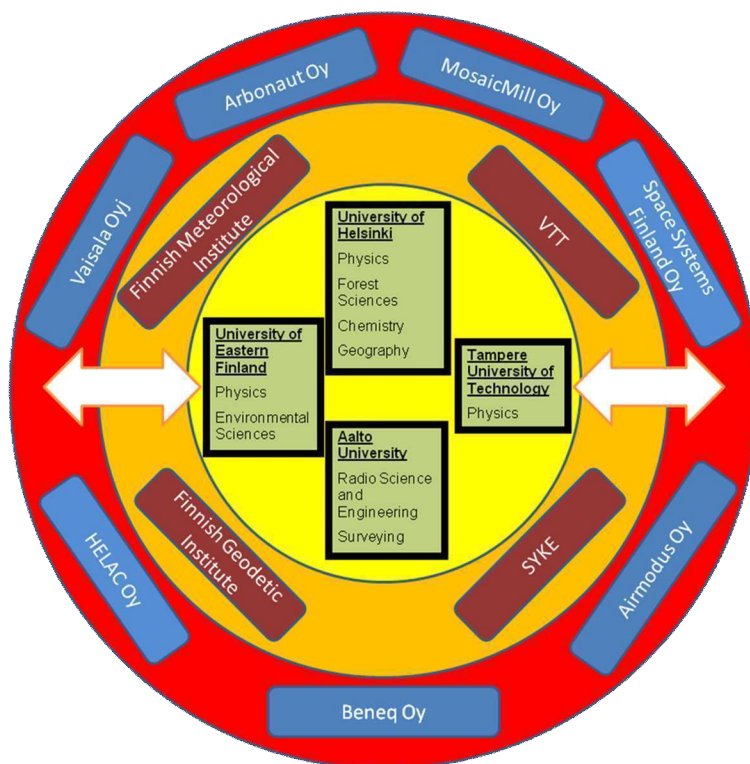


Figure 1. The current composition of the ACCC Doctoral Programme.

In Fig. 1, the four universities are in the core – all the Doctoral Programme students are enrolled as doctoral students in one of these four universities, and also the majority of the ACCC students (77% in 2008-2009) are being employed by one of these universities. The universities are also responsible in providing the required formal training including courses and transferable skills. The four participating research institutes are placed in the middle shell. In 2008-2009, 23% of the ACCC students were employed by these research institutes. The research institutes are strongly connected with the universities – there are common guidance groups, joint research projects, and joint professors and other senior staff members. The seven private enterprises are in the outermost shell. They operate with issues related to the research questions within the Doctoral Programme, but each of them has a more specific focus (e.g. instrument development). The enterprises are full members of the ACCC consortium, they participate actively in the Doctoral Programme, and they have strong connections with both the universities and research institutes involved.

In 2008-2009, a total of 24 doctors graduated in the Doctoral Programme. The mean period used for doctoral studies was 7.4 years, while the median was 6.5 years. These exceptionally long periods are partly explained by the fact that several graduates had extensive tasks not directly related to their research. If these graduates are excluded, the mean and median values were 5.4 and 5.0 years, respectively. Concerning the graduated Ministry-funded students, the mean period used for doctoral studies was 4.0 years.

It is foreseen that the development of the supervision and follow-up of the Doctoral Programme students will result in a shortened doctoral study period. The general timeline of studies in the Programme is presented below:

Year 1: Summer school, winter school, courses, workshop, research

Year 2: Courses (focus on training in transferable skills), workshop, research

Year 3: Research, manuscripts, papers, workshop, seminar course

Year 4: Ph.D. thesis final papers ready, summary

Currently there are 32 foreign postgraduate students in our Doctoral Programme. Our research groups are internationally well-known and attractive for foreign students. Furthermore, it is comparatively easy for foreigners to adjust working in our research groups, since there is an existing population of foreign students, and the main teaching and research language at our institutes is English. Finally, the participating units have recognised the importance of providing support in practical arrangements (housing, immigration etc.), and there are persons dedicated to take care of these arrangements in the research groups. The Doctoral Programme units use also special grants to attract foreign students.

The ACCC consortium has been successful to recruit internationally well-known top scientists to work in Finland. There are currently two FiDiPro professors and 20 other foreign senior scientists within the Doctoral Programme. They participate very actively in supervision, and also give courses according to the same principles as Finnish senior scientists. Furthermore, there are currently six ACCC supervisors whose affiliation is abroad.

INTEGRATION TO RESEARCH ACTIVITIES

The Doctoral Programme is in a strong symbiotic relationship with the Finnish Centre of Excellence in Physics, Chemistry, Biology and Meteorology of Atmospheric Composition and Climate Change. The education and knowledge transfer of the Centre of Excellence is formalized in the Doctoral Programme. On the other hand, the Doctoral Programme enhances the visibility of the Centre of Excellence internationally, especially among young researchers and students. The Doctoral Programme is also well related and completely integrated to various other research activities and supported by infrastructures presented in Figure 2.

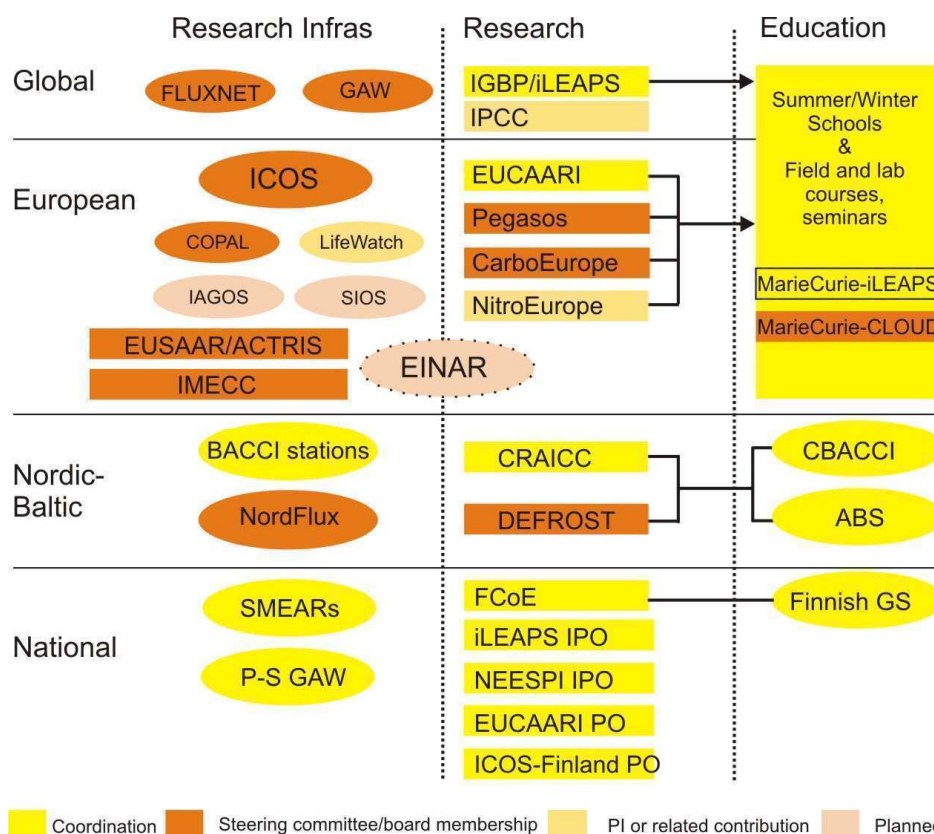


Figure 2. The current and planned activities related to the research infrastructures, major research projects and initiatives, and researcher training within the Doctoral Programme. Abbreviations: ABS=Nordic Master’s Degree Programme in Atmosphere-Biosphere Studies; ACTRIS = European aerosol and atmospheric chemistry infrastructure; BACCI= Research Unit on Biosphere-Aerosol-Cloud-Climate Interactions (former Nordic Centre of Excellence); CBACCI=Nordic-Baltic Graduate School on Carbon-Biosphere-Atmosphere-Cloud-Climate Interactions; CLOUD=Cosmics Leaving Outdoor Droplets (Marie Curie Initial Training Network); COPAL= COMMUNITY heavy-PAYload Long endurance Instrumented Aircraft for Tropospheric Research in Environmental and Geo-Sciences; CRAICC=Nordic Centre of Excellence on Cryosphere-Atmosphere Interactions in a Changing Arctic Climate; DEFROST=Impacts of a changing cryosphere - depicting ecosystem-climate feedbacks as affected by changes in permafrost, snow and ice distribution (Nordic Centre of Excellence); EINAR=European Institute of Atmospheric Sciences and Earth System Research; EUCAARI= European Integrated Project on Aerosol-Cloud-Climate-Air Quality Interactions; EUSAAR= European Supersites for Atmospheric Aerosol Research; FCoE=Finnish Centre of Excellence in Physics, Chemistry, Biology and Meteorology of Atmospheric Composition and Climate Change; GS= Finnish Doctoral Programme ACCC (Atmospheric Composition and Climate Change: from Molecular Processes to Global Observations and Models); IAGOS= In-service Aircraft for Global Observing System; ICOS =Integrated Carbon Observation System; IGBP= International Geosphere-Biosphere Program; iLEAPS=integrated Land Ecosystem Atmosphere Processes Study; IMECC= Infrastructure for Measurements of the European Carbon Cycle; P-S GAW= Pallas-Sodankylä Global Atmosphere Watch Station; PEGASOS= Pan-European Gas-Aerosols-climate interaction Study; SIOS= Svalbard Integrated Arctic Earth Observing System; SMEAR=Station for Measuring Ecosystem-Atmosphere Relations.

Figure 3 shows the spatial and temporal scales of the research methodology (observations, modelling, laboratory experiments).

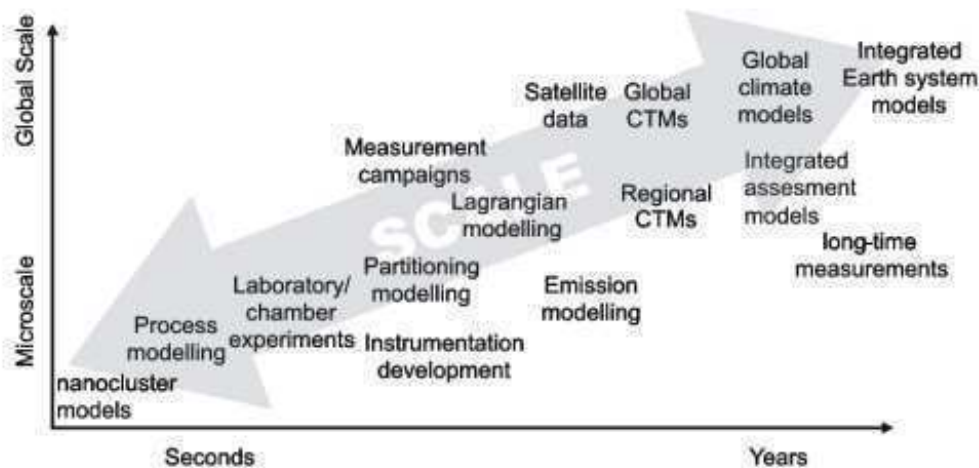


Figure 3. The temporal and spatial range of the research methods applied in the Doctoral Programme. Each partner is linked to one or more research method. The involved universities and research institutes cover a wider range of methods, whereas the private enterprises are more focused.

The Doctoral Programme emphasizes a conceptual approach to the research questions so that each student understands where his or her research is placed in Fig. 3, how it is related to other research topics and fields within the Doctoral Programme.

The specific research topics of the Doctoral Programme include:

- Atmospheric sciences
- Aerosol and environmental physics
- Aerosol technology
- Remote sensing
- Aerosol-cloud-climate interactions
- Biosphere-atmosphere interactions
- Global climate modelling
- Atmospheric chemistry
- Land use change quantification
- Development of aerosol, remote sensing, radar, and environmental technology
- Improved positioning to improve in-situ measurements
- Ubiquitous remote sensing
- Snow and ice studies: evolution of sea ice and snow conditions
- Carbon, water, nitrogen and aerosol cycles and balances
- Air quality

The ACCC Doctoral Programme has currently 111 supervisors/teachers. Thus, the student/teacher ratio is 1.08.

TRAINING AND SUPERVISION

Research and training within the Doctoral Programme includes joint analysis of results, transfer of good practices, and benchmarking. The partners are constantly using web-based tools like Moodle and Blackboard for e-learning, and Adobe Connect Pro for distributing seminars and lectures for a wider audience. In the Doctoral Programme context, new technologies to improve and support researcher education are developed and applied (e.g. Smart-SMEAR; Junninen et al., 2009).

Each Doctoral Programme student is working with the research topics listed in the previous section. In the beginning of doctoral studies, each student writes a study and research plan. The plans also identify the skills to be developed (the gap between the current situation and the desired outcome) and educational activities, including courses and training on transferable skills, which are needed to meet the goals in the specific time window (usually 4 years). The personalized projects often include inter-sectoral visits and/or secondments to another partner institution.

The study and research plan includes:

- conference visits including oral presentations or posters
- short laboratory visits
- international summer and winter schools
- measurement campaigns
- possible long-term visits to foreign universities or research institutes
- active participation in summer and winter schools, workshops and international conferences

The plan is carefully prepared together between the student and the supervisors, and international cooperation is implemented to support the students, their PhD work and further career plans in the best possible way.

During the studies, each student participates in joint courses and workshops. The study plans are designed by recognising the research career as a whole and as a part of that, the aim is that all PhD students finish the thesis in 4 years. Also the prospects for the postdoc period and after that are taken into account.

The joint training is carried out by the following actions:

- Guidance groups
 - Each student belongs to at least one
- Horizontal learning
 - Smooth and barrierless knowledge transfer between different disciplines and levels
- Inter-institutional supervision
 - Currently 40% of Doctoral Programme students
- Teacher workshops
 - Annually

The Doctoral Programme consortium organizes annually several scientific and training events:

- Joint summer and winter schools, field courses
 - 5-6 annually
- Ad hoc courses (courses with special emphasis on a very current research topic)
 - A few annually
- Workshops and conferences
 - Annual workshop for the Doctoral Programme
 - Annual workshop for teachers and supervisors
 - International early career scientist workshops
- Consortium units organize ~10 other conferences and workshops annually, and participate very actively in national and international conferences and workshops
- E-learning courses
 - 2-5 annually, usually organized jointly

The specific topics of the planned summer and winter schools and field courses include:

- Formation and growth of atmospheric aerosols
- Measurements of atmospheric aerosols: aerosol physics, sampling and measurement techniques
- Aerosol-cloud-climate interactions and modelling

- Ion and aerosol dynamics
- Physics and chemistry of air pollution and their effects: field course and data analysis
- Regional and global modelling
- Field course on micrometeorology and hydrology
- Remote sensing and radar technologies
- Land use change monitoring
- Phenology and plant stress
- Arctic air pollution
- Model-data assimilation
- Carbon, water, nitrogen and aerosol cycles
- Climate politics for scientists

These schools combine core and transferable skills, but always ensuring that these skills are learned actively and kept fully relevant to the students' own research. The key transferable skills in the Doctoral Programme are (i) working in the field, (ii) atmospheric instrument technology, (iii) data analysis, (iv) computer modelling, (v) writing articles, (vi) popular science writing, (vii) presentation skills including audiovisual skills, (viii) project management, (ix) writing proposals, and (x) commercialization of scientific ideas.

Each doctoral student participates in one or two guidance groups. A guidance group typically consists of 5-8 students and 2-3 supervisors. The group meets 2-4 times per month. In the group meetings the students report their progress, which is then discussed. Also senior scientist will give general and detailed comments and feedback to students. Currently altogether 13 guidance groups are operating.

The three-day annual meetings include a workshop for all the Doctoral Programme students and a steering committee meeting. In the workshop each Doctoral Programme student presents his/her research in oral and poster sessions to an audience involving the students, supervisors and interest groups. During the annual meeting the steering committee evaluates the functions of the past year, discusses the advancement of the Doctoral Programme students based on the supervisor reports, and decides about the implementation of the next year's activities.

Mobility is an integral part of the doctoral training in ACCC. On the national level mobility is planned on four different levels:

- mobility between Doctoral Programme sites (Helsinki-Kuopio-Tampere-Espoo)
- mobility between research fields (Ecology-Physics-Technology-Chemistry-Meteorology-Geography, in situ observations – space-based remote sensing observations)
- mobility between research methodologies (theory-modelling-experiments-observations)
- mobility between universities, research institutes and business

STRUCTURE, COLLABORATION AND QUALITY ASSURANCE

The ACCC Doctoral Programme has a clear structure, demonstrated by Fig. 4. The Programme is led by the Steering Committee, which includes the research group leaders of the partner universities (8 persons, chairman M. Kulmala) and research institutes (6 persons), and representatives of private enterprises (3 persons). The tasks of the Steering Committee include:

- selection of students
- decision of the joint and international courses and workshops within the Doctoral Programme
- general definitions of policy and decisions concerning the Doctoral Programme

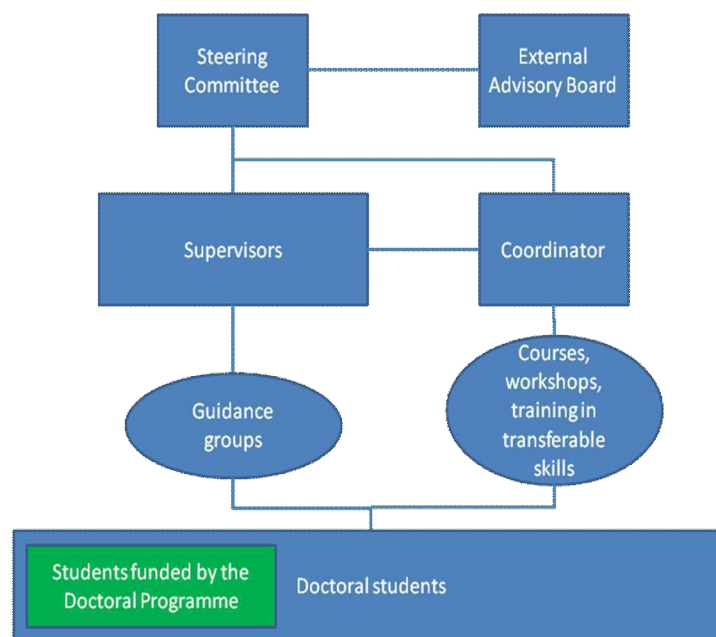


Figure 4. The structure of the ACCC Doctoral Programme.

The Doctoral Programme Steering Committee meets at least twice annually and monitors teaching activities at each host institution and helps the coordinator in joint teaching efforts. The advancement of each student is monitored annually by written reports by the supervisors to ensure early identification of problems. Students other than those funded by the funds allocated by the Academy of Finland are employed through their host organizations and follow the practices at their host institutions. With regard to their graduate education, they are full members of the Programme.

The External Advisory Board, which will start in the beginning of 2012, is a new component of the Doctoral Programme. The External Advisory Board will consist of four academic experts. The initial composition of the External Advisory Board will be the following:

- Prof. Ruprecht Jaenicke, Johannes Gutenberg Universität Mainz (chairperson)
- Prof. Neil M. Donahue, Carnegie Mellon University, USA
- Prof. Pavel Kabat, Wageningen University and Research Centre, the Netherlands
- Prof. Mark Sutton, Centre for Ecology and Hydrology, Edinburgh, UK

The ACCC Programme is constantly evaluated both by self-assessment, by the External Advisory Board and biannually by the Academy of Finland. In the self-evaluation, the following criteria are taken into account:

- Employability of graduates
- Quality and nature of core and transferable skills
- Universities' ability to foresee future challenges in science & society
- The graduates' ability to carry out independent, original research work
- Quality of research
- Publications in high-impact journals
- Number of publications
- Structured and dedicated supervision

Internal evaluation is carried out on different levels. During each classroom course, summer and winter school and workshop, student feedback is collected. The feedback is processed by the Coordinator after each event, and collected in a database. The steering committee discusses the feedback on an annual basis, and implements the improvements in the annual plan of activities.

The External Advisory Board (EAB) and Academy of Finland play the major roles in the external evaluation. EAB members participate in the annual workshop, and give direct feedback to the ACCC students and the Steering Committee. Furthermore, EAB prepares evaluation reports on a regular basis. The reports include suggestions for improvements in the current practices. The Academy of Finland evaluates the Doctoral Programme every second year in connection with the decision of possible new ministry-paid Doctoral Programme positions.

The general guidelines and good practices within the Doctoral Programme include:

- Maintenance, development and dissemination of best practices
- Open and transparent recruitment policy
- Active participation on the national and international policy and education system development
- Use of external evaluation
- Continuation of commitment on all levels (students, postdocs, senior scientists, professors)

In the latest evaluation report (Academy of Finland, 2011), the ACCC Doctoral Programme received the highest possible general grade (6 out of 6). However, it was noted that the other resources available for the Programme are generous. The ACCC Programme was granted three extra doctoral student positions from the beginning of 2012, increasing the total number to 15.

ACKNOWLEDGEMENTS

The funding from the Ministry of Education is gratefully acknowledged. The Graduate School activities have also been supported by the Academy of Finland (projects No. 118780 and 129663). The work has been supported also by the Academy of Finland Center of Excellence program (project number 1118615).

REFERENCES

- Academy of Finland (2011). Evaluation report, proposal #141209, 28 January 2011. Doctoral Programmes 2012-2015.
- CBACCI (2003). CBACCI education structure. Annex of the Steering Committee memorandum of the meeting 5.5.2003 in Oslo, Norway.
- Junninen, H., Lauri, A., Keronen, P., Aalto, P., Hiltunen, V., Hari, P., and Kulmala, M. (2009). Smart-SMEAR: on-line data exploration and visualization tool for SMEAR stations. *Boreal Environ. Res.* 14:447-457.

THE USE OF PARTICLE SIZE MAGNIFIER FOR DETECTION OF PARTICLES SMALLER THAN 2 NM AT THE CLOUD EXPERIMENT

K. LEHTIPALO^{1,2}, A. FRANCHIN¹, S. SCHOBESBERGER¹, J. VANHANEN², J. MIKKILÄ^{1,2}, T. NIEMINEN¹, D. WORSNOP^{1,3}, M. KULMALA¹, and the CLOUD collaboration

¹Department of Physics, University of Helsinki, Helsinki, Finland

²Airmodus Oy, Helsinki, Finland

³Aerodyne Research, Inc., Billerica, MA 01821-3976, USA.

Keywords: nucleation, CLOUD, condensation particle counters

INTRODUCTION

A reason why the molecular level processes leading to atmospheric new particle formation are not yet completely understood has been the inability to detect neutral particles smaller than about 3 nm, and thus directly observe the nucleating particles and their precursors. Condensation particle counters (CPCs) have recently been shown capable of measuring particles also in the sub-2 nm range (Sipilä *et al.*, 2008; Iida *et al.*, 2009; Vanhanen *et al.*, 2011). This allows deriving parameters describing the new particle formation process, *e.g.* the formation and growth rates, directly from measurements.

The CLOUD (Cosmics Leaving OUtdoor Droplets) experiment (Duplissy *et al.*, 2010) was designed to study the possible influence of galactic cosmic rays on the atmospheric new particle formation. A series of nucleation experiments were performed in a 26.1 m³ chamber, which could be exposed to the pion beam from the CERN Proton Synchrotron (PS) to simulate galactic cosmic rays (GCR). Since sulphuric acid has been identified as one of the key compounds in nucleation, the focus has been so far on investigating sulphuric acid nucleation in varying conditions. The measurement sequence allows comparing neutral experiments, in which all ions are filtered out from the chamber to experiments with exactly same conditions but ions created by GCR or the PS present in the chamber.

METHODS

The Airmodus A09 Particle Size Magnifier (PSM) was used at the CLOUD experiments to resolve the concentrations and size distribution of particles smaller than 2 nm. The PSM is a dual-stage mixing-type CPC using diethylene glycol for activating and initial growth of the particles. The cut-off size of the instruments was varied between about 1-2 nm by altering the mixing ratio of saturator and aerosol flow and thus changing the supersaturation created. The relation between the mixing ratio and activation diameter has been determined in laboratory calibrations using mobility standards (Ude and Fernandez de la Mora, 2005) and size-selected tungsten oxide and silver ions (Fig. 1). The nominal 50% cut-off size of the Particle Size Magnifier at the highest mixing ratio is about 1.5 nm (Vanhanen *et al.*, 2011).

The ion concentration and size distribution in the CLOUD chamber was measured with a Neutral cluster and Air Ion Spectrometer, (NAIS, Manninen *et al.*, 2009). The NAIS is able to measure the ion number size distributions in the mobility equivalent diameter range of 0.8 to 40 nm and corresponding neutral particle number size distributions from ~2 to 40 nm in mobility diameter. The ion mass spectra were simultaneously recorded with an Atmospheric Pressure interface Time-Of-Flight Mass Spectrometer (API-TOF; Junninen *et al.*, 2010).

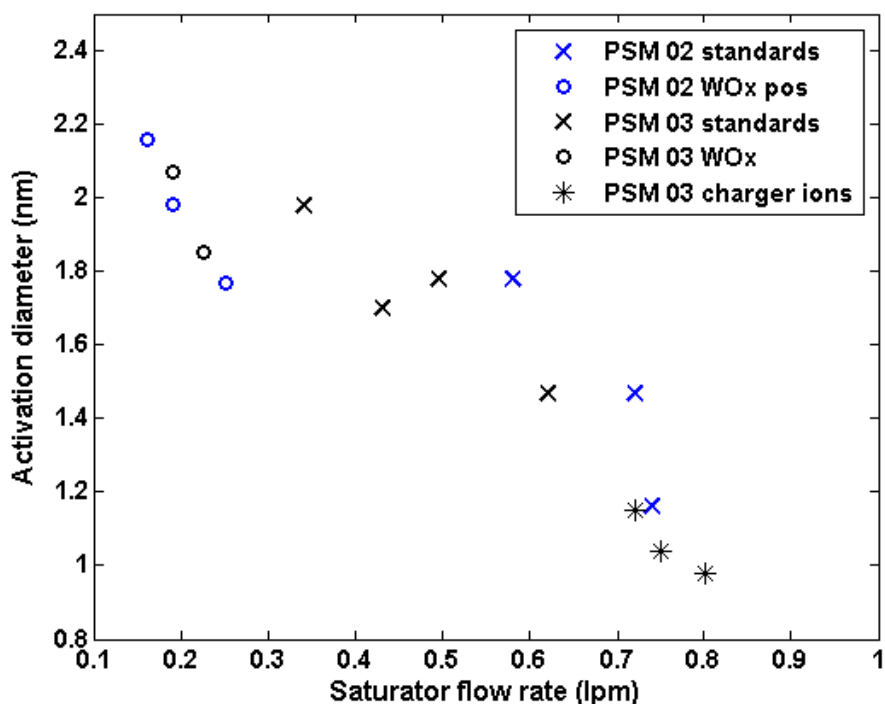


Figure 1. Saturator flow rate at which different sized calibration ions are activated in the PSM. At the CLOUD experiments, the saturator flow rate was scanned between 0.2-1 lpm.

CONCLUSIONS

The Particle Size Magnifier was able to detect clusters and particles right from the start of a nucleation experiment in the CLOUD chamber. The results can be compared to the ions detected with the ion spectrometers; however, the PSM is the only instrument capable of detecting electrically neutral particles smaller than 2 nm. For the first time, size-resolved formation rates and growth rates below 2 nm could be determined directly from measurements for the total particle population. The particle growth rates can also be compared to the growth of sulphuric acid containing clusters identified by the APi-TOF.

ACKNOWLEDGEMENTS

We thank CERN for supporting CLOUD with technical resources, and for providing a particle beam from the CERN Proton Synchrotron. This research has received funding from the EC's Seventh Framework Programme under grant agreement no. 215072 (Marie Curie Initial Training Network "CLOUD-ITN"), from the German Federal Ministry of Education and Research (project no. 01LK0902A), from the Swiss National Science Foundation, and from the Academy of Finland Center of Excellence program (project no. 1118615).

REFERENCES

Duplissy, J., Enghoff, M. B., Aplin, K. L., Arnold, F., Aufmhoff, H., Avngaard, M., Baltensperger, U., Bondo, T., Bingham, R., Carslaw, K., Curtius, J. David, A., Fastrup, B., Gagné, S., Hahn, F., Harrison, R. G., Kellett, B., Kirkby, J., Kulmala, M., Laakso, L., Laaksonen, A., Lillestol, E.,

- Lockwood, M., Mäkelä, J., Makhmutov, V., Marsh, N. D., Nieminen, T., Onnela, A., Pedersen, E., Pedersen, J. O. P., Polny, J., Reichl, U., Seinfeld, J. H., Sipilä, M., Stozhkov, Y., Stratmann, F., Svensmark, H., Svensmark, J., Veenhof, R., Verheggen, B., Viisainen, Y., Wagner, P. E., Wehrle, G., Weingartner, E., Wex, H., Wilhelmsson, M., and Winkler, P. M. (2010). Results from the CERN pilot CLOUD experiment. *Atmos. Chem. Phys.*, **10**, 1635–1647.
- Iida, K., Stolzenburg, M.R., and McMurry, P.H. (2009). Effect of working fluid on sub-2nm particle detection with a laminar flow ultrafine condensation particle counter. *Aerosol Sci. Technol.* **43**, 81-96.
- Junninen, H., M. Ehn, T. Petäjä, L. Luosujärvi, T. Kotiaho, R. Kostianen, U. Rohner, M. Gonin, K. Fuhrer, M. Kulmala and D.R. Worsnop (2010). A high-resolution mass spectrometer to measure atmospheric ion composition, *Atmos. Meas. Tech.* **3**, 1039–1053.
- Manninen, H. E., Petäjä, T., Asmi, E., Riipinen, I., Nieminen, T., Mikkilä, J., Hörrak, U., Mirme, A., Mirme, S. Laakso, L., Kerminen, V.-M., and Kulmala, M. (2009). Long-term field measurements of charged and neutral clusters using Neutral cluster and Air Ion Spectrometer (NAIS). *Boreal Env. Res.*, **14**, 591–605.
- Sipilä, M., Lehtipalo, K., Kulmala, M., Petäjä, T., Junninen, H., Aalto, P.P., Manninen, H.E., Vartiainen, E., Riipinen, I., Kyrö, E.-M., Curtius, J., Kürten, A., Borrmann, S., and O'Dowd C.D. (2008). Applicability of Condensation Particle Counters to measure atmospheric clusters. *Atmos. Chem. Phys.* **8**, 4049-4060.
- Ude S., and Fernandez de la Mora, J. (2005). Molecular monodisperse mobility and mass standards from electrosprays of tetra-alkyl ammonium halides, *J. Aerosol Sci.*, **36**, 1224–1237.
- Vanhanen, J., Mikkilä, J., Lehtipalo, K., Sipilä, M., Manninen, H. E., Siivola, E., Petäjä, T., Kulmala, M. (2011). Particle Size Magnifier for Nano-CN Detection. *Aerosol Sci. Tech.*, **45**, 4, 533-42.

INFLUENCE OF ASYMMETRIC CONCENTRATIONS OF SMALL IONS ON THE AEROSOL CHARGING STATE

J. LEPPÄ¹, S. GAGNÉ², L. LAAKSO^{1,2,3}, M. KULMALA² and V.-M. KERMINEN¹

¹Finnish Meteorological Institute, Climate Change, P.O. Box 503, 00101 Helsinki, Finland

²Department of Physics, University of Helsinki, P.O. Box 64, 00014 Helsinki, Finland

³School of Physical and Chemical Sciences, North-West University, Potchefstroom, South Africa

Keywords: Atmospheric aerosols, Charged particles, Aerosol dynamics, Aerosol modelling

INTRODUCTION

New particle formation has been observed to take place in various conditions in the atmosphere. The actual mechanisms of particle formation are still unknown, but they can be divided into two groups: electrically neutral and ion-induced mechanisms. One way to estimate the fraction of particles formed via ion-induced nucleation is to determine the fraction of charged particles at the size where particles are formed (Laakso *et al.* 2007). However, this fraction cannot usually be measured at such a small sizes due to instrumental limitations.

METHODS

Kerminen *et al.* (2007) derived an equation describing the behaviour of the charging state, S , (i.e. the quotient of the charged fraction, f^c , and the charged fraction in the bipolar equilibrium, f_{eq}^{\pm}) as a function of diameter using several simplifying assumptions. With the use of the equation, a curve can be fitted to the measured values of S to extrapolate the value of S at the size of particle formation, which can then be used to estimate the fraction of ion-induced nucleation. Iida *et al.* (2007) derived a method to determine also the diameter growth rate of particles based on the behaviour of the charged fraction.

Both Kerminen *et al.* (2007) and Iida *et al.* (2007) assumed symmetric concentrations of negatively and positively charged small ions (diameter $< \sim 2.0$ nm) as well as negatively and positively charged particles. In this study we have derived an equation describing the behaviour of charging state and developed a method to determine the particle growth rate from the charged fraction in a charge asymmetric framework.

To begin with, we modify the balance equations used by Kerminen *et al.* (2007) by allowing dissimilar values for negatively and positively charged small ions and particles. We also assume coagulation processes to be negligible, in which case the balance equations may be written as:

$$\frac{dN_0}{dt} = -\beta_0^- N_c^- N_0 - \beta_0^+ N_c^+ N_0 + \alpha N_c^- N_+ + \alpha N_c^+ N_- \quad (1)$$

$$\frac{dN_-}{dt} = \beta_0^- N_c^- N_0 - \alpha N_c^+ N_- \quad (2)$$

$$\frac{dN_+}{dt} = \beta_0^+ N_c^+ N_0 - \alpha N_c^- N_+ \quad (3)$$

where N_0 , N_- and N_+ are the concentrations of neutral, negatively charged and positively charged particles, respectively, N_c^- and N_c^+ are the concentrations of negatively and positively charged small ions, respectively, α is the attachment coefficient between a small ion and an oppositely charged particle, β_0^q is the attachment coefficient between a neutral particle and a small ion with charge state q .

The charged fractions are, by definition:

$$f_- = \frac{N_-}{N_0 + N_- + N_+} = \frac{N_-}{N_{\text{tot}}} \quad (4)$$

$$f_+ = \frac{N_+}{N_0 + N_- + N_+} = \frac{N_+}{N_{\text{tot}}} \quad (5)$$

In the atmosphere, the charged fractions evolve towards a value in a steady state. In the case of asymmetric concentrations of small ions, the steady state charged fractions, f_{asy}^\pm , can be calculated from Eqs. 1-5 by setting the time derivatives in Eqs. 1-3 to zero and substituting the resulting particle concentrations to Eqs. 4 and 5:

$$f_{\text{asy}}^- = \frac{\beta_0^- N_c^-}{\alpha N_c^+ + \beta_0^- N_c^- + \beta_0^+ \frac{(N_c^+)^2}{N_c^-}} \approx \frac{\beta_0^- N_c^-}{\alpha N_c^+} = f_{\text{eq}}^- \frac{N_c^-}{N_c^+} \quad (6)$$

$$f_{\text{asy}}^+ = \frac{\beta_0^+ N_c^+}{\alpha N_c^- + \beta_0^+ N_c^+ + \beta_0^- \frac{(N_c^-)^2}{N_c^+}} \approx \frac{\beta_0^+ N_c^+}{\alpha N_c^-} = f_{\text{eq}}^+ \frac{N_c^+}{N_c^-} \quad (7)$$

According to Eqs. 6 and 7, the ambient charged fractions do not evolve towards the bipolar charge equilibrium, f_{eq} , but towards values that depend on both the values in the charge equilibrium and the relative concentrations of small ions.

The charging state, S , is defined as the ratio of ambient charged fraction and the charged fraction in charge equilibrium. In the case where the concentrations of negatively and positively charged small ions are the same and the fractions of negatively and positively charged particles are the same the behavior of the charging state as a function of diameter is (Kerminen *et al.* 2007)

$$S = 1 - \frac{1}{k d_p} + \frac{(S_0 - 1) k d_0 + 1}{k d_p} e^{-k(d_p - d_0)}, \quad (8)$$

where

$$k = \frac{\alpha N_c}{GR} \quad (9)$$

Here GR is the particle diameter growth rate and S_0 is the charging state at size d_0 . The growth rate is assumed to be constant and same for both the neutral and the charged particles. For the charge asymmetric case, a similar derivation can be made by redefining the charging state as a ratio of ambient charged fraction and the steady state charged fraction presented by Eqs. 6 and 7. With these definitions, the charging states in the charge asymmetric case behave as

$$S_{\text{asy}}^{\pm} = 1 - \frac{1}{k^{\pm}d_p} + \frac{(S_{\text{asy},0}^{\pm}-1)k^{\pm}d_0+1}{k^{\pm}d_p} e^{-k^{\pm}(d_p-d_0)}, \quad (10)$$

where

$$k^{\pm} = \frac{\alpha N_c^{\mp}}{GR}. \quad (11)$$

Here it should be noted that the parameter k^q , which describes the population's ability to retain the charging state q , is dependent on the concentration of oppositely charged small ions.

The behaviors of the charging states as a function of diameter in charge symmetric and asymmetric cases are depicted in Figure 1. Regardless of the initial value at 2 nm, the charging state evolves towards unity in the charge symmetric case as the particles grow bigger. In the charge asymmetric case though, the charging states evolve towards values depending on the relative concentrations of small ions:

$$\lim_{d_p \rightarrow \infty} S^{\pm}(d_p) = \frac{N_c^{\pm}}{N_c^{\mp}}. \quad (12)$$

In order to determine the particle diameter growth rate, we change the coordinate system in Eqs. 1-3 as follows:

$$\frac{d}{dt} = \frac{dd_p}{dt} \times \frac{d}{dd_p} = GR(d_p) \times \frac{d}{dd_p} \quad (13)$$

By introducing the charged fractions defined in Eqs. 4 and 5, Eqs. 2 and 3 can be written in the new coordinate system as

$$GR \times \frac{dN_-}{dd_p} = GR \times N_{\text{tot}} \times \frac{df_-}{dd_p} = \beta_0^- N_c^- N_0 - \alpha N_c^+ N_- \quad (14)$$

$$GR \times \frac{dN_+}{dd_p} = GR \times N_{\text{tot}} \times \frac{df_+}{dd_p} = \beta_0^+ N_c^+ N_0 - \alpha N_c^- N_+ \quad (15)$$

The particle growth rates can then be expressed as

$$GR = \left(\frac{df_-}{dd_p} \right)^{-1} \left((1 - f_- - f_+) \beta_0^- N_c^- - \alpha f_- N_c^+ \right) \quad (16)$$

$$GR = \left(\frac{df_+}{dd_p}\right)^{-1} ((1 - f_- - f_+) \beta_0^+ N_c^+ - \alpha f_+ N_c^-). \quad (17)$$

Eqs. 16 and 17 can be used to estimate the particle growth rate and initial fractions of charged particles during a new particle formation event. This is done by iteratively adjusting the GR and the initial fractions in order to fit the charged fractions as a function of diameter obtained from solving Eqs. 16 and 17 to corresponding values obtained from the measurements.

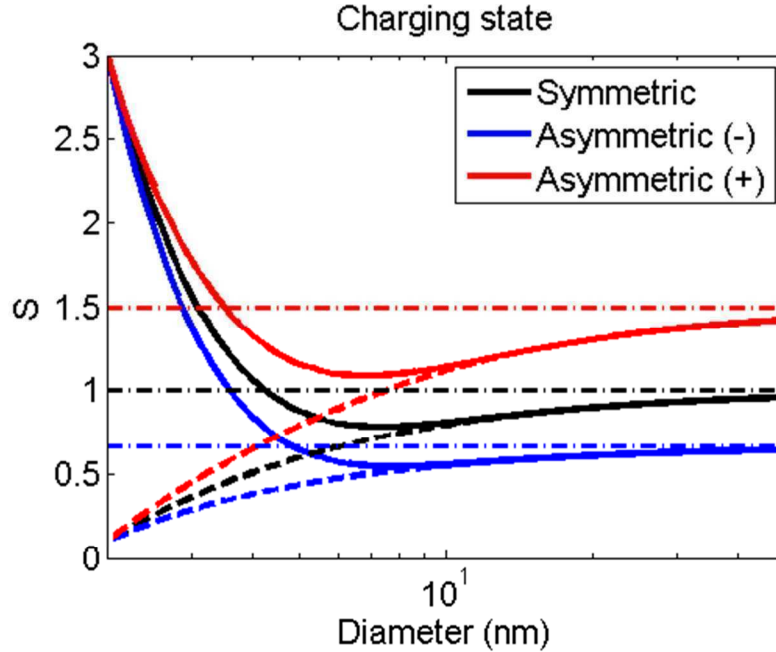


Figure 1. The charging state as a function of diameter. The particle growth rate was 6 nm h^{-1} and the initial charging state at 2 nm was 3 (solid lines) or 0.1 (dashed lines). The small ion concentrations were 500 cm^{-3} in symmetric case and 400 and 600 cm^{-3} for negative and positive ions, respectively, in the asymmetric case. The dashed-dotted lines correspond to values in the steady state.

RESULTS

A series of test simulations were conducted using the aerosol dynamical model Ion-UHMA (Leppä *et al.* 2009). Eq. 10 was used to estimate the initial charging states and Eqs. 16 and 17 were used to estimate the particle growth rate and the initial charged fractions from the simulated data. The estimated values were very close to the values used as input in the model, but it should be noted that the simulated cases were chosen to represent conditions where the assumptions needed when deriving the equations in this study hold. A more comprehensive set of test simulations will be conducted in the near future.

Similarly to many other environments, the average concentrations of negatively and positively charged small ions were observed to be substantially different in urban environment in Helsinki, Finland where charging states were measured using an Ion-DMPS instrument between December 2008 and February 2010 (Gagné *et*

al. 2011). The fraction of ion-induced nucleation and particle diameter growth rates were analyzed both assuming equal concentrations of small ions and without this assumption. The fractions of ion-induced nucleation did not depend much on this assumption. However, the growth rates determined from the charged fraction and particle size distribution agreed better in the charge asymmetric framework.

ACKNOWLEDGEMENTS

This work has been supported by European Commission 6th Framework program project EUCAARI, contract no. 036833-2 (EUCAARI), by Academy of Finland project ComQuaCC, project no. 135199, and the Academy of Finland Centre of Excellence program (project no. 211483, 211484 and 1118615).

REFERENCES

- Gagné, S., J. Leppä, T. Petäjä, M. J. McGrath, M. Vana, V.-M. Kerminen, L. Laakso and M. Kulmala (2011). Measurements of aerosol charging states in Helsinki, Finland, Submitted to *Atmos. Chem. Phys.*
- Iida, K., M. R. Stolzenburg, P. H. McMurry and J. N. Smith (2008). Estimating nanoparticle growth rates from size-dependent charged fractions: Analysis of new particle formation events in Mexico City, *J. Geophys. Res.*, **113**, D05207.
- Kerminen, V.-M., T. Anttila, T. Petäjä, L. Laakso, S. Gagné, K. E. J. Lehtinen and M. Kulmala (2007). Charging state of the atmospheric nucleation mode: Implications for separating neutral and ion-induced nucleation, *J. Geophys. Res.*, **112**, D21205.
- Laakso, L., S. Gagné, T. Petäjä, A. Hirsikko, P. P. Aalto, M. Kulmala and V.-M. Kerminen (2007). Detecting charging state of ultra-fine particles: instrumental development and ambient measurements, *Atmos. Chem. Phys.* **7**, 1333-1345.
- Leppä, J., V.-M. Kerminen, L. Laakso, H. Korhonen, K.E.J. Lehtinen, S. Gagné, H.E. Manninen, T. Nieminen and M. Kulmala (2009). Ion-UHMA: a model for simulating the dynamics of neutral and charged aerosol particles, *Boreal Env. Res.*, **14**, 559–575.

SIMULATION ON THE CONTRIBUTION OF BIOGENIC VOCs TO THE NEW PARTICLE FORMATION FROM JÜLICH PLANT CHAMBER MEASUREMENTS

L. LIAO¹, M. BOY¹, T. F. MENTEL², E. KLEIST², D. MOGENSEN¹, M. KULMALA¹, and M. DAL MASO¹

¹Department of Physics, University of Helsinki, P.O.Box 48, 00014, Helsinki, Finland

²Phytosphäre, Forschungszentrum Jülich, 52425, Jülich, Germany

Keywords: Aerosol, New particle formation, Terpenes, Sulphuric acid.

INTRODUCTION

Biogenic VOCs are substantially emitted from vegetation to atmosphere, and their emissions have been estimated to be of the order of 1150 Tg per year globally (Guenther *et al.*, 1995). Isoprenoids and terpenoids, including e.g. isoprene (C₅H₈), monoterpenes (C₁₀H₁₆), and sesquiterpenes (C₁₅H₂₄) are the most abundant BVOCs, accounting for over 50% of BVOC emissions (Guenther *et al.*, 1995). The oxidation of terpenes by OH, O₃, and NO₃ in air generating less volatile compounds may lead to the formation and growth of secondary organic aerosol, and thus presents a link to the vegetation, aerosol, and climate interaction system (Kulmala *et al.*, 2004). Studies including field observations, laboratory experiments and modelling have improved our understanding on the connection between BVOCs and new particle formation mechanism in some extent (see e.g. Tunved *et al.*, 2006; Mentel *et al.*, 2009). Nevertheless, the exact formation process still remains uncertain, especially from the perspective of BVOC contributions.

The purpose of this work is using the MALTE aerosol dynamics and air chemistry box model to investigate aerosol formation from reactions of direct tree emitted VOCs in the presence of ozone, UV light and artificial solar light in an atmospheric simulation chamber. The measured chamber data, including both gas and aerosol phase measurements are used to evaluate the model. This model employs up to date air chemical reactions, especially the VOC chemistry, which may potentially allow us to estimate the contribution of BVOCs to secondary aerosol formation, and further to quantify the influence of terpenes to the formation rate of new particles.

METHODS

Experiments were conducted in the plant chamber facility at Forschungszentrum Jülich, Germany (Jülich Plant Aerosol Atmosphere Chamber, JPAC). The facility consists of three Borosilicate glass chambers (164 L, 1150 L, and 1450 L) with Teflon floors. Either one of the two smaller chambers were served as plant chamber followed by the large chamber as reaction chamber (1450 L). The detail regarding to the chamber facility has been written elsewhere (Mentel *et al.*, 2009). During the experiments, gas phase sulphuric acid was measured by CIMS. VOC mixing ratios were measured by two GC-MS systems and PTR-MS. An Airmodus Particle size magnifier coupled with a TSI CPC and a PH-CPC were used to count the total particle number concentrations with a detection limit close to the expected size of formation of fresh nanoCN. A SMPS measured the particle size distribution. Several other parameters including ozone, CO₂, NO, temperature, relative humidity, and flow rates were also measured.

MALTE is a modular model to predict new aerosol formation in the lower troposphere, developed by Boy *et al.*, (2006). In this study, we use modules that include aerosol dynamics, air chemistry, and organic chemistry of VOCs as a MALTE box model for the chamber simulation. Considering that each individual terpene compound may react quite differently, the generalized parameterizations of terpene chemistry in

models are less used, and most biogenic VOCs will be accounted for individually when modelling the atmospheric new aerosol formation.

CONCLUSIONS

We first evaluate the modelled results with measurements, and further we investigate the influence of different order of magnitude of terpene mixing ratios, especially isoprene and monoterpenes to the most important parameter of new particles formation, i.e. the formation rate (J_1). Also, the influence of varying organic source rates on the sulphuric acid concentration available for particle formation is discussed.

ACKNOWLEDGEMENTS

The Authors wish to thank the Maj and Tor Nessling foundation for financial support (grant No. 2009362), as well as the Academy of Finland (Project No. 128731).

REFERENCES

- Guenther, A., Hewitt, C. N., Erickson, D., Fall, R., Geron, C., Graedel, T., Harley, P., Klinger, L., Lerdau, M., McKay, W. A., Pierce, T., Scholes, B., Steinbrecher, R., Tallamraju, R., Taylor, J., and Zimmerman, P. (1995). A Global-Model of Natural Volatile Organic-Compound Emissions, *Journal of Geophysical Research-Atmospheres*, 100, 8873-8892.
- Boy, M., Hellmuth, O., Korhonen, H., Nilsson, E. D., ReVelle, D., Turnipseed, A., Arnold, F., and Kulmala, M. (2006). MALTE - model to predict new aerosol formation in the lower troposphere, *Atmospheric Chemistry and Physics*, 6, 4499-4517.
- Kulmala, M., Suni, T., Lehtinen, K. E. J., Dal Maso, M., Boy, M., Reissell, A., Rannik, U., Aalto, P., Keronen, P., Hakola, H., Back, J. B., Hoffmann, T., Vesala, T., and Hari, P. (2004). A new feedback mechanism linking forests, aerosols, and climate, *Atmospheric Chemistry and Physics*, 4, 557-562.
- Tunved, P., Hansson, H.-C., Kerminen, V.-M., Ström, J., Dal Maso, M., Lihavainen, H., Viisanen, Y., Aalto, P. P., Komppula, M., and Kulmala, M. (2006). High Natural Aerosol Loading over Boreal Forests, *Science*, 312 (5771), 261-263.
- Mentel, T. F., Wildt, J., Kiendler-Scharr, A., Kleist, E., Tillmann, R., Dal Maso, M., Fisseha, R., Hohaus, T., Spahn, H., Uerlings, R., Wegener, R., Griffiths, P. T., Dinar, E., Rudich, Y., and Wahner, A. (2009). Photochemical production of aerosols from real plant emissions, *Atmospheric Chemistry and Physics*, 9, 4387-4406.

ENERGY AVAILABILITY INCREASES NITROGEN MINERALIZATION

A.S. LINDÉN¹, J. HEINONSALO^{1,2}, M. OINONEN³ and J. PUMPANEN¹

¹Department of Forest Sciences, Faculty of Agriculture and Forestry, P.O.Box 56, FIN-00014 University of Helsinki, Helsinki, Finland

²Viikki Biocenter, Department of Food and Environmental Sciences, Faculty of Agriculture and Forestry, P.O.Box 56, FIN-00014 University of Helsinki, Helsinki, Finland

³Finnish Museum of Natural History, Dating Laboratory, P.O. Box 64, FI-00014 University of Helsinki

Keywords: BOREAL, CARBON, NITROGEN, FEEDBACK, ECTOMYCORRHIZA

INTRODUCTION

We have studied the connection of underground labile energy input and the microbial nitrogen mineralization and decomposition using recalcitrant boreal forest topsoil in a controlled microcosm experiment. Study concentrates on a soil nitrogen pool, biological factors such as a bacterial biomass relationship to nematode worms, protease activity, ectomycorrhizal (EM) and non-mycorrhiza root tip numbers, and changes in root and shoots biomass in order to understand the connection between energy input and decomposition. Connection was studied by changing belowground energy input by using pulses of artificial C₄-glucose addition in bare soil and the presence of tree seedling. Transition in preferential substrate utilization and the substrate of microbial decomposition source were examined by using natural isotope ratios (¹³C/¹²C) and ¹⁴C radiocarbon dating for approximating the change in the age class of a substrate pool used for growth. The study highlights the importance of processes affecting the soil-atmospheric carbon-nitrogen exchange under current and future climatic conditions (IPCC). It is widely accepted that plant derived root exudates and microbial succession play a substantial role during the next decades, due their central role in natural carbon fluxes (Kirschbaum *et al.*, 2000, De Nobili *et al.*, 2001, Hogberg *et al.*, 2003, Hogberg & Read, 2006).

METHODS

We increased the energy obtainable for soil microbes by adding C₄-glucose to the soil in pulses at weekly intervals for a month and naturally by growing *P. sylvestris* seedlings in the microcosms for 6 months. We analysed the age of the respired ¹⁴CO₂ with AMS (Accelerator Mass Spectrometer) before and after glucose addition and incubation period of one month. Soil respiration (¹⁴CO₂) was trapped into molecular sieves (Hämäläinen *et al.*, 2010). In addition, soil cellular respiration rate and δ¹³C values were measured with cavity ring down spectrometer Picarro G1101-i (Picarro Inc., California, USA) in order to observe fluctuations in origins of respired CO₂.

Finally, photosynthesis of the seedlings, soil microbial biomass, quantity of nematodes, protease enzyme activity, mycorrhizal symbiosis, and total changes in root and shoot biomass as well as ¹³C, ¹⁴C and ¹⁵N contents were measured to study the changes in the decay of SOM C-pool.

C₄-glucose turnover rate was separately tested in a similar setup to exclude the possible ¹³C and ¹⁴C signals originating from the C₄-glucose addition.

CONCLUSIONS

Preliminary results suggest increase in the age of respired carbon similarly in boreal soils to that presented by Fontaine *et al.* (2007) by using agricultural soils with a cellulose addition as well as similar mechanism mentioned by Drake *et al.*, (2011) of belowground carbon stimulated nitrogen

uptake. We show that simple carbon substances can regulate nitrogen mineralization and possibly the decay rate of recalcitrant SOM pool. These results were obtained in circumstances where alternative easy nitrogen source was not available and where the nitrogen acquisition of trees through symbiotic relationship (Heinonsalo *et al.*, 2010) was possible. The result highlights the importance of dynamical root-microbe-soil cascade that should be accounted for in any carbon and nitrogen model or calculation concerning effects of ecosystem nutritional equilibrium and fluxes in particularly nitrogen limited boreal ecosystems. Further studies should be made to incorporate the effect of the increasing energy input belowground into ecosystem carbon and nitrogen models in order to estimate the changes taking place in the exchange of greenhouse gases and energy between the forests and the atmosphere.

ACKNOWLEDGEMENTS

The financial support by the Academy of Finland project number 218094 (FASTCARBON), Academy of Finland Centre of Excellence program (project no 1118615) is gratefully acknowledged.

REFERENCES

- De Nobili, M., Contin, M., Mondini, C. & Brookes, P. C. 2001. *Soil microbial biomass is triggered into activity by trace amounts of substrate*. Soil Biology & Biochemistry 33: 1163-1170.
- Drake et al. 2011. *Increases in the flux of carbon belowground stimulated nitrogen uptake and sustain the long-term enhancement of forest productivity under elevated CO₂*. Ecology Letters
- Fontaine, S., Barot, S., Barre, P., Bdioui, N., Mary, B. & Rumpel, C. 2007. *Stability of organic carbon in deep soil layers controlled by fresh carbon supply*. Nature 450: 277-280.
- Hämäläinen, K., Fritze, H., Jungner, H., Karhu, K., Oinonen, M., Sonninen, E., Spetz, P., Tuomi, M., Vanhala, P. and Liski, J. 2010. *Molecular sieve sampling of CO₂ from decomposition of soil organic matter for AMS radiocarbon measurements*. Nuclear Instruments and Methods in Physics Research Section B 268: pp. 1067-1069. doi:10.1016/j.nimb.2009.10.099.
- Heinonsalo, J., Pumpanen, J., Rasilo, T., Hurme, K. & Ilvesniemi, H. 2010. *Carbon partitioning in ectomycorrhizal Scots pine seedlings*. Soil Biology & Biochemistry. 42:1614-1623.
- Hogberg, M. N., Baath, E., Nordgren, A., Arnebrant, K. & Hogberg, P. 2003. *Contrasting effects of nitrogen availability on plant carbon supply to mycorrhizal fungi and saprotrophs - a hypothesis based on field observations in boreal forest*. New Phytologist 160: 225-238.
- Högberg P. and Read D.J. 2006. *Towards a more plant physiological perspective on soil ecology*. Trends in Ecology and Evolution. 21 (10):548-554.
- IPCC report, <http://www.ipcc.ch/>
- Kirschbaum M.U.F. 2000. *Will changes in soil organic carbon act as a positive or negative feedback in global warming*. Biogeochemistry 48: 2151.13

A FORESTRY-DRAINED PEATLAND IN SOUTHERN FINLAND IS A LARGE CO₂ SINK

A. LOHILA¹, K. MINKKINEN², M. AURELA¹, J.-P. TUOVINEN¹, T. PENTTILÄ³, and T. LAURILA¹

¹Finnish Meteorological Institute, Climate Change Research, PO Box 503, FI-00101 Helsinki, Finland.

²Department of Forest Sciences, University of Helsinki, PO Box 27, 00014 University of Helsinki, Finland.

³Finnish Forest Research Institute, Vantaa Research Unit, PO Box 18, FI-01301 Vantaa, Finland

Keywords: organic matter decomposition, peatland forestry, methane, nitrous oxide.

INTRODUCTION

Forestry-drainage of peatlands is one of the most important land-use practices affecting the greenhouse gas balance of the forestry sector in Finland. Due to methodological difficulties in determining the whole-ecosystem carbon dioxide (CO₂) balance of these forests, and partly due to large spatial and site-type dependent variation in the CO₂ exchange processes, the magnitude and even the sign of the CO₂ balance is highly uncertain. To fill in this gap, we measured the net ecosystem exchange (NEE) of CO₂ in a nutrient-poor forestry-drained peatland in southern Finland. Here we report the annual CO₂ balance measured at this site in the calendar year of 2005.

METHODS

Our measurement site Kalevansuo, which is located in Loppi in southern Finland (60°38'49"N, 24°21'23"E; elevation 129 m), was originally a dwarf shrub pine bog. It was drained in 1969, which resulted in a lowered water table (on average 40 cm below the ground) and increased the growth of the natural tree stand. The average peat depth was 2.2 m. The tree stand consisted of a dominant Scots pine (*Pinus sylvestris*) stand of 835 stems ha⁻¹ and an understorey of pubescent birch (*Betula pubescens*) trees. The pine stand had a dominant height of 15 m. The annual increment of live tree stand was 160 g C m⁻² yr⁻¹. The all-sided leaf area index of the needles was 5 m² m⁻². The relatively dense field layer consisted of different shrubs and mosses.

Fluxes of CO₂, H₂O, sensible heat and momentum were measured with the eddy covariance technique on top of a 21.5-m telescopic mast. Fluctuations of wind velocity components were measured with a sonic anemometer/thermometer (SATI-3SX, Applied Technologies, Inc.) and those of CO₂ concentration with a LI-7000 CO₂/H₂O analyzer (LI-COR, Inc.). The storage flux of CO₂ was calculated from the concentrations measured at the top of the mast and at a height of 4 m, and was added to the measured turbulent flux.

A spectrum of supporting meteorological measurements, such as radiation, soil and air temperature, and water level depth, were also conducted at the study site.

CONCLUSIONS

The drained peatland forest was a net sink of -871 g CO₂ m⁻² in 2005. The ecosystem acted as a carbon (C) sink over a 6-month period, from the beginning of April to the end of October. The highest total

ecosystem respiration (R_{tot}) and gross photosynthesis (GPP) were observed in the end of July, coinciding with the temperature maximum and water level depth minimum (Fig. 1).

If the amount of C annually fixed into the trees (160 g C m^{-2}) is subtracted from the yearly NEE (240 g C m^{-2}), we obtain 80 g C m^{-2} as an estimate of the annual peat+ground vegetation CO_2 balance. This result suggests that the site is a considerable net C sink. Our finding supports the observations from C stock studies that nutrient-poor peatland types may continue to sequester C after their drainage for forestry (Minkkinen and Laine, 1998; Minkkinen *et al.*, 1999). This result can be attributed to (1) the low nutrient status of the site, which decreases the peat decomposition rate and increases the allocation of C into the roots and (2) actively photosynthesising and dense ground vegetation. The peat decomposition may be lowered due to the relatively high water level at the site; at nutrient-poor sites like Kalevansuo, drainage is not as efficient as in the mire margins. This is because, after the drainage, the peat subsides and the functioning of ditches on a flat terrain tends to deteriorate due to vegetation. On the other hand, the growth rate of trees remains slow because of the low nutrient concentration. Consequently, the tree stand transpiration remains low, which keeps the water table at a relatively high and the peat decomposition rates at a moderate level (Silvola *et al.*, 1996; Ojanen *et al.*, 2010).

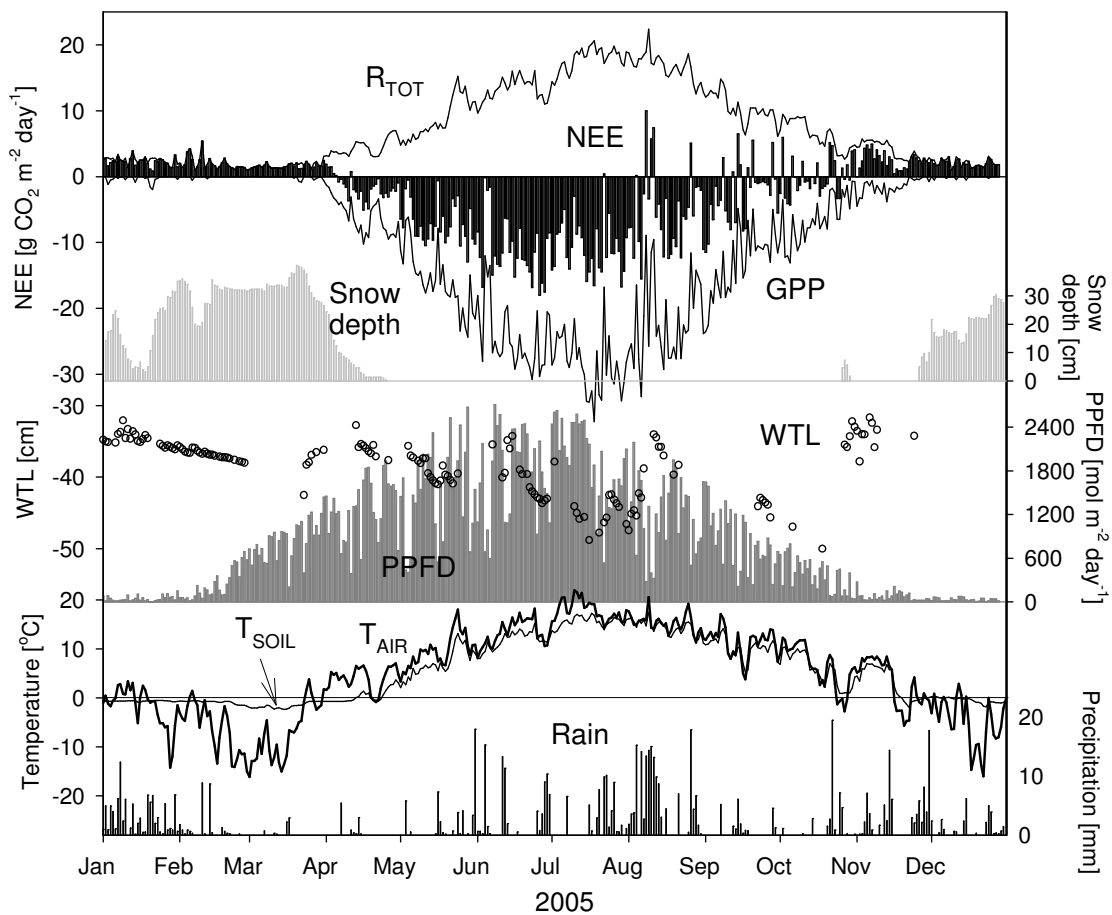


Figure 1. Annual course of NEE, its components R_{tot} and GPP, snow depth, water level depth, irradiation (PPFD), air and soil temperature, and precipitation at the Kalevansuo drained peatland forest.

ACKNOWLEDGEMENTS

The financial support by the European Commission through the project GHG Europe (244122), and by the Academy of Finland Centre of Excellence program (project 1118615) are gratefully acknowledged.

REFERENCES

- Minkkinen, K. and Laine, J. (1998). Long-term effect of forest drainage on the peat carbon stores of pine mires in Finland. *Canadian J. For. Res.*, **28**, 1267–1275.
- Minkkinen, K., Vasander, H., Jauhiainen, S., Karsisto, M., and Laine, J. (1999). Post-drainage changes in vegetation composition and carbon balance in Lakkasuo mire, central Finland. *Plant Soil*, **207**, 107–120.
- Ojanen, P., Minkkinen, K., Alm, J., and Penttilä, T. (2010). Soil-atmosphere CO₂, CH₄ and N₂O fluxes in boreal forestry-drained peatlands. *For. Ecol. Manage.*, **260**, 411–421.
- Silvola, J., Alm, J., Ahlholm, U., Nykänen, H., and Martikainen, P.J. (1996). CO₂ fluxes from peat in boreal mires under varying temperature and moisture conditions. *J. Ecol.*, **84**, 219–228.

CHEMICAL COMPOSITION AND CORRELATION OF IONS IN A MARINE ATMOSPHERE

G. LÖNN¹, M.J. MCGRATH¹, H. JUNNINEN¹, S. SCHOBESBERGER¹, A. FRANCHIN¹, T. PETÄJÄ¹,
D.R. WORSNOP^{1,2} AND M. KULMALA¹

¹Department of Physics, University of Helsinki, P.O. Box 64, 00014, Helsinki, Finland

²Aerodyne Research Inc., Billerica, MA, USA

Keywords: atmospheric aerosols, cluster ions, field measurements.

INTRODUCTION

Coastal new particle formation is a frequent phenomenon (O'Dowd and Hoffmann, 2005) that has a strong connection to coastal tides, air mass origin and sun radiation. The aim of this study was to identify atmospheric ions present in a marine and coastal environment and to observe how their concentrations change over time. A strong connection between halogen ion concentration and tide phase was observed. During low tide, the halogens are thought to be released by marine organisms (McFiggans et al. 2010). The data was collected during the MaCLOUD Inc project in December, 2010 at Mace Head, situated on the west coast of Ireland.

METHODS

We used an Atmospheric Pressure interface- time-of-flight mass spectrometer (APi-TOF, Junninen et al. 2010, Ehn et al. 2010b) to determine the composition and concentration of both positive and negative atmospheric ions. The APi-TOF is able to detect charged clusters and molecules at mass range 1-3000 Th, which provides insight into the chemical composition of the marine atmosphere.

We processed the data using tofTools, a data analysis package for MATLAB. The data is analysed in several steps, of which mass calibration and peak fitting are the most important. Although the instrument is roughly calibrated during measurement, the calibration will shift with time owing to temperature changes. tofTools allows recalibration of spectra using known peaks, which makes it possible to identify ions by their mass. The accuracy of the instrument is <20 ppm (Junninen et al. 2010).

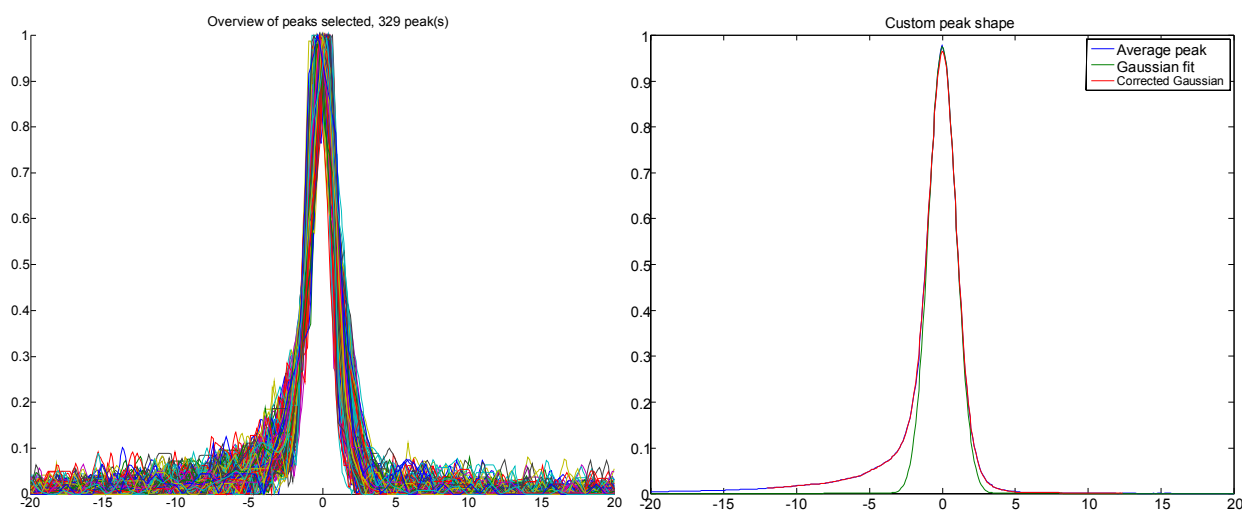


Figure 1. Example of determining a custom peak shape using tofTools. The left graph shows the 329 peaks used for calculating the peak shape shown in the right graph (in red).

The development of tofTools is ongoing. We have now also implemented automatic peak detection and fitting. A standard Gaussian fit can be used for simplicity, but it is also possible to calculate and use a custom peak shape. The determination of a custom peak shape is based on averaging all the significant and pure (single) peaks from one or more spectra and calculating the deviation from a normal Gaussian curve. An example of this can be seen in figure 1. The ability to automatically fit peaks also gives the opportunity to easily examine time series of ions.

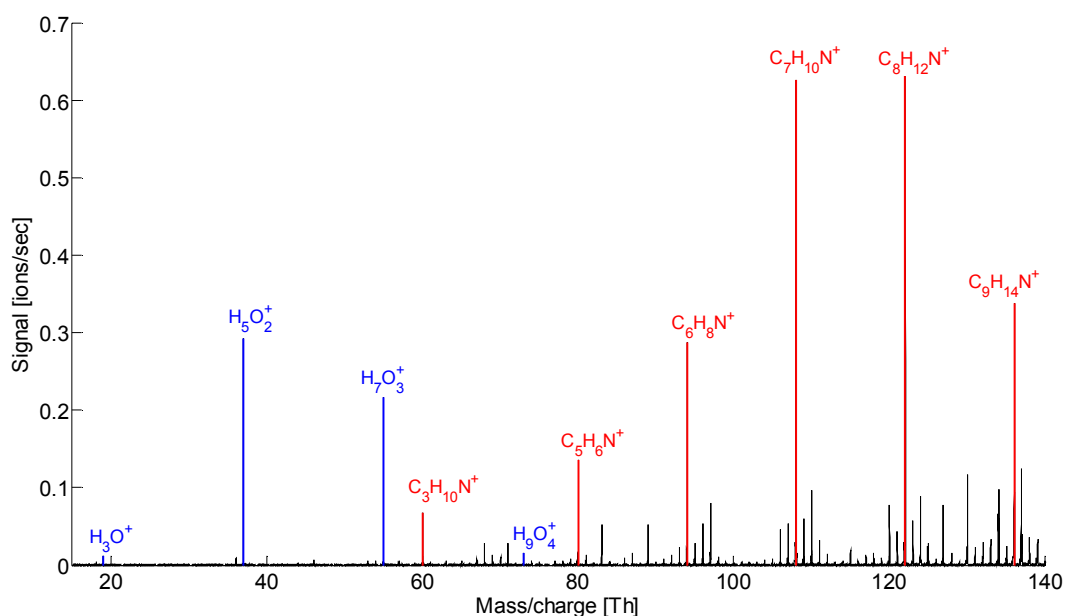


Figure 2. Positive ion spectra from Mace Head at midnight December 9th 2010 averaged over 60 minutes. The blue peaks are the hydronium ion and its clusters and the red ones are various organic ions.

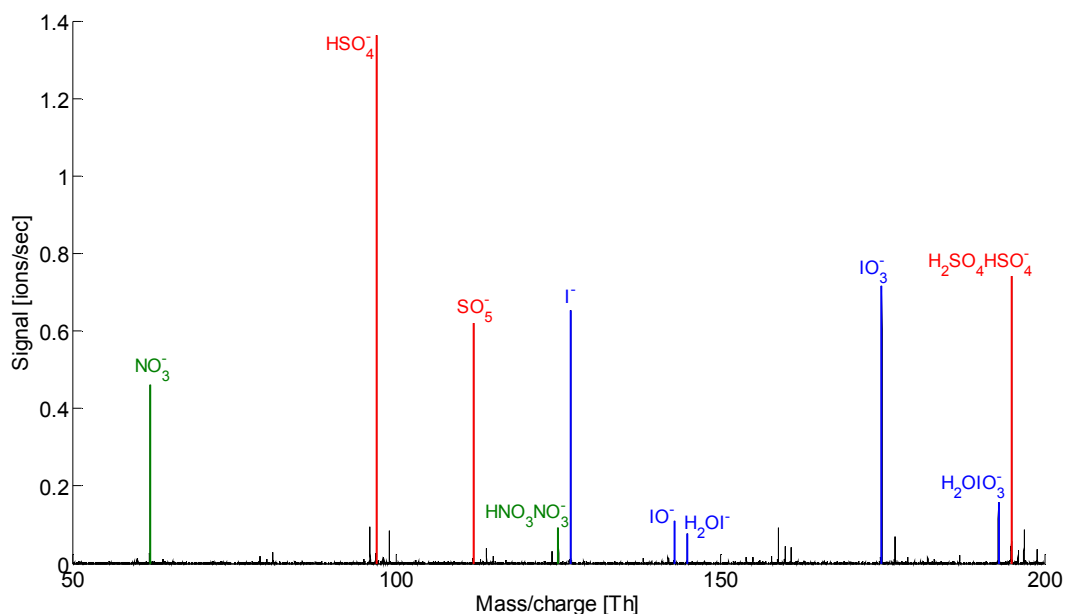


Figure 3. Negative ion spectra from Mace Head at noon December 1st 2010 averaged over 60 minutes. Notice the strong presence of ions containing iodine.

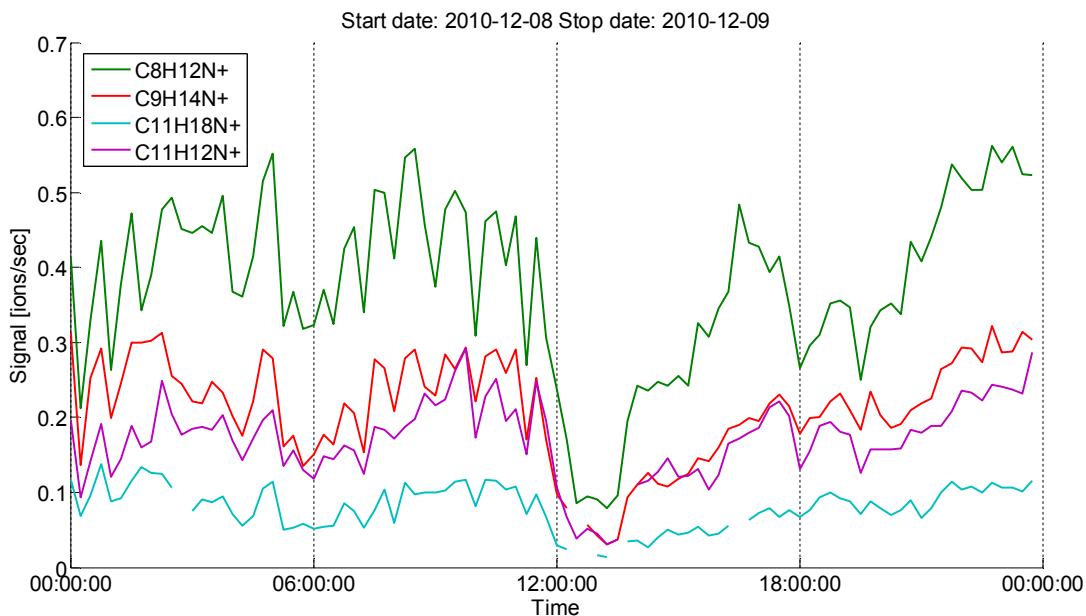


Figure 4. Time series of certain positive organic ions for one day. Notice the good correlation between these ions.

CONCLUSIONS

We were able to identify a large part of the ions, both positive and negative ones, by their mass. Some of the identified positive ions are presented in figure 2 and some of the negative in figure 3. The complete results will be compared to those of the boreal area of Hyytiälä (Ehn et al. 2010b). Initial analysis has revealed compounds containing iodine and bromine, which is to be expected.

We calculated time series for the most abundant ions and compared these to each other. For the positive ions, results show strong correlations between the hydronium ion and its clusters, but also between different organic ions. An example of this is presented in figure 4.

Several higher mass clusters were also identified through this technique. As the mass of the cluster increases, the number of possible atomic combinations for the given mass also increases, which makes identification of higher-mass ions more difficult. However, some of these ions were observed to correlate very well with smaller ions, suggesting that the smaller ions are building blocks for the larger ions. Further analysis revealed that the higher-mass ions could be explained by the smaller ions combining with abundant neutral species, such as sulphuric acid.

Meteorological data (e.g. temperature, sun radiation, humidity) was also collected during the campaign and correlations between these variables and ion concentrations will also be presented. In particular, several compounds (such as sulphuric and nitric acid) are well known to have diurnal cycles. It is expected that this will be confirmed in this dataset. Tidal variations of halogen-containing compounds would also support the hypothesis of halogen-emitting organisms being abundant at low tide.

ACKNOWLEDGEMENTS

This work was supported by the Academy of Finland Center of Excellence program under project number 1118615 and the Academy of Finland under grant agreement number 1133872.

REFERENCES

- Ehn, M., Junninen, H., Petäjä, T., et al. (2010b), *Atmos. Chem. Phys.*, **10**, 8513-8530.
Junninen, H., Ehn, M., Petäjä, T., et al. (2010), *Atmos. Meas. Technol.*, **3**, 1039-1053.
McFiggans, G., Bale, C.S.E, Ball, S.M., et al. (2010), *Atmos. Chem. Phys.*, **10**, 2975-2999.
O'Dowd, C.D. and Hoffmann, T. (2005), *Environ. Chem.*, **2**, 245-255.

sPARCK - SIMPLE PROGRAM FOR ATMOSPHERICALLY RELEVANT CLUSTER KINETICS

V. LOUKONEN, M. J. MCGRATH, R. VÄÄNÄNEN, R. KARINKANTA, K. VIISANEN,
M. DAL MASO and H. VEHKAMÄKI

Division of Atmospheric Sciences, Department of Physics, University of Helsinki, Helsinki,
P.O. Box 64, FI-00014 University of Helsinki, Finland.

Keywords: NUCLEATION KINETICS, CLASSICAL NUCLEATION THEORY.

WHAT?

We have developed a simple Program for Atmospherically Relevant Cluster Kinetics (sPARCK) which solves the birth-death equation

$$\frac{dc_i}{dt} = \sum_{jk} \beta_{jk} c_j c_k - \sum_j \beta_{ij} c_i c_j + \sum_j \gamma_{ij} c_j - \sum_j \gamma_{ji} c_i$$

for the two-component system of sulfuric acid and water. In sPARCK the time-development of the concentrations of different clusters c_i is solved with the help of classical condensation and evaporation coefficients β_{ij} and γ_{ij} , respectively. The coefficients are related by the detailed balance assumption, e.g. for the evaporation of one sulfuric acid molecule one has

$$\gamma_{\text{sa}} = \beta_{\text{sa}} \frac{c^e(1, 0) c^e(n_{\text{sa}}, n_{\text{w}})}{c^e(n_{\text{sa}} + 1, n_{\text{w}})},$$

and the condensation coefficient is given as

$$\beta_{\text{sa}} = (8\pi k_B T)^{1/2} \left(\frac{1}{m(n_{\text{sa}}, n_{\text{w}})} + \frac{1}{m_{\text{sa}}} \right)^{1/2} (r(n_{\text{sa}}, n_{\text{w}}) + r_{\text{sa}})^2$$

where $m(n_{\text{sa}}, n_{\text{w}})$ and $r(n_{\text{sa}}, n_{\text{w}})$ are the mass and the radius of a cluster containing n_{sa} sulfuric acid and n_{w} water molecules and m_{sa} and r_{sa} are those of sulfuric acid monomer and c^e are the concentrations of the particular clusters in equilibrium (Vehkamäki, 2006).

However, in sPARCK the kinetics are not limited only to the monomers but all the possible collisions and evaporations are taken into account. From a physical point of view this is a great strength, especially in the sulfuric acid-water system where hydrates are known to form. On the other hand, this also poses a challenge: when all the clusters are allowed to participate into the dynamics of the system, the problem becomes computationally very demanding.

HOW?

It is clear from the birth-death equation that the development of any one concentration depends on the concentrations of the other clusters. Thus to find out how the cluster distribution evolves, one must solve a system of coupled differential equations. As the number of clusters in the system grows as $(n_{\text{sa}} + 1)(n_{\text{w}} + 1) - 1$, for atmospherically relevant systems the number of equations to

solve is at least on the order of 10^4 , indeed turning the physical problem into a very non-trivial computational task.

To solve the problem for larger systems in any reasonable time, the program used should be parallelized. Towards this end, we have utilized the PETSc libraries (Balay *et al.*, 1997) in the development of sPARCK. The PETSc (Portable, Extensible Toolkit for Scientific Computation) libraries use the MPI standard for all message-passing communication and offer data structures and routines as building blocks for large-scale application codes, making parallel programming at least in principle more efficient.

WHY?

To properly understand particle formation through nucleation, it is not enough to study only the thermodynamics of the system – also the kinetics must be taken into consideration. The approach described here will yield not only the steady-state cluster distributions, but in addition to that, nucleation rates with minimal amount of approximations.

However, sPARCK uses classical nucleation theory for all the thermodynamics. Ideally the energetics of at least the smallest of clusters would be obtained from quantum mechanics, although the classical theory is likely to be the only possibility for larger clusters in the foreseeable future.

sPARCK – work still under progress – is also likely to find applications from different larger-scale models (e.g. aerosol models, air quality models), where nucleation rate parameterizations are needed.

ACKNOWLEDGEMENTS

The financial support by the Maj and Tor Nessling Foundation, the Academy of Finland (Center of Excellence program, project no 1118615 and project no 135054) and the ERC StG 257360-MOCAPAF is gratefully acknowledged. MJM gratefully acknowledges support from a National Science Foundation International Research grant (OISE-0853294).

REFERENCES

- Vehkamäki, H., (2006). *Classical Nucleation Theory in Multicomponent Systems*. (Springer–Verlag Berlin Heidelberg).
- Balay, S., Gropp, W. D., McInnes, L. C. and Smith, B. F. (1997) Efficient Management of Parallelism in Object Oriented Numerical Software Libraries, in: *Modern Software Tools in Scientific Computing*, Arge, E., Bruaset, A. M. and Langtangen, H. P. (Eds.), 163–202, Birkhäuser Press.

THE FIRST NUCLEATION THEOREM WITH COAGULATION SCAVENGING OF PRECRITICAL CLUSTERS

J. MALILA¹, K.E.J. LEHTINEN^{1,2}, I. NAPARI³, R. MCGRAW⁴ and A. LAAKSONEN^{1,5}

¹Department of Applied Physics, University of Eastern Finland, P.O. Box 1627, 70211 Kuopio, Finland

²Finnish Meteorological Institute, Kuopio Unit, P.O. Box 1627, 70211 Kuopio, Finland

³Division of Atmospheric Sciences, Department of Physics, P.O. Box 64, 00014 University of Helsinki, Finland

⁴Atmospheric Sciences Division, Environmental Sciences Department, Brookhaven National Laboratory, Upton, New York 11973, U.S.A.

⁵Finnish Meteorological Institute, Climate Change Unit, P.O. Box 503, 00101 Helsinki

Keywords: nucleation, coagulation, nucleation theorem, scavenging

INTRODUCTION

Atmospheric new particle formation (NPF) from both natural and anthropogenic vapours (Kulmala and Kerminen, 2008) has been shown to enhance cloud condensation nuclei (CCN) concentrations in various environments, and modelling results suggest that NPF may lead to substantial increase of both CCN concentration and cloud albedo globally. However, a major source of uncertainty is that all nucleation parameterisations applied in regional and global models perform relatively poorly (Zhang *et al.*, 2010). Resolving this uncertainty may even be crucial for determination of the sensitivity of Earth’s climate (Schwartz *et al.*, 2010).

An obvious way to improve nucleation parameterisations would be to resolve the molecular mechanism behind an actual NPF event. Applications of the first nucleation theorem (Kashchiev, 2000) to field and laboratory data have led to a still lasting debate on the molecular nature of the process and speculation of involved species (though sulphuric acid seems still to be a good bet), especially whether the same species are responsible for nucleation and growth. However, the first nucleation theorem is typically used in form

$$\left(\frac{\partial \ln J}{\partial \ln n_{c,1}} \right)_{T, n_{i \neq c, 1}} = g_c^* + \epsilon_c, \quad (1)$$

where J is the nucleation rate, $n_{c,1}$ number concentration of condensing species monomers, and g_c^* number of condensing species monomers in the so-called critical cluster with $1 \leq \epsilon_c \leq 0$ being a residual kinetic factor. Although usually considered as a general result, Eq. (1) includes several implicit assumptions: One of these, existence of a unique extremum in the free-energy surface for the work of formation for clusters of g -molecules, *i.e.* g -mers, was recently challenged by Vehkamäki *et al.* (2011), who noticed that if this condition is not fulfilled—which may well be the case for the tropospheric NPF—Eq. (1) may not be valid. Here we tackle another issue, the role of coagulation scavenging of precritical clusters by the background aerosol; Kulmala *et al.* (2006) note “that the derivatives should be taken at constant temperature and gas phase activities of other species participating in the nucleation process, and in atmospheric conditions, also at constant condensation sink,” a statement that we further quantify in the next section.

THEORY

The effect of scavenging due to background aerosol on the nucleation rate is reasonably well known in the framework of the classical nucleation theory (see, for instance, Seinfeld and Pandis, 2006, and references

therein). Here we follow McGraw and Marlow (1983), who give the expressions for concentrations of various g -mers in exact continued fraction form, and use these to extend the kinetic derivation (McGraw and Wu, 2003) of the first nucleation theorem. For simplicity, we assume isothermal, stationary nucleation from single component ideal vapour as well as constant coagulation sink.

The extended Becker–Döring–Zeldovich model for our system reads

$$\frac{\partial n_g}{\partial t} = J_g - J_{g+1} - Q_g, \quad (2)$$

where $J_g = \beta_{g-1}n_{g-1} - \gamma_g n_g$ is the current from $(g-1)$ -mers to g -mers with concentration n_g , and $Q_g = q_g n_g$, where β_g , γ_g and q_g are the condensation, evaporation and scavenging rates for a g -mer. At steady state $\partial n_g / \partial t = 0$ for all sizes g , and after imposing boundary conditions $n_1 = \text{constant}$ and $n_G = 0$ for some (large) $G \gg g^*$ we get (details will be provided in a separate publication: Malila *et al.*, 2011)

$$\begin{aligned} \frac{n_{g-1}}{n_g} &= \frac{\beta_g + \gamma_g + q_g}{\beta_{g-1}} - \frac{\gamma_{g+1}}{\beta_{g-1} \frac{n_g}{n_{g+1}}} \\ &= \dots = A_{g-1} - \mathbf{K}_{j=g}^{G-1} \left(\frac{B_g}{A_g} \right), \end{aligned} \quad (3)$$

where $A_{g-1} = (\beta_g + \gamma_g + q_g) / \beta_{g-1}$ and $B_g = \gamma_{g+1} / \beta_{g-1}$ and \mathbf{K} is an operator symbol for continued fraction. After some manipulation and denoting the nucleation rate pass the critical size as $J_{g^*+1} = J$, we get

$$\left(\frac{\partial \ln J}{\partial \ln n_1} \right)_{T, \{q_i\}} = \frac{J + \sum_{i=2}^{g^*} Q_i (1 + g^*) - \sum_{i=2}^{g^*} Q_i}{J} = 1 + \tilde{g}, \quad (4)$$

where \tilde{g} is now the apparent excess number of molecules in the critical cluster. It is straightforward to see that always $\tilde{g} \geq g^*$, where the equality holds if $Q_i = 0$ for all $i = 2, \dots, g-1$. To apply the obtained form of the first nucleation theorem [Eq. (4)], we first need to solve individual n_g :s starting from n_{G-1} using Eq. (3), after what we can evaluate both g^* and \tilde{g} .

Another way to look the problem is to use the kinetic potential $\Phi_g = \ln(n_g/n_1)$ that generalizes the thermodynamic free energy cost (in units of kT) to overcome nucleation barrier (Wu, 1996). For our system we get

$$\Phi_g = \ln \left(\frac{n_2 n_3 \dots n_g}{n_1 n_2 \dots n_{g-1}} \right) = \ln \left(\prod_{k=2}^g \frac{1}{A_{k-1} - \mathbf{K}_{j=k}^{G-2} \left(\frac{B_j}{A_j} \right)} \right). \quad (5)$$

AN EXAMPLE APPLICATION AND FUTURE PROSPECTS

To exemplify the obtained results, we have performed some model calculations using water vapour at 260 K in 1 atm nitrogen atmosphere with monodisperse, spherical aerosol particles of varying size and concentration as a model system. Coagulation rates were calculated using Fuchs–Sutugin expression and for the “observed” nucleation rate J classical theory was used (Seinfeld and Pandis, 2006); condition of detailed balance was used to relate γ_g and β_{g-1} .

In Fig. 1, the ratio \tilde{g}/g^* for three different background aerosol size distributions is given. As can be seen, the apparent critical size may well be orders of magnitude larger than the true critical size. This can be understood considering the relative rate sensitivity (*i.e.* the first nucleation theorem) at the very verge of on-set separating total scavenging of g^* -mers ($J_{g^*+1} = 0$) and observable nucleation ($J_{g^*+1} > 0$). Figure 2 enlightens the observed phenomenon using the kinetic potential concept: On the x -axis, true size of the cluster is depicted. Coagulation scavenging scales various n_g down (arrow “A”) to the extend that maximum in Φ_g occurs at the same height than for scavenging-free nucleation taking place at higher

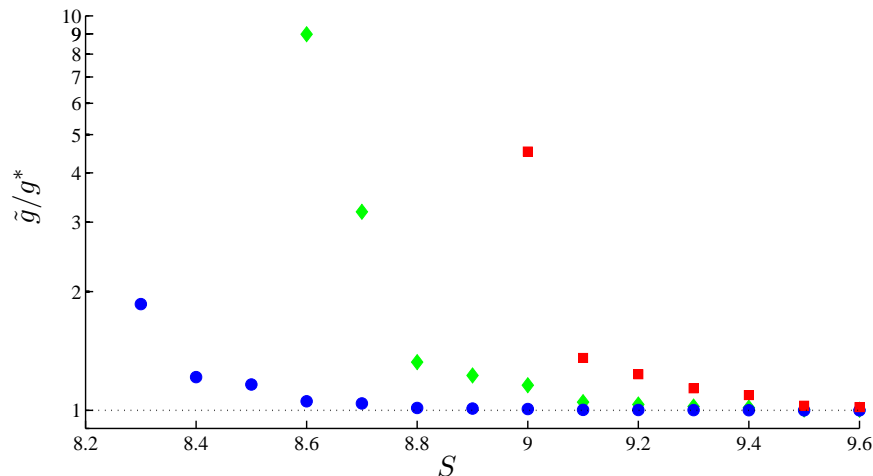


Figure 1: Ratio of apparent and true critical sizes with different background aerosol number concentration and size as a function of saturation ratio S : 10 m^{-3} , $1 \mu\text{m}$ (diamonds); 10 m^{-3} , $0.1 \mu\text{m}$ (circles); and 1000 m^{-3} , $0.1 \mu\text{m}$ (squares).

supersaturation (arrow “B”). The true critical size, determined by the location of maximum in Φ_g , is not affected. However, inappropriate application of Eq. (1) leads the critical size g^* to be observed at higher supersaturation, corresponding maximum of Φ_g in the scavenging-free system.

Coagulation scavenging of precritical clusters due to background aerosol can have a major impact on the analysis of NPF using the first nucleation theorem. To extend the provided formalism into multicomponent systems is work at progress that may allow one to analyse *e.g.* recent observations of NPF inside tropical upper tropospheric clouds (Weigel *et al.*, 2011). For boundary layer NPF, one should most probably incorporate the provided formalism with the possibility several extrema in Φ_g , non-stationary nucleation, cluster–cluster interactions, *etc.*

ACKNOWLEDGEMENTS

J.M. acknowledges support from the Graduate School “Atmospheric Composition and Climate Change: From Molecular Processes to Global Observations and Models.”

REFERENCES

- Kashchiev, D., (2000). *Nucleation: Basic Theory with Applications*. (Butterworth–Heinemann, Oxford, U.K.).
- Kulmala, M., K.E.J. Lehtinen and A. Laaksonen, (2006). Cluster activation theory as an explanation of the linear dependence between formation rate of 3 nm particles and sulphuric acid concentration. *Atmos. Chem. Phys.*, **6**, 787.
- Kulmala, M. and V.-M. Kerminen, (2008). On the formation and growth of atmospheric nanoparticles. *Atmos. Res.*, **90**, 132.
- Malila, J., K.E.J. Lehtinen, I. Napari, R. McGraw and A. Laaksonen, (2011). Accounting for precritical cluster loss processes in the first nucleation theorem. In preparation.
- McGraw, R. and W.H. Marlow, (1983). The multistate kinetics of nucleation in the presence of an aerosol. *J. Chem. Phys.*, **78**, 2542.

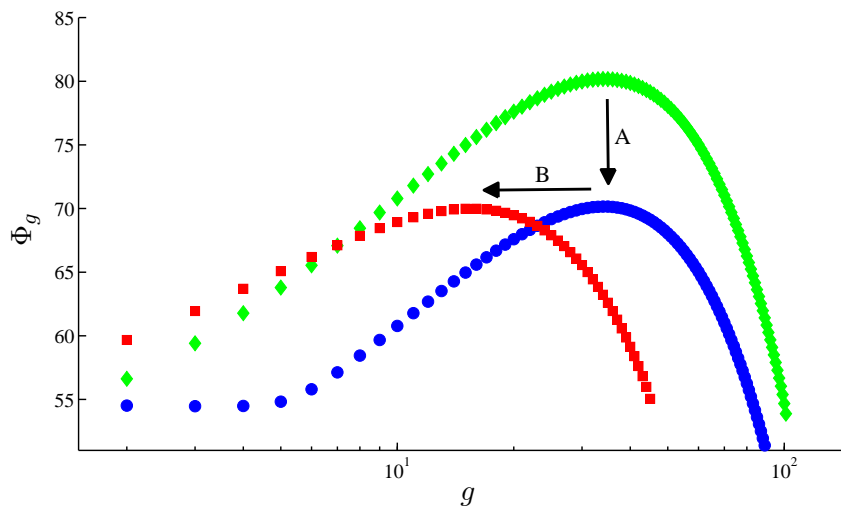


Figure 2: Kinetic potentials Φ_g as a function of cluster size: $S = 8$ (diamonds), no background particles; $S = 8$, 10 m^{-3} $10\text{-}\mu\text{m}$ background particles (circles); and $S = 15$, no background particles (squares). For the arrows, see the text.

McGraw, R. and D.T. Wu, (2003). Kinetic extensions of the nucleation theorem. *J. Chem. Phys.*, **118**, 9337.

Schwartz, S., R.J. Charlson, R.A. Kahn, J.A. Ogren and H. Rodhe, (2010). Why hasn't Earth warmed as much as expected? *J. Climate*, **23**, 2453.

Seinfeld, J.H. and S.N. Pandis, (2006). *Atmospheric Chemistry and Physics*, 2nd ed. (John Wiley & Sons, New York, U.S.A.).

Vehkamäki, H., M.J. McGrath, T. Kurten, M. Kulmala and K.E.J. Lehtinen, (2011). Rethinking the application of the first nucleation theorem to atmospheric nucleation. Preprint.

Weigel, R., S. Borrmann, J. Kazil, A. Minikin, A. Stohl, J.C. Wilson, J.M. Reeves, D. Kunkel, M. de Reus, W. Frey, E.R. Lovejoy, C.M. Volk, S. Viciani, F. D'Amato, F. Cairo, H. Schlager, K.S. Law, G.N. Shur, G.V. Belyaev and J. Curtius, (2011). In situ observations of new particle formation in the tropical upper troposphere: the role of clouds and the nucleation mechanism. *Atmos. Chem. Phys. Disc.*, **11**, 9249.

Wu, D.T., (1996). Nucleation theory. *Solid State Phys.*, **50**, 37.

Zhang, Y., P.H. McMurry, F. Yu and M.Z. Jacobson, (2010). A comparative study of nucleation parameterizations: 1. Examination and evaluation of the formulations. *J. Geophys. Res.*, **115**, D20212.

EDDYUH – AN ADVANCED SOFTWARE FOR EDDY COVARIANCE FLUX CALCULATIONS

I. MAMMARELLA, O. PELTOLA, A. NORDBO, Ü. RANNIK AND T. VESALA

Department of Physics, P.O. Box 48, FI-00014, University of Helsinki, Finland

Keywords: EDDY COVARIANCE (EC) TECHNIQUE, EC FLUXES, EC SOFTWARE, EC POST-PROCESSING METHODS AND CORRECTIONS.

INTRODUCTION

The Eddy Covariance (EC) technique is the most common and worldwide used method for measuring vertical turbulent fluxes of momentum, energy and gases between the atmosphere and any ecosystem. Recently, the number of EC stations all over the world has dramatically increased and is thought to increase more in the next few years. EC is a mathematically complex technique, which analyzes high-frequency wind and scalar atmospheric data series (often called “raw data”), which are usually saved in hard drive devices for post-processing and final estimations of turbulent flux values. Although in the past several years great efforts of the EC flux community have led to a standard methodology (Aubinet et al., 2000) for post-processing steps (at least for CO₂ and energy fluxes), the harmonization of post-processing is quite difficult, since most of the required steps and corrections are site- and instrument- (gas analyzer and sonic anemometer) specific. Systematic differences in EC flux estimates strongly depend on the selection, application and order of processing steps (Mauder et al., 2008). Moreover, a standard methodology for CH₄ and N₂O is not yet established in the EC flux community, and analysis and quality control (QA/QC) tools need be developed for inclusion into the international database for non-CO₂ flux measurements and to extend the methodological approach already taken in the CarboEurope database for CO₂.

METHODS

With this in mind, we recently developed the software EddyUH, a new post-processor for EC measurements. EddyUH is written in Matlab and includes a graphical user interface (Fig. 1), which allows the user to upload all relevant information concerning the site, the EC system configuration, and the related methods and corrections to be used. Such information is then saved in a project file. As shown in Fig.2, the software includes a number of modules, which operate at different levels of post-processing:

- *EddyUH_Preprocessor* performs several operations on the EC raw data. The module needs ancillary information passed as input from the project file. The outputs are wind and gas raw signals statistics (mean, standard deviation, co-variance, skewness, kurtosis), spectra and co-spectra for each raw data file, time lag estimates, quality statistics parameters (flux non-stationarity, flux intermittency, random flux error). All these data are saved in monthly binary files, and then used by other modules.
- *EddyUH_High frequency spectral transfer function estimator* lets the user to empirically estimate the low pass filter time constant of the EC system, by using the previously estimated co-spectral data. For water vapour fluxes, measured by a closed path EC system, the analysis is performed on different classes of relative humidity (RH). Then the H₂O time constant is parameterized as a function of RH following the method of Mammarella et al. (2009). The estimated time constants are then used in the *EddyUH_Flux calculation* module in order to perform the spectral correction to the final flux values.

- *EddyUH_Time lag optimizer* contains several statistical and visual tools to optimize the time lag windows, which were used in the *EddyUH_Preprocessor* and to validate the estimated values of the time lag (especially for closed path EC systems).
- *EddyUH_Spectral analysis* is a powerful module allowing the user to perform ogive analysis, to parameterize empirical spectra/co-spectra models relevant for the actual site, to calculate turbulent parameters like the integral time scale of turbulence and the dissipation of turbulent kinetic energy.
- *EddyUH_Flux calculation* is the module for calculating the final corrected fluxes. It uses the outputs and the information from all the other modules and performs remaining relevant corrections to the fluxes. An automatic and visual quality screening of the fluxes is also performed at this stage. For each processed month, the outputs are then saved in two ascii files, one containing the full dataset (not only the corrected fluxes), and another one having a user defined format.

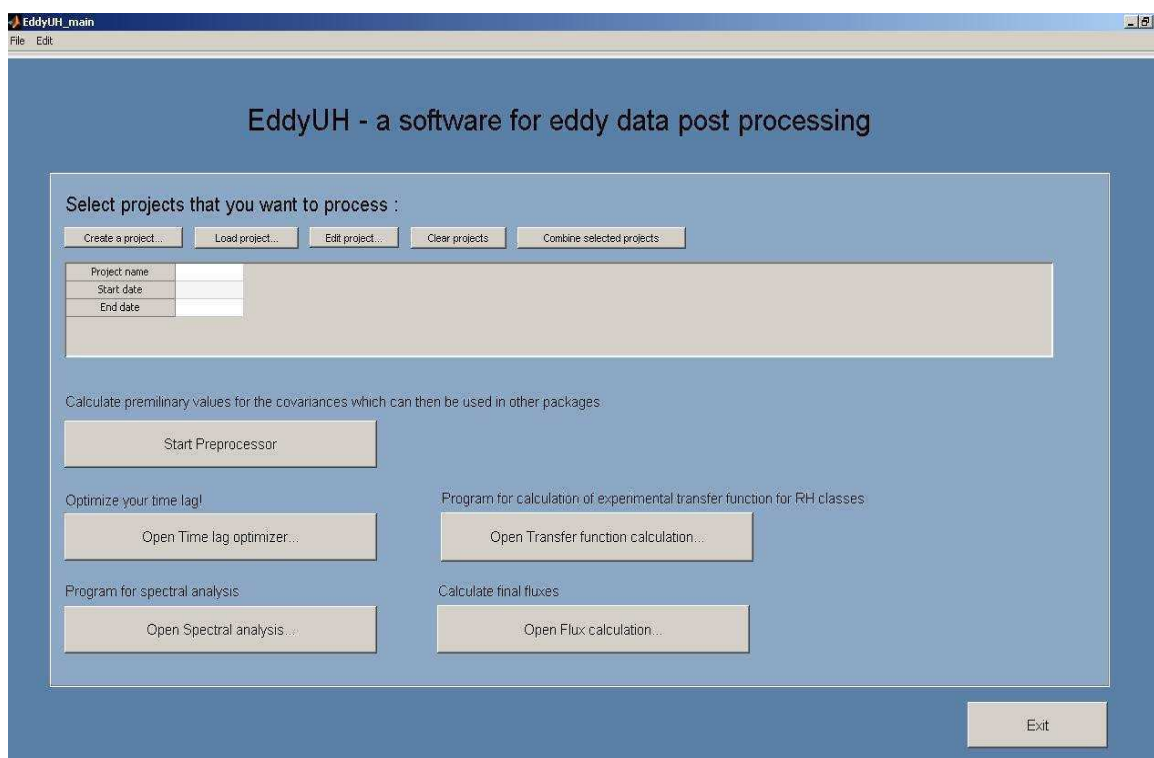


Figure 1. The main interface of EddyUH.

A substantial amount of instruments (sonic anemometers and gas analyzers) are supported, and standardized procedures are fully implemented in EddyUH. In order to advance methodical issues concerning especially CH₄ and N₂O fluxes, most updated corrections and methods for EC flux estimates for these gases have been also included. The main features of EddyUH are summarized in Table 1.

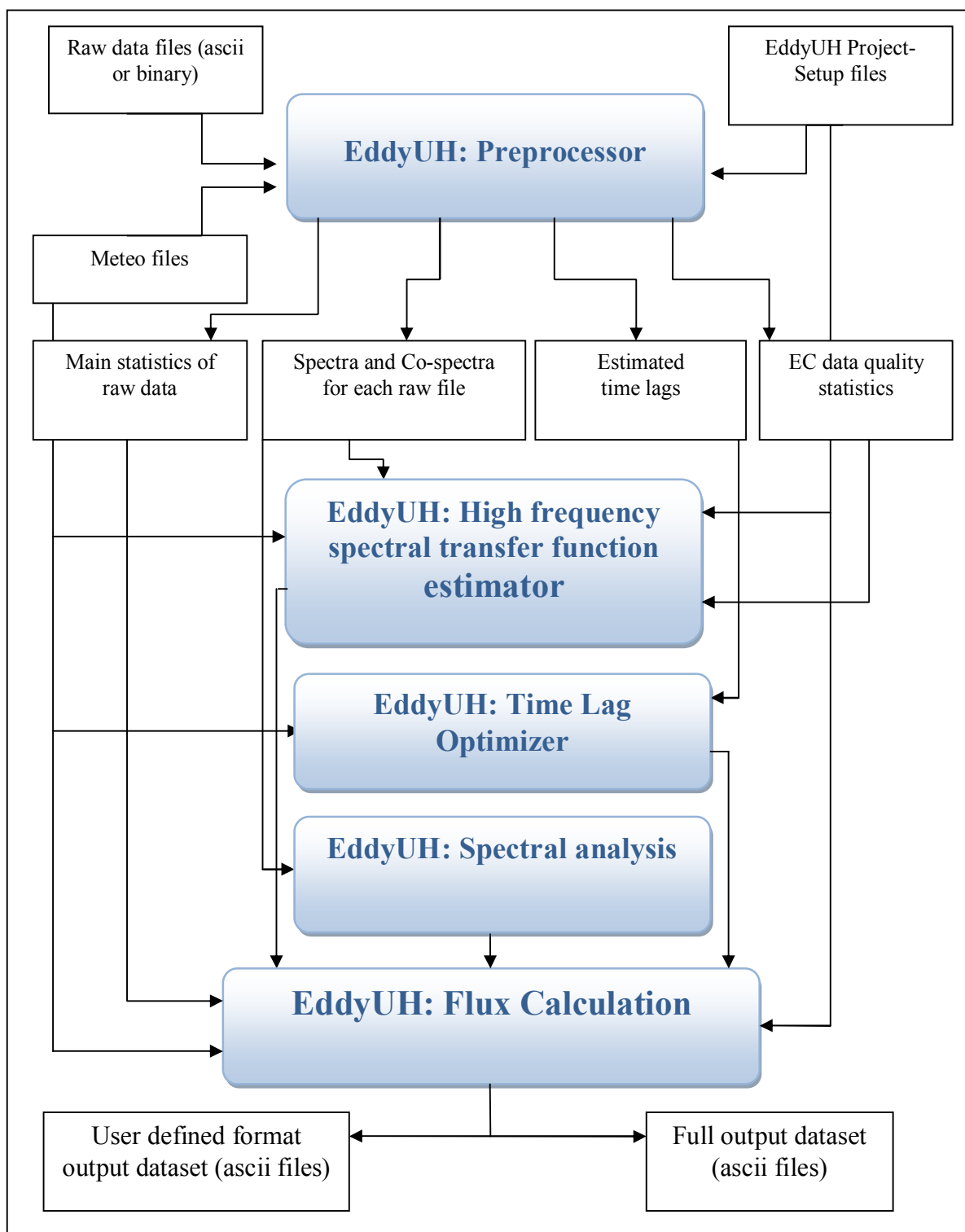


Figure 2. Flow chart of EddyUH.

Supported instruments	
Sonic anemometers	Gill-R2, Gill-R3, Gill-HS, Campbell CSAT3, Metek-USA-1
Gas analyzers	Licor-6262 (CO ₂ , H ₂ O), Licor-7000 (CO ₂ , H ₂ O), Licor-7500 (CO ₂ , H ₂ O), Licor-7200 (CO ₂ , H ₂ O), Licor-7700 (CH ₄), Campbell TGA100 (CH ₄ , N ₂ O), Los Gatos -FMA (CH ₄), Picarro G2301-f (CH ₄ , CO ₂ , H ₂ O), Aerodyne QCLAS (N ₂ O, CO ₂ , H ₂ O, CH ₄)
Implemented methods/corrections	
Raw data level	Units conversion and Calibration; Spike detection; Cross-wind correction (Liu et al., 2001); Dilution correction point by point; Angle of attack correction (Nakai et al., 2006); Block averaging, linear detrending and autoregressive running mean filter; Time lag estimation
Coordinate rotation of sonic wind components	Planar fit (Wilczak et al., 2001); Streamwise rotation (1D, 2D or 3D) according to McMillen (1988)
Quality statistics	Skewness, kurtosis, flux non-stationarity, random flux error, flux intermittency (Foken and Wichura, 1996; Vickers and Mahrt, 1997)
High frequency loss	Theoretical (Moncrieff et al., 1987, Moore et al., 1986); Empirical estimation of the transfer function (Aubinet et al., 2000; Mammarella et al., 2009)
Low frequency loss	According to Rannik (1999)
Humidity correction to sensible heat flux	According to Schotanus et al. (1983)
WPL correction	Based on Webb et al.(1980), Ibrom et al.(2007) for closed-path gas analyser, additional cross-talk correction for Licor-7700, Los Gatos -FMA and Aerodyne QCLAS

Table 1. Main features of EddyUH.

The new software was validated against the Eddy Covariance Community software (ECO₂S), recently developed within the IMECC-EU project (<http://gaia.agraria.unitus.it/eco2s/>). The software intercomparison was performed using one month of raw data, measured at the SMEAR II station, Hyytiälä, Finland. The resulting flux datasets show close agreement (Figure 3). Finally, EddyUH can potentially expand the use of the EC method beyond the micrometeorology community and prove a valuable tool for plant physiologists, hydrologists, biologists, and other non-micrometeorological areas of research.

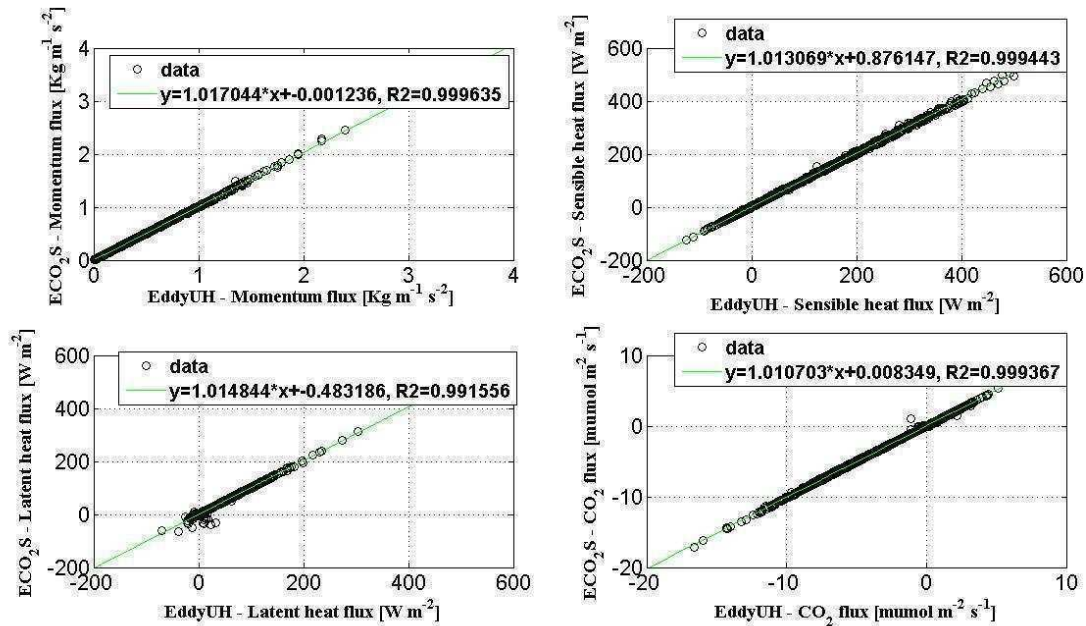


Figure 3. Comparison of EC flux values calculated by EddyUH and ECO₂S post-processing software. EC data were measured above a Scots Pine forest in Hyytiälä, Finland in May 2006.

ACKNOWLEDGEMENTS

The financial supports by the Academy of Finland Centre of Excellence program (project no 1118615) and EU projects ICOS, IMECC and GHG-Europe are gratefully acknowledged.

REFERENCES

- Aubinet, M., A. Grelle, A. Ibrom, U. Rannik, J. Moncrieff, T. Foken, A. S. Kowalski, P. H. Martin, P. Berbigier, C. Bernhofer, R. Clement, J. Elbers, A. Granier, T. Grünwald, K. Morgenstern, K. Pilegaard, C. Rebmann, W. Snijders, R. Valentini, and T. Vesala (2000). Estimates of the annual net carbon and water exchange of forests: The EUROFLUX methodology, *Adv. Ecol. Res.*, 30, 113–175.
- Foken, T. and B. Wichura (1996). Tools for quality assessment of surface-based flux measurements, *Agric. and For. Meteorol.*, 78, 83-105.
- Ibrom, A., E. Dellwik, S. E. Larsen and K. Pilegaard (2007). On the use of the Webb–Pearman–Leuning theory for closed-path eddy correlation measurements. *Tellus B*, 59: 937–946.
- Liu, H., G. Peters, and T. Foken (2001). New equations for sonic temperature variance and buoyancy heat flux with an omnidirectional sonic anemometer, *Bound.-Lay. Meteorol.*, 100, 459–468.
- Mammarella I., S. Launiainen, T. Gronholm, P. Keronen, J. Pumpanen, Ü. Rannik and T. Vesala (2009). Relative humidity effect on the high frequency attenuation of water vapour flux measured by a closed-path eddy covariance system, *Journal of Atmospheric and Oceanic Technology*, 26(9), 1856-1866.
- Mauder, M., T. Foken, R. Clement, J. A. Elbers, W. Eugster, T. Grünwald, B. Heusinkveld, and O. Kolle (2008). Quality control of CarboEurope flux data - Part 2: Inter-comparison of eddy-covariance software, *Biogeosciences* 5, 451-462.
- McMillen, R. T. (1988). An eddy correlation technique with extended applicability to non-simple terrain, *Bound.-Lay. Meteorol.*, 43, 231-245.
- Moncrieff, J. B., J. M. Massheder, H. DeBruin, J. Elbers, T. Friborg, B. Heusinkveld, P. Kabat, S. Scott, H. Søgaard and A. Verhoef (1997). A system to measure surface fluxes of momentum, sensible

- heat, water vapor and carbon dioxide, *J. Hydrol.*, 188–189, 589–611.
- Moore, C. J. (1986). Frequency response corrections for eddy correlation systems, *Bound.-Lay. Meteorol.*, 37, 17–35.
- Nakai, T., M.K. van der Molen, J.H.C. Gash and Y. Kodama (2006). Correction of sonic anemometer angle of attack errors, *Agric. and For. Meteorol.*, 136, 19-30.
- Rannik, Ü., and T. Vesala (1999). Autoregressive filtering versus linear detrending in estimation of fluxes by the eddy covariance method, *Bound.-Lay. Meteorol.*, 91, 259-280.
- Schotanus, P., F. T. M. Nieuwstadt, and H. A. R. DeBruin (1983). Temperature measurement with a sonic anemometer and its application to heat and moisture fluctuations, *Bound.-Lay. Meteorol.*, 26, 81–93
- Vickers, D. and L. Mahrt (1997). Quality control and flux sampling problems for tower and aircraft data. *J. Atmos Oceanic Technol.*, 14, 512-527
- Webb, E. K., G. I. Pearman, and R. Leuning (1980). Correction of the flux measurements for density effects due to heat and water vapour transfer, *Q. J. Roy. Meteorol. Soc.*, 106, 85–100.
- Wilczak, J. M., S. P. Oncley and S. A. Stage (2001). Sonic anemometer tilt correction algorithms, *Bound.-Lay. Meteorol.*, 99, 127–150.

DIRECT DETECTION OF ATMOSPHERIC PARTICLE FORMATION USING ION SPECTROMETERS

H.E. MANNINEN¹, A. HIRSIKKO¹, T. NIEMINEN¹, T. YLI-JUUTI¹, E. ASMI², J. KONTKANEN¹, A. FRANCHIN¹, S. GAGNÉ¹, K. LEHTIPALO¹, V.-M. KERMINEN², T. PETÄJÄ¹, and M. KULMALA¹

¹Department of Physics, University of Helsinki, P.O. BOX 64, 00014 University of Helsinki, Finland

²Finnish Meteorological Institute, Research and Development, P.O. BOX 503, FI-00101, Finland

Keywords: AIR IONS, PARTICLE FORMATION, ION-INDUCED NUCLEATION.

INTRODUCTION

Aerosol particles exist everywhere in the atmosphere, they are diverse and complex, and they are in a constant movement and interaction with their surroundings. Aerosol particle sizes range from nanometer sized molecular clusters up to approximately 100 μm cloud droplets. Aerosol particles have global effects on Earth's climate and regional effects on air quality. The main characterizing parameters of atmospheric particles are their size, concentration, and composition. Secondary new particle formation (NPF) increases the total particle concentration and decreases the median particle size. Under favorable conditions, nucleated particles grow into sizes in which they are able to act as cloud condensation nuclei.

From a physical point of view, two very different particle types can be distinguished: charged (air ions or ion clusters) and neutral particles. The existence of atmospheric ion clusters as small as 0.5-1 nm in diameter has been known for decades, and measurements with ion spectrometers, such as the Air Ion Spectrometer (AIS, Mirme et al., 2007) and Balanced Scanning Mobility Analyzer (BSMA, Tammet et al., 2006), have demonstrated that such clusters are present practically all the time (Hirsikko et al., 2011). The production rates of ion clusters are, however, generally too low to explain the observed particle formation rate (Hirsikko et al., 2011). In view of the insufficient numbers of ion clusters, the key to understanding the atmospheric NPF is clearly the presence of neutral clusters. Direct measurement at the size range where the nucleation occurs infers the possible mechanism for NPF (relative contribution of ions or neutral particles to total particle formation).

METHODS

Ion spectrometers were used to measure the mobility distributions of charged aerosol particles and clusters down to molecular sizes. Atmospheric nucleation and cluster activation takes place in the mobility diameter range of 1.5–2 nm (Nieminen et al., 2009). Therefore, ion spectrometers allow direct measurements exactly at the size where atmospheric nucleation occurs. In addition to characterizing the spatial and temporal variability of the nucleation events, this enables the investigation of several parameters relevant to nucleation events, including the particle formation and growth rates. Understanding the temporal variation of the NPF phenomenon and quantifying its effect on the climate and air quality requires both intensive field campaigns and long-term, continuous field measurements.

RESULTS AND CONCLUSIONS

Although a large number of observations have shown that atmospheric NPF takes place frequently in the continental boundary layer, the role of ions in this process is not well quantified. Therefore, ion spectrometers have been measuring in many different locations for example in continuous measurements in Hyytiälä, Finland (Manninen et al., 2009), and in EUCAARI (European Integrated project on Aerosol Cloud Climate and Air Quality interactions) campaign one-year-long time series

from 12 continental measurement sites (Manninen et al., 2010). The data set presented by Manninen et al. (2010) is unique. To date, the EUCAARI ion spectrometer measurements are the most comprehensive effort to experimentally characterize nucleation and growth of atmospheric clusters and particles at ground-based observation sites on a continental scale. The twelve field sites represent a wide variety of environments, such as marine, coastal, remote continental, suburban, rural and mountainous regions. The field sites are located at different altitudes ranging from sea level to several thousands of meters above sea level. NPF was observed to occur at all the sites and the observations were used as indicators of the particle formation mechanisms. Particle formation rates and size-dependent growth rates were examined to obtain information on NPF and subsequent growth.

The recently developed Neutral cluster and Air Ion Spectrometer (NAIS, Kulmala et al., 2007; Manninen et al., 2010) can be reliably used to measure ions and neutral species near the sizes where atmospheric particle formation begins. The main purposes of the NAIS are to: (1) charge particles efficiently in sub-3 nm size range, (2) detect the fraction concentration of charged particles down to 10 cm^{-3} in air, (3) measure with a high enough time resolution that enables the detection of rapid changes in size spectra during particle formation bursts, and (4) cover the whole size range from cluster molecules up to 42 nm, which approaches the climatically relevant sizes where the particles act as cloud condensation nuclei. In the case of parallel ion and neutral cluster measurements, also the contribution of ions to the NPF can be investigated.

One of the key problems in elucidating the atmospheric nucleation is the importance of ion-induced nucleation. As a solution, simultaneous measurement of the concentrations of charged and neutral nanoparticles is a viable method to detect it. Based on our study, neutral particle formation seems to dominate over ion-induced and ion-mediated nucleation, at least in the continental boundary layer. The results obtained from the NAIS particle and ion measurements agree well with separate independent measurements performed with other electrical mobility spectrometer (Gagné et al., 2011) and condensation based (Lehtipalo et al., 2009) techniques. The formation rates of charged particles at 2 nm accounted for 1-30 % of the respective total particle formation rates. As a significant new result, we found out that the total particle formation rate varied much more between the different sites than the formation rate of charged particles (Manninen et al., 2010).

In order to understand the role of atmospheric aerosol particles in the climate change and radiative forcing and feedbacks related to it, long-term measurements are crucially needed. Continuous time series are essential to understanding difference between seasonal and long-term interannual variability. As an example, continuous (particle and) ion number size distribution measurements at SMEAR II in Hyytiälä since (1997 and) 2003 can be seen as a good starting point towards the right direction. The instrumental developments described here, observing neutral clusters about a nanometer smaller than any earlier measurement technique, offer a chance to test the existing nucleation theories against real atmospheric data. By conducting measurements similar to those reported here in a few carefully-selected locations, it should be possible to develop simple yet sufficiently accurate nucleation parameterizations for large-scale modeling (Paasonen et al., 2010; Nieminen et al., 2011).

ACKNOWLEDGEMENTS

This work has been supported by European Commission 6th Framework program projects: EUCAARI, contract no 036833-2 (EUCAARI). The financial support by the Academy of Finland Centre of Excellence program (project no 1118615) is also gratefully acknowledged.

REFERENCES

Gagné, S., Lehtipalo, K., Manninen, H.E., Nieminen, T., Schobesberger, S., Franchin, A., Yli-Juuti, T., Boulon, J., Sonntag, A., Mirme, S., Mirme, A., Hörrak, U., Petäjä, T., Asmi, E., and Kulmala, M.: Intercomparison of air ions spectrometers: a basis for data interpretation (2011). *Atmos. Meas. Tech. Discuss.*, 4, 1139-1180.

- Hirsikko, A., Nieminen, T., Gagné, S., Lehtipalo, K., Manninen, H. E., Ehn, M., Hörrak, U., Kerminen, V.-M., Laakso, L., McMurry, P. H., Mirme, A., Mirme, S., Petäjä, T., Tammet, T., Vakkari, V., Vana, M., and Kulmala, M. (2011). Atmospheric ions and nucleation: a review of observations. *Atmos. Phys. Chem.*, 11, 767–798.
- Kulmala, M., Riipinen, I., Sipilä, M., Manninen, H.E., Petäjä, T., Junninen, H., Dal Maso, M., Mordas, G., Mirme, A., Vana, M., Hirsikko, A., Laakso, L., Harrison, R.M., Hanson, I., Leung, C., Lehtinen, K.E.J. and Kerminen, V.-M.: Towards direct measurement of atmospheric nucleation. *Science*, 318, 89-92, 2007.
- Lehtipalo, K., Sipilä, M., Riipinen, I., Nieminen, T., and Kulmala, M.: Analysis of atmospheric neutral and charged molecular clusters in boreal forest using pulse-height CPC, *Atmos. Chem. Phys.*, 9, 4177-4184, 2009.
- Manninen, H.E., Petäjä, T., Asmi, E., Riipinen, I., Nieminen, T., Mikkilä, J., Hörrak, U., Mirme, A., Mirme, S., Laakso, L., Kerminen, V.-M. & Kulmala, M.: Long-term field measurements of charged and neutral clusters using Neutral cluster and Air Ion Spectrometer (NAIS). *Boreal Env. Res.* 14, 591–605, 2009.
- Manninen, H. E., Nieminen, T., Asmi, E., Gagné, S., Häkkinen, S., Lehtipalo, K., Aalto, P., Vana, M., Mirme, A., Mirme, S., Hörrak, U., Plass-Dülmer, C., Stange, G., Kiss, G., Hoffer, A., Törő, N., Moerman, M., Henzing, B., de Leeuw, G., Brinkenberg, M., Kouvarakis, G. N., Bougiatioti, A., Mihalopoulos, N., O'Dowd, C., Ceburnis, D., Arneth, A., Svenningsson, B., Swietlicki, E., Tarozzi, L., Decesari, S., Facchini, M. C., Birmili, W., Sonntag, A., Wiedensohler, A., Boulon, J., Sellegri, K., Laj, P., Gysel, M., Bukowiecki, N., Weingartner, E., Wehrle, G., Laaksonen, A., Hamed, A., Joutsensaari, J., Petäjä, T., Kerminen, V.-M., and Kulmala, M.: EUCAARI ion spectrometer measurements at 12 European sites – analysis of new particle formation events, *Atmos. Chem. Phys.*, 10, 7907-7927, 2010.
- Mirme, A., Tamm, E., Mordas, G., Vana, M., Uin, J., Mirme, S., Bernotas, T., Laakso, L., Hirsikko, A., and Kulmala, M. (2007). A wide-range multi-channel Air Ion Spectrometer. *Boreal Environ. Res.*, 12, 247–264.
- Nieminen, T., Manninen, H. E., Sihto, S.-L., Yli-Juuti, T., Mauldin, III, R. L., Petäjä, T., Riipinen, I., Kerminen, V.-M., and Kulmala, M.: Connection of sulfuric acid to atmospheric nucleation in boreal forest, *Environ. Sci. Technol.*, 43, 4715–4721, 2009.
- Nieminen, T., Paasonen, P., Manninen, H. E., Sellegri, K., Kerminen, V.-M., and Kulmala, M.: Parameterization of ion-induced nucleation rates based on ambient observations, *Atmos. Chem. Phys.*, 11, 3393-3402, 2011.
- Paasonen, P., Nieminen, T., Asmi, E., Manninen, H., Petäjä, T., Plass-Dülmer, C., Birmili, W., Hörrak, U., Metzger, A., Baltensperger, U., Hamed, A., Laaksonen, A., Kerminen, V.-M., and Kulmala, M.: On the role of sulphuric acid and low-volatility organic vapours in new particle formation at four European measurement sites, *Atmos. Chem. Phys.*, 10, 11223-1124, 2010.
- Tammet, H.: Continuous scanning of the mobility and size distribution of charged clusters and nanometer particles in atmospheric air and the Balanced Scanning Mobility Analyzer BSMA, *Atmos. Res.*, 82: 523–535, 2006.

Historical trends in global and regional CCN concentrations from 1850 to 2000

J. MERIKANTO¹, C. CARSLAW², H. KORHONEN³ and M. KULMALA¹

¹ Division of Atmospheric Sciences, University of Helsinki, Finland.

² School of Earth and Environment, University of Leeds, UK.

³Department of Physics and Mathematics, University of Eastern Finland, Kuopio, Finland.

Keywords: Global aerosols modelling, CCN.

INTRODUCTION

Atmospheric aerosols are derived from particles emitted directly into the atmosphere (primary emissions) or from formation of new particles through nucleation from precursor gases. Aerosols interact with climate directly by scattering and absorbing sunlight, and indirectly by acting as cloud condensation nuclei (CCN). Increased CCN concentrations leads to enhanced reflectivity of warm clouds, which results in negative climate forcing. Industrialization has resulted in large increases in both primary aerosol and aerosol precursor gas emissions around the globe. However, these increases have not been uniform around the globe, nor have they taken place as a smooth function of time. Therefore, changes in aerosol-related climate forcings are spatially and temporally inhomogeneous, and importantly, their forcing trends differ from much smoother (and positive) forcing trends of greenhouse gases.

Here we investigate the trends in CCN concentrations from early industrialization (1850) close to modern day (2000) in global and regional (continental-wide) levels. In our study we use a global aerosol model GLOMAP (Spracklen et al., 2005) paired with latest historical emission inventories.

METHODS

We use a global microphysics model GLOMAP to simulate the CCN concentrations in years 1850, 1910, 1930, 1950, 1970, 1980, 1990, and 2000. GLOMAP is an extension to a 3-D offline chemical transport model TOMCAT (Chipperfield, 2006), and has a horizontal resolution of 2.8×2.8 deg with 31 vertical levels between the surface and 10 hPa. The model meteorology is obtained from ECMWF analysis for the year 2000. Same meteorology is used for all years. Aerosol is modelled using two different sectional distributions with 20 size bins spanning from 3nm to 25 μm , and consists of sulfate (SU), sea salt (SS), elemental carbon (EC), and organic carbon (OC). One of the distributions is hydrophobic containing freshly emitted EC and OC, and the other distribution is hydrophilic and contains SU, SS, and aged EC and OC. The condensing vapors include sulfuric acid and secondary organics that is derived from first stage oxidation products of monoterpenes (Guenther et al., 1995) with the assumed yield of 13 %. Secondary organics emissions are assumed to be the same for all years. Historical EC and OC emissions from anthropogenic combustion are obtained from the emission inventory of Bond et al. (2007) and are further divided into fossil fuel and biofuel components using the inventory of Fernandes et al. (2007). Historical anthropogenic sulfur emissions are obtained from the inventory of Smith et al. (2004), with 2.5% of sulphur emitted as primary sulfate and the remaining sulphur as gaseous SO_2 . Historical wildfire emissions are obtained from the inventory of (Dentener et al., 2006) for years 1750 and 2000, and are taken as the population weighted average for the studied years. Other emission including constantly erupting volcanoes, SS, and marine dimethylsulfide (DMS) are assumed to be the same for all

years. Volcanic emissions obtained from AeroCom emission inventory (Dentener et al., 2006). For SS emissions we follow the scheme of Gong (2003), and for DMS we use the scheme of Kettle et al. (1999).

Aerosol is produced by the combination of primary particle emissions and atmospheric nucleation. For nucleation we use a combination of homogeneous H₂SO₄-H₂O scheme by Kulmala et al. (1998) (mainly taking place in the upper free troposphere) and activation nucleation in the boundary layer (Kulmala et al., 2006), where the the proportionality constant $A = 2 \cdot 10^6 \text{ cm}^{-3}$ is used. CCN concentrations are calculated using the method presented by Petters and Kreidenweis (2007) for a constant supersaturation of 0.2%, typical for warm stratocumulus clouds considered to be most susceptible for changes in their albedo.

CONCLUSIONS

According to our calculations shown in Figure 1, industrialization has resulted the global CCN concentrations to roughly double. However, changes have been larger over continental regions, while marine regions are also effected due to shipping and long range transport of aerosols.

The changes in CCN concentrations result from the combined changes in anthropogenic sulfur and particulate organic emissions. Global anthropogenic sulfur emissions grew strongly from the start of industrialization until late 1970's, but have declined since (Smith et al., 2004). On the other hand, global particulate organic emissions have continued to climb (Bond et al., 2007). According to our study, the combined effect has been the rise in global CCN concentrations until 1980, after which they have stayed nearly constant.

Regional trends in changes have been strongest over continental Europe, where early industrialization tripled CCN concentrations from 1850 to 1910. European CCN concentrations peaked in 1970-1980, but have since declined strongly due to reductions in European sulfur emissions. On the other hand, CCN concentrations over South-East Asia have continued to rise strongly in recent decades.

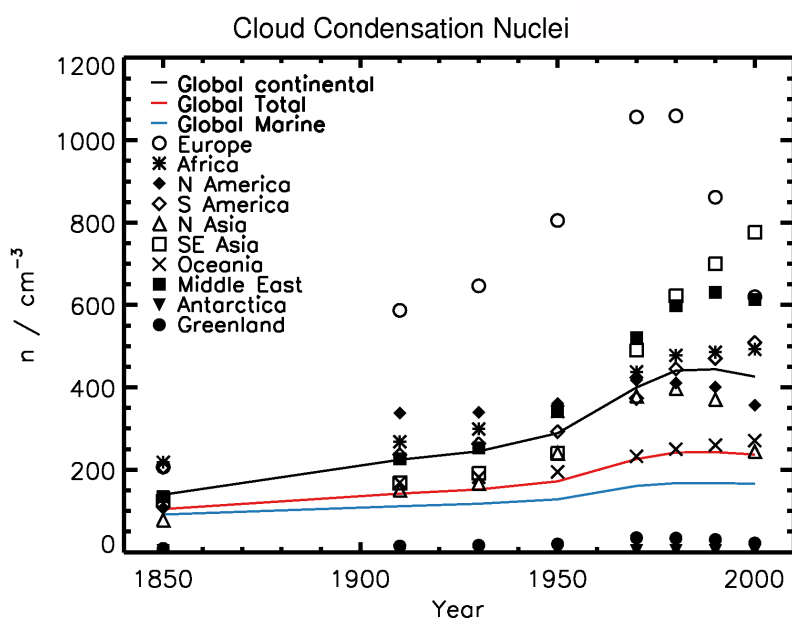


Figure 1: Calculated global and regional trends in CCN at 0.2% supersaturation due to changes in anthropogenic emissions.

REFERENCES

- Bond, T., E. Bhardwaj, R. Dong, R. Jogani, S. Jung, C. Roden, D. G. Streets, and N. M. Trautmann (2007), Historical emissions of black and organic carbon aerosol from energy-related combustion, 1850-2000, *Global Biogeochem. Cycles*, *21*, GB2018.
- Chipperfield, M. (2006), New version of the TOMCAT/SLIMCAT off-line chemical transport model: Intercomparison of stratospheric tracer experiments, *Q. J. R. Meteorol. Soc.*, *132*, 1179–1203, doi:10.1256/qj.05.51.
- Dentener, F., S. Kinne, T. Bond, O. Boucher, J. Cofala, S. Generoso, P. Ginoux, S. Gong, J. Hoelzemann, A. Ito, L. Marelli, J. Penner, J.-P. Putaud, C. Textor, M. Schulz, G. v.d Werf, and J. Wilson (2006), Emissions of primary aerosol and precursor gases in the years 2000 and 1750 prescribed data-sets for AeroCom, *Atmos. Chem. Phys.*, *6*, 4321–4344.
- Fernandes, S. D., N. M. Trautmann, D. G. Streets, C. A. Roden, and T. C. Bond (2007), Global biofuel use, 1850-2000, *Global Biogeochem. Cycles*, *21*, GB2019.
- Gong, S. L. (2003), A parameterization of sea-salt aerosol source function for sub- and super-micron particles, *Global Biogeochem. Cycles*, *17*(4), 1097.
- Guenther, A., C. N. Hewitt, D. Erickson, et al (1995), A global model of natural volatile organic compound emissions, *J. Geophys. Res.*, *100*, 8873–8892.
- Kettle, A. J., Andreae, M. O., Amouroux, D., et al (1999), A global database of sea surface dimethyl sulfide (DMS) measurements and a procedure to predict sea surface DMS as a function of latitude, longitude, and month, *Global Biogeochem. Cycles*, *13*(2), 399-444.
- Kulmala, M. , Laaksonen, A. , and Pirjola, L. (1998), Parameterization for sulfuric acid/water nucleation rates, *J. Geophys. Res.*, *103*, 8301-8308.
- Kulmala, M., K. E. J. Lehtinen, and A. Laaksonen (2006), Cluster activation theory as an explanation of the linear dependence between formation rate of 3 nm particles and sulfuric acid concentration, *Atmos. Chem. Phys.*, *6*, 787–793.
- Petters, M.D., and Kreidenweis, S.M., A single parameter representation of hygroscopic growth and CNN activity (2007), *Atmos. Chem. Phys.*, *7*, 1961-1971.
- Smith, S. J., R. Andres, E. Conception, J. and Lurz (2004), Historical sulfur dioxide emissions 1850-2000: Methods and results, *PNNL Research Report*, PNNL-14537.
- Spracklen, D. V., K. J. Pringle, K. S. Carslaw, M. P. Chipperfield, and G. W. Mann (2005), A global off-line model of size-resolved aerosol microphysics: I. Model development and prediction of aerosol properties, *Atmos. Chem. Phys.*, *5*, 2227–2252.

AEROSOL SIZE RESOLVED VERTICAL FLUX MEASUREMENTS

P MIETTINEN¹, P TIITTA¹, A JAATINEN¹, A KORTELAINEN¹, L HAO¹, J SMITH^{1,2,3}
AND A LAAKSONEN²

¹Department of applied physics, University of Eastern Finland, 70210, Kuopio, Finland

²Finnish Meteorological Institute, 00101, Helsinki, Finland

³National Center for Atmospheric Research, 80307, Boulder, CO USA

Keywords: AEROSOL, FLUX, SIZE-RESOLVED, FMPS

INTRODUCTION

One of the largest uncertainties in the estimation of the Earth's radiation budget is caused by incomplete understanding of aerosol induced cooling effect (IPCC, 2007). Numerous properties of aerosol population such as the size distribution, number concentration, and chemical composition affect the interactions of aerosols and radiation. In addition to aerosol properties, knowledge of particle origin and transport are essential for gaining a better understanding of aerosol's impact on atmospheric processes. Aerosol vertical flux measurements can give new information about spatial and temporal evolution of the aerosol population. Using flux measurement data, not only the location and strength of aerosol sinks and sources can be investigated, but the analysis can be extended to, e.g., estimation of particle deposition velocities.

METHODS

The eddy covariance method provides a direct method to estimate vertical aerosol fluxes. Early aerosol flux measurements were aimed at studying total particle number fluxes and it was not until recent years that size resolved particle flux measurements gained attention and real instruments that accomplished this were tested. A major problem prohibiting the use of size resolved particle flux techniques has been absence of suitable instrumentation that must be applied. Size resolved aerosol eddy covariance measurements involve high speed sampling of 3D wind components as well as particle number size distribution information. While high sampling frequency 3D anemometers have been at disposal for decades, the high speed particle sizing instruments have been brought to market just few years ago.

Several methods have been developed to overcome the demand for high frequency particle sizing. Methods like Relaxed Eddy Accumulation and Disjunct Eddy Covariance use special particle sampling strategy to capture high frequency signal information with slow response instrumentation. We demonstrate the direct use of FMPS (Fast Mobility Particle Sizer) for vertical size resolved aerosol flux measurements. While maximum sampling frequency of FMPS is 1 Hz it closes the gap between commonly used 10 Hz sampling frequency of eddy covariance systems and 0.01 Hz which is typical sampling frequency of DMPS systems. In order to find which part of particle size data signal was lost due to 1 Hz sampling we used fast response particle counter (TSI 3010) in parallel to DMPS to monitor total particle number vertical flux.

We report field measurements of size resolved aerosol flux at two sites in central Finland: Puijo Tower (fall 2008, Kuopio, Finland) and Hyytiälä (summer 2009, Juupajoki, Finland). We found that direct sampling with FMPS can provide a decent approximation to the total frequency spectra of size resolved particle flux signal when the measurement site location and meteorological conditions are suitable for EC measurements (Figure 1). In addition, by using a fast response particle counter in parallel with the FMPS it is possible to estimate the lost portion of signal due to 1 Hz sampling.

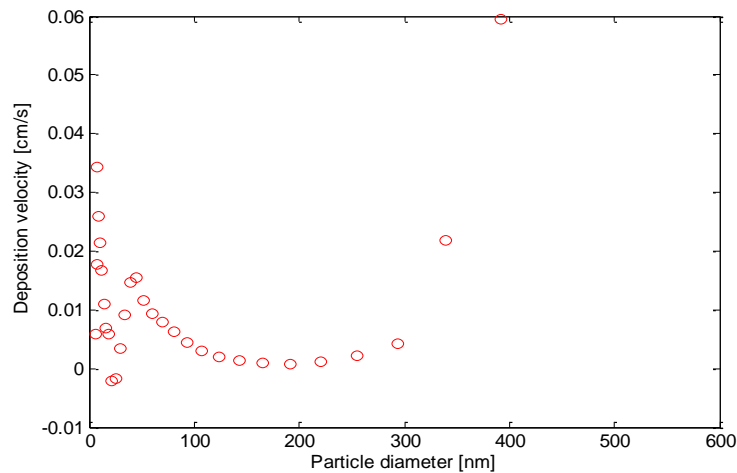


Figure 1. Example of size resolved deposition velocities measured by FMPS in Puijo.

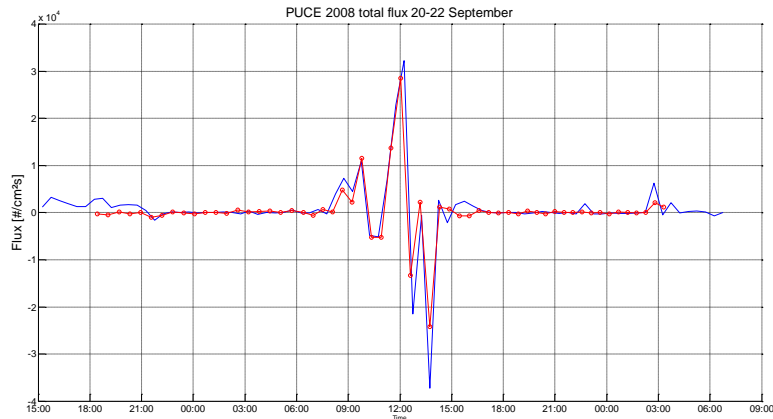


Figure 2. Example of FMPS induced flux (red) vs. CPC induced particle vertical flux.

CONCLUSIONS

FMPS induced vertical aerosol particle flux provides an alternative method for size resolved flux measurements. The use of FMPS simplifies sampling systems compared to e.g. REA or DEC and if used with CPC total particle flux measurements for reference signal, high frequency signal losses can be estimated accordingly to the reference signal.

ACKNOWLEDGEMENTS

This work was supported by the Academy of Finland.

REFERENCES

IPCC (2007). The Physical Science Basis. Cambridge University Press, Cambridge, United Kingdom and New York, NY, USA, 996 pp.

STATISTICAL PROXY FOR SULPHURIC ACID CONCENTRATION

S. MIKKONEN¹, S. ROMAKKANIEMI¹, J. N. SMITH^{1,2}, H. KORHONEN³, T. PETÄJÄ⁴, C. PLASS-DUELMER⁵, M. BOY⁴, P. H. MCMURRY⁶, K.E.J. LEHTINEN^{1,3}, J. JOUTSENSAARI¹, A. HAMED¹, R.L. MAULDIN III², W. BIRMILI⁷, F. ARNOLD⁸, M. KULMALA⁴, and A. LAAKSONEN^{1,9}

¹Department of Applied Physics, University of Eastern Finland, POB 1627, FIN-70211 Kuopio, Finland

²Atmospheric Chemistry Division, National Center for Atmospheric Research, Boulder, CO, USA

³Finnish Meteorological Institute, Kuopio unit, P.O.B. 1627, FIN-70211 Kuopio, Finland

⁴Department of Physics, University of Helsinki, POB 64, FIN-00014 Helsinki, Finland

⁵Hohenpeissenberg Meteorological Observatory, Hohenpeissenberg, Germany

⁶Department of Mechanical Engineering, University of Minnesota, Minneapolis, MN, USA

⁷Leibniz Institute for Tropospheric Research, Permoserstrasse 15, 04318 Leipzig, Germany

⁸Max-Planck-Institute for Nuclear Physics, Heidelberg, Germany

⁹Finnish Meteorological Institute, P.O.B. 503, 00101 Helsinki, Finland

First author email: santtu.mikkonen@uef.fi

Keywords: Sulphuric acid, proxy, statistical prediction

INTRODUCTION

Sulphuric acid has been shown to be involved in nucleation (Kulmala et al., 2004; Kerminen et al., 2010;) and growth of newly formed particles (Laaksonen et al., 2008) and the number concentration of freshly nucleated particles is found to have a strong dependency on sulphuric acid levels (Weber, et al. 1997, Kuang et al., 2008). The problem is that gas phase sulphuric acid concentration is difficult to measure and in many measurement sites no H₂SO₄ data are available. A technique for measuring the gas-phase sulfuric acid concentration even down to about 10⁴ molec cm⁻³ has already been available for more than a decade (Eisele and Tanner, 1993; Berresheim et al., 2000; Sorokin and Arnold, 2007) but the Chemical Ionization Mass Spectrometer (CIMS) devices, used in the measurements, have been quite rare. In addition there are differences between the CIMS devices in use, which causes variation to results of measurements.

Several studies have provided evidence that high SO₂ and radiation levels give a significant contribution to particle formation (Mikkonen et al., 2006; Petäjä et al., 2009) and growth (Boy et al., 2005; Mikkonen et al., 2011) most probably due to their effect on the concentration of H₂SO₄. Hamed et al. (2010) provided evidence that lowered SO₂ concentrations reduced new particle formation (NPF) events in Melpitz, Germany. In addition, Jaatinen et al. (2009) found out that in polluted areas SO₂ concentration is higher on days when NPF occurs. This is most probably due to the fact that SO₂ is the main precursor of gaseous sulphuric acid. On the other hand in a clean environment, Hyytiälä, Finland, SO₂ concentration was lower in days when new particle formation occurred. In Hyytiälä NPF appears to take place usually when condensation sink is low, i.e. when air is clean.

The purpose of this study is to analyze data from six different measurement sites and find an applicable proxy for sulphuric acid concentration, thus expand the study made by Petäjä et al. (2009). Robustness of the analysis results will be tested for different datasets in order to find a proxy which can be used in further studies in places where direct H₂SO₄ measurements have not been made.

METHODS

In total seven datasets, consisting of six campaign datasets and one long term dataset, were analyzed for this study (Table 1). Chemical ionization mass spectrometer was used to measure the gas-phase sulfuric acid concentration in six measurement campaigns and in one long term measurement. The campaign datasets were measured in Hyytiälä, Finland, in San Pietro Capofiume (SPC), Italy, in Melpitz, Germany,

in Atlanta, USA, and in Niwot Ridge (NWR), USA. The long term data were measured in Hohenpeissenberg, Germany (Birmili et al., 2003).

Table 1. Measurement places and times of the campaigns

Measurement site	Measurement time	Coordinates
Hyytiälä, Finland	17.3. – 13.4. 2003	61_510 N, 24_170 E, 181m a.s.l.
	24.3. – 28.6. 2007	
San Pietro Capofiume (SPC), Italy	21.6. – 16.7.2009	44_390 N, 11_370 E, 11m a.s.l.
Melpitz, Germany	30.4. – 31.5.2008	51_320 N, 12_540 E, 87m a.s.l.
Niwot Ridge (NWR), USA	24.6. – 15.7.2007	40_62 N, 105_50 W, >3000 m a.s.l.
Atlanta, USA	30.7. – 31.8.2002	33_74 N, 84_38 W, 275 m a.s.l.
Hohenpeissenberg (HPB), Germany	1.4.1998 – 31.7.2000	47_480 N, 11_00 E, 985m a.s.l.

The main source of sulphuric acid in the atmosphere is the reaction chain induced by SO₂ and OH radical whereas its main sink is condensation to aerosol particles. A proxy for sulphuric acid concentration is based on a production mechanism that is described by the net reaction SO₂+OH→H₂SO₄+HO₂, and a deposition-based loss mechanism that is described by a first order rate constant, *CS*, also known as the condensation sink. Integrating the differential equation for sulphuric acid concentration

$$d[H_2SO_4]/dt = k \cdot [OH] \cdot [SO_2] - [H_2SO_4] \cdot CS,$$

where *k* is temperature dependent reaction constant, gives the sulphuric acid concentration at given time. To simplify the problem, it can be assumed that the H₂SO₄ production is in steady-state, which leads to proxy function given by

$$[H_2SO_4] = k \cdot [OH] \cdot [SO_2] \cdot CS^{-1}.$$

OH radical concentration is suggested to be strongly correlated with the intensity of ultraviolet radiation (Rohrer and Berresheim, 2006) despite the complex OH chemistry in the atmosphere. UV radiation is highly correlated with global radiation so due to UV-data availability issues we use the measurements of global radiation as a proxy for OH.

RESULTS

First we made tests with a linear fitting procedure in order to test different proxy functions L1-L5, introduced in Table 2. In all proxies *B* is a constant, calculated from the data, *k* is temperature depended reaction constant, [H₂SO₄] is sulphuric acid concentration in molec cm⁻³, *Radiation* is global radiation in W m⁻², [SO₂] is sulphur dioxide concentration in molec cm⁻³ and *CS* is the condensation sink in s⁻¹. All observations are 10 minute averages of the variables and only data points with *Radiation* higher than 10 W m⁻² and [SO₂] higher than 0.1 ppb were used in the analysis.

Table 2. Proxy functions for fitting procedures.

Proxy	Equation	Proxy	Equation
L1	$B \cdot k \cdot Radiation \cdot [SO_2] \cdot CS^{-1}$	N1	$a \cdot k \cdot Radiation^b \cdot [SO_2]^c \cdot CS^d$
L2	$B \cdot k \cdot Radiation \cdot [SO_2]$	N2	$a \cdot k \cdot Radiation^b \cdot [SO_2]^c$
L3	$B \cdot k \cdot Radiation \cdot [SO_2]^{0.5}$	N3	$a \cdot k \cdot Radiation^b \cdot [SO_2]^c \cdot RH^e$
L4	$B \cdot k \cdot Radiation \cdot [SO_2] \cdot RH^{-1}$	N4	$a \cdot k \cdot Radiation^b \cdot [SO_2]^c \cdot CS^d \cdot RH^e$
L5	$B \cdot k \cdot Radiation \cdot [SO_2] \cdot (CS \cdot RH)^{-1}$	N5	$a \cdot k \cdot Radiation^b \cdot [SO_2]^c \cdot (CS \cdot RH)^f$

In theory the Proxy L1 should give the best results but it is outperformed by another proxy in every dataset except Hohenpeissenberg. In SPC, Melpitz and both Hyytiälä data the best linear proxy was L3, with *Radiation* · [SO₂]^{0.5}, where correlation *R* between the observed [H₂SO₄] and predicted values given by the proxy were 0.88, 0.82, 0.74 and 0.86, respectively. The square root dependence of [SO₂] suggests that it acts also as an indicator for pollution i.e. the sinks of sulphuric acid. This is supported by the result that in NWR, where the air is the cleanest, the power of [SO₂] in the best proxy is 1 (*R*=0.67). In Atlanta high relative humidity in mornings may affect the sulphuric acid concentrations and it has to be taken account

in the proxy. The best prediction was gained with Proxy L5 ($R=0.82$) but also Proxy L3 performed well ($R=0.80$). Note that Proxy L4 outperformed Proxy L1 in Melpitz, Hyytiälä, NWR and Atlanta, which suggests that in these data RH might be better indicator for removal process of $[H_2SO_4]$ than CS .

Proxy L3 giving the best approximation in linear type fitting suggests that the steady state assumption is possibly somewhat unrealistic in atmospheric conditions and thus the linear fitting procedure may not be optimal for proxy construction. In order to find the optimal parameterization for the proxy, a nonlinear least squares fitting procedure was applied to all datasets, with fit functions N1-N5 given by Table 2. In these proxies a , b , c , d , e and f are parameters fitted from the data and k is temperature depended reaction constant.

If the steady state applies without any additional chemistry, then in Proxy N1 b and c should be unity and d should be -1, and as seen from results of Proxy L1 in some cases it turns out to be an adequate approximation. However, the fitting procedure results show that the powers vary a lot for the best predictive models and that they are quite far from the theoretical values; for Proxy N1 the powers b , c and d vary in ranges 0.17–1.41, 0.48–0.88 and -0.58–0.41, respectively.

Performance of the proxies varies slightly between the sites. Best correlations between observed and predicted sulphuric acid concentrations ($R>0.9$) were found with Proxy N4 in SPC and in Atlanta where the air is most polluted whereas the lowest correlations in general in campaign datasets was found in NWR which is the cleanest of the sites. Long term data from Hohenpeissenberg is the most difficult to predict due to seasonal variation of meteorological parameters and opposite seasonal variation of $[H_2SO_4]$ and $[SO_2]$: sulphuric acid concentration is at its highest in the summer, when solar radiation is at its highest, but SO_2 concentration is at its highest in winter time. Still, the correlation between observed and predicted value with proxies N4 and N5 can reach almost 0.7, which can be considered a good result for dataset this long. In SPC, Melpitz and Hyytiälä 2003 datasets the differences between prediction abilities of the proxies are negligible, which indicates that in these data Proxy N2 with only Radiation and $[SO_2]$ is capable to explain most of the variation of the sulphuric acid concentration and no further parameters are needed.

ACKNOWLEDGEMENTS

This work was supported by Alfred Kordelin foundation and The Academy of Finland Center of Excellence program (project number 1118615).

REFERENCES

- Berresheim, H., et al.: Chemical ionization mass spectrometer for longterm measurements of atmospheric OH and H_2SO_4 , *Int. J. Mass. Spectrom.*, 202, 91–109, 2000.
- Birmili, W., et al.: The Hohenpeissenberg aerosol formation experiment (HAFEX): A long-term study including size-resolved aerosol, H_2SO_4 , OH, and monoterpenes measurements, *Atmos. Chem. Phys.*, 3, 361–376, 2003
- Boy, M., et al.: Sulphuric acid closure and contribution to nucleation mode particle growth, *Atmos. Chem. Phys.*, 5, 863–878, doi:10.5194/acp-5-863-2005, 2005.
- Eisele, F. and Tanner, D.: Measurement of the gas phase concentration of H_2SO_4 and methane sulfonic acid and estimates of H_2SO_4 production and loss in the atmosphere, *J. Geophys. Res.*, 98, 9001–9010, 1993.
- Hamed, A., et al.: Changes in the production rate of secondary aerosol particles in Central Europe in view of decreasing SO_2 emissions between 1996 and 2006, *Atmos. Chem. Phys.*, 10, 1071–1091, 2010.
- Jaatinen, A., et al.: A comparison of new particle formation events in the boundary layer at three different sites in Europe. *Boreal Environ. Res.*, 14: 481–498, 2009.
- Kerminen, V.-M., et al.: Atmospheric nucleation: highlights of the EUCAARI project and future directions, *Atmos. Chem. Phys.*, 10, 10829–10848, doi:10.5194/acp-10-10829-2010, 2010.

- Kuang, C., et al.: Dependence of nucleation rates on sulfuric acid vapor concentration in diverse atmospheric locations, *J. Geophys. Res.*, 113, D10209, doi:10.1029/2007JD009253, 2008.
- Kulmala, M., et al.: Formation and growth rates of ultrafine atmospheric particles: a review of observations, *J. Aerosol Sci.*, 35, 143–176, 2004.
- Laaksonen, A., et al.: SO₂ oxidation products other than H₂SO₄ as a trigger of new particle formation – Part 2: Comparison of ambient and laboratory measurements, and atmospheric implications, *Atmos. Chem. Phys.*, 8, 7255-7264, 2008.
- Mikkonen, S., et al.: Using discriminant analysis as a nucleation event classification method, *Atmos. Chem. Phys.*, 6, 5549-5557, doi:10.5194/acp-6-5549-2006, 2006.
- Mikkonen, S., et al.: Meteorological and trace gas factors affecting the number concentration of atmospheric Aitken (D_p=50 nm) particles in the continental boundary layer: parameterization using a multivariate mixed effects model. *Geosci. Model Dev.* 4 1-13. doi:10.5194/gmd-4-1-2011, 2011
- Petäjä, T., et al.: Sulfuric acid and OH concentrations in a boreal forest site, *Atmos. Chem. Phys.*, 9, 7435-7448, doi:10.5194/acp-9-7435-2009, 2009.
- Sorokin, A. and Arnold, F.: Laboratory study of cluster ions formation in H₂SO₄-H₂O system: Implications for threshold concentration of gaseous H₂SO₄ and ion-induced nucleation kinetics, *Atmos. Environ.*, 41, 3740–3747, doi:10.1016/j.atmosenv.2007.01.017, 2007.
- Rohrer and Berresheim, Strong correlation between levels of tropospheric hydroxyl radicals and solar ultraviolet radiation, *Nature*, 442, 184–187, doi:10.1038/nature04924, 2006
- Weber, R. J., et al.: Measurements of new particle formation and ultrafine particle growth rates at a clean continental site. *J. Geophys. Res.*, 1997: 4375-4385.

OH-REACTIVITY AND CONCENTRATION IN SUMMERTIME BOREAL FOREST

D. MOGENSEN¹, S. SMOLANDER¹, A. NÖLSCHER², J. WILLIAMS², V. SINHA^{2,3}, L. ZHOU¹, A. GUENTHER⁴, T. NIEMINEN¹, M. KAJOS¹, J. RINNE¹, A. SOGACHEV⁵, M. KULMALA¹ and M. BOY¹

¹Division of Atmospheric Sciences, Department of Physics, University of Helsinki, P.O. Box 48, FIN-00014.

² Max Planck Institute of Chemistry, J. Becher Weg 27, 55128 Mainz, Germany.

³ Indian Institute of Science Education and Research (IISER) Mohali, MGSIPAP Complex, Sector 26, Chandigarh 160019.

⁴ National Center for Atmospheric Research, Boulder, CO 80307, USA.

⁵ Wind Energy Division, Risø National Laboratory for Sustainable Energy. Technical University of Denmark. Building 118, Box 49, DK-4000, Roskilde, Denmark.

Keywords: OH-REACTIVITY, OH CONCENTRATION, SOA, ATMOSPHERIC MODELLING.

INTRODUCTION

The hydroxyl radical (OH) is the most important oxidant in the atmosphere. Understanding both the sources and sinks of OH is key to assessing the atmosphere's capacity to oxidise gas phase organic trace gases and produce secondary organic aerosols (SOA). Currently, researchers believe that H₂SO₄ is taking part in both aerosol formation and growth, and it is therefore highly essential to predict correct OH concentrations by models, since it is from OH-oxidation of SO₂ that H₂SO₄ eventually is produced. Wrong H₂SO₄ concentrations in models lead to wrong modelled aerosol parameters, which among other effects, increase uncertainties on climate predictions from aerosols.

While the production term for OH has thought to be reasonably well constrained by radiometer measurements (JO¹D), the sink term (total OH-reactivity) was until recently only indirectly determined by summing the contributions of all available measured participating compounds.

The application of Laser Induced Fluorescence (LiF) has allowed total OH lifetime and hence total OH-reactivity (OH-reactivity = 1/ OH lifetime) to be determined directly in campaigns such as PROPHET 2000 (Di Carlo *et al.*, 2004), INTEX-B (Mao *et al.*, 2009), PMTACS-NY2001 (Ren *et al.*, 2003) and PRD (Lou *et al.*, 2009). The principle of the LiF instrument is to excite OH on-off in a low pressure chamber. When the excited OH transits to ground state, it emits fluorescence that is then detected (Faloona *et al.*, 2004). Measuring the total OH-reactivity using LiF is difficult, since it requires the rapid measurement of OH at very low concentrations and requires complicated corrections due to atmospheric NO to be taken into account.

Here we use a dataset acquired using an alternative method, namely the comparative reactivity approach (Sinha *et al.*, 2008). This technique circumvents the difficult task of measuring OH radicals directly and instead relies on the accurate measurement of pyrrole at high mixing ratios (> 15 ppbV) using a Proton Transfer Reaction – Mass Spectrometer (PTR-MS) (Sinha *et al.*, 2010). Since measurement techniques provide data at a specific point for a limited period, modelling is needed in order to develop an overall spatial and temporal understanding of the total reactivity and test the accuracy of chemical parametrizations by comparison with measurements.

OH-reactivity has previously been calculated in models, albeit with limited chemistry; (Apel *et al.*, 2010) (including 85 chemical species, and 196 reactions), and from field measurements by adding the OH-reactivity of the individually measured OH sinks (e.g. NMHCs, CO, CH₄, NO_x) (Lou *et al.*, 2009; Sinha *et al.*, 2010; Di Carlo *et al.*, 2004).

METHODS

We have modelled the atmospheric OH-reactivity and concentration in a boreal forest and investigated the contributions from atmospheric inorganic species, methane, isoprene, monoterpenes and other important VOCs. Daily and seasonal variations in the reactivity are also presented, as are the vertical reactivity profiles until the boundary layer.

We have used SOSA (Model to Simulate the concentrations of Organic vapours and Sulphuric Acid); a one-dimensional vertical chemistry-transport model (Boy *et al.*, 2011) which includes very detailed chemistry with chemical reaction equations selected from the Master Chemical Mechanism (<http://mcm.leeds.ac.uk/MCM/>) and processed using the Kinetic PreProcessor (KPP) (Damian *et al.*, 2002). In order to ascertain how well we understand the OH initiated photochemical processes, we have compared our calculated OH-reactivity and concentration with measured ambient data from the two campaigns; HUMPPA-COPEC-10 (Hyytiälä United Measurements of Photochemistry and Particles in Air – Comprehensive Organic Precursor Emission Concentration 2010) July-August, 2010 and BFORM (Boreal Forest OH Reactivity Measurements) August 2008. Both campaigns took place in Hyytiälä, SMEAR II station, Southern Finland (61 °N, 24 °E, 180 m a.s.l.). The forest around the station is dominated by 45-year-old Scots pine, and the canopy reaches a height of about 18 m. The total atmospheric OH-reactivity was measured using the Comparative Reactivity Method (Sinha *et al.*, 2008).

RESULTS AND DISCUSSION

Model simulations show that the main contributors to the OH-reactivity is seasonally dependent; the main contributors in summer are of organic origin whereas in winter they are inorganic compounds. The vertical OH-reactivity has been modelled and compared with directly measured vertical OH-reactivity at two different heights - one in canopy and one above canopy (in 2008 only measurements from one height inside the canopy are available). In Figure 1 we present daily averaged measured OH-reactivity for 12-14 m (measured in August 2008), 18 m and 24 m (measured in July-August, 2010) together with modelled OH-reactivity for 18 m (modelled for July-August, 2010). The daily pattern within the modelled reactivity is not as well pronounced as the measured data. However, a late afternoon peak due to higher isoprene emissions is observed. Also the modelled accumulated OH-reactivity until the boundary layer peaks in the middle of the day, which correlates with VOC emissions. As also seen from Figure 1, the modelled OH-reactivity is highly underestimated. Model simulations for both year 2008 and 2010 only account for ~ 30 – 50 % of the total measured OH sink, and we believe the reason for missing OH-reactivity (modelled OH-reactivity subtracted from measured OH-reactivity) is unmeasured unknown BVOCs, and limitations in our knowledge of atmospheric chemistry including uncertainties in rate constants.

The OH concentration has been both measured and modelled and is visualised in Figure 2. Model simulations seem to predict the measured OH concentration well, but overestimates the OH concentration at noon or early afternoon by up to a factor of 2 on some days, and during night time underestimate the concentration by up to 3×10^5 molecules/cm³. Most of the OH concentration overestimation can be explained by the missing OH-reactivity and uncertainties on the measurements (a factor of 2). However, on certain days, e.g. Julian day 216 and 217, the underestimation in the modelled OH-reactivity cannot account for the daytime overestimation in the modelled OH

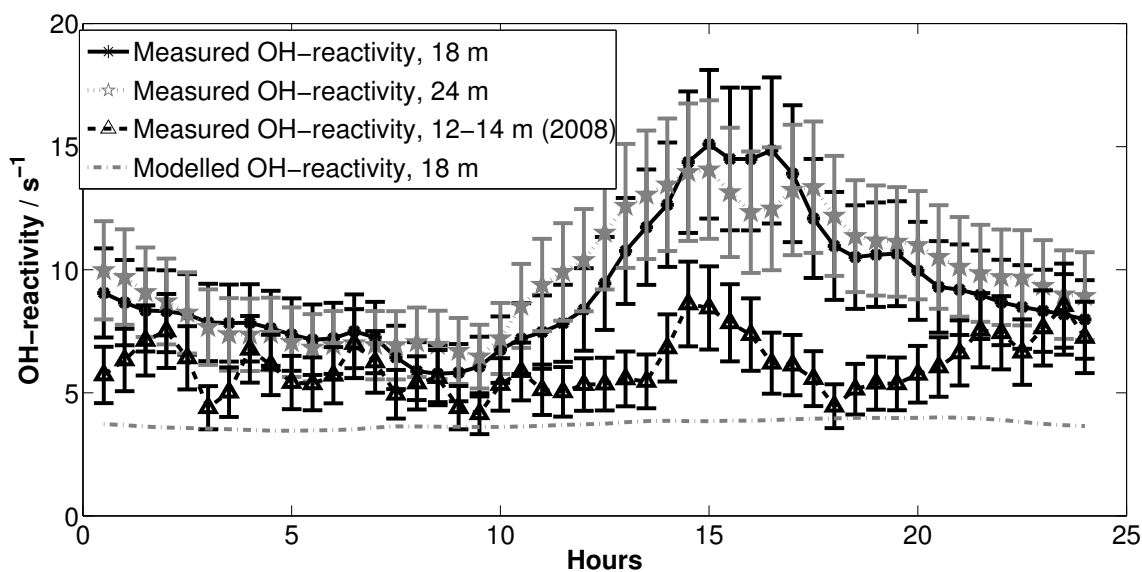


Figure 1: Daily averaged measured OH-reactivity for 12–14 m (measured in August 2008), 18 m and 24 m (measured in July–August, 2010) together with modelled OH-reactivity for 18 m (modelled for July–August, 2010).

concentration. On some days (e.g. Julian day 201, 211, and 222) the model underestimates the measured OH concentration, pointing in the direction of a missing OH source term (Taraborrelli *et al.*, 2010). One option is that the missing OH source is recycling of OH through isoprene reactions (Lelieveld *et al.*, 2008). Further, during night time we are lacking a mysterious OH source (during daytime OH is mainly produced through photolysis of ozone).

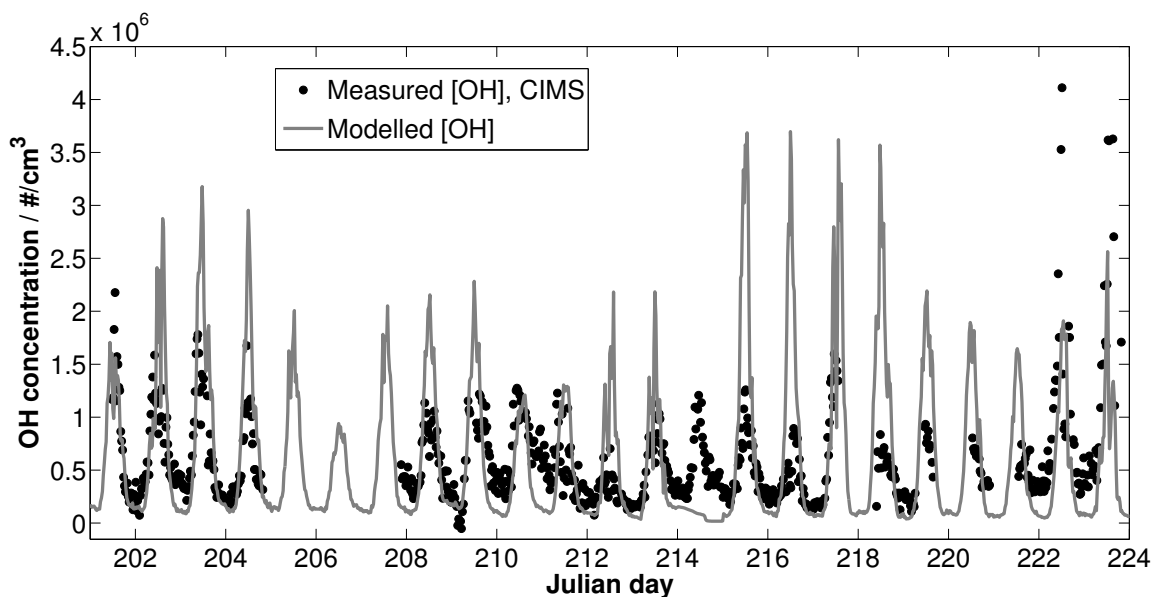


Figure 2: Modelled and measured OH concentration for July-August, 2010.

CONCLUSIONS

Model simulations only account for $\sim 30 - 50\%$ of the total measured OH sink, and we believe the reason for missing OH-reactivity (modelled OH-reactivity subtracted from measured OH-reactivity) is unmeasured unknown BVOCs, and limitations in our knowledge of atmospheric chemistry including uncertainties in rate constants.

ACKNOWLEDGEMENTS

This work was supported by the the Finnish Center of Excellence (FCoE) and the Helsinki University Centre for Environment (HENVI).

REFERENCES

- Apel, E. C., L.K. Emmons, T. Karl, F. Flocke, A.J. Hills, S. Madronich, J. Lee-Taylor, A. Fried, P. Weibring, J. Walega, D. Richter, X. Tie, L. Mauldin, T. Campos, A. Weinheimer, D. Knapp, B. Sive, L. Kleinman, S. Springston, R. Zaveri, J. Ortega, P. Voss, D. Blake, A. Baker, C. Warneke, D. Welsh-Bon, J. de Gouw, J. Zheng, R. Zhang, J. Rudolph, W. Junkermann, D.D. Riemer. (2010). Chemical evolution of volatile organic compounds in the outflow of the Mexico City Metropolitan area. *Atmos. Chem. Phys.*, **10**, 2353.
- Boy, M., A. Sogachev, J. Lauros, L. Zhou, A. Guenther and S. Smolander. (2011). SOSA - a new model to simulate the concentrations of organic vapours and sulphuric acid inside the ABL - Part I: Model description and initial evaluation. *Atmos. Chem. Phys.*, **11**, 43.
- Damian, V., A. Sandu, M. Damian, F. Potra and G.R. Carmichael. (2002). The Kinetic PreProcessor KPP – A software environment for solving chemical kinetics. *Comput. Chem. Eng.*, **26**, 1567.
- Di Carlo, P., W.H. Brune, M. Martinez, H. Harder, R. Leshner, X. Ren, T. Thornberry, M.A. Carroll,

- V. Young, P.B. Shepson, D. Riemer, E. Apel and C. Campbell. (2004). Missing OH Reactivity in a Forest: Evidence for Unknown Reactive Biogenic VOCs. *Science*, **304**, 722.
- Faloona, I.C., D. Tan, R.L. Leshner, N.L. Hazen, C.L. Frame, J.B. Simpas, H. Harder, M. Martinez, P. Di Carlo, X.R. Ren and W.H. Brune. (2004). A laser-induced fluorescence instrument for detecting tropospheric OH and HO₂: Characteristics and calibration. *J. Atmos. Chem.*, **47**, 139.
- Lelieveld, J., T.M. Butler, J.N. Crowley, T.J. Dillon, H. Fischer, L. Ganzeveld, H. Harder, M.G. Lawrence, M. Martinez, D. Taraborrelli and J. Williams. (2008). Atmospheric oxidation capacity sustained by a tropical forest *Nature*, **452**, 737.
- Lou, S., F. Holland, F. Rohrer, K. Lu, B. Bohn, T. Brauers, C.C. Chang, H. Fuchs, R. H \ddot{a} seler, K. Kita, Y. Kondo, X. Li, M. Shao, L. Zeng, A. Wahner, Y. Zhang, W. Wang and A. Hofzumahaus. (2009). Atmospheric OH reactivities in the Pearl River Delta â China in summer 2006: measurement and model results. *Atmos. Chem. Phys.*, **10**, 11243.
- Mao, J., X. Ren, W.H. Brune, J.R. Olson, J.H. Crawford, A. Fried, L.G. Huey, R.C. Cohen, B. Heikes, H.B. Singh, D.R. Blake, G.W. Sachse, G.S. Diskin, S.R. Hall and R.E. Shetter. (2009). Airborne measurement of OH reactivity during INTEX-B. *Atmos. Chem. Phys.*, **9**, 163.
- Ren, X. R., H. Harder, M. Martinez, R.L. Leshner, A. Oligier, Y. Shirley, J. Adams, J.B. Simpas and W.H. Brune. (2003). HO_x concentrations and OH reactivity observations in New York City during PMTACS-NY2001. *Atmos. Environ.*, **37**, 3627.
- Sinha, V., J. Williams, J.N. Crowley and J. Lelieveld. (2008). The Comparative Reactivity Method - a new tool to measure total OH Reactivity in ambient air. *Atmos. Chem. Phys.*, **8**, 2213.
- Sinha, V., J. Williams, J. Lelieveld, T.M. Ruuskanen, M.K. Kajos, J. Patokoski, H. Hellen, H. Hakola, D. Mogensen, M. Boy, J. Rinne, and M. Kulmala. (2010). OH Reactivity Measurements within a Boreal forest: Evidence for Unknown Reactive Emissions. *Env. Sci. Tech.*, **44**, 6614.
- Taraborrelli, D., M.G. Lawrence, T.M. Butler, R. Sander and J. Lelieveld. (2009). Mainz Isoprene Mechanism 2 (MIM2): an isoprene oxidation mechanism for regional and global atmospheric modelling *Atmos. Chem. Phys.*, **9**, 2751.

BAYESIAN FORECAST MODEL FOR SIZE-FRACTIONATED URBAN PARTICLE NUMBER CONCENTRATIONS

B. MØLGAARD¹, T. HUSSEIN^{1,2}, J. CORANDER³ and K. HÄMERI¹

¹Department of Physics, P.O.Box 48, FI-00014, University of Helsinki, Finland.

²Department of Physics, University of Jordan, Amman, 11942, Jordan.

³Department of Mathematics and Statistics, P.O.Box 68, FI-00014, University of Helsinki, Finland.

Keywords: FORECAST, PARTICLE NUMBER CONCENTRATION, STATISTICAL MODELLING, HELSINKI.

INTRODUCTION

Especially in cities people are exposed to high concentrations of air pollutants. In order to reduce this exposure forecasts of the concentrations are desirable. Such forecast may be produced by the aid of statistical models. There are several examples of forecast models for gaseous pollutants and particle mass concentrations, but not for particle number concentrations. We have developed a parametric regression model in the framework suggested by Chib (1993), and showed that it can be used for forecasting particle number concentrations. The forecasts are provided as probability distributions.

METHODS

In addition to local sources particle number concentrations are affected by weather conditions (Hussein *et al.*, 2006). Thus a statistical model should include parameters related to weather and sources as covariates (predictors). A simple regression model is not appropriate, however, because of autocorrelation of the concentrations. Autocorrelation is a general problem when dealing with time series, and a solution to this problem was suggested by Chib (1993). He considered a model of the form:

$$y_t = x_t^T \beta + \varepsilon_t, \quad \varepsilon_t = u_t + \phi_1 \varepsilon_{t-1} + \dots + \phi_p \varepsilon_{t-p},$$

where y_t is some observation at time t , x_t is a vector of covariates at time t , β is a vector of parameters, ϕ 's are autoregressive parameters, ε is the autocorrelated error, and u is an independent normally distributed error term with variance σ^2 . To apply this model to our problem we have set $y = \log(N)$, where N is the number concentration of some size fraction. For the covariate vector x_t we used 71 simple functions of temperature, wind speed, wind direction, relative humidity, traffic intensity, and time. The forecasting procedure is the following:

- Use a set of learning data and vague priors to obtain the posterior distribution of the parameters β , ϕ , and σ .
- Use the parameters and data from the past week to obtain distributions ε from the past week.
- Then use ε from the past week, the parameters β , ϕ , and σ , and forecasts of weather and traffic to produce forecasts of the particle number concentrations for the coming days.

To do this numerically we used a Markov Chain Monte Carlo (MCMC) algorithm (Chib, 1993) to obtain samples of the parameters according to the posterior distributions and Monte Carlo integration to produce forecasts.

We tested our forecasting model by using data from the SMEAR III station in Helsinki and traffic data (2005–2008). Forecasts were made for the years 2006–2008 for two size-fractions: ultra-fine particles (UFP, diameter < 100 nm) and accumulation mode (100–950 nm). We did not have old weather and traffic forecasts available, so we used the actual measurements. So we should expect our forecasts to be somewhat better than what can be obtained with this model in a real forecasting situation.

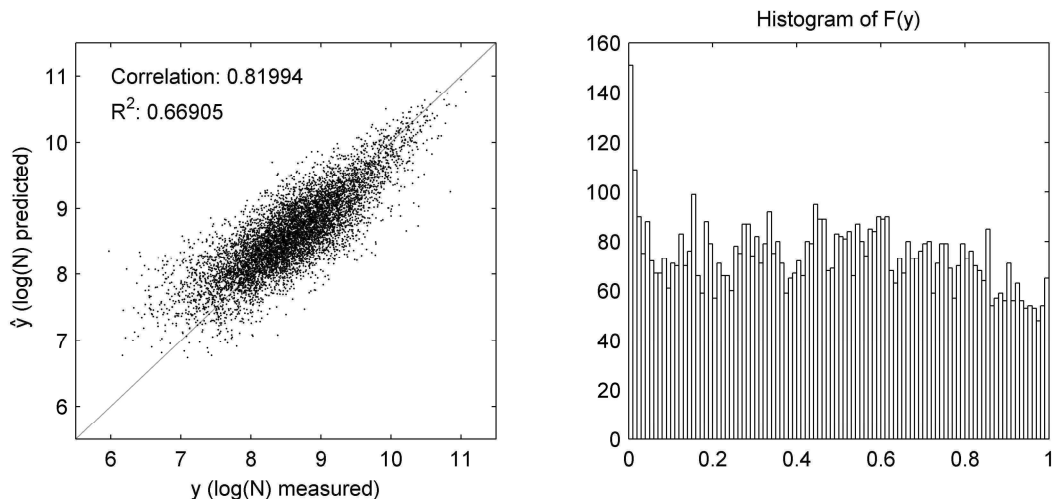


Figure 1: Left: Expected $\log(N)$ compared to measured $\log(N)$, where N is the number concentration of ultrafine particles measured in particles/cm³, and the natural logarithm is used. Right: Probability integral transform. Forecasted cumulative distribution functions evaluated at measured values.

RESULTS AND DISCUSSION

In the left side of figure 1 we have compared the expected value $\hat{y} = E[Y]$ with the measured value y ($= \log(N)$). The UFP forecasts for the upcoming day explain 67% of the variance of $\log(N)$ at three hour time resolution, and the forecasts seem to be slightly better for high than for low concentrations. To check whether the probabilistic description is appropriate we have evaluated the forecasted cumulative distribution functions F at the measured values y for all times t , where both forecast and measurement are available. Ideally, this would provide a sample from the uniform distribution $U(0,1)$. The histogram in figure 1 shows that the distribution of $F(y)$ deviates slightly from the uniform distribution. We do not consider this relatively small deviation problematic, however. For the accumulation mode the R^2 is smaller (0.57), and the distribution of $F(y)$ deviates less from the uniform distribution.

We have in different ways investigated whether the model description is adequate. For example, we have checked that the error term ε is autocorrelated and that u is not. The performance of the MCMC algorithm has also been assessed, and it converges fast enough and mixes well. On a PC our algorithm requires only a few minutes for extracting information from the learning data and producing a forecast for a few days.

CONCLUSIONS

Our model forecasts probability distributions for size-fractionated particle number concentrations. The probabilistic description is adequate, and forecasts capture a large part of the variance of the concentrations. The model is flexible and may be implemented in other urban locations.

ACKNOWLEDGEMENTS

This work was funded by the Ubicasting 2 project (TEKES).

REFERENCES

- Chib, S. (1993). Bayes regression with autoregressive errors – A Gibbs sampling approach, *J. Econometrics* **58**, 275–294.
- Hussein, T., A. Karppinen, J. Kukkonen, J. Härkönen, P.P. Aalto, K. Hämeri, V.M. Kerminen, M. Kulmala (2006). Meteorological dependence of size-fractionated number concentrations of urban aerosol particles. *Atmos. Environ.* **40**, 1427–1440.

PERFORMANCE OF SOME NUCLEATION THEORIES WITH A NON-SHARP DROPLET-VAPOR INTERFACE

I. NAPARI, J. JULIN and H. VEHKAMÄKI

Department of Physics, P.O. Box 64, 00014 University of Helsinki, Finland.

Keywords: Nucleation theories, Molecular Dynamics, Nucleation rate.

INTRODUCTION

The classical nucleation theory (CNT) has been the dominant nucleation theory for decades. In CNT several simplifying assumptions are made, including attributing several properties of the bulk liquid to the small droplets. Nonetheless, CNT succeeds in providing a qualitative description of nucleation. Its quantitative predictions are worse, however, and for example experimental nucleation rates can differ from CNT predictions by several orders of magnitude. To remedy this various alternate theoretical approaches have emerged. Some are specific to nucleation, such as the diffuse interface theory (DIT) (Gránásy, 1996) and the extended modified liquid drop model - dynamical nucleation theory (EMLD-DNT) (Reguera and Reiss, 2004a; Reguera and Reiss, 2004b), and some are more general theories that can also be applied to nucleation, such as density functional theory (DFT) (Zeng and Oxtoby, 1991) and square gradient theory (SGT) (Cahn and Hilliard, 1958; Cahn and Hilliard, 1959).

There are differences in the input data needed for the different theories. DIT requires the heat of evaporation, as well as the same thermophysical quantities as CNT. If the vapor can be considered ideal EMLD-DNT requires only the same quantities as CNT, but for a non-ideal vapor an equation of state (EoS) for the vapor is required. SGT requires always an EoS, and DFT needs the exact molecular interaction potential. What these four theories have in common is that, contrary to CNT, the vapor-liquid interface is not considered sharp.

Here we have compared the nucleation rate predictions of the aforementioned theories to recent molecular dynamics (MD) simulations of Lennard-Jones (LJ) argon (Horsch *et al.*, 2008; Horsch and Vrabec, 2009; Napari *et al.*, 2009). We have also compared critical cluster sizes. The simulations span several different temperatures.

METHODS AND RESULTS

The MD data set is comprised of three recent nucleation studies in LJ vapors, where the actual nucleation event is observed in a simulation box (so-called direct nucleation simulation). All these studies consider a LJ potential that is truncated and shifted at 2.5σ , where σ is the LJ length parameter. Simulated bulk thermodynamic properties for a LJ fluid with 2.5σ cutoff are given by Vrabec *et al.* (2006). The comparison between theory and simulation is done consistently: the theories either use or result in the same values of equilibrium vapor pressure, bulk liquid density and surface tension as the simulations. Finally, a realistic EoS is needed to account for the nonideality of the vapor. To be fully consistent in the comparison of the theories, we chose the DFT EoS to obtain pressure and chemical potential in all our calculations.

Logarithmic nucleation rates as a function of the chemical potential difference between the super-saturated and saturated vapors $\Delta\mu$ are depicted in Fig. 1 at reduced temperatures $T = 0.65$ and

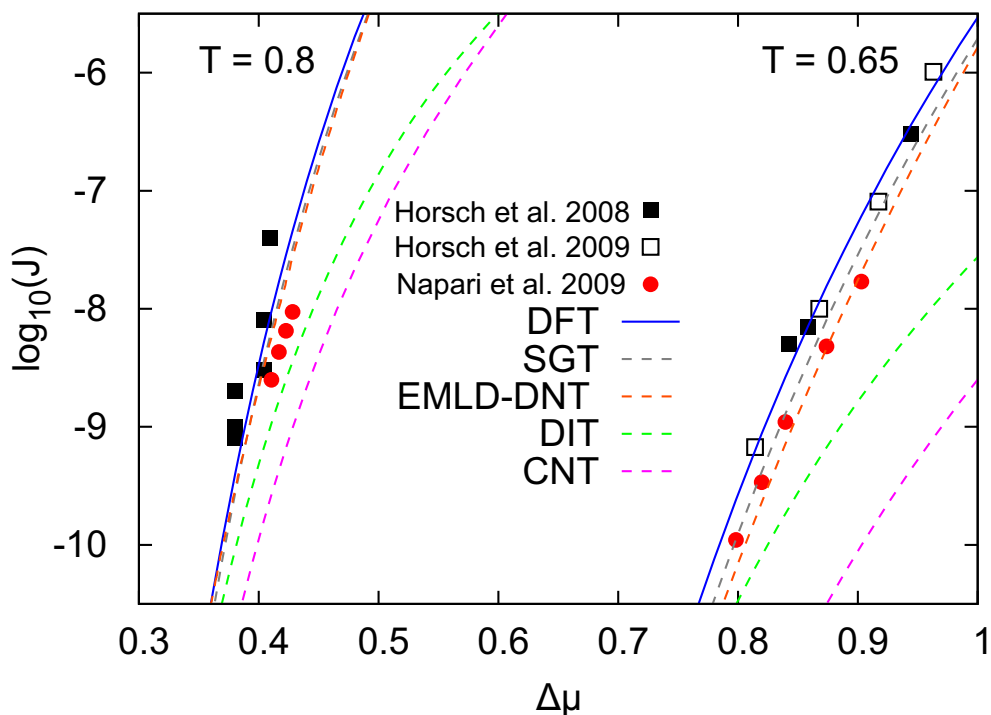


Figure 1: Nucleation rates for a LJ fluid truncated and shifted at 2.5σ as function of the chemical potential difference between supersaturated and saturated vapors. Shown are results from MD simulations and theoretical calculations. Temperature is given in units of ϵ/k_B and chemical potential in units of ϵ .

$T = 0.8$. The figure shows the MD nucleation rate data together with nucleation rates from the different theories, including CNT. We find that EMLD-DNT, DFT and SGT differ from MD results by less than one order of magnitude. DIT underestimates the MD values by up to two orders of magnitude, but is still a clear improvement to CNT.

Figure 2 shows the critical cluster sizes according to the theories and simulations at $T = 0.65$, $T = 0.7$, and $T = 0.8$. The MD critical sizes are calculated from the simulated nucleation rates using the nucleation theorem. DFT seems to give the best theoretical results, although at $T = 0.8$ the sizes are overestimated. DFT is closely matched by SGT with only slightly larger sizes. CNT and especially DIT underestimate the MD sizes and EMLD-DNT, in the range of supersaturations of these MD data sets, overestimates them.

For a more thorough discussion of the methods and results, see Napari *et al.* (2010).

CONCLUSIONS

The best results are obtained from DFT, which reproduces both the MD nucleation rates and critical cluster sizes rather well. DFT is unfortunately usually limited to rather simple fluids. SGT does not need an interaction potential, and the SGT nucleation rates and cluster sizes are close to DFT values. However, SGT is quite sensitive to the choice of EoS. DIT somewhat underestimates the nucleation rate, but it is still much better than CNT when predicting nucleation rates, and it is easy to use. EMLD-DNT almost equals DFT in predicting nucleation rates, but does not succeed in predicting cluster sizes at high vapor densities, where EMLD-DNT is also highly dependent on the EoS. EMLD-DNT is thus at its best when applied to nearly ideal vapors.

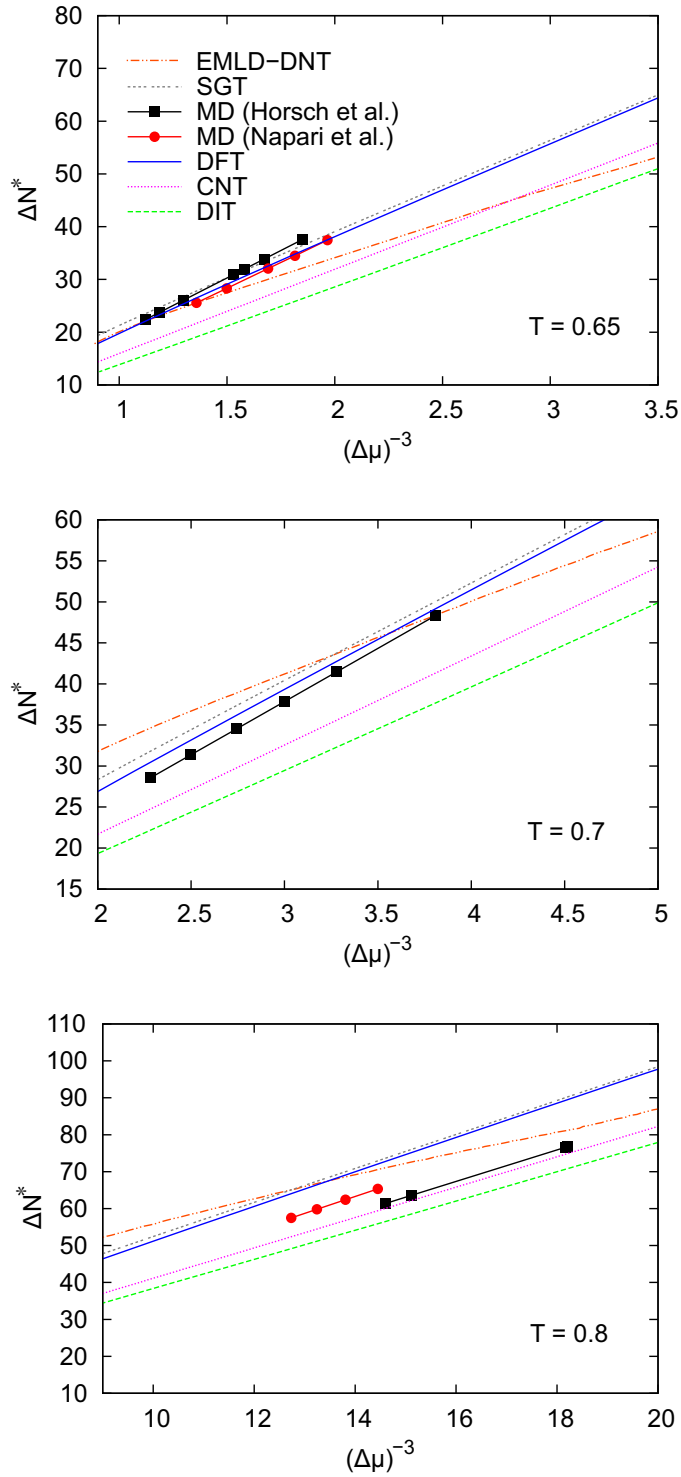


Figure 2: The theoretical and simulated excess number of particles in the critical cluster at $T = 0.65$, $T = 0.7$, and $T = 0.8$. The MD sizes are based on fitting the nucleation rate data and using the nucleation theorem.

ACKNOWLEDGMENTS

This research was supported by the Academy of Finland Center of Excellence program (project number 1118615) and ERC StG 257360-MOCAPAF.

REFERENCES

- Cahn, J. W. and Hilliard, J. E. (1958). Free energy of a nonuniform system. I. Interfacial free energy. *J. Chem. Phys.*, **28**, 258–267.
- Cahn, J. W. and Hilliard, J. E. (1959). Free energy of a nonuniform system. III. Nucleation in a two-component incompressible fluid. *J. Chem. Phys.*, **31**, 688–699.
- Gránásy, L. (1996). Diffuse interface theory for homogeneous vapour condensation. *J. Chem. Phys.*, **104**, 5188–5198.
- Horsch, M. and Vrabec, J. (2009). Grand canonical steady-state simulation of nucleation. *J. Chem. Phys.*, **131**, 184104.
- Horsch, M., Vrabec, J., and Hasse, H. (2008). Modification of the classical nucleation theory based on molecular simulation data for surface tension, critical nucleus size, and nucleation rate. *Phys. Rev. E*, **78**, 011603.
- Napari, I., Julin, J., and Vehkamäki, H. (2009). Cluster sizes in direct and indirect molecular dynamics simulations of nucleation. *J. Chem. Phys.*, **131**, 244511.
- Napari, I., Julin, J., and Vehkamäki, H. (2010). Performance of some nucleation theories with a non-sharp droplet-vapor interface. *J. Chem. Phys.*, **133**, 154503.
- Reguera, D. and Reiss, H. (2004a). Extended modified liquid drop-dynamical nucleation theory (EMLD-DNT) approach to nucleation: A new theory. *J. Phys. Chem. B*, **108**, 19831–19842.
- Reguera, D. and Reiss, H. (2004b). Fusion of extended modified liquid drop model for nucleation and dynamical nucleation theory. *Phys. Rev. Letters*, **93**, 165701.
- Vrabec, J., Kedia, G. K., Fuchs, G., and Hasse, H. (2006). Comprehensive study of the vapour-liquid coexistence of the truncated and shifted Lennard-Jones fluid including planar and spherical interface properties. *Molec. Phys.*, **104**, 1509.
- Zeng, X. C. and Oxtoby, D. W. (1991). Gas-liquid nucleation in Lennard-Jones fluids. *J. Chem. Phys.*, **94**, 4472–4478.

AMINES INHIBIT THE PARTICLE GROWTH: H₂SO₄-H₂O-AMINE FLOW TUBE EXPERIMENT

K. NEITOLA¹, D. BRUS^{1,3}, M. SIPILÄ², T. JOKINEN², P. PAASONEN² and H. LIHAVAINEN¹

¹Finnish Meteorological Institute, Erik Palménin aukio, P.O. Box 503, FI-00101 Helsinki, Finland

²Department of Physical Sciences, University of Helsinki, P.O.Box 64, FI-00101 Helsinki, Finland

³Laboratory of Aerosol Chemistry and Physics, Institute of Chemical Process Fundamentals Academy of Sciences of the Czech Republic, Rozvojová 135, CZ-165 02 Prague 6, Czech Republic

Keywords: homogeneous nucleation, sulphuric acid, amine, flow tube.

INTRODUCTION

Sulphuric acid is known to play a key role in atmospheric nucleation (gas to particle conversion). Homogeneous nucleation of sulphuric acid and water has been studied for several decades both in laboratory experiments and field. Only recently the laboratory simulations were able to explain the atmospheric nucleation rates measured in field (Sipilä *et al.*, 2010). The attention has shifted lately towards a third nucleating species (ammonia, amines) in addition to sulphuric acid and water. This is due to recent quantum chemical calculations that suggest a third species to thermodynamically stabilize sulphuric acid-water molecular clusters.

METHODS

Flow tube technique was used to study homogeneous nucleation of sulphuric acid and water with and without the presence of amines. Wide range of concentrations of trimethylamine (TMA) and dimethylamine (DMA) were separately used in two different relative humidities (30% and 50%). Sulphuric acid was produced using a thermally controlled one meter long saturator with I.D. of 6 cm which is filled with pure (97%) sulphuric acid. Dry, purified, and particle free air is flown through the saturator with constant flow rate (0.1 lpm) to saturate the flow with sulphuric acid vapour. The concentration of sulphuric acid is controlled by the temperature of the saturator. The sulphuric acid concentration was measured with CIMS (Petäjä *et al.*, 2009) or API-TOF (Junninen *et al.*, 2010).

The concentration of nucleated particles was monitored with Particle Size Magnifier (PSM, Vanhanen *et al.*, 2010). The size of the particles was measured with DMPS system (HAUKE DMA, UCPC, TSI model 3025A) in the range of 3 to 200 nm. Five different concentration levels of TMA and DMA were used (170, 480, 800, 1700 and 3600 ppt) with sulphuric acid concentration range between 10⁵ and 5·10⁷ mol./cm³. The flow tube was operated in several hour cycles with same conditions to ensure the stable state in flow tube. TMA or DMA concentration was changed only after a full cycle of saturator temperatures (0-45°C) was done for both RH's separately.

RESULTS

Figure 1 shows DMPS size distributions (upper panel) and total count (lower panel) data without TMA for one saturator temperature cycle at RH 30%. Figure 2 shows data from DMPS (upper panel) and PSM (lower panel) for exactly similar conditions as in figure 1, except the addition of TMA. The sizes of the particles are similar in both figures before adding TMA. After the addition of TMA the size decreases out of the DMPS size range and concentration of particles decreases to 1/3 of the original concentration. Increasing the RH to 50% increases the concentration temporarily but after stable state is achieved concentration is decreased to about 800 cm⁻³. Similar behaviour was observed for addition of DMA.

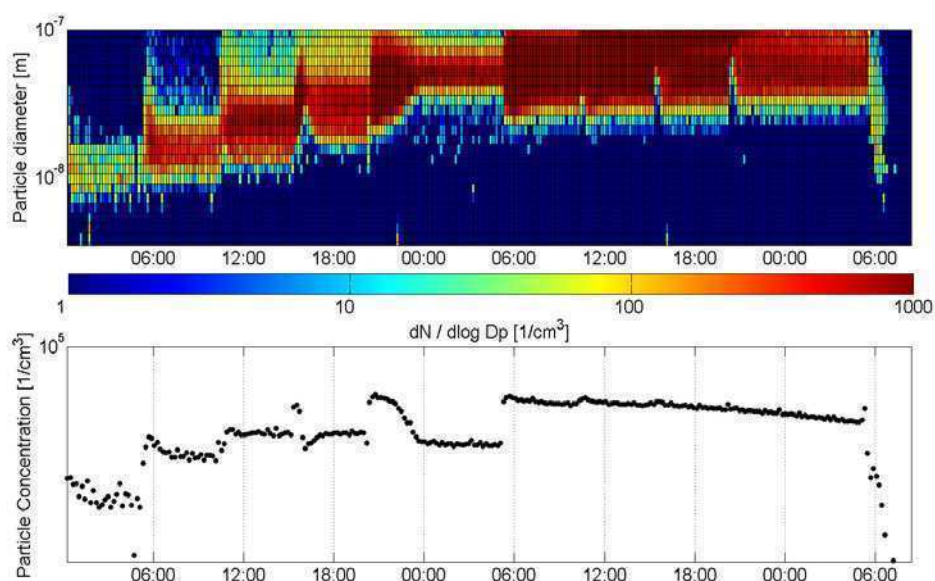


Figure 1. DMPS data for size distribution (upper panel) and total concentration (lower panel) for one saturator temperature cycle without TMA.

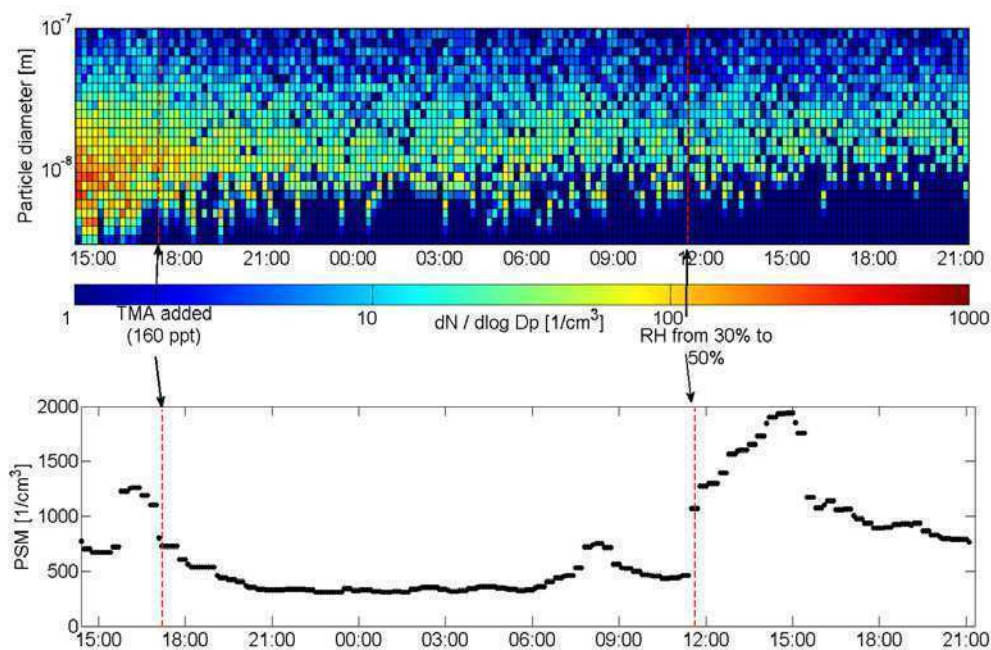


Figure 2. DMPS and PSM data over one cycle of saturator temperatures at RH 30% with lines when TMA (160ppt) was added and RH changed to 50%.

CONCLUSIONS

Results imply that addition of TMA or DMA form thermodynamically stable clusters in sulphuric acid water system with sizes below the detection limit of the PSM (~ 1.5 nm) suppressing the condensation of sulphuric acid to the surface of the particles and preventing the growth to detectable sizes. Such behaviour was predicted by Anttila *et al.*, (2005) for system containing sulphuric acid and ammonia.

ACKNOWLEDGEMENTS

This work was supported by the Maj & Torr Nessling and KONE foundations together with Finnish Center of Excellence.

REFERENCES

- Anttila, T., H. Vehkamäki, I. Napari and M. Kulmala (2005), Effect of ammonium bisulphate on atmospheric on water-sulphuric acid-ammonia nucleation, *Boreal Env. Res.*, 10: 511-523.
- Junninen, H., M. Ehn, T. Petäjä, L. Luosujärvi, T. Kotiaho, R. Kostianen, U. Rohner, M. Gonin, K. Fuhrer, M. Kulmala and D. R. Worsnop (2010), A high-resolution mass spectrometer to measure atmospheric ion composition, *Atmos. Meas. Tech.*, 3, 1039–1053, doi:10.5194/amt-3-1039-2010.
- Petäjä T., R. L. Mauldin, III, E. Kosciuch, J. McGrath, T. Nieminen, P. Paasonen, M. Boy, A. Adamov, T. Kotiaho and M. Kulmala (2009), Sulfuric acid and OH concentrations in a boreal forest site, *Atmos. Chem. Phys.*, 9, 7435–7448.
- Sipilä, M. T. Berndt, T. Petäjä, D. Brus, J. Vanhanen, F. Stratmann, J. Patokoski, R. L. Mauldin III, A.P.-Hyvärinen, H. Lihavainen and M. Kulmala, (2010) The role of sulfuric acid in atmospheric nucleation, *Science* 327, 5970, pp. 1243 - 1246, DOI: 10.1126/science.1180315,.
- Vanhanen, J., J. Mikkilä, K. Lehtipalo, M. Sipilä, H. E. Manninen, E. Siivola, T. Petäjä and M. Kulmala, (2011), Particle size magnifier for nano-CN detection, *Aerosol Sci. & Tech.*, Vol. 45, 4, 533-542, doi: 10.1080/02786826.2010.547889.

PHYSICAL AND CHEMICAL CHARACTERISTICS OF AIR IONS DURING AUTUMN 2010 IN HYYTIÄLÄ, FINLAND

TUOMO NIEMINEN¹, HEIKKI JUNNINEN¹, SIEGFRIED SCHOBESBERGER¹,
GUSTAF LÖNN¹, MIKAEL EHN^{1,2}, TUUKKA PETÄJÄ¹, DOUGLAS R. WORSNOP^{1,3} and
MARKKU KULMALA¹

¹Department of Physics, University of Helsinki, P.O. Box 64, FI-00014, Finland.

²Forschungszentrum Jülich, Germany

³Aerodyne Research, MA, USA

Keywords: air ions, mass spectrometry, sulphuric acid

INTRODUCTION

The HUMPPA-COPEC campaign was organized between 12th July and 15th August 2010 at the University of Helsinki Station for Measuring Ecosystem–Atmosphere Relations (SMEAR II) in Hyytiälä, Finland (see Hari and Kulmala (2005) for a description of the station) as a co-operation between the Max Planck Institute for Chemistry and University of Helsinki. The aim of the campaign was to obtain a detailed and comprehensive view of the atmospheric chemistry related to both gas-phase and particulate-phase. Comprehensive measurements of aerosols, ions and trace gases allows links between the oxidation chemistry and the particle size and composition to be established. Related to atmospheric aerosol particle formation and especially to the growth of newly formed secondary aerosol particles, summer is the most active time of the year (Dal Maso *et al.*, 2005).

METHODS

Aerosol spectrometers that have been operating continuously at the SMEAR II station from 2003 onwards are the Balanced Scanning Mobility Analyzer (BSMA) and Air Ion Spectrometer (AIS) (Tammets, 2006; Mirme *et al.*, 2007). These spectrometers measure the size distributions of negative and positive air ions in the mobility diameter range 0.8–8.0 nm (BSMA) and 0.8–40 nm (AIS). During the HUMPPA-COPEC campaign the recently developed atmospheric pressure interface mass spectrometer APi-TOF (Junninen *et al.*, 2010) was additionally measuring the chemical composition of the smallest air ions in the mass-to-charge ratio upto 1500 Th, the upper limit corresponding roughly to particle size of 2 nm in mobility diameter.

RESULTS

During the campaign the average concentration of negative and positive cluster ions smaller than 2 nm was around 500 cm⁻³ per polarity according to both the ion spectrometers and APi-TOF. The average mass spectra of negative ions at daytime and nighttime during the whole campaign are shown in Figure 1. There is a clear difference between these daytime and nighttime spectra. During daytime photochemistry driven by OH oxidation produces in the atmosphere e.g. sulphuric acid, which due to its high acidity will take up the negative charges effectively. Indeed, the highest peaks in the daytime negative ion spectra are de-protonated sulphuric acid monomer (HSO₄⁻ at integer mass 97 Th) and dimer (H₂SO₄·HSO₄⁻, 195 Th). Other major daytime species were malonic acid (103 Th), nitric acid dimer (125 Th), and a cluster of malonic acid and nitric acid (166 Th). In the night-time, when the sulphuric acid production decreases, other masses are seen to peak in the mass spectra. These include very strong peaks at mass-to-charge ratios 340, 342 and 372 Th, as well as a group of peaks in the range 500 – 600 Th.

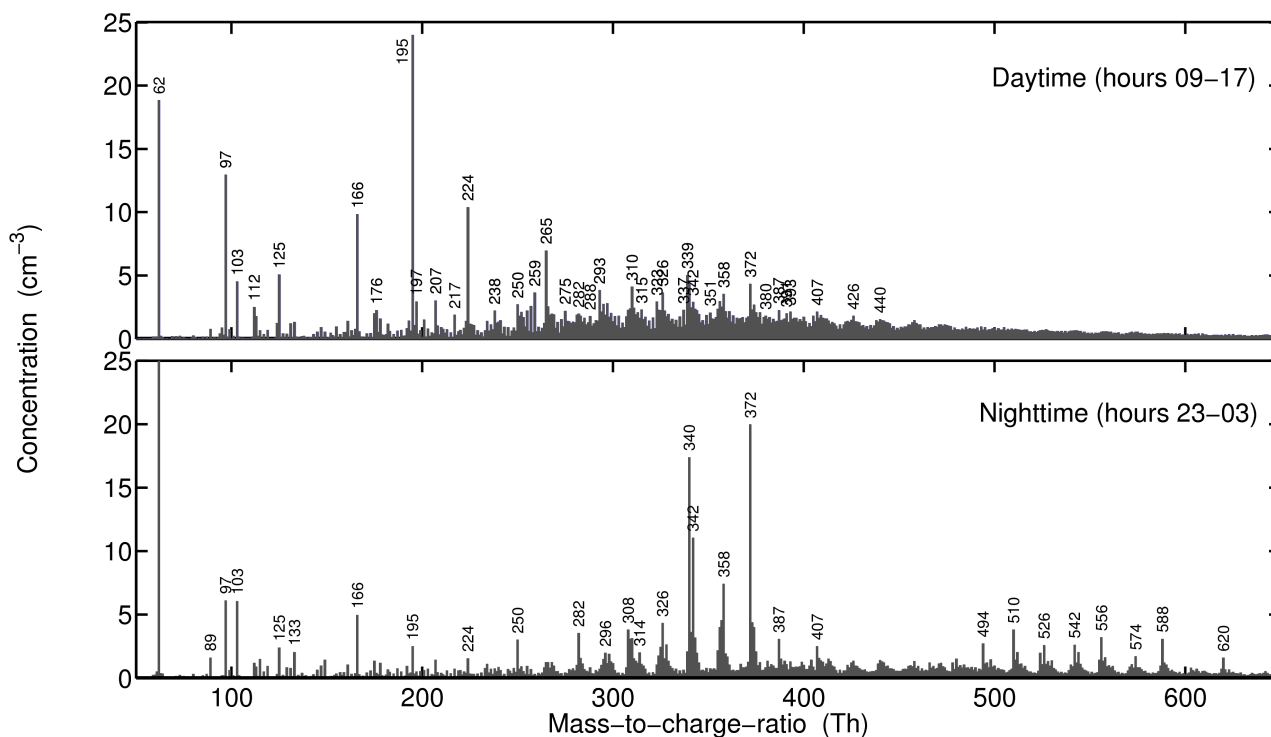


Figure 1. Average mass spectra of negative ions in the mass-to-charge-ratio 50– 650 Th during daytime (upper panel) and nighttime (lower panel) of the campaign. The strongest peaks are indicated by their mass-to-charge ratio.

REFERENCES

- Dal Maso M. *et al.* (2005). Formation and growth of fresh atmospheric aerosols: eight years of aerosol size distribution data from SMEAR II, Hyytiälä, Finland, *Boreal Environ. Res.* 10, 323–336.
- Hari P. and Kulmala M (2005). Station for Measuring Ecosystem–Atmosphere Relations (SMEAR II), *Boreal Environ. Res.* 10, 315–322.
- Junninen H. *et al.* (2010). A high-resolution mass spectrometer to measure atmospheric ion composition, *Atmos. Meas. Tech.*, 3, 1039–1053.
- Mirme A. *et al.* (2007). A wide-range multi-channel Air Ion Spectrometer, *Boreal Env. Res.* 12, 247– 264.
- Tammet H. (2006). Continuous scanning of the mobility and size distribution of charged clusters and nanometer particles in atmospheric air and the Balanced Scanning Mobility Analyzer BSMA, *Atmos. Res.* 82, 523–535.

MULTISITE ANALYSIS OF URBAN FLUX MEASUREMENTS IN HELSINKI

A. NORDBO, L. JÄRVI, S. HAAPANALA and T. VESALA

Department of Physics, University of Helsinki,
Erik Palmenin Aukio 1, 00014 University of Helsinki, Finland.

Keywords: EDDY COVARIANCE, URBAN, FLUX, TURBULENCE.

INTRODUCTION

Inadvertent climate modification in urban areas leads to increased air temperatures and affects pollution dispersion through changes in atmospheric stability. The climate modification is caused by altered vertical energy fluxes which stems from changes in land-use and the release of anthropogenic heat. Furthermore, urban climates are characterised by greater aerosol particle concentrations and large vertical particle and CO₂ fluxes originating from traffic and other combustion processes. These alterations in fluxes affect comfort of city dwellers and are a challenge for numerical weather prediction. Our aim is to study surface–atmosphere interactions through vertical turbulent fluxes at three urban sites during a cold winter. The study is the first multisite analysis of urban fluxes at such high latitudes.

METHODS

The measurements were conducted at three urban sites in Helsinki from November 2010 to January 2011. Two of the sites, Fire Station and Hotel Tornii, are in the centre of Helsinki and the third site, SMEARIII, is located four kilometres North-West of the centre (Figure 1). The area around SMEARIII can be divided into three surface cover sectors (buildings 320–40°, heavy traffic road 40–180° and vegetation 180–320°) designated according to the dominant surface cover, and the sectors have different roughness characteristics (Table 1). The Fire Station and Hotel Tornii sites, conversely, are both characterized by rough and impervious urban surface cover in all directions. The mean building heights in a 500 m radius circle around the two center sites were calculated with 1° steps for 20° windows and the averages are 21.7 m and 23.6 m (Figure 2, Table 1). The displacement heights and roughness lengths were determined according to MacDonald *et al.*, (1998) for the same sectors and the urban canopy can be said to be fairly homogeneous with average displacement heights of 14.4 m and 15.0 m and a standard deviation of 3.2 m for both sites.

Turbulent fluxes of momentum (τ), sensible heat (H), latent heat (LE), carbon dioxide (F_c) and particles (F_p) were measured using the eddy covariance technique at all sites. The setups consisted of a three-dimensional sonic anemometer (USA-1, Metek GmbH, Germany) for acquiring the three wind components and sonic temperature, a water condensation particle counter (TSI-3781, TSI Incorporated, USA) and infrared gas analyzers (IRGA) for measuring the fluctuations in CO₂ and H₂O concentrations. SMEARIII had a closed-path (LI7000, LI-COR, Lincoln, Nebraska, USA) and open-path (LI-7500) IRGA, Fire Station an enclosed-path (LI-7200) and open-path IRGA, and an enclosed-path IRGA was used at Hotel Tornii. Raw eddy covariance data were logged at 10 Hz for post processing and fluxes were calculated with 30-minute averaging according to widely accepted calculation procedures (Aubinet *et al.*, 2000). A 2-dimensional coordinate rotation was applied to wind speed data, all data were linearly detrended and the time lag between wind speed and scalar data was taken into account by maximization of the cross-correlation function. Furthermore, a density correction (Webb *et al.*, 1980) was done to open-path IRGA data, H was corrected for cross-wind effects and sonic heating (Liu *et al.*, 2001) and spectral corrections were applied to all fluxes. After flux calculations, quality screening was applied to flux values to ensure an adequate stationarity in the turbulent signal (Foken and Wichura 1996). In addition, flux data are omitted when wind is from a direction with flow distortion (Figure 1). Flux observations were continuous for all fluxes besides F_p for Fire Station (Jul 1st – Oct 27th 2010) and Hotel Tornii (Nov 4th 2010 – Jan 31st 2011).

	SMEARIII	Fire Station	Hotel Tornii
Coordinates	60°12'10.14"N 24°57'40.06"E	60° 09'54.74"N 24° 56'43.37"E	60° 10' 04.09"N 24° 56' 19.28"E
Height above sea level (m)	29	23.0	15.2
Mast height above ground level (m)	31	41.8	60.0
Building height (m)	20 ± 2, 0, 0	21.7 ± 3.6	23.6 ± 4.7
Displacement height (m)	13, 8, 6	14.4 ± 3.2	15.0 ± 3.2
Roughness length (m)	2	1.2 ± 0.3	1.4 ± 0.5
Flow distortion	0–50°	90–180°	85–140°

Table 1. Characteristics of three eddy covariance measurement stations. The building height, displacement height and roughness lengths are for a circle with a 500 m radius. Standard deviation indicated by \pm . Values for SMEAR III are from Vesala *et al.*, (2008) and three values corresponding to wind direction sectors (see

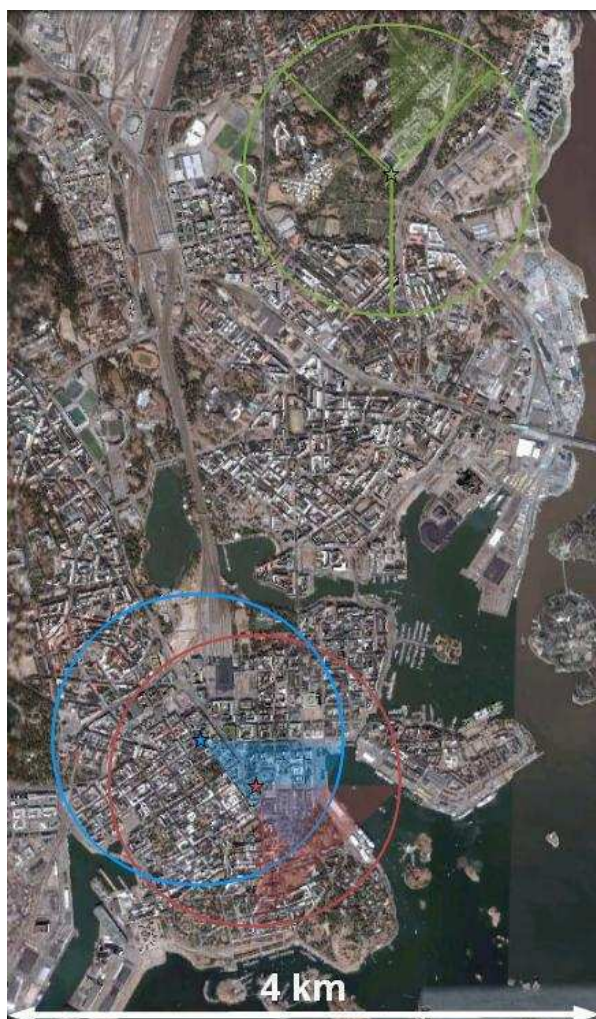


Figure 1. Three eddy covariance measurement stations in Helsinki: SMEARIII (green), Hotel Tornii (blue) and Fire Station (red). Stars indicate the tower location and circles show the area within 1 km from the tower. The circle of SMEARIII is divided to three wind direction sectors, namely, buildings 320–40°, road 40–180° and vegetation 180–320°. Wind directions with flow distortion are marked with translucent color. Background picture from Google Earth.

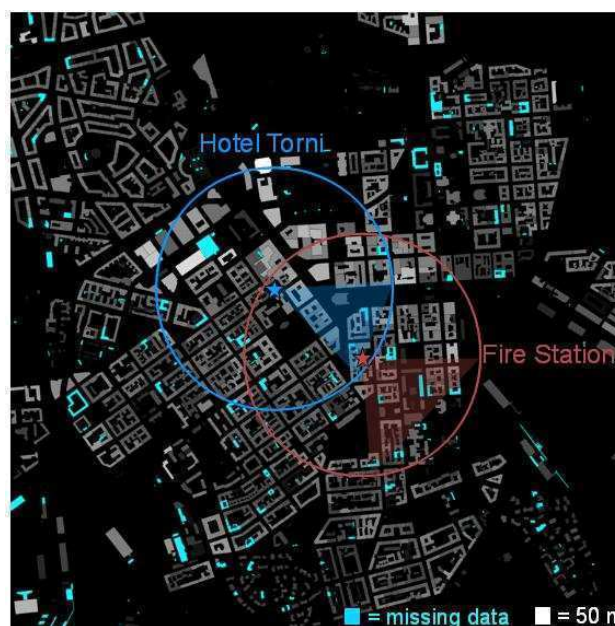


Figure 2. The Hotel Tornii and Fire Station measurement stations. Stars indicate the tower location and circles show the area within 500 m from the tower. Buildings are marked with gray shading where white corresponds to 50 m and black to 0 m (e.g. roads, sea).

CONCLUSIONS

The measurement period is characterized by the arrival of an exceptionally cold winter with half-hour temperatures ranging from -22.7°C to 14.0°C . The precipitative sum is 265 mm from which 53% came down as snow. The prevailing wind direction is from NNE, but other wind directions have about the same occurrence (Figure 4). The momentum flux is about the same for all sites and is governed by synoptic variation rather than wind direction.

The sensible heat flux shows on average much higher values for the city centre sites compared with SMEAR III (Figure 3). H also stays on average positive during night (40 Wm^{-2}) whereas negative values are observed for SMEAR III. Stable atmospheric stability ($H<0$) is observed half of the time at SMEAR III whereas the occurrence in the city centre is less than 5%. Opposite behaviour is observed for LE as daytime values for SMEAR III exceed the corresponding values for downtown by about 22 Wm^{-2} . The main reason for the differences in energy flux partitioning is the difference in land usage. The vegetation cover around SMEAR III favours evapotranspiration whereas downtown the impervious surfaces and water runoff favour energy transport via sensible heat flux. This can also be seen for mean fluxes as a function of wind direction for all sites (Figure 4). Largest evapotranspiration for SMEAR III is seen in the directions of high vegetation cover and the park SSE of Hotel Tornii can be seen in both of the downtown measurements. On the other hand, some of the differences in energy flux partitioning can also stem from anthropogenic sensible and latent heat release which is large in the road sector of SMEAR III and in all directions around the centre sites. Especially, the high night-time H downtown probably has an anthropogenic origin.

The carbon dioxide flux is on average twice as high for Hotel Tornii (mean \pm std, $12.5\pm 10.5\ \mu\text{mol m}^{-2}\text{ s}^{-1}$) and Fire Station ($10.4\pm 9.2\ \mu\text{mol m}^{-2}\text{ s}^{-1}$) compared with SMEAR III ($5.2\pm 4.7\ \mu\text{mol m}^{-2}\text{ s}^{-1}$) where anthropogenic sources are weaker. F_c in the road sector of SMEAR III, on the other hand, is about the same as the averages downtown (Figure 4). CO_2 emissions around Hotel Tornii are about the same for all wind directions whereas higher values for Fire Station are observed when the wind is from NNW. The diurnal variation shows weakest fluxes around five in the morning and peaks around four in the afternoon when the highest traffic rates in Helsinki are observed (Figure 3) (Järvi *et al.*, 2009).

The particle flux comparison is made difficult due to the shorter measurement periods at Fire Station and Hotel Tornii. Anyhow, the diurnal pattern of F_p follows that of F_c and the coefficients of determination are 0.53, 0.61 and 0.53 for SMEAR III, Fire Station and Hotel Tornii, respectively. The wind direction dependency of F_p shows the location of roads more clearly than F_c (Figure 4) and the average flux is again highest for Hotel Tornii ($0.35\pm 0.30\ 10^9\ \text{m}^{-2}\text{ s}^{-1}$) and about the same for Fire Station ($0.15\pm 0.14\ 10^9\ \text{m}^{-2}\text{ s}^{-1}$) and SMEAR III ($0.13\pm 0.20\ 10^9\ \text{m}^{-2}\text{ s}^{-1}$).

To conclude, the energy flux partitioning between sensible and latent heat fluxes is largely affected by changes in land use and by anthropogenic heat release. The changes are so profound that stable atmospheric stratification is very seldom observed in central Helsinki despite cold winter conditions. Furthermore, CO_2 and particle fluxes in the center of Helsinki correspond to those observed outside the center over a heavy traffic road. The changes in atmospheric stability and increased particle fluxes affect pollution and are especially important to investigate in high latitudes with shallow winter-time boundary layers. Thus, more measurements and numerical studies of flow in an urban boundary layer are needed in order to increase the comfort of city dwellers and to improve weather prediction.

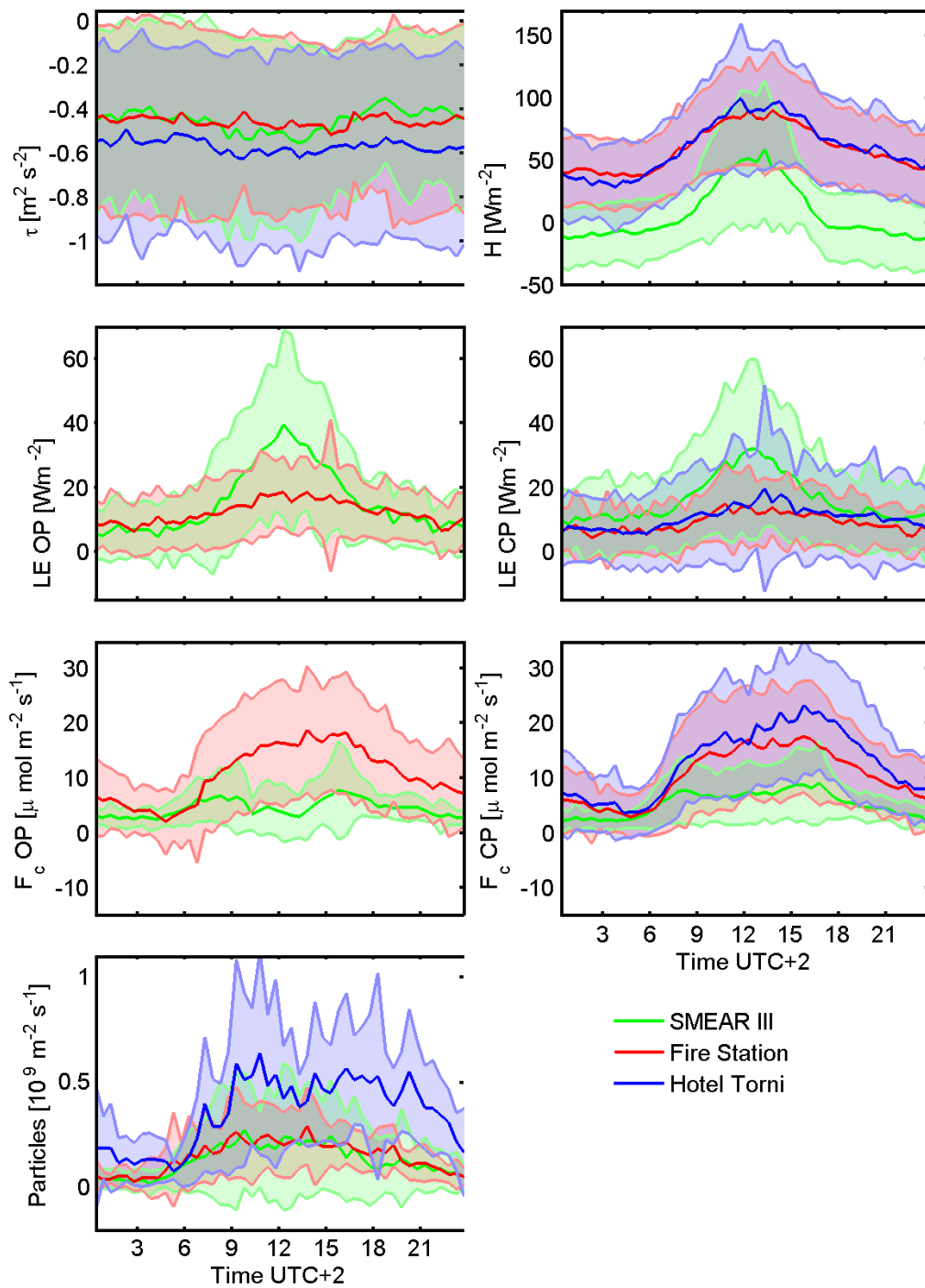


Figure 3. Average diurnal courses from Oct 2010 to Jan 2011 for momentum (τ), sensible heat (H), latent heat (LE), carbon dioxide (F_c) and particles (F_p). LE and F_c have measurements with open-path (OP) and closed-path (CP) analyzers. Shaded areas indicate standard deviations and diurnal courses are shown for all three stations.

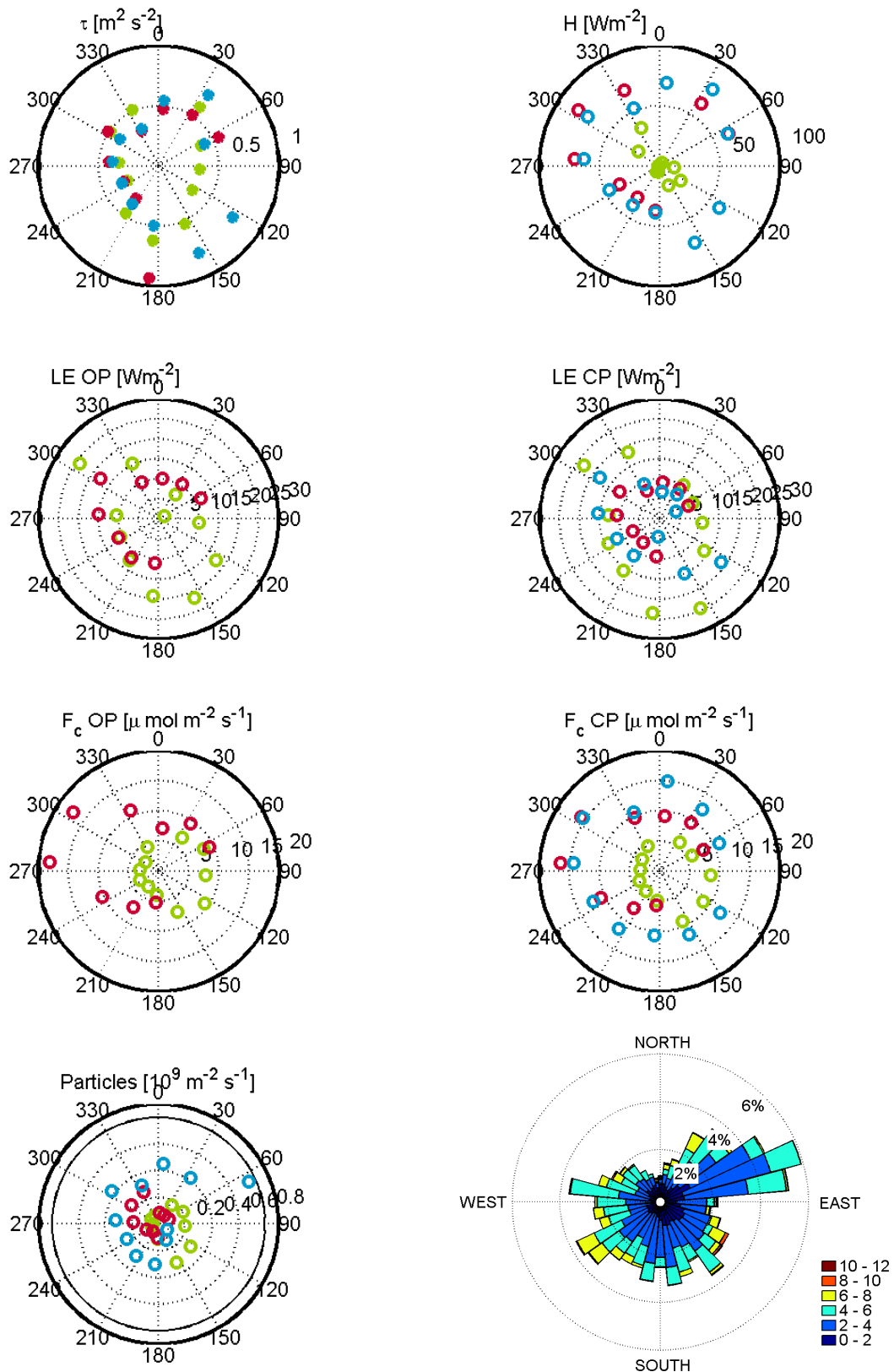


Figure 4. Average fluxes per wind direction from Oct 2010 to Jan 2011 for momentum (τ), sensible heat (H), latent heat (LE), carbon dioxide (F_c) and particles (F_p). LE and F_c have measurements with open-path (OP) and closed-path (CP) analyzers. Positive values are indicated by circles and negative values by dots. All three sites are included: SMEAR III (green), Fire Station (red) and Hotel Tornii (blue). The wind direction histogram for the measurement period is also given (lower right); bars indicate relative occurrence (%) and the wind speed is given in colors ($m s^{-1}$).

ACKNOWLEDGEMENTS

The financial support by the Academy of Finland Centre of Excellence program (project no 1118615) and Academy of Finland project 138328 are gratefully acknowledged.

REFERENCES

- Aubinet, M., A. Grelle, A. Ibrom, U. Rannik, J. Moncrieff, T. Foken, A.S. Kowalski, P.H. Martin, P. Berbigier, C. Bernhofer, R. Clement, J. Elbers, A. Granier, T. Grunwald, K. Morgenstern, K. Pilegaard, C. Rebmann, W. Snijders, R. Valentini and T. Vesala. (2000). Estimates of the annual net carbon and water exchange of forests: The EUROFLUX methodology, *Advances in Ecological Research, Vol30*, **30**, 113-175.
- Foken, T. and B. Wichura. (1996). Tools for quality assessment of surface-based flux measurements, *Agric. For. Meteorol.*, **78**, 83-105.
- Järvi, L., Ü. Rannik, I. Mammarella, A. Sogachev, P.P. Aalto, P. Keronen, E. Siivola, M. Kulmala and T. Vesala. (2009). Annual particle flux observations over a heterogeneous urban area, *Atmospheric Chemistry and Physics*, **9**, 7847-7856.
- Liu, H.P., G. Peters and T. Foken. (2001). New equations for sonic temperature variance and buoyancy heat flux with an omnidirectional sonic anemometer, *Bound. -Layer Meteorol.*, **100**, 459-468.
- MacDonald, R.W., R.F. Griffiths and D.J. Hall. (1998). An improved method for the estimation of surface roughness of obstacle arrays, *Atmos. Environ.*, **32**, 1857-1864.
- Vesala, T., L. Järvi, S. Launiainen, A. Sogachev, Ü. Rannik, I. Mammarella, E. Siivola, P. Keronen, J. Rinne, A. Riikonen and E. Nikinmaa. (2008). Surface-atmosphere interactions over complex urban terrain in Helsinki, Finland, *Tellus Ser. B-Chem. Phys. Meteorol.*, **60**, 188-199.
- Webb, E.K., G.I. Pearman and R. Leuning. (1980). Correction of Flux Measurements for Density Effects due to Heat and Water-Vapor Transfer, *Q. J. R. Meteorol. Soc.*, **106**, 85-100.

ECOSYSTEM AND ATMOSPHERIC MEASUREMENTS IN ICOS-FINLAND

M. NYMAN¹, T. LAURILA², L. KULMALA^{1,3}, E. JUUROLA^{1,3}, S. SORVARI¹, S. HAAPANALA¹, P. KERONEN¹, P. KOLARI^{1,3}, I. MAMMARELLA¹, M. KOMPPULA⁴, K. LEHTINEN⁴, S. JUUTI⁴, T. AALTO², M. AURELA², L. LAAKSO², Y. VIISANEN², and T. VESALA¹

¹Department of Physics, PL 48, FIN-00014, University of Helsinki, Finland.

²Finnish Meteorological Institute, Helsinki, Finland.

³Department of Forest Sciences, University of Helsinki, Finland.

⁴University of Eastern Finland, Kuopio, Finland.

Keywords: Greenhouse gases, long term observations, climate change, distributed research infrastructure

INTRODUCTION

The global mean temperature has increased and will continue to increase in the 21st century due to the increased concentrations of greenhouse gases such as carbon dioxide (CO₂), methane (CH₄) and nitrous oxide (N₂O) in the atmosphere (IPCC, 2007). Understanding about the driving forces of climate change requires full quantification of the greenhouse gas (GHG) emissions and sinks by long term and high precision observations in the atmosphere as well as on the land and ocean surfaces. There are major research challenges such as 1) what is the regional distribution of GHG fluxes, 2) how does environmental factors and human intervention impact the exchange of GHG, and 3) how will the sources and sinks of GHGs change in future.

Integrated Carbon Observation System (ICOS) has received funding by the EU to develop a strategic plan for constructing a European infrastructure to provide the long-term atmospheric and flux observations required to understand the present state and predict the future behaviour of the global carbon cycle and GHG emissions as well as to monitor and assess the effectiveness of carbon sequestration in GHG emission reduction activities. At the moment, Finland is aiming for ICOS headquarters and Atmospheric Thematic Centre (ATC) in collaboration with France. The host of the headquarters is suggested to Finland whereas the host of the ATC would be France.

METHODS

The ICOS-Finland is established by three national partners: University of Helsinki (UH), Finnish Meteorological Institute (FMI), and University of Eastern Finland (UEF). ICOS-Finland will have readiness for four atmospheric stations as well as two full and seven associate ecosystem stations for ICOS (Figure 1). The Finnish sites represent the boreal and sub-arctic Eurasian environments with both east-west and south-north transitions in eco-climatic features. The Finnish SMEAR (station for measuring ecosystem-atmosphere relationships) stations, especially the SMEAR II in Hyytiälä is an intensively equipped world-class observatory operating since 1995. The station is a full ecosystem station and being upgraded to become also an ICOS atmospheric station. Scots pine forest SMEARI in northern Finland and urban SMEARIII in Helsinki are associate ecosystem stations. The full measurement sites, level 1 sites, will measure the full suite of parameters based on the definition by ICOS preparatory work. The level 2 sites and associate sites will be measuring a subset of ICOS core parameters (see ICOS Stakeholder's handbook).

Atmosphere measurements include the precise determination of concentrations above the atmospheric surface layer. The spatial concentration variations measured the network of inter-calibrated towers

together with the atmospheric transport models enables to estimate sinks and sources on the scale of 100–1000 km. The Pallas-Sodankylä is the most northern of the four Finnish Atmospheric stations. It has been operating since 1994. In the Sodankylä observatory, atmospheric concentration measurements will be upgraded and a calibration gas cylinder filling station is under construction. New atmospheric sites are under preparation in the northern Baltic proper area (Utö) and in the eastern part of Finland (Koli).

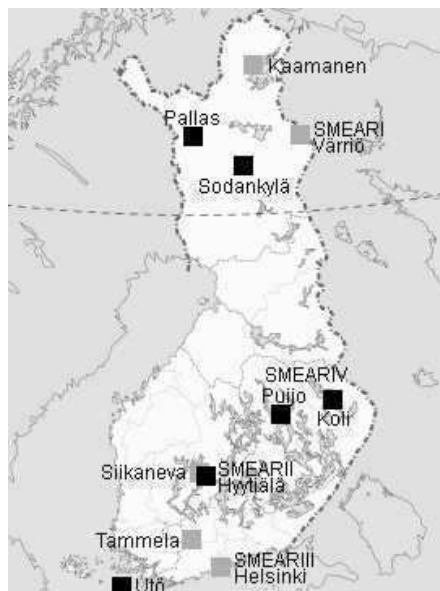


Figure 1: The research stations in Finland that contribute to the European ICOS. Pallas-Sodankylä, SMEARII Hyttiälä, Utö (Baltic Sea) and Puijo-Koli (SMEARIV) are the Finnish atmospheric stations of which Sodankylä and SMEARII Hyttiälä are also full ecosystem stations. SMEARI Värriö, SMEARIII Helsinki, Kaamanen, Tammela, Siikaneva, Lompolojännkä (Pallas) and Kenttäröva (Pallas) are associate ecosystem stations.

In order to interpret the atmospheric concentrations above continents in terms of GHG cycle processes, additional measurements are needed at the surface. Eddy covariance (EC) techniques allow continuous monitoring of CO₂, H₂O and heat fluxes over vegetation canopies. These fluxes, typically calculated on ½ h basis, form the core of ecosystem measurements. The source area (footprint) extends 0.1–1 km away from the measuring tower. The utilization and interpretation of flux measurements require the observations of tens of other variables related to meteorology, hydrology, ecophysiology of vegetation and soil processes. CH₄ and N₂O can be also measured by EC although this is not yet as routine work as it is for CO₂.

Temporal resolution of a day for eddy flux towers is sufficient to capture the variability in terrestrial fluxes driven by changing weather patterns (e.g. the effect of frost or drought on forests) and transform them into operational systems. ICOS network aims at obtaining GHG balances in a high-resolution grid, ultimately in 10 km resolution. However, terrestrial ecosystem carbon fluxes are so heterogeneous and variable that it will be impossible to measure fluxes over all kinds of ecosystems continually over Europe and adjacent regions. The network of micrometeorological flux measurement sites should represent the most typical ecosystems. Other integrating parameters, such as biomass and soil carbon inventories are needed to upscale the flux data, in combination with satellite images.

The GHG balance is achieved by combining atmospheric concentration and ecosystem flux observations in a modelling system. Observations of net ecosystem CO₂ balances, using micrometeorological methods, will constrain simulations of CO₂ uptake by photosynthesis and emission by respiration. In addition, we should have flux observations from ecosystems for which the simulations rely more on observations. Managed peatlands are such an extensive ecosystem type in Finland. Soil respiration measurements by chambers will help in segregating soil processes from net ecosystem balance observations.

The full ecosystem stations, SMEARII in southern Finland and Sodankylä in northern Finland are ready and running. At some associate ecosystem sites, flux measurements still needs to be developed to reach ICOS standards. New sensors for ancillary measurements, such as radiation and soil temperature probes, are added to most sites. A new automated chamber measurement system has been developed for forest floor vegetation gas exchange (Lohila et al. 2010). At the Pallas node of the Global Atmosphere Watch site, a new flux site representing the arctic mountain vegetation started in autumn 2010.

One key area for FMI flux studies is northern ecosystems with presently ongoing measurements in two forest ecosystems on mineral soils (Sodankylä Scots pine forest and Kenttäröva spruce forest) and on two pristine wetlands (northern boreal fen Lompolojänkki and subarctic fen Kaamanen). Another focus for FMI is the carbon balance of different ecosystems on organic soils. The northern wetlands and one southern boreal fen, Siikaneva, that is run in co-operation with the UH serve as a good reference for the measurements on managed peatlands. Measurements at a nutrient-rich forestry-drained peatland (Lettosuo) were started in 2009.

Two sites of ICOS-Finland, Puijo atmospheric station and Hyytiälä ecosystem station, are currently participating in the ICOS demonstration experiment together with selected set of stations around Europe. The purpose is to evaluate the communications and interactions between the stations and the Thematic Centers, identify the critical aspect and problems in the data acquisition and data flow, evaluate if it is possible to acquire the 95% of the data as specified in the project, and to compare the data processed centrally with the site level version. The demonstration experiment will last till October 2011

CONCLUSIONS

Climate change is one the most challenging problems that humanity will have to cope with in the coming decades. Long-term coordinated and standardized observations provided by ICOS help reduce the uncertainties of future projections and predict the future behaviour of the global carbon cycle and GHG emissions. ICOS will monitor and assess the effectiveness of carbon sequestration and GHG emission reduction activities on global atmospheric composition levels, including attribution of natural and anthropogenic sources and sinks by region and sector. ICOS-Finland has the readiness to contribute to the European research infrastructure with four atmospheric stations, two full and seven associate ecosystem stations in the boreal and subarctic environments.

ACKNOWLEDGEMENTS

The financial support by EU projects ICOS and IMECC and the Academy of Finland Centre of Excellence program (project no 1118615) and the Academy project “Integrated Greenhouse Gas Monitoring System” (project no 17352) are gratefully acknowledged.

REFERENCES

- IPCC: Contribution of Working Group I to the Fourth Assessment Report of the Intergovernmental Panel on Climate Change. In: Solomon, S., Qin, D., Manning, M., Chen, Z., Marquis, M., Averyt, K., Tignor, M.M.B. and Miller, H.L. (Eds.). (Cambridge University Press, Cambridge, UK and New York, USA.).
- Lohila A., K. Minkkinen, P. Ojanen, T. Penttilä, M. Koskinen, M. Kämäräinen, M. Aurela, M. Linkosalmi, J. Hatakka, J.-P. Tuovinen, and T. Laurila. 2010. Lettosuo supporting ecosystem ICOS station: greenhouse gas flux measurements at a forestry-drained peatland. Poster abstract in the First ICOS-Finland Science Workshop, Hyytiälä, November 16-17, 2010.
- ICOS Stakeholder’s handbook. October 2009.
http://www.icos-infrastructure.eu/doc/ICOS_stakeholders_handbook_final_2009_wc.pdf

INFLUENCE OF TEMPERATURE IN THE RECOVERY FROM PHOTODAMAGE IN *PINUS SYLVESTRIS* L.

B. OLASCOAGA, A. PORCAR-CASTELL, E. NIKINMAA

Department of Forest Sciences, University of Helsinki, Latokartanonkaari 7 PO Box 27 00014
Finland

Keywords: *Pinus sylvestris* L, photoinhibition, modeling,

INTRODUCTION

Light is an indispensable requisite in photosynthesis but also a potential source of damage that affects the photosynthetic machinery and plant physiology.

When light is absorbed by the chlorophylls of the light harvesting complex (LHC), the excitation energy associated can be transferred to reaction centers to drive photosynthesis, but also been re-emitted as chlorophyll fluorescence and released as heat in order to minimize the production of damaging reactive oxygen species (ROS), that will damage the D1 protein in PSII in a process called photoinhibition.

Photoinactivated reaction centers require repair (Andersson and Aro, 2001). D1 proteins that have been damaged must be removed from the PSII and degraded by many proteases (Adam 2001), while synthesis of new D1 proteins and their assembly into PSII is required to maintain their functionality and drive photosynthesis.

It is known that the level of photoinhibition can be affected by many environmental conditions and accelerates at low or high temperature, drought, etc (Mamedov and Styring, 2003). Nevertheless, there is no model that explains the response of photoinhibition throughout a wide range of temperature and light treatments.

In this experiment we will analyze the influence of temperature in the recovery after photodamage by strong light in Scots pine (*Pinus sylvestris* L.) shoots using fluorescence measurements.

METHODS

A total of 20 Scots pine shoots acclimated to summer condition ($F_v/F_m = 0,80 \pm 0,03$; $n=20$), with F_v/F_m value close to optimal 0,83 (Krause and Weis, 1991) were dark acclimated in a weather chamber for 2 hours before photoinhibitory treatment ($1500 \mu\text{mol photons m}^{-2} \text{s}^{-1}$ actinic light) throughout a range of temperatures from $-5 \text{ }^\circ\text{C}$ to $20 \text{ }^\circ\text{C}$.

Fluorescence data was recorded using a monitoring PAM fluorometer (MONI-PAM, Heinz Walz GmbH, Effeltrich, Germany) and MONI-heads were attached to current year needles in each Scots pine shoot.

A saturating pulse (1s, 4000 $\mu\text{mol photons m}^{-2} \text{s}^{-1}$ actinic light) was initially given and immediately followed by 7 min of illumination with 1500 $\mu\text{mol photons m}^{-2} \text{s}^{-1}$ actinic light treatment. After the light treatment a new saturating pulse was recorded and light source was switched off. Three saturating pulses were given in the darkness 5, 15 and 30 minutes after light treatment.

Values for F_0 and F_m obtained from each saturating pulse served to calculate reaction center (RC) no photochemical quenching (NPQ) values. The latter values were used to calculate the rate of recovery (k_{rec}) in the darkness and no photochemical quenching (NPQ) building during the photoinhibitory light treatment, using the equations:

$$A) \text{ RC} = (1/F_0 - 1/F_m) / (1/F_{0 \text{ initial}} - 1/F_{m \text{ initial}})$$

$$B) \text{ dRC/dt} = (k_{rec} \text{ RC}_{\text{dam}} / \text{RC}_{\text{tot}}) - (k_{pi} \text{ RC}_{\text{func}} / \text{RC}_{\text{tot}}), \text{ where}$$

k_{rec} : Rate of recovery

k_{pi} : Rate of photoinhibition

RC_{dam} : Amount of photoinhibited RC, unable to participate in electron transport

RC_{func} : Amount of functional RC, able to participate in electron transport

$$C) \text{ NPQ} = (F_{m \text{ initial}} / F_m) - 1$$

$$D) \text{ dNPQ/dt} = \{(\lambda_b(1-Q)S^{\text{off}} / S^{\text{on}} + S^{\text{off}}) - (\lambda_r QS^{\text{on}} / S^{\text{on}} + S^{\text{off}})\} \text{NPQ}_{\text{max}}, \text{ where}$$

λ_b : NPQ building rate

λ_r : NPQ relaxing rate

S^{off} : Amount of inactive energy quenching sites

S^{on} : Amount of active energy quenching sites

Q : Amount of functional reaction centers

CONCLUSIONS

Summer-acclimated Scots pines showed a peak in the rate of recovery around 15 °C (Fig.1), decreasing towards lower temperatures. The reduction might be linked to a decrease in the speed of enzymatic processes linked to the synthesis and assembly of the components of PSII in the recovery from photodamage. At 20 °C, the reduction in the rate of recovery might be linked to damage and loss of stability in the molecules and structures of the photochemical machinery.

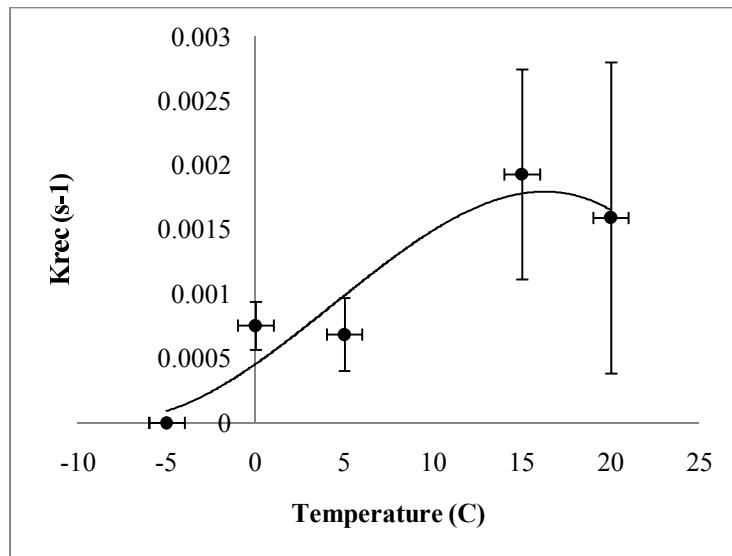


Fig.1 Recovery rate (Krec) values throughout a range of temperatures from -5 °C to 20 °C in summer-acclimated Scots pine shoots after 7 min of light treatment with 1500 $\mu\text{mol photons m}^{-2} \text{s}^{-1}$ actinic light . Each value is the average of 4 independent runs and the bars denote standard deviation.

NPQ building (Fig.2) during the 7 min actinic light treatment with 1500 $\mu\text{mol photons m}^{-2} \text{s}^{-1}$ showed the same pattern, reaching a peak around 15 °C. The low temperatures inhibit the enzymatic de-epoxidation reactions, thus decreasing NPQ building values. Interestingly a similar pattern happens at temperatures higher than 15 °C.

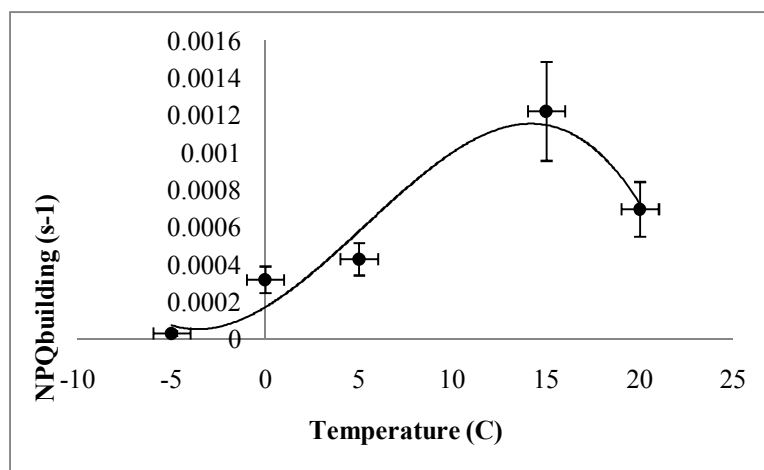


Fig.2 NPQ building throughout a range of temperatures from -5 °C to 20 °C in summer-acclimated Scots pine shoots during 7 min of actinic light treatment with 1500 $\mu\text{mol photons m}^{-2} \text{s}^{-1}$. Each value is the average of 4 independent runs and the bars denote standard deviation.

The test will be extended to a range of temperatures from -5 to 40 °C and light treatments from 50- to 1500 $\mu\text{mol photons m}^{-2} \text{ s}^{-1}$ in order to have more detailed information about the effect of temperature in the photoinhibitory rate, recovery rate and NPQ dynamic in Scots pines.

REFERENCES

- Andersson, B., and E-M. Aro (2001) *Regulation of Photosynthesis* (Kluwer Academic Publishers).
- Demmig-Adams, B., W.W. Adams III, and A.K. Mattoo (2008) *Photoprotection, photoinhibition, gene regulation and environment* (Springer).
- Horton, P., A.V. Ruban and R.G. Walter (1996). Regulation of light harvesting in green plants. *Annual Review of Plant Physiology and Plant Molecular Biology*. **47**, 655.
- Krause, G.H., and E. Weis (1991). Chlorophyll fluorescence and photosynthesis: the basics, *Annual Review of Plant Physiology Plant Molecular Biology*. **42**, 313.

USING QUANTUM MECHANICS TO IMPROVE OUR KNOWLEDGE ABOUT CLIMATE CHANGE

I.K. ORTEGA¹, T. KURTEN¹, O. KUPIAINEN¹, H. VEHKAMÄKI¹, and M. KULMALA¹

¹ Division of Atmospheric Sciences, Department of Physical Sciences, P.O. Box 64, FI-00014 University of Helsinki, Finland.

Keywords: MOLECULAR CLUSTERS, SULFURIC ACID, AMMONIA, AMINES, NUCLEATION.

INTRODUCTION

Climate change is currently one of the central scientific issues in the world, and the ability to reliably forecast climate is crucial for making political decisions that affect the lives of billions of people. According to the Intergovernmental Panel on Climate Change, aerosols remain the dominant uncertainty in predicting radiative forcing and climate change.

An important fraction of atmospheric aerosols are formed from condensable vapours by gas-to-particle nucleation, unfortunately, the actual birth mechanism of the particles is still unknown. In atmospheric conditions these nucleating clusters are small, consisting of only a few or a few tens of molecules. These clusters are therefore well below present detection limits if they are electrically neutral. Several theoretical methods have tried to describe those clusters, but probably the most successfully has been quantum mechanical calculations. The aim of our work is use quantum mechanical calculation to improve our knowledge about molecular mechanism behind atmospheric nucleation and identify the molecules responsible of this phenomenon.

METHODS

Our aim is to include in our calculations as large of clusters as possible. But on the other hand, we need as accurate results as possible. We need to look for the best tools to achieve good accuracy but keeping the computational cost in a reasonable limit (for example, a very accurate calculation that takes years is not useful at all). We have tested 7 different methods and compared the results against a high level calculation for sulfuric acid dimer.

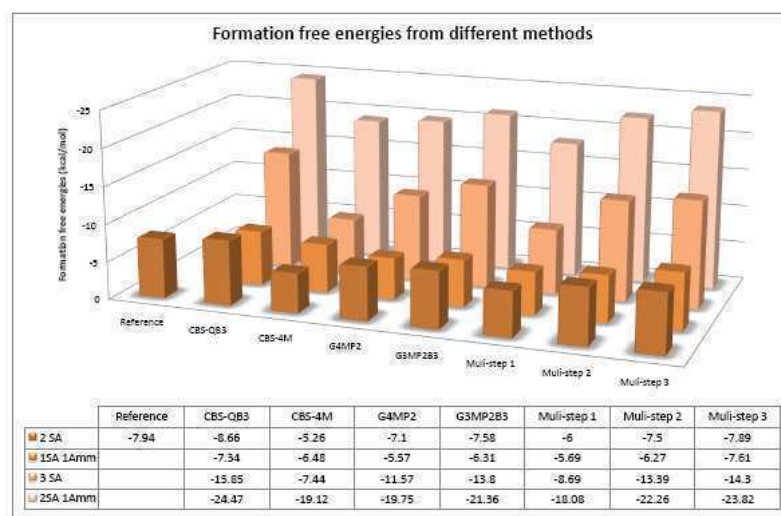


Figure 1. Comparison of different methods. Reference method consists on a combination of high level methods, including anharmonic corrections and relativistic effects, Multi step 1 correspond to

BLYP/DZP, multi step 2 correspond to B3LYP/6-31G** and multi step 3 correspond to B3LYP/CBSB7 all three combined with RICC2/aug-cc-pV(T+d)Z single point energy calculation.

The results shows that the multi-step procedure combining B3LYP/CBSB7 geometry and frequencies calculation with the high level RI-CC2/aug-cc-pV(T+d)Z single point calculation yield formation free energies close to the high level calculation for sulfuric acid dimer, and also close to CBS-QB3 results. As can be seen in the following figure, the computational cost for this combined procedure is by far smaller than the cost for CBS-QB3 calculations.

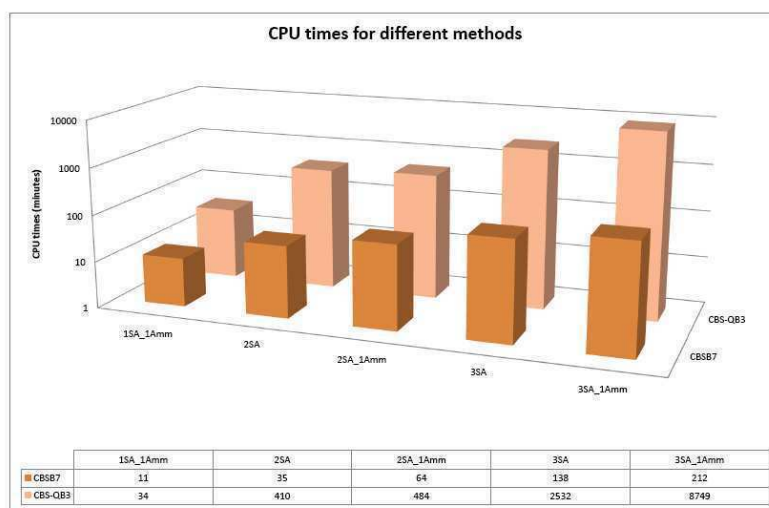


Figure 2. CPU times for different methods.

CONCLUSIONS

Using the formation free energies obtained from our calculations we have estimated the evaporation rates of negatively charged sulfuric clusters containing one base molecule. The results are shown in figures 3 and 4.

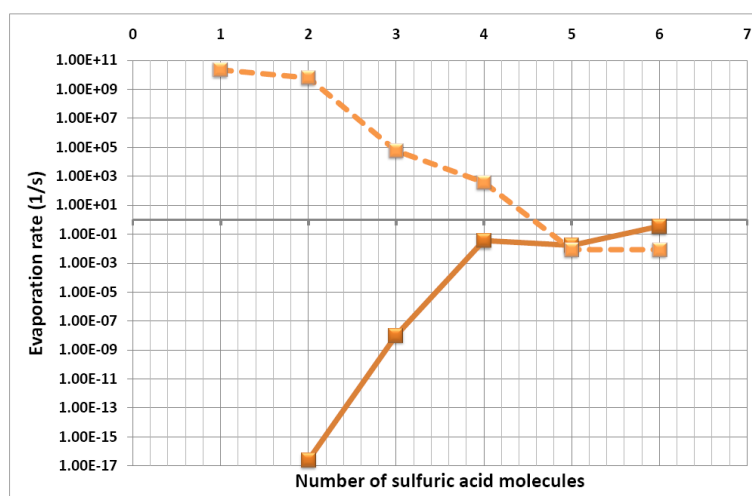


Figure 3. Evaporation rate of sulfuric acid (solid line) and ammonia (dashed line) from charged clusters containing one ammonia molecule.

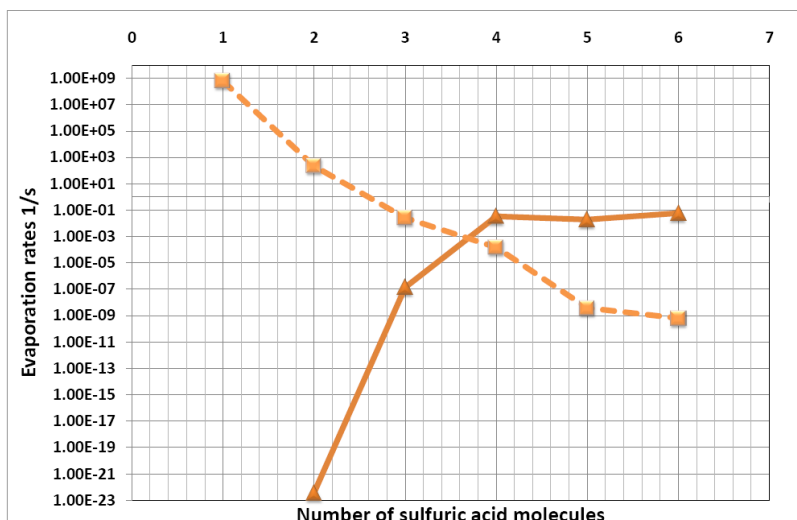


Figure 4. Evaporation rate of sulfuric acid (solid line) and DMA (dashed line) from charged clusters containing one DMA molecule.

The evaporation of sulfuric acid molecule is practically the same independent of the base molecule present in the cluster. The main difference between ammonia and DMA clusters is that DMA will stay in the cluster if it contains at least 4 sulfuric acid molecules while ammonia requires one extra acid molecule. These results can explain recent experimental results (Franchin et al. 2010), where they detected pure sulfuric acid clusters up to the trimer, DMA containing tetramers and ammonia containing pentamers.

ACKNOWLEDGEMENTS

This work was supported by the projects, FP7-ATMNUCLE project No 227463 (ERC Advanced Grant), Academy of Finland LASTU program project number 135054 and FP7-MOCAPAF project No 257360 (ERC Starting grant). The authors thank the Scientific Computing Center (CSC) in Espoo, Finland, for the computing time.

REFERENCES

Franchin, Alessandro; Schobesberger, Siegfried; Makhmutov, Vladimir; Stozhkov, Yuri; Gagné, Stéphanie; Nieminen, Tuomo; Manninen, Hanna E.; Petäjä, Tuukka; Kulmala, Markku: Ion measurements during the first H₂SO₄ nucleation experiments at the CLOUD chamber. Poster 11D6 International Aerosol Conference, Helsinki, Finland, 29.8-3.9.2010.

PARTICLE GROWTH RATE FROM NUCLEATION MODE TO CLOUD CONDENSATION NUCLEI IN BOREAL FOREST

P. PAASONEN, M. K. KAJOS, P. RANTALA, H. JUNNINEN, T. PETÄJÄ and M. KULMALA

Department of Atmospheric Sciences, University of Helsinki, Helsinki, Finland.

Keywords: Aerosol growth, VOC, Aitken mode, accumulation mode.

INTRODUCTION

The particle growth rate is an essential quantity in studying the effect of aerosols on the global climate change. The particles either formed from vapours in new particle formation process or emitted directly into atmosphere need to grow to Cloud Condensation Nuclei (CCN) sizes, with diameter of approximately 100 nm, in order to participate in cloud formation. The main component driving the aerosol growth seems to be the organic vapours (e.g. Riipinen et al, 2011). In this study we use data collected in Hyytiälä, Finland (Hari and Kulmala, 2005), during years 2007-2010. We determine growth rates for particles with diameters from below 10 nm to over 100 nm. From this growth rate we calculate the source rate of condensing vapour and compare it with temperature and measured concentrations of monoterpenes and isoprene.

METHODS

The particle growth rates (GR) were determined from the particle size distribution data measured with Differential Mobility Particle Sizer (DMPS). We used a mode fitting method for determining the GR. Up to 3 modes was fitted for every size distribution. A straight line was fitted into the maxima of these modes in those parts of the particle size distribution data in which a clear growing mode was seen (see Fig. 1). The growth rate of the particles was determined from these fitted lines in units nm/h. Unlike in most of the previous studies, in which GR is determined during the day and afternoon, we determined GR also during the nights. The measurements for monoterpene and isoprene concentrations were conducted with Proton Transfer Reaction Mass Spectrometer (PTR-MS).

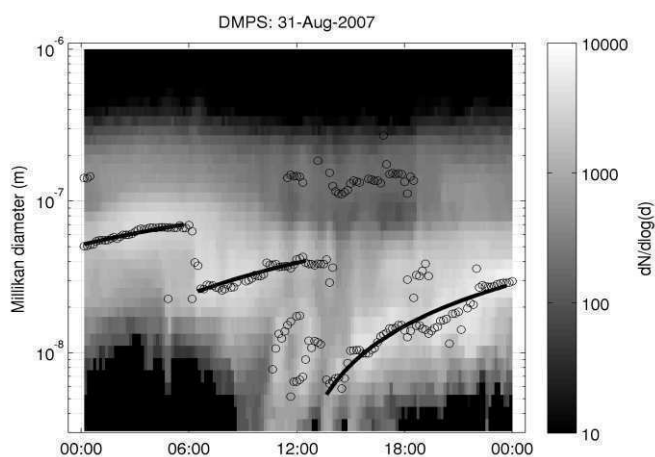


Figure 1. An example of the growth rate determination. Black circles describe the fitted mode maxima, and the lines are the growth rates fitted to these maxima.

The concentration of condensing vapour leading to a growth rate of 1 nm/h ($C_{1\text{nm/h}}$) can be calculated for particles with varying diameter by using the formula given by Nieminen et al. (2009). With this we calculated the prevailing concentrations of condensing vapour as

$$C_{\text{GR}} = \text{GR} * C_{1\text{nm/h}}.$$

Monoterpenes or isoprene as volatile vapours do not condense on particles, but instead some of their oxidation products are suggested to be main participants in particle growth (Tunved et al., 2006). Thus, we approximated a source rate Q_{GR} for the condensing vapour and compared that with the measured monoterpene and isoprene concentrations. By assuming a steady state for the condensing vapour concentration, the major sink being the condensation sink CS formed by the particle population, the source rate of the condensing vapour can be written as

$$Q_{\text{GR}} = C_{\text{GR}} * \text{CS}.$$

CONCLUSIONS

The temperature explains over 25 % of the variation in Q_{GR} throughout the year, both during day and night (Fig. 2), when those data points in which the RH was over 90 % were left out. Under very humid circumstances the correlation between Q_{GR} and T was completely lost and the Q_{GR} values were clearly higher than in dryer data points with same temperature. This might be due to a significant difference in the initial wet diameter and the observed dry diameter of these particles.

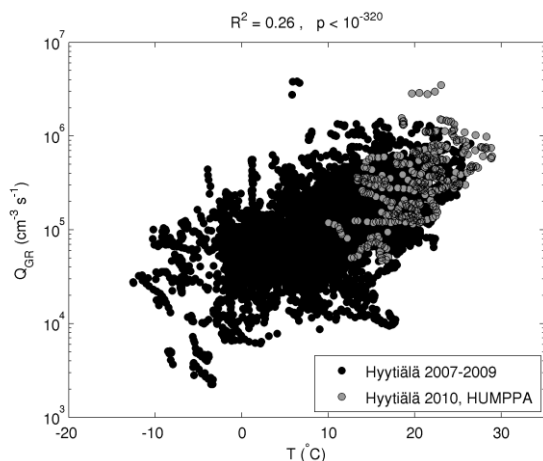
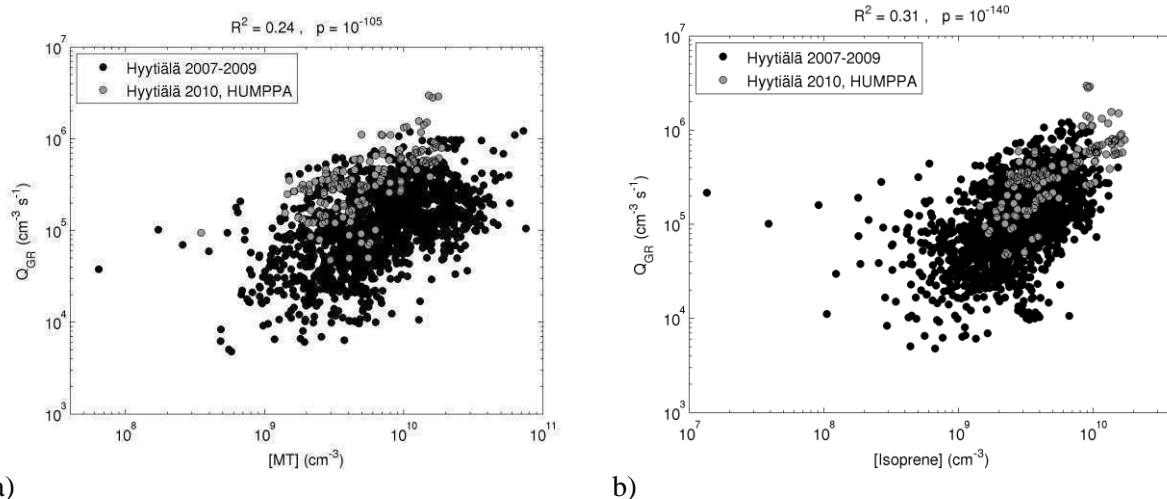


Figure 2. The source rate of condensing vapour as a function of temperature. The correlation coefficient R^2 and the p-value describing the probability of coincidental correlation are shown in the figure.

Source rate of condensing vapour Q_{GR} is depicted as a function of measured monoterpene (MT) and isoprene concentrations in Fig. 3. In both figures an increase of two orders of magnitude in measured vapour concentration causes approximately equal increase in Q_{GR} . However, Q_{GR} has stronger correlation with isoprene concentration than with monoterpene concentration. This is partly related to lower [MT] during the HUMPPA campaign than during the previous years with the corresponding temperatures. This uplifts the HUMPPA data points in Fig. 3a. Better correlation between Q_{GR} and isoprene seems to indicate that either isoprene or some other volatile organic compounds having very similar concentrations could be responsible for majority of the particle growth in boreal forest, instead of the most abundant monoterpenes α -pinene and 3-carene.



a) b)
 Figure 3. The source rate of condensing vapour as a function of a) monoterpene and b) isoprene concentration. The correlation coefficients R^2 and p-values describing the probability of coincidental correlation are shown in the figure.

According to our analysis the growth rate of particles with diameters between 10 and 100 nm in Boreal forest is closely connected to monoterpene and isoprene concentrations, and thus to temperature.

ACKNOWLEDGEMENTS

This work was supported by Maj and Tor Nessling Foundation (project number 2010212) and by the Academy of Finland Centre of Excellence program (project No. 1118615).

REFERENCES

- Hari, P. and Kulmala, M. (2005), Station for measuring ecosystem-atmosphere relations (SMEAR II), *Boreal Env. Res.*, **10**, 315-322.
 Nieminen, T. et al. (2009), Sub-10 nm particle growth by vapor condensation – effects of vapor molecule size and particle thermal speed, *Atmos. Chem. Phys.*, **10**, 9773-9779.
 Riipinen, I. et al. (2011), Organic condensation: a vital link connecting aerosol formation to cloud condensation nuclei (CCN) concentrations, *Atmos. Chem. Phys.*, **11**, 3865-3878
 Tunved, P. et al. (2006), High Natural Aerosol Loading over Boreal Forests, *Science*, **312**, 261-263.

THE ANALYSIS OF SIZE-SEGREGATED CLOUD CONDENSATION NUCLEI COUNTER (CCNC) DATA FROM SMEAR II AND ITS IMPLICATIONS FOR AEROSOL-CLOUD RELATIONS

M. PARAMONOV¹, T. PETÄJÄ¹, P.P. AALTO¹, V.-M. KERMINEN² and M. KULMALA¹

¹Department of Physics, University of Helsinki, P.O. Box 64, FI-00014, Helsinki, Finland.

²Finnish Meteorological Institute, P.O. Box 503, 00101, Helsinki, Finland.

Keywords: CCNC, aerosol, cloud, critical diameter.

INTRODUCTION

Aerosol particles are omnipresent in the atmosphere, and besides directly influencing the radiative balance of the Earth, they play a crucial role in cloud formation (Stevens and Feingold, 2009). Through a variety of microphysical processes aerosol particles influence the albedo, lifetime and precipitation patterns of clouds in what is known as indirect effects of aerosols on climate (Forster *et al.*, 2007). The ability of aerosol particles to act as cloud condensation nuclei (CCN) is strongly linked to their physical and chemical properties, with the most important parameters being CCN concentration, aerosol critical diameter and hygroscopicity (Seinfeld and Pandis, 2006).

METHODS

CCNC measurements have been conducted continuously at the SMEAR II (Station for Measuring Ecosystem-Atmosphere Relations) in Hyytiälä Forestry Field Station in Finland since June 2008, and they form a part of the comprehensive network of aerosol- and meteorology-related measurements in Southern Finland (Hari and Kulmala, 2005). The station (61° 50' 50.685"N, 24° 17' 41.206"E, 179 m a.m.s.l.) is located 220 km north-west of Helsinki on a flat terrain surrounded by a Scots Pine stand, and is, therefore, well representative of the boreal environment. The CCNC in question is a diffusion-type CCN counter, including a differential mobility analyzer (DMA), condensation particle counter (CPC), optical particle counter (OPC) and a saturator unit. Both non-size-segregated and size-segregated measurements are performed by the instrument, with the latter having started in February 2009 with an introduction of a DMA into the system. CCN concentrations are measured across 30 size channels, with particle diameters ranging from 20 to 300 nm for supersaturation levels of 0.1%, 0.2%, 0.4%, 0.6% and 1%. This measurement setup allows for a direct determination of critical diameter d_c and the hygroscopicity parameter κ . Starting in January 2010, CCN efficiency spectra are measured on average 66 times per day; previously they were measured 77 times per day.

Activated fractions A were calculated for each size channel in each spectrum by dividing the number concentration of CCN by the corresponding number concentration of CN. Each CCN efficiency spectrum was then fitted with a function proposed by Rose *et al.* (2008) in the form of

$$A = a \left(1 + \operatorname{erf} \left(\frac{D - D_a}{\sigma \sqrt{2}} \right) \right) \quad (1),$$

where a is half the maximum A for each spectrum, erf is error function, D is particle diameter, D_a is the particle diameter at $A = a$ and σ is the standard deviation of the cumulative Gaussian distribution function. Before the function was fitted, A values were normalized to unity by multiplying every A with $0.5/a$. In the function above the fit parameter D_a is the critical diameter of dry aerosol particles D_c , which in this study is defined as the diameter at which half of the incoming particles are activated at a certain level of

supersaturation. The described method allows for direct determination of critical diameter values from size-segregated CCNC data.

In previous studies, which dealt with CCN data from SMEAR II, D_c and κ values were calculated indirectly, either by applying the κ -Köhler theory to the hygroscopicity-tandem DMA (H-TDMA) data, or by combining the particle size distribution data with the CCNC data (Mikkilä *et al.*, 2010; Sihto *et al.*, 2010). This study will be the first to present the results of direct derivation of D_c and κ values from size-segregated CCNC measurements at SMEAR II, and will allow for a comparison of methods for their determination. Besides the temporal trends and the chemical analysis based on κ values, the study will also concentrate on the source apportionment of CCN based on the observed chemical variations utilizing the trajectory analysis. During the conditions of the well-mixed boundary layer, particle number size distributions will also be used simultaneously with CCNC data to investigate the occurrence of the Hoppel minimum as a result of the processing of particles by clouds. The study aims to provide the most comprehensive and up-to-date overview of the CCNC data for a boreal environment in Southern Finland by means of detailed analysis of size-segregated CCN data, aided by the incorporation of a variety of other datasets from SMEAR II deemed relevant.

ACKNOWLEDGEMENTS

This work is supported by the Maj and Tor Nessling Foundation project nr. 2010143 "*The effects of anthropogenic air pollution and natural aerosol loading to cloud formation*".

REFERENCES

- Forster, P., V. Ramaswamy, P. Artaxo, T. Berntsen, R. Betts, D.W. Fahey, J. Haywood, J. Lean, D.C. Lowe, G. Myhre, J. Nganga, R. Prinn, G. Raga, M. Schulz and R. Van Dorland (2007): Changes in Atmospheric Constituents and in Radiative Forcing. *In: Climate Change 2007: The Physical Science Basis. Contribution of Working Group I to the Fourth Assessment Report of the Intergovernmental Panel on Climate Change* [Solomon, S., D. Qin, M. Manning, Z. Chen, M. Marquis, K.B. Averyt, M. Tignor and H.L. Miller (eds.)]. Cambridge University Press, Cambridge, United Kingdom and New York, NY, USA.
- Hari, P. and M. Kulmala (2005). Station for measuring ecosystem-atmosphere relations. *Boreal Env. Res.* **10**, 315–322.
- Mikkilä, J., J. Vanhanen, S.-L. Sihto, M. Ehn, T. Mäkelä, T. Petäjä and M. Kulmala (2010). CCN properties from H-TDMA measurements in Hyytiälä, in Proc. Int. Aerosol Conf., Helsinki, Finland.
- Rose, D., S.S. Gunthe, E. Mikhailov, G.P. Frank, U. Dusek, M.O. Andreae and U. Pöschl (2008). Calibration and measurement uncertainties of a continuous-flow cloud condensation nuclei counter (DMT-CCNC): CCN activation of ammonium sulfate and sodium chloride aerosol particles in theory and experiment. *Atmos. Chem. Phys.* **8**, 1153–1179.
- Seinfeld, J.H. and S.N. Pandis (2006). *Atmospheric Chemistry and Physics. from air pollution to climate change* (2nd edition). (John Wiley & Sons, New York, USA).
- Sihto, S.-L., J. Mikkilä, J. Vanhanen, M. Ehn, L. Liao, K. Lehtipalo, P.P. Aalto, J. Duplissy, T. Petäjä, V.-M. Kerminen, M. Boy and M. Kulmala (2010). Seasonal variation of CCN concentrations and aerosol activation properties in boreal forest. *Atmos. Chem. Phys. Discuss.* **10**, 28231–28272.
- Stevens, B. and G. Feingold (2009). Untangling aerosol effects on clouds and precipitation in a buffered system. *Nature* **461**, 607–613.

TOTAL OH REACTIVITY MEASUREMENTS IN BOREAL FOREST

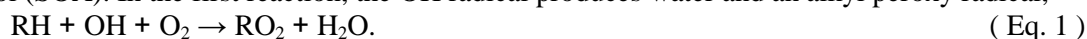
J. PATOKOSKI¹, M.K. KAJOS¹, T.M. RUUSKANEN, S. SCHALLHART¹, P. RANTALA¹, J. RINNE¹

¹Department of Physics, P.O. Box 64, FI-00014, University of Helsinki, Finland.

Keywords: TOTAL OH REACTIVITY, VOCS, BOREAL FOREST, PTR-MS.

INTRODUCTION

Hydroxyl radical (OH) oxidizes inorganic gases and VOCs to forms in which they can take part to aerosol formation. Globally boreal forests are important sources of biogenic volatile organic compounds (BVOCs) emitted to the atmosphere. Yearly about 1.3 billion tonnes of VOCs are released due to natural and anthropogenic emission to the atmosphere (Goldstein and Galbally, 2007). The reactions with organic compounds are the major sink of OH in boreal forest, where as in the winter reactions with inorganic species dominate (Mogensen et. al. 2011). The oxidation of VOCs, denoted R, by the OH radicals in the atmosphere starts a long chain of reactions that produce less volatile compounds that can form secondary organic aerosol (SOA). In the first reaction, the OH radical produces water and an alkyl peroxy radical,



The reaction can be followed by a reaction with NO that produces an alkoxy radical which in turn can react with O₂,



The alkyl peroxy radicals, RO₂ and HO₂, can also react with each other. This reaction produces alcohols, carbonyls and peroxides which again can react with OH,



METHODS

Total OH reactivity was measured by comparative reaction method (CRM) where proton transfer reaction mass spectrometer (PTR-MS) was used as a detector.

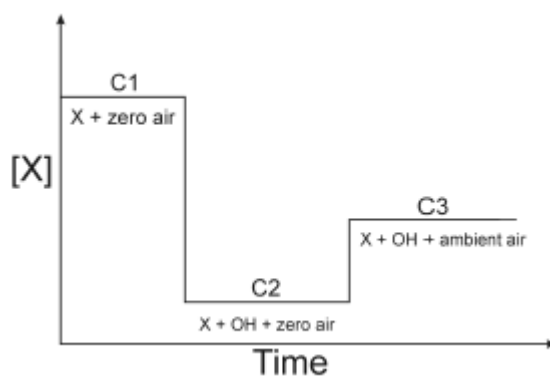


Figure 1. Different steps in CRM.

In CRM compound X which usually do not exists in the air is introduced to reactor. In this setup compound X was pyrrole. Concentration of pyrrole C1 was detected. When C1 level was constant enough OH radicals were generated and introduced to the reactor. Because of OH radicals C1 level decreased when OH radicals reacted with X. C2 level was detected. C1-C2 levels difference gave initial concentration of OH radicals. Next step was to introduce ambient air to reactor. Ambient air contained

reactive species which competed with X about OH radicals in the reactor so the concentration of X increased to level C3 (Figure 1 and 2) (Sinha et. al. 2008).

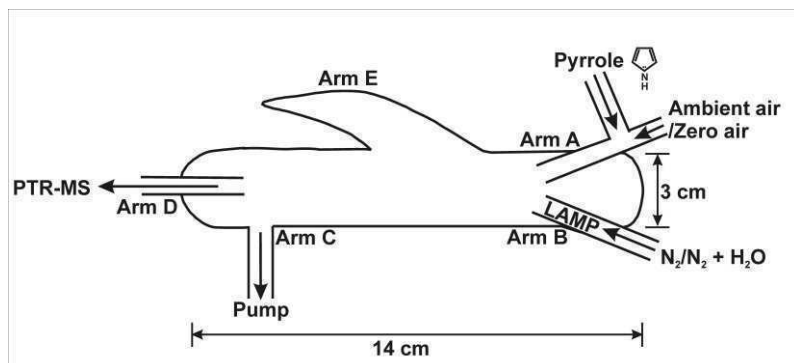


Figure2. Schematic picture of glass reactor used in CRM.

Loss reaction of OH radicals are



which leads to the rate expression

$$-\delta [\text{OH}]/dt = k_p[\text{OH}][\text{Pyrrole}] + k_{\text{OH+air}}[\text{OH}][\text{air}], \quad (\text{Eq. 7})$$

where k_p is the rate coefficient for reaction of OH with pyrrole, $k_{\text{OH+air}}$ is the effective rate coefficient of all reactive compounds in the sample and [air] is summed concentration. Change in pyrrole concentration (C1-C3) is given

$$(C1-C2) = (R_p/R_p+R_{\text{air}})[\text{OH}] \quad (\text{Eq. 8})$$

if all OH is lost in reaction between air and pyrrole. Reactivity is

$$R_p = ((C3-C2)/(C1-C3)) \cdot k_p C1 \quad (\text{Eq. 9})$$

This CRM has been used in boreal forest where the measured total OH reactivity was up to twice the OH reactivity calculated based on measured inorganic and trace gases (Sinha et. al. 2010). In the previous studies OH reactivity was measured only from one height in the top canopy and the campaigns were only during a month. However, the modeled OH reactivity results indicated large gradients within the canopy and close to the forest floor.

Measurements of total OH reactivities simultaneously with versatile measurements of trace gases in ambient air was measured during summer 2011 in SMEAR II station (Station for Measuring Ecosystem-Atmosphere Relations) which is a high latitude boreal measurement site in Hyytiälä, Finland. Total OH reactivities was measured at two different heights inside the canopy in monthly measurement campaigns during the summer. OH reactivity was calculated for the same heights from simultaneous inorganic gas measurements (Hari and Kulmala, 2005) and VOC measurements with a PTR-MS similar to the method described by Taipale et al (2008). Preliminary results of this study was to declare: 1) the variation of measured total OH reactivity over the summer months and 2) determine out how much reactivity is still missing from the comparison measured total OH reactivity to the calculated OH reactivity (Mogensen et. al, 2011) of the measured trace gases.

ACKNOWLEDGEMENTS

The financial support by the Academy of Finland Centre of Excellence program (project no 1118615) is gratefully acknowledged.

REFERENCES

- Goldstein, A. H. and Galbally, I. E. (2007), Known and unexplored organic constituents in the earth's atmosphere, *Environ. Sci. Technol.*, **41**, 1514–1521.
- Hari, P., and Kulmala, M. (2005). Station for Measuring Ecosystem–Atmosphere Relations (SMEAR II), *Boreal Environ. Res.*, **10**, 315–322.
- Mogensen, D., Smolander, S., Sogachev, A., Zhou, L., Sinha, V., Guenther, A., Williams, J., Nieminen, T., Kajos, M., Rinne, J., Kulmala, M. and Boy, M. (2011), Modelling atmospheric OH-reactivity in a boreal forest ecosystem, *Atmos. Chem. Phys. Discuss*, **11**, 9133–9163.
- Sinha, V., Williams, J., Crowley, J.N. and Lelieveld, J. (2008), The Comparative Reactivity Method – a new tool to measure total OH Reactivity in ambient air, *Atmos. Chem. Phys.*, **8**, 2213–2227.
- Sinha, V, Williams, J., Lelieveld, J., Ruuskanen, T.M., Kajos, M.K., Patokoski, J., Hellen, H., Hakola, H., Mogensen, D., Boy, M., Rinne, J. and Kulmala, M. (2010), OH Reactivity Measurements within a Boreal Forest: Evidence for Unknown Reactive Emissions, *Environ. Sci. Technol.*, **44**, 6614–6620.
- Taipale, R., Ruuskanen, T. M., Rinne, J., Kajos, M. K., Hakola, H., Pohja, T. and Kulmala, M.: (2008). Technical Note: Quantitative long-term measurements of VOC concentrations by PTR-MS-measurement, calibration and volume mixing ratio calculation methods, *Atmospheric Chemistry and Physics*, **8**, 6681–6698.

INTERCOMPARISON OF FOUR METHANE GAS ANALYSERS FOR EDDY COVARIANCE FLUX MEASUREMENTS

O. PELTOLA, I. MAMMARELLA, S. HAAPANALA and T. VESALA

Department of Physics, Division of Atmospheric Sciences, University of Helsinki, Helsinki, 00014, Finland.

Keywords: eddy covariance, methane flux, laser absorption spectroscopy.

INTRODUCTION

Amount of new state-of-the-art gas analysers able to measure also other greenhouse gases than CO_2 with high sampling frequency and precision has increased during the last decade. High sampling frequency is a necessity for eddy covariance measurements because with low sampling frequency all the turbulent eddies are not resolved. Thus measuring methane and nitrous oxide fluxes with eddy covariance technique has lately become more common. Even though the performance of the new gas analysers has already been tested in the laboratory and in the field, critical field intercomparisons of the novel instruments are still needed. This is due to the fact that validating trace gas flux retrieved from one gas analyser is quite challenging because there is no reliable reference for the measured flux. In addition even though the gas analyser might function well in laboratory conditions, functioning in the field circumstances might be another matter. Therefore methane fluxes were measured with four recently commercialised novel gas analysers simultaneously at Siikanen fen. The measurement system operated about six months between March and August 2010. The aim of this measurement campaign was to evaluate functionality, data quality and overall performance of the gas analysers and to provide an instrumentation recommendation for the European Research Infrastructure ICOS (Integrated Carbon Observation System).

METHODS

The methane gas analyser intercomparison was carried out between 1st of April and 26th of October in 2010 at Siikanen fen ($61^{\circ}49.961'N$, $24^{\circ}11.567'E$, 160 m a.s.l). Siikanen is a nutrient poor, i.e. oligotrophic, open fen. Distance from the study site to the tree line is in north and south directions about 200 m and east and west directions several hundred meters. Surrounding forest consists mainly of Scots pines. Peat depth varies from 2 m to 4 m, increasing toward the centre of the site. The surface topography is relatively flat with no pronounced slope and the methane sources are distributed quite uniformly around the measurement station (Aurela *et al.*, 2007). Due to this, in addition to relatively long homogeneous fetch, this location is well-suitable for eddy covariance measurements.

Micrometeorological measurement system used to observe trace gas fluxes usually consists of sonic anemometer and at least one gas analyser. In Siikanen site three-axis sonic anemometer/thermometer (USA-1, METEK, Germany) was used to measure three wind components and air temperature. CO_2 and H_2O concentrations were measured with a closed-path NDIR-based gas analyser (LI-7000, LI-COR Biosciences, Lincoln, NE, USA). Sonic anemometer was situated at 2.75 m height. All measurements related to eddy covariance were recorded at 10 Hz sampling rate.

The participating methane gas analysers were TGA100A (Campbell Scientific Inc.), G1301-f (Picarro Inc., USA), RMT-200 (Los Gatos Research Inc.) and LI-7700 (Li-Cor Inc.). Three first gas

	LI-7700	TGA100A	G1301-f	RMT-200
How many days operated	31	111	134	160
Percentage of good data	68 %	68 %	89 %	88 %

Table 1: Table including information on how long the gas analysers were functioning and how big fraction of these measurements were good data. Good data in this context is defined as those periods when the measured methane flux fulfilled turbulence stationarity criterion and the raw methane concentration data contained no spikes. Raw measurement was considered as a spike when the difference between two consecutive datapoints exceeded 0.5 ppm. The same limit was used for all the methane gas analysers.

analysers were closed-path and the last was a prototype of later commercialised open-path methane gas analyser. All of these gas analysers are based on different variations of laser absorption spectroscopy: TGA100A is based on TDLAS measurement technique employing lead-salt laser (e.g. Werle, 1998), G1301-f is based on wavelength-scanned cavity ring down spectroscopy (WS-CRDS), RMT-200 is based on off-axis integrated cavity output spectroscopy (off-axis ICOS) (Hendriks *et al.*, 2008) and LI-7700 is based on wavelength modulation spectroscopy (WMS) (McDermitt *et al.*, 2010). Only TGA100A employs tunable lead-salt diode laser and thus it was the only instrument that needed liquid nitrogen constantly in order to function properly. Water vapour was removed with a drier from TGA100A air samples before they reached the gas analyser measurement cell.

RESULTS

Three out of four methane gas analysers operated with occasional breaks through the whole measurement period. LI-7700 stopped working during June, thus the amount of LI-7700 methane flux data is smaller and this should be considered when the results are analysed. Fig. 1 shows scatter plots of methane flux measured with the four instruments. Picarro G1301-f was selected as a reference for the other gas analysers mainly because it is said to be free from water vapour effects and the measured CH_4 flux show small scatter. However the choice was more or less arbitrary, also RMT-200 or TGA100A could have been selected as reference. According to Fig. 1 a), RMT-200 and G1301-f measured almost identical methane flux throughout the measurement period. This means that they agreed during low flux periods at the beginning and at the end of summer when the flux was around zero, but also during high flux periods in the middle of summer when the magnitude of the flux was around $10 \text{ mg}/(\text{m}^2\text{h})$. Correlation between measured fluxes is high ($r^2 = 0.997$) and slope (approximately 1.007) of the fitted curve almost equals one. Median relative difference between methane fluxes measured by RMT-200 and G1301-f is approximately 3.4 %, meaning that RMT-200 fluxes are larger. However, this difference depends slightly on the magnitude of the flux: between 1st of April and 25th of May it is 8.3 %, while between 25th of May and 23rd of September it is 2.9 %. The former subperiod corresponds to low flux period, with average methane flux $0.5 \text{ mg}/(\text{m}^2\text{h})$ and the latter period corresponds to high flux period, with average flux of $3.1 \text{ mg}/(\text{m}^2\text{h})$. However RMT-200 data was not corrected for spectroscopic cross-talk effect caused by water vapour (Tuzson *et al.*, 2010), and thus the results may slightly change if this correction is applied. In any case, this effect should be small and the correlation should remain high.

Correlation between methane flux measured with TGA100A and G1301-f ($r^2 = 0.896$) is not as high as in the case of RMT-200 and G1301-f, but the datasets are still well correlated. Methane flux data measured by TGA100A has larger scatter than methane flux measured by the other instruments and this can also be seen in Fig. 1 b) if it is compared with the previous Fig. 1 a). Slope of the fitted line is 0.855 which is still quite near the optimal value of 1. Median relative

difference between TGA100A and G1301-f fluxes is 1.9 % and this difference in low (between 1st of April and 25th of May) and high (between 25th of May and 23rd of September) flux periods are 3.7 % and -0.3 %, respectively. Correlation between methane flux measured with LI-7700 and G1301-f is poor ($r^2 = 0.001$). This is due to the fact that LI-7700 was functioning only in the beginning of the measurement period, when the flux was small and LI-7700 was not able to measure small fluxes all the time properly.

CONCLUSIONS

From this preliminary data analysis it is difficult to assess which one of these instruments produces the most reliable estimates for methane fluxes. However, agreement between RMT-200 and G1301-f, in addition to small scatter in the retrieved flux data, indicate that these two instruments performed well and might be measuring methane fluxes more accurately than the other two instruments. TGA100A also performed well, even though the scatter in the data was more pronounced. However, one major downside in using TGA100A is the constant need for cooling the lead-salt laser. This increases the maintenance needs significantly, when compared to instruments that can operate in room temperatures, such as RMT-200, G1301-f and LI-7700.

ACKNOWLEDGEMENTS

The financial supports by the Academy of Finland Centre of Excellence program (project no 1118615) and EU projects ICOS, IMECC and GHG-Europe are gratefully acknowledged.

REFERENCES

- Aurela, M., Riutta, T., Laurila, T., Tuovinen, J.-P., Vesala, T., Tuittila, E.-S., Rinne, J., Haapanala, S. and J. Laine. (2007). CO_2 balance of a sedge fen in southern Finland - the influence of a drought period. *Tellus*, **59B**, 826-837.
- Hendriks, D.M.D., Dolman, A.J., van der Molen, M.K. and J. van Huissteden. (2008). A compact and stable eddy covariance set-up for methane measurements using off-axis integrated cavity output spectroscopy. *Atmos. Chem. Phys.*, **8**, 431-443.
- McDermitt, D., Burba, G., Xu, L., Anderson, T., Komissarov, A., Riensche, B., Schedlbauer, J., Starr, G., Zona, D., Oechel, W., Oberbauer, S. and S. Hastings. (2010). A new low-power, open-path instrument for measuring methane flux by eddy covariance. *Appl. Phys. B*, **102(2)**, 391-405.
- Tuzson, B., Hiller, R.V., Zeyer, K., Eugster, W., Neftel, A., Ammann, C. and L. Emmenegger. (2010). Field intercomparison of two optical analyzers for CH_4 eddy covariance flux measurements. *Atmos. Meas. Tech. Discuss.*, **3**, 2961-2993.
- P. Werle. (1998). A review of recent advances in semiconductor laser based gas monitors. *Spectrochim. Acta. A.*, **54**, 197-236.

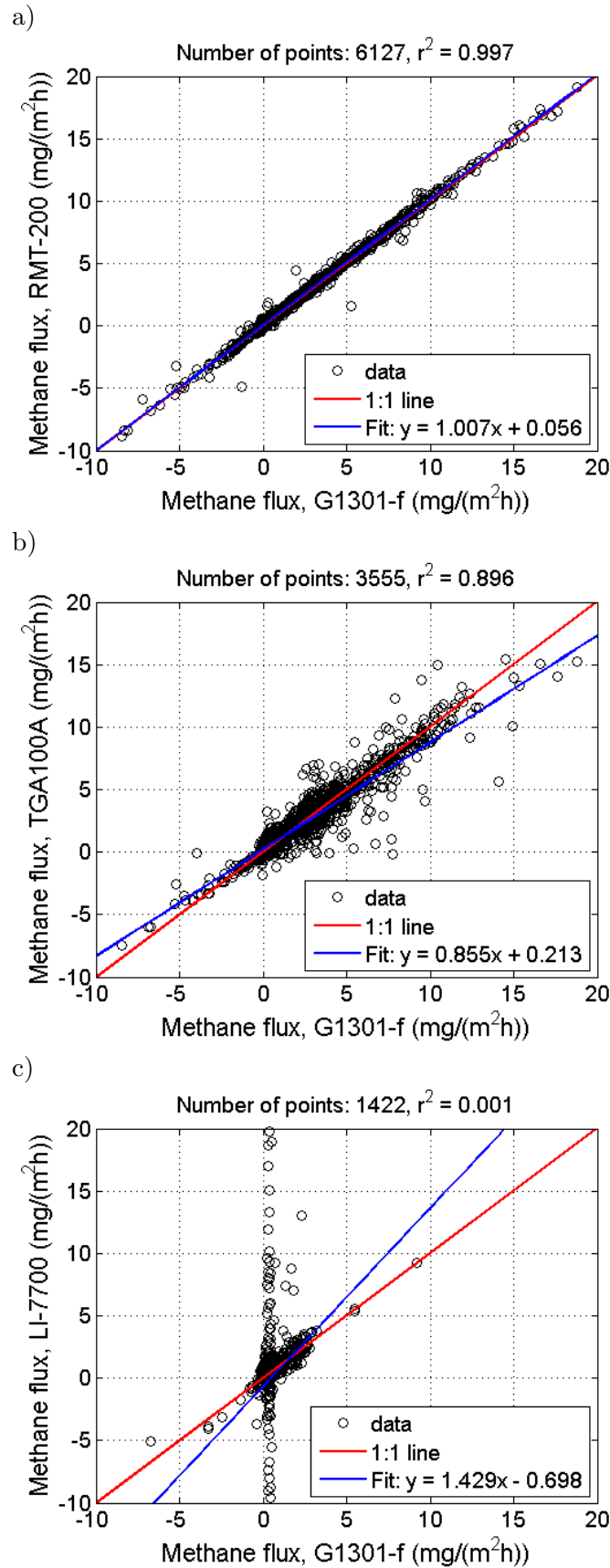


Figure 1: Scatter plots of methane flux. Data from the whole measurement period was used excluding periods when the amount of spikes in the raw methane data exceeded 100.

AN OVERVIEW OF RECENT INSTRUMENT DEVELOPMENT AT UNIVERSITY OF HELSINKI

T. PETÄJÄ¹, M. SIPILÄ¹, K. LEHTIPALO^{1,2}, H. E. MANNINEN¹, H. JUNNINEN¹, T. RUUSKANEN¹,
M. EHN³, J. VANHANEN², H. VEHKAMÄKI¹, D. R. WORSNOP^{1,4}, and M. KULMALA¹

¹Department of Physics, Division of Atmospheric Sciences, PL 64, 00014 University of Helsinki

²Airmodus Oy, Helsinki, Finland

³Forschungszentrum Jülich GmbH, Jülich, 52425, Germany

⁴Aerodyne Research, Inc., Billerica, MA 01821-3976, USA

Keywords:

ATMOSPHERIC AEROSOLS, ATMOSPHERIC IONS, CHARACTERIZATION, INSTRUMENT
DEVELOPMENT, FIELD EXPERIMENTS, LABORATORY EXPERIMENTS

INTRODUCTION

The atmosphere contains ubiquitous numbers of aerosol particles suspended in the air. Atmospheric aerosol particles affect the global climate directly by scattering incoming solar radiation and indirectly by acting as cloud condensation nuclei (CCN). Regionally, suspended particulate matter degrades visibility (Cabada et al. 2004) and has negative effects on human health (Brunekreef and Holgate, 2002, von Klot et al. 2005). In a larger scale, the aerosol particles affect the global albedo as well as precipitation patterns (Rosenfeld et al. 2008). The net effects depend on the number of particles, their chemical composition, and their physical size. The aerosol particle population is closely linked with the Earth's surface and reflects the regional emissions of both gaseous and particulate phase components. Due to the complexity of the connections between the surface exchange of gases and particles, and their transformation processes, they pose a large uncertainty in the current estimates on the global climate change (IPCC, 2007).

In order to assess the role of atmospheric aerosol particles in the global and regional scales, representative measurements in connection with global and regional modelling are needed. Furthermore, detailed laboratory systems need to be understood via measurements and modelling and these results need to be up-scaled to regional and even to global dimension (Kerminen et al. 2010). The aim of this study is to present the activities of the last few years in aerosol instrument development at the University of Helsinki (UHEL). Also the fundamental reasoning and behind this development is briefly discussed.

INSTRUMENT DEVELOPMENT

Our recent work in the instrumental development can be divided into three major areas: 1) atmospheric mass spectrometry, 2) Condensation Particle Counters, 3) improvement, development and verification of existing instrumentation. These activities are conducted in a close collaboration between UHEL and e.g. Airmodus, Aerodyne and TofWerk. The instrument development provides us with the state-of-the-art tools that are needed for the scientific breakthroughs.

In terms of atmospheric aerosol research, mass spectrometry has been proven to be crucial in both determining the aerosol particle chemical composition (Jimenez et al. 2009) as well as quantifying the precursor vapors (Petäjä et al. 2009, Ruuskanen et al. 2011, this issue). In this field, a major breakthrough

has been the Atmospheric Pressure interface Time-of-Flight mass spectrometer (APi-TOF, Junninen et al. 2010, Ehn et al. 2010). This instrument provides nearly a universal detector that is both sensitive and has a high mass accuracy to be able to determine the chemical composition of atmospheric ions. Currently we have committed ourselves in development of the ionization methods for the APi-TOF that will enable us to expand the repertoire of the APi-TOF from the atmospheric ion composition to neutral gas-phase components as well as to atmospheric clusters (Jokinen et al. 2011, this issue).

In the development of the ionization techniques, the interplay between the detailed quantum chemical modelling and the experiments is crucial. To illustrate the importance of the collaboration, for example Kurtén et al. (2011) theoretically showed that a strong gas phase base, if being present, can affect chemical ionization mass spectrometric method of determination of gaseous phase sulphuric acid.

The APi-TOF has provided us a clear link between mass of clusters and electrical mobility (Ehn et al. 2011). This is directly linked to the Condensation Particle Counter (CPC) development. Vanhanen et al. 2010 presented Particle Size Magnifier (PSM) incorporating a use of di-ethylene glycol (Iida et al. 2009) and a mixing type CPC (Sgro and Fernández de la Mora, 2004). The PSM is able to detect charged molecular ions (Ude and Fernández la Mora, 2005) down to 1.05 nm in electrical mobility equivalent size (Lehtipalo et al. 2011, this issue). For the unknown species, this corresponds to mass range of 70-250 amu (Ku and Fernández de la Mora, 2010, Ehn et al. 2010b). Without a doubt with this set of instruments we operate in the range where the atmospheric nucleation is occurring (Kulmala et al. 2007). This will be the key to solving the participating compounds in the new particle formation in the atmosphere.

Concurrent measurements with the APi-TOF and ion spectrometers are fruitful. While the APi-TOF provides a detailed chemical composition data, the ion spectrometers can determine ion concentrations (Asmi et al. 2009, Gagne et al. 2011). The ion spectrometer provides reference transmission information in the field for the mass spectrometers so the mass dependent loss correction can be applied. Furthermore, in the instrument calibration, the APi-TOF can be used to characterize the ion spectrometer corona ions which will shed light into the operation of the ion spectrometers and the data interpretation (Manninen et al. 2011).

The role of ions in the overall atmospheric nanoparticle formation is controversial (Gagné et al. 2008, Yu and Turco, 2011). Laakso et al. 2007 presented the ion-Differential Mobility Particle Sizer (ion-DMPS) that was able to determine charging state of atmospheric nanoparticles. We have developed this method further (Hakala et al. 2011, this issue) by implementing a nano-Differential Mobility Analyzer (Chen et al. 1998) and Pulse-Height Analysis (Sipilä et al. 2009). Kerminen et al. 2007 provided the theoretical framework stemming from balance equations and utilizing the aerosol dynamical modelling in addressing the relative roles of ion induced and neutral nucleation pathways to the observed atmospheric aerosol formation. Again, this illustrates the strong connection between modelling and measurements. You need both to fully utilize the results and connect them together to form a coherent picture of the atmospheric situation.

OUTLOOK

Clearly, the instrument development is important. However, one has to bear in mind that the development as such is more of an engineering task so it should be driven by the scientific needs. We need to incorporate the theoretical understanding already at the initial stages of development. This is particularly important when dealing with clusters, ions and particles in the nanoscale. Without a completely independent approach with quantum chemistry and molecular and aerosol dynamics we cannot interpret the data obtained with the state-of-the art instrumentation and thus cannot link the importance of our data to the global atmosphere.

The laboratory verification of the CPC and ion instrumentation with a cut-off size in the sub-2 nm size range has shown the utmost importance of mass spectrometric methods; the physical size by itself is not

enough, we need to know also the chemical composition of these nanoparticles as that will play a crucial role whether they can be detected or not. Along the same lines, also the full utilization of chemical composition information with high resolution mass spectrometers is needed to interpret the details of the ambient nanoparticle data. The integration of physical and chemical information from the state-of-the-art instrumentation with models of quantum chemistry and aerosol dynamics will be the key resolving the participating compounds in the atmospheric new particle formation.

Another aspect that has to be kept in mind is the importance of long-term monitoring. This activity is far from being easy and standard. The requirements of the modern instruments put pressure on the existing infrastructure both in terms of quality of the hardware and operation personnel. The benefit of running the instruments in the field will be redeemed as it will provide crucial data for resolving the role of chemistry, meteorology, ecology and physics in the fate of atmospheric air pollution in various temporal scales starting from seconds up to decadal scale.

A network of stations, such as SMEAR (Hari and Kulmala, 2005) should be utilized to characterize the chemical environment in the boundary layer at a variety of ecosystems, not only campaign-wise (e.g. Manninen et al. 2010), but in a continuous manner. This will pose challenges to both data storage as well as pre-processing and visualization. For this, we need tools like SMART-SMEAR (Junninen et al. 2009). Also, in the future, integration of the continuous field data with remote sensing (Sundström et al. 2011, this issue) will be important as well as targeted laboratory experiments (Kerminen et al. 2010, Neitola et al. 2011, this issue). A full benefit stemming from various national and international collaborations via various projects and networking activities should be taken advantage of.

REFERENCES

- Asmi, E., Sipilä, M., Manninen, H.E., Vanhanen, J., Lehtipalo, K., Gagné, S., Mirme, A., Mirme, S., Tamm, E., Uin, J., Komsaare, K., Attoui, M. and Kulmala, M. (2009) Results of the first air ion spectrometer calibration and intercomparison workshop, *Atmos. Chem. Phys.* 9, pp. 141-154.
- Brunekreef, B. and Holgate, S. (2002) Air pollution and health, *Lancet*, 360, pp. 1233-1242.
- Cabada, J. *et al.* (2004) Light scattering by fine particles during the Pittsburgh Air Quality Study: Measurements and modeling, *J. Geophys. Res.*, 109, D16S03, doi:10.1029/2003JD004155.
- Chen, D.-R., Pui, D.Y.H., Hummes, D., Fissan, H., Quant, F.R. and Sem, G.J. (1998) Design and evaluation of a nanometer aerosol differential mobility analyzer (Nano-DMA), *J. Aerosol Sci.* 29, pp. 497-509.
- Ehn, M., Junninen, H., Petäjä, T., Kurtén, T., Kerminen, V.-M., Schobesberger, S., Manninen, H.E., Ortega, I.K., Vehkamäki, H., Kulmala, M. and Worsnop, D.R. (2010a) Composition and temporal behavior of ambient ions in the boreal forest. *Atmos. Chem. Phys.* 10, pp. 8513-8530.
- Ehn, M., Junninen, H., Schobesberger, S., Manninen, H.E., Franchin, A., Sipilä, M., Petäjä, T., Kerminen, V.-M., Tammet, H., Mirme, A., Mirme, S., Hörrak, U., Kulmala, M. and Worsnop, D. (2011) An instrumental comparison of mobility and mass measurements of atmospheric small ions *Aerosol Sci. Technol.*, 45, pp. 522-532.
- Gagné, S., Laakso, L., Petäjä, T., Kerminen, V.-M. and Kulmala, M. (2008) Analysis of one year of Ion-DMPS data from SMEAR II station, Finland. *Tellus B* 60, pp. 318-329 doi: 10.1111/j.1600-0889.2008.00347.x.
- Gagné, S., Lehtipalo, K., Manninen, H.E., Nieminen, T., Schobesberger, S., Franchin, A., Yli-Juuti, T., Boulon, J., Sonntag, A., Mirme, S., Mirme, A., Hörrak, U., Petäjä, T., Asmi, E. and Kulmala, M. (2011)

Intercomparison of air ion spectrometers: a basis for data interpretation. *Atmos. Meas. Technol. Discuss.*, 4, pp. 1139-1180.

Hakala, J., Sipilä, M., Lehtipalo, K., Järvinen, E., Siivola, E., Kulmala, M. and Petäjä, T. (2011) A new nanoscale ion differential mobility particle sizer, *Report Series in Aerosol Science*, this issue.

Hari, P., and Kulmala, M. (2005) Station for Measuring Ecosystem-Atmosphere Relations (SMEAR II). *Boreal Environ. Res.* 10, pp. 315-322.

Iida, K., Stolzenburg, M.R. and McMurry, P.H. (2009) Effect of working fluid on sub-2 nm particle detection with a laminar flow ultrafine condensation particle counter, *Aerosol Sci. Technol.* 43, pp. 81-96.

IPCC, 2007: *Climate Change 2007: The Physical Science Basis. Contribution of Working Group I to the Fourth Assessment Report of the Intergovernmental Panel on Climate Change*, Eds. Solomon, S., D. Qin, M. Manning, Z. Chen, M. Marquis, K.B. Averyt, M. Tignor and H.L. Miller. Cambridge University Press, Cambridge, United Kingdom and New York, NY, USA, 996 pp.

Jimenez, J. L., *et al.* (2009), Evolution of organic aerosols in the atmosphere, *Science*, 326, 1525–1529, doi:10.1126/science.1180353.

Jokinen, T.B.A., Sipilä, M., Petäjä, T., Junninen, H., Mauldin III, R.L., Worsnop, D.R. and Kulmala, M. (2011) Sulfuric acid and sulfuric acid cluster detection with CI-API-TOF, *Report Series in Aerosol Science*, this issue.

Junninen, H., Lauri, A., Keronen, P., Aalto, P., Hiltunen, V., Hari, P. and Kulmala, M. (2009) Smart-SMEAR: on-line data exploration and visualization tool for SMEAR stations, *Boreal Environ. Res.* 14, pp. 447-457.

Junninen, H., Ehn, M., Petäjä, T., Luosujärvi, L., Kotiaho, T., Kostianen, R., Rohner, U., Gonin, M., Fuhrer, K., Kulmala, M. and Worsnop, D.R. (2010) API-ToFMS: a tool to analyze composition of ambient small ions. *Atmos. Meas. Technol.*, 3, pp. 1039-1053.

Kerminen, V.-M., Anttila, T., Petäjä, T., Laakso, L., Gagné, S., Lehtinen, K.E.J. and Kulmala, M. (2007) Charging state of the atmospheric nucleation mode: implications for separating neutral and ion-induced nucleation. *J. Geophys. Res.*, 112, D21205, doi: 10.1029 /2007JD008649.

Kerminen, V.-M., Petäjä, T., Manninen, H.E., Paasonen, P., Nieminen, T., Sipilä, M., Junninen, H., Ehn, M., Gagné, S., Laakso, L., Riipinen, I., Vehkamäki, H., Kurtén, T., Ortega, I.K., Dal Maso, M., Brus, D., Hyvärinen, A., Lihavainen, H., Leppä, J., Lehtinen, K.E.J., Mirme, A., Mirme, S., Hörrak, U., Berndt, T., Stratmann, F., Birmili, W., Wiedensohler, A., Metzger, A., Dommen, J., Baltensperger, U., Kiendler-Scharr, A., Mentel, T.F., Wildt, J., Winkler, P.M., Wagner, P.E., Petzold, A., Minikin, A., Plass-Dülmer, C., Pöschl, U., Laaksonen, A. and Kulmala, M. (2010) Atmospheric nucleation: highlights of the EUCAARI project and future directions. *Atmos. Chem. Phys.* 10, pp. 10829-10848.

Ku, B. K. and Fernández de la Mora, J. F. (2009). Relation between electrical mobility, mass, and size for nanodrops 1–6.5 nm in diameter in air, *Aerosol Sci. Technol.* 43, pp.241-249.

Kulmala, M., Riipinen, I., Sipilä, M., Manninen, H. E., Petäjä, T., Junninen, H., Dal Maso, M., Mordas, G., Mirme, A., Vana, M., Hirsikko, A., Laakso, L., Harrison, R. M., Hanson, I., Leung, C., Lehtinen, K. E. J., and Kerminen, V.-M. (2007). Towards direct measurement of atmospheric nucleation, *Science*. 318, pp. 90-92.

Kurtén, T., Petäjä, T., Smith, J., Ortega, I. K., Sipilä, M., Junninen, H., Ehn, M., Vehkamäki, H., Mauldin, L., Worsnop, D. R., and Kulmala, M.: The effect of H₂SO₄ - amine clustering on chemical ionization mass spectrometry (CIMS) measurements of gas-phase sulphuric acid, *Atmos. Chem. Phys.*, 11, pp. 3007-3019.

Laakso, L., Gagné, S., Petäjä, T., Hirsikko, A., Aalto, P.P., Kulmala, M. and Kerminen, V.-M. (2007) Detecting charging state of ultra-fine particles: instrumental development and ambient measurements. *Atmos. Chem. Phys.* 7, pp. 1333-1345.

Lehtipalo, K., et al. (2011) Report series in Aerosol Science, this issue.

Manninen, H.E., Nieminen, T., Asmi, E., Gagné, S., Häkkinen, S., Lehtipalo, K., Aalto, P., Vana, M., Mirme, A., Mirme, S., Hörrak, U., Plass-Dülmer, C., Stange, G., Kiss, G., Hoffer, A., Tärö, N., Moerman, M., Henzing, B., de Leeuw, G., Brinkenberg, M., Kouvarakis, G.N., Bougiatioti, K., Mihalopoulos, N., O'Dowd, C.D., Ceburnis, D., Arneth, A., Svenningsson, B., Swietlicki, E., Tarozzi, L., Decesari, S., Facchini, M.C., Birmili, W., Sonntag, A., Wiedensohler, A., Boulon, J., Sellegri, K., Laj, P., Gysel, M., Bukowiecki, N., Weingartner, E., Wehrle, G., Laaksonen, A., Hamed, A., Joutsensaari, J., Petäjä, T., Kerminen, V.-M. and Kulmala, M. (2010) EUCAARI ion spectrometer measurements at 12 European sites - analysis of new-particle formation events. *Atmos. Chem. Phys.*, 10, pp. 7907-7927.

Manninen, H.E., Franchin, A., Schobesberger, S., Hirsikko, A., Hakala, J., Skromulis, A., Kangasluoma, J., Ehn, M., Junninen, H., Mirme, A., Mirme, S., Sipilä, M., Petäjä, T., Worsnop, D.R. and Kulmala, M. (2011) Characterisation of corona-generated ions used in a Neutral cluster and Air Ion Spectrometer (NAIS). *Atmos. Meas. Technol. Discuss.* 4, pp. 2099-2125.

Neitola, K., Brus, D., Sipilä, M., Jokinen, T., Paasonen, P. and Lihavainen, H. (2011) Amines inhibit growth : H₂SO₄-H₂O-amine flow tube experiments, Report Series in Aerosol Science, this issue.

Petäjä, T., Mauldin III, R.L., Kosciuch, E., McGrath, J., Nieminen, T., Adamov, A., Kotiaho, T. and Kulmala, M. (2009) Sulfuric acid and OH concentrations in a boreal forest site. *Atmos. Chem. Phys.* 9, pp. 7435-7448.

Rosenfeld, R., Lohmann, U., Raga, G.B., O'Dowd, C.D., Kulmala, M., Fuzzi, S., Reissell, A. and Andreae, M.O. (2008) Flood or drought: How do aerosols affect precipitation? *Science*, 321, pp. 1309-1313.

Ruuskanen, T.M., Müller, M., Schnitzhofer, R., Karl, T., Graus, M., Bamberger, I., Hörtnagl, I., Wohlfahrt, G., and Hansel, A. (2011) Emission and deposition of VOC above grassland, eddy covariance fluxes with PTR-TOF, Report Series in Aerosol Science, this issue.

Sipilä, M., Lehtipalo, K., Attoui, M., Neitola, K., Petäjä, T., Aalto, P.P., O'Dowd, C.D. and Kulmala, M. (2009) Laboratory verification of PH-CPC's ability to monitor atmospheric sub-3nm clusters. *Aerosol Sci. Technol.*, 43, pp. 126-135.

Sgro, L. A., and Fernández de la Mora, J. (2004). A simple turbulent mixing CNC for charged particle detection down to 1.2 nm, *Aerosol Sci. Technol.* 38, pp. 1-11.

Ude, S., and Fernández de laMora, J. (2005) Molecular monodisperse mobility and mass standards from electrosprays of tetra-alkyl ammonium halides, *Aerosol Sci.* 36, pp. 1224-1237.

Vanhanen, J., Mikkilä, J., Lehtipalo, K., Sipilä, M., Manninen, H.E., Siivola, E., Petäjä, T. and Kulmala, M. (2011) Particle size magnifier for nano-CN Detection *Aerosol Sci. Technol.*, 45, pp. 533-542.

von Klot, S. *et al.* (2005). Ambient air pollution is associated with increased risk of hospital cardiac readmission of myocardial infarction survivors in five European cities. *Circulation*, 112, pp. 3073-3079.

Yu, F. and Turco, R. (2011) The size-dependent charge fraction of sub-3-nm particles as a key diagnostic of competitive nucleation mechanisms under atmospheric conditions, *Atmos. Chem. Phys. Discuss.*, 11, pp. 11281-11309.

COMPARISON OF STATIC CHAMBERS TO MEASURE CH₄ FLUXES FROM SOILS

M. PIHLATIE^{1, 15}, J. RIIS CHRISTIANSEN², H. AALTONEN³, J. KORHONEN¹, A. NORDBO¹, T. RASILO³, G. BENANTI⁴, M. GIEBELS⁵, M. HELMY⁴, J. HIRVENSALO⁶, S. JONES⁷, R. JUSZCZAK⁸, R. KLEFOTH⁹, R. LOBO DO VALE¹⁰, A.P. ROSA¹¹, P. SHREIBER¹², D. SERGA¹³, S. VICCA¹⁴, B. WOLF¹⁵, and J. PUMPANEN³

¹Department of Physics, Division of Atmospheric Sciences, FI-00014 University of Helsinki, Finland

²Department of Forest & Landscape Ecology, University of Copenhagen, Denmark

³University of Helsinki, Department of Forest Sciences, FI-00014 University of Helsinki, Finland

⁴School of Biology and Environmental Science, University College Dublin, Dublin 4, Ireland

⁵Leibniz-Centre for Agricultural Landscape Research, Institute for Landscape Matter Dynamics, Germany

⁶MTT Agrifood Research Finland, Plant Production Research, FI-31600 Jokioinen, Finland

⁷Scottish Agricultural College, Edinburgh, Bush Estate, Penicuik, Midlothian EH26 OPH

⁸Meteorology Department, Poznan University of Life Sciences, Piatkowska 94, 60-649 Poznan, Poland

⁹Wageningen UR, Environmental Sciences, Soil Science Centre, P.O. Box 47, 6700 AA, Wageningen, the Netherlands

¹⁰ISA, Universidade Técnica de Lisboa, Tapada da Ajuda 1349-017, Lisboa, Portugal

¹¹Centro de Ecologia e Biologia Vegetal, Departamento de Biologia Vegetal, Lisboa, Portugal

¹²University of Hamburg, KlimaCampus, Institute of Soil Science, Allende-Platz 2, 20146 Hamburg, Germany

¹³Laboratoire d'Aérodologie - Observatoire Midi-Pyrénées, FR-31400 Toulouse, France

¹⁴University of Antwerp, Research Group of Plant and Vegetation Ecology, Universiteitsplein 1, 2610 Wilrijk, Belgium.

¹⁵Institute for Meteorology and Climate Research (IMK-IFU), Karlsruhe Institute of Technology, Kreuzeckbahnstraße 19, 82467 Garmisch-Partenkirchen, Germany

Keywords: NON-CO₂ GREENHOUSE GASES, CHAMBER METHOD, CHAMBER DESIGN, FLUX CALCULATION.

INTRODUCTION

The static chamber method is the most commonly used method to measure greenhouse gas (GHG) fluxes, especially methane (CH₄) and nitrous oxide (N₂O), from soils. The basic principle of this technique is to cover an area of soil with a closed box of known volume and measure the change in the concentration of a gas over time. The change in the headspace concentration over time is then translated to a flux rate, representing the diffusive flux into or out of the soil.

Debates on how to design an optimal chamber and how to calculate the gas fluxes from soils have been going on more than 30 years. Inter-comparisons of different chamber designs in controlled conditions in combination with different flux calculation methods are scarce and the focus has been in CO₂. Even though the studies dealing with CO₂ have identified critical issues regarding chamber design and sampling, the results are not directly applicable to chambers used for CH₄ and N₂O. Thus, in order to minimize the errors related to the measurements of non-CO₂ greenhouse gas exchange, there is an urgent need to perform similar evaluation for CH₄ and N₂O as for CO₂ under controlled laboratory conditions.

We organized a chamber comparison campaign for static chambers used for N₂O and CH₄ flux measurements. We tested 18 static chambers against five CH₄ flux levels replicated for three soil types. The aims of the study were 1) to quantitatively assess the uncertainties and errors related to static chamber measurements and chamber designs, and 2) to compare the suitability of different flux calculation methods.

METHODS

Calibration campaign took place at Hyytiälä Forestry Field station (61°51'N, 24°17' E) August and October 2008. The calibration system was originally built for CO₂ chamber calibration (see Pumpanen *et al.* 2004), and part of the results from this campaign are reported in Christiansen *et al.* (2011). Here we present the results of the comparison of 18 static chambers.

We measured the chamber fluxes with three different sand types and five different flux levels ranging between 60 to 2000 µg of CH₄ m⁻² h⁻¹. The chambers were from different research groups across Europe. They varied with size, shape, material, and they were operated with different headspace mixing strategies (fan, syringe). Chamber fluxes of CH₄ were calculated using linear and exponential functions, and these fluxes were compared to a known reference flux. This allowed us to quantify chamber specific under- or overestimations in the fluxes.

CONCLUSIONS

The tested static chambers underestimated the CH₄ fluxes by up to 42% depending on the way of headspace mixing and flux calculation method. The degree of flux underestimation decreased by the use of fan to mix the chamber headspace, and by the use of non-linear flux calculation method. The non-linear concentration development within chamber headspace indicate that the flux from the soil decreases during the enclosure and hence the chamber placement affected the gas concentration gradient between the soil and the atmosphere. The non-linearity within the chamber headspace decreased with increasing chamber height. This shows that smaller chambers are more prone to underestimation of the fluxes, especially when linear flux calculation methods are used. The underestimation of the fluxes was independent on flux level, allowing us to extrapolate the chamber specific underestimations to flux values outside the experiment.

ACKNOWLEDGEMENTS

We wish to thank the staff at the Hyytiälä forestry field station for letting to occupy the storage hall for the campaign and helping in numerous technical questions. This research was financially supported by Nitrogen in Europe (NinE) program of the European Science Foundation, ACCENT BIAFLUX EU-project, GREENFLUX-TOK project “Micrometeorological techniques for In-situ measurements of greenhouse gases” (contract no. MTKD-CT-2006-042445), Maj and Tor Nessling Foundation, and the Academy of Finland Centre of Excellence program (project number 1118615), the post-doctoral project 1127756, and the Academy Fellow project 130984.

REFERENCES

- Christiansen, J.R., Korhonen, J.F.J., Juszczak, R., Giebels, M., Pihlatie M. (2011). Assessing the effects of chamber placement, manual sampling and headspace mixing on CH₄ fluxes in a laboratory experiment. *Plant and Soil*, In press, DOI 10.1007/s11104-010-0701-y.
- Pumpanen, J., Kolari, P., Ilvesniemi, H., Minkkinen, K., Vesala, T., Niinisto, S., Lohila, A., Larmola, T., Morero, M., Pihlatie, M., Janssens, I., Yuste, J.C., Grunzweig, J.M., Reth, S., Subke, J.A., Savage, K., Kutsch, W., Ostreng, G., Ziegler, W., Anthoni, P., Lindroth, A., Hari, P., 2004. Comparison of different chamber techniques for measuring soil CO₂ efflux. *Agricultural and Forest Meteorology* 123, 159-176.

PHYSIOLOGICAL FACTORS UNCOUPLING THE PHOTOCHEMICAL REFLECTANCE INDEX (PRI) FROM THE PHOTOSYNTHETIC LIGHT USE EFFICIENCY (LUE).

A. PORCAR-CASTELL¹, I. GARCIA-PLAZAOLA², C. NICHOL³, P. KOLARI¹, B. OLASCOAGA¹, R. ESTEBAN², E. NIKINMAA¹

¹ Department of Forest Sciences, University of Helsinki, Latokartanonkaari 7 PO Box 27
00014 Finland

² Department of Plant Biology and Ecology, University of the Basque Country, Spain

³ School of Geosciences, University of Edinburgh, UK

Keywords: Leaf reflectance, chlorophyll fluorescence, Photosynthetic light use efficiency, Remote sensing

INTRODUCTION

The photochemical reflectance index (PRI) is regarded as a non-destructive optical proxy to determine the photosynthetic light use efficiency (LUE) of vegetation [1]. The linkage between PRI and LUE is based on a regulatory process known as non-photochemical quenching (NPQ) that takes place in the photosynthetic antennae [2]. NPQ decreases the LUE by promoting the thermal deactivation of absorbed excitation energy and it has been associated, among others, to the operation of the xanthophylls-cycle. The relationship between PRI and LUE has been probed at different spatial (leaf to canopy) and temporal scales (diurnal to seasonal) and in a wide number of species with very variable results [3]. The PRI index is based on the normalized differences in reflectance in two spectral bands, one around 531 nm that is affected by carotenoid absorption and a reference band that is expected to remain constant at 570 nm, yet it is affected by chlorophyll absorption. The PRI has been shown to track both rapid variation in the de-epoxidation of the xanthophylls cycle pigments on a daily basis, as well as slow changes in carotenoid and chlorophyll contents [4]. But do these adjustments affect NPQ and PRI in a equal fashion? Does the relationship between PRI and NPQ remain constant at the seasonal time scale when strong changes in pigment contents occur in overwintering evergreen foliage? Understanding the linkage between optical or remotely sensed data and the physiological acclimation of photosynthesis is a key requisite for the successful implementation of remotely sensed data to the study of biophysical processes. A great deal of research is currently going on in the field of remote sensing of biophysical parameters that seeks to overcome technical (i.e. how to obtain a high signal to noise ratio) or physical issues related to the acquisition of optical data (i.e. characterizing the complex radiative transfer processes that affect the signal before it reaches the sensor). However, little emphasis has been placed so far in the study of the physiological links between optical data and biophysical processes at the time-scale of interest to remote sensing (i.e. seasonal). The aim of this study was to assess the impact of physiological factors that may potentially decouple the relationship between PRI and light use efficiency in boreal Scots pine throughout the year.

METHODS

We combine leaf level measurements of pigment concentrations, chlorophyll fluorescence, needle reflectance and gas exchange, and canopy level measurements of PRI and flux data to ascertain the potential implications of the decoupling factors at different spatial scales. For this purpose, different parameters from adult Scots pine trees growing in SMEAR-II Station were measured throughout the year. Leaf level measurements were carried out both during night and day to facilitate the separation between seasonal and diurnal acclimation processes. Chlorophyll fluorescence measurements were

performed with a portable fluorometer, FMS-2 Hansatech (UK); needle reflectance was measured at the needle level with a portable spectroradiometer equipped with a plant probe and an external light source (ASD, Boulder CO), and at the canopy level with a pair of two band PRI sensors (531nm, 570nm) (Skye Instruments, UK), photosynthesis was measured at the shoot level with a system of custom made automated chambers and at the canopy level with an eddy covariance system; needle pigment concentration were quantified by means of HPLC.

CONCLUSIONS

The main findings were that NPQ is mainly modulated by the state of de-epoxidation of the xanthophyll-cycle pigments (DEPS) (Fig 1A) whereas the PRI is mainly modulated by the total pool of xanthophyll pigments (VAZ) on a chlorophyll basis (Fig. 1D). It is known that plants respond to different types of stress by upregulating leaf level concentrations in xanthophyll-cycle pigments (VAZ), and by increasing the de-epoxidation status (DEPS) of these pigments. However, under certain conditions VAZ and DEPS may change independently of each other, thus causing a decoupling between PRI and NPQ. We show that this is the case in Scots pine needles during Spring recovery, where needle xanthophyll-cycle pigment concentrations increase drastically in April (decrease in PRI), while DEPS remains constant (no change in NPQ). The result is an uncoupling between PRI and NPQ (Fig. 2), during April prior to the Spring recovery of photosynthesis that affects the relationship between PRI and LUE, this uncoupling can be seen both at the leaf and canopy levels.

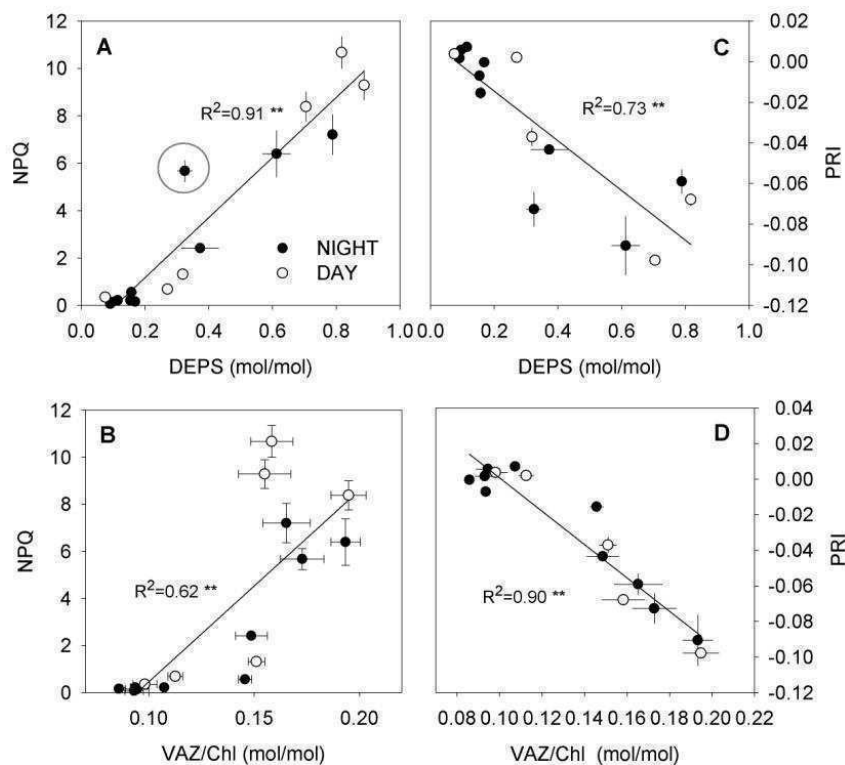


Fig. 1. Relationship between the de-epoxidation state of the xanthophyll-cycle pigments (DEPS) and NPQ (A) or PRI (C), and between the total pool of xanthophyll-cycle pigments on a chlorophyll basis (VAZ/Chl) and NPQ (B) or PRI (D). Points represent means and SE (N=3 biological replicates).

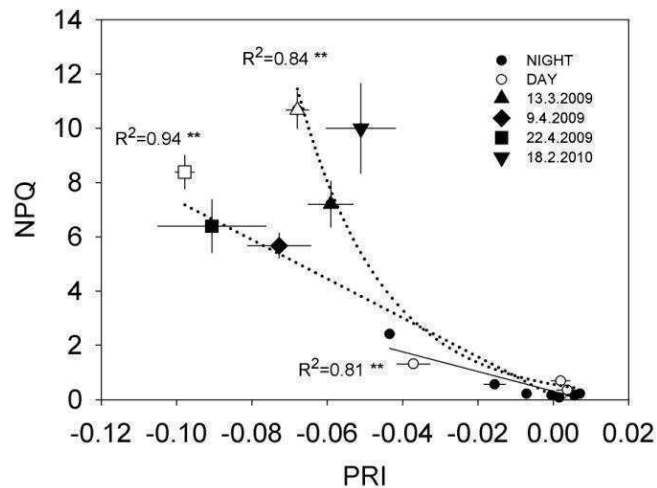


Fig. 2. Annual relationship between the PRI and NPQ. A curvilinear relationship would be expected between PRI and NPQ, where NPQ increases faster than the PRI decrease during winter due to xanthophyll-independent forms of NPQ. Yet, this relationship breaks down during April when xanthophyll-cycle pigment pool increases independently of NPQ. Points during winter and Spring are represented with different symbols to facilitate the visualization of the uncoupling process. Rest of the year points are represented by circles.

REFERENCES

- [1] J.A. Gamon, J. Peñuelas and C.B. Field, 1992, *Rem. Sens. Environ.*, 41, 35-44.
- [2] W. Bilger and O. Björkman, 1991, *Planta*, 184, 226-234.
- [3] M.F. Garbulsky, J. Peñuelas, J.A. Gamon, Y. Inoue and I. Filella, 2011, *Rem. Sens. Environ.*, 115, 281-297.
- [4] I. Filella, A. Porcar-Castell, S. Munné-Bosch, J. Bäck, M.F. Garbulsky and J. Peñuelas, 2009, *Int. J. Rem. Sens.*, 30, 4443-4455.

IMPORTANCE OF SURFACTANT REPRESENTATIONS FOR PREDICTED CLOUD DROPLET NUMBERS IN GLOBAL SCALE SIMULATIONS

N. L. Prisle¹, D. Topping², S. Romakkaniemi³, M. Dal Maso¹, G. McFiggans², and H. Kokkola⁴

¹ University of Helsinki, Department of Physics, P.O. Box 48, 00014, University of Helsinki, Finland.

² University of Manchester, Centre for Atmospheric Science, Simon building, Oxford road, Manchester, M13 9pl, UK.

³ University of Eastern Finland Kuopio, Department of Physics, P.O. Box 1627, 70211, Kuopio, Finland.

⁴ Finnish Meteorological Institute, Kuopio Unit, P.O. Box 1627, 70211, Kuopio, Finland.

Keywords: SURFACTANTS, ORGANIC AEROSOL, CCN ACTIVITY, GLOBAL MODELING.

INTRODUCTION

Indirect radiative effects of atmospheric aerosols via their influence on cloud drop formation and cloud properties account for the major uncertainties in predictions of the anthropogenic influence on global climate and future climate changes (IPCC, 2007). Aerosol cloud condensation nucleus (CCN) activity is determined by both particle size and chemical composition, but CCN properties of the organic aerosol fraction in particular remain to be firmly constrained (Hallquist et al., 2009). One challenge in this respect involves the tendency of some organic aerosol components to preferentially accumulate in the surface region (the surface activity) of aqueous solutions (Shulman et al., 1996; Facchini et al., 1999; Sorjamaa et al., 2004). Such surface active compounds (surfactants) have been demonstrated in atmospheric aerosol and cloud and fog water samples (Yassaa et al., 2001; Mochida et al., 2003; Cheng et al., 2004; Facchini et al., 2000) and their aqueous extracts (Oros and Simoneit, 2000; Mochida et al., 2002; Kiss et al., 2005; Dinar et al., 2006; Asa-Awuku et al., 2008), from marine and rural and urban/polluted continental environments, and can collectively comprise a significant fraction of the organic aerosol mass.

Accumulation of surfactant molecules in the surface can cause reduction in solution surface tension. For sub-micrometer sized droplets with large surface-area-to-bulk-volume ratios (A/V), the resulting partitioning between the solution bulk and surface phases can furthermore deplete droplet bulk concentrations of dissolved surfactant molecules (Prisle et al., 2010b, and references therein). Bulk phase depletion from surface partitioning may significantly change droplet solution properties, compared to macroscopic solutions (where $A/V \rightarrow 0$ [length]⁻¹) with the same overall composition (Seidl and Hanel, 1983; Bianco and Marmur, 1992; Laaksonen, 1993). Laboratory experiments, in combination with comprehensive thermodynamic model calculations, have shown that surface activity can significantly affect organic aerosol CCN potential (Prisle et al., 2010b, 2008; Sorjamaa et al., 2004). This may occur via both surface tension reduction and surfactant surface partitioning in activating cloud droplets, but the combined effect of these mechanisms and the variation with aerosol size and composition is highly non-linear and thus non-trivial to predict (Prisle et al., 2010b, 2008; Sorjamaa et al., 2004).

Both equilibrium surface partitioning and surface tension of activating cloud droplets can be determined from numerical solutions to thermodynamically consistent relations (Prisle et al., 2010b, and references therein). Unfortunately, such calculations with several nested iterations are com-

putationally much too demanding for implementation into atmospheric models (Kokkola et al., 2006). Recently, Topping (2010), Raatikainen and Laaksonen (2011), and Prisle et al. (2010a) have presented different parameterizations to account for the combined effects of surfactant properties in cloud droplet activation of organic aerosols. These representations involve different approximations to the detailed thermodynamic description of surfactant bulk-surface partitioning (Gibbs et al., 1928) and droplet activation from equilibrium Köhler theory (Köhler, 1936), and thus have somewhat different scope.

In this work, we compare global model predictions of cloud droplet number concentrations, applying different representations of the influence of surface active organic aerosol on cloud droplet activation. In addition to the commonly applied approaches of either simply disregarding aerosol component surfactant properties altogether, or using reduced droplet surface tension corresponding to a macroscopic solution of equivalent composition (Prisle et al., 2010b, and references therein), we also use the novel parameterizations accounting for the detailed surfactant effects within activating cloud droplets. The aim is to investigate the significance of accounting for surfactant properties of organic aerosol in global scale simulations of cloud droplet numbers, as well as any differences in results and applicability of the novel parameterizations including comprehensive surfactant effects.

METHODS

Simulations were made using the aerosol-climate model ECHAM5.5-HAM2, which consists of fifth generation general circulation model ECHAM5.5 (Roeckner et al., 2003), with aerosol model HAM2 (Stier et al., 2005; Zhang, 2010). The aerosol number size-distribution is described by a superposition of seven log-normal modes and accounts for aerosol emissions, removal, radiative effects, chemistry, relative humidity, and aerosol microphysics. Chemical compounds included are: sulfate (SU), black carbon (BC), organic carbon (OC), sea salt (SS), and mineral dust (DU). Aerosol microphysical processes (condensation, coagulation, nucleation, and hydration) are calculated within the modal aerosol microphysics module M7 (Vignati et al., 2004), which is coupled to HAM2.

The model includes aerosol-cloud interactions by a double-moment cloud microphysics scheme (Lohmann et al., 2007, and references therein), which calculates cloud droplet and ice nuclei number concentrations (CDNC and ICNC, respectively). Activated cloud droplet numbers are calculated using the cloud activation parameterization by Abdul-Razzak and Ghan (2000), with aerosol size distribution and composition, and updraft velocity as inputs. The parameterization estimates the maximum supersaturation according to the critical supersaturation of the individual aerosol modes, taking into account the kinetic effect of condensation. For the purposes of this work, we have extended the cloud activation parameterization to account for effects of organic surface activity on critical supersaturation of different aerosol sizes according to four different approaches (see Table 1). The parameterizations of Topping (2010) and Raatikainen and Laaksonen (2010) give practically identical results in test calculations of Köhler activation, so only the first was used here.

Representation	surface partitioning	surface tension
(0) traditional Köhler (base case)	-	-
(1) macroscopic solution	-	x
(2) Topping (2010)	x	x
(3) Prisle et al. (2010a)	x	-

Table 1: Surfactant properties included in the different representations of CCN activity, as implemented to the cloud activation parameterization by Abdul-Razzak and Ghan (2000).

RESULTS AND DISCUSSION

We have made five-year simulations for the years 1998–2002 with prescribed meteorology, initially assuming that the entire organic aerosol fraction is surface active with properties corresponding to Suwannee River Fulvic Acid (SRFA). SRFA is a commercial reference compound that has often been invoked as a better-characterized model substance for humic-like atmospheric organics (Dinar et al., 2007; Hatch et al., 2008). Results for predicted cloud droplet number concentrations at the cloud top (CDNC) are shown in Figure 1, for the macroscopic solution approach (1), and in Figure 2, using the parameterization of Topping (2010) (2), both relative to the base case of disregarding organic surfactant properties altogether (0). The parameterization of Prisle et al. (2010a) (3) give qualitatively similar results to the latter, and is not shown here.

The results obtained so far clearly demonstrate that surfactant effects, and how they are accounted for, can make a significant difference for predicted cloud drop numbers, also on a global scale. Facchini et al. (1999) estimated the potential magnitude for the effect of organic aerosol surface activity on cloud droplet numbers and resulting radiative forcing. To our knowledge, the present results are however the first actual global model predictions that include comprehensive surfactant effects of organic aerosol. These simulations are made feasible by the development and implementation of the novel surfactant CCN activity parameterizations (Topping, 2010; Raatikainen and Laaksonen, 2011; Prisle et al., 2010a) to the ECHAM framework. Each parameterization reduces the computational demand of considering detailed surfactant effects, but as mentioned, the underlying simplifying assumptions differ. Those of Topping (2010) and Raatikainen and Laaksonen (2011) both consider surface tension reduction and bulk phase depletion of surfactant, but thus still require knowledge of composition and composition-dependent properties for the organic fraction and are able to consider a limited number of components. On the other hand, that of Prisle et al. (2010a) neglects surface tension effects and only includes bulk phase depletion, but since organic composition is therefore not required for the calculations, this approach is thus potentially applicable to realistic ambient aerosol of unresolved composition and properties.

The global distribution of differences between predictions with the different surfactant CCN activity parameterizations, the underlying mechanisms, and the sensitivity of our results, especially to assumptions regarding the organic surfactant fraction and nature, is the focus of further investigations. Activated cloud droplet numbers have been seen in previous studies not to be very sensitive to variations in aerosol composition, due to buffering from feedbacks with meteorological parameters (Reutter et al., 2009). Due to the non-linearity of the combined surfactant effects on CCN activation with aerosol size and composition, the variation of surfactant CCN activity within an aerosol population, and its evolution over time, is not readily anticipated. Extreme surfactant properties may therefore not necessarily also imply an extreme effect for organic CCN activity, let alone for global predictions of cloud droplet numbers.

ACKNOWLEDGEMENTS

N. L. Prisle gratefully acknowledges the funding received for this work from the Carlsberg Foundation (grants 2009_01_0366 and 2010_01_0391).

REFERENCES

- Abdul-Razzak, H. and Ghan, S. (2000). A parameterization of aerosol activation 2. Multiple aerosol types. *JOURNAL OF GEOPHYSICAL RESEARCH-ATMOSPHERES*, 105(D5):6837–6844.
- Asa-Awuku, A., Sullivan, A., Hennigan, C. J., Weber, R. J., and Nenes., A. (2008). Investigation

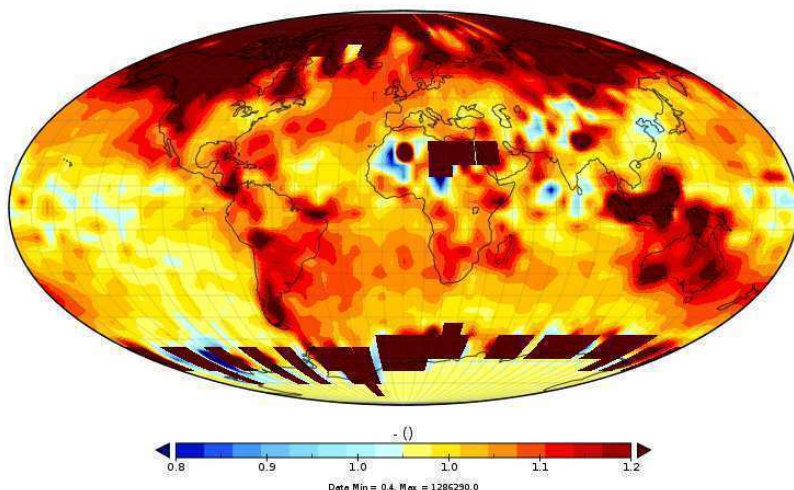


Figure 1: Difference in cloud droplet number concentrations (CDNC, [$\text{m}^{-3}/\text{m}^{-3}$]) at the cloud top, predicted using the macroscopic solution approach (1) relative to the base case (0).

of molar volume and surfactant characteristics of water-soluble organic compounds in biomass burning aerosol. *Atmospheric Chemistry and Physics*, 8:799–812.

Bianco, H. and Marmur, A. (1992). The Dependence of the Surface Tension of Surfactant Solutions on Drop Size. *Journal of Colloid and Interface Science*, 151:517–522.

Cheng, Y., Li, S.-M., Leithead, A., Brickell, P. C., and Leitch, W. R. (2004). Characterizations of *cis*-pinonic acid and n-fatty acids on fine aerosols in the Lower Fraser Valley during Pacific 2001 Air Quality Study. *Atmospheric Environment*, 38:5789–5800.

Dinar, E., Taraniuk, I., Graber, E. R., Anttila, T., Mentel, T. F., and Rudich, Y. (2007). Hygroscopic growth of atmospheric and model humic-like substances. *Journal of Geophysical Research*, 112:D05211.

Dinar, E., Taraniuk, I., Graber, E. R., Katsman, S., Moise, T., Anttila, T., Mentel, T. F., and Rudich, Y. (2006). Cloud Condensation Nuclei properties of model and atmospheric HULIS. *Atmospheric Chemistry and Physics*, 6:2465–2481.

Facchini, M., Decesari, S., Mircea, M., Fuzzi, S., and Loglio, G. (2000). Surface Tension of Atmospheric Wet Aerosol and Cloud/Fog Droplets in Relation to their Organic Carbon Content and Chemical Composition. *Atmospheric Environment*, 34:4853–4857.

Facchini, M., Mircea, M., Fuzzi, S., and Charlson, R. (1999). Cloud Albedo Enhancement by Surface-Active Organic Solutes in Growing Droplets. *Nature*, 401:257–259.

Gibbs, J., Bumstead, H., Longley, W., and Name, R. V. (1928). *The Collected Works of J. Willard Gibbs*. Longmans, Green and Co.

Hallquist, M., Wenger, J. C., Baltensperger, U., Rudich, Y., Simpson, D., Claeys, M., Dommen, J., Donahue, N. M., George, C., Goldstein, A. H., Hamilton, J. F., Herrmann, H., Hoffmann, T., Iinuma, Y., Jang, M., Jenkin, M. E., Jimenez, J. L., Kiendler-Scharr, A., Maenhaut, W., McFiggans, G., Mentel, T. F., Monod, A., Prevot, A. S. H., Seinfeld, J. H., Surratt, J. D., Szmigielski, R., and Wildt, J. (2009). The formation, properties and impact of secondary organic aerosol: current and emerging issues. *Atmospheric Chemistry and Physics*, 9:5155–5236.

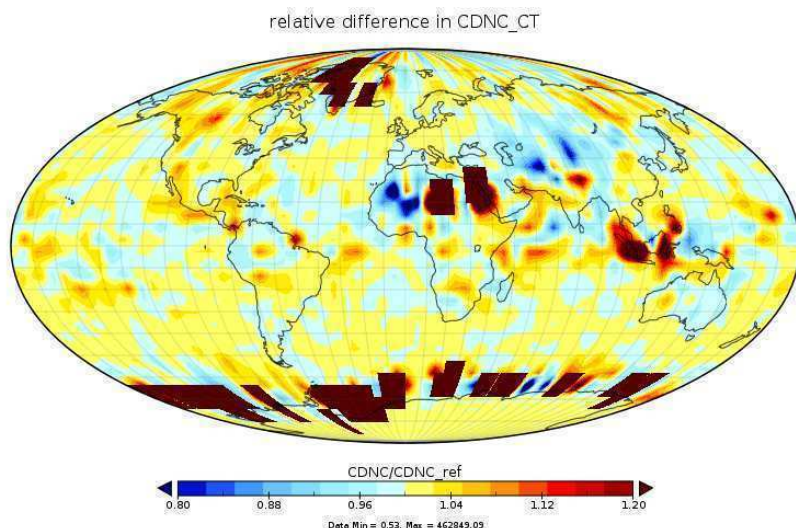


Figure 2: Difference in cloud droplet number concentrations (CDNC, $[\text{m}^{-3}/\text{m}^{-3}]$) at the cloud top, predicted using the approach of Topping (2010) (2) relative to the base case (0).

Hatch, C. D., Gierlus, K. M., Schuttlefield, J. D., and Grassian, V. H. (2008). Water adsorption and cloud condensation nuclei activity of calcite and calcite coated with model humic and fulvic acids. *Atmospheric Environment*, 42:5672–5684.

IPCC (2007). *Climate Change 2007, The Physical Science Basis, Contribution of Working Group I to the Fourth Assessment Report of the Intergovernmental Panel on Climate Change*. Cambridge University Press, New York.

Kiss, G., Tombacz, E., and Hansson, H.-C. (2005). Surface Tension Effects of Humic-Like Substances in the Aqueous Extract of Tropospheric Fine Aerosol. *Journal of Atmospheric Chemistry*, 50:279–294.

Köhler, H. (1936). The Nucleus in and the Growth of Hygroscopic Droplets. *Transactions of the Faraday Society*, 32:1152–1161.

Kokkola, H., Sorjamaa, R., Peräniemi, A., Raatikainen, T., and Laaksonen, A. (2006). Cloud Formation of Particles Containing Humic-Like Substances. *Geophysical Research Letters*, 33:L10816,1–5.

Laaksonen, A. (1993). The Composition Size Dependence of Aerosols Created by Dispersion of Surfactant Solutions. *Journal of Colloid and Interface Science*, 159:517–519.

Lohmann, U., Stier, P., Hoose, C., Ferrachat, S., Kloster, S., Roeckner, E., and Zhang, J. (2007). Cloud microphysics and aerosol indirect effects in the global climate model ECHAM5-HAM. *ATMOSPHERIC CHEMISTRY AND PHYSICS*, 7(13):3425–3446.

Mochida, M., Kawamura, K., Umemoto, N., Kobayashi, M., Matsunaga, S., Lim, H.-J., Turpin, B., Bates, T., and Simoneit, B. (2003). Spatial distributions of oxygenated organic compounds (dicarboxylic acids, fatty acids, and levoglucosan) in marine aerosols over the western Pacific and off the coast of East Asia: Continental outflow of organic aerosols during the ACE-Asia campaign. *Journal of Geophysical Research*, 108:D23S8638.

Mochida, M., Kitamori, Y., Kawamura, K., Nojiri, Y., and Suzuki, K. (2002). Fatty acids in the marine atmosphere: Factors governing their concentrations and evaluation of organic films on sea-salt particles. *Journal of Geophysical Research*, 107:D17S4325.

- Oros, D. and Simoneit, B. (2000). Identification and emission rates of molecular tracers in coal smoke particulate matter. *Fuel*, 79:515–536.
- Prisle, N. L., Maso, M. D., and Kokkola, H. (2010a). A simple representation of surface active organic aerosol in cloud droplet formation. *Atmos. Chem. Phys. Discuss.*, 10:23601–23625.
- Prisle, N. L., Raatikainen, T., Laaksonen, A., and Bilde, M. (2010b). Surfactants in cloud droplet activation: mixed organic-inorganic particles. *Atmos. Chem. Phys.*, 10:5663–5683.
- Prisle, N. L., Raatikainen, T., Sorjamaa, R., Svenningsson, B., Laaksonen, A., and Bilde, M. (2008). Surfactant partitioning in cloud droplet activation: a study of C8, C10, C12 and C14 normal fatty acid sodium salts. *Tellus*, 60B:416–431.
- Raatikainen, T. and Laaksonen, A. (2010). A simplified treatment of surfactant effects on cloud drop activation. *Geosci. Model Dev. Discuss.*, 3:11391159.
- Raatikainen, T. and Laaksonen, A. (2011). A simplified treatment of surfactant effects on cloud drop activation. *Geosci. Model Dev.*, 4:107–116.
- Reutter, P., Su, H., Trentmann, J., Simmel, M., Rose, D., Gunthe, S. S., Wernli, H., Andreae, M. O., and Pöschl, U. (2009). Aerosol- and updraft-limited regimes of cloud droplet formation: influence of particle number, size and hygroscopicity on the activation of cloud condensation nuclei (CCN). *Atmos. Chem. Phys.*, 71:738–745.
- Roeckner, E., Bäuml, G., Bonaventura, L., Brokopf, R., Esch, M., Giorgetta, M., Hagemann, S., Kirchner, I., Kornbluh, L., Manzini, E., Rhodin, A., Schlese, U., Schulzweida, U., and Tompkins, A. (2003). The atmospheric general circulation model ECHAM5. PART I: Model description. *MPI-Report*, 349:127 pp.
- Seidl, W. and Hanel, G. (1983). Surface-Active Substances on Rainwater and Atmospheric Particles. *Pure and Applied Geophysics*, 121:1077–1093.
- Shulman, M., Jacobson, M., Charlson, R., Synovec, R., and Young, T. (1996). Dissolution Behavior and Surface Tension Effects of Organic Compounds in Nucleating Cloud Droplets. *Geophysical Research Letters*, 23:277–280.
- Sorjamaa, R., Svenningsson, B., Raatikainen, T., Henning, S., Bilde, M., and Laaksonen, A. (2004). The Role of Surfactants in Köhler Theory Reconsidered. *Atmospheric Chemistry and Physics*, 4:2107–2117.
- Stier, P., Feichter, J., Kinne, S., Kloster, S., Vignati, E., Wilson, J., Ganzeveld, L., Tegen, I., Werner, M., Balkanski, Y., Schulz, M., Boucher, O., Minikin, A., and Petzold, A. (2005). The aerosol-climate model ECHAM5-HAM. *Atmos. Chem. Phys.*, 5:1125–1156.
- Topping, D. (2010). An analytical solution to calculate bulk mole fractions for any number of components in aerosol droplets after considering partitioning to a surface layer. *Geoscientific Model Development*, 3(2):635–642.
- Vignati, E., Wilson, J., and Stier, P. (2004). M7: An efficient size-resolved aerosol microphysics module for large-scale aerosol transport models. *J. Geophys. Res.*, 109(D22202).
- Yassaa, N., Meklati, B. Y., Cecinato, A., and Marino, F. (2001). Particulate n-alkanes, n-alkanoic acids and polycyclic aromatic hydrocarbons in the atmosphere of Algiers City Area. *Atmospheric Environment*, 35:1843–1851.
- Zhang, K. (2010). Simulated aerosol microphysical properties in ECHAM5.5-HAM2 and their effects on radiative flux perturbation calculation. *in preparation*.

SATELLITE CAL-VAL ACTIVITIES AND FACILITIES OF FMI AT SODANKYLÄ

J. PULLIAINEN¹, E. KYRÖ¹ and Y. VIISANEN¹

¹Finnish Meteorological Institute
Finland.

Keywords: Earth Observation, satellite calibration and validation.

During recent years, Finnish Meteorological Institute (FMI) has developed the atmospheric and environmental research infrastructure at northern Finland in particular to enable the extensive long-term calibration and validation of current and future Earth observing satellite instruments. As an outcome, Sodankylä-Pallas is currently a unique research data provider representing at high latitude continental environment. Additionally, the Sodankylä-Pallas super-site has been promoted for ground reference concerning numerous satellite missions of European Space Agency (ESA), NASA, EUMETSAT and Jaxa (Japan). The satellite CAL-VAL activities are focused to the FMI research facility at Sodankylä that is also equipped with ground-based satellite instrument reference systems operating at UV-, VIS-, IR- and μ W-wavelengths.

The location of Sodankylä-Pallas at Finnish Lapland is ideal for the atmospheric and environmental research of boreal and sub-arctic zone. The principal observation infrastructure of Finnish Meteorological Institute (FMI) is deployed to two main areas: Arctic Research Centre at Sodankylä (67°22 'N, 26°39 'E) and Pallas clean air research station (67° 58'N, 24°07 'E). The Sodankylä facility hosts programs addressing upper air chemistry and physics, atmospheric column measurements, snow/soil hydrology, biosphere-atmosphere interaction and satellite calibration-validation studies. The Pallas station focuses to the monitoring the near-surface air chemistry and physics as well as greenhouse gas exchange.

Observations collected at Sodankylä and Pallas stations support several international research networks and projects concerning arctic and boreal environment such as:

- WMO GAW: Global Atmospheric Watch
- WMO GRUAN: GCOS Reference Upper Air Network. Sodankylä is among the initial stations of the reference network established in 2008.
- GEWEX: Global Energy and Water Cycle Experiment
- NDACC: Network for the Detection of Atmospheric Composition Change
- EU-ICOS: International Carbon Observation System
- TCCON (Total Carbon Column Observing Network): A network of ground-based Fourier Transform Spectrometers recording direct solar spectra in the near-infrared spectral region.
- ESA GlobSnow and EUMETSAT H-SAF: Climate databases and near-real-time services for hemispheric snow mapping

The new development at Sodankylä also includes the establishment of systems for cryospheric research and monitoring, which includes the participation as a primary station to the planned WMO Global Cryospheric Watch (GCW) initiative; as well as development of satellite systems for the monitoring of cryospheric processes and arctic atmosphere. Currently, reference systems and measurements are provided e.g. for ESA SMOS, ESA CoReH2O, NASA AURA, NASA/Jaxa AMSR-E, NASA MODIS and ESA AATSR.

The Sodankylä CAL/VAL data are used to support numerous Earth observation missions. Relevant activities include:

- Long-term measurements of geo-physical variables related to surface, atmosphere and near-Earth space.
- Balloon sounding launch facility for meteorology and atmospheric chemistry.
- Measurements towers, masts and platforms with versatile instrumentation.
- High-resolution information on surface characteristics of the Sodankylä-Pallas area (land use and land cover).
- Observation time-series with ground-based reference systems of satellite instruments (UV, VIS, IR, μ W).

Particularly for the study of cryospheric processes the relevant monitoring data consists of:

- Continuous automatic (distributed) data on:
 - Soil moisture profiles (several locations representing open and forested areas on mineral soil; regional extension during 2011)
 - Soil temperature and soil frost profiles (several locations representing open and forested areas on mineral soil as well as bogs (peat soil); regional extension during 2011)
 - Snow depth and SWE (several locations representing open and forested areas on mineral soil as well as bogs)
 - Snow temperature profiles (one location, new locations will be added during 2011)
 - Automatic weather station observations (including WMO synoptic station)
 - Radiation observations (incoming and reflected)
 - Atmospheric soundings (troposphere and stratosphere)
 - CO₂ and methane fluxes between the atmosphere and soil-vegetation system for different ecosystems
- The manual in situ monitoring programme provides data on (with varying frequency of observation)
 - SWE and snow depth on snow pits (forest and bog sites)
 - Snowpack layering and snow grain size on snow pits
 - Soil frost depth at several locations
 - Distributed snow observations on a 4 km-long snow course
- The available reference also includes static data sets such as digital land cover maps (at the spatial resolution of 25 m)
- Continuous reference measurements for space-borne sensors by ground-based remote sensing instruments:
 - ESA Elbara-II reference radiometer for SMOS (ESA campaign activity ongoing, started on 2009); application area: soil moisture and cryospheric processes.
 - ESA SnowScat reference radar for the planned CoReH₂O mission (ESA campaign activity ongoing, 2009-2011); application area: snow monitoring with X- and Ku-band radar.
 - SODRAD tower-based radiometer of FMI, reference e.g. to AMSR-E (X-, K-, Ka- and W-band dual-pol. radiometer); will be expanded to include 21 and 150 GHz channels; application area: snow and soil processes and atmospheric monitoring (future).
 - Mast-borne VIS/NIR spectrometer of FMI, reference e.g. to MODIS; application area: effects of forest canopy and snow to space-borne imaging and satellite products concerning boreal forest zone
 - Reference instruments for various atmosphere observing satellites (Brewer spectrometer, FTIR for greenhouse gas columnar observations, tropospheric lidar, visiting instruments, currently e.g. a stratospheric lidar).

Data archiving and distribution system is established and in use, it can be directly used or linked to other existing data distribution systems (see **litdb.fmi.fi**). Most of the data sets are already freely available for research purposes (including long observation time-series).

EFFECT OF INCREASED SOIL TEMPERATURE ON CO₂ EXCHANGE AND NET BIOMASS ACCUMULATION IN NORWAY SPRUCE, SCOTS PINE AND SILVER BIRCH; PRELIMINARY RESULTS OF A MICROCOSM EXPERIMENT

J. Pumpanen¹, J. Heinonsalo², T. Rasilo¹ and H. Ilvesniemi³

¹Department of Forest Sciences, P.O. Box 27, FI-00014, University of Helsinki, Finland.

²Viikki Biocenter, Department of Food and Environmental Sciences, Faculty of Agriculture and Forestry, P.O. Box 56, FI-00014 University of Helsinki, Finland.

³Finnish Forest Research Institute, Vantaa Research Station, P.O. Box 18, FI-01301 Vantaa, Finland.

Keywords:

Carbon, allocation, soil temperature, photosynthesis, respiration

INTRODUCTION

The aim of this study was to investigate in a microcosm experiment the effect of soil temperature on CO₂ exchange and carbon allocation pattern of *Pinus sylvestris*, *Picea abies* and *Betula pendula* seedlings and on the species composition of associated ectomycorrhizal (ECM) fungi. We studied the effect of soil temperature on carbon balance of soil column where the tree roots were growing in humus. We measured soil respiration, needle or leaf photosynthesis and biomass carbon allocation pattern of the seedlings in controlled temperature, moisture and light conditions and determined the species composition of associated ECM fungal species. We hypothesized that high soil temperature affects the photosynthesis of the plant by increasing the belowground carbon sink according to the earlier presented hypothesis e.g. by Körner (2003) and this mechanism is related to the root associated ECM biomass and ECM species composition. We also hypothesized that the belowground carbon sink strength depends on the ECM species and could be seen in the carbon allocation pattern of different tree and ECM species.

METHODS

The soils used in this study were collected from Hyytiälä Forestry Field Station in southern Finland (61° 84' N, 24° 26' E) from individual stands dominated by *P. sylvestris* or *B. pendula* and *P. abies*. The soil was sieved through a 4 mm mesh and applied in thin microcosms consisting of separate root and shoot compartments allowing separate measurements of CO₂ exchange of belowground and aboveground parts. The seedlings (n=15) were grown at 7-11.5 °C, 12-16 °C and 16-22 °C soil temperatures. During the growing period microcosms were placed into growth chambers (300x300x400 mm with transparent lids) equipped with a cooling system maintaining soil temperatures described above. The soil part of the microcosms was covered with opaque white polyethylene lids to protect the root system from the light and isolating the root system from the aboveground part. The isolation was also needed for controlling the belowground part temperature. Seedlings were exposed to a day/night photoperiod of 19/5 h and photon irradiance was 170-300 μmol m⁻² s⁻¹ during the day period. Microcosms were watered three times a week with distilled water spray to maintain sufficient soil moisture. The above and below ground CO₂ exchange was measured at the end of the 7 month growth period using the gas exchange laboratory system described in Pumpanen et al. (2009). The biomass of the seedlings was harvested in the end of the experiment and separated to following compartments: needles, stems, roots and ectomycorrhizal root tips. For ECM analyses, one ectomycorrhizal root tip from ten randomly selected root pieces was taken, pooled and used for DGGE analysis in order to identify different species and their occurrence in the samples as described in Heinonsalo et al. (2010).

PRELIMINARY RESULTS

Net photosynthesis and shoot and root respiration generally increased along with increasing temperature. However, the temperature did not affect significantly net biomass accumulation, suggesting higher turnover rate of assimilated carbon at high soil temperatures. Ectomycorrhizal species composition and mass did not show correlation with soil temperature and below ground carbon sink. Our results suggest that *P. sylvestris* benefits from warmer soil temperature, since its biomass accumulation seemed to be higher in the warmest soil temperature especially in the belowground.

ACKNOWLEDGEMENTS

This work was supported by the Academy of Finland grants number 212915, 213093, 206085 and 130984.

REFERENCES

- Heinonsalo, J., J. Pumpanen, T. Rasilo, K.-R. Hurme and H. Ilvesniemi (2010). Carbon partitioning in ectomycorrhizal Scots pine seedlings. *Soil Biology & Biochemistry* 42 (9): 1614-1623.
- Körner, C. (2003). Carbon limitations in trees. *J. Ecology* 91: 4-17.
- Pumpanen, J.S., J. Heinonsalo, T. Rasilo, K.-R. Hurme and H. Ilvesniemi (2009). Carbon balance and allocation of assimilated CO₂ in Scots pine, Norway spruce and Silver birch seedlings determined with gas exchange measurements and ¹⁴C pulse labelling in laboratory conditions. *Trees-Structure and Function* 23: 611-621. doi:10.2136/sssaj2007.0199.

ECOSYSTEM SCALE VOC EMISSIONS MEASURED BY SURFACE LAYER GRADIENT TECHNIQUE

Pekka Rantala¹, Maija K. Kajos¹, Johanna Patokoski¹, Taina M. Ruuskanen¹,
Simon Schallhart¹, Risto Taipale² and Janne Rinne¹

¹Division of Atmospheric Sciences, Department of Physics, University of Helsinki, Finland.

²Research Center Jülich, IEK-8: Troposphere, Germany.

Keywords: Gradient method, VOC, PTR-MS, Hyytiälä.

INTRODUCTION

The gradient method is a very traditional way to measure fluxes and it is based on the parametrization of the surface layer turbulence and so called first order closure. It means that the turbulent transport and the molecular transport are assumed to be similar and therefore the vertical turbulent transport term $\overline{c'w'}$ can be determined in a form

$$\overline{c'w'} = -K_h \frac{\partial \bar{c}}{\partial z}, \quad (1)$$

where K_h is a turbulent transfer coefficient for heat and c a concentration. According to the Monin-Obukhov similarity theory

$$K_h = \frac{ku_*(z-d)}{\phi_h[(z-d)/L]}, \quad (2)$$

where k is Von Kármán constant, u_* friction velocity, L Monin-Obukhov length, d zero displacement height and $\phi_h[(z-d)/L]$ a universal function.

Using these equations and a concentration profile measurements, it is possible to calculate fluxes without any fast response instruments. However, the gradient method has several requirements (like a strong horizontal homogeneity) for a measurement site. (e.g. see Foken, 2006)

In this work, we studied whether it is possible to use gradient method, Monin-Obukhov similarity theory and proton-transfer-reaction mass spectrometry (Lindinger *et al.*, 1998) for a long-term VOC flux measurements in Hyytiälä at SMEAR II station (61° 51' N, 24° 17' E, 180 m a.m.s.l.).

METHODS

We started our measurements at the end of May in 2010, and the PTR-MS was measuring 27 different compounds from six different measurement levels of the 73 m high tower. Two of the measurement levels (4.2 m and 8.4 m) were below the canopy and four of them (16.8 m, 33.6 m, 50.4 m and 67.2 m) above the canopy. The calibrations were done using a gas standard and the automatic calibration unit (GCU, Ionimed Analytik). The calibration and volume mixing ratio calculation procedures have been described by Taipale *et al.* (2008).

The fluxes were calculated using the profile measurements and the gradient method (see e.g. Rinne *et al.*, 2000). Due to a tall canopy height (approximately 18 m in summer 2010), a roughness sublayer corrections were made for the flux calculations using a method by Rinne *et al.* (2000). The zero displacement height was determined using a method by Bruin and Verhoef (1997).

According to the preliminary results, the concentration measurements succeeded very well and flux calculations are looking promising for some compounds. A clear positive cumulative flux was observed for a protonated masses (atomical mass per charge units) 33, 45, 47, 59, 69, 81 and 137 which are assumed to be related to the compounds methanol, acetaldehyde, ethanol/formic acid, acetone, MBO-fragment/isoprene, monoterpene fragments and monoterpenes respectively.

CONCLUSIONS

The gradient method showed fluxes of several VOCs including emissions of methanol, acetone and monoterpenes in the same range as observed previously by chamber and disjunct eddy covariance methods. However, gradient method is an indirect flux measurement technique and the reliability of the gradient fluxes should be evaluated by comparing them with direct eddy covariance flux results. Therefore, we are going to measure VOC-fluxes in next summer 2011 using gradient method as well as the disjunct eddy covariance method (see J. Rinne *et al.*, 2007) and the eddy covariance method. The eddy covariance measurements will be done by the new fast response proton-transfer-reaction time-of-flight mass spectrometer (Ionicon Analytik GmbH).

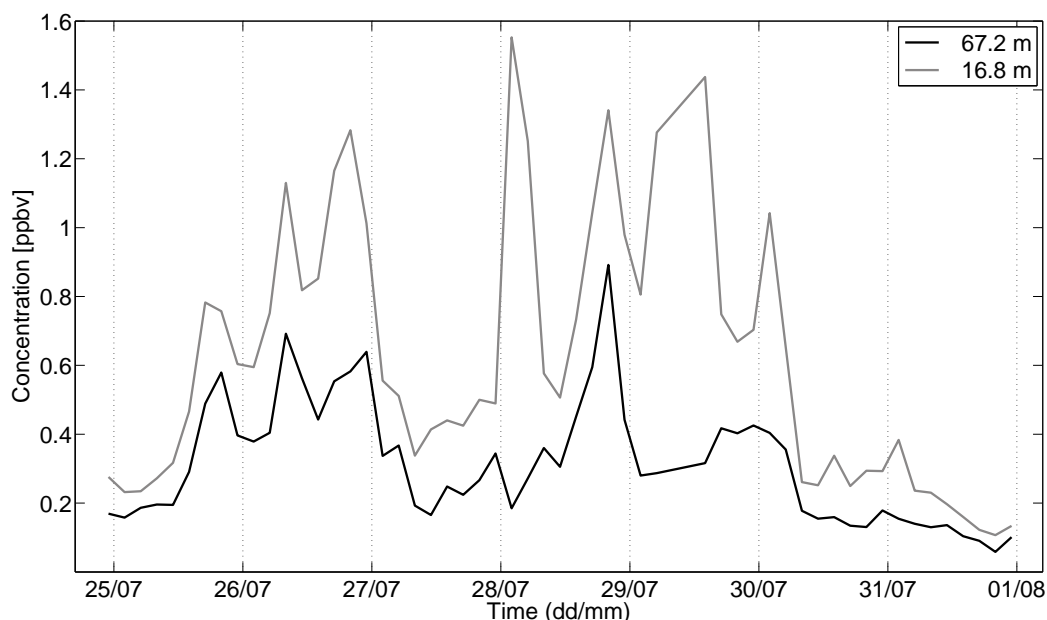


Figure 1: Concentration of monoterpenes (protonated mass 137 amu) at levels 16.8 m (grey line) and 67.2 m (black line) during 25.7.-31.7.2010.

REFERENCES

- Foken, T. (2006). 50 Years of the Monin-Obukhov Similarity Theory. *Boundary-Layer Meteorology*, **119**, 431–447.
- Lindinger, W., A. Hansel and A. Jordan (1998). On-line monitoring of volatile organic compounds at pptv levels by means of Proton-Transfer-Reaction Mass Spectrometry (PTR-MS)—Medical applications, food control and environmental research. *Int. J. Mass Spectrom.*, **173**, 191–241.
- Rinne, J., J-P. Tuovinen, T. Laurila, H. Hakola, M. Aurela and H. Hypén (2000). Measurements

of hydrocarbon fluxes by a gradient method above a northern boreal forest. *Agricultural and Forest Meteorology*, **102**, 25–37.

Rinne, J., R. Taipale and T. Markkanen and T. M. Ruuskanen, H. Hellen, M. Kajos, T. Vesala and M. Kulmala (2007). Hydrocarbon fluxes above a Scots pine forest canopy : measurements and modeling. *Atmospheric Chemistry and Physics*, **7**, 3361–3372.

Taipale, R., T. M. Ruuskanen, J. Rinne, M. K. Kajos, H. Hakola, T. Pohja and M. Kulmala (2008). Technical note : quantitative long-term measurements of VOC concentrations by PTR-MS - measurement, calibration, and volume mixing ratio calculation methods. *Atmospheric Chemistry and Physics*, **8**, 6681–6698.

DOC CONCENTRATION AND QUALITY IN THE RIPARIAN ZONE OF A FORESTED BOREAL CATCHMENT

T. RASILO¹, A. OJALA², M. STARR¹ and J. PUMPANEN¹

¹Department of Forest Sciences, University of Helsinki,
P.O. Box 27, FI-00014 University of Helsinki, Finland.

²Department of Environmental Sciences, University of Helsinki, Lahti, Finland.

Keywords: DOC, Boreal forest, catchment.

INTRODUCTION

Terrestrial and aquatic ecosystems are closely connected and the role of freshwater environments to the carbon budget of boreal landscape is important but not very well known (e.g. Richey *et al.*, 2002; Ometto *et al.*, 2005; Billett *et al.*, 2004). Most of the lakes in the boreal zone are heterotrophic, i.e. they process terrestrial carbon and thus a significant part of carbon from surrounding forest is released back into the atmosphere through the lakes. Carbon from the catchment area carried by water can be in particulate (organic POC), dissolved (organic or inorganic DOC, DIC) or gaseous (free CO₂, CH₄) form. Bulk of particulate carbon is sedimented to the bottom of waterbodies, but DOC can be used as a source of energy in the water column and CO₂ is formed. Part of DOC forms complicated, stable humic and fulvic compounds. They are important e.g. for light conditions in aquatic environments and transport of heavy metals. Organic acids are one fraction of DOC and form part of the buffer capacity against acidity. When acidic deposition has decreased, the amount of DOC in surface waters has increased (Vuorenmaa *et al.*, 2006).

There is quite little DOC in the precipitation, in Finland the concentrations range from 1 to 4 mg L⁻¹, (Lindroos *et al.*, 1999; Lindroos *et al.*, 2007) but also higher concentrations have been measured in boreal region (Moore 2003). When passing through the canopy and flushing carbon from the foliage DOC concentration of water increases (Michalzik and Matzner, 1999). However most of the carbon enters the catchment through photosynthesis which turns inorganic CO₂ to organic form. Organic carbon then enters soil through litter fall and root turnover. Highest DOC concentrations are found in soil where concentration in soil water decreases with increasing depth (Wu *et al.*, 2010). DOC is removed from soil solution by decomposition or adsorption (Michalzik *et al.*, 2001), or it is transported to lakes and streams.

There are several ways water can pass through the catchment area. It can move in surface flows or infiltrate deep into groundwater level. Origin and transformations during transport influence the quality of dissolved organic matter (DOM) in the lake ecosystems. Water signatred by surface soils is generally rich in DOM and has low pH. Usually such water has a short residence time, but can contribute significantly to the storm runoff at the basin outlet. Transit times also vary markedly from storm to storm. The wetter the soil and the higher the groundwater table, the larger the contribution of short-residence time water to the runoff (Moldan and Cerný, 1994).

The physico-chemical significance of DOM in waters is often neglected because lack of good characterization methods. Organic matter in the soil goes through decomposition and organic breakdown products form humic substances. In addition to decomposition, organic matter is altered also by resynthesizing microbes and abiotic degradation by e.g. UV radiation (McKnight and Aiken 1998). Thus, DOC is very inhomogeneous material and consists of many different kind of organic molecules. Therefore its characterization is a complicated process. Yet, a widely used simple tool in soil science to estimate the degree of aromaticity and molecular size of DOC is spectrophotometry. The

ratio of absorbances at 465 nm (E4) and 665 nm (E6) is inversely proportional to the degree of humification, condensation, aromaticity and molecular weight (Chen *et al.*, 1977). This means that a high E4/E6 ratio corresponds to a low aromaticity and vice versa.

In this study we measured DOC concentration in various water compartments in the riparian zone of the pristine lake Valkea-Kotinen. Because DOC consists of many different kind of organic molecules and goes through transformations in the soil, we used the spectrophotometric method to analyze the changes in its quality. Later we will calculate the flow of DOC from the terrestrial catchment into the aquatic ecosystem.

METHODS

The study site Valkea-Kotinen is situated in southern boreal zone in Finland (61°14' N, 25°04' E) and belongs to Evo nature reserve area. It consists of a catchment area (30 ha) with a head-water lake Valkea-Kotinen (surface area 3.6 ha) and its small outlet brook. 76% of the terrestrial area is natural state oldgrowth forest dominated by Norway spruce with some Scots pine, birch and aspen and the rest is covered by peatland. The annual mean temperature is 3.1 °C and annual mean precipitation is 618 mm. The growing period ($T > 5^{\circ}\text{C}$) is 112 days long and the lake is ice-covered for 170 days between November and April.

Rainwater and throughfall samples were collected into polyethylene bags with 15 funnels (diameter 197 mm) installed at 130 cm height below canopy or in an open fen nearby. The amount of precipitation/throughfall was measured and samples were pooled for further analyses. Soil water was collected with suction cup lysimeters (model 653X01-B02M2; Soil Moisture Corporation, California, USA) installed at 10 and at 30 cm depths in spring 2007. Half of the lysimeters were installed 2 m from the shore line (shore) and half 12 m from the shore line (forest). Nine perforated plastic tubes (diameter 20 mm) were installed in soil to measure the level of groundwater and to take samples from it. They were at 2 m (shore), at 7 m (middle) and at 12 m (forest) from the shore line. All the samples were taken once a week throughout the open-water periods in 2007–2009.

The samples were transported to the laboratory and analyzed within 24 hours for pH (Ag/AgCl sureflow electrode, Orion Research Incorporation, USA) and conductivity (YSI 3200 conductivity instrument, YSI Incorporated, USA). For DOC analysis samples were filtered (GF/C Whatman, Millex-HA 0.45 μm Millipore) and either measured immediately or frozen (-20°C) for later analysis. The DOC concentration of all water samples was analyzed with total organic carbon analyzer (TOC-5000A, Shimadzu Corporation, Australia). Two replicates of each water compartment were analyzed and before the analysis the pH of the samples was decreased by adding 30 μl hydrochloric acid (2 mol L^{-1}) to 10 ml of sample. The absorbance of water at 465 nm and 665 nm wavelength was measured with spectrophotometer (UV-1650PC, Shimadzu Instruments Manufacturing Co. Ltd, China) from samples using distilled water as a blank. The absorbance ratio of 465 nm/665 nm (E4/E6) was calculated.

RESULTS AND DISCUSSION

The mean DOC concentration was lowest in the rainwater and highest in the soil water near the shore line (Fig 1). The DOC concentration in rainwater was more or less stable during the ice free period but that in throughfall varied a lot. High concentrations were observed as a consequence of dry periods, when dry deposition (e.g. pollen) was accumulating on branches and foliage and rain flushed it into the collectors. As rain water and throughfall collectors were emptied only once in a week, evaporation during sunny periods might have increased DOC concentration by condensating the samples. On the other hand heavy rain events with large amounts of water can dilute and decrease DOC concentrations of the samples.

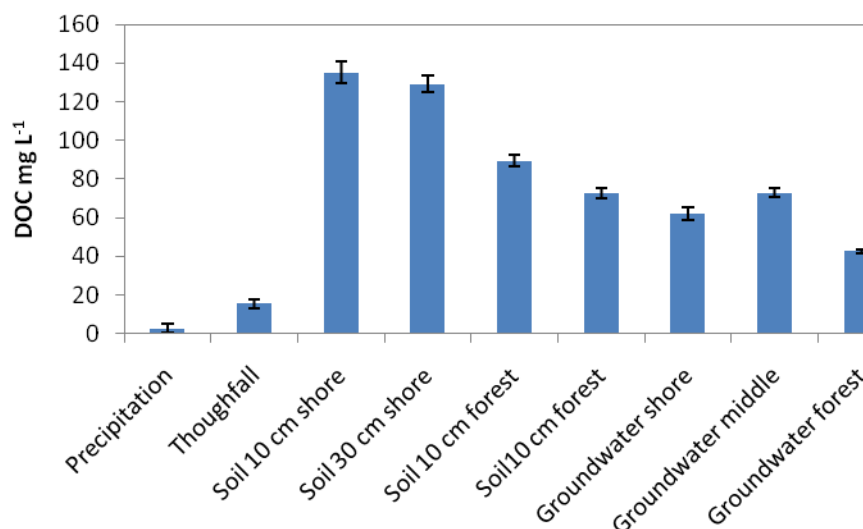


Figure 1. DOC concentration of different water compartments in the riparian zone of Valkea-Kotinen catchment (mean and standard error 2007–2009).

The DOC concentration in soil water varied a lot between different lysimeters. Large variation in the concentrations indicates high spatial heterogeneity of the soil. However, DOC concentration was in general higher at 10 cm than at 30 cm and close to the shore line than at 12 m distance from it at both depths (Fig 1). This highlights the importance of the riparian zone, which is shown to act also as a hot spot of green house gas emissions (Larmola *et al.*, 2003). As water passes through the riparian zone, it is often rich in nutrients providing good circumstances for plant growth and microbial activity; water is always plentiful as lake is just next to it and the level of groundwater is often close to soil surface. Riparian zone is also an important filter for nutrients leached from forest (or agricultural fields) and these zones have been successfully used for protecting waterbodies. There was less variation in the DOC concentration of groundwater than in soil water but DOC concentration in groundwater was also higher close to the shore line than in the forest (Fig 1). The highest groundwater DOC concentrations were measured at 7 m from the shore line.

Even though the DOC concentration in rainwater was rather low, the total input of DOC by precipitation is not negligible. The annual flux of organic carbon through precipitation in Valkea-Kotinen catchment area (30 ha) varied from 235 to 530 kg, which is approximately one fifth of total flux to forest floor by throughfall. Photosynthesis turns inorganic carbon to organic form which can be leached from the canopy, and thus the amount of DOC reaching forest floor is several times higher than the DOC input in precipitation. Soil gains carbon also through litterfall, root turnover and root exudates. The DOC concentration in soil water was clearly higher than in throughfall because DOC was leached from the thick organic layer of the soil. Respiration and decomposition returns the organic carbon bound in the biomass back to inorganic form.

The E4/E6 ratio was highest in the soil water and lowest in the rain water (Fig 2). In groundwater the ratio was higher near the shore line than in the forest. Near the shore line groundwater might be influenced by lake water, which can alter DOC composition. In soil water the aromaticity seems to decrease with the depth at 2 m distance from the shore line as the E4/E6 ratio increases, but the situation is opposite in the forest. Usually aromaticity increases when decomposition proceeds as simple molecules are used first and microbes can also resynthesize complex forms of DOC. Near the shore line soil water might be mixed with lake water bringing fresh DOC. The effect of proceeding decomposition and increasing aromaticity is clearly seen in the difference between soilwater and groundwater. The low values of E4/E6 ratios in rain water and throughfall do not follow the expected pattern of proceeding decomposition, but tell that the quality of DOC is different from that in soil water.

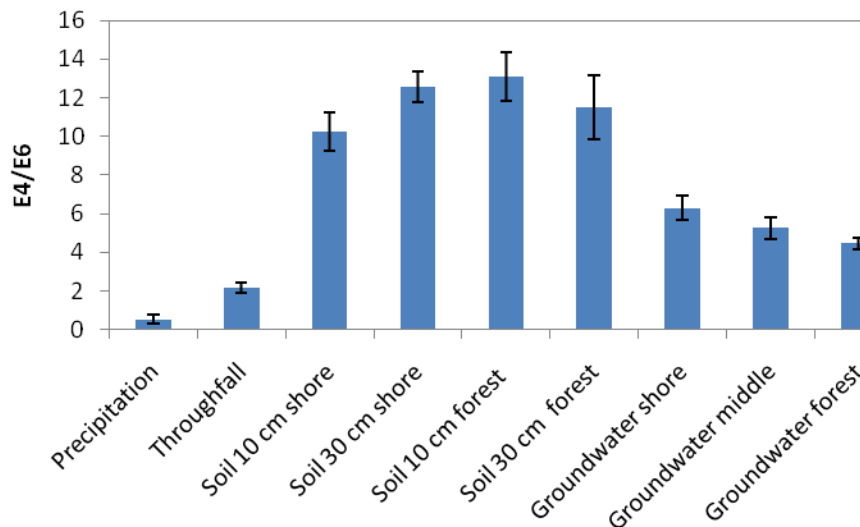


Figure 2. The ratio of absorbances at 456 nm and 665 nm (E4/E6) different water compartments in the riparian zone of Valkea-Kotinen catchment (mean and standard error).

ACKNOWLEDGEMENTS

This work is part of the project TRANSCARBO funded by the Academy of Finland (1116347) and University of Helsinki research funds project VESIHIISI (490032).

REFERENCES

- Billett, M.F., S.M. Palmer, D. Hope, C. Deacon, R. Storeton-West, K.J. Hargreaves, C. Flechard and D. Fowler (2004). Linking land-atmosphere-stream carbon fluxes in a lowland peatland system. *Global Biogeochemical Cycles* **18**, doi: 10.1029/2003GB002058.
- Chen, Y., N. Senesi and M. Schnitzer (1977). Information provided on humic substances by E4/E6 ratios. *Soil Science Society of America Journal* **41**, 352–358.
- Larmola, T., J. Alm, S. Juutinen, P.J. Martikainen and J. Silvola (2003). Ecosystem CO₂ exchange and plant biomass in the littoral zone of a boreal eutrophic lake. *Freshwater Bioogy* **48**, 1295–1310.
- Lindroos, A.-J., J. Derome, K. Derome, and K. Niska (1999). Deposition on the forests and forest floor in 1999, in Raitio, H. and T. Kilponen (eds.) Forest Condition Monitoring in Finland – National report 1998. *The Finnish Forest Research Institute, Research Papers* **743**, 72–77.
- Lindroos, A.-J., J. Derome and K. Derome (2007). Open area bulk deposition and stand throughfall in Finland during 2001–2004, in Merilä, P., T. Kilponen and J. Derome, (eds.) Forest condition monitoring in Finland – National report 2002–2005. *Working Papers of the Finnish Forest Research Institute* **45**, 81–92.
- McKnight, D.M. and G.R. Aiken (1998). Sources and age of aquatic humus, in: Hessen, D.O. and L. J. Tranvik, (eds) Aquatic Humic Substances. Springer-Verlag, Berlin Heidelberg; *Ecological Studies*, **133**, 9–39.
- Moldan and J. Cerný (eds.) (1994). *Biogeochemistry of Small Catchments* (SCOPE 51, Wiley, New York).
- Michalzik, B., and E. Matzner (1999). Dynamics of dissolved organic nitrogen and carbon in a central European Norway spruce ecosystem. *European Journal of Soil Science* **50**, 579–590.
- Michalzik, B., K. Kalbitz, J.H. Park, S. Solinger and E. Matzner (2001). Fluxes and concentrations of dissolved organic carbon and nitrogen - a synthesis for temperate forests. *Biogeochemistry* **52**, 173–205.
- Ometto, J.P.H.B., A.D. Nobre, H.R. Rocha, P. Artaxo and L.A. Martinelli (2005). Amazonian and the modern carbon cycle: lessons learned. *Oecologia* **143**, 483–500.

- Richey, J.E., J.M. Melack, A.K. Aufdenkampe, A.K., V.M. Ballester and L.L. Hess (2002). Outgassing from Amazonian rivers and wetlands as a large tropical source of atmospheric CO₂. *Nature* **416**, 617–620.
- Wu, Y., N. Clarke and J. Mulder (2010). Dissolved organic carbon concentrations in throughfall and soil waters at level II monitoring plots in Norway: Short- and long-term variations. *Water Air & Soil Pollution* **205**, 273–288.
- Vuorenmaa, J., M. Forsius and J. Mannio (2003). Increasing trends of total organic carbon concentrations in small forest lakes in Finland from 1987 to 2003. *Science of the Total Environment* **365**, 47–65.

LAND–USE–INDUCED LAND–COVER CHANGES AND FUNCTIONING OF THE EARTH SYSTEM

ANNI REISSELL¹, NATHALIE DE NOBLET–DUCOUDRÉ², PAVEL KABAT³ and DAN YAKIR⁴

¹iLEAPS International Project Office, Department of Physics, University of Helsinki, Finland

²Laboratoire des Sciences du Climat et de l’Environnement, Unité mixte CEA–CNRS–UVSQ, Gif–sur–Yvette, France

³Climate Change and Biosphere Centre, Wageningen University and Research Centre, Wageningen, Netherlands

⁴Environmental Sciences & Energy Research, Weizmann Institute of Science, Rehovot, Israel

Keywords: land use, land cover, climate change, global change

INTRODUCTION

It is imperative to develop a fundamental understanding of Land–Use–induced Land–Cover Changes (LULCC): its interactions with the human, biogeochemical and biogeophysical dynamics, and its impacts at the regional scale and on the planetary climate system. Here, we briefly summarise a new initiative, the LULCC synthesis topic plan for the 2nd International Geosphere-Biosphere Programme (IGBP) Synthesis “Planet Under Pressure: Knowledge and Solutions”. The LULCC synthesis is lead by the Integrated Land–Ecosystem–Atmosphere Processes Study (iLEAPS), planning and implementation in collaboration with several international research organisations, communities and other stakeholders.

The 2nd IGBP synthesis will identify gaps in our knowledge and contribute to a baseline for international research and policy in the area of global environmental change in the coming decades. The synthesis initiative will be undertaken during 2010–2014. The synthesis will involve a broad range of stakeholders, organisations and individuals, right from its planning stages to its completion, including natural and social scientists from within and outside of the IGBP community and individuals from the policy community. Key results will be presented, for example, in high-level scientific synthesis articles, summaries for various stakeholders, and at the global change open science conference to be held 26–29 March 2012 in London, UK.

BACKGROUND

Humans have a major role in environmental changes, including the influence on the climate system (IPCC, 2007). The observed effects of this human influence are largely due to increased industrial emissions of greenhouse gases, trace gases, and aerosol particles into the atmosphere. While emissions have increased, global land cover has continuously changed since the first human settlements because of various ways to use the land, for example for cropland, urban constructions, pasture, and forestry. Changes in vegetation distribution have large local and regional effects on the terrestrial water cycle, soil erosion, biodiversity, water quality, urban pollution, and mesoscale and regional features of the atmospheric circulation (Takata *et al.*, 2009, Feddema *et al.*, 2005).

LULCC has contributed substantially to anthropogenic emissions in the past (Houghton, 2003). At present, LULCC contributes to both emissions and carbon sequestration—affected by continuous tropical deforestation, expanding temperate and boreal forests, as well as by enhanced productivity resulting from a combination of CO₂–fertilisation and uses of fertilisers. Studies on land–climate interactions also suggest

that changes in the land properties (for example albedo, roughness, moisture content) can significantly influence climate variability at the regional scale and also have an effect on nature of extreme events [Narisma and Pitman, 2003; Seneviratne *et al.*, 2006]—of key relevance in climate change.

OBJECTIVES

The overall objective of our initiative is to achieve a synthesis of existing knowledge, coordinate current and initiate future research efforts that will serve as a roadmap for future LULCC activities and its effective integration into the IPCC scheme and global change research.

The main motivation for this initiative is the need to analyse and synthesise existing knowledge on LULCC as guidance for international global change policy. It is also important to launch appropriate coordinated numerical experiments to determine the robustness of assessments of LULCC–climate interactions and influence.

The aims of this LULCC synthesis are to:

- Achieve a synthesis of existing knowledge based on available datasets and modelling studies;
- Coordinate current and initiate future research efforts, again looking simultaneously at datasets and models;
- Ensure effective integration of LULCC into the IPCC (Intergovernmental Panel on Climate Change) scheme and global change research;
- Set up and/or enforce interactions with stakeholders and decision makers to make the products of our research useful outside our scientific community;
- Help define priorities (draw a roadmap) that will serve both ends (science and decision) for future LULCC activities.

KEY QUESTIONS

LULCC will focus on changes in: a) weather and atmospheric processes, b) biogeochemical cycles, c) water cycle, and d) atmospheric load of aerosols. All these are integral components of the climate system [Radiative forcing of climate change, 2005; Kabat *et al.* Eds., 2004]. We intend to look at both past and future changes with the expectation to deliver valuable information to the stakeholders, for example the IPCC 5th assessment report.

We will focus on five key questions:

1. How well do the climate models simulate the influence of LULCC on trace gas and energy exchange between the biosphere and the atmosphere; and how well do the land–surface models capture the different sensitivities of the land–use system to climate forcing?
2. Which types of LULCC feedbacks within the climate system are important?
3. What have been the rate, magnitude and type of land cover and land use changes over the past thousand years?
4. Is there evidence of LULCC being an important forcing agent of the climate in the past?
5. What are the plausible options to manage future LULCC to mitigate and adapt to climate variability, including extremes and longer–term change?

These five questions span the entire field of LULCC; addressing the research field in its entirety is important. The first two questions are core activities at the start of the LULCC synthesis project.

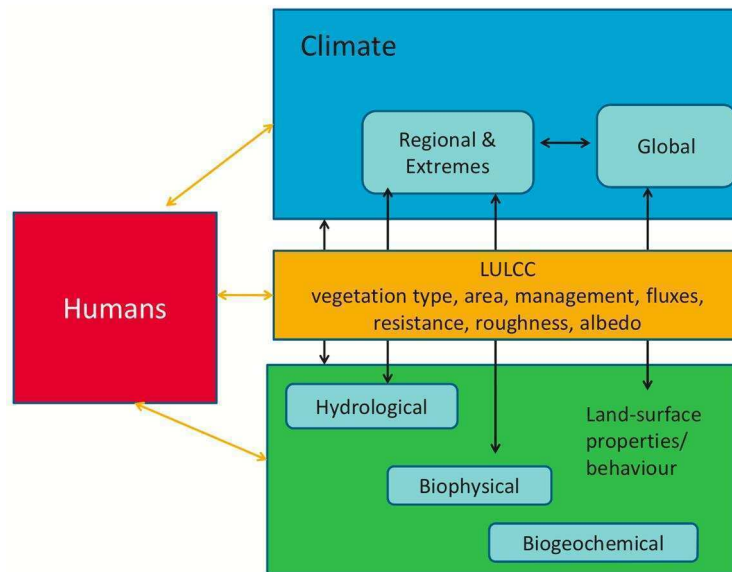


Figure 1. General conceptual figure of LULCC domain: interactions among land–surface properties/behaviour, climate and humans. Figure by Markus Reichstein and Dan Yakir.

IMPLEMENTATION AND OUTCOMES

The LULCC objectives will be achieved by gathering key scientists from IGBP, several international research communities, and involving a variety of other stakeholders from the start of the project.

The action plan includes:

- Evaluation and synthesis of available datasets and numerical experiments in the form of peer-reviewed papers or specific reports;
- Definition and production of relevant diagnostics (metrics) that will be useful for decision makers;
- Design of experimental protocols and launch of the associated modelling experiments;
- Model intercomparison studies such as LUCID (Pitman *et al.*, 2009) to a) assess the confidence we can have in the various models when they are used to evaluate the impacts of LULCC on for example climate, b) robustly evaluate the climatic effects of LULCC;
- A literature review of the feedbacks that have been identified as being important and that relate to LULCC and that should be properly evaluated.

The implementation will include workshops that bring together modelers and experimentalists, other stakeholders, for example. The kick-off meeting aimed at various policy and decision-making stakeholders will be held 21 September 2011, in connection with the iLEAPS Science Conference (18-23 September 2011), in Garmisch-Partenkirchen, Germany.

The longer-term outcomes will include high-profile review articles, journal special issues, summaries for policy makers, online resources, press releases, articles in popular press aimed at the general public, international and national policy briefings, educational products.

Several of the products will be published in time for the next IPCC Assessment Report (AR5) and the major international science conference in London, 26-29 March 2012, “Planet Under Pressure – new knowledge towards solutions”.

This synthesis project will be carried out in collaboration among several stakeholders: Integrated Land Ecosystem–Atmosphere Processes Study (iLEAPS), Analysis, Integration and Modeling of the Earth System (AIMES,) Past Global Changes (PAGES), International Global Atmospheric Chemistry (IGAC),

Global Land Project (GLP), Global Land/Atmosphere System Study of the Global Energy and Water Cycle Experiment (GEWEX/GLASS), Land-Use and Climate, Identification of robust impacts (LUCID), Climate of the 20th Century (C20C), global network of micrometeorological tower sites FLUXNET, Evaluation and intercomparison of existing land evapotranspiration products (LandFlux-EVAL), International Land Model Benchmarking (iLAMB) as well as with non-IGBP researchers and organisations in this wide interdisciplinary field.

For the project other stakeholders are the Food and Agriculture Organization (FAO) of the United Nations, United Nations Environment Programme (UNEP), Intergovernmental Panel on Climate Change (IPCC), US National Aeronautics and Space Administration (NASA), European Space Agency (ESA), for example.

SUMMARY

The LULCC synthesis project gathers the leading scientists from around the world and is lead by an international Scientific Committee.

For updated information about LULCC and the IGBP Synthesis, please see the websites: [LULCC Synthesis](http://www.ileaps.org/multisites/lulcc/) (<http://www.ileaps.org/multisites/lulcc/>) and [IGBP 2nd Synthesis](http://www.igbp.net/page.php?pid=510) (<http://www.igbp.net/page.php?pid=510>).

For more information and if you are interested in contributing to the project, please contact Nathalie de Noblet-Ducoudré (nathalie.de-noblet@lsc.ipsl.fr) or Anni Reissell (anni.reissell@helsinki.fi).

REFERENCES

- Feddema et al. (2005). The importance of land-cover change in simulating future climates. *Science* 310, 1674–1678.
- Houghton RA (2003). Revised estimates of the annual net flux of carbon to the atmosphere from changes in land use 1850–2000. *Tellus* 55(B), 378–390.
- IPCC (2007). *Climate Change 2007, The Physical Science Basis*. Working Group 1 Contribution to the Fourth Assessment Report of the Intergovernmental Panel on Climate Change. Cambridge University Press. Edited by S. Solomon et al.
- Kabat P et al. Eds (2004). *Vegetation, water, humans and the climate: A new perspective on an interactive system*. Springer, Berlin, Global Change – The IGBP Series, 566 pp.
- Narisma GT and Pitman AJ (2003). The impact of 200 years of land-cover change on the Australian near-surface climate. *Journal of Hydrometeorology* 4, 424–436.
- Pitman AJ et al. (2009). Uncertainties in climate responses to past land cover change: First results from the LUCID intercomparison study. *Geophysical Research Letters* 36, L14814, doi:10.1029/2009GL039076.
- Radiative forcing of climate change (2005). *Radiative forcing of climate change: Expanding the concept and addressing uncertainties*. Committee on Radiative Forcing Effects on Climate Change. Climate Research Committee, Board on Atmospheric Sciences and Climate, Division on Earth and Life Studies, The National Academies Press, Washington DC, 208 pp.
- Seneviratne SI et al. (2006). Land-atmosphere coupling and climate change in Europe. *Nature* 443, 205–209.
- Takata K et al. (2009). Changes in the Asian monsoon climate during 1700–1850 induced by preindustrial cultivation. *Proceedings of the National Academy of Sciences of the United States of America*, PNAS 106(24), 9586–9589, doi:10.1073/pnas.0807346106.

RECENT ADVANCES IN SAMPLING AND IN CHEMICAL ANALYSIS OF ATMOSPHERIC AEROSOLS

M.-L. RIEKKOLA¹, K. HARTONEN¹, J. PARSHINTSEV¹, T. LAITINEN^{1,2}, J. RUIZ-JIMENEZ¹, T. PETÄJÄ² and M. KULMALA²

¹Laboratory of Analytical Chemistry, Department of Chemistry, P.O.Box 55, FI-00014, University of Helsinki, Finland

²Division of Atmospheric Sciences, Department of Physics, P.O.Box 64, FI-00014, University of Helsinki, Finland

Keywords: ATMOSPHERIC AEROSOLS, SAMPLING, ANALYSIS, DATA EVALUATION.

INTRODUCTION

Atmospheric aerosol particles have become a topic of keen interest for researchers in the field of climate change. The main reason for this interest is the ability of these particles to affect climate through direct and indirect processes, including absorbing and reflecting radiation and changing the properties of clouds. Aerosols are highly complex, since their size dependent chemical composition differs in time and space. Because of the complexity, quantification of the climate effects of aerosols continues to be highly uncertain and a great challenge to researchers [Pöschl et al. 2005, Ayash et al. 2009].

Over a half of the submicron aerosol mass in the troposphere consists of organic material, especially oxygenated compounds [Zhang et al. 2007, Jimenez et al. 2009]. Highly oxidized compounds, such as carboxylic acids and keto- and dicarboxylic acids, are of greatest interest because of their low saturation pressure and consequent high aerosol forming potential. Gas-phase oxidation products with sufficiently low vapour pressure can form secondary organic aerosols (SOA) by condensing/partitioning onto pre-existing particles, or they can undergo nucleation to form new particles [Hoffmann et al. 1997]. It is widely recognized that acids, formed by the oxidation of terpenes, play a major role in biogenic SOA formation because of their abundance in the atmosphere and low vapour pressure. In view of their importance, the acids formed from oxidation of terpenes in ambient aerosol particles have attracted special attention.

The collection of aerosol particles is one of the most difficult steps in the analytical procedure. Atmospheric aerosols are usually collected on a filter or an impactor plate and analyzed either off-line by various techniques or directly with aerosol mass spectrometer.

The overall aim of the study was to develop tools for the clarification of the chemistry involved in biogenic aerosol formation and growth, so allowing more precise determination of biosphere-atmosphere interactions. Targeted aims of the research were development of laser aerosol mass spectrometer for direct measurement of chemical composition of ultrafine particles, utilization of differential mobility analyzer for size separation before filter sampling, optimization of particle-into-liquid sampler for the on-line chemical analysis by conventional chromatographic-mass spectrometric techniques, optimization of two-dimensional gas-chromatography and liquid chromatography-mass spectrometry with different ionization sources for off-line analysis and development of data analysis techniques for handling the information produced by various analytical methods in order to find correlations between physical properties of aerosols and their chemical composition.

METHODS

Laser AMS

The laser aerosol mass spectrometer (laser AMS) has been recently described (Laitinen, 2009) and its applicability tested in laboratory experiments (Laitinen, 2010). Briefly, charged and size-separated (with DMA) particle flow from ambient air was directed to an oppositely charged polished stainless steel collection surface, which is part of a custom designed sampling valve. Collected samples were introduced to the high vacuum (10^{-8} torr) of the mass spectrometer (MS) by rotating the sampling valve. The sample was desorbed from the collection surface with an IR-laser (1064 nm wavelength) and ionized with a UV-laser (193 nm wavelength). The ions were then guided with an ion lens system (15 cm) to the orthogonal TOFMS (Tofwerk AG, Switzerland) and detected according to their flight times. Ions were pulsed into the TOF with frequency of 12 kHz from the ion extraction region. Total analysis of each sample included 10 to 30 desorption/ionization events to vaporize the sample completely. All single spectra were later calibrated and added together to form a complete mass spectrum for each sample. Background signal was extracted from each sample before any compound identification and correlation analysis.

Particles of 10- to 50-nm were continuously collected from one hour to a few days depending on the available particle mass, and then analyzed. The collected particle mass was first approximated from particle size distributions calculated from the SMEAR II station DMPS data. After the measurements, the sampled mass was calculated from sample flow rate, sample collection efficiency, and actual particle concentration. The particle concentrations were measured with a condensation particle counter (TSI 3025 CPC, MN, USA). The collected samples did not need any sample treatment and all spectra were analyzed on-line. The laser AMS system was used for compound identification and semi-quantitative analysis. The samples were collected with +2.5 kV collection voltage while the aerosol flow rate was set to 4 L min^{-1} and the DMA sheath air flow to 10 L min^{-1} . Altogether 26 samples were collected and analyzed (Laitinen, 2011).

Aerosol sampling with PILS

A full description of the aerosol sampling with PILS can be found elsewhere (Orsini, 2003; Parshintsev, 2009). Briefly, the sampling system consisted of an ADI2081 particle-into-liquid sampler (Applikon Analytical, Schiedam, The Netherlands) coupled with an eight-channel peristaltic pump (Watson Marlow 205S, Wilmington, USA). DirectQ-UV water (Millipore, USA) was used as a working liquid and for transport flow. To remove gas-phase compounds, three-channel annular denuders (242 mm length, Teflon coated, stainless steel sheath, URG, Chapel Hill, USA) with different coatings (XAD for organic gases, potassium iodide in glycerol for ozone) were added to the sampling line and were recoated when the colour of the potassium iodide denuder changed to yellow. Aerosols were size separated before the denuder with a cyclone (PM2.5, URG, Chapel Hill, USA), which was cleaned once a day. During collection, the transport flow containing the aerosol sample was divided into two parts. One part was collected off-line to a pre-weighed beaker, while the other was directed to the conditioning/sampling valve of the solid-phase extraction step (see Parshintsev, 2010 for more information).

Figure 1 shows a schematic of the constructed on-line coupled PILS-SPE-HPLC-MS apparatus. All connections were made with PEEK capillaries (1.6 mm O.D., 0.5 mm I.D.). The analytical procedure was the following: Step 1: Conditioning of the solid-phase trap. Methanol 4 min, 1 ml/min and MilliQ water 4 min, 1 ml/min. For greater convenience, two Jasco PU-980 pumps (Tokyo, Japan) were used and connected with a three-way valve to the conditioning/sampling valve.

Step 2: Sampling. The liquid flow was connected directly to the conditioning/sampling valve. At the end of the PILS sampling, the internal standard was added to the trap manually by syringe.

Step 3: Elution and analysis. The loop (500 μl) was filled with elution solvent for desorption of the trapped analytes. When HPLC-MS analysis was turned on, the main valve was switched to the analysis mode (position A). As can be seen from Figure 1, eluent from the HPLC system flushes the trap in the

opposite direction to sampling. Two minutes after injection, the valve was switched back to the conditioning/sampling mode (position B) and a new analysis was started from step 1.

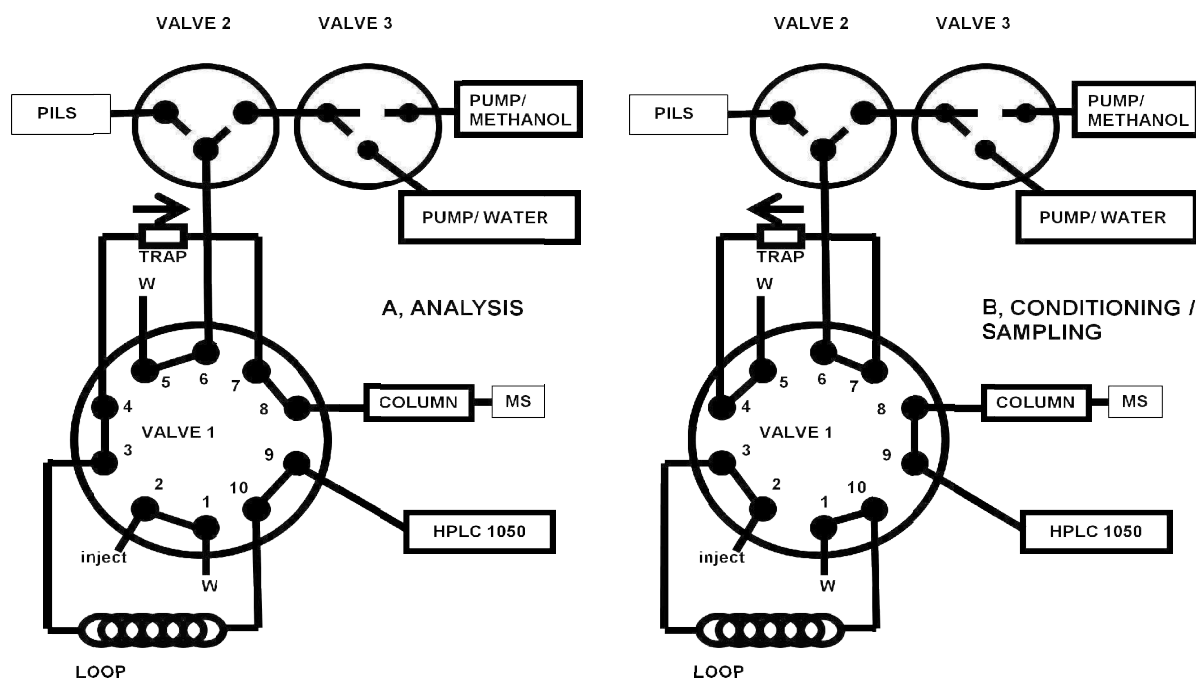


Figure 1. Schematic of the constructed on-line coupled PILS-SPE-HPLC-MS apparatus. A- procedure for sample analysis, B- procedure for conditioning the trap and PILS sampling.

Size-selective filter sampling

Since DMA assisted filter sampling was already employed by our group (Laitinen, 2010), it was decided to evaluate the possible artefacts during the collection of ultrafine particles. The aerosol sampling system was modified as depicted in Figure 2. A Vienna-type differential mobility analyzer was the basic element in the size segregation in the filter collection system.

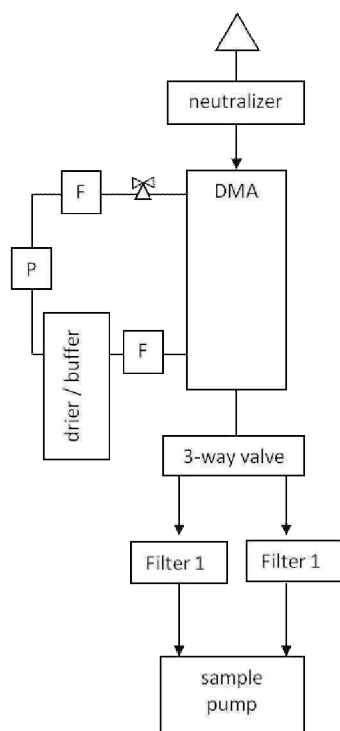


Figure 2. Schematic of the size-selective aerosol collection system. P indicates a pump and F a high efficiency particulate filter (HEPA) in the sheath flow of the differential mobility analyzer (DMA).

The DMA was operated in a closed loop flow arrangement with a sheath flow of 24 l/min. Voltages, corresponding to particle sizes of 30 nm, 40 nm, and 50 nm were preselected to collect particles onto a filter placed downstream of the DMA sample flow (4 l/min). A timer was connected to the high voltage (HV) supply and to a three-way valve that turned off the HV supply and, simultaneously, switched the 3-way valve to another direction. Thus, 30 nm (or 40 or 50 nm) particles were collected onto one filter for a 15 min period and particle-free air was sampled onto a second filter for a further 15 min period. This measurement cycle was maintained for the whole collection period. Before size segregation, the particles to be sampled were brought to a known charge distribution with an Am-241 alpha-source (60 MBq). Filter samples were extracted for 20 minutes with acetone/methanol mixture (1 ml/min, 1:1 v/v) with use of dynamic ultrasonic assisted extraction. Samples were analyzed by liquid chromatography-mass spectrometry and gas-chromatography-mass spectrometry. More detailed explanation of the methods is presented elsewhere (Parshintsev, 2011).

Comprehensive two dimensional gas chromatography-mass spectrometry

DMA size separated samples were also analyzed by comprehensive two-dimensional gas chromatography (GC×GC-TOF). Experiments were carried out on an Agilent 7890A gas chromatograph (Santa Clara, USA) equipped with a split/splitless injector and interfaced with a LECO Pegasus® 4D TOFMS system (LECO, St. Joseph, MI, USA). The Agilent GC was equipped with a secondary oven and a liquid N₂ quad-jet dual-stage modulator. A nonpolar HP-5 column (29 m × 0.25 mm i.d., 0.25 μm film thickness) was used as the first-dimension column and a semipolar RTX-17 column (1 m × 0.1 mm i.d., 0.1 μm film thickness) as the second-dimension column (housed in the secondary oven). Two columns were connected with a Silket® Treated Universal Press-Tight® connector (Restek, Bellefonte, PA, USA). A 2m×0.53mm i.d. DPTMDS deactivated retention gap was connected to the first-dimension column.

The data acquisition and the first step of the data processing were accomplished with LECO® ChromaTOFTM optimized for the Pegasus® 4D software (version 3.34). After data processing, the software generates a peak table which displays information about the peaks found. Peak name, retention time, retention index (I) value, CAS registry number, unique mass, height, signal-to-noise ratio (S/N),

area, similarity and mass spectra are examples of the specific information given for each peak in the table. In this work, data processing was used to find all peaks with an S/N larger than 10. Unique mass was used for area/height calculations and the peak width was set at 0.5 s. The NIST05 electron ionization mass spectral database was used for the spectral search. In order to identify one compound the fit between the experimental mass spectrum and the database spectrum should be higher than 700 in normal search mode.

The I value for each compound was calculated using linear hydrocarbons and PAHs as reference in the case of the semi-volatile compounds and silylated polyols, and carboxylic acids in the case of the low-volatility compounds. These reference compounds were not added to the samples since atmospheric aerosol contains them naturally and they could be easily identified by comparing the retention times with those of the standards. I values were calculated on the basis of the retention time.

The peak table provided by LECO software was used as input data for Guineu 0.8.1 software. Briefly, the peak tables obtained for the analysis of the same group of compounds, semi-volatile or non-volatile, were combined into a single peak table which contains the same information provided by the original peak tables in addition to mean similarity and similarity standard deviation. The compounds which present a mean spectral similarity lower than 750 were removed from the peak table. The experimental I value, for each compound, was compared with the value provided in the literature. For this purpose, I value library was constructed containing the experimental and/or theoretical I values for approximately 1500 compounds. The cut-off limit for I difference was set to 200 units and these compounds with I difference larger than 200 units were deleted from the list. The remaining compounds were accepted as identified compounds.

The mass spectra and I values obtained for the compounds deleted from the peak list in the previous steps (unknowns) were analyzed using the Golm metabolome database. The identification conditions were the same used previously (spectral search fit higher than 750 and I difference less than 200 units).

In the last step, the compounds classified as unknowns in the previous step were re-analyzed in the Golm metabolome database searching in this case for the main functional groups present in the molecule.

Laboratory-made Visual Basic (VB) software was used for the combination of the peak lists provided for the analysis of semi-volatile and low-volatility compounds by Guineu software. The main property of the VB software is the classification of compounds according to their chemical composition. First the compounds were classified by their main functional group present in the molecule into seven different groups such as, hydrocarbons, halogenated compounds, nitrogen compounds, sulphur compounds, carboxyl, carbonyl and hydroxyl compounds. Then the compounds previously classified were further sub-classified, according to the specific element and functionality present in the molecule. In addition, so called unknown compounds whose main functional groups were only identified, were classified by the VB software into ten chemical groups such as, aldehydes, alcohol, alkenes, amines, carboxylic acids, carbonyl compounds, aromatic compounds, phenols, hydroxyl compounds and acetals.

CONCLUSIONS

Laser AMS

Two main findings from the laser AMS samples were black carbon and the possible presence of amines. The black carbon was seen as a distinct plume in the spectrum produced by the desorption laser (black carbon was ionized with desorption laser) at mass range about 150-400 amu. Black carbon compounds are known to absorb infrared radiation strongly. The black carbon did not correlate with anything else; it was observed in particle sizes from 10 to 50 nm both during the new particle formation events and also when there was no new particle formation. We assume that the black carbon probably came from local sources (cars, saunas etc.) and in bigger particles it was transported within air masses from elsewhere. Most abundant amines were found with mass peaks of 143, and 185 amu, and they were tentatively assigned to alkyl-substituted amines (spectrum shown in Fig. 3). Several other ions possibly originating from amines were recorded during the measurements as well, but their concentrations were several fold smaller compared to ions 143 amu and 185 amu. In previous measurements at the SMEAR II station (Smith, 2010), amines were sometimes found during the new particle formation events. Here, some of the amines were found in nearly all samples, but relatively, concentrations were the highest in particles of 10 to 25 nm

and on the samples when one or more new particle formation events occurred during the collection of these laser AMS samples. With such limited data, however, it is too early to claim for sure that these amines have something to do with the new particle formation. More measurements on fine particles and longer data sets are needed before a connection between amines and new particle formation events can be confirmed.

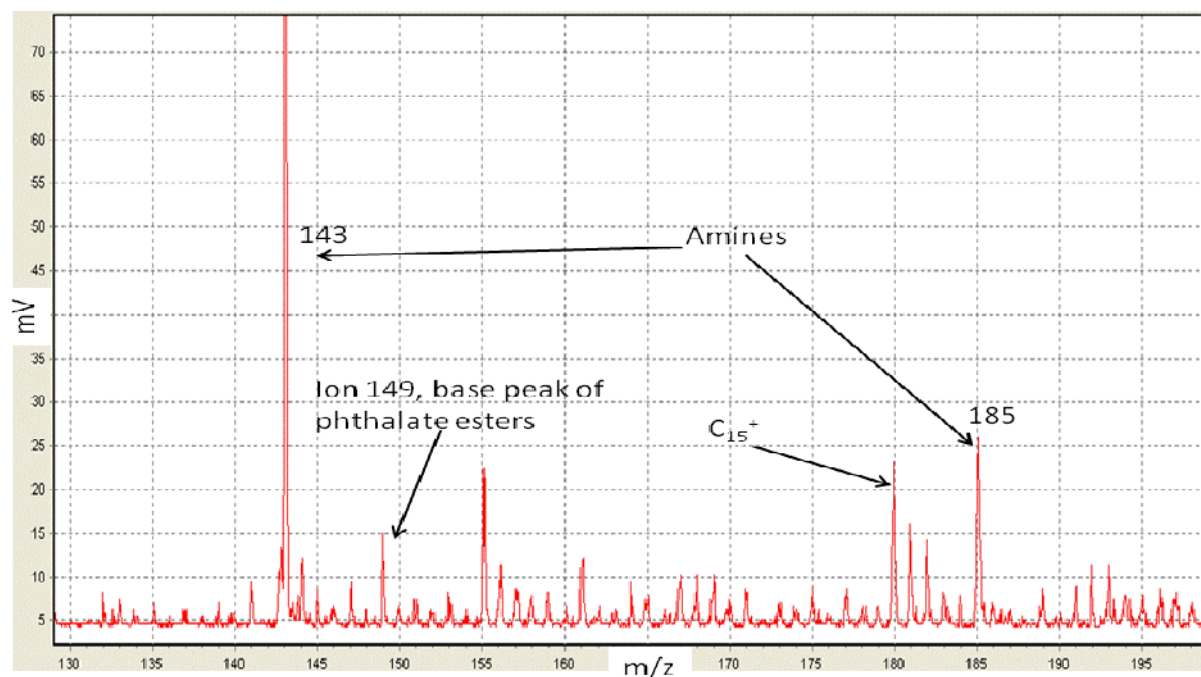


Figure 3. Laser AMS spectrum measured during a nucleation events. Particle size was 20 nm and the collection time was 96.5 hours.

PILS-SPE-HPLC-MS

Atmospheric aerosol samples were collected and analysed to test the performance of the constructed on-line system. Also, off-line analysis was conducted for purposes of comparison. Concentrations of the studied acids measured by the two techniques are presented in Parshintsev et al, 2010. The results achieved with the two techniques were in good agreement. In addition, except for pinic and *cis*-pinonic acids, the concentrations of the acids found in the aerosol samples agree with concentrations reported in the literature. Pinic and *cis*-pinonic acid usually contribute to aerosol mass during the growing season of coniferous trees. However, the weather in Finland in February was cold, with no biological activity of the trees. Relatively high concentrations of these acids indicate transport from distant areas or that the acids are chemically stable. Two samples, one collected on February 5, 2010, at 12.45pm- 3pm and the other on February 8, 2010, 11.50am- 2.15pm, contained unusually high concentrations of hydroxyglutaric acid, which is considered to be an oxidation product of pinic acid. In the same two samples, the concentration of pinic acid was lower than in other samples taken on the same day. This finding, suggesting that oxidation was still going on, is not in agreement with chemical stability of the compounds. To clarify this issue, much more samples need to be collected and analysed on-line and the correlation of the results with various atmospheric parameters need to be studied. On-line coupled PILS-SPE-HPLC-MS would be an excellent tool for this type of research.

DMA for size separation before filter sampling

As can be seen from Table 1 (Parshintsev, 2011), gas-phase compounds contribute significantly to the particle mass found on the filters containing both phases, regardless of the filter medium. As expected, however, adsorption is much higher on quartz than on teflon. Polar gas-phase compounds are readily adsorbed on polar quartz filters because of the various interactions that are possible (dipole-dipole,

electrostatic, etc). Such adsorption occurs for all-sized and PM_x particles, and aerosols under 50 nm in diameter would clearly not be an exception. Only 50 nm particle samples were selected for the comparison between quartz and teflon, since the adsorption behaviour was assumed to be the same for the other samples.

The group of Kirchstetter et al. (2001) found adsorption to depend on the vapour pressure of the compound. However, our results do not always show such a dependency. The adsorption of pinic and *cis*-pinonic acid did not depend on vapour pressure (here pinic < *cis*-pinonic), and in general, the adsorption of other compounds followed the same trend. This discrepancy between our and their results might be due, in part, to our failure to calculate the sampling deviation. Calculating of sampling deviation would have required simultaneous collection of samples with at least two DMA systems and we had only one system at our disposal. In some cases, the hypothesis of adsorption dependence on vapour pressure nevertheless works nicely. For instance, in the second set of samples collected on quartz filters (February 22-26), the adsorption of aldehydes from hexanal to nonanal is proportional to their vapour pressures (1330, 507, 280, and 71 Pa). The adsorption of these compounds did not, however, show any correlation with vapour pressure in the collection onto teflon. Levoglucosan (vapour pressure 24.10 μPa) and mannose (vapour pressure 2.44 μPa), in turn, showed a good correlation for both filter media. The results with teflon are surprising due to its non-polar nature. Perhaps the gas-phase polyols adsorb onto already collected particles, which then serve as an additional filtering layer. In other words, the aerosol layer may behave as a gas chromatographic stationary phase, mostly polar, and adsorb gas-phase compounds in the manner quartz does. Differences in the adsorptions of benzoic acid and benzaldehyde support this suggestion. Our results suggest that neither filter can clearly be preferred since chemical alteration of samples occurs in both cases. The described sampling system nevertheless allows determination of the true amounts of compounds in aerosol phase. Results can be then presented as absolute amounts of analytes in nanograms after subtraction of gas-phase amounts, or, using the amount of sampled air, as concentrations in ng/m³.

GC×GC-TOF

The most relevant compounds, in terms of concentrations, present in the semi-volatile and non-volatile fractions of the aerosol particles were identified. Two different classifications, based on the composition and the main functional groups, or specific element were developed for the identified compounds. These classifications allowed the clarification of the aerosol particle composition and the influence of the aerosol size on the chemical composition of the particles. Significant differences were found in the compound profile for TS, 50-nm and 30-nm particles. In most of the cases, the highest number of compounds and highest value for the sum of the normalized peak area were found for 30-nm particles, which were collected in a different season of the year. The study showed the potential of this methodology to access the aerosol chemistry and compositional changes occurring during the particle growth process. In all the cases, the number of compounds was increased with the particle size opposite to the sum of normalized peak areas that were mostly decreased with the exception of aldehydes. The chemical composition of aerosol particles was studied using two different parameters, the number of compounds and the sum for the normalized peak areas. The average values and the ranges obtained for each group, according to the main functional group present in the molecule, of the identified compounds are shown in Figure 4, where ranges are expressed as error bars. There is a clear difference between 30-nm particles and the rest of the samples. Hydrocarbons, aldehydes, halogenated and nitrogen containing compounds showed higher values in terms of number of compounds and sum of normalized peak areas in the 30-nm particles. On the other hand, TS and 50-nm particles demonstrated the highest values for these parameters in the case of acids, alcohols and sulphur containing compounds. Although explanations can be given to these differences, we should keep in mind that the different collection season of the year for 30-nm particles affects their composition. A detailed study of the aerosol particle composition according to the specific elements present in the molecule is presented elsewhere (Ruiz-Jimenez, 2011). It is usual that the group which contains the highest values for the number of compounds has also a highest value for the sum of the normalized peak area, but there are some exceptions. It is clear that alkenes, thio compounds, amino acids, esters, alcohols and ketones are the most abundant compounds in the aerosol particles under study. It is not possible to find any clear trend for halogenated compounds. Similar number was found for fluorinated

and iodinated compounds. The contribution of free acids, whose number is similar to the esters, to the composition of the particles should also be emphasized. Alkenes, amino acids, alcohols and ketones have also the highest values in terms of relative peak area. Results which differ from those provided by the number of compounds were found in the case of halogenated compounds, sulphur containing compounds and acids. Chlorinated compounds, thio compounds and esters are the most abundant in the case of 50 and 30-nm particles. On the other hand, the relative peak area is higher in the case of the fluorinated compounds, sulphonamides and free acids for TSP.

Here, the most recent research on atmospheric aerosol chemical composition, done in Laboratory of Analytical Chemistry of the Helsinki University is presented. As it was shown, many different approaches were chosen to achieve the goal of the research. Even though, results are encouraging, more trials are clearly needed in order to develop techniques suitable for routine analysis.

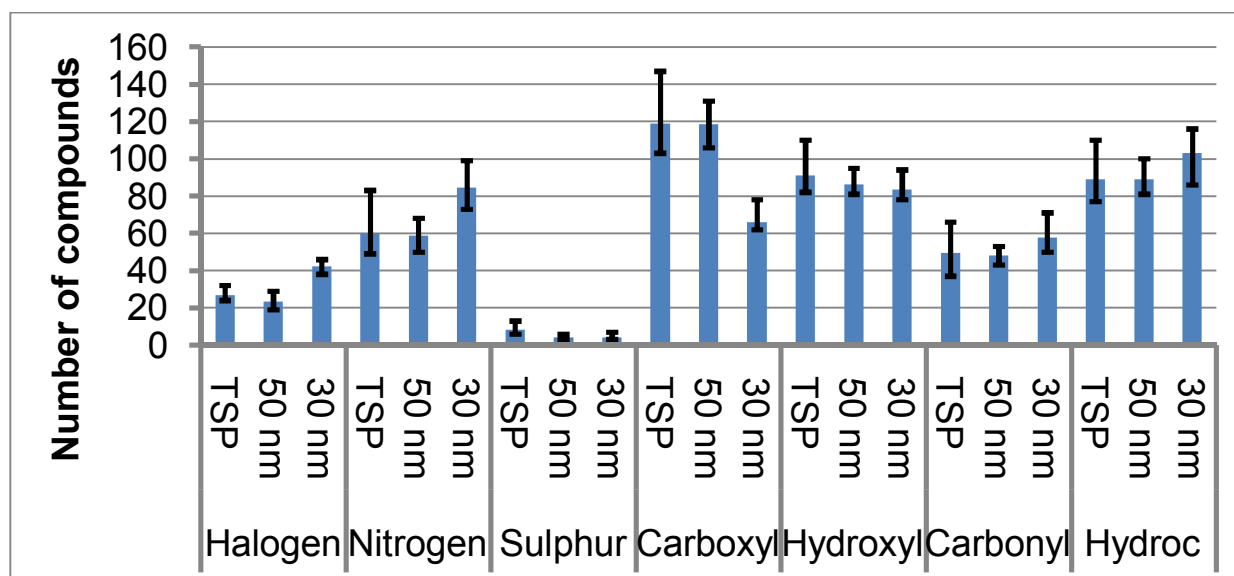


Figure 4. Number of compounds according to the aerosol size.

Table 1. Contribution of gas-phase compounds to the total mass of compounds in aerosol samples in percents. Q-quartz, T-teflon. from Parshintsev et al.2011

Compound	18.02-22.02	22.02-26.02	26.02-03.03	03.03-09.03	09.03-16.03	16.03-22.03	22.03-29.03	29.03-07.04	07.04-13.04	13.04-19.04
	50nm Q	50nm Q	50nm Q	50nm T	50nm T	50nm T	40nm T	40nm T	40nm T	30nm T
Levogluconan	91.7	73.2	64.4	20.8	32.1	41.8	41.5	22.9	45.5	31.4
L-Mannose	70.8	87.0	69.2	47.5	87.8	99.1	52.1	32.4	59.2	53.8
D-Mannose	-	57.3	74.4	77.2	43.7	49.9	27.1	22.9	29.2	-
Malonic acid	100.0	100.0	93.2	64.1	30.2	22.2	31.4	27.1	48.1	35.2
Maleic acid	-	-	-	-	-	-	-	9.2	23.4	24.4
Malic acid	37.7	83.0	100.0	50.5	100.0	28.4	2.9	3.3	21.8	50.1
Adipic acid	100.0	83.2	100.0	100.0	97.3	69.0	36.9	20.2	42.8	44.7
Azelaic acid	100.0	69.8	80.3	84.6	84.8	13.0	47.0	16.1	38.8	40.8
Tartaric acid	-	6.4	60.0	100.0	100.0	58.2	0.9	5.6	-	-
Octanoic acid	73.7	76.0	61.7	46.0	67.7	33.6	22.5	19.8	20.6	28.5
Palmitic acid	61.4	74.3	81.5	55.4	63.3	46.6	24.8	20.9	24.6	24.0
Vanillic acid	-	-	-	-	-	-	-	-	-	-
cis-Pnonic acid	67.7	87.2	93.3	-	-	-	-	-	-	-
3-Hydroxyglutaric acid	66.8	91.0	76.8	67.1	64.8	44.5	-	-	-	-
Pinic acid	42.6	43.0	52.0	26.3	74.7	34.7	21.9	-	-	-
Benzoic acid	75.5	81.9	100.0	35.8	55.1	33.9	17.7	3.8	18.6	47.6
Mandelic acid	-	-	-	-	-	-	-	-	-	-
Sebacic acid	-	-	-	88.9	84.4	38.0	42.0	60.0	32.0	64.7
Hexanal	55.9	32.3	42.2	25.4	24.6	41.2	98.6	19.2	34.7	24.6
Benzaldehyde	35.5	27.9	28.8	20.9	12.2	21.3	55.3	34.3	22.1	12.2
Heptanal	88.4	32.6	47.6	38.6	47.8	43.1	99.5	38.4	97.2	47.8
Octanal	-	39.8	34.7	35.8	47.4	35.5	66.1	22.6	63.3	47.4
Nonanal	80.6	49.2	34.0	56.9	32.3	28.7	58.1	27.2	75.4	32.3
Pinonaldehyde	54.0	28.8	27.2	19.0	22.8	44.0	96.4	20.3	29.1	22.8
Tridecanal	-	-	-	30.7	29.8	61.5	61.3	39.1	68.0	29.8
β -Caryophyllene aldehyde	47.2	30.4	44.3	20.3	50.4	47.0	71.6	34.4	80.3	50.4
β -Nocaryophyllene aldehyde	-	39.1	42.8	-	43.2	52.9	100.7	15.9	63.7	43.2
Ethylenediamine	37.8	93.0	30.7	88.8	50.5	84.9	56.5	20.8	50.9	50.5
Diethylamine	34.4	69.0	92.6	76.5	14.7	95.9	54.0	72.2	41.2	14.7
Dipropylamine	5.2	16.3	84.5	91.1	52.4	47.5	73.3	57.0	37.4	52.4
para-Aminophenol	44.8	81.3	100.0	95.4	43.6	72.2	90.1	56.3	95.9	43.6
Isopropylamine	87.7	-	6.1	-	44.6	21.8	71.5	10.3	73.4	44.6
Isopropylaniline	45.7	69.7	76.5	84.3	41.6	40.9	55.9	43.7	79.2	41.6

ACKNOWLEDGEMENTS

This research was supported by the Academy of Finland Center of Excellence program (project number 1118615). Financial support was also provided by the Emil Aaltonen Foundation.

REFERENCES

- Ayash, T. *et al.* (2009) Understanding climatic effects of aerosols: modeling radiative effects of aerosols, *ACS Symposium Series*, **1005**, 149. doi: 10.1007/s00216-011-5041-0
- Hoffmann, T. *et al.* (1997) Formation of organic aerosols from the oxidation of biogenic hydrocarbons, *J. Atmos. Chem.* **26**, 189.
- Jimenez, J.L. *et al.* (2009) Evolution of organic aerosols in the atmosphere, *Science* **326**, 1525.
- Kirchstetter, T.W. *et al.* (2001) Laboratory and field investigation of the adsorption of gaseous organic compounds onto quartz filters. *Atmos. Environ* **35**, 1663.
- Laitinen, T. *et al.* (2009) Aerosol time-of-flight mass spectrometer for measuring ultrafine aerosol particles, *Boreal Env. Res.* **14**, 539.
- Laitinen, T. *et al.* (2010) Determination of organic compounds from wood combustion aerosol nanoparticles by different gas chromatographic systems and by aerosol mass spectrometry, *JC Chromatogr A* **1217**, 151.
- Laitinen, T. *et al.* (2011) Characterization of organic compounds in 10 to 50 nm aerosol particles in a boreal forest with laser desorption ionization aerosol mass spectrometer and comparison with other techniques. *Atmos Environ*, (2011), doi: 10.1016/j.atmosenv.2011.04.023
- Orsini, D.A. *et al.* (2003) Refinements to the particle-into-liquid sampler (PILS) for ground and airborne measurements of water-soluble aerosol composition, *Atmos. Environ.* **37**, 1243.
- Parshintsev, J. *et al.* (2009) Analysis of organic compounds in ambient aerosols collected with the particle-into-liquid sampler, *Boreal Environ. Res.* **14**, 630.
- Parshintsev, J. *et al.* (2010) Particle-into-liquid sampler on-line coupled with solid-phase extraction-liquid chromatography-mass spectrometry for the determination of organic acids in atmospheric aerosols, *J.C Chromatogr. A* **1217**, 5427.
- Parshintsev, J. *et al.* (2011) Comparison of quartz and teflon filters for simultaneous collection of size-separated ultrafine aerosol particles and gas-phase zero samples, *Anal. Bioanal. Chem.* (2011), doi: 10.1007/s00216-011-5041-0
- Pöschl, U. (2005) Atmospheric aerosols: composition, transformation, climate and health effects. *Angew Chem* **117**, 7520.
- Ruiz-Jimenez, J. *et al.* (2011) Comprehensive GCxGC, a valuable technique for the screening of different chemical compounds in ultrafine aerosol particles, Submitted to *Environ. Monitoring*
- Smith, J. N. *et al.* (2010) Observations of ammonium salts in atmospheric nanoparticles and possible climatic implications, *PNAS* **107**, 6634.
- Zhang, Q. *et al.* (2007) Ubiquity and dominance of oxygenated species in organic aerosols in anthropogenically-influenced Northern Hemisphere midlatitudes, *Geophys. Res. Lett.* **34**

LONG TERM MEASUREMENTS OF METHANE EMISSION FROM A BOREAL FEN BY EDDY COVARIANCE METHOD

J. RINNE¹, S. HAAPANALA¹, O. PELTOLA¹, M. PIHLATIE¹, M. AURELA², J. HATAKKA², C. SCHURIG¹, I. MAMMARELLA¹, T. LAURILA², E.-S. TUITTILA³, T. VESALA¹

¹University of Helsinki, Department of Physics, PL 48, 00014 University of Helsinki, Finland

²Finnish Meteorological Institute, Climate Change Research, Helsinki, Finland

³University of Helsinki, Department of Forest Sciences, Finland

Keywords: peatland, carbon cycle, flux measurement.

INTRODUCTION

Northern wetlands are important for the global climate system not only because they store vast amounts of carbon, but also because they emit high amounts of methane into the atmosphere. However, continuous long-term measurements of ecosystem scale methane emissions from these ecosystems are still quite sparse. We have measured methane emissions from a boreal fen by eddy covariance method continuously since 2005. First year of the measurements of methane has been published earlier (Rinne *et al.*, 2007). The aims of this study were to determine the annual ecosystem scale methane emission from a boreal fen and seasonal and inter-annual variation of the emission.

METHODS

The measurement site is located at the eastern end of the Siikaneva fen, which is a boreal oligotrophic fen located in Ruovesi in Southern Finland (61°50'N, 24°12'E, 162 m a.s.l.). The peat depth at the measurement site is up to four meters and has accumulated since the end of the last ice age, in about 9000 yr. The vegetation at the site is dominated by *Sphagnum* mosses, Sedges (*Carex rostrata* Stokes, *C. limosa* L., *Eriophorum vaginatum* L.) and Rannochrush (*Scheuchzeria palustris* L.). A more detailed description of the vegetation at the site is given by Riutta *et al.*, (2007). The site has a relatively flat topography with no pronounced string and hollow structures. The homogenous fetch extends some 200 m in the north and south and several hundred meters in east and west. The annual mean temperature during 1971–2000 at Hyttiälä weather station, located 5 kilometres from Siikaneva, was 3.3°C and the annual precipitation 713 mm.

The methane fluxes were measured using the eddy covariance technique. Methane concentrations were measured at a rate of 10 Hz by a tunable diode laser absorption spectrometer (Campbell TDLAS, TGA-100, years 2005-2007) or integrated cavity ring down laser spectrometer (Los Gatos RMT-200, years 2008-2010). The three-dimensional wind vector was measured at the rate of 10 Hz by an acoustic anemometer (USA-1, METEK, Germany). Also carbon dioxide and water vapour fluxes were measured by eddy covariance technique utilizing the same acoustic anemometer and a closed path infrared gas analyser (IRGA, Li-Cor 7000). The acoustic anemometer was placed 3 m above the peat surface.

RESULTS

Monthly average methane fluxes (Figure 1) show clear seasonal cycle with low emissions during winter and highest emissions in summer. The emissions show exponential dependence on peat temperature (Figure 2). Best correlation was found with temperature measured at the depth of 35 cm with Q_{10} of 6.1. Similar dependencies are found for daily average fluxes. No direct dependence of emission on water table

position was found. However, rapid rises of water table depth were often associated with transient reduction of methane emission (Figure 3). There are two possible reasons for this behaviour. First, a layer of methane poor rainwater on top of the older peat water can reduce the diffusive flux until a quasi-stationary gradient is re-established. Second, the rise of water table leads to increased hydrostatic pressure in the peat water thus contracting the existing bubbles. This leads to decrease of ebullition until the bubbles have again reached the critical size needed for their release.

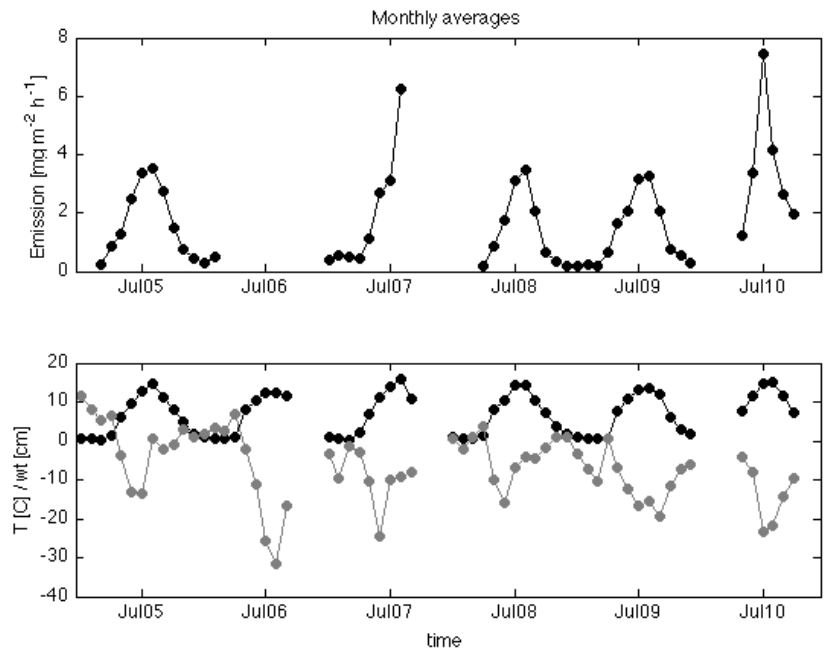


Figure 1. Monthly average methane emission, peat temperature at 35 cm depth, and water table position.

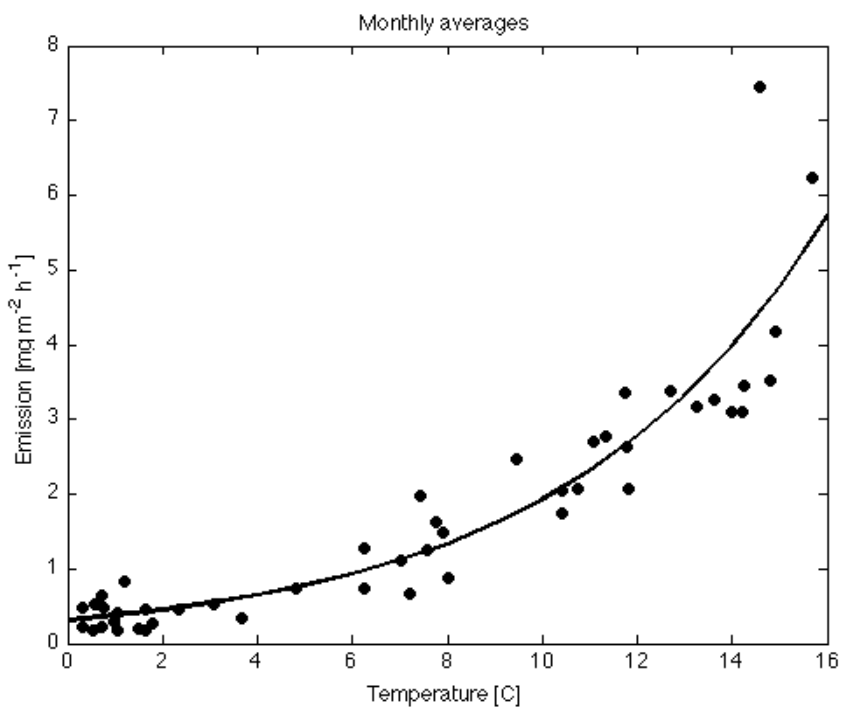


Figure 2. Monthly average methane emission against peat temperature at 35 cm depth.

By using temperature dependence of monthly emissions we can gapfill the emission timeseries and estimate the annual methane emissions. The annual methane emissions range from 10 to 18 gC m⁻² y⁻¹ (Table 1). Aurela et al. (2007) reported the annual carbon dioxide sink of the site to be 50-60 gC m⁻² y⁻¹ in 2004 and 2005. Thus the methane emission appears to be a significant part of the carbon balance of this fen.

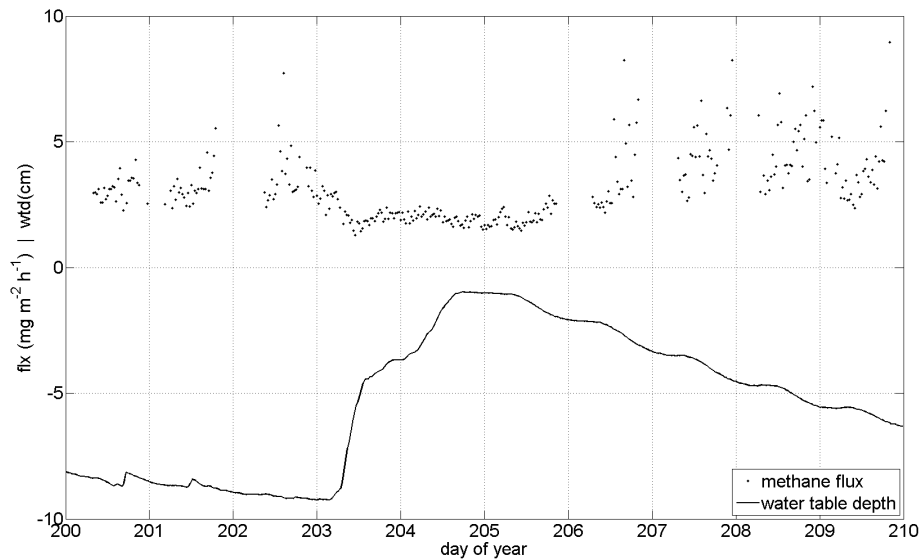


Figure 3. Detail of timeseries (2008) of half-hourly methane emission and water table depth.

CONCLUSIONS

The preliminary results presented here indicate that methane is an important part of the carbon balance of this boreal fen ecosystem. The ecosystem scale methane emissions depend on peat temperature both on daily and monthly scales. No direct correlation between temporal variations of ecosystem scale methane emission and water table position was observed. Water table changes may exert a more complicated effect on methane emission.

Year	Methane emission (gC m ⁻² a ⁻¹)
2005	13.4
2006	(11.8)
2007	14.7
2008	10.3
2009	11.2
2010	17.6

Table 1. Annual methane emissions. Note that the value for 2006 is based solely on temperature dependence of the emission.

ACKNOWLEDGEMENTS

We acknowledge the Academy of Finland Center of Excellence program and the Academy Fellow grant (J. Rinne) for Financial support (211483, 120434, 125238, 1118625).

REFERENCES

- Aurela, M., T. Riutta, T. Laurila, J.-P. Tuovinen, T. Vesala, E.-S. Tuittila, J. Rinne, S. Haapanala, & J. Laine, (2007). CO₂ balance of a sedge fen in southern Finland – the influence of a drought period. *Tellus*, **59B**, 826-837.
- Rinne, J., T. Riutta, M. Pihlatie, M. Aurela, S. Haapanala, J.-P. Tuovinen, E.-S. Tuittila & T. Vesala, (2007). Annual cycle of methane emission from a boreal fen measured by the eddy covariance technique. *Tellus*, **59B**, 449-457.
- Riutta, T., J. Laine, M. Aurela, J. Rinne, T. Vesala, T. Laurila, S. Haapanala, M. Pihlatie & E.-S. Tuittila, (2007). Spatial variation in plant communities and their function regulates carbon gas dynamics in boreal fen ecosystem. *Tellus*, **59B**, 838-852.

ECOSYSTEM SCALE VOC EMISSION FROM SCOTS PINE FOREST

J. RINNE¹, T.M. RUUSKANEN¹, R. TAIPALE¹, M.K. KAJOS¹, J. PATOKOSKI¹, A. GHIRARDO², J.-P. SCHNITZLER², J. AALTO³, H. AALTONEN³, H. HAKOLA⁴, J. BÄCK³, M. BOY¹

¹University of Helsinki, Department of Physics, PL 48, 00014 University of Helsinki, Finland

²Helmholtz Zentrum München, Germany

³University of Helsinki, Department of Forest Sciences, Finland

⁴Finnish Meteorological Institute, Air Quality Research, Helsinki, Finland

Keywords: monoterpene, methanol, hydrocarbon emission, flux measurement.

INTRODUCTION

Coniferous forests are a major source of volatile organic compounds (VOC), including monoterpenes, into the boreal atmosphere (Rinne et al., 2009). These compounds contribute to the growth of secondary aerosol growth (Tunved et al., 2006). Thus it is important to understand the processes driving these emissions, which can be achieved with detailed emission measurements (see e.g. Aalto et al., this issue) and controlled experiments. For model and algorithm development leaf level emission measurements in controlled environment have proved essential. For deeper understanding of processes underlying the emission the laboratory work in cellular level has been conducted.

From the perspective of atmospheric chemistry we need quantitative data on VOC emissions mostly in ecosystem or landscape scales. Thus we need to be able to upscale our understanding of cellular and leaf level emission processes to yield quantitative emissions in these larger scales. For this, emission models of varying complexity are used. In order to evaluate the performance of these models independent measurements of VOC emissions in ecosystem or landscape scales are essential. While longer term measurement of landscape scale emissions is very challenging, we are able to measure ecosystem scale VOC emissions using surface layer flux measurement techniques.

METHODS

We have employed disjunct eddy covariance technique with proton transfer reaction quadrupole mass spectrometer at a boreal Scots pine forest at SMEAR II station in Hyytiälä, Finland. Detailed description of the measurement system is given by Rinne et al. (2007) and Taipale et al. (2008; 2010). In addition we have used surface layer gradient (SLG) technique with PTR-QMS.

The contributions of de novo and evaporative emissions have been obtained by ¹³C labelling experiment conducted in laboratory conditions (Ghirardo et al., 2010). The contributions of canopy and soil emissions are estimated using automated enclosure measurements (e.g. Ruuskanen et al., 2005, Aaltonen et al., 2011). The insight into the processes underlying the emissions, atmospheric transport and processing can be combined using a numerical model model such as SOSA (e.g. Boy et al., 2011). The data used for evaluate the importance of various emission processes and models include surface layer fluxes and atmospheric concentrations.

RESULTS

The results from flux measurements show that monoterpenes make up over 50% of the ecosystem scale VOC emission measured by the DEC-PTR-QMS (Figure 1). Other compounds emitted are methanol, acetone, isoprene and acetaldehyde. However, the magnitudes measured with different surface layer techniques differ considerably from each other.

The ^{13}C labelling experiment with tree seedlings has shown that monoterpene emissions from boreal evergreen coniferous trees originate from two parallel pathways, one directly from synthesis and the other from storage pools (Ghirardo et al., 2010). The former pathway is in close connection with photosynthesis. However, the ecosystem scale contribution of these pathways is difficult to separate using flux data due to strong correlation between the driving environmental parameters and to similar functional forms of the corresponding algorithms (Taipale et al., 2011). ^{13}C labelling did not show acetone and methanol emission to be closely connected to photosynthesis.

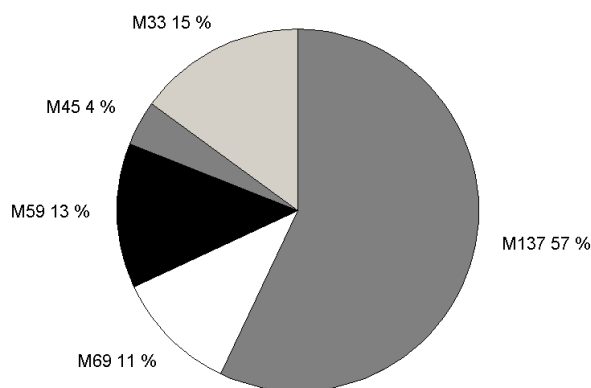


Figure 1. Contribution of different VOCs to the total ecosystem scale VOC emission, in mass basis, from a Scots pine forest in July 2007. M33: methanol; M45: acetaldehyde; M59: acetone; M69: isoprene, M137: sum of monoterpenes.

CONCLUSIONS

The results show that accurate determination of ecosystem scale VOC emission at low emission environment, such as boreal forest, is still a challenge. Depending on a measurement method the magnitude of emission as well as the dynamics can be different. However, combining results from various experiments, field measurement techniques and model work we can discern following general features in the ecosystem scale VOC emission from boreal Scots pine forest: 1) The major compounds emitted are monoterpenes, with significant contributions of methanol, acetone, isoprene and acetaldehyde. 2) The monoterpene emission from evergreen coniferous forest originates partially directly from monoterpene synthesis and partially as evaporation from large specialized storage structures. 3) The dominant monoterpene measured at stand scale in the Scots pine forest is α -pinene (Rinne et al., 2000; see also Bäck et al., this issue). There is a large tree-to-tree variation in magnitude of monoterpene emission as well as in monoterpene composition emitted. 4) The VOC emission from forest soil may be of importance especially in spring and autumn (Aaltonen et al., 2011). Future improvements of ecosystem scale emission measurement by surface layer flux measurement methods include application of conventional eddy covariance method with proton transfer reaction – time of flight mass spectrometer at Hyytiälä site (see e.g. Ruuskanen et al., 2011).

ACKNOWLEDGEMENTS

We acknowledge the Academy of Finland Center of Excellence program and the Academy Fellow grant (J. Rinne) for financial support (grant nos 211483, 120434, 125238, 1118625).

REFERENCES

- Aalto, J., P. Kolari, H. Aaltonen, J. Bäck, P. Hari and E. Nikinmaa (2011) Continuous measurements of Scots pine shoots show huge variation in voc emissions during year 2010. Report Series in Aerosol Sciences vol XX, pp. yy
- Aaltonen H., Pumpanen J., Pihlatie M., Hakola H., Hellén H., Kulmala L., Vesala T. & Bäck J. (2011) Boreal pine forest floor biogenic volatile organic compound emissions peak in early summer and autumn. *Agricultural and Forest Meteorology* 151: 682-691
- Bäck, J., J. Aalto, P. Kolari, E. Juurola, M. Henriksson and H. Hakola (2011) Temporal and between-tree variability of Scots pine monoterpene emissions in a boreal forest stand. Report Series in Aerosol Sciences vol XX, pp. yy
- Boy, M., A. Sogachev, J. Lauros, L. Zhou, A. Guenther & S. Smolander (2011) SOSA – a new model to simulate the concentrations of organic vapours and sulphuric acid inside the ABL – Part 1: Model description and initial evaluation *Atmospheric Chemistry and Physics* 11: 43-51.
- Ghirardo, A., K. Koch, R. Taipale, I. Zimmer, J.-P. Schnitzler & J. Rinne, (2010) Determination of de novo and pool emissions of terpenes from four common boreal/alpine trees by ¹³CO₂ labeling and PTR-MS analysis. *Plant, Cell & Environment* 33: 781-792.
- Rinne, J., H. Hakola, T. Laurila & Ü. Rannik, (2000) Canopy scale monoterpene emissions of *Pinus sylvestris* dominated forests. *Atmospheric Environment* 34: 1099-1107.
- Rinne, J., R. Taipale, T. Markkanen, T.M. Ruuskanen, H. Hellén, M.K. Kajos, T. Vesala & M. Kulmala, (2007) Hydrocarbon fluxes above a Scots pine forest canopy: measurements and modeling. *Atmospheric Chemistry and Physics* 7: 3361-3372.
- Rinne, J., J. Bäck & H. Hakola, (2009) Biogenic volatile organic compound emissions from Eurasian taiga: Current knowledge and future directions. *Boreal Environment Research* 14: 807-826.
- Ruuskanen, T.M., P. Kolari, J. Bäck, M. Kulmala, J. Rinne, H. Hakola, R. Taipale, M. Raivonen, N. Altimir, P. Hari (2005) On-line field measurements of monoterpene emissions from Scots pine by proton transfer reaction - mass spectrometry. *Boreal Environment Research* 10: 553-567.
- Taipale, R., T.M. Ruuskanen, J. Rinne, M.K. Kajos, H. Hakola, T. Pohja & M. Kulmala, (2008) Technical Note: Quantitative long-term measurements of VOC concentrations by PTR-MS – measurement, calibration, and volume mixing ratio calculation methods. *Atmospheric Chemistry and Physics* 8: 6681-6698.
- Taipale, R., T.M. Ruuskanen, & J. Rinne, (2010) Lag time determination in DEC measurements with PTR-MS. *Atmospheric Measurement Technology* 3: 853-862.
- Taipale, R., M.K. Kajos, J. Patokoski, P. Rantala, T.M. Ruuskanen, & J. Rinne, (2010) Role of de novo biosynthesis in ecosystem scale monoterpene emissions from a boreal Scots pine forest. *Biogeosciences Discuss.* 7: 8019-8040.
- Tunved, P., H.-C. Hansson, V.-M. Kerminen, J. Ström, M. Dal Maso, H. Lihavainen, Y. Viisanen, P.P. Aalto, M. Komppula, & M. Kulmala (2006) High natural aerosol loading over Boreal forests, *Science* 312: 261-263.

ADSORPTION ACTIVATION OF INSOLUBLE AEROSOL PARTICLES

S. ROMAKKANIEMI¹, H. KESKINEN¹, A. JAATINEN¹, J.N. SMITH^{1,2,3}, J. JOUTSENSAARI¹ and A. LAAKSONEN^{1,3}

¹Department of Applied Physics, University of Eastern Finland, PO BOX 1627, 70211 Kuopio, Finland

²National Center for Atmospheric Research, P.O. Box 3000, Boulder, CO USA

³Finnish Meteorological Institute, P.O. Box 503, 00101 Helsinki, Finland

Keywords: ADSORPTION, AEROSOL CLOUD INTERACTION, CCN

INTRODUCTION

Commonly it has been thought that only aerosol particles with substantial amount of water soluble matter can form cloud droplets at the ambient conditions. However, recently it has been proposed that also insoluble, but hydrophilic, particles can act as a cloud condensation nucleus (CCN) even at atmospheric supersaturations (Sorjamaa and Laaksonen, 2007, Henson, 2007). This could potentially affect the aerosol cloud interactions on areas with dust concentrations.

METHODS

In the theory water adsorption is described by isotherms which give the amount of adsorbed water on the particle surface as a function of relative humidity in subsaturated conditions. One example of such an equation is the so called FHH-isotherm giving the number of adsorbed water layers on the surface as:

$$\ln \frac{1}{S} = \frac{A}{\Theta^B}, \quad (1)$$

where S is the gas saturation ratio, Θ is the surface coverage, i.e. the number of water layers, and A and B , are fitted parameters dependent on the surface properties. In the traditional Köhler equation the term describing the solute effect (Raoult's effect) can be replaced by solving the S from Eq. 1 [Sorjamaa and Laaksonen, 2007],

$$S = \exp\left(\frac{4\sigma M_w}{RT\rho_w D}\right) \exp(-A)\Theta^{-B}, \quad (2)$$

from which the critical supersaturation can be calculated. Thus if the isotherm describing the amount of water on the surface can be determined, the cloud droplet formation potential of particles can be calculated from equation 2.

It has been shown by Romakkaniemi et al. [2001] that the hygroscopic differential mobility analyzer (HTDMA) can be used to study water uptake by adsorption on aerosol particles at subsaturated conditions. With small enough particles it is possible to detect the formation of water layers, although the depth of monolayer is approximately only 3 Å. In this study we produced silica particles from an aqueous solution. The amount of water adsorbed on the particles at RH's between 40 and 90% was measured with nano-HTDMA, The growth of particles at super-saturated conditions was measured by CCN counter to test the validity of equation 2.

RESULTS

The adsorption of water on small aerosol particles composed of silica follows FHH-adsorption isotherm. Based on the HTDMA measurements for 8nm and 10 nm particles, the parameters A and B in Eq. 1 are found to be 4.82 and 2.16, respectively. These values are slightly higher than values reported in Kumar et

al. [2010] for typical dust and mineral samples. By using parameters A and B in Eq. 2 we get the critical supersaturation as a function of particle size.

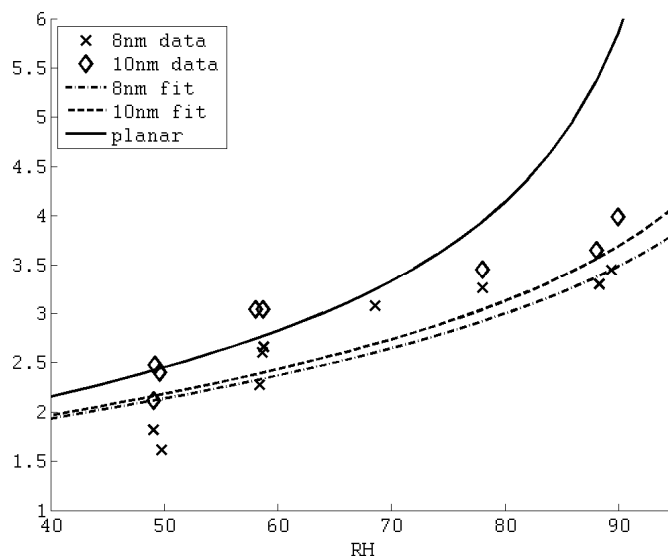


Figure 1. Number of adsorbed water layers on the surface of 8nm and 10 nm particles, and the fitted isotherm.

In Figure 2 we present the activated fraction of 114nm and 150nm particles as a function of supersaturation. For this type of curve a sigmoidal function can be fitted and from that we can determine D50, the diameter at which half of the aerosol are activated. Also presented are expected values for critical supersaturations calculated from Eq. 2 with parameters from HTDMA measurements. As can be seen the particles activate in slightly lower supersaturation than expected. However, at the moment data is still uncorrected for the effects of shape and multiple charging in DMA. As silica particles are formed from aggregates, the surface area is actually larger than for spherical particles. Multiple charging will let larger particles to pass DMA and thus the number of activated particles of certain size seems to be larger than actually is. Thus both corrections would move activation curves to right (Kumar et al 2010).

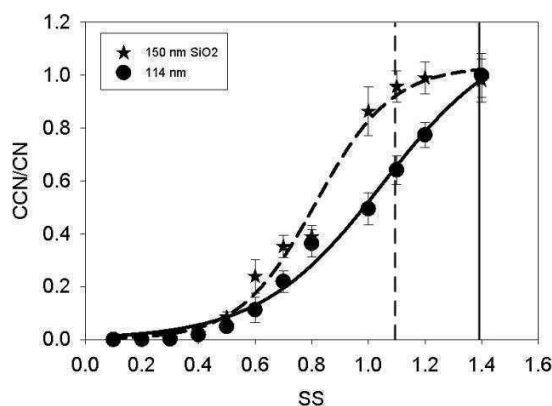


Figure 2. Activation curves from CCN counter. The data are not corrected for shape or multiple charges in the DMA.

CONCLUSIONS

Our preliminary results support the theory and results by Kumar et al. (2010) stating that equation 2 is valid for estimating CCN properties of insoluble particles. We will continue the work by coating particles with small amount of soluble compounds and study how the transition from adsorption activation to traditional Köhler theory takes place.

ACKNOWLEDGEMENTS

This work was supported by the Academy of Finland (projects 123466 and 138951), the Kone Foundation and the Saastamoinen Foundation.

REFERENCES

- Henson, B. F. (2007). An adsorption model of insoluble particle activation: Application to black carbon, *J. Geophys. Res.*, 112, D24S16, doi:10.1029/2007JD008549.
- Kumar, P., I.N. Sokolik, and A. Nenes (2010), Measurements of cloud condensation nuclei activity and droplet activation kinetics of fresh unprocessed regional dust samples and minerals, *Atmos. Chem. Phys. Discuss.*, 10, doi:10.5194/acpd-10-31039-2010.
- Romakkaniemi, S., K. Hämeri, M. Väkevä, and A. Laaksonen (2001), Adsorption of water on 8–15 nm NaCl and (NH₄)₂SO₄ aerosols measured using an ultrafine tandem differential mobility analyzer, *J. Phys. Chem. A*, 105, 8183–8188, 2001.
- Sorjamaa, R. and A. Laaksonen(2007) The effect of H₂O adsorption on cloud drop activation of insoluble particles: a theoretical framework, *Atmos. Chem. Phys.*, 7, doi:10.5194/acp-7-6175-2007.

EMISSION AND DEPOSITION OF VOC ABOVE GRASSLAND, EDDY COVARIANCE FLUXES WITH PTR-TOF

T. M. RUUSKANEN^{1,2}, M. MÜLLER^{2,3}, R. SCHNITZHOFFER^{2,3}, T. KARL^{2,4}, M. GRAUS², I. BAMBERGER², L. HÖRTNAGL⁵, G. WOHLFAHRT⁵, and A. HANSEL²

¹Division of Atmospheric Sciences, Department of Physics, University of Helsinki, Finland

²Institute of Ion Physics and Applied Physics, University of Innsbruck, Austria

³Ionicon Analytik, Innsbruck, Austria

⁴Atmospheric Chemistry Division, National Center for Atmospheric Research, Boulder, CO 80307, USA

⁵Institute of Ecology, University of Innsbruck, Innsbruck, Austria

INTRODUCTION

Volatile organic compounds (VOCs) take part in atmospheric processes from formation of atmospheric oxidants, such as ozone and OH, to secondary organic aerosol particle formation. Biogenic emissions make up for three quarters of the total release to the atmosphere (Guether et al). Monoterpene and oxidized VOC fluxes have been measured at SMEAR II using proton-transfer-reaction – quadrupole-mass-spectrometer (PTR-QMS) combined with disjunct eddy covariance (Rinne et al., 2007). In addition to monoterpenes, plants emit a number of other organic compounds, including more reactive sesquiterpenes that are only semi-volatile. The amount of carbon released by plants as biogenic VOCs is uncertain (Chapin et al., 2006). Biogenic VOCs have been suggested as an important part of the missing reactivity observed in OH-reactivity measurements (e.g. Sinha et al., 2010), and wildest arguments suggest that the current emission inventories may miss up to half of the reactive carbon as a VOC flux entering the atmosphere (Goldstein and Galbally, 2007).

METHODS

Proton transfer reaction ionizes a wide range of VOCs; and in combination with a time of flight mass spectrometer (PTR-TOF) (Jordan et al., 2009) it was used to measure at 10 Hz frequency full mass spectra up to m/z 315. Fast (5-20Hz) measurements enable use of eddy covariance (EC) that is the preferred direct flux determination method. The mass resolution of the PTR-TOF (Graus et al., 2010) enabled the identification of chemical formulas and separation of oxygenated and hydrocarbon species exhibiting the same nominal mass. From the full mass spectra, we determined 481 ion mass peaks (Ruuskanen et al., 2011) from ambient air concentration above a managed, temperate mountain grassland in Neustift, Stubai Valley, Austria. Eddy covariance fluxes were calculated for all of the ion mass peaks for time periods of fully grown grass, harvesting (cutting and drying) as well as during the start of re-growth after harvesting. Unexpected deposition of monoterpenes (Fig. 1) and sesquiterpenes was observed to the grassland outside the grass harvesting period (Bamberger et al., 2011).

RESULTS

During the harvesting the fluxes of terpenoids turned to an emission (Fig. 2) and we found significant fluxes of 18 compounds distributed over 43 ions, including protonated parent compounds, as well as their isotopes and fragments and VOC-H⁺-water clusters. The dominant BVOC fluxes were emissions of methanol, acetaldehyde, ethanol, hexenal and other C₆ leaf wound compounds, acetone, acetic acid,

monoterpenes and sesquiterpenes. We conducted laboratory studies on several of the grassland plant species grown from the seeds of the field site and confirmed that they were the source of emissions during cutting (Brilli et al., 2011). The smallest reliable fluxes we determined were less than $0.1 \text{ nmol m}^{-2} \text{ s}^{-1}$, as in the case of sesquiterpene emissions from freshly cut grass. During cutting, total VOC emission fluxes up to $200 \text{ nmol m}^{-2} \text{ s}^{-1}$ were measured. Previous measurements with a PTR-QMS have shown continuous methanol emission over the growing season that is enhanced by the harvesting (Bamberger et al., 2010). Methanol emissions accounted for half of the emissions of oxygenated VOCs and a third of the carbon of all measured VOC emissions during harvesting.

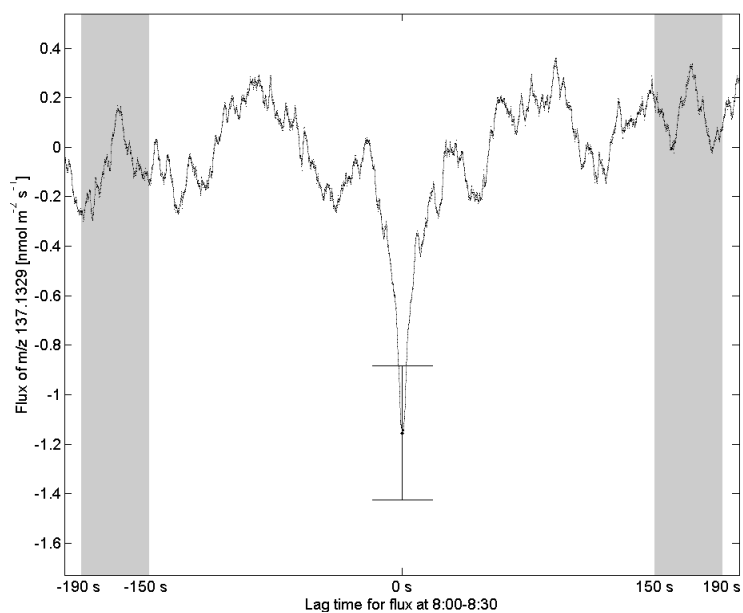


Figure 1. Deposition flux determined from the minimum covariance around 0 s lag time of monoterpene (m/z 137.1329 Th) and vertical wind during a 30 minute above intact grass. The uncertainty of the flux shown (bar) was determined from covariance far from the true lag (gray areas).

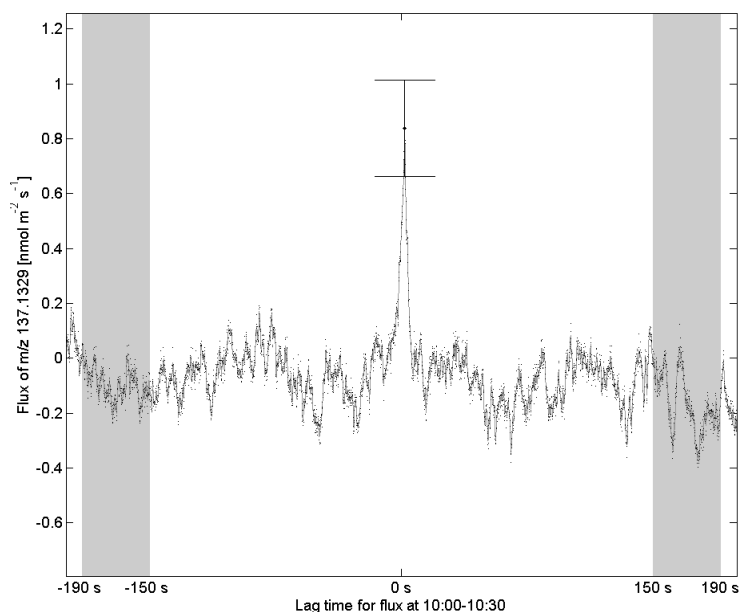


Figure 2. Emission flux determined from the minimum covariance around 0 s lag time of monoterpene (m/z 137.1329 Th) and vertical wind during a 30 minute during grass harvesting. The uncertainty of the flux shown (bar) was determined from covariance far from the true lag (gray areas).

ACKNOWLEDGEMENTS

The work of Marie Curie fellow Dr. Taina Ruuskanen was funded by the European Commission as a part of the Industry-Academia Partnerships and Pathways (IAPP; 218065).

REFERENCES

- Bamberger, I., Hörtnagl, L., Schnitzhofer, R., Graus, M., Ruuskanen, T. M., Müller, M., Wohlfahrt, G., and Hansel, A. (2010). BVOC fluxes above mountain grassland, *Biogeosciences*, 7, 1413–1424.
- Bamberger, I., Hörtnagl, L., Ruuskanen, T. M., Schnitzhofer, R., Müller, M., Graus, M., Karl, T., Wohlfahrt, G., and Hansel, A. (2011). Deposition fluxes of terpenes over grassland, *J. Geophys. Res.*, in review.
- Brilli, F., Ruuskanen, T. M., Schnitzhofer, R., Müller, M., Breitenlechner, M., Bittner, V., Wohlfahrt, G., Loreto, F., and Hansel, A. (2010). Ultrafast detection of biogenic volatile organic compounds by Proton Transfer Reaction “Time-of-Flight” Mass Spectrometry (PTR-TOF) after leaf wounding and darkening, submitted, *PLoS ONE*.
- Chapin, F. S. III, Woodwell, G. M., Randerson, J. T., Rastetter, E. B., Lovett, G. M., Baldocchi, D. D., Clark, D. A., Harmon, M. E., Schimel, D. S., Valentini, R., Wirth, C., Aber, J. D., Cole, J. J., Goulden, M. L., Harden, J. W., Heimann, M., Howarth, R. W., Matson, P. A., McGuire, A. D., Melillo, J. M., Mooney, H. A., Neff, J. C., Houghton, R. A., Pace, M. L., Ryan, M. G., Running, S.W., Sala, O. E., Schlesinger, W. H., and Schulze, E.-D. (2006). Reconciling carbon cycle concepts, terminology and methods, *Ecosystems*, 9, 1041–1050.
- Goldstein, A. H. and Galbally, I. E. (2007). Known and unexplored organic constituents in the earth’s atmosphere, *Environ. Sci. Technol.*, 41, 1514–1521.
- Graus, M., M. Müller and A. Hansel (2010). High resolution PTR-TOF quantification and formula confirmation of VOC in real time, *J. Am. Soc. Mass Spectr.*, 21, 1037-1044.
- Jordan, A., S. Haidacher, G. Hanel, E. Hartungen, L. Märk, H. Seehauser, R. Schottkowsky, P. Sulzer and T.D. Märk (2009). A high resolution and high sensitivity proton-transfer-reaction time-of-flight mass spectrometer (PTR-TOF-MS), *Int. J. Mass Spectrom.*, 286, 122-128.
- Müller, M., M. Graus, T.M. Ruuskanen, R. Schnitzhofer, I. Bamberger, L. Kaser, T. Titzmann, L. Hörtnagl, G. Wohlfahrt, T. Karl, A. Hansel (2010). First eddy covariance flux measurements by PTR-TOF, *Atmos. Meas. Tech.*, 3, 387-398.
- Rinne, J., Taipale, R., Markkanen, T., Ruuskanen, T. M., Hellén, H., Kajos, M. K., Vesala, T., and Kulmala, M. (2007). Hydrocarbon fluxes above a Scots pine forest canopy: measurements and modeling, *Atmos. Chem. Phys.*, 7, 3361–3372.
- Ruuskanen, T. M., M. Müller, R. Schnitzhofer, T. Karl, M. Graus, I. Bamberger, L. Hörtnagl, F. Brilli, G. Wohlfahrt, and A. Hansel (2011). Eddy covariance VOC emission and deposition fluxes above grassland using PTR-TOF. *Atmos. Chem. Phys.*, 11, 611-625.
- Sinha, V., Williams, J., Lelieveld, J., Ruuskanen, T. M., Kajos, M. K., Patokoski, J., Hellen, H., Hakola, H., Boy, M., Rinne, J., Kulmala, M.: OH Reactivity Measurements within a Boreal forest (2010). Evidence for Unknown Reactive Emissions, *Env. Sci. Tech.*, 44, 6614–6620.

STABILITY OF CLUSTERS CONTAINING WATER, PYRIDINE AND AMMONIA

K. RUUSUVUORI¹, T. KURTÉN¹, M. J. MCGRATH¹, I.K. ORTEGA¹, H. VEHKAMÄKI¹ and M. KULMALA¹

¹Department of Physics, P.O. Box 64, FI-00014, University of Helsinki, Finland

Keywords: Heterogeneous nucleation, Magic Numbers, Quantum chemistry, Modelling,

INTRODUCTION

Understanding of the processes involving atmospheric aerosols is essential if we are to understand the Earth's atmosphere, climate change or the health effects of air impurities. Aerosols are, by definition, solid or liquid particles (or combinations of these) uniformly distributed in a finely divided state in a gas, usually air. Their size ranges from nanometers to tens of micrometers. Unfortunately, both the birth and interaction mechanisms of atmospheric aerosols are varied and often also poorly understood.

Even though the majority of atmospheric nucleation is believed to happen via neutral pathways (Kulmala et al., 2007, Mirme et al, 2010), ion-induced nucleation may play some part, especially in regions where air ion or ion cluster concentrations are relatively high. There are several molecular ion species in the atmosphere, but Schulte and Arnold (1990) have identified protonated pyridine as the most abundant molecular ion in the middle troposphere over Europe. Several atmospheric reaction channels have been proposed which could lead to large positive cluster ions containing eg. water, pyridine and ammonia (Beig and Brasseur, 2000). Thus, understanding the properties of nitrogen containing organic molecules is important and with the help of quantum chemical calculations, we can gain useful insight on the details of ion-induced nucleation.

Our objective is to study $H^+(NH_3)_1(C_5H_5N)_1(H_2O)_n$ clusters with $n=1-5$, and see how the stability of the clusters behaves as a function of the amount of water molecules in the cluster.

COMPUTATIONAL DETAILS

Our calculations have been performed using the Gaussian 09 (Frisch et al., 2009) quantum chemistry program and CP2K (<http://cp2k.berlios.de/>), a freely available molecular simulations program.

RESULTS

We have started the study of the structure of clusters containing (protonated) pyridine, ammonia and 1-5 water molecules. Optimized geometries for the single pyridine ion, ammonia and water molecules were obtained with Gaussian 03 using density functional theory at the B3LYP/3-21G level. These geometries were used as "building blocks" for generating cluster geometries. Cluster geometries were generated randomly within the limits of cluster definitions (i.e. the generated configurations were always true clusters, according to the Stillinger criterion) and checked for uniqueness. Energies for the generated cluster configurations were calculated with CP2K using the density functional based tight binding (DFTB) method. For each case of $H^+(NH_3)_1(C_5H_5N)_1(H_2O)_n$, 10 000 random geometries were generated, out of which 50 lowest energy geometries were selected for each $H^+(NH_3)_1(C_5H_5N)_1(H_2O)_n$. These geometries were then optimized with CP2K using the DFTB method. The next step is to study these optimized geometries and select the most promising ones (eg. the ones with the most hydrogen bonds) for geometry optimization and energy calculations using higher level methods.

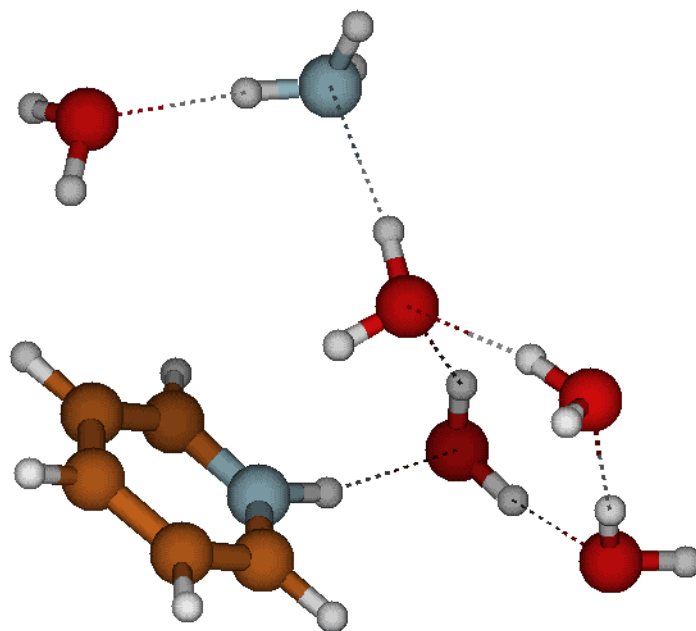


Figure 1. An example of a $\text{H}^+(\text{NH}_3)_1(\text{C}_5\text{H}_5\text{N})_1(\text{H}_2\text{O})_5$ geometry. The geometry has been optimized with CP2K at the DTFB level.

CONCLUSIONS

Using randomly generated geometries with the molecular simulations program CP2K has proven to be an efficient way of generating initial geometries. Further cluster stability studies are still underway.

ACKNOWLEDGEMENTS

We thank the CSC – IT Center for Science Ltd. for computer time and technical assistance. The financial support by the Academy of Finland Centre of Excellence program (Project No. 1118615) and ERC StG 257360-MOCAPAF is gratefully acknowledged.

REFERENCES

- Kulmala, M., Riipinen, I., Sipilä, M., Manninen, H.E., Petäjä, T., Junninen, H., Dal Maso, M., Mordas, G., Mirme, A., Vana, M., Hirsikko, A., Laakso, L., Harrison, R.M., Hanson, I., Leung, C., Lehtinen, K.E.J. and Kerminen, V.-M. (2007) Toward Direct Measurement of Atmospheric Nucleation, *Science*, 318, 89-92
- Mirme, S., Mirme, A., Minikin, A., Petzold, A., Hörrak, U., Kerminen, V.-M. and Kulmala, M. (2010) Atmospheric Sub-3nm Particles at High Altitudes, *Atmos. Chem. Phys.*, 10, 437–451
- Schulte, P. and Arnold, F. (1990) Pyridinium Ions and Pyridine in the Free Troposphere, *Geophys. Res. Lett.*, 17, 1077–1080
- Beig, G. and Brasseur, G.P. (2000) Model of Tropospheric Ion Composition: A First Attempt, *J. Geophys. Res.*, 105, 22671–22684
- Frisch, M.J. *et al.* (2004) Gaussian 03, Revision E.01, Gaussian, Inc., Wallingford CT

VOC FLUX AND CONCENTRATION MEASUREMENTS WITH PTR-TOF IN HYYTIÄLÄ

S. SCHALLHART, T. M. RUUSKANEN, M. K. KAJOS, H. JUNNINEN, J. RINNE, M. KULMALA

Department of Physics, University of Helsinki, Finland

INTRODUCTION

Per year over 1100 million tons carbon of non-methane volatile organic compounds (VOCs) are emitted from biogenic sources world-wide. About half of all global VOC emissions are from tropical woodlands and in the northern hemisphere the boreal zone is the largest forested area and a major source of biogenic VOCs (Guenther et al., 1995).

The emitted VOCs react during the day with OH and O₃, during the night with NO₃ and O₃. This chemistry is very complex and especially the reactions of higher photo-oxidized biogenic VOCs are not well known. The oxidation products of biogenic VOCs, like isoprene and monoterpenes, can condense on secondary organic aerosol (SOA) particles (e.g Kourtchev et al., 2006) or contribute to wet or dry deposition. Till now only a few of those products could be measured and indentified.

In addition of the soft ionization and the relative small fragmentations of the proton-transfer-reaction quadrupole (PTR- quad) instrument, the proton-transfer-reaction time-of-flight (PTR-TOF) mass spectrometer has a better transmission especially at high masses and is able to measure whole spectra in a time resolution of 10 Hz. This enables the PTR-TOF to look for fluxes in the whole mass spectra not, like in the PTR quad, for only a dozen preselected masses. With its high resolution of ~4500 $\Delta m/m$ (determined of the full width at half maximum of the ion peak) the instrument is capable of separating isobaric compounds, but cannot distinguish between isomeric compounds. The high mass accuracy of < 20 ppm enables the identification of the chemical composition of the mass peaks.

METHODS

To get more information on the nucleation process and the involved compounds, a PTR-TOF mass spectrometer measured from March to May 2011 in SMEAR II, Hyytiälä, Finland.

In Hyytiälä the PTR-TOF was measuring ambient air from three meters above the top of the canopy (see Figure 1). The air was sampled through a heated (~5°C above ambient temperature) 10 mm (o.d.) Teflon PTFE tube with a flow of over 15 l/min, to reduce the wall losses. Changes in the flight path, caused by temperature fluctuations, lead to expansion and contraction of the TOF. Changes in the path length influences the time of flight and causes mass scale shifts. To calibrate the mass scale a low concentration of trichlorobenzene was continuously added to the sample flow in the instrument through a diffusion limited capillary. In the ambient air over a hundred different compounds up to a mass/charge ratio of 500 Th were measured. In addition zero gas was measured, to identify instrumental background as well as peaks produced by the ion source. Preliminary results of the measurements will be presented in a poster.

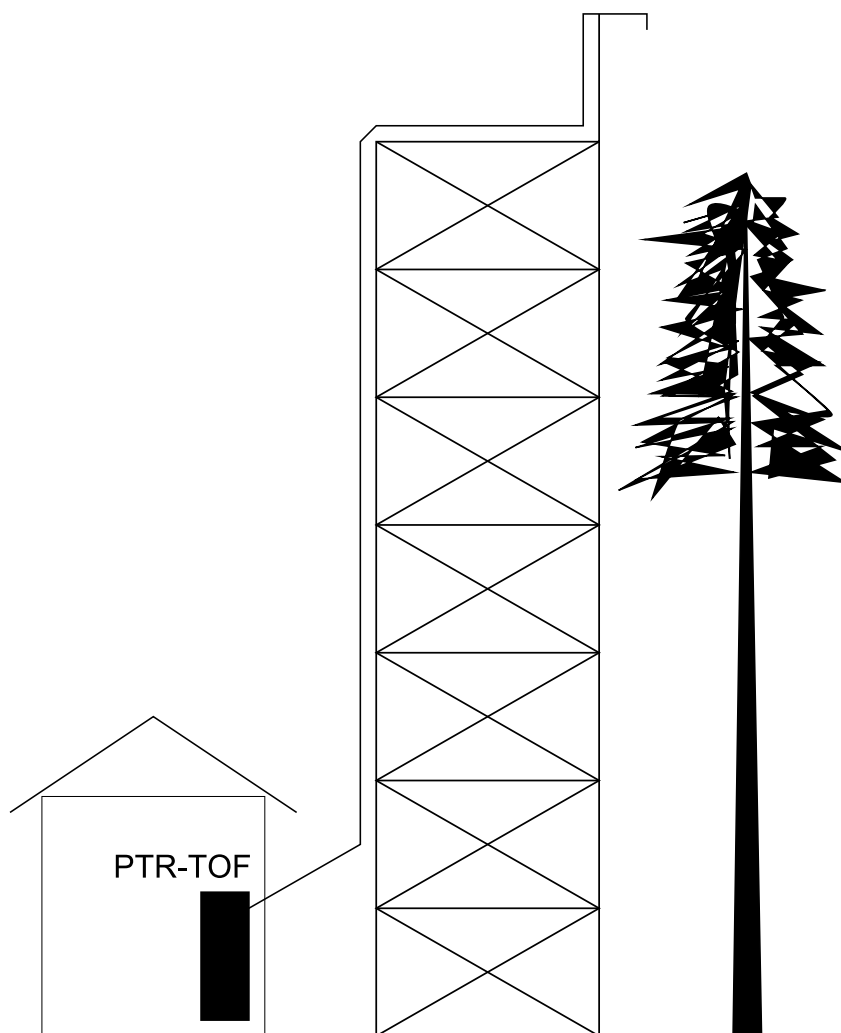


Figure 1: A schematic picture of the measurement setup

ACKNOWLEDGEMENTS

The financial support by the Academy of Finland Centre of Excellence program (project no 1118615) is gratefully acknowledged.

REFERENCES

- Guenther, A., C. Hewitt, D. Erickson, R. Fall, C. Geron, T. Graedel, P. Harley, L. Klinger, M. Lerdau, W. McKay, (1995). A global model of natural volatile organic compound emissions. *J. Geophys. Res.*, 100 (D5), 8873-8892.
- Kourtchev, I., T. M. Ruuskanen, P. Keronen, L. Sogacheva, M. Dal Maso, A. Reissell, X. Chi, R. Vermeylen, M. Kulmala, W. Maenhaut, M. Claeys (2006). Determination of isoprene and α -/ β -pinene oxidation products in boreal forest aerosols from Hyytiälä, Finland: diel variations and possible link with particle formation events, *Plant Biology*, 10, 138–149.

MEASUREMENTS OF IONS AND ION CLUSTERS BY MASS SPECTROMETRY DURING SULFURIC ACID-INDUCED NUCLEATION IN THE CLOUD CHAMBER AT CERN

S. SCHOBESBERGER¹, A. FRANCHIN¹, H. JUNNINEN¹, M. EHN^{1,2}, K. LEHTIPALO¹, S. GAGNÉ¹, T. NIEMINEN¹, T. PETÄJÄ¹, M. KULMALA¹, D.R. WORSNOP^{1,3}, and the CLOUD collaboration.

¹Division of Atmospheric Sciences, Department of Physics, University of Helsinki, Helsinki, FI-00014, Finland.

²Forschungszentrum Jülich GmbH, Jülich, 52425, Germany.

³Aerodyne Research, Inc., Billerica, MA 01821-3976, USA.

Keywords: nucleation, sulfuric acid, cluster ions, mass spectrometry.

INTRODUCTION

Several studies have shown a very good correlation between past variations in climate, and solar and cosmic ray variability (Kirkby, 2007). Aerosols and clouds still represent a large uncertainty in our understanding of climate change (Intergovernmental Panel on Climate Change, 2007), and several proposed mechanisms link solar variability with changes in the climate through possible effects of cosmic rays on weather, aerosols and clouds (Carslaw *et al.*, 2002). However, the details, as well as the significance, of those mechanisms remain unclear.

The CLOUD (Cosmics Leaving Outdoor Droplets) experiment was designed to investigate in particular the possible influence of galactic cosmic rays on the formation of new aerosol particles in the atmosphere and their growth to climatically relevant sizes. It provides exceptionally clean and well-defined experimental conditions in an aerosol chamber of 26.1 m³. Situated at the CERN Proton Synchrotron (PS) it adds the possibility of simulating cosmic rays “on demand” by making use of the synchrotron’s pion beam. Nucleation from gaseous precursors has been found to be an important source of aerosol particles in the atmosphere, and it has been shown that sulfuric acid (H₂SO₄) plays a crucial role in atmospheric nucleation (Kulmala *et al.*, 2004, Riipinen *et al.*, 2007). Therefore the focus of the experiments conducted so far was to investigate sulfuric acid nucleation under different conditions. These include varying beam intensity, concentration of ammonia (NH₃), temperature, and relative humidity.

METHODS

The Atmospheric Pressure interface Time-Of-Flight Mass Spectrometer (APi-TOF) is described in detail in Junninen *et al.* (2010). It is a high-resolution mass spectrometer produced by ToFwerk AG, (Switzerland) and Aerodyne Research, Inc. (MA, USA). Sampling occurs from atmospheric pressure through a critical orifice. The sampled ions pass through differentially pumped chambers and are focused and guided to the mass spectrometer by quadrupoles and an ion lens assembly. Note that in the setup used, no ionization of the sampled aerosol was performed. The sole purpose of the Atmospheric Pressure interface (APi) is to guide sampled ions through a progressively higher vacuum to the Time-Of-Flight mass spectrometer (TOF). Therefore only naturally charged ions are detected by this setup.

In the course of the experiments, sulfuric acid nucleation events were produced in the CLOUD chamber. Nucleation was usually initiated by significantly increasing concentrations of H₂SO₄, which was produced by photolytic oxidation of SO₂. [H₂SO₄] could hence be controlled by adjusting UV irradiation inside the chamber. At low concentrations of NH₃, nucleation occurred mainly by negative ions, while at higher levels of NH₃, nucleation of positive ions became significant. The composition of these ions could be determined based on their exact masses and isotopic patterns, facilitated by the cleanliness of the chamber.

CONCLUSIONS

For negative polarity, the compositions of practically all small ions could be determined during all experimental conditions. These were almost exclusively sulfur-containing compounds, such as SO_5^- and HSO_4^- . In the positive spectra, most ions could be identified as well and were found to be dominated by protonated nitrogen-containing organic molecules, such as pyridine and amines.

During nucleation events in the chamber, the ion species registered by the APi-TOF were almost exclusively sulfur-containing compounds or molecular clusters in both polarities. With a time resolution of less than 1 minute, the growth of clusters of negative and positive polarity was observable, starting at the single HSO_4^- ion (for the negative case), up to 3300 Da, corresponding to mobility equivalent diameters up to approximately 2 nm. The larger cluster ions were characteristic of on-going new particle formation, as detected by other instruments, and were found to always contain H_2SO_4 molecules. Depending on exact experimental conditions, they also contained NH_3 , organic compounds (mainly amines), or both. A portion of a typical spectrum during one experiment is shown in Figure 1.

Correlations between features of the steady-state cluster distributions during nucleation and experimental variables give detailed insights into the early steps of new (charged) particle formation driven by sulfuric acid.

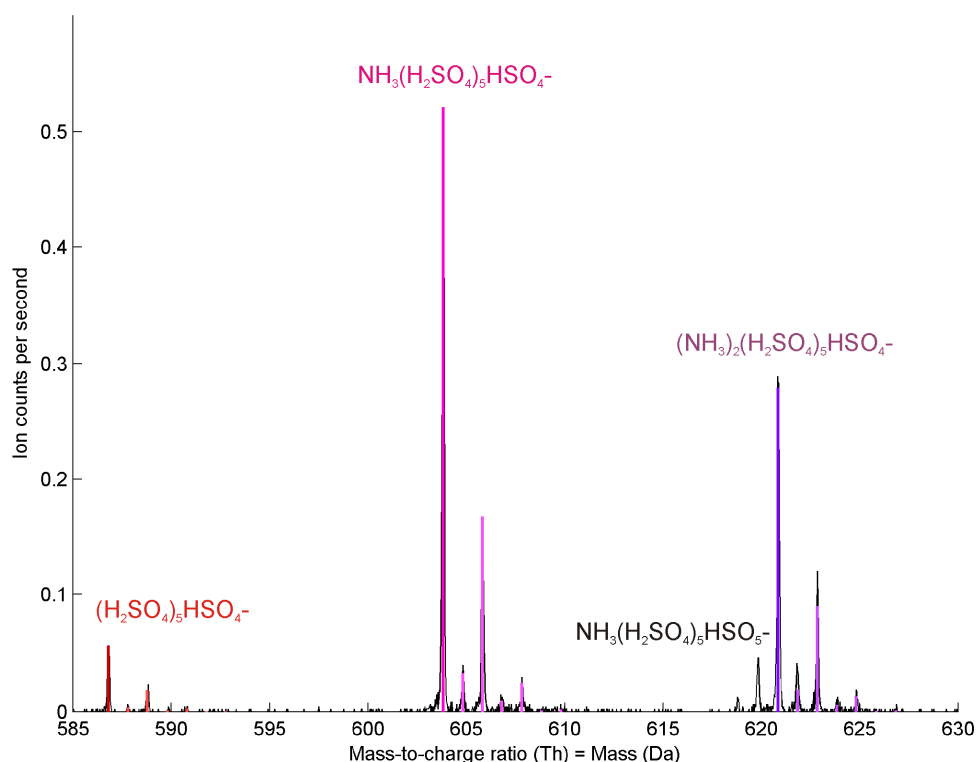


Figure 1. A portion of the negative ion spectrum, as recorded during a nucleation experiment in the CLOUD chamber. The raw data is displayed in black. Clear peaks are visible, originating from molecular clusters, as labelled. Predicted isotopic patterns are shown in colors for the three most abundant ion clusters visible in this portion.

One noteworthy issue of mass spectrometry of ion clusters with the APi-TOF is fragmentation processes in the low pressure regions inside the instrument. We are certain that evaporation of molecules from clusters occurs at some degree after sampling. H_2O molecules, for instance, were almost never found bound to ions (with the exception of pure water clusters). Comparisons to ion mobility spectrometers (as in Ehn *et al.*, 2011) can be made and help assessing the significance of post-sampling fragmentation.

ACKNOWLEDGEMENTS

This research was funded by the EC's 7th Framework Programme under grant agreement number 215072 (Marie Curie Initial Training Network "CLOUD-ITN"), by the Academy of Finland Center of Excellence program under project number 1118615, by the Academy of Finland under grant agreement number 1133872, by the German Federal Ministry of Education and Research under project number 01LK0902A and the Swiss National Science Foundation. CERN's support of CLOUD with important technical resources and provision of a particle beam from the PS is gratefully acknowledged.

REFERENCES

- Carslaw, K.S., R.G. Harrison and J. Kirkby (2002). Cosmic rays, clouds, and climate, *Science* **298**, 1732.
- Ehn, M., H. Junninen, S. Schobesberger, H.E. Manninen, A. Franchin, M. Sipilä, T. Petäjä, V.-M. Kerminen, H. Tammet, A. Mirme, S. Mirme, U. Hörrak, M. Kulmala and D.R. Worsnop (2011). An instrumental comparison of mobility and mass measurements of atmospheric small ions, *Aerosol Science and Technology* **45**, 522-532.
- Intergovernmental Panel on Climate Change, Solomon, S. *et al.*, Eds. (2007). Contribution of Working Group I to the Fourth Assessment Report of the Intergovernmental Panel on Climate Change, 2007 (Cambridge University Press, Cambridge, United Kingdom and New York, NY, USA).
- Junninen, H., M. Ehn, T. Petäjä, L. Luosujärvi, T. Kotiaho, R. Kostianen, U. Rohner, M. Gonin, K. Fuhrer, M. Kulmala and D.R. Worsnop (2010). A high-resolution mass spectrometer to measure atmospheric ion composition, *Atmos. Meas. Tech.* **3**, 1039–1053.
- Kirkby, J. (2007). Cosmic rays and climate, *Surv. Geophys.* **28**, 333-375.
- Kulmala, M., H. Vehkamäki, T. Petäjä, M. Dal Maso, A. Lauri, V.-M. Kerminen, W. Birmili and P.H. McMurry (2004). Formation and growth rates of ultrafine atmospheric particles: a review of observations., *J. Aerosol Sci.* **35**, 143-176.
- Riipinen, I., S.-L. Sihto, M. Kulmala, F. Arnold, M. Dal Maso, W. Birmili, K. Saarnio, K. Teinilä, V.-M. Kerminen, A. Laaksonen and K.E.J. Lehtinen (2007). Connections between atmospheric sulphuric acid and new particle formation during QUEST III–IV campaigns in Heidelberg and Hyytiälä, *Atmos. Chem. Phys.* **7**, 1899–1914.

AEROSOL OPTICAL PROPERTIES OVER CHINA OBSERVED WITH SATELLITE REMOTE SENSING

A.-M. SUNDSTRÖM¹, P. KOLMONEN², L. SOGACHEVA², E. RODRIGUEZ², M. HANNUKAINEN¹, K. ATLASKINA¹, and G. de LEEUW^{1,2,3}

¹Department of Physics, University of Helsinki, Helsinki, Finland.

²Finnish Meteorological Institute, Helsinki, Finland.

³TNO Environment and Geosciences, Utrecht, The Netherlands.

Keywords: Aerosol remote sensing, aerosol optical depth, China.

INTRODUCTION

Aerosols affect Earth's radiation budget directly by scattering and absorbing solar radiation, and indirectly by modifying the microphysical properties of clouds. However, large uncertainties still exist in current estimates of the aerosol effects on climate, mainly due to aerosols strong temporal and spatial variation. Satellites offer the opportunity to observe the spatial distribution of aerosols with adequate resolution and coverage on regional to global scales. The primary aerosol parameter retrieved from the satellite measurements is the aerosol optical depth (AOD), which describes quantitatively the column-integrated extinction of solar light caused by atmospheric aerosols. It can be determined from the top of the atmosphere (TOA) reflectance by an inversion algorithm over a cloud-free area.

In this work we present a study on aerosols in China using satellite data. China is one of the fastest growing economies in the world. Along with the continuously increasing population and strong economic growth, the increase of anthropogenic pollutants is evident. The key city centers in China are located mainly in the eastern and southern part of the country. The Beijing area in the north east, Shanghai and Yangtse River Delta in the east, Pearl River Delta in the south, and Sichuan basin in the center inland are having tens of millions inhabitants. Several studies have shown, that in major cities in China the mean aerosol mass concentration can be well above national and international standards (e.g. Xu *et al.*, 2002, Guinot *et al.*, 2007). Large amounts of aerosol and precursor gases exported from these areas can have significant impacts on air quality and climate on both regional and global scales (Takekawa *et al.*, 2009).

METHODS

The AATSR instrument (Advanced Along Track Scanning Radiometer) on board ENVISAT (ENVironmental SATellite) was initially designed for observing sea surface temperatures with high accuracy; however, the measurements made at two different viewing angles (at nadir and at 55° forward) renders the instrument suitable for the retrieval of aerosol properties as well. AATSR has seven wave bands in the visible and infrared regions, centered at 0.555, 0.659, 0.865, 1.61, 3.7, 11.0, and 12.0 μm . With a swath width of 512 km and nadir resolution of 1 x 1 km², AATSR reaches global coverage in about five days. The overpassing is about 10 am local time.

The AATSR Dual View (ADV) algorithm used at the Finnish Meteorological Institute and University of Helsinki is developed to retrieve aerosol optical properties over land. The dual view property is used in the ADV algorithm to eliminate the surface contribution from the top of the atmosphere

(TOA) reflectance. Hence, an additional surface reflectance model is not needed. For a cloud-free pixel the ADV algorithm produces the AOD over land at two different wavelengths: 0.555, and 0.659 μm . In addition to AOD, the retrieved parameters include mixing ratio, Ångström coefficient, and surface reflectance (optional). In this context the mixing ratio refers to the contribution of fine mode aerosols (particles having effective radius of about 0.1 μm) to the total aerosol extinction. It is noted that the ADV retrieves continuous mixing ratio, i.e. the mixtures of two different aerosol types used in the retrieval are not fixed but adjusted along the iteration.

The ADV input consists of two user-defined, pre-calculated aerosol models. The selection of the most representative aerosol models for the retrievals over China is based the results obtained in the study of (Sundström *et al.*, 2011). Both aerosol models, one representing the fine, and the other coarse mode aerosol, are described by a log-normal size distribution (geometrical mean radius and standard deviation) and a complex refractive index as given in Table 1.

Aerosol name	mode	r_g [μm]	(σ)	$Re(m)$	$Im(m)$	Reference
Industrial pollution	fine	0.092	1.526	1.410	0.006	(Omar <i>et al.</i> , 2005)
Neutral	coarse	0.590	2.115	1.430	0.008	(Levy <i>et al.</i> , 2007)

Table 1: The aerosol models used for the ADV retrieval input. The aerosol size distribution is assumed to be log-normal, described by the geometrical radius r_g and standard deviation σ . $Re(m)$ and $Im(m)$ indicate the real and imaginary part of the aerosol refractive index.

CONCLUSIONS

The AATSR data was retrieved for selected years between 2003 and 2009. To study the results over Eastern China, the AATSR retrievals were averaged to a $0.1 \times 0.1^\circ$ grid. It should be noted, that in the winter the AATSR retrieval at high latitude is affected by the large solar zenith angle and occasionally by snow on the ground. The ADV does not produce credible results for such highly reflecting surfaces. Therefore, northern China (including the Beijing area) lacks AATSR observations from about mid-December to mid-January.

Results show a clear difference in AOD between the densely populated/ industrialized regions in the eastern and southern parts of China, and rural areas in the north west (Fig. 1). The seasonal variation of the AOD pattern is most noticeable over areas having major anthropogenic activity; whereas, over the rural areas the AOD at 0.555 μm remains below 0.3 for the whole year. Generally lowest AODs are observed during the winter over the major part of the Eastern China; whereas, during the summer the AOD is higher than in other seasons over most areas.

The seasonal variation of the AOD over Beijing is stronger than in other key city areas. The AODs observed over Beijing area during the summer can be twice as high (the mode AOD at 0.555 μm about 0.8) as late winter or early spring (the mode AOD at 0.555 μm about 0.3). The AOD over Beijing is highly dependent on the direction of the air flow, which also explains the observed seasonal variation. During winter and spring clean airmasses from the north is advected frequently to Beijing, resulting in low AODs. On the other hand, during summer the airmasses over Beijing often originate from the heavily polluted areas in the south. Over Shanghai, Sichuan basin (Chengdu), and Pearl River Delta (Guangzhou) the AOD at 0.555 μm remains mainly over 0.5 throughout the seasons.

The AATSR mixing ratios indicate a clear dominance of the fine mode particles over Eastern China. Over urban areas the fine mode aerosols contribute 0.6-1.0 to the total aerosol extinction; whereas, in rural areas the mixing ratio is mainly below 0.5.

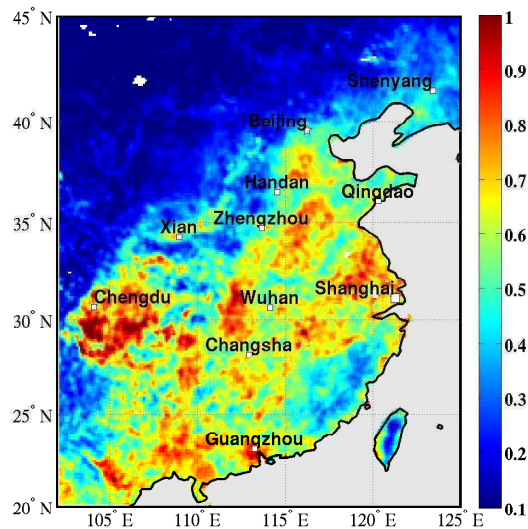


Figure 1: An example of the aggregate AOD over Eastern China obtained from AATSR for 2009 at $0.555 \mu\text{m}$ wavelength. The resolution is $0.1 \times 0.1^\circ$. White areas designate missing observations.

ACKNOWLEDGEMENTS

This work was supported by the projects EUCAARI, AMFIC, Megapoli and MACC.

REFERENCES

- Curier, L., G. de Leeuw, P. Kolmonen, A.-M. Sundström, L. Sogacheva, and Y. Bennouna (2009). Aerosol retrieval over land using the AATSR dual-view algorithm, In *Satellite Aerosol Remote Sensing Over Land*. (Springer Verlag), 135–159.
- Guinot, B., H. Cachier, J. Sciare, Y. Tong, W. Xin, and Y. Jianhua (2007). Beijing aerosol: Atmospheric interactions and new trends. *J. Geophys. Res.*, **112**, D14314.
- Levy, R. C. L. A. Remer, and O. Dubovik (2007). Global aerosol optical properties and application to Moderate Resolving Imaging Spectroradiometer aerosol retrieval over land. *J. Geophys. Res.*, **112**, D13210.
- Omar, A.H., J.-G. Won, D. M. Winker, S.-C. Yoon, O. Dubovik, and M.P. McCormick (2005). Development of global aerosol models using cluster analysis of AERONET measurements. *J. Geophys. Res.*, **110**, D10S14.
- Sundström, A.-M., P. Kolmonen, L. Sogacheva, and G. de Leeuw (2011). Aerosol retrievals over China with the AATSR Dual-View Algorithm. *accepted to Rem. Sens. Environ.*
- Takekawa, N., T. Miyakawa, M. Kuwata, Y. Kondo, Y. Zhao, S. Han, K. Kita, Y. Miyazaki, Z. Deng, R. Xiao, M. Hu, D. van Pinxteren, H. Herrmann, A. Hofzumahaus, F. Holland, A. Wahner, D. R. Blake, N. Sugimoto, T. Zhu (2009). Variability of submicron aerosol observed at a rural site in Beijing in the summer of 2006. *J. Geophys. Res.*, **114**, D00G05.
- Xu, J., M. H. Bergin, X. Yu, G. Liu, J. Zhao, C. M. Carrico, and K. Baumann (2002). Measurement of aerosol chemical, physical and radiative properties in the Yangze delta region of China. *Atm. Environ.*, **36**, 161–173.

Methane Emissions from Boreal Wetlands: A modelling study with the JSBACH model

Marin Tomašić¹, Teemu Hölttä¹, Robert Getzieh², Victor Brovkin²
Timo Vesala¹, Sampo Smolander¹, Thomas Kleinen², Christian Reick²
Maarit Raivonen¹, Jouni Susiluoto³, Álvaro Valdebenito⁴

1 Division of Atmospheric Sciences, Department of Physics, Helsinki University, Finland

2 Land in the Earth System, Max-Planck-Institute for Meteorology, Hamburg, Germany

3 Finish Meteorological Institute, Helsinki

4 Norwegian Meteorological Institute, Oslo

Abstract

Wetland are one of the main land sources for emitting methane. Estimated values of the global methane emission range from 100 to 231 Tg CH₄ yr⁻¹ which is considered together with emissions from other natural sources (termites, oceans etc.) between 28 to 43 % of the emissions ([1]). Peatland ecosystems have a very crucial role in estimating the potential overall CH₄ emission flux. Although covering only about 3 % of the globe, they are a carbon storage reserve pool for up to 30 % of the global terrestrial land carbon ([4]). Further temperature rise and its following microbial activities in peat will cause higher anaerobic CH₄ production levels and thus have a strong coupled feedback on global warming in general. Especially boreal peatlands have a large potential to contribute to this process due to the high carbon storage during the Holocene. The CBALANCE carbon tool is part of the JSBACH land component of the MPI Earth System Model (MPI-ESM) and is currently amended to include biogeochemical transport in peatlayers and its release into the atmosphere. The main CH₄ transport processes (1. Diffusion in the soil layers, 2. plant mediated transport of CH₄ and 3. Bubbling) have been described already in previous works (e.g. by [2] using the LPJ-WHY-ME model, [3]) and we will follow them as a benchmark in a first order approach. The second emission process (plant mediated transport) will be modelled and tested with different parametrizations to simulate the change from the water phase into the plant and its further CH₄ transport within aerenchyma. We will check the different ways to model the transfer of CH₄ into the atmosphere (via piston velocity as well as with a diffusion-equilibrium approach). The ebullition described by [2] is currently developed and we will present model runs. If possible, a new way to simulate the bubble formation ([5]) will also be shown.

References

- [1] K. L. Denman, G. Brasseur, A. Chidthaisong, P. Ciais, P. M. Cox, R. E. Dickinson, D. Hauglustaine, C. Heinze, E. Holland, D. Jacob, U. Lohmann, S. Rmachandran, P. L. da Silva Dias, S. C. Wofsy, and X. Zhang. Couplings between changes in the climate system and biogeochemistry. In *In Solomon et al. [2007], chapter 7, pages 499–588.*
- [2] Wania, R., I. Ross, and I. C. Prentice (2009), Integrating Peatlands and Permafrost into a dynamic global vegetation model: 1. Evaluation and sensitivity of physical land surface processes In *Global Biogeochem. Cycles 23*
- [3] Walter, B., and M. Heimann, A process-based climate sensitive model to derive the methane emissions from natural wetlands: Application to five wetland sites, sensitivity to model parameters and climate In *Global Biogeochem. Cycles 14, 745–766*
- [4] Rydin, H., and Jeglum, J. The Biology of Peatlands *Oxford University Press, New York*
- [5] T. Hölttä, T. Vesala, M. Perämäki, E. Nikinmaa (2002). Relationship between Embolism, Stem Water Tension and Diameter Changes. *Journal of Theoretical Biology 215: 23-38*

LARGE EDDY SIMULATION MODEL FOR STUDYING ATMOSPHERIC TURBULENCE

M. K. TU¹, A. HELLSTEN², T. MARKKANEN² and T. VESALA¹

¹Department of Physics, University of Helsinki, Helsinki, Finland.

²Finnish Meteorological Institute, Finland.

Keywords: LES, TURBULENCE, FINITE-DIFFERENCE METHOD.

INTRODUCTION

Large Eddy Simulation (LES) is an efficient tool to study atmospheric boundary layer (ABL) phenomena. Our ultimate plan is to study flux footprints using LES over simplified homogeneous urban-like surface topography consisting of a large array of rectangular obstacles. So far, footprints have been estimated using LES over homogeneous flat terrain (Steinfeld *et al.*, 2008; Leclerc *et al.*, 1997). Footprint estimation is based on Lagrangian-stochastic (LS) particle modelling coupled with LES. A large ensemble of particles is released from near ground surface and then followed in time as the turbulent flow field advects the particles. The footprint can then be calculated using the method proposed by Rannik *et al.* (2003).

The strategy of this study is to repeat one of the cases studied previously by Steinfeld *et al.* (2008) firstly. Only after this step we will start working with the more complex topography. We are using the PALM LES model (Raasch and Schröter, 2001) as did Steinfeld *et al.* (2008) as well. They reported that the second-order central differencing scheme of Piaseck and Williams (1970) (PW) for the advection terms is not suitable to be employed with the LS particle model as unphysical high particle accelerations occurred. This is very likely owing to the dispersive and non-dissipative nature of the numerical error of the PW-scheme. Therefore, they used the upstream-spline scheme (Mahrer and Pielke, 1978) (UPS) which involves dissipative numerical error. On the other hand, the numerical dissipation is usually considered harmful in LES and therefore undesired. Other disadvantages of the UPS scheme in PALM are the larger required computing time and the fact that it can only be used with the first-order Euler time marching scheme while the PW-scheme is normally used with the fourth-order Runge-Kutta time marching. The aim of this paper is to compare convective ABL results computed using both the UPS and PW schemes to find out how strongly the numerical dissipation manifests itself in the results. Moreover, the latest version of PALM (version 3.8) includes a new fifth-order accurate upwind-type scheme (Wicker and Skamarock, 2002) (WS) which is also slightly dissipative. We will also compare the results computed using the WS-scheme with those using the PW- and UPS-schemes. It is assumed that the WS-scheme could be suitable to be used with the LS-particle simulations, although we have not yet tested this. If this assumption holds, it might be a good alternative to the WS-scheme to be used in our planned footprint study.

DESCRIPTION OF THE TEST CASE

The research will be based on the Large Eddy Simulation model (PALM) (Raasch and Schröter, 2001), of which the latest version (version 3.8) is employed here. Table 1 shows the most important physical and numerical parameter setting of the study. The model domain extended 8,640 m in each of the two horizontal directions and 1,440 m vertically. The resolution used was 10 m in all directions and the geographic latitude was set for 46 deg. N for setting the Coriolis parameter. In PALM, u - and v -wind components were initialized with values of 4 m/s and 0 m/s, respectively. At the bottom surface, kinematic sensible heat flux of 0.05 K m/s was prescribed as well as the roughness length was set to 0.14 m. In this study, we initialized the potential temperature field with a linearly increasing function with surface value

of 300 K and lapse rate of 3 K/km. All parameters were fixed for three different schemes of PW, UPS, and WS.

Model Initial Data Setting	
model domain, x, y, z	(8640 m) x (8640 m) x (1440 m)
resolution, $\Delta x, \Delta y, \Delta z$	10 m
latitude	46 deg. N
geostrophic wind components	$u = 4$ m/s ; $v = 0$ m/s
surface roughness length	0.14 m
kinematic surface temperature flux	0.05 K m/s
surface potential temperature	300 K
free-atmosphere potential-temperature gradient	3 K/km

Table 1. Description of the physical and numerical parameters setting.

RESULTS AND DISCUSSION

The horizontally averaged vertical profiles of wind components, wind-wise component of the momentum flux and variances of the velocity-component fluctuations are shown in Fig. 1. Potential temperature and sensible heat flux profiles are shown in Fig. 2. According to Figs. 1 and 2, all the profiles computed using the WS-, UPS-, and PW-schemes look qualitatively correct. However, the v -component of wind velocity in the UPS-result is smaller compared to the PW- and WS-schemes. Moreover, the wind velocity fluctuations in the UPS-result are clearly smaller than the velocity perturbations in the PW- and WS-results. The patterns of vertical momentum flux of u - and v -components have differences between the UPS- and WS-results. In the UPS-result, the u -component of the total momentum flux increases along the height under 700 meters height but showing the transition between 20 and 50 meters height. In the WS-result, the v -component values of the total momentum flux are much larger than the values in the UPS-result. The simulation results of vertical profiles of potential temperature obtained with the PW- and WS-schemes are similar to each other, but the UPS-scheme gives somewhat lower temperature in the mixed layer. This is a consequence of the reduced mixing by the convective and turbulent motion owing to the numerical dissipation of the kinetic energy. Figures 3, 4 and 5 illustrate the velocity components and potential temperature distributions on vertical cross sections using the PW-, UPS-, and WS-schemes, respectively. These colour plots show that the PW- and WS-results involve clearly more small-scale motion than the UPS-result in which the smallest eddies have mostly smeared out owing to the numerical dissipation. In general, the WS-result looks qualitatively quite similar to the PW-result. However, a more careful spectral analysis is still needed for a more detailed comparison of the numerical properties of these schemes.

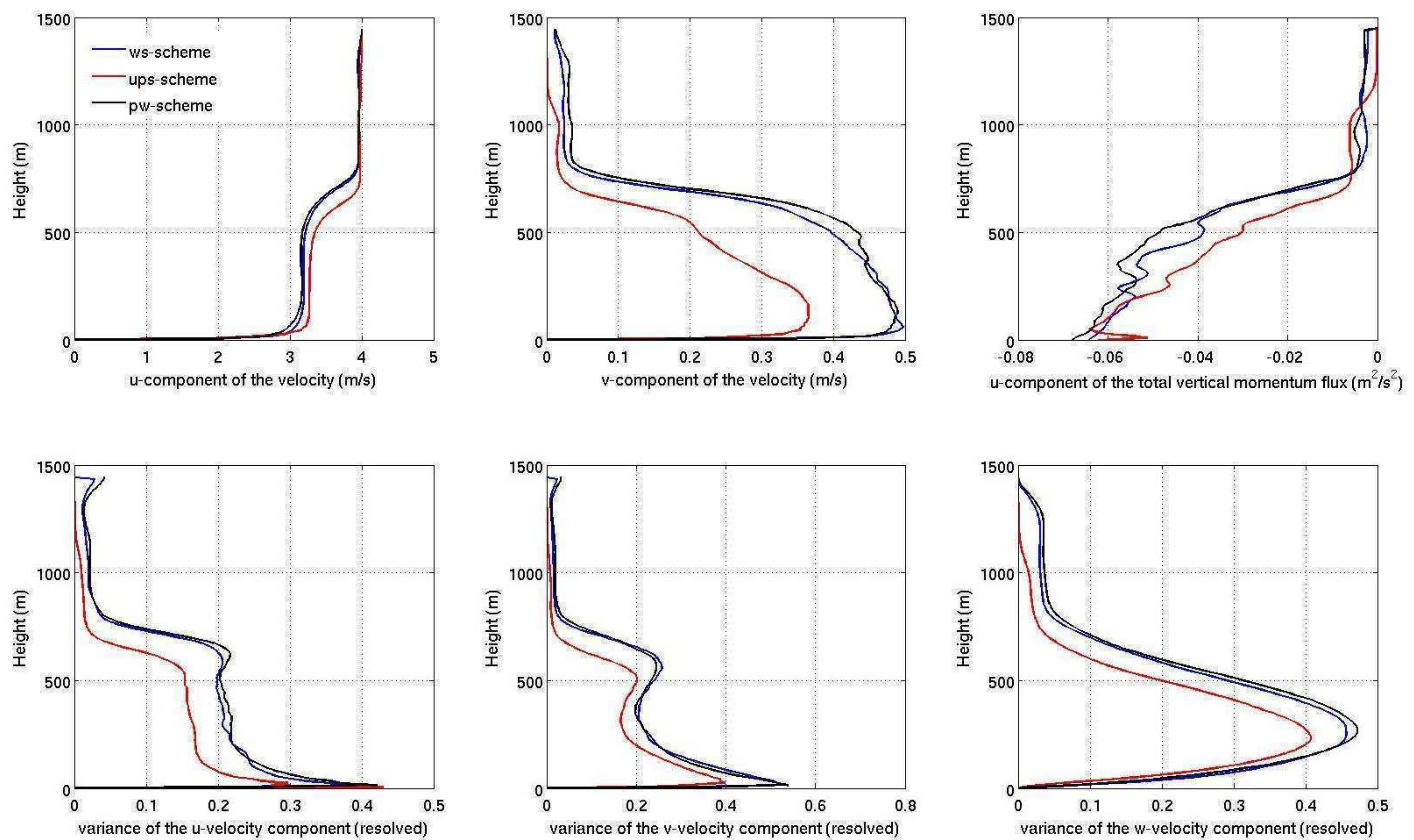


Figure 1. The vertical profiles of u- and v-components for the WS-, UPS-, and PW-schemes.

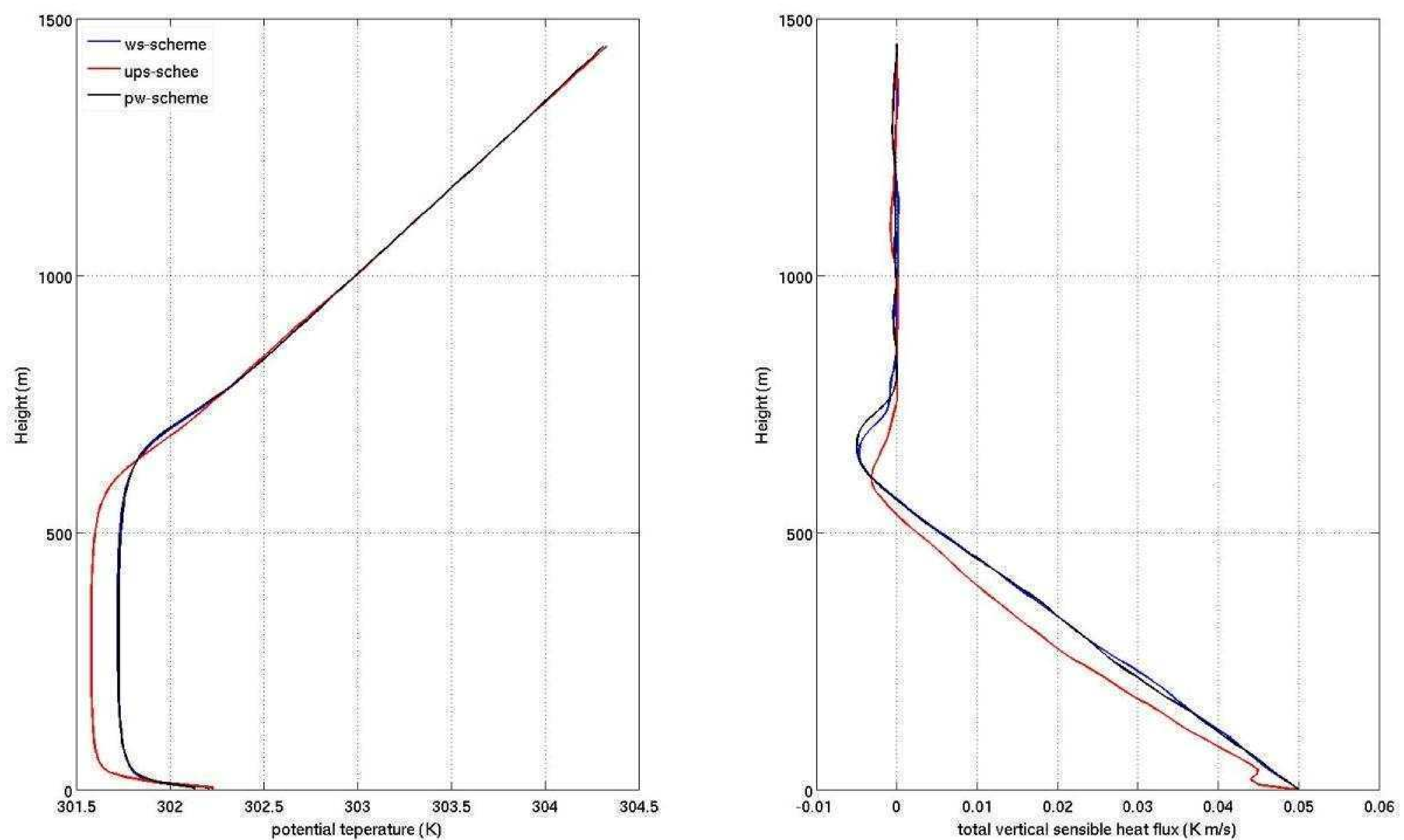


Figure 2. The vertical profiles of potential temperature and total vertical sensible heat flux for the WS-, UPS-, and PW-schemes.

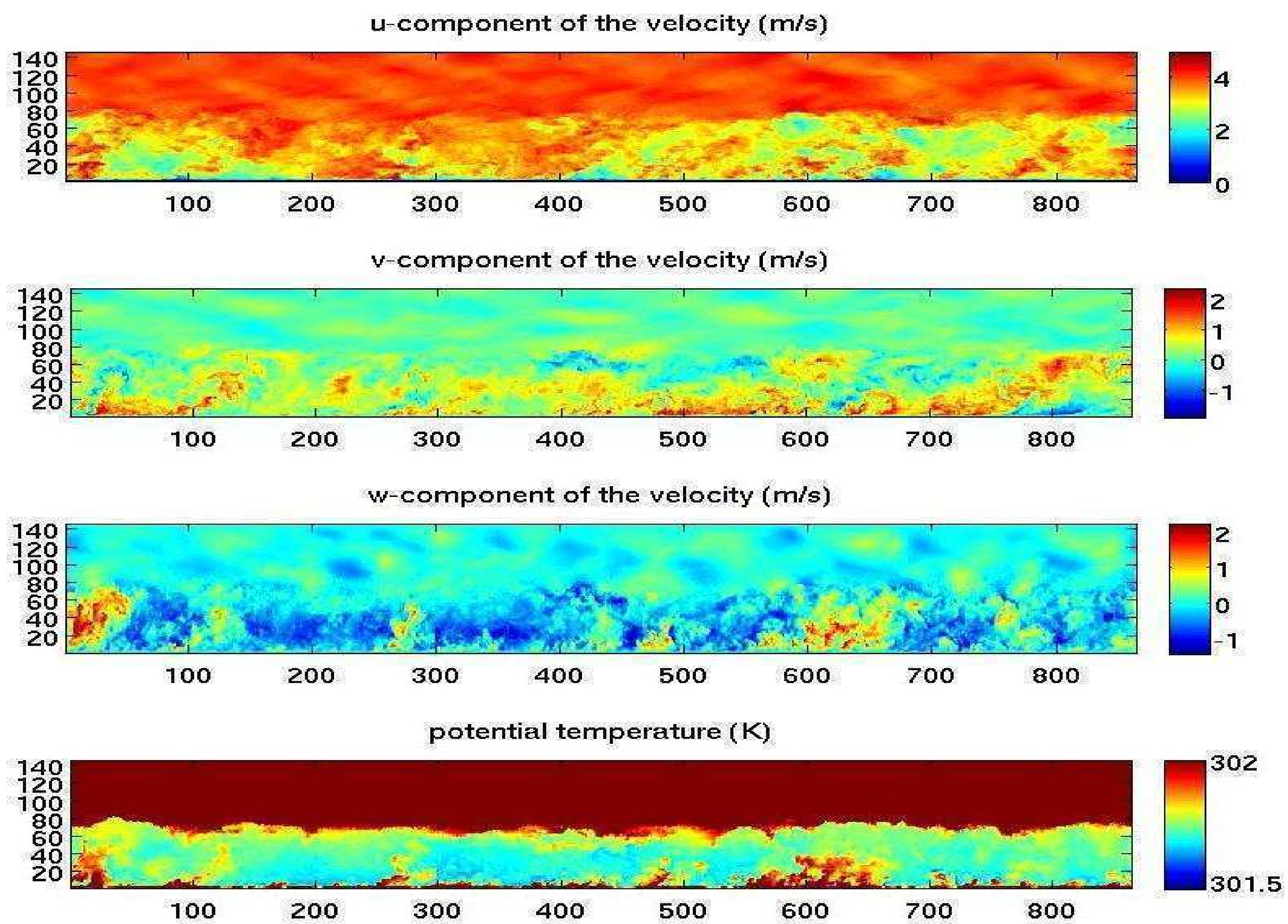


Figure 3. The vertical cross sections of wind velocity components and potential temperature by using the PW-scheme. Horizontal axis is the grid point number in x -direction. Vertical axis is the grid point number in z -direction.

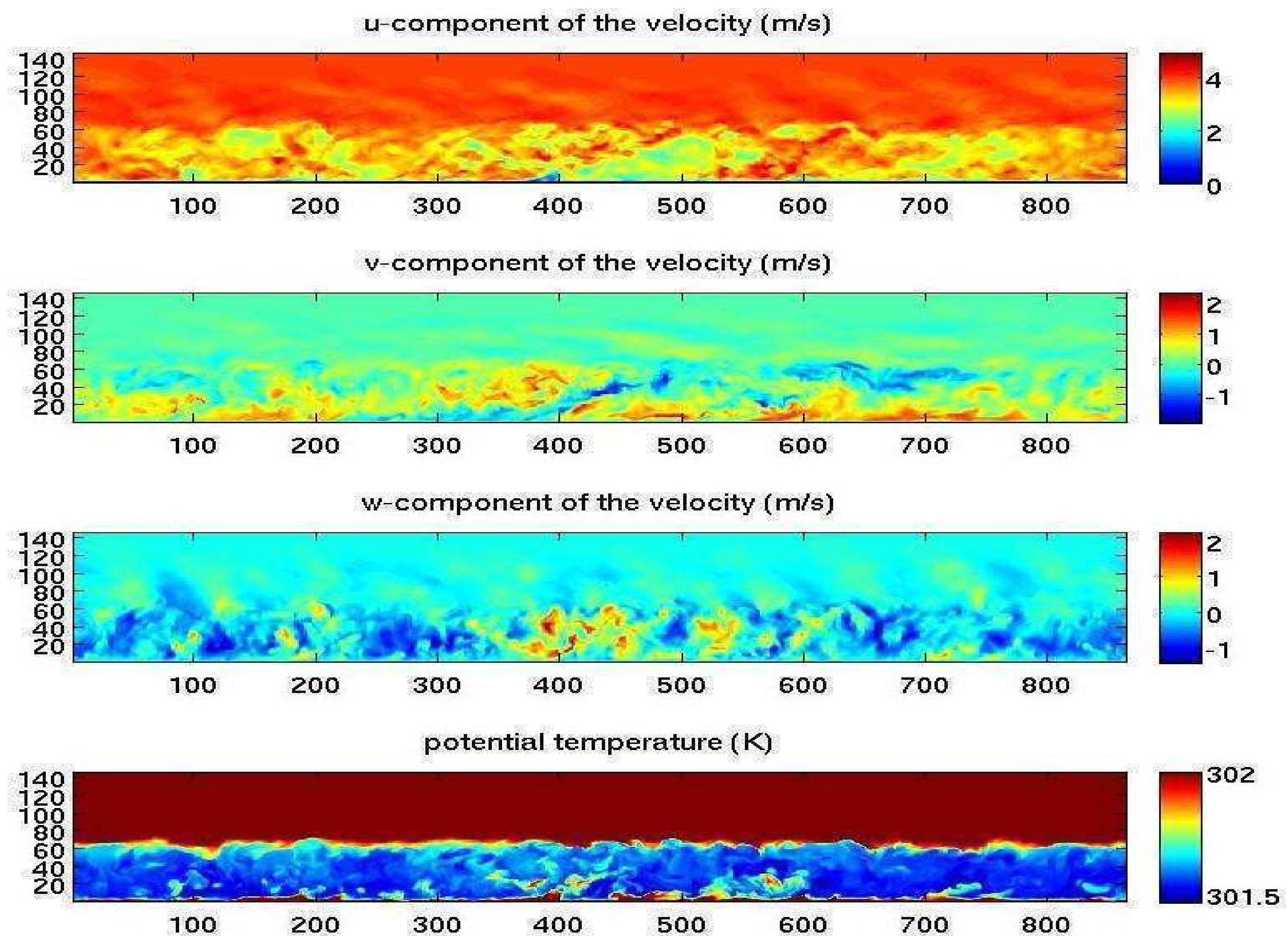


Figure 4. The vertical cross sections of wind velocity components and potential temperature by using the UPS-scheme. Horizontal axis is the grid point number in x -direction. Vertical axis is the grid point number in z -direction.

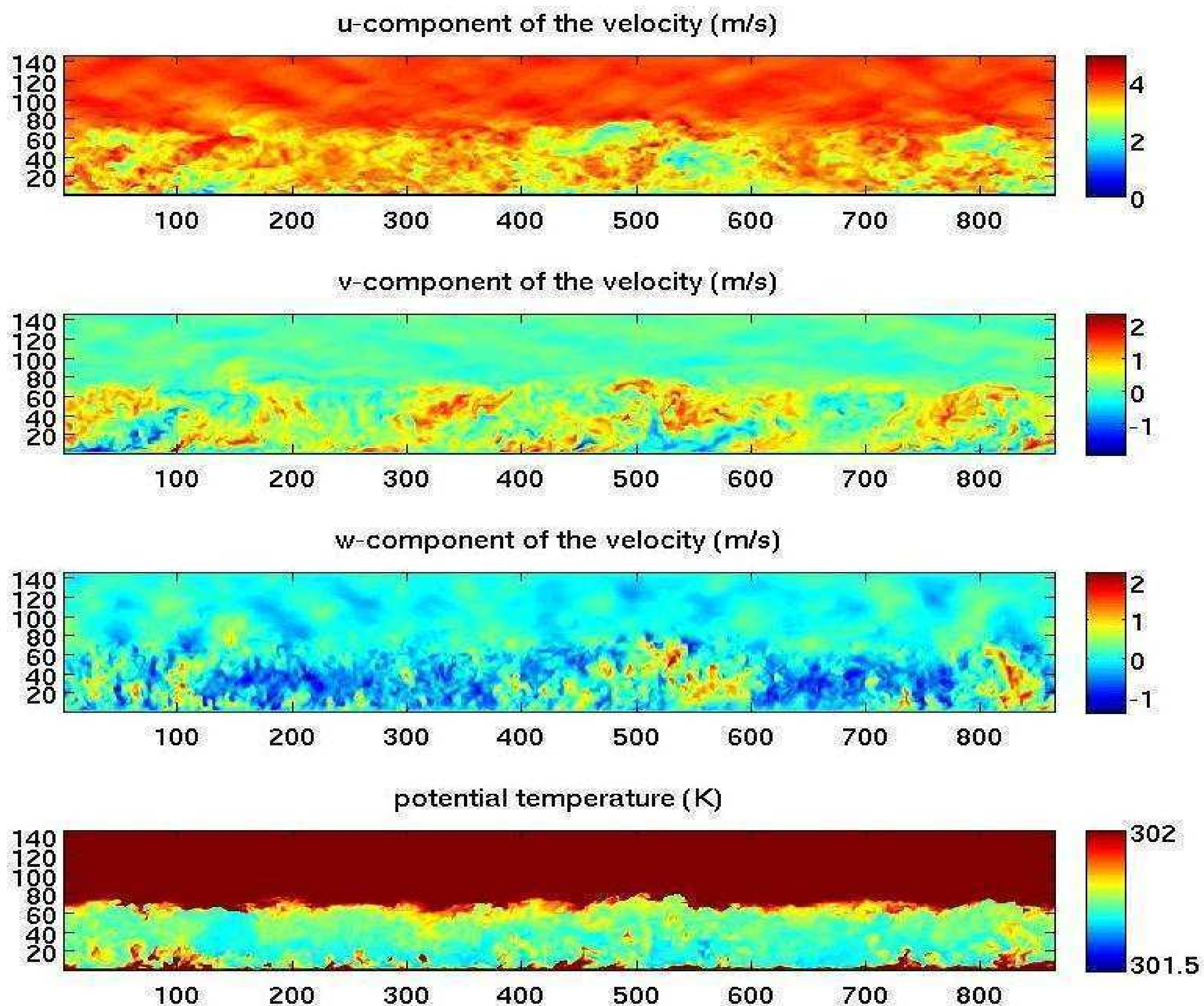


Figure 5. The vertical cross sections of wind velocity components and potential temperature by using the WS-scheme. Horizontal axis is the grid point number in x -direction. Vertical axis is the grid point number in z -direction.

CONCLUSIONS

A convective ABL has been simulated using the PALM LES code. Results computed using three different finite-difference advection schemes are compared. These schemes are: central scheme (Piaseck and Williams, 1970) (PW), upstream-spline scheme (Mahrer and Pielke, 1978) (UPS) and fifth-order upwind scheme (Wicker and Skamarock, 2002) (WS). The UPS-result show quite strong effects of numerical dissipation compared with the PW- and WS-schemes. In general, the WS-result looks qualitatively quite similar to the PW-scheme. However, a more careful spectral analysis is still needed for a more detailed comparison of the numerical properties of these schemes.

REFERENCES

- Leclerc M.Y., Shen S.H., and Lamb B. (1997). Observations and large-eddy simulation modeling of footprints in the lower convective boundary layer, *J Geophys Res Atmos*, **102**, 9323–9334.
- Mahrer, Y., and R. A. Pielke (1978). A test of an upstream spline interpolation technique for the advective terms in a numerical mesoscale model, *Wea. Rev.*, **106**, 818-830.
- Piascek S. A. and Williams G. P. (1970). Conservation properties of convection difference schemes. *J. Comput. Phys.*, **6**, 392-405.
- Rannik Ü., Aalto P., Keronen P., Vesala T. and Kulmala M. (2003). Interpretation of aerosol particle fluxes over a pine forest: Dry deposition and random errors, *J. Geophys Res.*, **108**, 4544.

- Raasch, S. and Schröter, M. (2001). PALM – A large eddy simulation model performing on massively parallel computers, *Z. Meteorol.*, **10**, 363–372.
- Steinfeld G., Raasch S., and Markkanen T. (2008). Footprints in homogeneously and heterogeneously driven boundary layers derived from a Lagrangian stochastic particle model embedded into large-eddy simulation, *Boundary-Layer Meteorol.*, **129**, 225–248.
- Wicker, L. J. and Skamarock, W. C. (2002). Time splitting methods for elastic models using forward time schemes, *Monthly Weather Review*, **130**, 2088–2097.

CO₂ ANOMALIES ALONG FOREST AND MIRE HYDROLOGICAL ECOTONE

B. ĀTUPEK¹, K. MINKKINNEN¹, P. KOLARI¹, M. STARR¹, J. ALM^{2a}, T. VESALA¹, J. PUMPANEN¹,
M. PULKKINEN¹, J. LAINE^{2b} and E. NIKINMAA¹

¹Department of Forest Sciences, P.O. Box 27, 00014 University of Helsinki, Finland.

^{2a}Finnish Forest Research Institute, P.O. Box 68, 80101 Joensuu, Finland.

^{2b}Finnish Forest Research Institute, Kaironiementie 54, 39700 Parkano, Finland

Keywords: Carbon balance, Landscape, Forest and peatland ecotone, Hydrological gradient.

INTRODUCTION

Although the boreal zone CO₂ exchange has been studied in detail by chamber and eddy covariance (EC) methods for decades on typical ecosystems (Kolari *et al.* 2006, Kolari *et al.* 2009, Pumpanen *et al.* 2004, Riutta *et al.* 2007, Vesala *et al.* 1998, Vesala *et al.* 2010), the mesoscale spatial variation of adjacent transitional forests and mires is still poorly known. Especially little is known of the contribution of the forest and mire margin, frequently fluctuating between wet and dry conditions, into the mesoscale CO₂ budget of the ecotone stretching between the upland xeric forest and lowland sparsely forested wet mire. Is the boreal forest - mire margin acting as a sink or source of CO₂? Is the forest - mire margin tree assimilation larger than organic matter decomposition (when water table draws down) during dry year? Is the soil approaching water saturation (when water table draws up) during wet year limiting the forest - mire margin tree assimilation, and at the same time non-restricting the decomposition of more than 20 cm deep organic horizon? The answers to corresponding questions are not evident from typical forest or typical mire Carbon balance studies.

This study brings insights on CO₂ exchange processes for forest - mire transitional forest types in comparison to typical upland forest types and sparsely forested open mire types during typical (2005), exceptionally wet (2004), and dry (2006) years. Additionally this study evaluates the role of forest floor vegetation along the forest and mire ecotone as a potential trigger-point in mesoscale CO₂ balance sensitive to moisture variation.

METHODS

The Vatiharju-Lakkasuo ecotone of nine forest and mire stations ECOGRAD forms a gradient in vegetation distribution, soil moisture and nutrient conditions in Central Finland (61° 47', 24° 19') (Ātupek *et al.* 2008). The SMEARII eddy covariance station for continuous measurements of forest-atmosphere relations recorded since 1996 (<http://www.honeybee.helsinki.fi/smear>) (Vesala *et al.* 1998, Mäkelä *et al.* 2006) is located 6km apart north-west from ECOGRAD. The environmental data (light, temperature, moisture) between ECOGRAD and SMEARII are strongly correlated. The ECOGRAD forests are situated along 450 m transect with a relative relief of 15 meters and a 3.3 % slope facing NE (Figure 1). The forest types range upland forests on mineral soil, forest and mire transitions on gleyic soil, and sparsely forested mires on histosol. Hydrological conditions are ranging from the upslope xeric Scots pine forest situated on the crest of glacial sandy esker through midslope subxeric Scots pine Norway spruce forest, through mesic and herb-rich spruce dominated types, through forest and mire transitions of paludified mixed spruce pine birch forests, and downslope to permanently wet tall-sedge pine fens (Figure 1)

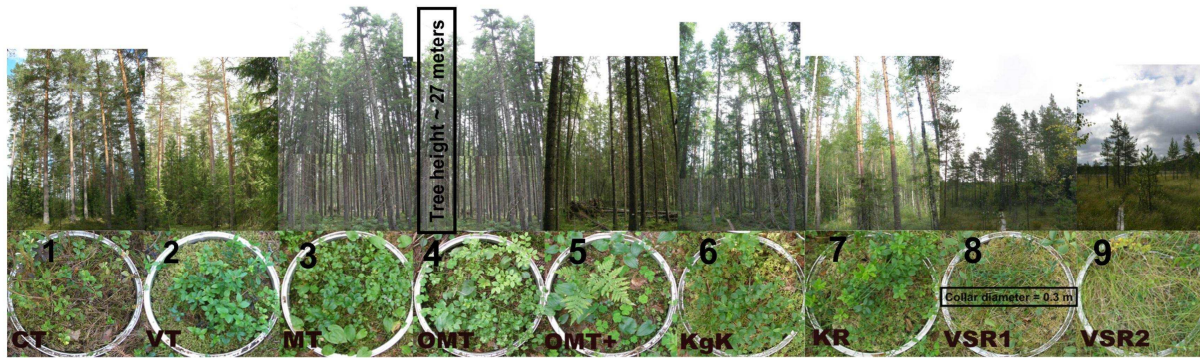


Figure 1. Photographs of nine stations of 450 m long Vatiharju - Lakkasuo forest - mire ecotone in Finland. Photographs of tree stands and ground vegetation encircled in metallic collars for upland xeric, subxeric, mesic and herb-rich forest types (1 CT - Calluna, 2 VT - Vitis Idea, 3 MT - Myrtillus, 4 OMT - Oxalis-Myrtillus); paludified forest - mire margin types (5 OMT+ - Oxalis-Myrtillus Paludified, 6 KgK - Myrtillus Spruce Forest Paludified); sparsely forested wet mire types: 7 KR - Spruce Pine Swamp, 8 VSR1 and 9 VSR2 - Tall Sedge Pine Fen). Forest types were classified according to classification system of Cajander (1949), and Laine *et al.*(2004).

The ECOGRAD micrometeorological and gas exchange measurements were taken weekly during summers of 2004 (July-November), 2005 (May-November), 2006 (May-September), and occasionally during winters. The measurements of the forest floor photosynthetically active radiation (PAR_{ff}), the soil temperatures in 5 cm depth (T_5), the volumetric soil water content in 10 cm depth, the depth of water level, the forest floor photosynthesis and respiration (P_{ff} , and R_{ff}) and the forest floor net exchange (NE_{ff}) followed the same procedure as described by Tupek *et al.* (2008).

RESULTS

The dynamics of upland forest and lowland mire were in meteorological terms highly comparable (Fig. 2 and Fig.3) Daily patterns of air temperatures, precipitation sums, and photosynthetically active radiation above the forest canopy were identical between forest and mire. Except for winter, and exceptionally early spring in 2006, the soil temperature profiles measured in subxeric pine forest (SmearII station) were around summer peak colder by 2 °C on average from temperatures of wet mire (Lakkasuo station), while temperatures during whole autumn followed same pattern. Figures 2a and 2b shows contrasting temporal variations between 3 consecutive years. Therefore years were generally classified as '2004 - wet and cold', '2005 - intermediate' or 'typical', and '2006 - dry and warm'. The dynamic patterns of forest and mire ecosystem daily air temperatures and precipitation sums are autocorrelated.

The measured instantaneous half hourly meteorological differences in photosynthetically active radiation intercepted onto the forest floor (PAR_{ff}), soil temperature at 5 cm (T_5), soil water content at 10 cm (SWC θ_{10}), and water table depth (WT), forest floor photosynthesis and respiration (P_{ff} , and R_{ff}) and the forest floor net exchange (NE_{ff}) between forest types along the ecotone are shown on Figure 3).

The prevailing minimum forest floor light along ecotone was observed in the subxeric and herb rich upland Spruce-Pine Vaccinium vitis idea type forest (VT), Spruce Myrtillus type forest (MT), and Spruce Oxalis-Myrtillus type forest (OMT) on mineral soils and on frequently paludified gleyic soils with deeper organic horizon of the forest - mire edge stations, Oxalis - Myrtillus paludified type (OMT+) and Spruce Myrtillus paludified forest type (KgK). The xeric and wet edge of ecotone with sparser forest canopies more than doubled intercepted forest floor light, while mire with scarce pines Tall-sedge Pine Fen type (VSR2) received almost the same unobstructed light levels as measured forest canopy of SmearII, or open mire station Lakkasuo. The PAR_{ff} measurements of 2006 often doubled the measured amount of received light by forest floor in 2005, in 2004 PAR_{ff} weren't measured (Figure 3a).

Beside PAR_{ff} extremities, the highly noticeable environmental difference along the ecotone between upland forest and mire types was increasing soil moisture (Figure 3c, and 4d) and rising water table level (Figure 3d, and 4e). Water table depth of 2004 of all forest and mire types was similar to WT of 2005, while 2006 drought was mainly affecting forest mire transitions and mires (Figure 3d; OMT+, KgK, KR, VSR1, and VSR2). Temporal soil moisture and water table dynamics were in agreement to dynamics of upland forest station SmearII and mire station Lakkasuo (Figures 2b, 4c, and 4d) showing for all years typical spring maximum after snowmelt, summer minimum, and soil water recharge in late summer and autumn. Although trends of soil water dynamics were typical, wet conditions of 2004 contrasting to drought in 2006 were exceptional.

The forest floor respiration (R_{ff}) measurements as total ground level CO_2 efflux determined from the increasing concentration gradient in non-transparent chamber showed dynamic synergies of soil carbon pool decomposition, and respiration of tree and ground vegetation roots. Spatial variation of R_{ff} oscillation showed lower amplitude than other two component CO_2 fluxes (Figure 3e). Generally during all years, no distinct trend in spatial variation between ecosystems R_{ff} was observed. The ecosystems could not be easily ranked by R_{ff} for example according to increased soil moisture levels or by other common single environmental factor. The R_{ff} spatial variation of ecotone forest and mire types showed in each moisture group of ecosystems (upland forest, transitions, and mires (Figures 3c and 3d)) site types with dominant R_{ff} fluxes (CT, OMT, KgK, VSR2) and site types with lower R_{ff} (VT, OMT+, VSR1) (Figure 3e). The R_{ff} measurements during 2004 wet and 2005 intermediate moisture conditions ranged in similar patterns along the ecotone, while in 2006 eight forest and mire types forest floor respiration levels dropped except for only one increased response of R_{ff} to drought in Tall-sedge pine fen (VSR2 mire station).

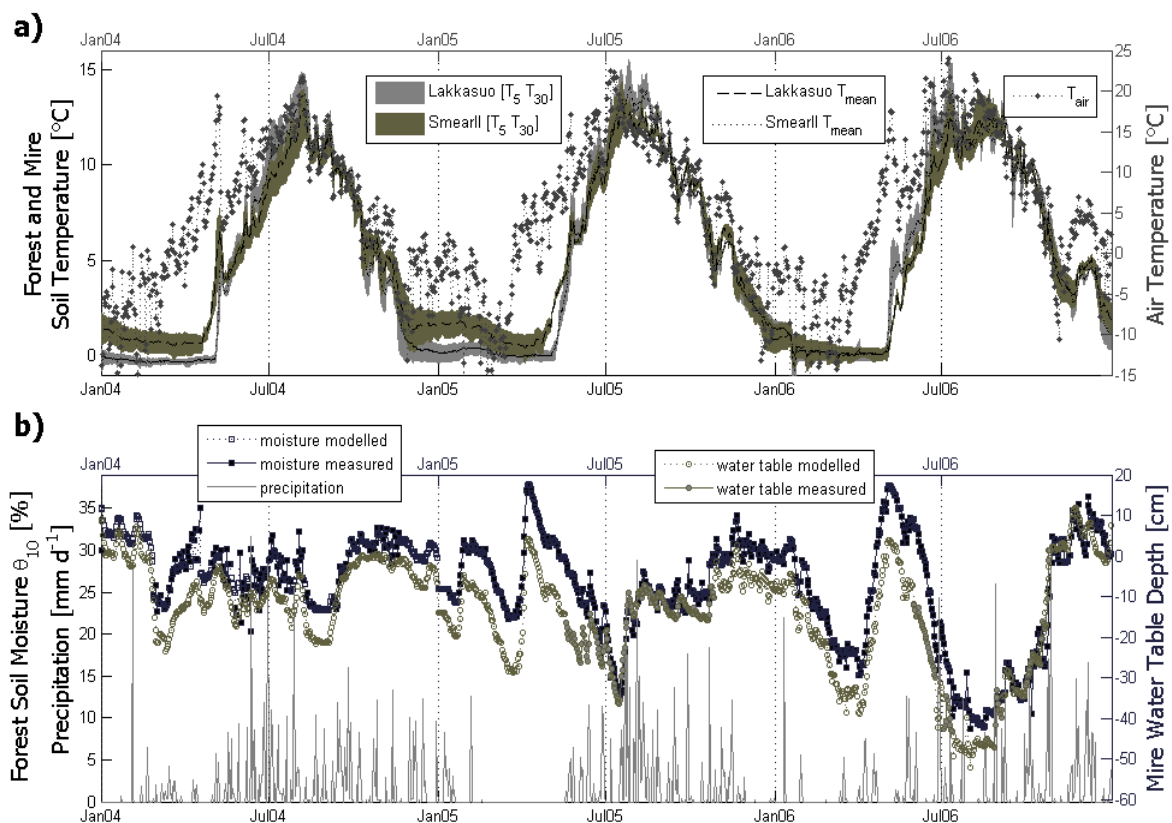


Figure 2. The comparison of meteorological factors between contrasting typical subxeric Scots pine forest in Hyytiälä (SMearII eddy covariance station) and 6km away located typical wet mire Lakkasuo (Tall sedge pine fen, VSR2 station of ECOGRAD) during 2004 (wet/cold), 2005 (typical), and 2006 (dry/warm) years. a) Daily trends of soil temperature intervals at 5, 30 cm depths, and air temperature. b) Daily trends of SmearII soil water content at 10 cm depth, Lakkasuo water table depth, and precipitation sums.

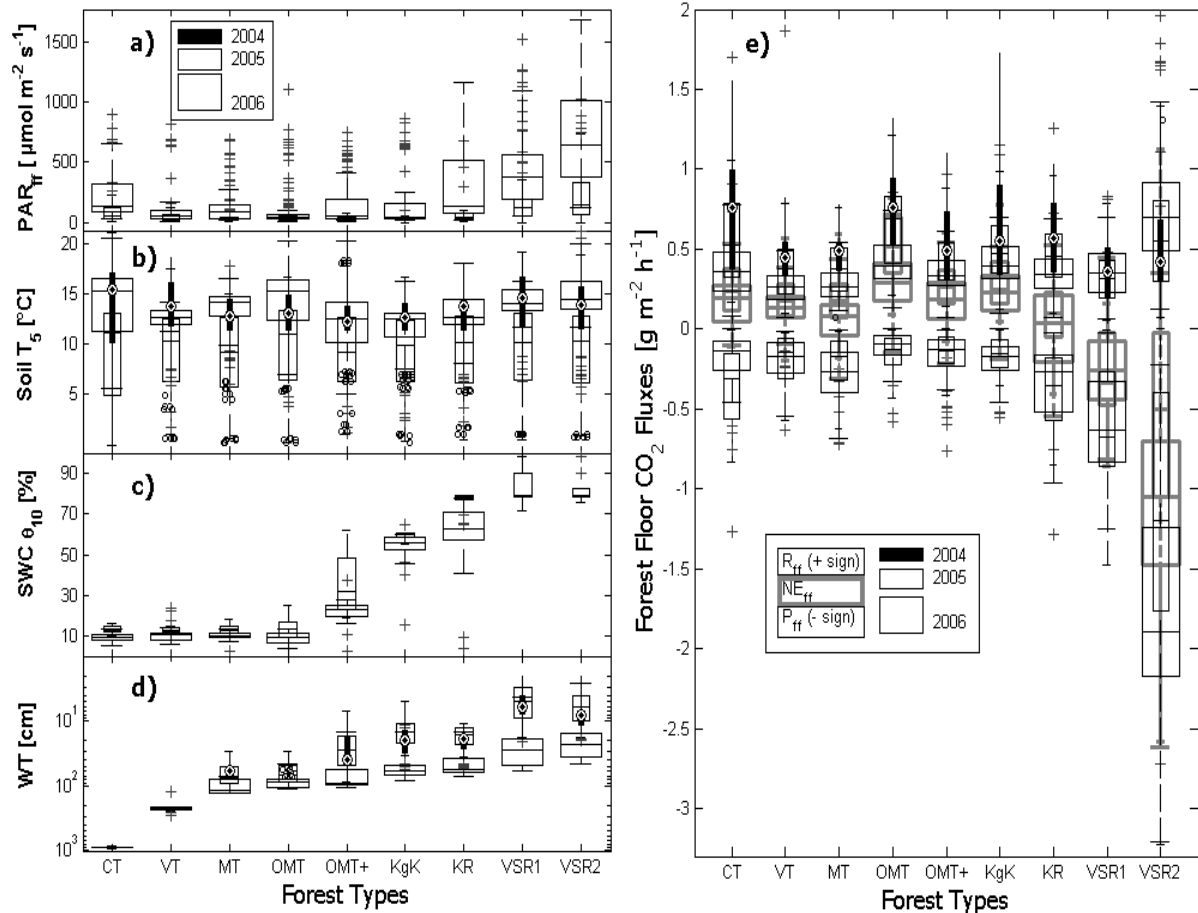


Figure 3. The range of instantaneous measurements collected during years 2004 (compact narrow box), 2005 (open narrow box), 2006 (open wide box) and grouped into quarters around the median for each forest and mire type. The figure panels show a) the forest floor photosynthetically active radiation (PAR_{ff}), b) the soil temperatures in 5 cm depth (T₅), c) the volumetric soil water content in 10 cm depth, d) the water level, and e) the forest floor photosynthesis and respiration (P_{ff}, and R_{ff}, black box) and the forest floor net exchange (NE_{ff}, graybox). Note, that lower soil temperature measurements in 2005 were result of prolonged measuring season into colder spring and autumn periods and were not a result of colder growing season.

The forest floor net exchange (NE_{ff}) as total ground level CO₂ efflux determined from the increasing concentration gradient in transparent chamber showed dynamic synergies of R_{ff}, plus photosynthesis of forest floor vegetation (P_{ff}, negative sign). Differences in NE_{ff} dynamics and spatial variation among forest and mire types along the ecotone observed in increasing manner between forested mires primarily reflected patterns of P_{ff} (Figure 3e). Obviously, the P_{ff} measured values of sparsely forested mires were larger than P_{ff} of forest - mire transition, and P_{ff} of upland forest types under denser tree stand canopies and lower PAR_{ff} values (Figures 3a and 3e).

Although general pattern of NE_{ff} and P_{ff} along the ecotone during two 2005 and 2006 measurement seasons was the same, distinct contrasting responses of forest and mire types CO₂ flux measurements to drought conditions were observed. For example forested mires VSR1, and KR both slightly reduced carbon sequestration during season affected by drought, while VSR2 resulted in increased P_{ff} values. Forest-mire transitions KgK and OMT+ P_{ff} measurements were almost identical in both seasons. For upland forests types the major drought response was P_{ff} reduction in Calugna type (CT) xeric pine forest versus P_{ff} increase in Myrtillus type (MT) spruce forest. Interestingly, generally stronger reduction of R_{ff} than P_{ff} of ecotone ecosystems during dry year 2006 generally weakened NE_{ff} source character of upland forests and transitions, and strengthened NE_{ff} sink character of sparsely forested mires (Figure 3e). Worth noticing were also negative instantaneous net forest floor CO₂ exchanges especially in upland forests

during 2006; e.g. large forest floor sequestration capacity of Myrtillus type (MT) spruce forest strongly overwhelming forest floor synergic CO₂ sources including supposedly large component of tree root respiration.

ACKNOWLEDGEMENTS

This work was supported by the Nordic Centre for Studies of Ecosystem Carbon Exchange and its Interactions with the Climate System (NECC), Nordic Centre of Excellence (NCoE), REBECCA by Helsinki University Environmental Research Centre (HERC), Finnish Centre of Excellence in Physics, Chemistry, Biology and Meteorology of Atmospheric Composition and Climate Change (FCoE).

REFERENCES

- Cajander, A. K. (1949). Forest types and their significance. *Acta Forestalia Fennica* **56**, 1–69.
- Kolari, P., Pumpanen, J., Kulmala, L., Ilvesniemi, H., Nikinmaa, E., Grönholm, T. and Hari, P. (2006). Forest floor vegetation plays an important role in photosynthetic production of boreal forests. *Forest Ecology and Management* **221**, 241-248.
- Kolari P, Kulmala L, Pumpanen J, Launiainen S, Ilvesniemi H, Hari P, Nikinmaa E (2009). CO₂ exchange and component CO₂ fluxes of a boreal Scots pine forest. *Boreal Environment Research* **14**, 761-783.
- Laine, J., Komulainen, V.-M., Laiho, R., Minkkinen, K., Rasinmäki, A., Sallantausta, T., Sarkkola, S., Silvan, N., Tolonen, K., Tuittila, E.-S., Vasander, H., and Päivänen, J. (2004) Lakkasuo, a guide to mire ecosystems. Helsingin Yliopiston Metsäekologian Laitoksen Julkaisuja, 31. Helsinki, Finland. 123 p.
- Mäkelä A., Kolari P., Karimäki J., Nikinmaa E., Perämäki M. and Hari P (2006). Modelling five years of weather-driven variation of GPP in a boreal forest. *Agr. Forest Meteorol.* **139**, 382-398.
- Pumpanen, J., Westman, C.J. and Ilvesniemi, H. (2004). Soil CO₂ efflux from a podzolic forest soil before and after forest clear-cutting and site preparation. *Boreal Environment Research* **9**, 199-212
- Riutta, T., Laine, J. & Tuittila, E.-S. 2007. Sensitivity of CO₂ exchange of fen ecosystem components to water level variation. *Ecosystems* **10**: 718-733.
- Župek, B., Minkkinen, K., Kolari, P., Starr, M., Chan, T., Alm, J., Vesala, T., Laine, J. and Nikinmaa, E. (2008), Forest floor versus ecosystem CO₂ exchange along boreal ecotone between upland forest and lowland mire. *Tellus B*, **60**: 153–166.
- Vesala T., Haataja J., Aalto P., Altimir N., Buzorius G., Garam E., Hameri K., Ilvesniemi H., Jokinen V., Keronen P., Lahti T., Markkanen T., Makela J.M., Nikinmaa E., Palmroth S., Palva L., Pohja T., Pumpanen J., Rannik U., Siivola E., Ylitalo H., Hari P., and Kulmala M. (1998). Long-term field measurements of atmosphere-surface interactions in boreal forest combining forest ecology, micrometeorology, aerosol physics and atmospheric chemistry. *Trends in Heat, Mass, Momentum Transfer* **4**, 17–35.
- Vesala T, Launiainen S, Kolari P, Pumpanen J, Sevanto S, Hari P, Nikinmaa E, Kaski P, Mannila H, Ukkonen, E., Piao, S. L., and Ciais, P (2010). Autumn temperature and carbon balance of a boreal Scots pine forest in Southern Finland. *Biogeosciences* **7**: 163–176.

SURFACE SOUTHERN PACIFIC OCEAN SOA

P. VAATTOVAARA^{1,2}, L. CRAVIGAN², N.TALBOT³, G. OLIVARES³, C. LAW⁴, M. HARVEY⁴, Z.

RISTOVSKI² and A. LAAKSONEN^{1,5}

¹Department of Applied Physics, University of Eastern Finland, Kuopio, FI-70211, Finland

²ILAQH, Queensland University of Technology, Brisbane, 4000, Australia

³National Institute of Water and Atmosphere, Auckland, New Zealand

⁴National Institute of Water and Atmosphere, Wellington, 6021, New Zealand

⁵Finnish Meteorological Institute, Helsinki, FI-00101, Finland

Keywords: MARINE AEROSOLS, SECONDARY ORGANICS, ULTRAFINE, COMPOSITION.

INTRODUCTION

Marine biologically active regions (e.g., coasts, ice edges, frontal regions and open water areas with plankton blooms) are known to produce a range of compounds that interact with atmosphere affecting directly and indirectly particle production, composition, and wider properties of the marine atmosphere. Whilst the CLAW hypothesis (Charlson et al., 1987) supports the idea of the importance of marine biological activity on ultrafine ($d < 100\text{nm}$) particle composition and effects through secondary sulfate production via DMS, this hypothesis does not take into account the secondary organic fraction in the composition of the ultrafine particles. So far recent observations about the presence of a remarkable marine-origin secondary organic fraction in ultrafine particles have been identified down to nucleation mode size particles ($d < 15\text{nm}$) over Irish coastal waters of the Atlantic Ocean (Vaattovaara et al., 2006), and Arctic Ocean close to ice edges (Vaattovaara et al., ICNAA 2009), and Australian sub-tropical Pacific Ocean waters (Modini et al., 2009). In spite of the importance of a secondary fraction to the properties of radiatively active sizes in marine environments, marine produced particle composition is very unknown in various other marine biologically active locations around the world.

METHODS

This study about the composition of nucleation ($d < 15\text{nm}$) and the lower end of Aitken ($20\text{nm} < d < 60\text{nm}$) modes particles was focused on particle production in one such region the Chatham Rise region (New Zealand; latitude 42°S - 44°S , longitude 174°E - 177°W) during the SOAP (Surface Ocean Particle Production) pilot project voyage (austral summer period from 1.2.2011 to 12.2.2011). The location was in the southern Pacific Ocean over the Sub-Tropical Convergence (STC) to the east of New Zealand. The region experiences intensive austral summer phytoplankton blooms. Figure 1 shows the measurement route with observed plankton blooms during the expedition.

The ultrafine particle composition was studied using the Ultra Fine Organic Tandem Differential Mobility Analyser (UFO-TDMA; Vaattovaara et al., 2005) and the Volatility Humidity Tandem Differential Humidity Analyser (VH-TDMA; Johnson et al. 2005) methods on board of RV Tangaroa (New Zealand). Auxiliary data were collected from the ships weather station, underway instrument suite and marine information observations, SMPS (Scanning Mobility Particle Sizer) particle size distribution measurements, total particle count CPC (Condensation Particle Counter) measurements with 5 nm and 10 nm cut-off sizes, and black carbon measurements. Marine biological activity was checked with MODIS

satellite data and supported by in situ chlorophyll and dissolved DMS measurements. Marine air mass origin was followed with HYSPLIT (Rolph, 2003; Draxler and Rolph, 2003) trajectories.

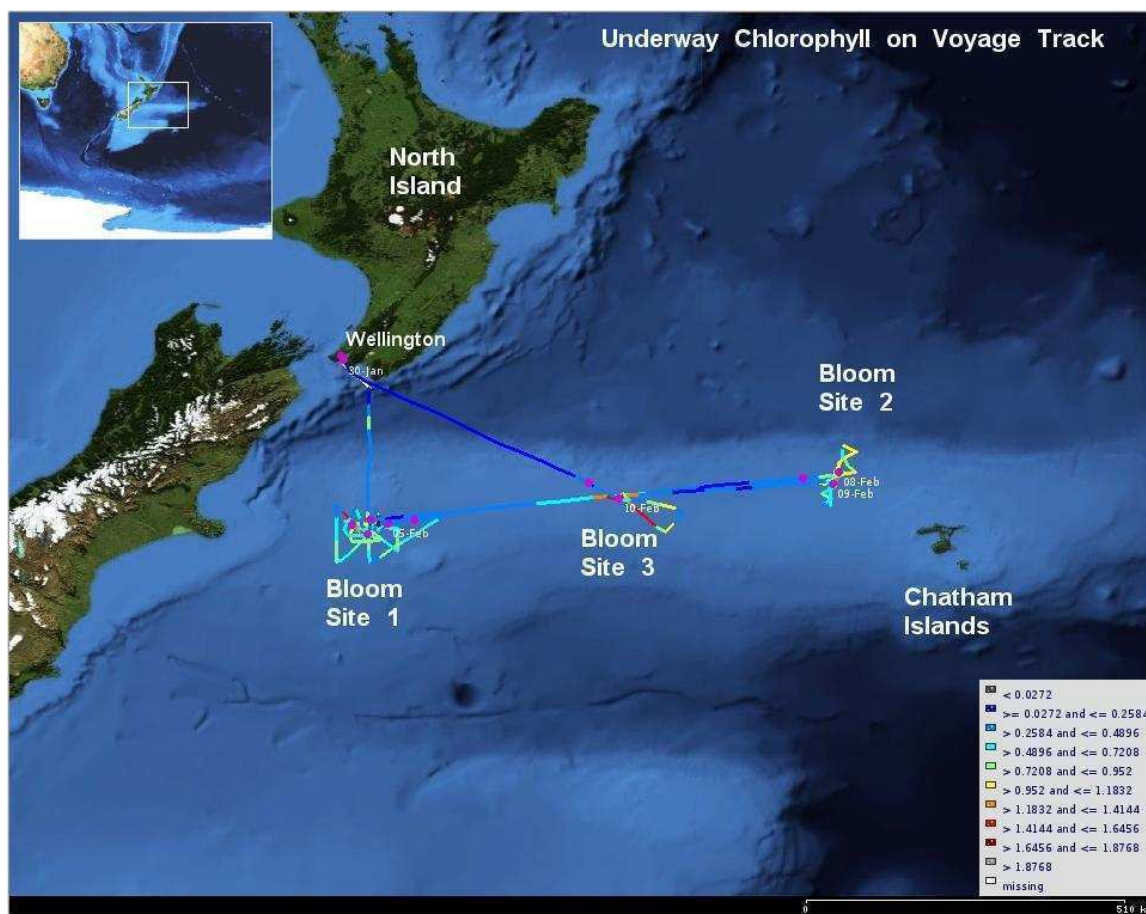


Figure 1. The measurement route with observed plankton blooms during the pre-SOAP expedition (1.2.-12.2.2011).

CONCLUSIONS

The TDMA measurements showed that in the biologically active marine area observed nucleation and Aitken mode sized particles include a clearly detectable organic fraction. Due to intensive solar radiation (e.g., 4.2., 6.2., 9.2., and 10.2.) secondary organic fraction was highly probable in those ultrafine particles. Furthermore, the comparison between in situ bubble burst chamber and atmospheric particles composition measurements strongly support secondary origin of the atmospherically observed ultrafine particles. The comparison of the secondary organic fraction observations on Atlantic, Arctic, and Pacific Oceans reveals that even though the secondary organic fraction clearly exists in ultrafine particle phase in the different biologically active marine regions, the exact properties of the fraction can be dependent on local marine area conditions.

ACKNOWLEDGEMENTS

This study was supported by EU COST action 735, QUT (Queensland University of Technology, Australia), and NIWA (National Institute of Water and Atmosphere, New Zealand), the Academy of Finland through the Center of Excellence and through the grant no. 136841. We thank whole research team and the crew and captain of RV Tangaroa for pleasant expedition. The authors also gratefully acknowledge Sea-WiFs and MODIS Aqua and Terra (NASA/Goddard Space Flight Center and

ORBIMAGE) for satellite data and the NOAA Air Resources Laboratory (ARL) for the provision of the HYSPLIT transport and dispersion model and READY web site (<http://www.arl.noaa.gov/ready.html>) used in this study.

REFERENCES

- Charlson, R.J., J.E. Lovelock, M. Andreae and S.G. Warren (1987). Oceanic phytoplankton, atmospheric sulphur, cloud albedo and climate, *Nature*, **326**, 6114, 655–661.
- Draxler, R.R. and G.D., Rolph (2003). HYSPLIT (HYbrid Single-Particle Lagrangian Integrate Trajectory). Model access via NOAA ARL READY Website (<http://www.arl.noaa.gov/ready/hysplit4.html>), Silver Spring, MD: NOAA Air Resources Laboratory.
- Johnson, G.R., Z.D. Ristovski, B. D'Anna and L. Morawska (2005). Hygroscopic behavior of partially volatilized coastal marine aerosols using the volatilization and humidification tandem differential mobility analyzer technique. *J. Geophys. Res.*, 110, D20203.
- Modini, R., Z.D. Ristovski, G.R. Johnson, C. He, N. Surawski, L. Morawska, T. Suni and M. Kulmala (2009). *Atmos. Chem. Phys.* **9**, 19, 7607-7621.
- Rolph, G.D. (2003). Real-time Environmental Applications and Display sYstem (READY) Websit, SilverSpring,, MD: NOAA Air Resources Laboratory.
- Vaattovaara, P., M. Räsänen, T. Kühn, J. Joutsensaari. and A. Laaksonen (2005). A method for detecting the presence of organic fraction in nucleation mode sized particles. *Atmos. Chem. Phys.*, **5**, 3277-3287.
- Vaattovaara, P., P.E. Huttunen, Y.J. Yoon, J. Joutsensaari, K.E.J. Lehtinen, C.D. O'Dowd, A. Laaksonen (2006). The composition of nucleation and Aitken modes particles during coastal nucleation events: evidence for marine secondary organic contribution. *Atmos. Chem. Phys.* **6**, 4601-4616.

SUB-MICRON AEROSOL PARTICLE SIZE DISTRIBUTIONS IN CLEAN AND POLLUTED SOUTHERN AFRICAN SAVANNAH

V. VAKKARI¹, H. LAAKSO¹, M. KULMALA¹, D. MABASO² and L. LAAKSO^{1,3,4}

¹University of Helsinki, Dept. Physics, P. O. Box 64, 00014 Univ. of Helsinki, Finland

²Rustenburg Local Municipality, Rustenburg, Republic of South Africa

³Finnish Meteorological Institute, Research and Development, P.O. BOX 503, FI-00101, Finland

⁴School of Physical and Chemical Sciences, North-West University, Potchefstroom, Republic of South Africa

Keywords: aerosol size distribution, Southern Africa, savannah.

INTRODUCTION

Sub-micron aerosol particles effect climate via direct and indirect mechanisms (Seinfeld and Pandis, 1998) and pose a threat for human health (Pope and Dockery, 2006). Depending on their size, they may scatter light, act as cloud condensation nuclei, or penetrate at different depths in human lungs.

Due to their large variability in size and dynamically driven tendency to occur in different separate size-ranges, modes, the particle size distribution is often expressed as a sum of multiple log-normal modes. Smallest particles (< 25 nm) are classified as nucleation mode, slightly larger (25–100 nm) as Aitken mode, next accumulation mode (100–1000 nm) and particles above 1000 nm as coarse mode particles. Especially for modelling purposes the modal representation of aerosol particle size distribution provides clear benefits in e.g. reduced number of differential equations (e.g. Korhonen *et al.*, 2004). For large observational datasets, the modal representation provides a simple way to study the behaviour of aerosols.

We present here a unique data set of a total of four years of sub-micron aerosol particle size distribution measurements conducted in clean and polluted savannah environments in Southern Africa and combine the results with air mass history from HYSPLIT back-trajectories and compare them with satellite-obtained aerosol optical depth from MODIS data.

METHODS

The sub-micron particle size distribution measurements were carried out in the Republic of South Africa during the period July 2006 – May 2010. The period until February 2008 represents semi-clean background savannah (Botsalano game reserve) (Laakso *et al.*, 2008; Vakkari *et al.*, 2011), whereas the second part of the measurements is from a polluted mining area (Marikana village next to Rustenburg) with a strong impact from domestic biomass burning in informal settlements (Venter *et al.*, 2011).

The particle number size distributions were observed with a Differential Mobility Particle Sizer with a size range from 10 to 840 nm. The modal fittings were calculated with the method described in (Vartiainen *et al.*, 2007). All the measurements and the environment are discussed in detail in (Laakso *et al.*, 2008) and (Vakkari *et al.*, 2011). In addition to the in-situ measurements, particle size distributions and their representativeness are analyzed as a function of air mass origin utilizing 96-hour back-trajectories calculated with the HYSPLIT 4.8 model (Draxler and Hess, 2004) and compared with the aerosol optical depth from MODIS satellite data.

RESULTS

On a regional scale the difference between the semi-arid Karoo region and the Highveld is clear, Figure 1. In the Karoo region – a 90 degree sector ranging from due west to due south from Botsalano in Figure 1 – anthropogenic emissions are small and also biogenic activity is lower than in the Highveld (Friedl *et al.*, 2002) and therefore it supports a significantly lower concentration of Aitken and accumulation mode particles than the Highveld. The highest Aitken mode concentrations originate in the industrialized Highveld, around and east of Rustenburg and Johannesburg. The highest accumulation mode concentrations originate in the semi-permanent anticyclonic re-circulation path (Garstang *et al.*, 1996) following the border of the Republic of South Africa and in the direction of the Kalahari Desert west and north-west of Botsalano.

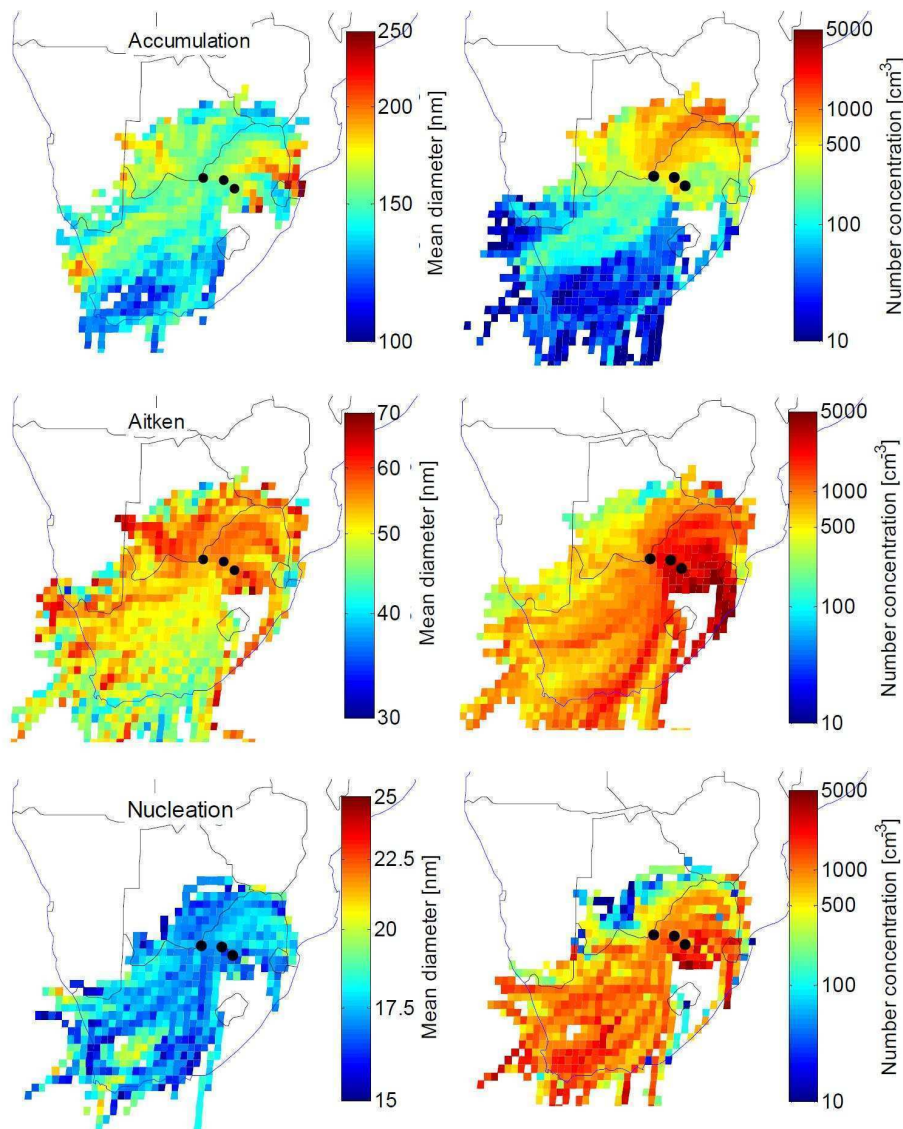


Figure 1. Accumulation, Aitken and nucleation modes as a function of the origin of air masses for Botsalano game reserve, Republic of South Africa. The black dots are (from left to right) Botsalano, Marikana and Johannesburg.

Although the nucleation mode particle concentration do not have clear differences between the Karoo and Highveld, we have found seasonal and spatial differences in particle formation and growth rates indicating the importance of biogenic organics and sulphuric compounds (Vakkari *et al.*, 2011).

The source areas of aerosol particles obtained from in-situ measurements combined with air mass trajectories agree on a qualitative level with the satellite produced aerosol optical depth, as is seen comparing Figure 1 and Figure 2.

CONCLUSIONS

The sub-micron aerosol size distributions clearly reflect the different landscapes of the Southern Africa and also the effect of anthropogenic activities as well as the prevailing meteorological conditions is clearly seen. All in all this dataset provides unique opportunities for modelling purposes in an environment with very few previous observations.

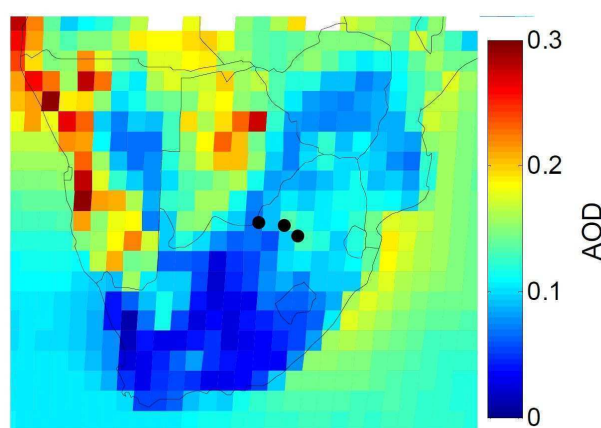


Figure 2. Aerosol optical depth from MODIS satellites. AOD has been averaged over the time period of July 2006 – May 2010 and both Aqua and Terra satellites. The black dots are (from left to right) Botsalano, Marikana and Johannesburg.

REFERENCES

- Draxler, R.R., and G.D. Hess (2004). Description of the HYSPLIT_4 Modelling System, NOAA Technical Memorandum ERL ARL-224.
- Friedl, M.A., D.K. McIver, J.C.F. Hodges, X.Y. Zhang, D. Muchoney, A.H. Strahler, C.E. Woodcock, S. Gopal, A. Schneider, A. Cooper, A. Baccini, F. Gao and C. Schaaf (2002). Global land cover mapping from MODIS: algorithms and early results, *Remote Sens. Environ.*, **83**, 287-302.
- Garstang, M., M. Tyson, R. Swap, M. Edwards, P. Källberg and J.A. Lindesay (1996). Horizontal and vertical transport of air over southern Africa, *J. Geophys. Res.*, **101**, 23721-23736.
- Korhonen, H., K.E.J. Lehtinen and M. Kulmala (2004). Multicomponent aerosol dynamics model UHMA: model development and validation, *Atmos. Chem. Phys.*, **4**, 757-771.
- Laakso, L., H. Laakso, P.P. Aalto, P. Keronen, T. Petäjä, T. Nieminen, T. Pohja, E. Siivola, M. Kulmala, N. Kgabi, M. Molefe, D. Mabaso, D. Phalatse, K. Pienaar, and V.-M. Kerminen (2008). Basic characteristics of atmospheric particles, trace gases and meteorology in a relatively clean Southern African Savannah environment, *Atmos. Chem. Phys.* **8**, 4823-4839.
- Seinfeld, J.H. and S.N. Pandis (1998). *Atmospheric Chemistry and Physics: From Air Pollution to Climate Change* (Wiley, New York).
- Pope, C.A. and D.W. Dockery (2006). Health effects of fine particulate air pollution: Lines that connect, *J. Air Waste Manag. Assoc.*, **56**, 709-742.

- Vakkari, V., H. Laakso, M. Kulmala, A. Laaksonen, D. Mabaso, M. Molefe, N. Kgabi and L. Laakso (2011). New particle formation events in semi-clean South African savannah, *Atmos. Chem. Phys.* **11**, 3333-3346.
- Vartiainen, E., M. Kulmala, M. Ehn, A. Hirsikko, H. Junninen, T. Petäjä, L. Sogacheva, S. Kuokka, R. Hillamo, A. Skorokhod, I. Belikov, N. Elansky and V.-M. Kerminen (2007). Ion and particle number concentrations and size distributions along the Trans-Siberian railroad, *Boreal Env. Res.*, **12**, 375–396.
- Venter, A., V. Vakkari, P. Tiitta, M. Josipovic, J.P. Beukes and L. Laakso (2011). *in prep.*

On eddy covariance flux measurements over lakes

T. VESALA¹, A. NORDBO¹, S. HAAPANALA, I. MAMMARELLA¹, J. PUMPANEN², W. EUGSTER³,
J. HUOTARI⁴ and A. OJALA⁵

¹Department of Physics, University of Helsinki

²Department of Forest Sciences, University of Helsinki

³Institute of Plant, Animal and Agroecosystem Sciences, ETH, Switzerland

⁴Lammi Biological Station, University of Helsinki

⁵Department of Environmental Sciences, University of Helsinki

Keywords: Lake-atmosphere exchange, eddy covariance, CO₂ fluxes

We give an overview on the status of eddy covariance measurements over lake surfaces with a focus on CO₂ fluxes. Inland waters have a significant role in the sequestration, transport and mineralization of organic carbon (Battin et al., 2009, Tranvik et al., 2009). Although inland waters are especially important in lateral transporters of carbon, their direct carbon exchange with the atmosphere, so called outgassing, has also been recognized to be a significant component in the global carbon budget (Tranvik et al., 2009, Bastviken et al., 2011). Lakes also store carbon (C) effectively in their sediments but for instance in the boreal zone annual CO₂ emissions are 17-43 times higher than the net sedimentation of C (Kortelainen et al., 2006). In forested catchments, the annual CO₂ efflux from lakes has been estimated to be up to 14 % of the annual net ecosystem exchange (Hanson et al., 2004).

Lakes cover only about 3% of the Earth's surface (Downing et al., 2006), but in the boreal zone lakes cover on average 7 % of land area, and furthermore in some parts in Finland (Raatikainen et al., 1990) and northern Canada (Spence et al., 2003) they occupy up to 20 % and 30 % of the landscape, respectively. Many of the water bodies are small. The average number in Finland – the country in Europe which probably has the highest density of lakes per unit area – is 56 lakes per 100 km² (Raatikainen and Kuusisto, 1990) and the number of lakes with a surface area less than 0.01 km² is over 130 000. More importantly, the arctic tundra is similarly occupied by numerous small ponds and lakes, the response of which to high-latitude warming and the resulting changes in CO₂ and CH₄ effluxes is very uncertain (Walter et al., 2007). MacIntyre et al. (2010) concludes that regional and global fluxes of greenhouse gases from lakes may be considerably larger than current estimates.

The present outgassing estimates are still provisional and probably underestimated (Alsdorf et al., 2007). The eddy covariance (EC) technique would be an indispensable tool for directly assessing the fluxes from lakes, rather than using chambers, although there is the expectation that agreement between methods can be found with appropriate chamber design (Cole et al. 2010). Beside chambers, gas exchange models are applied based on the measured CO₂ partial pressure difference between the air and water and parameterized bulk transfer coefficients, but the transfer coefficient is difficult to experimentally determine (MacIntyre et al., 2010). However, long-term EC flux measurement data are very scarce and much more data from lakes of different sizes, lake types (like water colour) and meteorological conditions are urgently needed to assess the role of lakes in local, regional, and global carbon budgets. There is a negative relationship between lake size and the gas saturation (i.e. surface water CO₂ concentration relative to atmospheric equilibrium) and especially small lakes, are a relatively large source of CO₂ (Kelly et al., 2001; Kortelainen et al., 2006). To guarantee the best achievements, the EC-related work should be carried out in close collaboration of atmospheric physicists/meteorologists and limnologists and aquatic ecologists.

Six articles are reporting on EC measurements of CO₂ fluxes over lakes. Anderson et al. (1999) (AN) have used the method over a small woodland lake in Minnesota, USA, Morison et al. (2000) (MO) studied the productivity of a tropical *Echinochloa* grassland in high-water phase in Amazon floodplain, Eugster et al.

(2003) (EU) determined exchange rates over an Arctic Alaskan and an isolated (no inlet and no outlet) mid-latitude Swiss lake, Vesala et al. (2006) (VE) report fluxes for a full open-water period for a small boreal uppermost (no inlet) lake, Guerin et al. (2007) (GU) investigated a tropical reservoir in French Guiana and in Jonsson et al. (2008) (JO) the studied lake was located in Sweden, north of the Arctic Circle in the boreal forest zone. The lengths of the records are rather short. In AN lake-atmosphere exchanges were measured over 5 weeks in spring, summer and fall, over a 3-yr period. MO reports two weeks for aquatic phase of the grassland and about one month for terrestrial low-water period when the study site cannot be regarded as an inland water body. EU covers three separate periods of few days, primarily looking at the process of outgassing rather than its long-term relevance for C budgets. During the first one (2 days), the instruments were mounted on Toolik Lake (Alaska) shore requiring the exclusion of data when the mean wind was from the land. The second period, also at Toolik Lake, covers 5 days, but the equipment was mounted in the center of the lake on a moored float. During the third period at Lake Soppensee (Switzerland), the measurements were carried out over 3 days, again with instruments mounted on a moored float. GU reports data only for 24 hours measured a few hundred meters upstream of the dam of the studied reservoir. In JO the measurements were made over about 3 months and the shortest fetch to the shore was 350 m. The longest available data set published in a peer-reviewed journal is a full open-water period from April to November 2003 from Finland, Lake Valkea-Kotinen in VE. However, the article, based on Valkea-Kotinen data set, showing the first long-term record of EC measurements over five consecutive open-water periods is under preparation.

Nordbo et al. (2011) have stressed the importance and scarcity of data on small lakes. The sizes on the reported studies excluding MO study are, in the order of increasing size: Lake Valkea-Kotinen (VE) is about 460 m long and 130 m wide (average depth (ad) 2.5 m), Lake Soppensee (EU) is about 800 m long and 400 m wide (ad 12 m), Williams Lake (AN) is ellipsoidal with 900-m major axis and 550-m minor axis (ad 5.2 m), Toolik Lake (EU) has a surface area of 1.5 km² (ad 7 m), Lake Merasjärvi (JO) has a surface area of 3.8 km² (ad 5.1 m), the average surface of the Petit-Saut dam reservoir at Sinnamary River (GU), owing to high and low water levels, is 300 km². An overview of long (> 5 months) and short-term sensible and latent heat flux measurements by EC over lake, tabulated by Nordbo et al. (2011) in their Table 1, lists besides the already mentioned studies (VE, EU, AN, JO and GU) three long-term and six short-term energy flux records. EC flux measurements of CH₄ have only recently been started, but no studies have been published in the peer-reviewed literature so far.

For proper interpretations of EC fluxes, one also needs to monitor various other variables in addition to the CO₂ flux. Anyone planning to set a lake EC facility should consider a “shopping list” of sensors for basic meteorological variables. The following list shows the ultimate desire of scientists wishing to understand the processes behind the outgassing from a lake. For a simple quantification of CO₂ effluxes alone, a reduced set of variables will also do in most cases. The ultimate list includes downwelling and upwelling radiation components (short-wave and long-wave components separately), inclinometer, buoy/platform orientation, air CO₂ concentration gradient, water temperature profile, sediment temperature (or water temperature close to the lake bottom), water velocities, water conductivity, water CO₂ concentration profile, dissolved inorganic carbon (DIC) and nitrogen (DIN), dissolved organic carbon (DOC) and nitrogen (DON), particulate organic matter (POM) for lakes with relevant inflows, dissolved oxygen profile/redox potential, pH, chlorophyll concentration, total nitrogen, total phosphorous and sediment samplers. It would be desirable to measure fluxes also by chambers for inter-comparison. The monitoring of CO₂, DIC, DOC and POM from inlet and outlet water allows for a full carbon balance estimate. One should also note that flux footprints (source areas) tend to be long over smooth lake surfaces due to low levels of mechanical turbulence and measurements over small water bodies may face the problem with long enough fetches. However, Vesala et al. (2006) studied the small Lake Valkea-Kotinen and demonstrated that source areas can be relatively short because of the presence of turbulence generated by the surrounding forest, compared to a larger lake with an extended smooth surface.

The earliest article (AN) concludes “In view of the uncertainty in predicting lake-atmosphere CO₂ transfer and its important global implications in air-water exchange, we strongly encourage other investigators to

make comparative measurements of CO₂ flux in an effort to better understand and quantify the environment controls regulating air-water gas transfer in natural settings”, in 1999. After 12 years, we still must agree with this statement.

ACKNOWLEDGEMENTS

We acknowledge the Centre of Excellence program (project no 1118615) and EU projects ICOS, IMECC and GHG-Europe.

REFERENCES

- Alsdorf, D., Bates P, Melack J, et al. (2007) Spatial and temporal complexity of the Amazon flood measured from space. *Geophys. Res. Letters* 34, DOI: 10.1029/2007GL029447.
- Anderson, D.E., R.G. Striegl, D.I. Stannard, C.M. Micherhuizen, T.A. McConnaughey, and J.W. LaBaugh (1999) Estimating lake-atmosphere CO₂ exchange. *Limnol. Oceanogr.* 44, 988-1001.
- Bastviken, D., Tranvik, L. J., Downing, J. A., Crill, P. M. and Enrich-Prast, A. (2011) Freshwater methane emissions offset the continental carbon sink. *Science*, 331, 50.
- Battin, T.J., S. Luysaert, L.A. Kaplan, A.K. Aufdenkampe, A. Richter L.J. and Tranvik (2009) The boundless carbon cycle. *Nature Geoscience*, 2, 598-600.
- Cole, J. J., Bade, D. L., Bastviken, D., Pace, M. L. and Van de Bogert, M. (2010) Multiple approaches to estimating air--water gas exchange in small lakes. *Limnol. Oceanogr. : Methods*, 8, 285-293.
- Downing, J.A., Y.T. Prairie, J.J. Cole, C. M. Duarte, L.J. Tranvik, R.G. Striegl, W.H. McDowell, P. Kortelainen, N.F. Caraco, J.M. Melack, J.J. Middelburg (2006) The global abundance and size distribution of lakes, ponds, and impoundments. *Limnol. Oceanogr.*, 51(5), 2388–2397.
- Eugster, W., Kling, G., Jonas, T., McFadden, J. P., Wüest, A., MacIntyre, S. and Chapin, III, F. S. (2003) CO₂ exchange between air and water in an arctic Alaskan and midlatitude Swiss lake: Importance of convective mixing *J. Geophys. Res.*, 108 , 4362-4380
- Guerin F, Abril G. Significance of pelagic aerobic methane oxidation in the methane and carbon budget of a tropical reservoir (2007) *J. Geophyscial Res. Biogeosciences*, 112, G03006.
- Hanson, P. C., Pollard, A.I., Bade, D. L., Predick, K., Carpenter, S. R. and Foley, J. A. (2004) A model of carbon evasion and sedimentation in temperate lakes. *Global Change Biol.*, 10, 1285-1298
- Jonsson, A., J. Åberg, A. Lindroth, and M. Jansson (2008) Gas transfer rate and CO₂ flux between an unproductive lake and the atmosphere in northern Sweden, *J. Geophys. Res.*, 113, G04006, doi:10.1029/2008JG000688.
- Kelly, C. A., Fee, E., Ramlal, P. S., Rudd, J. W. M., Hesslein, R. H., Anema, C. & Schindler, E. U. (2001). Natural variability of carbon dioxide and net epilimnetic production in the surface waters of boreal lakes of different sizes. *Limnol. Oceanogr.* 46: 1054-1064.
- Kortelainen, P. et al. (2006) Sediment respiration and lake trophic state are important predictors of large CO₂ evasion from small boreal lakes. *Global Change Biol.* 12, 1554-1567.

- MacIntyre, S., Jonsson, A., Jansson, M., Aberg, J., Turney, D.E. and Miller, S.D. (2010) Buoyancy flux, turbulence, and the gas transfer coefficient in a stratified lake. *Geophys. Res. Letters* 37, L24604, doi: 10.1029/2010GL044164.
- Morison, J.I.L., M.T.F Piedade, E. Müller, S.P. PLong, W.J. Junk, and M.B. Jones, (2000). Very high productivity of the C₄ aquatic grass *Echinochloa polystachya* in the Amazon floodplain confirmed by net ecosystem CO₂ flux measurements. *Oecologia* 125, 400-411.
- Nordbo, N., S. Launiainen, I. Mammarella, M. Leppäranta, J. Huotari, A. Ojanen and T. Vesala (2011) Long-term energy flux measurements and energy balance over a small boreal lake using eddy covariance technique. *J. Geophys. Res.* 116, DOI: 10.1029/2010JD014542.
- Raatikainen, M and Kuusisto E. (1990) Suomen järvien lukumäärä ja pinta-ala [The number and surface area of the lakes in Finland]. *Terra* 102, 97-110. [In Finnish with English summary].
- Spence, C., Rouse, W. R., Worth, D. and Oswald, C. (2003) Energy budget processes of a small northern lake. *J. Hydrometeorol.* 4, 694-701.
- Tranvik, L. J., Downing, J. A., Cotner, J. B., Loiselle, S. A., Striegl, R. G., Ballatore, T. J., Dillon, P., Finlay, K., Fortino, K., Knoll, L. B., Kortelainen, P. L., Kuster, T., Larsen, S., Laurion, I., Leech, D. M., McCallister, S. L., McKnight, D. M., Melack, J. M., Overholt, E., Porter, J. A., Prairie, Y., Renwick, W. H., Roland, F., Sherman, B. S., Schindler, D. W., Sobek, S., Tremblay, A., Vanni, M. J., Verschoor, A. M., van Wachenfeldt, E. and Weyhenmeyer, G. A. (2009) Lakes and reservoirs as regulators of carbon cycling and climate. *Limnol. Oceanogr.*, 54, 2298-2314.
- Vesala, T., Huotari, J., Rannik, Ü, Suni, T., Smolander, S., Sogachev, A., Launiainen, S. and Ojala, A. (2006) Eddy covariance measurements of carbon exchange and latent and sensible heat fluxes over a boreal lake for a full open-water period. *J. Geophys. Res.-Atmospheres*, 111, D11101
- Walter, K.M., L.C. Smith, F.S. Chapin III. (2007) Methane bubbling from northern lakes: present and future contributions to the global methane budget. *Phil. Trans. R. Soc. A*, 365, 1657-1676.

SOURCES OF PERSISTENT ORGANIC POLLUTANTS IN ATMOSPHERE AT PALLAS, FINLAND

M. VESTENIUS¹, P. ANTTILA¹, K. HANSSON², H. HELLÈN¹, E. BRORSTRÖM-LUNDEN²
and H. HAKOLA¹.

¹Finnish Meteorological Institute, P.O. BOX 503,
FI-00101 HELSINKI, FINLAND

² IVL Swedish Environmental Research Institute Ltd., Box 5302,
SE-400 14 GÖTEBORG, SWEDEN

Keywords: POP, PAH, PMF, AIR QUALITY.

INTRODUCTION

Source apportionment of atmospheric pollutants was studied at the Finnish Meteorological Institute's (FMI) Global Atmosphere Watch (GAW) station, Pallas. The station is located at the northernmost limit of the northern boreal forest zone and represents well the continental background air of the subarctic region (Hatakka et al., 2003). Matorova station (68°00'00''N, 24°14'24''E) at an elevation of 340 m a.s.l. is situated on top of a small hill covered by coniferous forest in the middle of a hectare clearing. The dataset from 1996 to 2009 (one week in a month) contains trace elements, the major inorganic ions, ozone, nitrogen dioxide, sulphur dioxide, and persistent organic pollutants (POP) including polycyclic aromatic hydrocarbons (PAH).

Samples for persistent organic pollutants (POP) including polycyclic aromatic hydrocarbons (PAH) analysis were collected at Matorova and analyzed in the laboratory of the IVL Swedish Environmental Research Institute (IVL). Gases and main ions as well as trace metals were analyzed by FMI. Positive Matrix Factorization (PMF) was applied in source apportionment and the source sector frequency distribution using EMEP air mass trajectories was calculated for each PMF factor in order to identify source directions.

RESULTS AND DISCUSSION

Positive matrix factorization was applied to the complete weekly dataset between 1996-2009 so that analogous weekly time series were compiled from the supportive inorganic components. Most, over 90 % of measured POP mass consisted of PAHs (Figure 1).

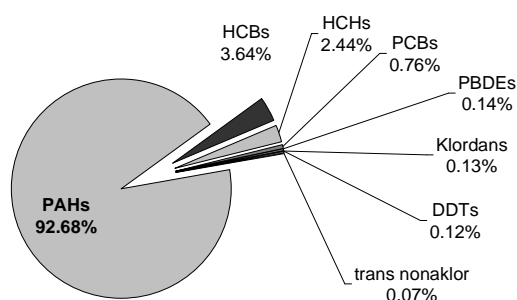


Figure 1: Average proportions of the measured POP compound mass.

PMF-analysis of weekly samples yielded five potential source factors (Fig.2). These factors were identified as Kola factor (F1), insecticide factor (F2), sea spray factor (F3), soil factor (F4) and traffic and LRT factor (F5).

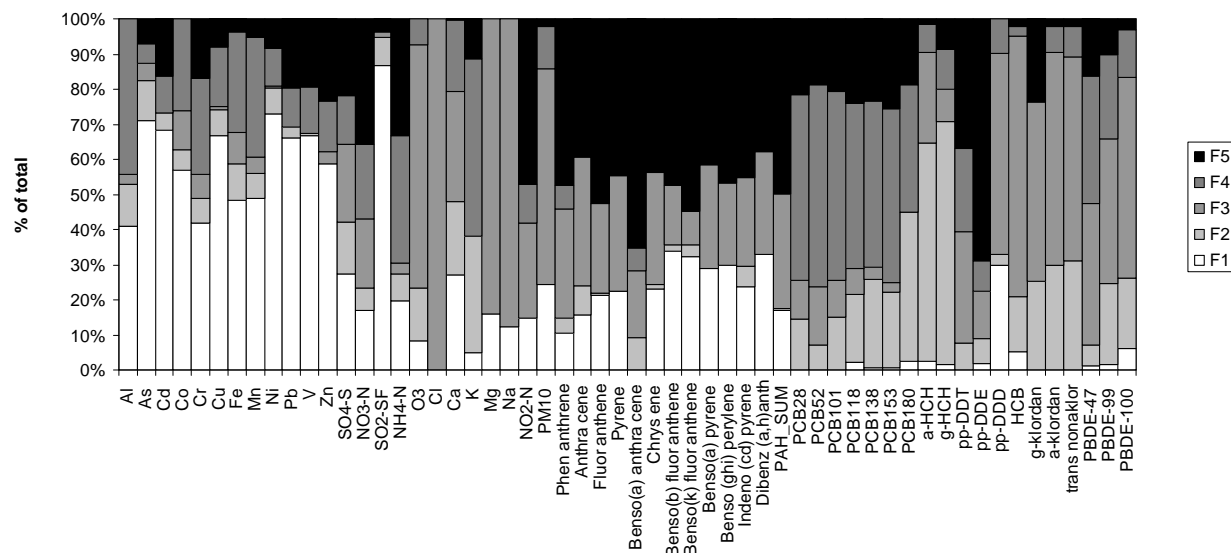


Figure 2: Source factors for the weekly samples at Pallas, 1996-2009.

Factor 1 contains large amount of trace elements (As, Ni, Cu, Pb, V, Zn) with most of gaseous SO₂ and 30-40% of the heavier PAH pollution. These pollutants are characteristic to the metal industries and air masses for this factor came from east. The source profile and the air mass trajectory analysis suggest that the industry in Kola peninsula was the major source for Factor 1.

Factor 2 contains most of the insecticides a-HCH and g-HCH (lindane) with high summer contribution, but without any specific source direction. This factor had a decreasing trend due to the reduction of the production and use of these compounds and the slow extinction of these pollutants from the ecosystem. (Li *et al.*, 2002).

Factor 3 is the sea spray factor without clear seasonal variation. The source direction was the Arctic Ocean and the northern Atlantic Ocean. 60% of PM₁₀ was associated to this factor, which indicates that a major fraction of PM₁₀ detected at Pallas was related to maritime air masses and sea salt particles during the study period 1996-2009. Majority of organochlorine compounds and 30% of the lighter PAH compounds were associated with this factor.

Factor 4 is a soil source; high loadings of aluminium, manganese, ammonium, potassium and PCBs with a systematic summer maximum. PCBs are found in contaminated soil particles and/or evaporation from the soil (Yi *et al.*, 2008). The air masses related to this factor originated mainly from south and west.

Factor 5 includes approximately half of PAHs and NO₂. The factor contribution was highest in winter and the dominating source directions were south and southwest. The high loadings of NO₂ and long-range transfer (LRT) nitrate and ammonium particles suggest reasonably remote traffic sources. The high contribution of DDT and DDE also refers to LRT air masses from the southern areas, where DDT is still in use (ATSDR, 2002).

REFERENCES

- Hatakka, J., Aalto, T., Aaltonen, V., Aurela, M., Hakola, H., Komppula, M., Laurila, T., Lihavainen, H., Paatero, J., Salminen, K. & Viisanen, Y. 2003. Overview of the atmospheric research activities and results at Pallas GAW station. *Boreal Env. Res.* **8**, 365–383.
- Li Y-F, Macdonald RW, Jantunen LMM, Harner T, Bidleman TF, Strachan WMJ, 2002. The transport of h-hexachlorocyclohexane to the western Arctic Ocean: a contrast to a-HCH. *Sci Total Environ* **291**:229–4
- Yi, S.-M., Reddy Pagilla, S., Seo, Y.-C., Mills, W.J., Holsen, T.M., 2008. Emissions of polychlorinated biphenyls (PCBs) from sludge drying beds to the atmosphere in Chicago. *Chemosphere* **71**, p.1028.
- ATSDR, 2002. *Toxicological Profile for DDT, DDE, and DDD*. Agency for Toxic, Substances and Disease Registry, Atlanta, US.

PREScribed FOREST BURNING EXPERIMENT IN JUNE 2009

A. VIRKKULA^{1,4}, J. LEVULA^{2,3}, T. POHJA², G. DE LEEUW^{1,4}, D. SCHULTZ^{1,4}, C. CLEMENTS⁵,
J. KUKKONEN⁴, J. NIKMO⁴, M. SOFIEV⁴, L. PIRJOLA⁶, L. KULMALA^{3,1}, J. PUMPANEN³,
T. VESALA¹, A.-J. KIELOAHO¹, H. AALTONEN³, M. PIHLATIE¹, S. HÄKKINEN¹,
H.E. MANNINEN¹, H. JUNNINEN¹, T. NIEMINEN¹, and M. KULMALA¹

¹Department of Physics, University of Helsinki, FI-00014, Helsinki, Finland

²Hyytiälä Forestry Field Station, University of Helsinki, FI-35500, Korkeakoski, Finland

³Department of Forest Sciences, P.O. Box 27, FI-00014, University of Helsinki

⁴Finnish Meteorological Institute, FI-00560, Helsinki, Finland

⁵Department of Meteorology, San José State University, 95192, San José, CA, USA

⁶Department of Technology, Metropolia University of Applied Sciences, FI-00079, Helsinki, Finland

Keywords: Wildland fire, Dispersion, Chemical composition, Number concentration, Hyytiälä.

INTRODUCTION

A controlled prescribed burning of forest was conducted near the SMEAR II station (Hari and Kulmala, 2005) in Hyytiälä on 26 June 2009. The experiment was part of both the EUCAARI and the Integrated Monitoring and Modelling System for Wildland Fires (IS4FIRES) projects. The general goal was to provide data for estimating the effect of natural forest fires on air quality and climate. More detailed goals were to study aerosol chemical composition and physical characteristics, concentrations of gaseous compounds, their processes, detection of fires using satellite remote sensing, modelling both fire spreading and atmospheric dispersion of the fire plume. The experiment was also designed to study the recovery of forest after burning. An additional important part of forest-atmosphere interactions is soil respiration. In this experiment the changes taking place in soil respiration following clear-cutting and prescribed burning were quantified.

METHODS

The forest was first cut clear in February 2009. Most tree trunks were transported away; some of them and all tree tops and branches were left on the ground in the burn area, so the amount of fuel was high. The amount of burned organic material was ~46.8 tons. About 64% of the burned material consisted of the cut tree material, 32% of organic litter and hummus layer and about 4% of surface vegetation. The burned area was approximately 0.8 ha.

During the burning measurements were conducted on the ground with both fixed and mobile instrumentation, and from an aeroplane. Ground-based instrumentation included the SMEAR II station together with meteorological and ecological measurements on and around the site. Ground-level dispersion of particles and trace gases was measured both by using the research van, “Sniffer”, and by people walking in the forest with portable particle counters at different distances from the burning area. Vertical and horizontal dispersion were measured with instruments installed in a Cessna 172, described in detail by Schobesberger, et al. (2009). Soil respiration, i.e., CO₂ exchange was measured with automatic chambers both before the clear cut of the forest, after cutting it before the burning and after the burning (Kulmala et al., 2011). These measurements still continue. The forest floor VOC measurements were started already a year before the prescribed burning and continued a year after. The VOC fluxes were

measured on five permanently installed collars with a manual steady-state chamber system. The VOC sampling and analyse method is explained detail by Aaltonen et al. (2011).

So far the dispersion of the plume was modeled by using two models: 1) the BUOYANT model of the Finnish Meteorological Institute (FMI) (Kukkonen et al. 2000) and 2) the Fire Emission Production Simulator (FEPS, 2011). The latter is a web-based model which manages data concerning consumption, emissions and heat release characteristics of prescribed burns and wildland fires.

RESULTS AND DISCUSSION

The area was set on fire on 26 June 2009 at 07:45 East European Time (UTC +2 hours), the flaming was over at 10:00 EET and there was only little visible smoke at 13:00 EET. Wind direction was favourable (175 - 215°) for steering the smoke to SMEAR II only during the start of the experiment and the again during the late phase of the experiment (Figure 1A).

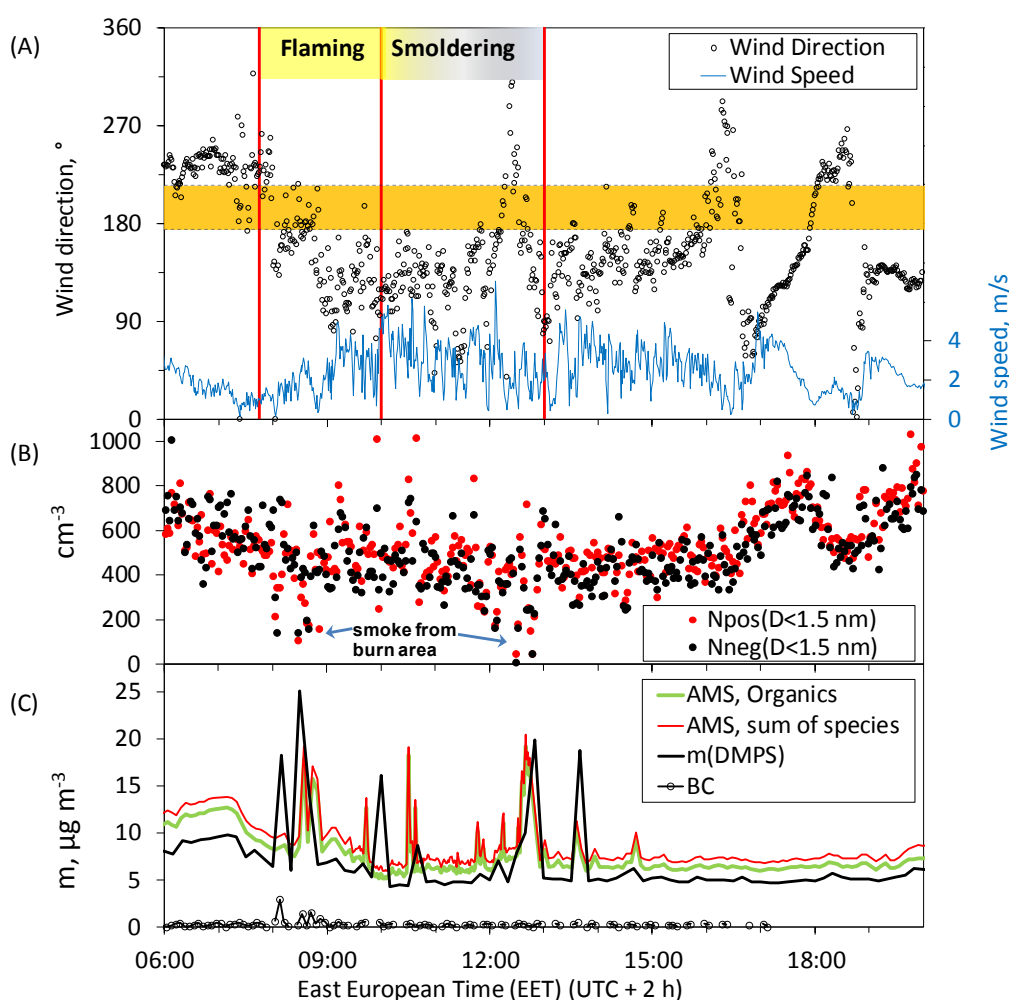


Figure 1. Data of selected ground-based measurements at SMEAR II on 26 June 2009. (A) Wind direction and speed at 34 m AGL. The red vertical lines indicate the start and end of the flaming and clear smoldering phases. The dark yellow line indicates the wind direction sector that would bring smoke from the fire to SMEAR II. (B) Positive and negative cluster mode particle concentrations measured with a NAIS. (C) Concentrations of organics and the sum of all compounds measured with an AMS, mass concentration of particles smaller than 600 nm measured with a DMPS and using the density of 1.5 g cm^{-3} , and black carbon concentration measured with an aethalometer.

There were 6 – 7 periods when smoke clearly arrived at the ground-based fixed instrumentation at SMEAR II. The Neutral Air Ion Spectrometer (NAIS) measurements showed that cluster mode ($D_p < 1.5$ nm) particle number concentrations decreased clearly in the smoke plume (Figure 1B). The Aerosol Mass Spectrometer (AMS) measurements showed that of the measured compounds (SO_4^{2-} , NO_3^- , Cl^- , NH_4^+ , and organics) the concentrations of only organics were considerably higher in the smoke plume than outside of it, and also nitrate slightly. The concentration of black carbon increased only for a short period in one of the periods when smoke arrived at SMEAR II.

In the middle of the burning area CO_2 concentration peaks were around 200–300 ppm above the baseline and peak vertical flow velocities were ~ 10 m/s (6 ± 3 m/s), as measured with a 3D sonic anemometer placed within the burn area (Clements et al. 2009). Peak particle number concentrations were approximately $1 - 2 \times 10^6 \text{ cm}^{-3}$ in the plume at the distance of 100–200 m from the burn area. These concentrations were consistently measured with both the "Sniffer" on the ground and in the aeroplane. At SMEAR II, however, the total particle number concentrations increased from ~ 1000 – 2000 cm^{-3} to 5000 – 15000 cm^{-3} only and scattering coefficients increased from 20 – 30 Mm^{-1} to 50 – 100 Mm^{-1} . These values were approximately two orders of magnitude lower than those measured inside the plume with the aeroplane.

SMOKE PLUME RISE

The transport of the smoke plume was studied by flying through it at several altitudes from about 70 m above ground level to > 1500 m AGL. The heat lifted the smoke so that clearly enhanced particle number concentrations could be observed at an altitude of > 1500 m AGL (Figure 2). At higher altitudes the plume was not detected any more. The plume rise modeled with the FEPS was clearly lower than the observed one. Also the Buoyant model predicts lower plume rise than the observed although the agreement was better. One of the input values to the Buoyant model is the fraction of the area burning at each moment. If it was assumed that 50% of the area is burning at the same time, the modeled plume rise agreed well with the observations (Figure 2).

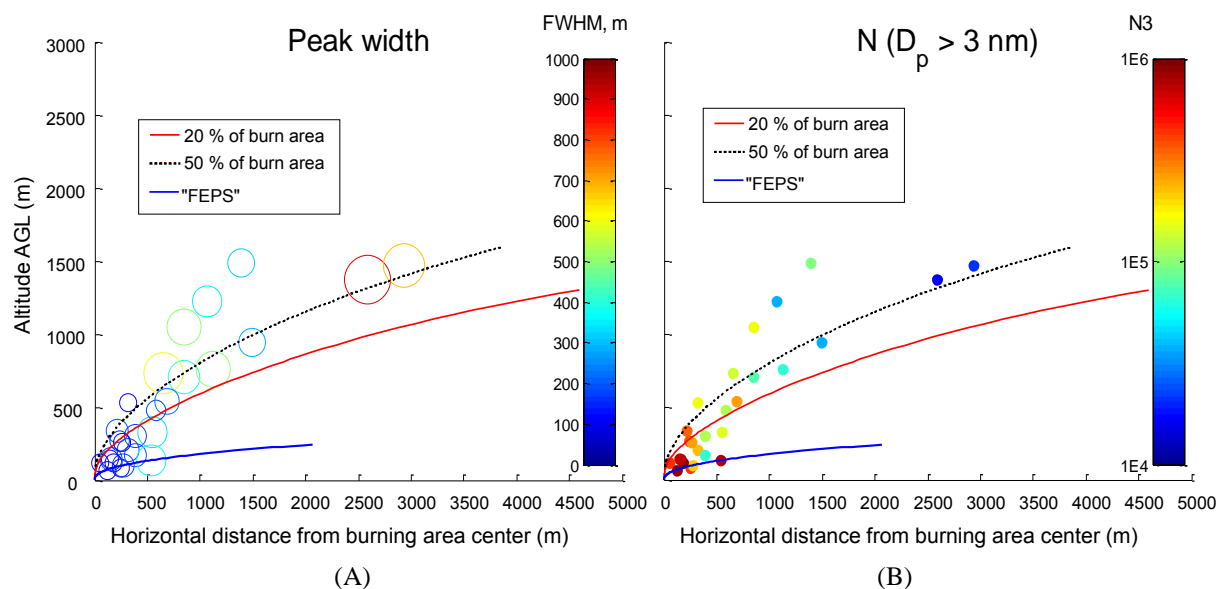


Figure 2. The measured (circles) and modeled (lines, see text) plume rise. In (A) the empty circles represent the full width of half maximum (FWHM) of each plume passage by the aeroplane, the width is coded both by the color and the diameter of the circle. In (B) the color of the filled circle represents the peak particle number concentration above the background value at the same altitude ($[N] = \text{cm}^{-3}$) measured in each plume passage.

EMISSION ESTIMATES FROM AIRBORNE MEASUREMENTS

The amount of CO₂, black carbon, number and mass of particles emitted during the experiment was estimated by combining information from the airborne measurements and the vertical flow velocity measured on ground in the middle of the burning area. The diameter of the smoke plume at various altitudes was determined from the particle number concentration measurements in the Cessna. The average concentration *c* of CO₂, BC, particle number and mass in each plume passage was multiplied with the plume area *A*. There was roughly a linear relationship between altitude and the product *cA* (Figure 3).

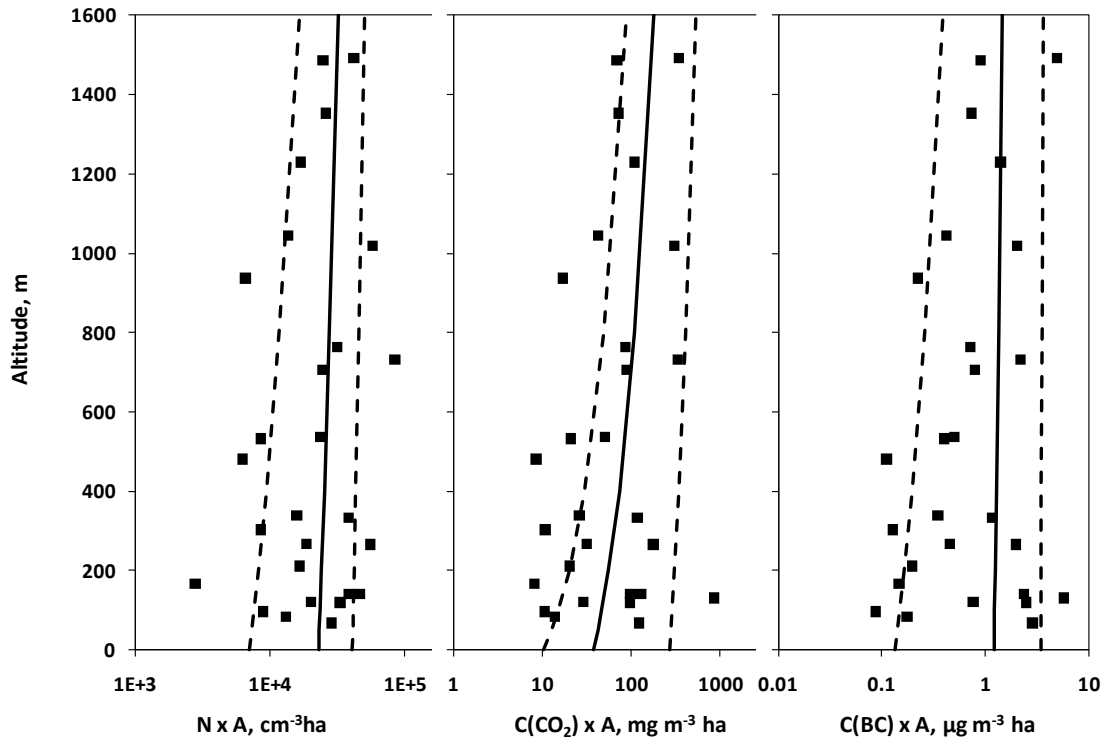


Figure 3. The product of average concentration and plume area in each passage of the plume. The continuous line is the linear fit of $(cA)_Z = k \times z + (cA)_0$ to the data, the dashed lines are calculated by using the same slope *k* but as offsets the 10th and 90th percentiles of the *pA* products in the passages at altitudes < 200 m agl.

When multiplied by the vertical flow velocity *w*₀ measured in the middle of the fire (Clements et al. 2009) on ground and integrating over the burning time $T \approx 2^h15'$ the total mass emitted may be calculated from

$$m_{TOT} = \int_0^T c_0 A_0 w_0 dt \approx c_0 A_0 w_0 T \approx (cA)_0 w_0 T$$

For example, with *w*₀ = 6 m/s and the extrapolated (*cA*)₀ product of 38 mg m⁻³ ha for CO₂(carbon) this procedure yields an estimated total emission of 18.5 tons of carbon, i.e., 67.7 tons of CO₂. When this is divided by 46.8 tons, i.e., the estimated total burned biomass, we get an estimated emission factor of 1.45 kg(CO₂)/kg(burned dry biomass). The linear regression yields a standard error for (*cA*)₀. This was used in the above formula to calculate an uncertainty estimate for the emission factors.

The same procedure was used also for particle number concentrations, particulate organic matter (POM) and black carbon (BC). The latter two were estimated from the scattering and absorption measurements, respectively. The results are shown in Table 1.

Table 1. Emission factors estimated from the airborne measurements and groundbased vertical flow velocity measurements.

	Emission Factor	\pm SE	
CO ₂	1625	747	g/kg(dry biomass)
N	4.88E+15	1.81E+15	N/kg(dry biomass)
POM	10.9	6.9	g/kg(dry biomass)
BC	2.1	0.8	g/kg(dry biomass)

CONCLUSIONS

The controlled burning campaign on 26 June 2009 at Hyytiälä was partially successful, partially not. The ground-based aerosol measurements showed that cluster-mode particles are mainly absent in wildland fire smoke and that the aerosol consists mainly of organics. The mobile measurements made both on ground with the Sniffer van and in air with the Cessna provided three-dimensional and time-dependent data on the dispersion of both aerosols and trace gases emitted from the fire. Analyses will be made, e.g., to derive particle emission factors as well as the fractionation of carbon into gas and aerosol phases, and to dispersion modeling. As an example of the type of analyses that can be made with the data, the airborne measurements were used here for estimating the CO₂ emissions during the experiment and for validating a plume rise model.

The forest floor measurements were also successful. The VOC fluxes were generally low and consist mainly on monoterpenes, but clear peak was observed after the burning. After a year the fluxes were stabilised close to the level before burning. The soil respiration measurements still continue. So far the preliminary results of Kulmala et al. (2011) show for instance that the burning had clear effects on the temperature dependence of soil respiration.

The non-successful part of the experiment was that the smoke arrived at the ground-based fixed instrumentation of SMEAR II only during short periods and even then not with its full power. As a result the experiment did not give answers to how the chemical composition and physical properties of the emissions evolve with the burning. Another non-successful part of the experiment was that it was not observed by satellites, at least according to the first analyses of available satellite images. The reason is that the time of the burning was between the overpasses of the satellites that measure aerosols.

ACKNOWLEDGEMENTS

The financial support by the Academy of Finland as part of the Centre of Excellence program (project no 1118615) and as part of the IS4FIRES project (decision no 122870) is gratefully acknowledged. The experiment was also supported by the European Commission 6th framework program project (EUCAARI), contract 036833-2, European Research Council, University of Helsinki, Finnish Meteorological Institute, Academy of Finland, TEKES, San José State University, CA, USA, and Institute for Tropospheric Research, Leipzig, Germany.

REFERENCES

- Aaltonen, H., J. Pumpanen, M. Pihlatie, H. Hakola, H. Hellén, L. Kulmala, T. Vesala and J. Bäck (2011). Boreal pine forest floor biogenic volatile organic compound emissions peak in early summer and autumn, *Agr. Forest Meteorol.* 151, 682-691.
- Clements C.B., Kukkonen, J., De Leeuw, G., Virkkula, A., Levula, J., Schultz, D.M., and Kulmala M. (2009) An overview of atmospheric measurements made during the IS4FIRES experiment at Hyytiälä, Finland. 8th Symposium on Fire and Forest Meteorology, (12-15 October 2009) (Kalispell, MT), p1.19
- FEPS, 2011. Fire emission production simulator [online]. [cited 2 Mar 2011]. Available from World Wide Web: <<http://www.fs.fed.us/pnw/fera/feps/>>.
- Hari, P. and Kulmala, M. (2005). Station for measuring ecosystem-atmosphere relations (SMEAR II), *Boreal Env. Res.* 10, 5, 315-322.
- Kukkonen, J., Nikmo, J., Ramsdale, S.A., Martin, D., Webber, D.M., Schatzmann, M. and Liedtke, J., 2000. Dispersion from strongly buoyant sources. In: Gryning, S.-E. and Batchvarova, E. (eds.), *Air Pollution Modeling and its Application XIII*, Kluwer Academic/Plenum Publishers, pp. 539-547.
- Kulmala L., Pumpanen J., Levula J., Rantanen S., Laakso H., Siivola E., Kolari P., and Vesala T. (2011) CO₂ efflux before and after a clear cut and prescribed burning of a boreal spruce forest. Abstracts of the annual FCoE workshop 2011, Report Series in Aerosol Science. In print.
- Schobesberger, S., Virkkula, A., Pohja, T., Aalto, P.P., Siivola, E., Franchin, A., Petäjä, T., and Kulmala, M. (2009). Airborne measurements of aerosols in the boundary layer and lower troposphere over Southern Finland, Proc. 2009 EUCAARI Annual Meeting, Stockholm, 17.-20.11.2009, Lappalainen, H.K., Asmi, A., Nieminen, T., and Kulmala, M. (Editors; 2010), Report Series in Aerosol Science, 107, 286-289.

GAS AND AEROSOL MEASUREMENTS WITH MARGA IN URBAN AND RURAL ENVIRONMENTS IN FINLAND

A. VIRKKULA, U. MAKKONEN, J. MÄNTYKENTTÄ, AND H. HAKOLA

Finnish Meteorological Institute, FI-00560, Helsinki, Finland

Keywords: Aerosol chemical composition, Trace gas, Nitrogen, Ammonia.

INTRODUCTION

Sulphur dioxide (SO₂) is the precursor of sulfuric acid and thus of new particle formation. Ammonia (NH₃) plays a key role in neutralizing acidic atmospheric compounds and in aerosol formation. The concentrations of semi-volatile aerosol species such as ammonium nitrate (NH₄NO₃) and ammonium chloride (NH₄Cl) are strongly dependent on the gas phase precursors ammonia (NH₃) nitric acid (HNO₃) and hydrochloric acid (HCl). Nitrous acid (HNO₂ or HONO) is of atmospheric importance due to its expected significant contribution to the production of OH radicals. It is obvious from the above that all these gases are important for atmospheric chemical processes and should be measured at a good time resolution.

NH₃ and acidic gases (SO₂, HCl, HNO₃, HNO₂) are water soluble. In water they form the respective ions ammonium (NH₄⁺), sulphate (SO₄²⁻), chloride (Cl⁻), nitrate (NO₃⁻), and nitrite (NO₂⁻) that can all be detected by ion chromatography (IC). On the other hand, the major inorganic constituents of aerosols are the water-soluble anions SO₄²⁻, Cl⁻, NO₃⁻, and the cations NH₄⁺, Na⁺, K⁺, Ca²⁺, and Mg²⁺, all of which can also be detected with an IC. It makes sense to analyze all of them with one instrument, as is done in the Monitor for AeRosols and Gasses in Ambient air (MARGA) (Ten Brink et al., 2007). It is an on-line analyzer for semi-continuous (1-hour time resolution) measurement of gases and water-soluble ions in aerosols.

The Finnish Meteorological Institute acquired a MARGA instrument in 2009. It was first used at the SMEAR III station in Helsinki from November 2009 to May 2010. It was then moved to a rural forest station, the SMEAR II station in Hyytiälä, southwestern central Finland. One purpose of this study was to investigate if MARGA instrument could be used to replace the traditional EMEP filter pack method. The other goal is to study diurnal and seasonal cycles of nitrogen-containing gases and aerosols.

MEASUREMENTS

The MARGA utilizes a Wet Rotating Denuder (WRD) to collect acid gasses and ammonia by diffusion into a liquid film. Particles pass through the denuder and are collected in a Steam Jet Aerosol Collector (SJAC). Within the SJAC, a supersaturated environment is created growing particles by deliquescence allowing them to be collected by inertial separation. As cooling takes place, steam condenses and washes the particles into a liquid sample that is subsequently analyzed by ion chromatography for water-soluble anions and cations. Absorption solutions are drawn from the WRD and SJAC to syringes (25 ml) in the analytical box. Each hour after the syringes have been filled, samples are injected to the Metrohm anion (250 µl loop) and cation chromatographs (500 µl loop) with the internal standard (LiBr).

In front of the instrument there are two inlets, PM10 and PM2.5, and there are two identical sampling boxes. For gases this setup is an online quality control since the gas concentrations should be the same after both inlets. For aerosols the two size fractions mainly give information of the contribution of large,

soil-originated or sea-salt particles, and of long-range-transported particles and of particles that have their origin in gas-to-particle conversion – the latter two groups are essentially all in the particle size range $D_p < 2.5 \mu\text{m}$.

The SO_2 concentration measured with the MARGA is compared with that measured with a conventional monitor. At SMEAR III SO_2 is measured also by using a TEI 43iTL (Thermo Fisher Scientific, USA) instrument that is based on UV-induced fluorescence. Aerosol phase measurements are compared with standard EMEP stacked 47 mm filters that were analyzed for the same ions as given by the MARGA.

RESULTS OF URBAN MEASUREMENTS

Selected time series of gases and aerosols measured at SMEAR III are shown in Figure 1. A major pathway in the formation of HNO_3 is the reaction $\text{NO}_2 + \text{OH} \cdot + \text{M} \rightarrow \text{HNO}_3 + \text{M}$ where the hydroxyl radical $\text{OH} \cdot$ is originated from photochemical reactions. In other words, when there is sunlight, the expected HNO_3 concentrations are higher than in the darkness. This is in agreement with our observations. During the darkest months (November - January) when solar radiation is low in the northern latitudes the concentration of nitric acid was mostly below 0.1 ppb and stayed stable throughout day and night. In the beginning of February variation of HNO_3 increased and peaks of 1 – 1.5 ppb were detected. In March and April the concentrations varied below 0.5 ppb. In May HNO_3 concentration increased again and peaked until 1 ppb.

Nitrous acid HNO_2 on the other hand is dissociated by solar radiation: $\text{HNO}_2 + h\nu \rightarrow \text{OH} \cdot + \text{NO}$. Also this is in agreement with our observations at the SMEAR III station: in winter they were highest and they decreased clearly towards spring.

Ammonia had a very clear seasonal cycle: in winter it was most of the time below detection limit. The significant sources of NH_3 are animal waste, ammonification of humus followed by emission from soils, losses of ammonium-containing fertilizers from soils, and industrial emissions (Seinfeld and Pandis, 1998). The agriculture-related and soil-related sources are strongest in summer, which as such already leads to a seasonal cycle. The additional explanation for the seasonal cycle of ammonia is related to temperature in another way: at warm temperatures at daytime ammonium nitrate particles may volatilize and at cold temperatures the other way round so the reaction $\text{NH}_3 + \text{HNO}_3 (\text{g}) \leftrightarrow (\text{NH}_4\text{NO}_3) (\text{s})$ has a temperature-dependent balance. This is also in agreement with our observations: the concentrations of ammonium and nitrate were highest in winter.

The comparison of SO_4^{2-} , NO_3^- , and NH_4^+ with the same ions from filter samples and SO_2 from a conventional monitor show that mainly the agreement is very good. There were some periods, however, when NH_4^+ seems to be missing totally, which is unrealistic. The respective raw data needs re-evaluation to study the reasons for this.

The contribution of the various nitrogen-containing species to their sum is studied in Figure 2. The variation is large but one observation can be made: in the coldest months January and February most nitrogen is in the aerosol phase, the balance turns to the gas phase when temperature increases. This is a general trend but large variations from this are also obvious in Figure 2. An interesting observation is that the contribution of nitrate is largest in March, which is not in any of the extremes either for temperature or solar radiation.

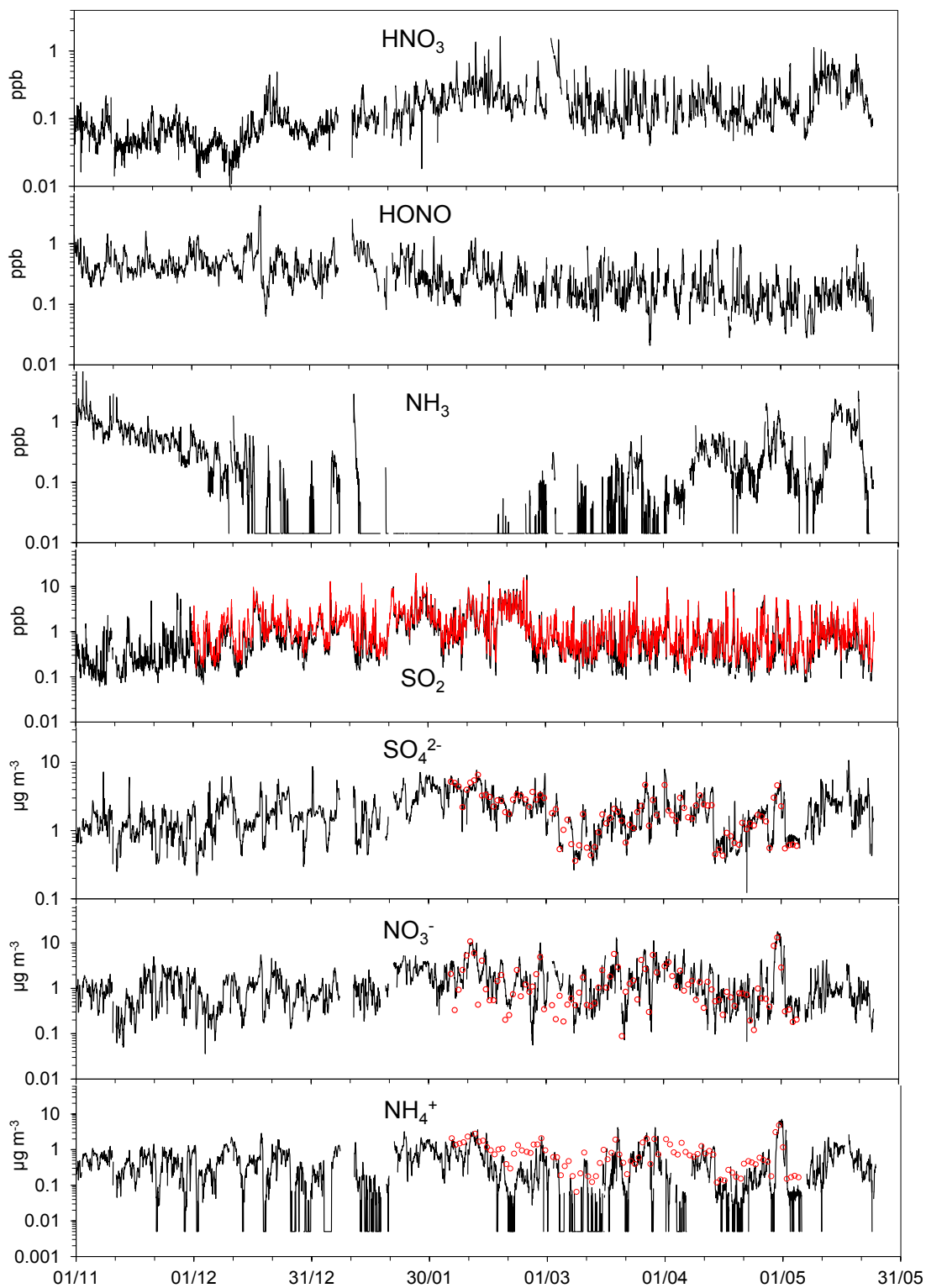


Figure 1. Hourly-averaged concentrations of selected gases (HNO_3 , HNO_2 , NH_3 , and SO_2) and aerosols ($D_p < 10 \mu\text{m}$) measured with the MARGA at SMEAR III from 1 November, 2009 to 25 May 2010. The red dashed line in the SO_2 time series is the data measured with a TEI 43iTL monitor. The red circles are respective concentrations analyzed from 24-hour EMEP PM10 filters.

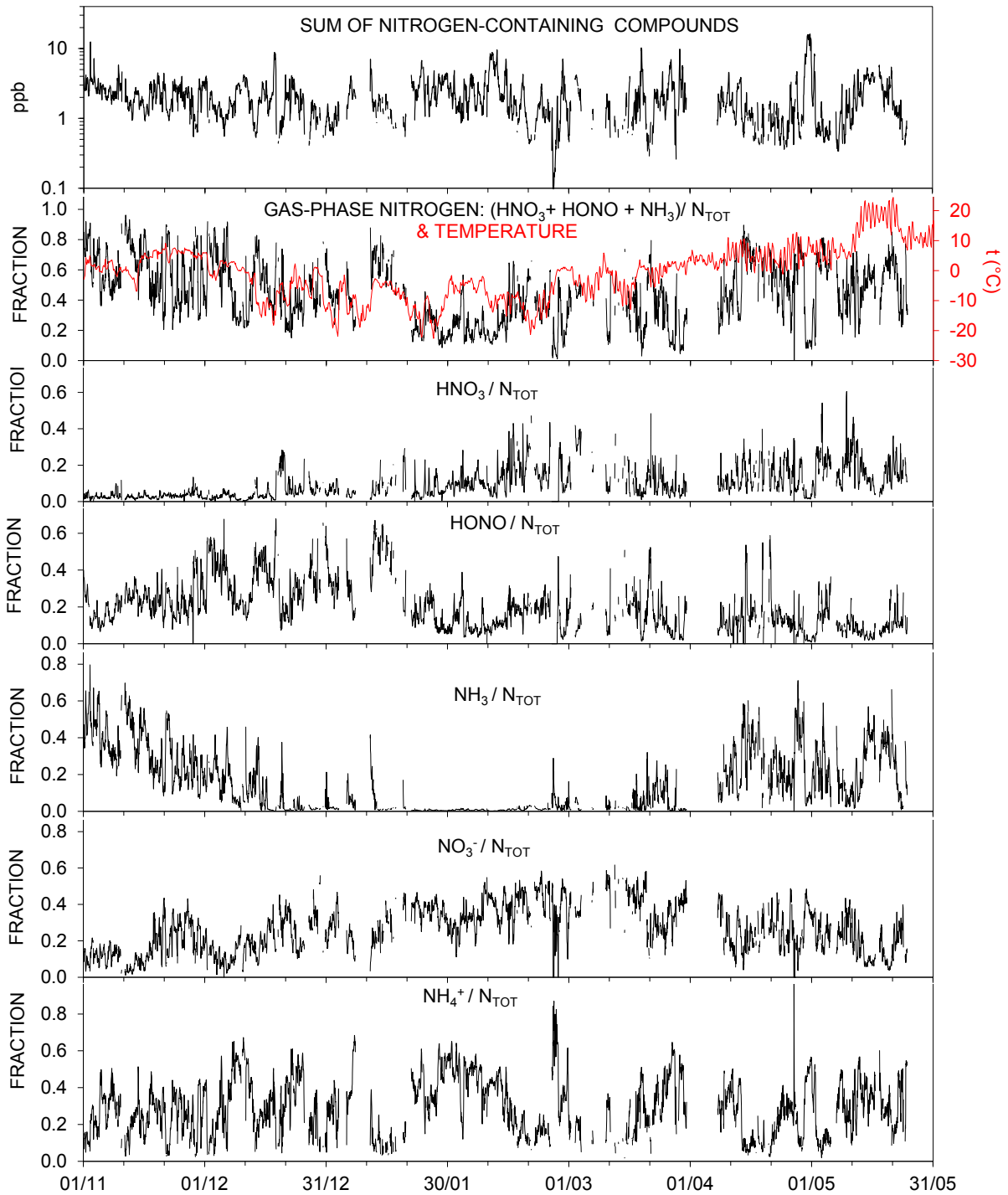


Figure 2. Nitrogen balance. Upper panel: Sum of nitrogen-containing gases ($\text{HNO}_3 + \text{HONO} + \text{NH}_3$) and aerosols in PM10 ($\text{NO}_3^- + \text{NH}_4^+$) all in ppb. The panels below that: fractions of nitrogen-containing compounds of the sum of all of them.

RESULTS OF RURAL MEASUREMENTS

Time series of selected MARGA measurements at SMEAR II in summer 2010 are shown in Figure 3. This covers a somewhat larger period than the large campaign “Hyytiälä United Measurements of Photochemistry and Particles in Air - Comprehensive Organic Precursor Emission Concentration 2010 (HUMPPA – COPEC-10)”, that was conducted at the SMEAR II In July – August 2010. The campaign was organized by the Max Planck Institute for Chemistry and the University of Helsinki.

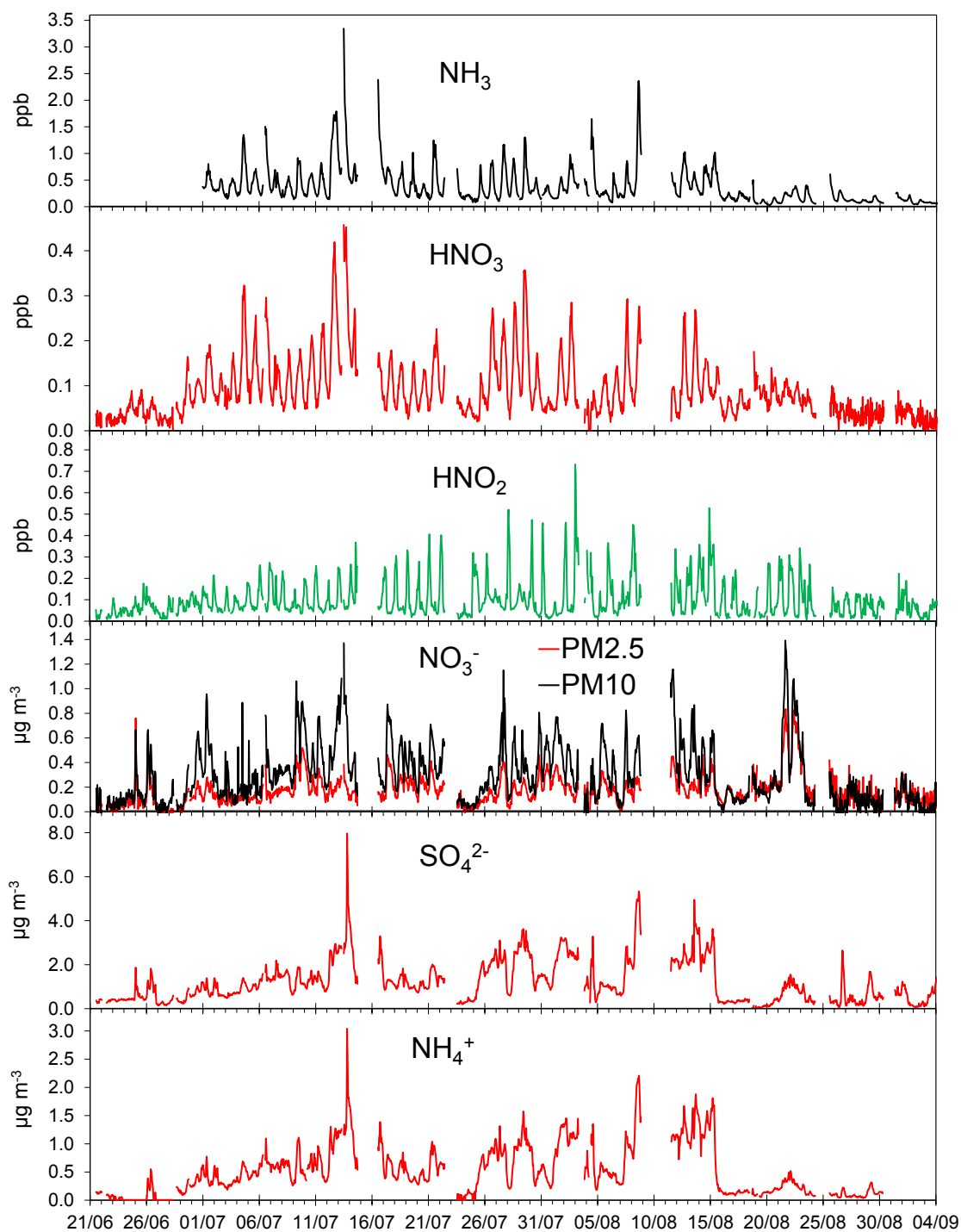


Figure 3. Hourly-averaged concentrations of selected gases (HNO₃, HNO₂, NH₃) and aerosols measured with the MARGA at SMEAR III from 1 November, 2009 to 25 May 2010.

A very clear diurnal cycle of NH_3 , HONO and HNO_3 was observed, especially in July. The data were classified according to the hour of the day. In July the highest median concentration of NH_3 , 0.59 ppb was observed in the afternoon at 15:00 and the lowest, 0.17 ppb at 05:00. Similarly, the highest median concentration of HNO_3 , 0.32 ppb was observed at 15:00 and the lowest, 0.20 ppb at 04:00. The clear diurnal cycles of ammonia and nitric acid suggest that they may at least partly be due to evaporation of ammonium nitrate particles in the hottest time of the warm July 2010 and condensation on particles at the cooler night. For HONO the diurnal variation was the opposite: the highest median concentration 0.20 ppb was observed very early in the morning at 03:00 and the minimum concentration 0.045 ppb in the evening at 18:00, in agreement with the photolysis of HONO. Towards the end of the campaign both the concentrations and their diurnal variations decreased. In 25 August to 04 September the median concentrations of ammonia, nitrous acid and nitric acid were 0.10 ppb, 0.061 ppb, and 0.18 ppb, respectively. From the 24-hour classification the medians of daily maximum and minimum concentrations were 0.16 and 0.069 ppb for ammonia, 0.094 and 0.021 ppb for nitrous acid, and 0.20 and 0.17 ppb for nitric acid.

There were large variations in the concentrations of anthropogenic-related major inorganic aerosol ions SO_4^{2-} , NO_3^- , and NH_4^+ , suggesting variations in source areas and transport routes of air masses. The main difference between the temporal variation of the gas phase species and the aerosol species was that the former clearly had a strong diurnal cycle whereas the latter remained roughly at the same level, either high or low, for a longer period, even though also nitrate had a period with a stronger diurnal cycle at the end of July until 15 August. Towards the end of the campaign both the concentrations and their diurnal variations decreased very clearly.

CONCLUSIONS

We have presented the first MARGA measurements made both at an urban and a rural site in Finland. The most important new information that can be obtained from this instrument is the concentration of the trace gases NH_3 , HNO_3 , HNO_2 , and HCl at a 1-hour time resolution so that for instance diurnal cycles can be observed. The aerosol species analyzed from the MARGA were most of the time in reasonable agreement with the same species analyzed from simultaneously taken filter samples.

The measurements at the urban and rural sites were made with the same instrument so it is clear that a direct comparison is not possible. However, the data do show common features: both the diurnal cycles of HNO_3 and HONO at the rural site and the seasonal cycle of them at the urban site were in agreement with photochemical production of HNO_3 and dissociation of HONO. Similarly, the seasonal cycle of NH_3 at the urban site is in line with the diurnal cycles observed at the rural site: there is obviously a temperature dependence of its concentration. The rural site is far from animal farms so, ammonification of humus followed by emission from soils is the most probable explanation for the cycle at SMEAR II.

ACKNOWLEDGEMENTS

The financial support by the Academy of Finland as part of the Centre of Excellence program (project no 1118615) is gratefully acknowledged.

REFERENCES

- Ten Brink H., Otjes R., Jongejan P., Slanina S. (2007) An instrument for semi-continuous monitoring of the size-distribution of nitrate, ammonium, sulphate and chloride in aerosol, *Atm. Environ.* 41, 2768-2779.
- Seinfeld J.H. and Pandis S.N. (1998) *Atmospheric chemistry and physics: from air pollution to climate change*, Wiley.

UHMAEMO – UNIVERSITY OF HELSINKI MULTICOMPONENT AEROSOL MODULE: A REVISED AND MODULARIZED VERSION

H. VUOLLEKOSKI¹, H. KORHONEN^{2,3}, L. ZHOU¹, K. E. J. LEHTINEN^{2,3}, V.-M. KERMINEN⁴, M. BOY¹ and M. KULMALA¹

¹Department of Physics, University of Helsinki, Helsinki, 00014, Finland

²Department of Physics and Mathematics, University of Eastern Finland, Kuopio, 70211, Finland

³Finnish Meteorological Institute, Kuopio Unit, Kuopio, 70211, Finland

⁴Finnish Meteorological Institute, Helsinki, 00560, Finland

Keywords: MODELING, AEROSOL DYNAMICS, PARTICLE FORMATION AND GROWTH.

INTRODUCTION

In their most recent assessment report, the Intergovernmental Panel for Climate Change (2007) states that aerosols have a potentially significant cooling effect in global warming. Additionally, there is an increasing public concern e.g. about the health effects of fine particles. In order to investigate these and many other unknowns related to both primary and secondary particle formation and growth, aerosol dynamical models are often applied. We have further developed an established aerosol dynamics model for wider usability.

MODEL DESCRIPTION

The original UHMA (University of Helsinki Multicomponent Aerosol) model was developed for studies of tropospheric new particle formation in clear sky conditions (Korhonen *et al.*, 2004). The size-segregated, sectional box model included all basic aerosol dynamical processes: nucleation, condensation, coagulation and dry deposition, and has been used quite extensively and successfully to study new particle formation characteristics particularly in the boreal forest environment of Hyytiälä, Finland.

Since the first UHMA description paper (Korhonen *et al.*, 2004), the program code has evolved due to e.g. addition of new minor processes, such as organic nucleation (Vuollekoski *et al.*, 2010) and snow scavenging (Kyrö *et al.*, 2009) parameterizations, which have both proven reasonable.

From a more technical perspective, the program code has gone through significant changes. For example, the coagulation coefficients are now recalculated only after significant changes in the sizes of particle bins have occurred, which typically causes a drastic reduction in computing time.

The new version is capable of directly using measurement and other input data to e.g. continuously set the vapor concentrations or initialize the particle distribution.

The condensation routine has been partially rewritten in an effort to describe the discrete general dynamic equation governing particle dynamics more accurately. As a result, all model dynamics are now described by differential equations, which makes the adaptation of differential equation solvers easier. In addition to the original Euler forward, the current version also includes the algorithms known as Euler–Cauchy and the 4th order Runge–Kutta. The improved condensation routine also includes a safety check: the time step of the model is automatically lowered, if too high growth rates threaten the numerical stability of the model.

The most significant difference between the original UHMA and the new version, aptly dubbed UHMAEMO, is, however, in structure: the code has been divided in more, shorter source files, and is now completely modularized. There are no global variables that would be visible outside of the scope of each function. Instead, all important variables are input and output via *ad hoc* data types. This means that UHMAEMO can be coupled with the majority of e.g. meteorological and chemical models with little effort.

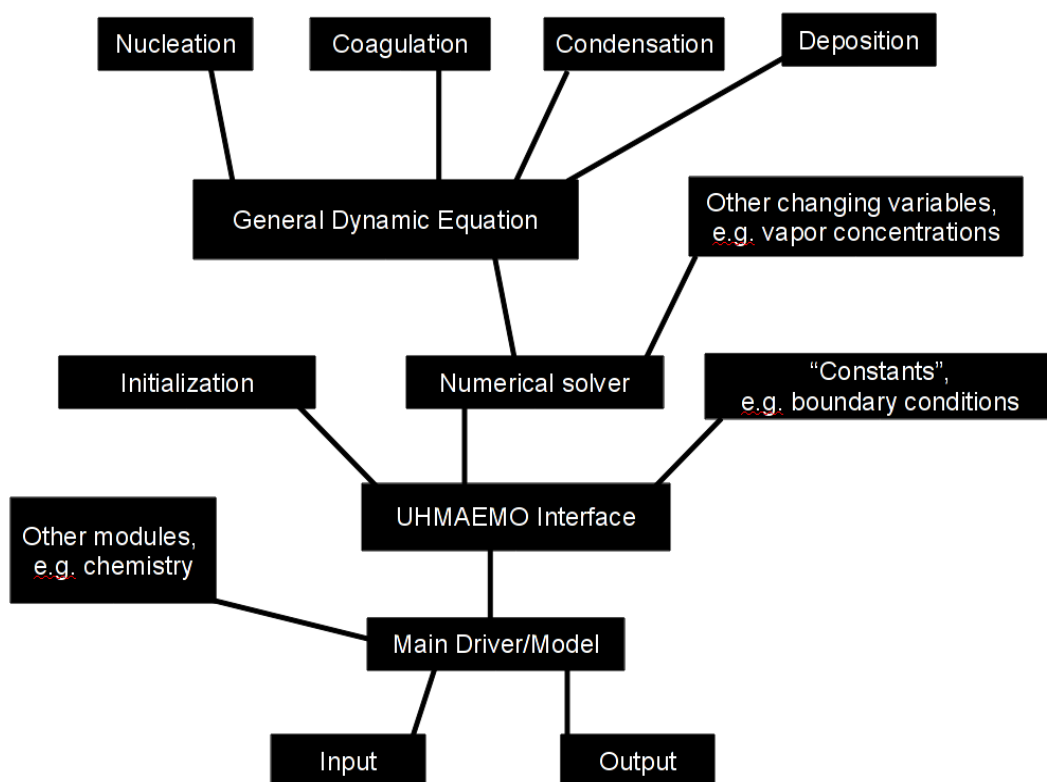


Figure 1: A schematic of UHMAEMO.

CONCLUSIONS

The established University of Helsinki Multicomponent Aerosol model (UHMA) has been further developed into an easily applicable module UHMAEMO. Currently, it is being coupled with a chemistry module in an effort to create a detailed box model, as well as with chemical, emission and meteorological modules aiming for regional models.

ACKNOWLEDGEMENTS

The financial support by the Academy of Finland Centre of Excellence program (project no 1118615) is gratefully acknowledged. This work has been partially funded by European Commission 6th Framework programme project EUCAARI, contract no 036833-2 (EUCAARI).

REFERENCES

- IPCC (2007). *Fourth Assessment Report: Climate Change 2007: Working Group I Report: The Physical Science Basis* (IPCC, Geneva, Switzerland).
- Korhonen, H., K. E. J. Lehtinen and M. Kulmala (2004). Multicomponent aerosol dynamics model UHMA: model development and validation, *Atmos. Chem. Phys.*, **1**, 757-771.
- Kyrö, E.-M., T. Grönholm, H. Vuollekoski, A. Virkkula, M. Kulmala and L. Laakso (2009). Snow scavenging of ultrafine particles: field measurements and parameterization, *Boreal Env. Res.*, **14**, 527-538.
- Vuollekoski, H., T. Nieminen, P. Paasonen, S.-L. Sihto, M. Boy, H. Manninen, K. E. J. Lehtinen, V.-M. Kerminen and M. Kulmala (2010). Atmospheric nucleation and initial steps of particle growth: numerical comparison of different theories and hypotheses, *Atmos. Res.*, **98**, 229-236.

AIRBORNE AEROSOL MEASUREMENTS OVER SOUTHERN FINLAND AT OCTOBER 2010 AND APRIL 2011

R. VÄÄNÄNEN¹, K. PAANANEN¹, T. PETÄJÄ¹, A. VIRKKULA^{1,2}, P.P. AALTO¹, T. POHJA¹,
L. KORTETJÄRVI¹, M. KULMALA¹

¹Department of Physics, University of Helsinki, Helsinki, Finland

¹Finnish Meteorological Institute, Helsinki, Finland

Keywords: Aerosols, airborne, SMPS.

INTRODUCTION

Atmospheric aerosols can be either primary particles, e.g. soot from combustion, street dust from traffic, or salt particles from sea spray; or secondary particles, which nucleate and condense from gas molecules. Plausible candidates for the nucleating vapours include sulfur acid (Sipilä et al, 2010) and for the vapours participating to the growth include volatile organic compounds (VOCs) (Metzgera et al, 2010). VOCs are shown to have an important role in the growth of the nucleated particles in boreal forests (Tunved et al, 2004).

Aerosol group at University of Helsinki has a long experience in ground-level aerosol measurements (see, e.g. Hari and Kulmala, 2005). However, there is only a few data measured in lower troposphere over Finnish boreal forests (O'Down et al, 2009; Schobesberger et al, 2010; Virkkula et al, 2010). In this study, our aim is to supplement the on-ground measurements with airborne measurements performed by a small Cessna 172 one-engine aircraft with slow velocity (air velocity around 130 km/h) operating between altitudes of 30 m and 3.5 km.

INSTRUMENTATION

Our measuring system includes sample air inlet mounted under the right wing of the aircraft, and instruments located inside the cabin. Together with the inlet there is an outside temperature, a relative humidity, and a photosynthetically active radiation (PAR) sensor. Instruments installed inside a rack behind the pilot and the operator include: A Scanning Mobility Particle Sizer (SMPS) with measuring range of 10 – 350 nm; an ultrafine CPC TSI 3776 with cut-off value of 3 nm; a CO₂/H₂O analyzer Li-Cor LI-840; and a pressure sensor. A triple wavelength (467,530 and 660 nm) particle/soot absorption photometer (PSAP, Radiance Research), and a nephelometer (Radiance Research Model 903) were not included the campaigns in 2010 but were again in the setup of 2011. An external vacuum pump and a venturi tube located at the outlet flow generate the needed vacuum for the instruments. Additionally, a GPS receiver records the flight track.

MEASUREMENT CAMPAIGNS

We will analyze the results of two measurements campaigns, namely, one performed in October 2010, and the second campaign in April 2011. The campaign during 4th Oct and 15th Oct, 2010 included 50 vertical profiles and total amount of flight hours was 38 h. The spring 2011 campaign started at 4th April, and ended at 26th of April with total amount of flight hours 37 h. In both campaigns we measured vertical profiles up to 3.5 km above the countryside of Southern Finland – which is a mosaic of boreal forests of different ages, mires, small lakes, and cultivated land.

The weather conditions separated the October 2010 campaign to two periods: 4th -7th Oct warmer airmasses originating from South or South-West arrived to Southern Finland in all air levels up to 3000 m,

and during 11th -15th Oct colder airmasses arrived from North or North-West in corresponding air levels. The trajectories of the airmasses are calculated using HYSPLIT4 model (Draxler, 1999). During the latter period a new particle formation events were observed at Hyytiälä SMEAR II station.

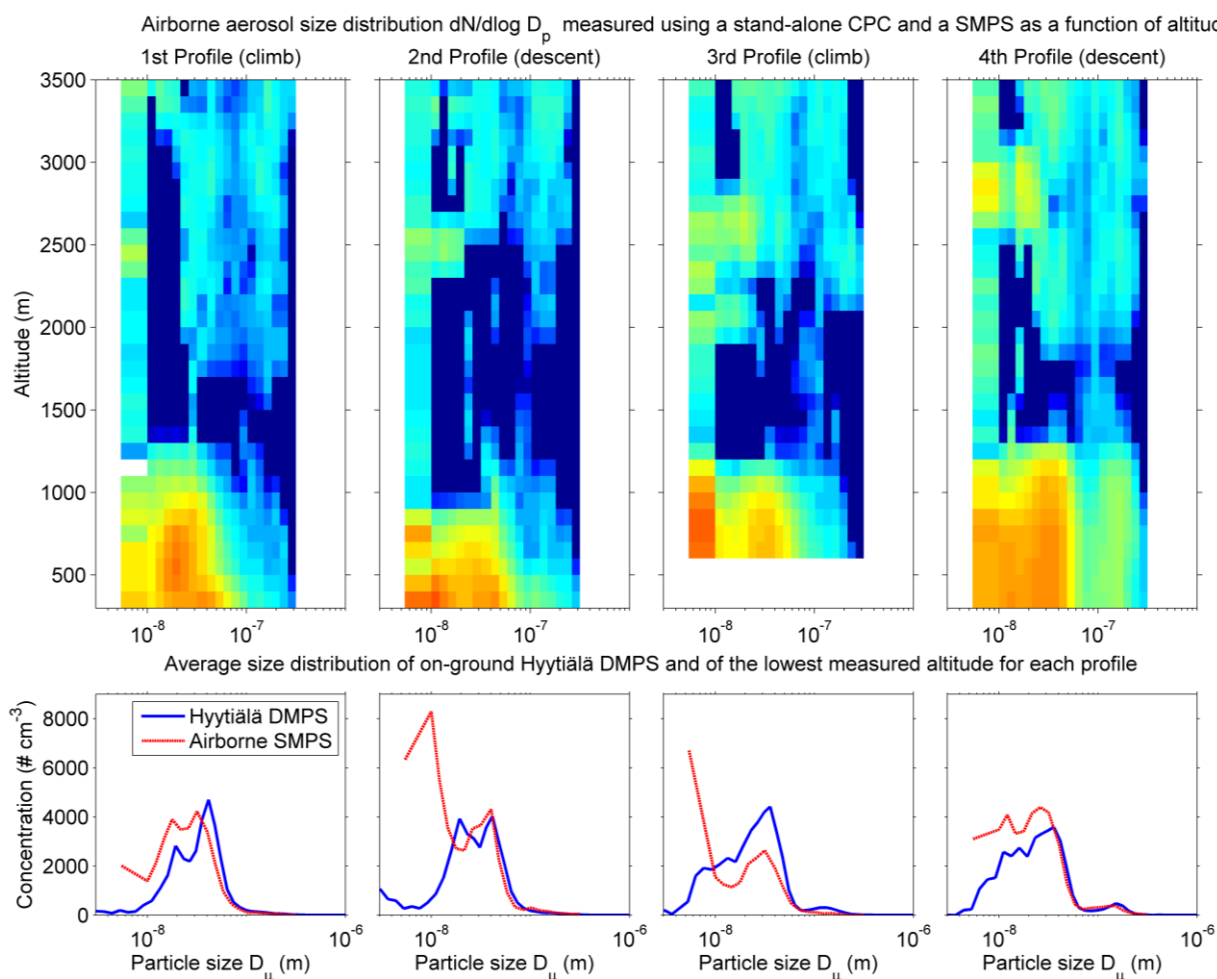


Figure 1. In the first row are the particle size distribution measured with airborne SMPS and ultrafine CPC during four vertical flight profiles at 13th Oct, 2010. In the second row are the particle size distributions of the lowest measured altitude compared to the average measured DMPS particle size distribution at Hyytiälä during the time of the corresponding profile. The concentration scale of the particle size distributions is same as in Figure 2B.

PRELIMINARY RESULTS

In Figure 1 is an example of vertical particle size distribution profiles for 13th of Oct, 2010. The flight routes are shown in the Figure 2A, the number indicates the corresponding profile. The plots at the first row of Figure 1 show the particle size distribution during four vertical profiles. For these plots, the altitude axis is divided to 100 m bins, and the mean distribution for each bin is calculated. The SMPS covers the size range of 10-350 nm, and the bin with the smallest diameter is calculated from the difference between the total particle concentration measured with the stand-alone CPC, and the concentration measured with SMPS. In the second row, the means of the DMPS particle size distributions measured at Hyytiälä SMEAR II station during each profile are compared to the airborne SMPS and CPC data measured at the lowest altitude of each profile. In that day, there were new particles growing at Hyytiälä Smear II station between 10 am and 3 pm, as can be seen from Figure 2B. One can see the largest differences between the airborne measurements and the ground-based measurements at the smallest particle sizes in profiles 2

and 3, whereas otherwise the shapes of the distributions (lower row of Fig.1) are quite similar. The profiles 2 and 3 are at low altitudes near Tampere City, and the anthropogenic pollution can be a source of the high concentrations of the sub-25 nm particles.

The highest concentrations are measured inside the boundary layer at altitudes below 1300 m. Above that, in the free troposphere, one can see first a layer of low concentration (total concentration below 100 cm^{-3}) and between 2-3.5 km again concentrations with $10^2\text{-}10^3 \text{ cm}^{-3}$.

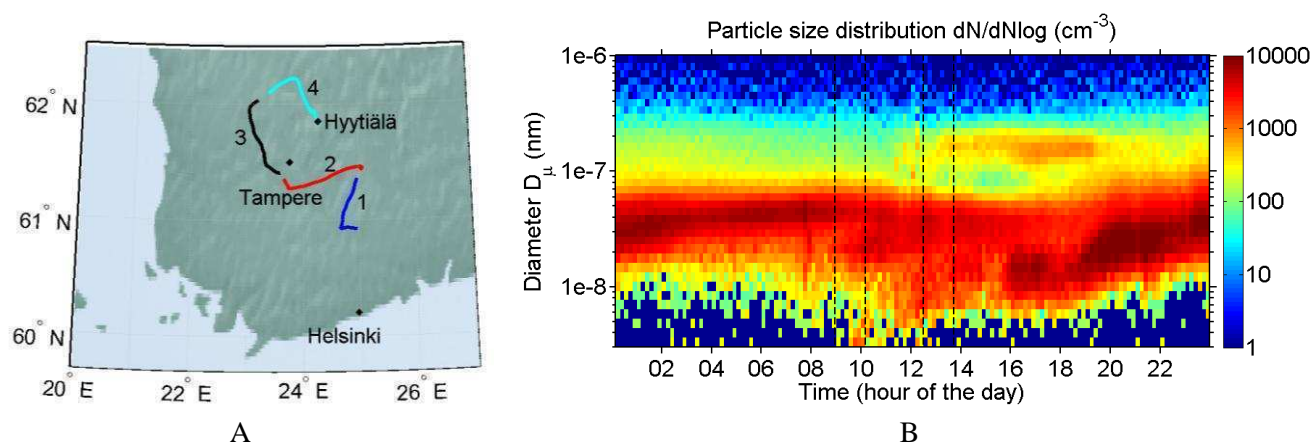


Figure 2. In figure A are the flight routes of four profile shown in Figure 1. In figure B is the particle size distribution at Hyytiälä during 13th Oct 2010. The first two profiles are measured at time between the first two dashed lines and the third and the fourth profile are measured between the latter dashed lines.

CONCLUSIONS

Two measurement campaigns were performed with a Cessna aircraft in October 2010 and in April 2011. The measured data included the size distribution, concentration and optical properties of airborne particles, together with CO₂/H₂O gases and meteorological parameters. Altitudes reached were from 300 m up to 3.5 km, and the airborne measurements are supported by the data from SMEAR II stations. The preliminary analysis of the October 2010 data shows some differences between the airborne size distributions when the airmasses came from different directions, however, more detailed analysis is needed.

ACKNOWLEDGEMENTS

The financial support by the Academy of Finland Centre of Excellence program (project no 1118615) is gratefully acknowledged.

REFERENCES

- Draxler, R.R. (1999): HYSPLIT4 user's guide. NOAA Tech. Memo. ERL ARL-230
- Hari, P. and Kulmala M. (2005). Station for measuring ecosystem-atmosphere relations (SMEAR II), *Boreal Env. Res.* **10**: 315.
- Metzgera, A., et al. (2010), Evidence for the role of organics in aerosol particle formation under atmospheric conditions. *PNAS*, **107** (15) 6646
- O'Dowd, C.D., et al. (2009). Airborne measurements of nucleation mode particles II: boreal forest nucleation events. *Atmos. Chem. Phys.*, **9**, 937.
- Schobesberger S., et al. (2010), Airborne measurements of aerosols in the lower troposphere over Southern Finland during 2009 in Proceedings of the Finnish Center of Excellence and Graduate

School in 'Physics, Chemistry, Biology and Meteorology of Atmospheric Composition and Climate Change' Annual Workshop 17.-19.5.2010. Report Series in Aerosol Science. Vol **109**.
Sipilä, M., et al. (2010), The Role of Sulfuric Acid in Atmospheric Nucleation. *Science*, **327** (5) 1243.
Tunved, P., et al. (2004), High Natural Aerosol Loading over Boreal Forests. *Science*, **312** (5771) 261.
Virkkula, A et al. (2010), Arrangement and preliminary results of a prescribed forest burning experiment in South-western Finland in June 2009 in Proceedings of the Finnish Center of Excellence and Graduate School in 'Physics, Chemistry, Biology and Meteorology of Atmospheric Composition and Climate Change' Annual Workshop 17.-19.5.2010. Report Series in Aerosol Science. Vol **109**.

ORGANIC ACID – INORGANIC SALT AQUEOUS SOLUTION DROPLETS: A STUDY ON EQUILIBRIUM VAPOUR PRESSURE OF SUCCINIC ACID

T. YLI-JUUTI¹, A.A. ZARDINI², M. KULMALA¹, M. BILDE², J. PAGELS³, A. ERIKSSON³, E. SWIETLICKI⁴, D. WORSNOP⁵ and I. RIIPINEN^{1,6}

¹Department of Physics, University of Helsinki, Helsinki, Finland.

²Department of Chemistry, University of Copenhagen, Copenhagen, Denmark.

³Faculty of Engineering, Lund University, Lund, Sweden.

⁴Department of Physics, Lund University, Lund, Sweden.

⁵Aerodyne Research Inc., Billerica, Massachusetts, USA.

⁶Department of Chemical Engineering, Carnegie Mellon University, Pittsburgh, USA.

Keywords: EVAPORATION, ORGANIC AEROSOLS, DICARBOXYLIC ACIDS, VAPOUR PRESSURE.

INTRODUCTION

Atmospheric aerosol particles affect the Earth's radiation balance directly by scattering and absorbing radiation and indirectly by acting as cloud condensation nuclei (CCN). Aerosol particles also have adverse health effects and lower the visibility. All these aerosol effects are largely dependent on the particle size and composition. These properties of aerosol particles depend on the origin of the particles, but also on the other processes modifying the aerosol population. The lack of knowledge on these properties potentially results in significant uncertainties for instance when modelling cloud condensation nuclei concentrations.

Growth of particles by condensation is one of the most important processes shaping the existing aerosol size distribution. It does not only increase the average size of the particles but also affects greatly on the life time of the smallest atmospheric particles: the fraction of the nanometre sized particles formed in atmospheric gas-to-particle phase transitions that survive to the large enough sizes to act as CCN is determined by how fast they grow compared to their loss rate by coagulation (Kerminen and Kulmala, 2002). Therefore, in the modelling of atmospheric aerosol particles it is crucial to consider the growth in a reasonable way (Riipinen *et al.*, 2011). This requires knowledge of the physical and chemical properties of aerosol components, which is currently scantily available especially for the organic constituents.

There is vast number of organic compounds in the atmosphere, and although many studies have addressed their thermodynamic properties we still lack a complete characterization of their physico-chemical properties. Although including the detailed information of all of these compounds in global models is unrealistic, it is of great benefit to know the properties of some of these compounds properly. Among the most important properties are the saturation vapour pressures for pure substances, and also the activities in particles consisting of many compounds, as atmospheric aerosol particles are typically mixtures of inorganic and organic compounds (Jimenez *et al.*, 2010)

One group of low-volatility organic compounds typically found from atmospheric aerosol particles are dicarboxylic acids. So far, the studies on these water soluble compounds have focused mainly on the saturation vapour pressures of pure compounds and the results from different studies have discrepancies. Even less is known about their equilibrium vapour pressures in multi-component mixtures. In this study,

the effect of inorganic salts on the evaporation of succinic acid (a dicarboxylic acid) from aqueous solution is studied and the saturation vapour pressure of succinic acid is determined testing different activity models.

METHODS

The evaporation rates of solution droplets were measured using a Tandem Differential Mobility Analyzer (TDMA) system modified to study sub-cooled droplets (Koponen *et al.*, 2007). The TDMA system is coupled with a 3.5 m long laminar flow tube that provides residence times of up to several minutes. Briefly, a monodisperse droplet population is selected with a Differential Mobility Analyzer (DMA) and let to the flow tube where the droplets evaporate. The size change of the droplets is measured with a Scanning mobility Particle sizer (SMPS) along the flow tube at 4 points as well as at the beginning and in the end of the tube. The droplets were atomized either from binary solution with succinic acid and water or from one of the ternary solutions containing both organic and inorganic solutes: succinic acid – sodium chloride – water and succinic acid – ammonium sulphate – water. In part of the measurements with ammonium sulphate as the inorganic compound the SMPS measurements were accompanied by an Aerosol Mass Spectrometer (AMS) to monitor the temporal evolution of the chemical composition of the droplets. The measurements were performed at room temperature and relative humidity inside the measurements setup was altered between 60-80 %. The initial organic molar fraction of the solute, F_{org} , was varied for the ternary droplet measurements from 0.33 to 0.90 in the experiments with sodium chloride as the inorganic compound and from 0.50 to 0.90 in the experiments with ammonium sulphate.

The measured change in particle size is compared to that predicted by a theoretical dynamical evaporation model based on mass transport from the droplet (Zardini *et al.*, 2010). In the model, the reduction in particle size is due to evaporation of succinic acid and water as the inorganic compound is assumed to stay in the liquid phase. Water is assumed to be equilibrated with the droplet and its partitioning between vapour and liquid phase is calculated using the Extended Aerosol Inorganic Model, E-AIM (www.aim.env.uea.ac.uk, see references therein), which is a phase equilibrium model including both organic and inorganic compounds. Due to the long time scale of the evaporation and low number concentration of particles the temperature of the particles and the gas in the flow tube are assumed to be equal and to stay constant.

Activity coefficients of succinic acid and water are calculated using E-AIM. Three activity coefficient models incorporated in E-AIM were tested: Redlich-Kister fitted activity equation, group contribution method UNIFAC with the standard set of parameters and UNIFAC with the modified set of parameters by Peng *et al.* (2001). In the binary cases these were compared also to Dortmund version of UNIFAC (Gmehling *et al.*, 1990). All the applied activity models consider interaction between the organic compound and water and between the inorganic compound and water neglecting the organic – inorganic interaction. Therefore, a difference between predicted and observed evaporation rates in the ternary cases might indicate that inorganic compound affects the activity of the organic compound.

In the evaporation model time step of 1 ms is used. The activity coefficients of water and succinic acid and the molar fraction of water in the liquid phase are updated from the E-AIM with 5 s intervals. The formation of solid phase and dissociation of succinic acid are not considered in the evaporation model. Physicochemical properties of succinic acid used in the evaporation model can be found from previous publications (Riipinen *et al.*, 2006; Koponen *et al.*, 2007; and references therein). Density of solution is calculated as a mass fraction weighted average of binary aqueous solution densities.

RESULTS AND DISCUSSION

The saturation vapour pressure of succinic acid $p_{sat,SA}$ was extracted from the binary succinic acid – water droplet experiments by using $p_{sat,SA}$ as a fitting parameter. The $p_{sat,SA}$ values obtained from the measurements performed at room temperatures were transformed to the $p_{sat,SA}$ values at 298.15 K by

utilizing the latent heat of vaporization of succinic acid that Koponen *et al.* (2007) determined using UNIFAC Dortmund activity model. The mean values and the relative variation of $p_{sat,SA}$ at 298.15 K determined by using the different activity models are presented in the Table 1. In general, the determined saturation vapour pressures had slightly increasing trend with relative humidity (RH). This was most pronounced when using UNIFAC with Peng *et al.* modified parameterization which resulted in 25 % variation in the $p_{sat,SA}$ values within the relative humidity range 60-80 %. It should be noted that these results are based on only four measurements, each in different RH, and therefore the uncertainty associated in the results may be larger than suggested by variation in the obtained $p_{sat,SA}$. The $p_{sat,SA}$ at 298.15 K determined by Koponen *et al.* (2007) using Dortmund version of UNIFAC was $0.98 \cdot 10^{-3}$ Pa and the $p_{sat,SA}$ obtained in this study using the same activity model is in reasonable agreement with this value.

Activity model	$p_{sat,SA}$ at 298.15 K mean (Pa)	relative variation (max.-min.)/mean*100%
Activity fitted equation	$1.29 \cdot 10^{-3}$	11 %
UNIFAC, Standard	$1.15 \cdot 10^{-3}$	9 %
UNIFAC, Peng <i>et al.</i> (2001) modified	$1.95 \cdot 10^{-3}$	25 %
UNIFAC, Dortmund	$0.90 \cdot 10^{-3}$	7 %

Table 1. Mean of the obtained saturation vapour pressures of succinic acid at 298.15 K and the relative variation of the values when using the four activity models.

The saturation vapour pressures of succinic acid obtained from the binary experiments with the three activity models included in the E-AIM were used for modelling the evaporation of the ternary organic – inorganic aqueous solution droplets. Figure 1 shows measured and modelled changes in size for droplets with succinic acid, ammonium sulphate and water with three initial organic molar fractions of solute and in two relative humidities. In general, the model captures the evaporative behaviour reasonably well. However, the model overestimates the evaporation rate when the molar fraction of succinic acid is comparative to or smaller than that of the inorganic compound. This was seen also with sodium chloride as the inorganic compound (Zardini *et al.*, 2010). In the cases with ammonium sulphate the agreement between the measured and modelled size changes seems to get better as RH increases. Therefore, it seems that the difference between the predicted and the observed size changes gets larger when the molar fraction of ammonium sulphate gets larger, i.e. when the effect of the inorganic compound would be expected to increase. Model runs presented in Fig. 1 correspond to fitted activity equation as the activity model.

There are at least two obvious possible sources of error, of which neither explains the difference between the measured and modelled evaporation rates completely. First, uncertainty in $p_{sat,SA}$ does not explain the overestimation of evaporation rate in the ternary cases since the agreement between the model and measurement is good with large succinic acid fraction. Second, the AMS measurements revealed that the composition of the droplets at the beginning of the flow tube is not what it would be assumed to be based on the organic fraction in the atomization solution. This is most probably due to part of the succinic acid evaporating from the droplets before they reach the DMA, which lowers the initial F_{org} from the expected one. This would lead to the predicted evaporation rate being too high. However, based on the analysis of the AMS data, the amount of succinic acid evaporated before the DMA is too low to solely explain the differences between the measure and modelled size changes. Therefore, the results might indicate that the activity of succinic acid is lowered by the inorganic solute in the mixture droplets. However, possible dissociation of succinic acid and formation of organic salts in the droplets as well as impurities in the droplets would decrease the evaporation rate and result in qualitatively the observed difference between the measured and modelled evaporation rates. Therefore, the effects of these, along with other uncertainties related to the measurement setup need to be studied more before drawing strong conclusions.

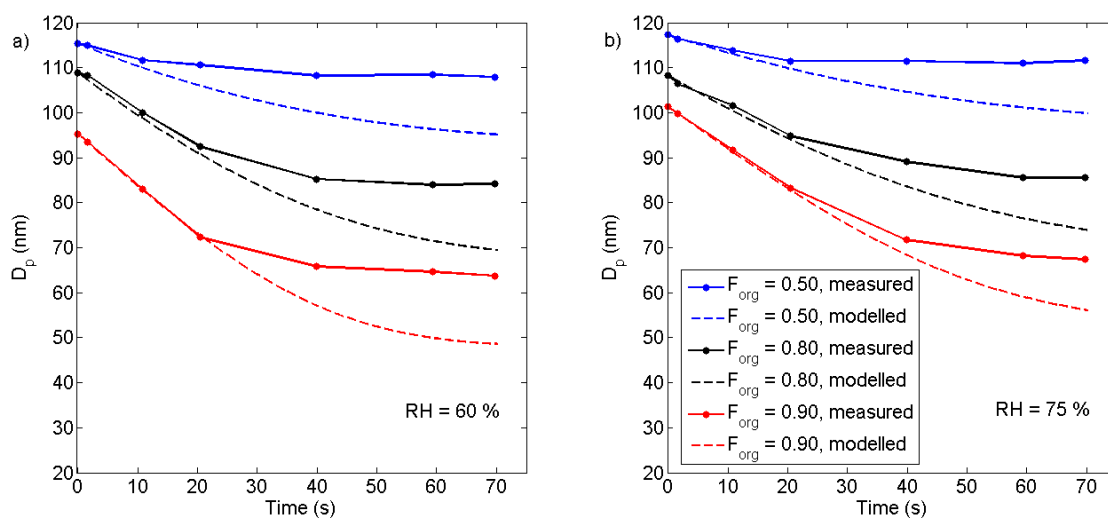


Figure 1. Measured and modelled size change of ternary droplets consisting of succinic acid, ammonium sulphate and water with three initial organic molar fractions of solute (F_{org}) in relative humidity of a) 60 % and b) 75 %.

ACKNOWLEDGEMENTS

This work was supported by EUCAARI (project no 036833), the Academy of Finland Centre of excellence program (project no 1118615) and Maj and Tor Nessling foundation.

REFERENCES

- Gmehling, J., Tiegs, D. and Knipp, U. (1990). A comparison of the predictive capability of different group contribution methods. *Fluid Phase Equilib.* **54**, 147-165.
- Jimenez, J.L., Canagaratna, M.R., Donahue, N.M., Prevot, A.S.H., Zhang, Q., Kroll, J.H., DeCarlo, P.F., Allan, J.D., Coe, H., Ng, N.L., Aiken, A.C., Docherty, K.S., Ulbrich, I.M., Grieshop, A.P., Robinson, A.L., Duplissy, J., Smith, J.D., Wilson, K.R., Lanz, V.A., Hueglin, C., Sun, Y.L., Tian, J., Laaksonen, A., Raatikainen, T., Rautiainen, J., Vaattovaara, P., Ehn, M., Kulmala, M., Tomlinson, J.M., Collins, D.R., Cubison, M.J., Dunlea, E.J., Huffman, J.A., Onasch, T.B., Alfarra, M.R., Williams, P.I., Bower, K., Kondo, Y., Schneider, J., Drewnick, F., Borrmann, S., Weimer, S., Demerjian, K., Salcedo, D., Cottrell, L., Griffin, R., Takami, A., Miyoshi, T., Hatakeyama, S., Shimojo, A., Sun, J.Y., Zhang, Y.M., Dzepina, K., Kimmel, J.R., Sueper, D., Jayne, J.T., Herndon, S.C., Trimborn, A.M., Williams, L.R., Wood, E.C., Middlebrook, A.M., Kolb, C.E., Baltensperger, U. and Worsnop, D.R. (2009). Evolution of organic aerosols in the atmosphere. *Science* **326**, 1525-1529.
- Kerminen, V.-M. and Kulmala, M. (2002). Analytical formulae connecting the "real" and "apparent" nucleation rate and the nuclei number concentration for atmospheric nucleation events. *J. Aerosol Sci.* **33**, 609-622
- Koponen, I.K., Riipinen, I., Hienola, A., Kulmala, M. and Bilde, M. (2007). Thermodynamic properties of malonic, succinic, and glutaric acids: Evaporation rates and saturation vapour pressures, *Environ. Sci. Technol.* **41**, 3926.
- Riipinen, I., Svenningsson, B., Bilde, M., Gaman, A., Lehtinen, K.E.J. and Kulmala M. (2006). A method for determining thermophysical properties of organic material in aqueous solutions: Succinic acid, *Atmospheric Res.* **82**, 579.
- Riipinen, I., Pierce, J.R., Yli-Juuti, T., Nieminen, T., Häkkinen, S., Ehn, M., Junninen, H., Lehtipalo, K., Petäjä, T., Slowik, J., Chang, R., Shantz, N.C., Abbatt, J., Leaitch, W.R., Kerminen, V.-M., Worsnop, D.R., Pandis, S.N., Donahue, N.M. and Kulmala, M. (2011). Organic

condensation – a vital link connecting aerosol formation to climate forcing. *Atmos. Chem. Phys. Discuss.* **11**, 387-423.

Peng, C., Chan, M.N. and Chan C.K. (2001). The hygroscopic properties of dicarboxylic and multifunctional acids: Measurements and UNIFAC predictions, *Environ. Sci. Technol.* **35**, 4495.

Zardini, A.A., Riipinen, I., Koponen, I.K., Kulmala, M. and Bilde, M. (2010). Evaporation of ternary inorganic/organic aqueous droplets: Sodium chloride, succinic acid and water, *J. Aerosol Sci.* **41**, 760.

THE FIRST LONG-TERM MODEL STUDY OF PARTICLE FORMATION AND GROWTH WITH DETAILED CHEMISTRY AND AEROSOL DYNAMICS IN AND ABOVE BOREAL FOREST

L.ZHOU¹, M.BOY¹, H.VUOLLEKOSKI¹, C.WATCHARAPASKORN¹, D.MOGENSEN¹,
S.SMOLANDER¹, A.SOGACHEV² and M.KULMALA¹

¹Department of Physics, University of Helsinki, Finland.

²Wind Energy Division, Risø National Laboratory for Sustainable Energy, Technical University of Denmark, Denmark.

Keywords: BOUNDARY LAYER MODELLING, PARTICLE FORMATION AND GROWTH, AEROSOL DYNAMICS.

INTRODUCTION

Natural and anthropogenic aerosols may have a great impact on climate as they can directly interact with solar radiation and indirectly affect the Earth's radiation balance and precipitation by modifying clouds. In order to quantify the direct and indirect effects, we must understand the complex processes that connect an aerosol particle to a cloud droplet. However, while modern measurement techniques are able to detect particle sizes down to nanometer all the way from ground up to the stratosphere, the data do not serve for all of our needs for understanding the processes. Hence we will demonstrate a modelling approach to investigate the complex processes of aerosols in the atmospheric boundary layer (ABL).

METHODS

SOSAA (model to **S**imulate the concentration of **O**rganic vapours, **S**ulphuric Acid, and **A**erosol) is the first column model existing in the world with detailed chemistry and aerosol dynamics parallelized. It can be used to study aerosol processes in the ABL for long period. The model includes the aerosol dynamics module UHMAEMO (**U**niversity of **H**elsinki **M**ulticomponent **A**erosol **M**odule) coupled with the chemistry-transport column model SOSA (model to **S**imulate the concentration of **O**rganic vapours, **S**ulphuric Acid, Figure 1).

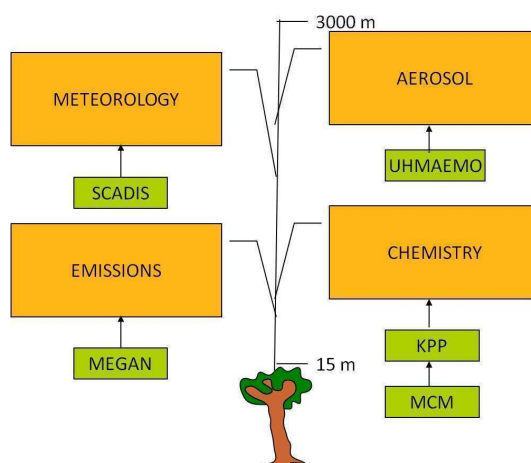


Figure 1. SOSAA model structure

SOSA attempts to reconstruct the emissions, transport, and chemistry in the ABL in and above a vegetation canopy using meteorological measurements (Boy et al., 2011). UHMAEMO simulates tropospheric new particle formation in clear sky conditions. It is developed from the UHMA model which includes all basic aerosol dynamical processes: nucleation, condensation, coagulation and dry deposition (Korhonen et al., 2004).

As a first application of the model, we present nucleation studies for the year 2010 in Hyytiälä, Finland with different nucleation theories including homogeneous nucleation of sulphuric acid and water, kinetic nucleation, and activation nucleation (Figure 2). Modelled particle growth rates and sulphuric acid concentrations have also been compared with measurements from HUMPPA-COPEC campaign, which was carried in Hyytiälä from 5th July to 13th August, 2010.

CONCLUSIONS

Simulation has shown that the particles mainly form in the lower boundary layer and their evolution follow the boundary layer development (Figure 2), which agree well with observations.

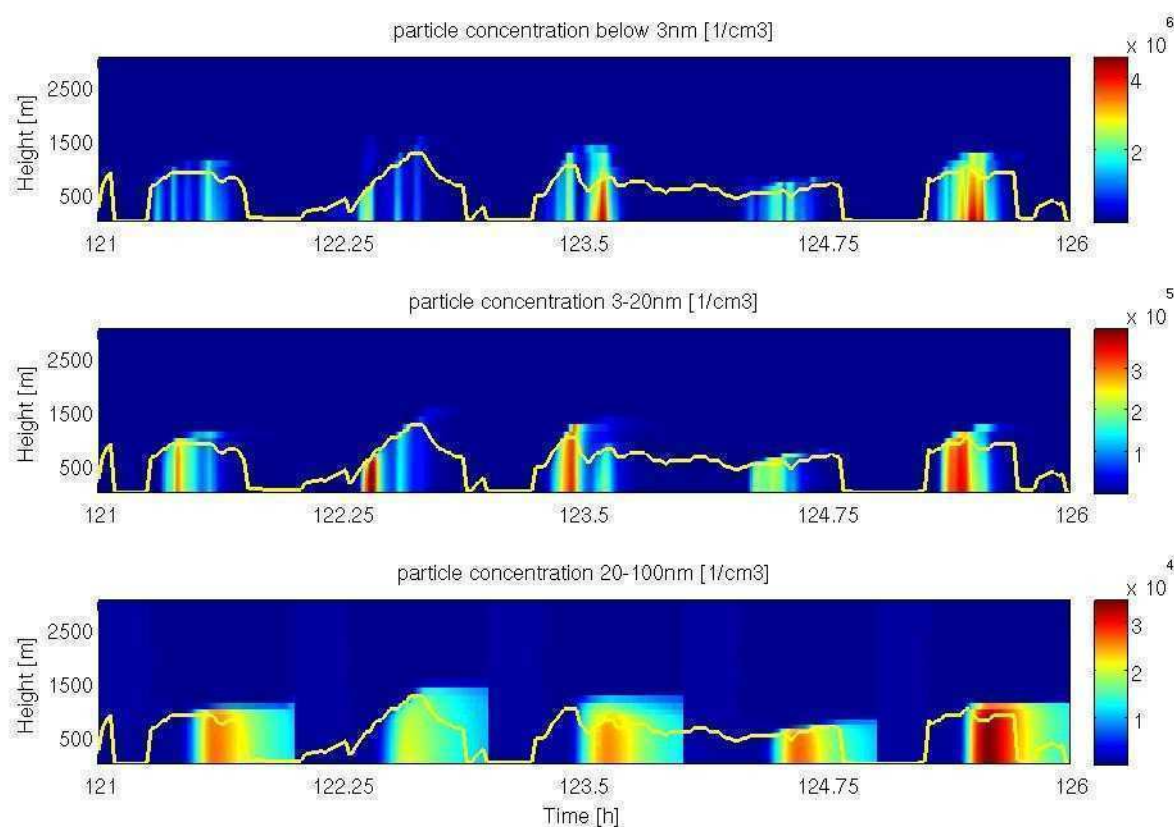


Figure 2. Simulated vertical particle distribution in the atmosphere for May 1—5, 2007, for size range below 3 nm, 3 – 20 nm and 20 – 100 nm respectively. Simulated boundary layer height is presented as well by the yellow line.

ACKNOWLEDGEMENTS

The financial support by Helsinki University Centre for Environment (HENVI), the Academy of Finland Centre of Excellence program (project no. 1118615), and the European Commission 6th Framework program project EUCAARI is gratefully acknowledged.

REFERENCES

Boy, M., Sogachev, A., Lauros, J., Zhou, L., Guenther, A. and Smolander (1975). SOSA – a new model to simulate the concentrations of organic vapours and sulphuric acid inside the ABL – Part 1: Model description and initial evaluation. *Atmos. Chem. Phys.* **11**, 43-51.

Korhonen, H., Lehtinen, K. E. J. and Kulmala, M (2004). Multicomponent aerosol dynamics model UHMA: model development and validation. *Atmos. Chem. Phys.* **1**, 757-771.

AEROSOL CHEMICAL COMPOSITION MEASUREMENTS AT A BOREAL FOREST SITE IN SOUTHERN FINLAND DURING DIFFERENT SEASONS

M. ÄIJÄLÄ¹, H. JUNNINEN¹, M. EHN¹, T. PETÄJÄ¹, P.P. AALTO¹, M. KULMALA¹ and D.R WORSNOP^{1,2}

¹Department of Physics, University of Helsinki, P.O. Box 64, FI-00014 Helsinki, Finland

²Aerodyne Research Inc, Billerica, MA 01821, USA

Keywords: RURAL AEROSOL, BOREAL FOREST, AEROSOL MASS SPECTROMETRY, AMS

INTRODUCTION

Boreal forests are an important biome, covering vast areas of the northern hemisphere and affecting the global climate change via various feedbacks (Bonan, 2001). Despite having relatively few anthropogenic primary aerosol sources, the boreal forest acts as a major source of climate-relevant aerosol particles (Tunved et al., 2006). This study describes aerosol chemical composition measurements using an Aerosol Mass Spectrometer (AMS, Jayne et al. 2000), carried out at a boreal forest area in Hyytiälä, Southern Finland. The site, Helsinki University SMEAR II measurement station (Hari & Kulmala, 2005), is situated at a homogeneous Scots pine (*Pinus sylvestris*) forest stand, and is equipped with a range of aerosol, meteorological and gas phase instruments. A continuous time series of aerosol number size distributions in the sub-micron size range, measured with a twin-DMPS, already spans 14 years. However, aerosol chemical composition has only been measured during relatively short campaigns (Allan et al., 2006), and has not been monitored in a more continuous fashion until recent years. The measurements presented here were taken in 2008 and 2009 as a part of the EUCAARI project (European integrated project on aerosol cloud climate air quality interactions, Kulmala et al., 2009).

METHODS

During the EUCAARI campaign an Aerodyne AMS was used to resolve aerosol chemical composition. The AMS features an aerodynamic lens for concentrating the sample particles to a narrow beam, a particle time-of-flight (PToF)-chamber for size distribution measurement, thermal vaporization of the sample particles, electron impact (EI) for ionizing the obtained vapor, combined with a compact time-of-flight mass spectrometer (C-ToF-MS) to obtain a mass spectrum of the ions (Drewnick et al., 2005). The original sample aerosol chemical composition is then obtained using data inversion and analysis (Allan et al., 2004). An example of the final aerosol mass spectrum is presented in Figure 1.

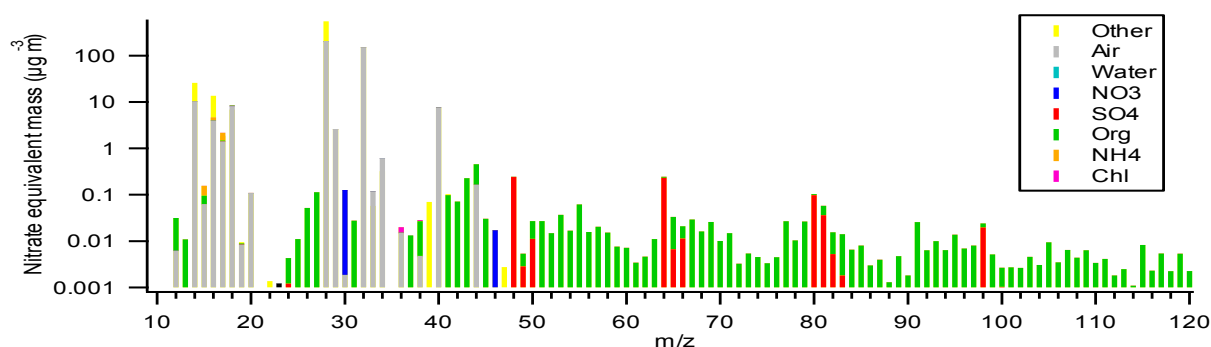


Figure 1. An example of an AMS average mass spectrum, from 22th September 2008, during a period of relatively high ($15 \mu\text{g}/\text{m}^3$) total mass concentrations.

RESULTS

The measured total mass concentrations in Hyytiälä were observed to vary from close to zero up to 17 $\mu\text{g}/\text{m}^3$. The average mass concentration and relative contribution of typical aerosol constituents for the two measurement periods are presented in Table 1 and Figure 2.

Table 1. Aerosol average chemical composition in Hyytiälä during two measurement periods.

Time period	average mass concentration ($\mu\text{g}/\text{m}^3$)					
	total	SO ₄	org	NH ₄	NO ₃	chl
29. Apr - 7. Jun 2008	2.92	0.80	1.63	0.32	0.17	0.000
3. Mar - 31. Mar 2009	3.40	1.43	1.37	0.36	0.23	0.008
10. Sep - 15. Oct 2008	2.21	0.41	0.60	0.14	0.08	0.004

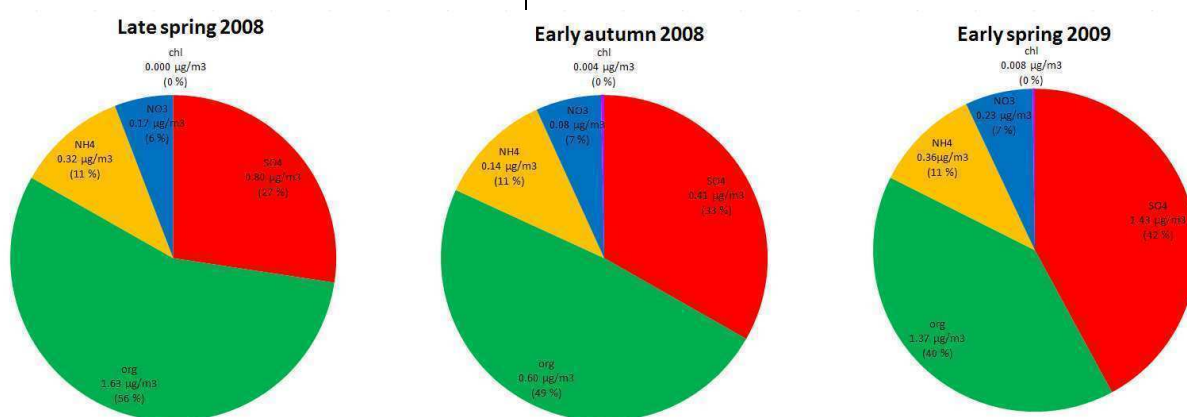


Figure 2. Relative contribution of organics, sulfates, nitrates, ammonia and chloride in Hyytiälä in autumn 2008 and early spring 2009.

For all of the campaigns, organics and sulfate together accounted for 82-83% of total mass. In late spring and early autumn, more organic aerosol was observed than during very early spring, both as fraction of total and in absolute amounts. Ammonia and nitrate fractions remained the same for all campaigns, with 11% and 6-7% total mass fractions respectively. The total aerosol mass loadings were somewhat higher during spring, averaging 2.92 and 3.40 $\mu\text{g}/\text{m}^3$ versus 2.21 $\mu\text{g}/\text{m}^3$ measured during the autumn campaign. The AMS time traces for different chemical species in March 2009 is presented in Fig 3. Both periods of relatively high loadings and those with little aerosol mass were observed, including events with high sulfate and nitrate concentrations.

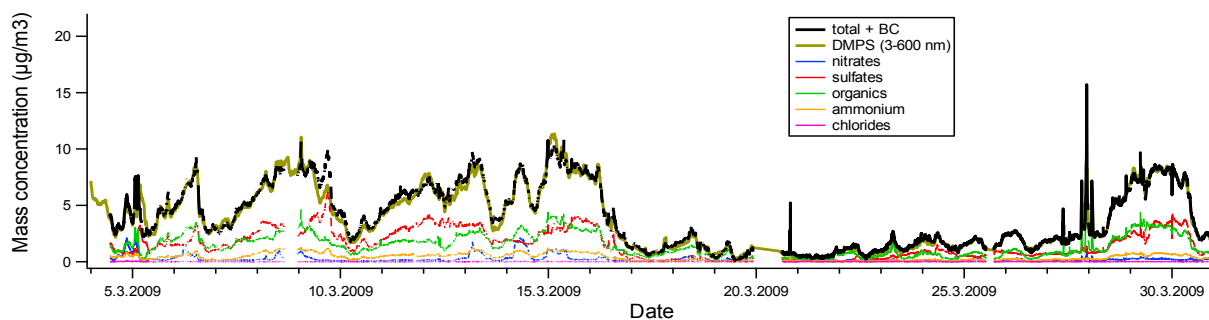


Figure 3. A time trace of aerosol mass loadings for measured chemical species in March 2009. Black carbon (BC) data is measured with an aethalometer, and is added to AMS total for DMPS comparison.

Mass concentrations measured with the AMS in the particle size range of 40-600 nm correlate well with DMPS measurements (Fig 4). The few differences between the two during some time periods are mostly explained by the different definition of particle diameter in the DMPS (electrical mobility equivalent diameter) and the AMS (vacuum aerodynamic diameter).

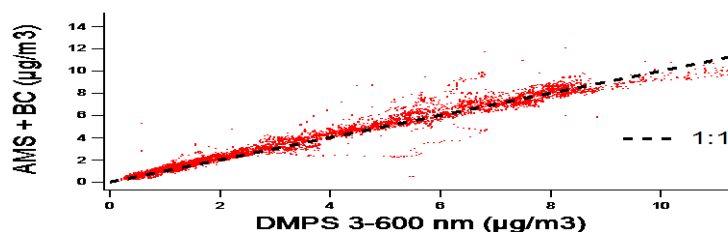


Figure 4. Correlation between the AMS and DMPS derived mass concentrations in March 2009.

CONCLUSIONS

In this study aerosol chemical composition was measured with an AMS at a boreal forest stand in Hyytiälä, Southern Finland. The most abundant chemical species for the measurement periods were organics and sulfates, making up most of the total aerosol mass. Their relative fractions of total mass, however, were different for different campaigns. Other components' mass loadings were smaller and their relative amounts remained almost the same for all three campaigns. The average total aerosol mass loadings were a little higher during spring campaigns. The AMS and DMPS measured mass loadings were found to correlate well. A more detailed analysis of the Hyytiälä AMS results, including positive matrix factorization (PMF) analysis, of the EUCAARI campaign AMS results is ongoing.

REFERENCES

- Allan J.D., Delia A.E., Coe H., Bower K.N., Alfarra M.R., Jimenez J.L., Middlebrook A.M., Drewnick F., Onasch T.B., Canagaratna M.R., Jayne J.T., and Worsnop D.R. (2004) A generalised method for the extraction of chemically resolved mass spectra from aerodyne aerosol mass spectrometer data. *J. Aer. Sci.*, 35:909-922.
- Allan J.D., Alfarra M.R., Bower K.N., Coe H., Jayne J.T., Worsnop D.R., Aalto P.P., Kulmala M., Hyotylainen T., Cavalli F. and Laaksonen A. (2006). Size and composition measurements of background aerosol and new particle growth in a Finnish forest during QUEST 2 using an Aerodyne Aerosol Mass Spectrometer. *Atm. Chem. Phys.*, 6, 315–327.
- Bonan, G.B. (2008). Forests and climate change: Forcings, feedbacks, and the climate benefits of forests *Science*, 320, 1444-1449.
- Drewnick F., Hings S.S., DeCarlo P., Jayne J.T., Gonin M., Fuhrer K., Weimer S., Jimenez J.L., Demerjian K.L., Borrmann S. and Worsnop D.R. (2005). A new time-of-flight aerosol mass spectrometer (TOF-AMS) - Instrument description and first field deployment. *Aer. Sci. Tech.*, 39, 637-658.
- Hari, P. & Kulmala, M. (2005). Station for measuring ecosystem-atmosphere relations (SMEAR II) *Boreal Environ. Res.*, 10, 315–322.
- Jayne J.T., Leard D.C., Zhang X.F., Davidovits P., Smith K.A., Kolb C.E. and Worsnop D.R. (2000). Development of an aerosol mass spectrometer for size and composition analysis of submicron particles. *Aer. Sci. Tech*, 33, 49-70.
- Kulmala M., Asmi A., Lappalainen H.K., Carslaw K.S., Poschl U., Baltensperger U., Hov O., Brenguier J-L., Pandis S.N., Facchini M.C., Hansson H-C., Wiedensohler A. and O'Dowd C.D. (2009). Introduction: European Integrated Project on Aerosol Cloud Climate and Air Quality interactions (EUCAARI) - integrating aerosol research from nano to global scales. (2009) *Atm. Chem. Phys.* 9, 3443-3444.
- Tunved P., Hansson H.C., Kerminen V.-M., Strom J., Dal Maso M., Lihavainen H., Viisanen Y., Aalto P.P., Komppula M. and Kulmala M. (2006). High natural aerosol loading over boreal forests. *Science*, 312, 261-263.